

Analysis of phylogenetic relationships among diploid Triticeae grasses

Von der Fakultät für Mathematik und Naturwissenschaften
der Carl von Ossietzky Universität Oldenburg zur Erlangung des
Grades und Titels eines

Doctor rerum naturalium (*Dr. rer. nat.*)

angenommene Dissertation

von Frau Nadine Bernhardt
geboren am 31.08.1985 in Lutherstadt Wittenberg

Gutachter: Prof. Dr. Dirk Carl Albach
Zweitgutachter: Dr. Frank R. Blattner

Tag der Disputation: 07. März 2016

CONTENTS

1	Introduction	5
1.1	Taxonomic treatments of Triticeae	5
1.1.1	The tribe Triticeae	5
1.1.2	Short introduction to taxonomy, phylogenetics and nomenclature	8
1.1.3	Taxonomic treatments from Linnaeus (1753) to Tzvelev (1976)	9
1.1.4	Löve's and Dewey's genomic systems of generic classification	10
1.1.5	Criticism and impact of the genomic system	11
1.1.6	The era of molecular phylogenies	12
1.1.7	'Chaotic' taxonomic treatments in Triticeae	12
1.1.7.1	The genus <i>Hordeum</i>	13
1.1.7.2	The <i>Aegilops-Triticum-Amblyopyrum</i> complex	14
1.2	Objectives	16
1.3	Molecular markers and phylogenetic inferences	17
1.3.1	Molecular markers and why one (kind) is not enough	17
1.3.2	Methods for gene and species tree inference	19
1.3.2.1	Single gene tree reconstructions	19
1.3.2.2	Multiple genes for species relationship estimations	21
1.4	Laboratory methods	24
1.4.1	The principle of flow cytometry	24
1.4.2	Sequence capture and Illumina sequencing	25
2	Materials and Methods	29
2.1	Selection of taxa and accessions	29
2.2	Flow-cytometric estimation of the genome size	32
2.3	Sequence capture	34
2.3.1	Designing the library of sequence capture probes	34
2.3.2	Accomplishment of the sequence capture	36
2.3.2.1	Optimizing the DNA fragment length	36
2.3.2.2	Library preparation and Illumina sequencing	38
2.4	Sequence assembly and data analyses	40
2.4.1	On-target assembly	40
2.4.2	Off-target assembly	40
2.4.3	Filtering of on-target loci and dataset partitioning	42
2.4.4	Inference of phylogenetic trees and topological comparisons	43
2.4.5	Estimation of reticulations	44
2.4.6	Coalescent-based species tree estimation	44
3	Results	47
3.1	Genome sizes	47
3.2	Sequencing output and sequence assembly	49
3.2.1	On-target	49
3.2.1.1	Read statistics and capture efficiency	49
3.2.1.2	Low-copy number loci and dataset partitioning	50
3.2.2	Off-target	52
3.2.2.1	The nrDNA tandem-repeat region	52

3.2.2.2	The whole chloroplast genome.....	53
3.3	Phylogenetic analyses	54
3.3.1	Low-copy number nuclear gene phylogenies	54
3.3.2	Rooted phylogenetic networks.....	56
3.3.3	Coalescent-based species trees.....	58
3.3.4	The nrDNA tandem-repeat and the chloroplast phylogeny.....	61
4	Discussion	67
4.1	Seed material.....	67
4.2	Sequence capture performance and data assembly	68
4.3	Genome plasticity	70
4.3.1	Origin and identification of paralogues.....	70
4.3.2	Chromosomal rearrangements	70
4.3.3	Gene and/or genome duplications and functional adaptation.....	71
4.4	Phylogenetic relationships among diploid Triticeae.....	72
4.4.1	Main topological groupings	73
4.4.2	The evolution of <i>Australopyrum</i> and its implications.....	73
4.4.3	<i>Eremopyrum</i> and <i>Agropyron</i>	74
4.4.4	<i>Pseudoroegneria</i>	74
4.4.5	<i>Secale</i>	75
4.4.6	<i>Thinopyrum</i>	75
4.4.7	The <i>Aegilops-Triticum-Amblyopyrum</i> complex	76
4.4.7.1	<i>Amblyopyrum</i> , <i>Aegilops speltoides</i> and the section <i>Sitopsis</i>	76
4.4.7.2	<i>Triticum</i> and its relationships to <i>Aegilops</i>	77
4.4.7.3	<i>Aegilops tauschii</i> and species involved in its formation.....	78
5	Conclusions.....	79
5.1	Hybridization-based enrichment approach for Triticeae	79
5.2	Markers and methods for phylogenetic inferences	80
5.3	Phylogenetic relationships among diploid Triticeae.....	82
5.3.1	The main clades and their estimated ages	82
5.3.2	Possible scenarios of speciation in Triticeae	83
5.4	Implications for taxonomic treatments.....	85
	Abstract	89
	Zusammenfassung	91
	References.....	93
	Acknowledgements	112
	Abbreviations	114
	Figures	116
	Tables.....	118
	Supplementary information	119
	Curriculum Vitae & Publications	140

1 INTRODUCTION

1.1 Taxonomic treatments of Triticeae

The content of this section is largely in accord with a book chapter by me in: Molnar M, Ceoloni C, Doležel J (eds.) *Alien Introgression in Wheat: Cytogenetics, Molecular Biology, and Genomics* (Switzerland, Springer International Publishing) that is currently in press.

1.1.1 The tribe Triticeae

The economically important grass tribe Triticeae Dumort. consists, depending on taxonomic treatment, of approximately 360 species and several subspecies in 20-30 genera, adding up to 500 taxa. Triticeae occur in temperate regions all over the Earth and harbour the important cereals, bread wheat (*Triticum aestivum*), barley (*Hordeum vulgare*), rye (*Secale cereale*) and their wild relatives, many forage grasses, species crucial for soil stabilization, and important elements of diverse plant communities. Morphologically they are characterized by the possession of open leaf sheath margins on culm leaves, membranous ligules, inflorescences having sessile spikelets, and ovaries with a hairy top. The tribe comprises annual as well as perennial species, with the annual members being most abundant in Western Asia and the Mediterranean, while the highest species diversity for the perennial members is reported in Central (and to a lesser extent in East) Asia, particularly China (Seberg & Frederiksen, 2001; Barkworth & Bothmer, 2009). There are self- as well as cross-pollinating species (Escobar *et al.*, 2010). Within Triticeae all taxa have a chromosome base number of

$x = 7$ and $2n$ chromosome numbers are 14 or multiples of 14. Supernumerary or B chromosomes are reported in only a few genera such as *Secale* and seem to be a result of major karyotype reorganizations (Martis *et al.*, 2012). The genomes vary in size, but are generally very large. For instance, the genome size of *Triticum aestivum* amounts to more than 100 times that of *Arabidopsis thaliana*.

The tribe is of interest in many areas of research, including archaeology, domestication research, crop breeding, and evolutionary biology. Approximately 12,000 years ago barley (*Hordeum vulgare*), einkorn wheat (*Triticum monococcum*), and emmer wheat (*Triticum turgidum*) were domesticated in the Fertile Crescent in Southwest Asia, marking the transition of human society from hunter-gatherer to a sedentary lifestyle (Kilian *et al.*, 2010). Triticeae species are also of research interest due to their potential for crop improvement by understanding and utilisation of the genetic diversity of wild relatives to ensure global food security (Kellogg *et al.*, 1996; Mochida & Shinozaki, 2013). Furthermore, the tribe exhibits a complex evolutionary history that is not well understood and adds to its appeal for evolutionary biologists.

Approximately 80 species of the tribe are diploid, while the majority of species are allopolyploid, i.e. combining parental genomes from different diploid species or genera of the tribe. Polyploid species are likely to have originated repeatedly, involving genetically different parent species and thus resulting in genetically diverse polyploid species-complexes (Soltis & Soltis, 1999; Mason-Gamer, 2004; Jakob & Blattner, 2010; Brassac *et al.*, 2012). *Triticum aestivum* is the most prominent allopolyploid species, formed by recurrent hybrid speciation involving three diploid species of the tribe and thereby combining three related genomes (named **A**, **B** and **D**) (Petersen *et al.*, 2006; Marcussen *et al.*, 2014). In Triticeae and many other crops such genomes were defined through cytogenetic characterization of chromosomes together with the analysis of their pairing behaviour in interspecific and intergeneric crosses. In comparison to other grass tribes Triticeae show a low barrier against hybridization and other introgressive events (i.e. gene flow between different species). This, together with large- and small-scale genome duplications and incomplete lineage sorting of ancestral polymorphisms, result in diverse genealogical histories for different parts of the genome (e.g. Escobar *et al.*, 2011).

The tribe Triticeae belongs to the Poaceae family and the subfamily of Pooideae. It is generally accepted to be monophyletic (Watson *et al.*, 1985; Kellogg, 1989; Soreng *et al.*, 1990; Seberg & Frederiksen, 2001), which means all taxa of the tribe are derived from a most recent common ancestor. However, the taxonomic treatment of the tribe's members continues to be under long-standing debate. Due to its economic importance in combination with its worldwide distribution, the tribe has always been of interest to researchers. Taxonomists differ in their opinion regarding the relationships of taxa, as well as in the changing methods and perceptions for good classificatory systems. This has resulted in various taxonomic treatments that in several cases have led to numerous correct scientific names for the same taxon. The circumscription of several of the tribe's genera is also under debate (e.g. to include the genus *Aegilops* into *Triticum* or to split it into several genera). The most recent description of Triticeae genera and a discussion of their level of acceptance can be found in Barkworth & Bothmer (2009), and is summarised in **Table 1.1**.

Table 1.1 List of genera and genomes in Triticeae (modified from Barkworth & Bothmer, 2009 and Barkworth & Jacobs, 2011).

Genus	Genomic composition
<i>Aegilops</i> L.	B[#], S, C, D, N, M, U, X
<i>Agropyron</i> Gaertn.	P
<i>Amblyopyrum</i> (Jaub. & Spach) Eig	T
<i>Anthosachne</i> Steud.	StHW
<i>Australopyrum</i> (Tzvelev) A. Löve	W
<i>Connorochloa</i> Barkworth, S.W.L. Jacobs & H.Q. Zhang	StYHW
<i>Crithopsis</i> Jaub. & Spach	K
<i>Dasypyrum</i> (Coss. & Durieu) T. Durand	V
<i>Douglasdeweya</i> C. Yen, J.L. Yang, & B.R. Baum	StP
<i>Elymus</i> L.	St plus at least one of H, W, Y
<i>Elytrigia</i> * Desv.	St, E, H, N
<i>Eremium</i> Seberg & Linde-Laursen	Ns
<i>Eremopyrum</i> (Ledeb.) Jaub. & Spach	F, Xe
<i>Festucopsis</i> (C.E. Hubb.) Melderis	L
<i>Henrardia</i> C.E. Hubb.	O
<i>Heterantherium</i> Hochst.	Q
<i>Hordelymus</i> (Jess.) Harz	Ns
<i>Hordeum</i> L.	H, I, Xa, Xu
<i>Hystrix</i> * Moench	StH or Ns
<i>Kengyilia</i> C. Yen & J.L. Yang	StPY
<i>Leymus</i> Hochst.	Ns
<i>Pascopyrum</i> A. Löve	St, H, N
<i>Peridictyon</i> Seberg, Fred. & Baden	Xp
<i>Psathyrostachys</i> Nevski	Ns
<i>Pseudoroegneria</i> (Nevski) A. Löve	St
<i>Roegneria</i> * K. Koch	St, Y
<i>Secale</i> L.	R
<i>Stenostachys</i> Turcz.	HW
<i>Taeniatherum</i> Nevski	Ta
<i>Thinopyrum</i> A. Löve	E sometimes with P, St, or L
<i>Triticum</i> L.	A, B, D

Generic names marked with an asterisk were not accepted by Barkworth & Bothmer (2009): The type species of *Elytrigia* and *Hystrix* were moved to *Elymus*, hence the generic names are no longer valid. Genome designations for *Eremopyrum* follow Wang *et al.* (1994) and Seberg & Frederiksen (2001). *Leymus* genome designation is given following Fan *et al.* (2014). *Roegneria* was not accepted because of e.g. a lack of morphological distinctions from *Elymus*. *Eremium* resembles *Leymus* genomically, and some taxa do so also morphologically. Löve's (1984) usage of the 'N' genome for *Leymus* had been replaced by 'Ns'. The 'N' genome in *Aegilops* was designated 'L' by Löve (Yen & Yang, 2009). #The B genome in *Aegilops* might be referred to as S or G in other treatments.

Today, there is common consent that a good classification of a taxonomic unit such as Triticeae starts with a thorough evaluation of phylogenetic relationships. This should be based on the analyses of different portions of the genome and include taxa of all genera or genomic groups, thereby covering their whole distribution area (Barkworth, 2000; Mason-Gamer, 2005; Petersen *et al.*, 2006). So far, there is no study available that resolves the tribe's evolutionary history in such a manner that it can be used as a basis for a conclusive taxonomic treatment. Published studies largely agree, however, that *Bromus*, the only genus in the tribe Bromeae, is the sister group to all Triticeae (Kellogg, 1992; Schneider *et al.*, 2009) and that the genera *Psathyrostachys* and *Hordeum* diverged early on from the rest of Triticeae. *Aegilops* and *Triticum* are closely related and of rather recent origin (Kellogg *et al.*, 1996; Petersen & Seberg, 1997; Mason-Gamer & Kellogg, 2000; Escobar *et al.*, 2011). Furthermore, it can be assumed that diploid species and monogenomic taxa (i.e. taxa possessing a single genome type in di- and polyploids) are the basic units within Triticeae and that heterogenomic polyploids (mostly intergeneric allopolyploids that combine different genomes in various combinations) form a second level of taxonomic entities (Kellogg, 1989; Seberg & Frederiksen, 2001).

The remainder of this section presents a short review of the important taxonomic treatments of Triticeae over time.

1.1.2 Short introduction to taxonomy, phylogenetics and nomenclature

Taxonomy in a broad sense is the theory and practice of identifying, describing and classifying organisms into a hierarchical system of taxa (e.g. genera, species, subspecies). It includes phylogenetics, which uncovers evolutionary relationships among organisms, systematics, which infers how to group them, and nomenclature, which is how to correctly name an organism. Taxonomy is not static and its treatments may change whenever new knowledge is gained that more appropriately reflects the evolutionary history of taxa. The rationale behind the objective to anchor taxonomy in the evolutionary history of organisms, is the assumption that in the long-term this will result in a stable system, as all taxa should originate through a single evolutionary process. There is general agreement that taxonomic decisions should therefore be made by integrating all available knowledge from different scientific disciplines including ecological, morphological, cytogenetic and molecular data. This combination of conceptual and methodological achievements was described as integrative taxonomy (Padial *et al.*, 2010). There are, however, no formal rules to follow on how to classify tribes into lower-ranked taxa (Barkworth & Bothmer, 2009). Taxonomists working on the same group of taxa may disagree on which kind of data, and to what extent that data, should be taken into account for taxonomic decisions, and if few large or many smaller taxonomic units should be preferred. Taxonomists may even differ in their opinion regarding what a species actually is. There are several contemporary and partially conflicting species concepts. Some might prioritize the phylogenetic species concept that a species is the smallest unit for which a monophyly (i.e. a clade comprising an ancestor and all of its descendants, which is inferred by the possession of shared derived characteristics, so called synapomorphies) can be found (Rosen, 1979; Cracraft,

1983). Recently, de Queiroz (2007) proposed a unifying species concept, based on the common denominator of all concepts. He stated that species are evolutionary lineages independent of other such lineages and that, for instance, crossing behaviour, ecology, and phylogeny are tools to infer such independence of lineages.

Despite the main objective of the International Code of Nomenclature for algae, fungi and plants (ICN; McNeill *et al.*, 2012) to ensure that there is only one correct scientific name for every taxon, the existence of several different and incompatible taxonomic treatments result in the existence of many formally correct names in use concurrently. This is especially true for taxa within Triticeae, as a reliable system of evolutionary relationships that can be used as a base for decision-making is still lacking. Moreover, the priority rule of the ICN states “for any taxon from family to genus inclusive, the correct name is the earliest legitimate one with the same rank.” Although intended to result in taxonomic stability, it may lead to changes of names even for taxonomic ranks not under debate if older legitimate names are detected. A striking example in wheatgrasses is the recent confusion about the tribe’s name: Reveal (2004, 2011) stated that Martinov designated the name Hordeae (as “Hordeaceae”) at the rank of tribe in 1820, implicating that Triticeae would be a younger and therefore illegitimate name given by Dumortier in 1824. This resulted in a gradual renaming of the tribe from Triticeae into Hordeae till a recent survey by Welker *et al.* (2014) revealed a misreading of Martinov’s work, in which no specific taxonomic rank was assigned to Hordeae. Hence, Triticeae Dumortier (1824) remains the valid name for the tribe.

1.1.3 Taxonomic treatments from Linnaeus (1753) to Tzvelev (1976)

Since the beginning of the Triticeae taxonomy, many considerably different classificatory systems have been proposed by diverse authors. The treatments reflect different aims of taxonomists, the state of the art of classificatory concepts, employed methods, and recognized taxa at the time in which they were published. When Linnaeus published his *Species Plantarum* in 1753, it was the start of modern biological (binomial) nomenclature, providing the names for plant classifications. Other early taxonomists aimed for a classification that would allow taxa to be easily recognized morphologically. They grouped species similar to each other and different from others into genera, thereby following a typological taxonomic concept (Linnaeus, 1753; Bentham, 1882).

With the development of new species concepts and analysis techniques, taxonomists aimed for their classification to reflect the evolutionary history of the tribe. Nevski (1934) was the first to propose a classification for Triticeae that reflects the tribe’s phylogeny. Thus it was largely different from earlier generic treatments (e.g. Bentham, 1882) in the number of accepted genera and their description. Nevski was well aware of the fact that morphological traits might evolve independently and hence, might not necessarily reflect evolution correctly. In addition to morphological data he included phytogeographic and cytogenetic data in his proposal. Noteworthy is the taxon sampling, which covered the centre of diversity of perennial Triticeae. His work was adopted in the Flora of the USSR, but its application in the West was delayed by several years. Taxonomic treatments in North America were mainly based on Hitchcock (1935, 1951), which in

turn were based on Bentham (1882) and Hackel (1887). On the basis of observations made studying crossing-relationships in the tribe, Stebbins (1956) argued that all taxa of the tribe might be subsumed into a single genus *Triticum*. His proposal was made under the influence of the biological species concept (Mayr, 1942) that defines a species as members of populations that can produce fertile offspring, and that are reproductively isolated from other such populations. Although a perfectly defensible proposal, it was not adopted and considered impractical to describe the diverse Triticeae. The treatment of the Russian taxonomist Tzvelev (1976) considered several additional annual and perennial genera in comparison to Hitchcock (1951) and was quickly adopted in the USSR (for a review see Barkworth, 2000).

1.1.4 Löve's and Dewey's genomic systems of generic classification

Until the 1980's several classificatory systems for members of the Triticeae had been proposed. They differed in goals, taxonomic and regional scope and were adopted differently in different parts of the world. Furthermore, since the start of genome analysis (Kihara, 1930) a large amount of cytogenetic data had been accumulated. To overcome existing taxonomical inconsistencies, Löve (1984) and Dewey (1984) independently proposed a generic classification for Triticeae that was solely based on the recognition of so called *genomes* (i.e. the monoploid set of chromosomes). They analysed the pairing behaviour of homologous chromosomes in metaphase I of meiosis in interspecific hybrids and recorded the number of chiasmata in a particular number of cells (often 50). Homologous chromosomes showing near complete pairing are defined as belonging to the same genome. Both authors considered hybrids sharing the same genome or genome combination to be congeneric, i.e. to be placed in the same genus. In contrast, hybrids showing little or no pairing of homologous chromosomes have different genomes and were considered intergeneric. Distinct genomes were depicted by different bold upper case letters, while genomes considered related but not identical are depicted with the same capital letter, extended by lower case letters or a superscript extension (Baum *et al.*, 1987).

Dewey's revision treated perennial Triticeae, while Löve's work was based on the whole tribe. Thereby Löve summarised extremely valuable information regarding all synonyms of which he was aware, together with their original citation, including chromosome number and genomic constitution. He also provided descriptions for all genera and subgenera (Barkworth & Bothmer, 2005). Löve recognized 37 genera, 13 of which are treated as *Aegilops* by most taxonomists today. He defined one genus per genome combination (**A**, **AB**, **ABD**) or ploidy level, respectively, for what is unified in *Triticum* s.str. today (van Slageren, 1994). Although Löve was not completely consistent (e.g. *Elymus* consisted of three different genome constitutions; Dewey 1984) and genus affiliations were partly inferred from morphological similarities (as at that time the genome composition was not analysed for all taxa) this treatment was the start of the modern taxonomy of Triticeae (Barkworth & Bothmer, 2009).

1.1.5 Criticism and impact of the genomic system

The genomic concept was sharply criticized, mainly because (1) the pairing behaviour of homologous chromosomes was interpreted as single-character classification by most taxonomists. Löve and Dewey themselves interpreted pairing behaviour as an indication of overall genetic similarity along the chromosomes, and therefore as a result of multiple characters (Barkworth & Bothmer, 2005). Severe disapproval was also mentioned, when (2) interpreting the extent of chromosomal pairing as an indicator for similarity between the genomes. This was considered a random division of a continuum, and therefore not a reliable taxonomic trait. Further criticism (3) was based on the fact that the failure of chromosomes to pair does not necessarily indicate dissimilarity. At this time, it was already known that a number of loci control the pairing behaviour and recombination of chromosomes. It was suggested that 50 loci might have an impact on the chromosomal pairing in *Pisum* (Gottschalk, 1973; Farooq *et al.*, 1990; Seberg & Petersen, 1998). Today, *Ph1* is the most extensively studied locus involved in this trait (Moore, 2009). Additionally, (4) the system was considered overall unstable, meaning each time new genomes or combinations of them are recognized species need to be transferred between genera, and (5) impractical in the field, when each time a new species is discovered, an appropriate name can only be given after the genome compositions have been identified (Baum *et al.*, 1987; Kellogg, 1989; Frederiksen & Petersen, 1998; Barkworth, 2000; Barkworth & Bothmer, 2005).

After publication of the genomic system of generic classification, taxonomists split into two opposite directions. On the one hand, the group rejecting the genomic concept, due to the lack of complete understanding of pairing behaviour of chromosomes in meiosis. On the other hand, the group acknowledging the additional information it provides, e.g. considering the possible convergent evolution of morphological and physiological traits. Regardless, Löve's revision was recognized as a valuable and comprehensive collection of names of members of Triticeae, and the information about pairing behaviour of chromosomes, i.e. the potential of species to exchange genetic information, was definitely of use to plant breeders.

Although heavily criticized, the genomic system contributed in the clarification and understanding of evolutionary relationships within the tribe. Kellogg (1989) argued that the genomic designations are good indicators of phylogenetic relatedness, as Löve treated them as discrete characters, i.e. as an "all-or-nothing phenomenon" of complete pairing of chromosomes vs. nearly complete failure to pair. However, genome data should never be used on its own. It should be combined with additional data from other disciplines to overcome differences in genetic regulation of chromosome pairing found among some taxa. In this manner, species groups that share a single genome and are also morphologically uniform can be considered monophyletic, and in several cases were found to form such groups through later phylogenetic analyses (e.g. Petersen *et al.*, 2004; Blattner, 2004, 2009). In contrast, heterogenomic species (i.e. species that combine two or more different genomes) are clearly the result of hybridization. Therefore they are in conflict with the monophyly criterion of the phylogenetic species concept, as more than one parental clade was involved in their formation. Heterogenomic taxa can be treated as units on their own in plant groups with a high extent of hybrid formation like Triticeae. They can be included as reticulations in cladistic analyses, for a review

see Kellogg (1989). Löve and Dewey's work showed that evolutionary relationships are not necessarily strictly based on bifurcating ancestral lineages and hence, cannot be covered by a classificatory system that allows only for hierarchical relationships.

1.1.6 The era of molecular phylogenies

The taxonomy within the tribe continued to evolve, particularly as improved phylogenetic analyses started to shed light on species relationships. Different kinds of molecular data were generated using isozymes (McIntyre, 1988; Jarvie & Barkworth, 1990), DNA/DNA hybridizations, and restriction-site analyses (Ogihara & Tsunewaki, 1988; Monte *et al.*, 1993; Mason-Gamer & Kellogg, 1996). In particular, DNA sequencing resulted in fast advances in molecular phylogenies within the tribe. In the last decades a multitude of molecular markers have been employed using coding and non-coding, nuclear and plastid, single- or low-copy number genes and repetitive loci (Hsiao *et al.*, 1995; Kellogg *et al.*, 1996; de Bustos & Jouve, 2002; Mason-Gamer *et al.*, 2002; Blattner, 2004; Petersen *et al.*, 2006, 2011; Golovnina *et al.*, 2007; Mason-Gamer, 2008, 2013; Jakob & Blattner, 2010; Bordbar *et al.*, 2011; Brassac *et al.*, 2012; Yan & Sun, 2012). Studies have mainly aimed for a better understanding within single genera (e.g. *Hordeum*, *Elymus*) of the tribe and/or a small subset of related genera with the main focus being *Hordeum*, *Pseudoroegneria* and *Elymus*, or the *Aegilops-Triticum-Amblyopyrum* complex.

Generally, the comparison of studies dealing with a similar set of taxa rarely revealed similar phylogenetic relationships. Possible reasons for incongruences between different studies are (1) true but different evolutionary histories of the distinct genes used as phylogenetic markers, (2) differently conducted analyses, and (3) limited, biased and variations of taxon sampling (Kellogg *et al.*, 1996; Petersen *et al.*, 2006; Blattner, 2009). Although not including all diploid genera, Escobar *et al.* (2011) have to date published the most comprehensive multi-genic dataset including one chloroplast and 26 nuclear loci, most of which are probably located on a single chromosome. This study resulted in the recognition of up to five major clades in diploid Triticeae and agrees with other studies, for instance in the basal positions of *Psathyrostachys* and *Hordeum* in the phylogenetic trees. Furthermore, it pinpoints clades that are particularly affected by reticulate evolution or incomplete lineage sorting (e.g. *Aegilops*, *Dasypyrum*, *Secale*, and *Triticum*). Although providing essential new insights, the still limited marker and taxa choice in Escobar *et al.* (2011) leaves many open questions regarding speciation processes in Triticeae.

1.1.7 'Chaotic' taxonomic treatments in Triticeae

The nomenclature of nearly all taxa within Triticeae is affected by confusion due to various taxonomic treatments. Several attempts were made to provide an overview of all synonyms under use, e.g. Löve (1984), The International Plant Name Index (IPNI; www.ipni.org), and eMonocot.org. Even assuming all taxonomists working on the tribe could be convinced to follow the same treatment, it requires extensive and careful literature search to ensure that only valid names (in agreement with the priority rule of

the ICN) will be given to taxa. However, once established, a single and conclusive taxonomic treatment that is generally used would greatly simplify the understanding of researchers working on Triticeae taxa. The same is true for the usage of the genomic symbols. Generally, genome designations offer an efficient and abbreviated way to depict relationships between allopolyploids and their progenitors. For this reason, they are used in nearly every study dealing with polyploids in Triticeae. Nonetheless, since Löve's (1984) revision of the tribe, several suggestions have already been made to rename some of the genomes (**Table 1.1**). Often, these suggestions have been followed by only some scientists, which led to another level of confusion. Depending on the publication at hand it can be difficult to track back the change(s) of a genome name and the reasons for it.

Nomenclatural conflicts as the result of different taxonomic treatments will be illustrated in detail for *Hordeum* and the species complex of *Aegilops*, *Triticum* and *Amblyopyrum*.

1.1.7.1 The genus *Hordeum*

The genus *Hordeum* L. comprises about 33 species, two subgenera and five sections. Almost half of the species are tetra- and hexaploid (allo- or autopolyploid) species (Blattner, 2009; Brassac & Blattner, 2015). As for other genera of Triticeae many different taxonomic treatments have been proposed during the last decades, e.g. based on morphological features and life cycle or the distribution of the species (e.g. Nevski, 1941; Covas, 1949; Bothmer & Jacobsen, 1985). Due to the economic importance of barley (*Hordeum vulgare*) many crossing experiments and analyses of seed fertility have been conducted. Based on genomic and karyological results it was suggested that the genus *Hordeum* should consist only of *Hordeum vulgare* (Löve, 1982, 1984) or *Hordeum vulgare* and *Hordeum bulbosum* (Dewey, 1984) and that all other species should be united under the genus *Critesion* Raf. While in both cases *Hordeum* is monophyletic, recent phylogenetic analyses have shown, that these treatments would result in a paraphyletic genus *Critesion*. Thus, most taxonomists currently reject to split *Hordeum* into smaller units (Bothmer *et al.*, 1995; Blattner, 2009), particularly as it is morphologically well defined.

Based on cytogenetic studies four different genomic groups were initially defined: **H**, **I**, **X**, and **Y** (Bothmer *et al.*, 1995) and their monophyly could be shown (e.g. Blattner, 2004; Petersen & Seberg, 2009; Brassac *et al.*, 2012). However, genome designation changes were proposed several times by different authors. Blattner (2009) proposed the usage of **H** for the genome occurring in *Hordeum vulgare* and *Hordeum bulbosum*, **Xa** for *Hordeum marinum*, **Xu** for *Hordeum murinum* and **I** for all remaining *Hordeum* species. This resulted in swapping the genome nomenclature for the **I** and **H** genomes from that of earlier studies (e.g. Wang *et al.*, 1994; Bothmer *et al.*, 1995). Although meant to decrease confusion by achieving consistency of the chromosome nomenclature of barley (i.e. 1H, 2H, etc.), it added confusion with respect to the whole tribe. In allopolyploid species such as *Elymus*, *Hystrix* (**Table 1.1**) the **H** genome is referring to the **I** genome of *Hordeum* and not to **H**. Generally, the comparison of molecular phylogenetic studies trying to unravel the evolution within the genus revealed several conflicting infrageneric phylogenies (for a review see Blattner, 2009). Brassac & Blattner (2015) presented a phylogeny including relationships for all di- and polyploid

Hordeum taxa based on one chloroplast and 12 nuclear single-copy loci making *Hordeum* the best understood genus in Triticeae at the moment.

1.1.7.2 The *Aegilops-Triticum-Amblyopyrum* complex

Regarding the wheat genus, *Triticum*, two different nomenclatural interpretations exist. Depending on the taxonomic treatment under use, *Triticum* either includes taxa that are otherwise described under *Amblyopyrum* and *Aegilops* (i.e. *Triticum* s.l.) or is restricted to species having the **A** genome or one of the genome combinations **AB**, **AAB**, or **ABD** (**Table 1.1**; Barkworth & Bothmer, 2009). In the past *Aegilops* and *Triticum* were rarely subsumed into one genus (Bowden, 1959; Dvořák & Zhang, 1992; Yen *et al.*, 2005) as proposed by Stebbins (1956). However, treating them separately makes *Aegilops* paraphyletic, as not all descending lineages are included in the same genus, and *Triticum* polyphyletic, since *Aegilops* played a key role in the formation of tetraploid and hexaploid wheats. Thus, *Aegilops tauschii* contributed the **D** genome to *Triticum aestivum*, the **B** genome (also referred to as **S** in the parental species, or **G** in other polyploid species) stems from *Aegilops speltoides* (Petersen *et al.*, 2006). Agreement on the congeneric status of *Aegilops* and *Triticum* would solve this nomenclatural problem. However, there is a long tradition in keeping both genera separate because of their clear morphological distinction. Of 153 inspected floristic treatments that were published between 1753 and 1994 approximately 86% considered them as different genera (van Slageren, 1994). In this work I adopt the traditional view and treat *Triticum* as separate from *Aegilops* (also following Barkworth & Bothmer, 2009).

In addition to the two different interpretations of the genus *Triticum* (i.e. keeping *Aegilops* and *Triticum* separate vs. their unification in one genus), different and incongruent taxonomic treatments for *Triticum* s.str. exist leading to confusion for the international research community. A good classificatory system for *Triticum* seems pivotal to unravel its origin but also to efficiently preserve its morphological and genetic diversity. Thus it has been argued that an especially detailed taxonomic system is needed that also meets the needs for future wheat breeding (Goncharov, 2002, 2011). Additionally, the lack of consistent rules on how to treat natural and artificial hybrids resulted in many unnamed artificial hybrids as well as hybrids with invalid names (Goncharov, 2011).

There are two main opposing classificatory systems, which both take into account genomic data. On the one hand, there is the latest monograph from Dorofeev *et al.* (1979) that is based on a very fine discrimination of morphological characters, but was also influenced by Flaksberger's (1935) treatment founded on the division of taxa into groups by ploidy level (di-, tetra- and hexaploids). Dorofeev *et al.* recognized 27 *Triticum* species in two subgenera, and no less than 1,054 infraspecific taxa.

On the other hand, Mac Key (1966, 1977, 1989, 2005) formulated his concept based on classical (Mendelian) genetics, i.e. observations made on a small number of genes that play a role in the development of distinct morphological characters in wheat (Goncharov, 2011). In his most recent treatment, Mac Key (2005) recognized ten species and 20 infraspecific taxa. He defined the subdivision *Triticosecale* for three artificial intergeneric hybrid species of *Triticum* and *Secale*. The treatment was acknowledged as an open

system that allows adjustment (van Slageren, 1994) or as a “plausible and workable concept” (Hammer *et al.*, 2011). Van Slageren (1994) followed Mac Key (1977, 1989), in that taxa at the species and subspecies level should only contain “commercially” cultivated wheat and their closest wild relatives. Artificial auto- or amphiploids should be included in a nothogenus (i.e. a “bastard” species) and excluded from *Triticum*. The same accounts for interspecific crosses that should be subsumed into nothospecies. He described a total of six species, and 17 subspecies. Van Slageren’s revision is the most consistent and most used treatment to date (e.g. Matsuoka, 2011; Zohary *et al.*, 2012; Feldman & Levy, 2012).

The traditional taxonomic treatments of the genus *Aegilops* L. subsumes 22 species (10 diploids and 12 polyploids) that occur in the Mediterranean and in western Asia. The species *Amblyopyrum muticum* is often included in *Aegilops* as *Aegilops mutica*. Morphologically *Aegilops* can be well differentiated from *Triticum* s.str. having no well developed keels on the glumes, while *Amblyopyrum muticum* can be distinguished from *Aegilops* by having a spike completely without awns or teeth (van Slageren, 1994; Kilian *et al.*, 2011). In *Aegilops* five sections have been defined based on morphological traits and genomic constitutions. *Aegilops speltoides* and *Amblyopyrum muticum* are the only (frequently) outcrossing species (for a review see Kilian *et al.*, 2011). To date no molecular study is available that resolves the phylogeny of the *Aegilops-Triticum-Amblyopyrum* complex satisfactory. The comparison between published molecular phylogenies is severely hampered by the differences in taxon sampling among studies. Petersen *et al.* (2006) used two single-copy nuclear genes and one plastid marker including tetraploid and hexaploids *Aegilops* and *Triticum* species, as well as species that represent all diploid genomes of Triticeae for phylogenetic analyses. All employed markers resulted in another tree topology. As a result of that study, Petersen *et al.* (2006) suggested that neither *Aegilops* and *Triticum* separately nor the combination of both genera can be assumed monophyletic.

1.2 Objectives

There is a consensus that a good taxonomic treatment of the tribe's members has to start with a robust phylogeny that is based on a combination of data from different parts of the genome (Mason-Gamer, 2005). This includes all representative genera, to provide conclusive results, as well as several accessions per species to test for monophyly within species (Petersen *et al.* 2006). So far, only a few molecular phylogenies have been published trying to understand the tribe's history as a whole, leaving many questions unanswered. These studies have only considered diploid taxa, with rarely more than one accession per species and only a small part of or biased fractions of the genome (Hsiao *et al.*, 1995; Petersen & Seberg, 1997, 2000, 2002; Escobar *et al.*, 2011). Recently, the advent of methods that retrieve sequence information from many different portions of the genome for many accessions and species group(s) under study at the same time coupled with high-throughput sequencing platforms offer new possibilities for a better understanding of speciation in taxonomically complex groups, such as the grass tribe Triticeae.

The aim of this dissertation is to (1) evaluate if a hybridization-based enrichment approach coupled with next-generation sequencing that targets sequence information from several hundred low-copy number genes is appropriate to (2) understand relationships among the diploid members of the tribe Triticeae. Thereby, (3) the best-suited kinds and combinations of molecular markers as well as efficient ways to analyse them will be identified. The generated data will be used to assess (4) if the generated phylogenetic data verifies the separate taxonomic treatment of *Aegilops* and *Triticum* and of *Amblyopyrum* and *Aegilops*, respectively, and (5) if the data can be used to make future classificatory decisions that reduce recent taxonomic confusion within Triticeae.

1.3 Molecular markers and phylogenetic inferences

A good understanding of evolutionary relationships between species requires the integration of information from several scientific disciplines (e.g. morphology, genome size, genetic information). Then, phylogenetic analyses can help to improve the understanding of species relationships. Because single molecular markers evolve under different evolutionary constraints, they only display a limited part of the true species relationships. Hence, for good species tree estimates, it is not sufficient to focus on sequence information from a single or few molecular markers. In the following, molecular markers commonly used in phylogenetic studies are introduced. Subsequently, potential reasons for incongruences between tree topologies from different markers or genes and the most frequently used methods for phylogenetic inference are shortly reviewed.

1.3.1 Molecular markers and why one (kind) is not enough

Early molecular phylogenetic studies were limited by the amount of sequence information that could be produced or efficiently analysed. Hence, they were usually based on single molecular marker regions to approximate the species tree. The highly variable and fast evolving internal transcribed spacer regions (ITS1 and ITS2) of the 18S-5.8S-26S nuclear ribosomal DNA (nrDNA) unit and chloroplast markers, e.g. the large subunit of ribulose-1,5-bisphosphate carboxylase/oxygenase (*rbcL*) or maturase K (*matK*), were frequently used for early phylogenetic inferences in plants. The nrDNA occurs as a tandem repeat of hundreds to thousands of copies in one or more chromosomal locations. Although it is bi-parentally inherited, unequal crossing over and/or high-frequency gene conversions lead to homogenization of the parental sequences (i.e. concerted evolution; Dubcovsky & Dvorák, 1995; Álvarez & Wendel, 2003), thus blurring the evolutionary pathway especially in polyploid taxa.

In contrast to the nrDNA tandem-repeat region, the chloroplast genome is usually maternally inherited in angiosperms, and therefore, the dispersal is limited to seeds. It is not recombining and due to the low rates of sequence divergence, its use in phylogenetic inference is limited to higher taxonomic levels (Sang, 2002). ITS and chloroplast markers have been frequently used in past studies. They are relatively easy to amplify via polymerase chain reaction (PCR), primarily due to conserved primer binding sites that enable their use over a broad taxonomic scale (Baldwin *et al.*, 1995) and also because they occur in high number in the cell (e.g. Stoof-Leichsenring *et al.*, 2014 for *rbcL*). Recently, studies that employ the highly variable external transcribed spacer (ETS) of the nrDNA unit as a molecular marker, able to better resolve phylogenies, have been more frequently published (e.g. Friesen *et al.*, 2015; Schulte *et al.*, 2015; Steffen *et al.*, 2015).

However, the increasing number of phylogenetic studies and usage of additional nuclear molecular markers showed that single markers often provide only little insight into species relationships. Incongruences between gene trees are frequently reported and are the result of different evolutionary forces acting on the analysed molecular markers. The four main reasons for conflicting gene trees are (1) gene flow (hybridization/recom-

ination/horizontal gene transfer), (2) incomplete lineage sorting, (3) differential gene duplication and loss and (4) differences in selective constraints. The reasons for gene tree conflict are briefly explained in the next paragraph, for a comprehensive review see Degnan & Rosenberg (2009).

Introgression or introgressive hybridization defined as “the permanent incorporation of genes from one set of differentiated populations into another” (Rieseberg & Wendel, 1993), might result in mosaic-like genomes, i.e. a new combination of parts of different genomes with different histories. The term “hybrid species” usually refers to polyploid speciation implying that newly formed hybrids are reproductively isolated from their parent species due to a change in ploidy level (Soltis & Soltis, 1999; Mallet, 2007). However, homoploid hybrid speciation occurs when species hybridize and form a new species that is reproductively isolated from the parental species without change in ploidy level. It was hypothesized, that reproductive isolation might result from reciprocal translocations that lead to novel but fit gametes that show lower fertility to the parental species (Rieseberg, 1997; Coyne & Orr, 2004). As a consequence different parts of a genome or even different parts of a gene can have varying histories. Additionally, it was shown that genes might move between diploid species via polyploid species that act as bridges (Kellogg *et al.*, 1996).

Another reason for gene tree incongruences resides in the existence of polymorphisms at speciation events and a differential fixation of the alleles in subsequent speciation events by drift and/or selection (i.e. incomplete lineage sorting (ILS); Kingman, 1982; Hudson, 1990). The chance of ILS in the data increases if divergence times of the studied taxa are short. Also, the larger the effective population size (N_e) is for a species, the more generations back are required for the lineages under study to coalesce into a common ancestral copy (Maddison, 1997; Sang, 2002; Degnan & Rosenberg, 2009). ILS is said to be the major challenge for phylogeny-based analyses at the inter- and intraspecific level (Sang, 2002).

Moreover, gene trees can only correctly reflect species relationships if orthologous sequences were sampled. Gene duplications that are followed by paralog diversification and a speciation event with differential gene loss afterwards in descendant species, may result in the sampling of paralogous sequences that result in conflicting species trees (e.g. Maddison, 1997). Misunderstood orthology was suggested to be more likely for deeper phylogenetic levels, as the longer the time scale since species divergence allows for more cycles of gene duplications and deletions (Sang, 2002).

The use of multiple nuclear protein coding single- or low-copy number genes is considered a good strategy for species tree reconstructions. They are bi-parentally inherited and the use of more conserved exons, where deleterious mutations are eliminated by purifying selection, and/or introns, that are evolutionary less constraint and therefore more variable, allow for their application at all taxonomic levels (Doyle & Doyle, 1999; Sang, 2002). In contrast to nrDNA and chloroplast markers, many independent phylogenetic hypotheses can be retrieved and hybrid speciation can be detected (Wendel *et al.*, 1995; Sang, 2002; Álvarez & Wendel, 2003). However, due to their possibly complex evolutionary history, results based on low-copy number genes have to be interpreted with caution.

It has also been shown that evolutionary forces affect parts of the genome differently. For instance, less gene flow is to be expected in a genomic island of divergence or speciation, i.e. regions involved in reproductive isolation or species-specific ecological adaptation (Via & West, 2008; Nosil *et al.*, 2009; Cruickshank & Hahn, 2014). There is general agreement that loci located in centromeric regions of chromosomes are less frequently involved in recombination. Consequently, they are expected to show a lower effective population size and ancestral polymorphisms coalesce faster. In contrast, telomeric regions of a chromosome are considered to be more frequently introgressed. Loci located in recombining regions are therefore characterized by a higher effective population size and should be more strongly affected by ILS (Kaplan *et al.*, 1989; Escobar *et al.*, 2011; Charlesworth, 2012).

The discussion of whether loci from high or from low recombining regions make the best markers for species tree reconstructions remains controversial. Intuitively, it may appear that loci located in low-recombining regions are better suited for species tree reconstructions, as they are less affected by introgression and less conflicting tree topologies are to be expected (Escobar *et al.*, 2011). On the other hand, loci in centromeric regions are under linkage disequilibrium, i.e. not independently segregating during meiosis. This means, that neutral variability is reduced at linked sites by selective forces such as selective sweeps or background selection (Charlesworth *et al.*, 1993; Nater *et al.*, 2015). In contrast, loci in telomeric regions are in linkage equilibrium and hence have a higher chance for an independent segregation during meiosis. Therefore, they provide several autonomous hypotheses for species tree inferences. Although potentially more affected by hybridization, it was suggested that the higher rate of intra-specific recombination at the telomeres lowers the probability of permanent maintenance of introgressed loci after inter-specific gene exchange. Accordingly, enhanced gene flow might be considered beneficial for species maintenance (Petit & Excoffier, 2009) and these regions might therefore be superior for phylogenetic inference.

1.3.2 Methods for gene and species tree inference

1.3.2.1 Single gene tree reconstructions

Given a set of sequences of one or more molecular markers of species (groups) under study, there is a vast choice of phylogenetic inference methods that can be used to analyse the phylogenetic relationships. There are distance-based methods that determine relationships between taxa by pairwise comparisons of sequence (dis)similarities, e.g. Neighbor-joining (Saitou & Nei, 1987). In contrast, Maximum Parsimony methods assume that the simplest explanation (e.g. the least number of character transformations) consistent with the data reflect the best phylogenetic hypothesis (Stewart, 1993).

Currently, the most frequently used methods to estimate single gene trees are Maximum-Likelihood (ML) and Bayesian phylogenetic inference (BI) approaches. These methods rely on models that describe the sequence evolution (i.e. the nucleotide frequencies and the different probabilities of nucleotide substitutions along the branches of a tree) to reconstruct gene tree topologies and branch length that correspond best to

the assumed model of evolution (Holder & Lewis, 2003). There is a multitude of models that describe the molecular DNA sequence evolution. The most complex model, the general time reversible model (GTR; Tavaré, 1986), uses individual parameters to describe all possible nucleotide frequencies and substitution probabilities. Additionally, for all models, parameters can be implemented that describe the fraction of invariable sites (Hasegawa *et al.*, 1985) and site dependent rate variation (for review see, e.g. Strimmer *et al.*, 2009). Different strategies to statistically select the best-fitting model are implemented in various programs like JMODELTEST (Posada, 2008) or PARTITIONFINDER (Lanfear *et al.*, 2012). Frequently used selection strategies are the Akaike information criterion (AIC; Akaike, 1974) or the Bayesian information criterion (BIC; Schwarz, 1978), that identify the best-fitting model by a high likelihood, but constrained by the number of parameters used (Liò & Goldman, 1998; Posada & Crandall, 2001; Posada, 2009).

ML and BI are similar in the way that both use likelihood estimations as the basis for tree inferences. ML is asking which hypothesis (i.e. tree topology and branch length) has the highest probability of producing the observed data (Felsenstein, 1981). This probability is the likelihood of the tree. Confidence can be assessed using bootstrap replications by a random re-sampling of the original data matrix with replacement. The tree-building algorithm is then applied to each replicate dataset (Whelan *et al.*, 2001; Holder & Lewis, 2003; Wiley & Lieberman, 2011). Although ML has proven to accurately resolve phylogenetic hypothesis, it is computationally very demanding and therefore slow. However, there are now fast algorithms that can handle large datasets in reasonable time (e.g. RAXML; Stamatakis, 2014). Nevertheless, ML relies on heuristics (e.g. the strictly hill-climbing algorithm) and returns only one best tree that might have originated from a local optimum in the tree space (Chor *et al.*, 2000; Guindon & Gascuel, 2003).

In BI the optimality-criterion is defined as finding the best hypothesis that maximized the posterior probability given the data and the model. The Bayes theorem (Bayes, 1763) could only be applied to phylogenetics in 1996 (Li, 1996; Rannala & Yang, 1996). Without reference to the actual data, first, a prior distribution is defined, e.g. that all alternative trees are equally probable (Ronquist *et al.*, 2009). BI uses Markov chain Monte Carlo algorithms (MCMC; Metropolis *et al.*, 1953; Hastings *et al.*, 2009) which aim at finding area(s) in a probability space where the probability density is the highest, and hence, the trees with highest posterior probability are supposed to be located (Wiley & Lieberman, 2011). In contrast to ML, BI returns more than one probable tree topology. The Metropolis coupled MCMC algorithm, as implemented, for example, in MRBAYES (Ronquist & Huelsenbeck, 2003), employs *heated* chains to accelerate mixing of the *cold* chain (i.e. to reach convergence on the target distribution). The *heated* chains can be pictured as exploring a hilly tree probability space that is flattened out in comparison to the actual landscape. Shallower valleys separate the hills in this landscape and moving between the peaks becomes easier. *Cold* and *heated* chains regularly exchange information (i.e. swapping of states between them). If the *heated* chain finds a tree topology with higher probability, the *cold* chain will move onto this hill. Since the remote tree space can be effectively explored, it is less likely that the algorithm gets trapped in local optima. Since the outcome of BI may be dependent on the starting point, several independent runs are typically employed (for a review see Ronquist *et al.*, 2009).

1.3.2.2 Multiple genes for species relationship estimations

Since individual gene trees represent a narrow part of the species evolution, it is important to consider information from several parts of the genome in species tree reconstructions. However, even if independent sequence information from multiple genetic locations is available, the choice of the best method for phylogenetic inferences is not an easy task. An increasing number of methods aiming at species tree reconstructions were developed that differ in the basic assumptions, advantages and limitations. The accuracy of these methods is often subject to severe criticism. What follows is an overview of frequently used species tree estimation methods, the underlying principles and limitations.

Phylogenetic networks are frequently drawn to unravel the evolutionary history of haplotypes of a single locus. They can be generally defined as a representation of taxa as nodes and their evolutionary relationships as edges (Huson & Bryant, 2006; Francis & Steel, 2015). Phylogenetic networks may be reconstructed from sequences, distances or from a set of gene trees from multiple loci. Phylogenetic trees represent a special type of network where edges are denoted as branches. Phylogenetic trees force the data into a bifurcating scheme. In the case of reticulated events involved in speciation other types of networks that allow relationships to be not strictly dichotomous are better suited to explore these relationships. Split networks are frequently used to visualize incompatible information in the source data using parallel edges, which may form nodes that do not point to an ancestral taxon. In contrast, reticulate networks are depicted as phylogenetic trees with all internal nodes representing ancestral species. Nodes connected with additional edges may indicate recombination or hybridization (Huson & Bryant, 2006). There is a multitude of programs able to produce phylogenetic networks e.g. PHYLONET (Than *et al.*, 2008), DENDROSCOPE (Huson & Scornavacca, 2012) and SPLITSTREE (Huson, 1998), but interpretation of the depicted discordance within and between datasets is difficult (Knowles & Kubatko, 2011). For a review on different phylogenetic networks see Huson & Bryant (2006) and Huson & Scornavacca (2011).

A widely used method to approximate the species tree is the combination of multiple sequence alignments (concatenation) of different parts of the genome into a single supermatrix. Due to its simplicity, concatenation is a standard approach for species tree inference. However, it has been criticized, because it hypothesizes that all data at hand evolved according to a single evolutionary tree and thereby ignores the biological reality (Kubatko & Degnan, 2007; Degnan & Rosenberg, 2009). Moreover, it was shown that it could produce incorrect tree topologies with high confidence (Kubatko & Degnan, 2007) and could be statistically inconsistent under the multispecies coalescent model (Roch & Steel, 2014).

Supertrees belong to another family of species tree inference methods. Traditionally, partially overlapping source trees obtained from different (kinds of) datasets and studies were combined to produce a larger supertree. Some supertree reconstruction approaches aim to achieve a minimum of the overall disagreement between source trees, while others follow the method of matrix representation with parsimony (MRP; for a review see Bininda-Emonds, 2004). In the past, the accuracy of supertree methods has been controversially discussed, because they often revealed poorly resolved supertrees when the source trees contained a large number of topological conflicts or

because they can result in a tree showing relationships in conflict to all input trees (Scornavacca *et al.*, 2008; Kupczok *et al.*, 2010). Recently, with more information available, the application of supertree methods shifted to taxa sets with higher overlap. The accuracy of supertree methods improved with the development of multilocus bootstrapping approaches to assess confidence or by approaches combining MRP with likelihood estimations (Nguyen *et al.*, 2012; Swenson *et al.*, 2012; Haeseler, 2012).

There are other methods that rely on multiple gene trees as input data that account for the stochastic history of genes, such as the Bayesian concordance analysis (BCA; Ané *et al.*, 2007) and the multispecies coalescent (Degnan & Rosenberg, 2009; Heled & Drummond, 2010). The BCA summarises individual Bayesian gene trees and provides a primary concordance tree that consists of the clades that are supported in most gene trees and hence, represents the main vertical phylogenetic signal in the data. It thereby assumes no specific biological reasons for gene tree conflict. BCA is implemented in the program BUCKY (Larget *et al.*, 2010). However, BUCKY tends to underestimate the concordance factors for datasets with many taxa and poorly resolved trees (C. Ané in response to the “BUCKY users”, 2012). In contrast, coalescence methods explicitly consider ILS as the only source of gene tree discordance (Heled & Drummond, 2010). ILS is modelled mathematically using the coalescent model (Kingman, 1982), which analyses the evolutionary history of a set of alleles in a manner that progresses backwards through time (Kubatko, 2009). Coalescence-based methods can be divided into two kinds: Short-cut coalescence methods (or summary methods) that integrate individual gene trees that were previously estimated, and Bayesian coalescence methods that co-estimate gene and species trees from multiple sequence alignments. Bayesian coalescence methods, e.g. BEST (Liu, 2008) and *BEAST (Heled & Drummond, 2010), are known to provide accurate species trees on simulated and biological data, but due to computational requirements their application is limited to relatively small datasets (i.e. maximally 25 species and less than 100 loci; McCormack *et al.*, 2013; Zimmermann *et al.*, 2014; Roch & Warnow, 2015). BEST and *BEAST are powerful programs since they integrate uncertainties in their species tree estimations. They estimate population sizes as well as calibrated phylogenies by modelling the molecular evolution on each branch in the tree.

Recently more and more short-cut coalescence methods are emerging to overcome limitations in the size of the datasets that can be analysed, e.g. STEM (Kubatko *et al.*, 2009), MP-EST (Liu *et al.*, 2010) and ASTRAL (Mirarab *et al.*, 2014c; Mirarab & Warnow, 2015). Simulation studies of summary methods have shown that they are statistically consistent under the multispecies coalescent model and able to return the correct species tree, if a large enough number of correct gene trees randomly sampled over the genome is provided. Concern has been raised regarding the use of summary methods in general. Multispecies coalescence methods are based on the assumption of free recombination between and no recombination within loci (Heled & Drummond, 2010; Liu *et al.*, 2015), hence the use of large contiguous sequences sampled from many regions of the genome have a high probability of recombination either between or within genes (Gatesy & Springer, 2013, 2014). On the other hand short sequences that have low probability of recombination are likely affected by gene tree estimation error (GTEE) due to a lack of phylogenetically relevant information. Both, loci under recombination and/or GTEE, may lower the accuracy of short-cut coalescence methods

(Roch & Warnow, 2015; Xi *et al.*, 2015). While it was suggested that summary methods should be avoided in favour of concatenation (Gatesy & Springer, 2014), it was also argued that there are programs with greater robustness to GTEE that are at least as accurate as concatenation methods (Roch & Warnow, 2015; Mirarab & Warnow, 2015). The inclusion of more genes was shown to make summary methods more robust, also under GTEE (Xi *et al.*, 2015).

Simultaneously to the development of summary-based methods, effort has been made to extend the usage of Bayesian coalescence methods to genome-scale analyses. Datasets are randomly divided into smaller subsets, then gene and species trees are coestimated for each data partition separately, as in *BEAST. The data obtained for every subset is subsequently merged using a summary method (Zimmermann *et al.*, 2014). Other strategies of binning have been proposed as well. Naive binning employs supermatrices formed by combining randomly selected gene sequences into supergenes (Bayzid & Warnow, 2013; Bayzid *et al.*, 2014) and statistical binning refers to the combination of gene sequences displaying gene trees with the same history defined by having no strongly supported conflicts (Mirarab *et al.*, 2014a). Liu *et al.* (2015) argue that both approaches may result in misleading species tree estimations because they are statistically inconsistent and biased.

Apart from methods that do not account for any or for only one reason of gene tree conflict, supertree strategies exist that infer species trees from whole gene families. These methods are consistent under gene loss/duplication and orthologues do not need to be identified (Chen *et al.*, 2000; Boussau *et al.*, 2013; de Oliveira Martins *et al.*, 2014). Because paralogues can be included, such tools make use of more available data and have proven to be robust under limited ILS (Boussau *et al.*, 2013).

To sum up, choosing the best method for estimating a species tree is difficult and highly dependent on the phylogenetic question (e.g. shallow vs. deep phylogeny), the data at hand (e.g. the amount of missing data, length and informativeness of loci and gene family data) and available prior knowledge (e.g. extent of ILS and/or hybridization). The application most advisable will utilise several independent approaches that complement each other and to then compare the results.

1.4 Laboratory methods

1.4.1 The principle of flow cytometry

Genomes in plants can exhibit a 2400-fold size difference. The smallest known genome is 63 Mb in *Genlisea margareta* (Lentibulariaceae; Doležel *et al.*, 2007) while the largest is 148,852 Mb in *Paris japonica* (Liliaceae; Bennett & Leitch, 2011). In Triticeae genome sizes range from about $2C = 6.9$ pg in diploid *Hordeum* to about $2C = 44$ pg in polyploid *Thinopyrum* (values from <http://data.kew.org/cvalues>). The biological meaning for these genome size differences is not yet unravelled and also known as the “C-value paradox” (Thomas, 1971; Eddy, 2012). It was suggested that genome size variations exist due to different amounts of repetitive elements, as the gene number in higher plants is similar with about 30,000 (e.g. Jakob *et al.*, 2004).

Flow cytometry (FCM) is a technology that is applied to analyse the optical properties of microscopic particles (i.e. cells or organelles) in an aqueous suspension. It can be used to sort different subpopulations of particles, but also represents a standard technique for the estimation of the nuclear DNA content in plants (Doležel, 2005; Doležel *et al.*, 2007).

In FCM the particles of interest are first stained with a fluorochrome. Then, a particle free fluid (sheath) is forced to flow under pressure through a small port of a cuvette (**Figure 1.1**) and the sample fluid is injected into the flowing stream. The sheath fluid flows reasonably faster than the sample fluid and the particles get separated and aligned due to hydrodynamic focussing. The particles can then be individually excited by a laser (i.e. a monochromatic light source). The excited dye molecules emit photons, which will be separated according to their wavelength (i.e. energy level) and redirected to photo detectors (photomultiplier tubes, PMT) that amplify and convert the light signals into electronic signals (voltages). Finally, they are converted into digital numbers that will be assigned a channel number. Besides fluorescence, the intensity of light scattered by each particle can be measured in forward (forward side scatter, FSC) or sideward (side scatter, SSC) direction from the light source. The scatter is a measure for the cell size, morphology and granularity or internal complexity, which allows the differentiation of different cell types (Robinson & Grégori, 2007).

The DNA quantity is usually given as C-value. The DNA content of an unreplicated haploid nucleus (i.e. holoploid genome size) is $1C$ (“C” standing for “constant”) with a chromosome number of n . The nucleus of a diploid individual before DNA replication has a DNA content of $2C$, respectively, and a chromosome number of $2n$. In polyploid species, the DNA amount can be given also as the homoploid genome size of a monoploid set of chromosomes x ., e.g. the $6Cx$ value for somatic cells of hexaploid *Triticum aestivum* is equivalent to the $2C$ value ($2n = 6x = 42$). The DNA content is assessed in absolute values of picograms or the number of base pairs (1 pg DNA = 0.978×10^9 bp).

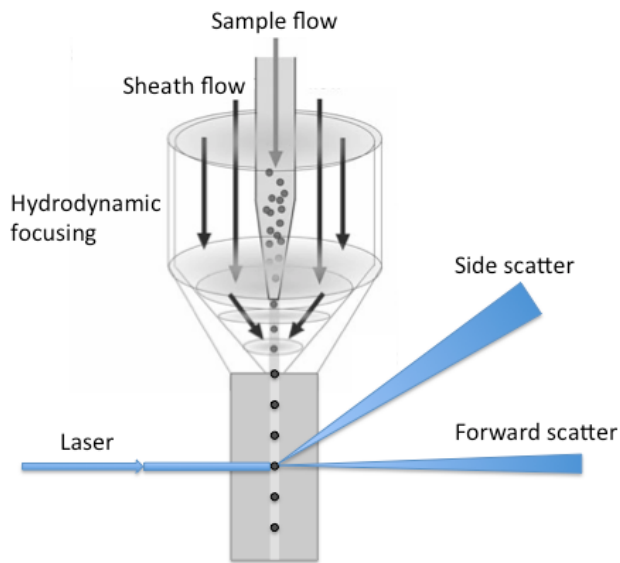


Figure 1.1 Schematic overview of the cuvette in a flow cytometer (modified from Robinson & Grégori, 2007). A particle free fluid (sheath) is under pressure forced to flow through a small port. The sample fluid is injected into the flowing stream. Sample particles are separated and aligned due to differences in the velocity of sheath and sample fluid (hydrodynamic focusing). A laser individually excites the particles of interest. The emitted fluorescence is assigned to different intensity classes.

A precise estimation of the DNA quantity requires a reference standard with known nuclear DNA quantity. The standard and sample nuclei need to be simultaneously isolated and stained (internal standardization) with a fluorochrome, that binds selectively and stoichiometrically to DNA. FCM then simultaneously records relative fluorescence intensities of reference standard and sample.

There are species in Triticeae that hold more than one ploidy level. The estimation of the genome sizes allows distinguishing polyploid accessions from diploids.

1.4.2 Sequence capture and Illumina sequencing

Although the sequencing costs for next-generation sequencing (NGS) technologies are constantly dropping, the sequencing of whole genomes is still too cost-intensive to be applied to a high number of species and individuals with large genomes and a high genomic repeat content as found in Triticeae. A targeted hybridization-based enrichment approach (also known as sequence capture) that reduces the genomic complexity is a powerful technique to simultaneously capture several hundred of nuclear low-copy number loci from all over the genome and up to several hundred kilobases (Gnirke *et al.*, 2009; Cummings *et al.*, 2010; Mamanova *et al.*, 2010; Grover *et al.*, 2012; Cronn *et al.*, 2012).

In general, target enrichment protocols apply short biotinylated DNA or RNA oligonucleotides (called baits or capture probes) that are complementary to genomic DNA regions of interest (e.g. exons, organelle genomes). Baits can be obtained in different sizes from different manufacturers, e.g., 60-90 bp (NimbleGen) or 120 bp (Agilent

Technologies) and are designed based on available sequence information from one or more related species. Genomic DNA is sheared into short fragments and hybridized in solution with these custom oligonucleotides. The excess of these single-stranded non-self-complementary RNA baits drives the hybridization. The formed DNA–RNA-bait hybrids can be separated from the non-desired fraction using magnetic beads that carry streptavidin on their surface, followed by a PCR step to amplify the desired DNA (Gnirke *et al.*, 2009; Lemmon & Lemmon, 2013). Unique barcodes that facilitate pooling and the later simultaneous sequencing of several dozens of samples can be added during this step. There are protocols that allow the barcoding of samples before the actual capture process as well. The enriched fractions of multiple samples can then be sequenced on a high-throughput next-generation sequencing platform. Early target enrichment protocols used captured probes that were immobilised on a microarray (e.g. Fu *et al.*, 2010; Burbano *et al.*, 2010; Salmon *et al.*, 2012). More recent studies applied hybrid enrichment in solution (Faircloth *et al.*, 2015; Stephens *et al.*, 2015a,b). The general scheme of such a target enrichment procedure is depicted in **Figure 1.2**.

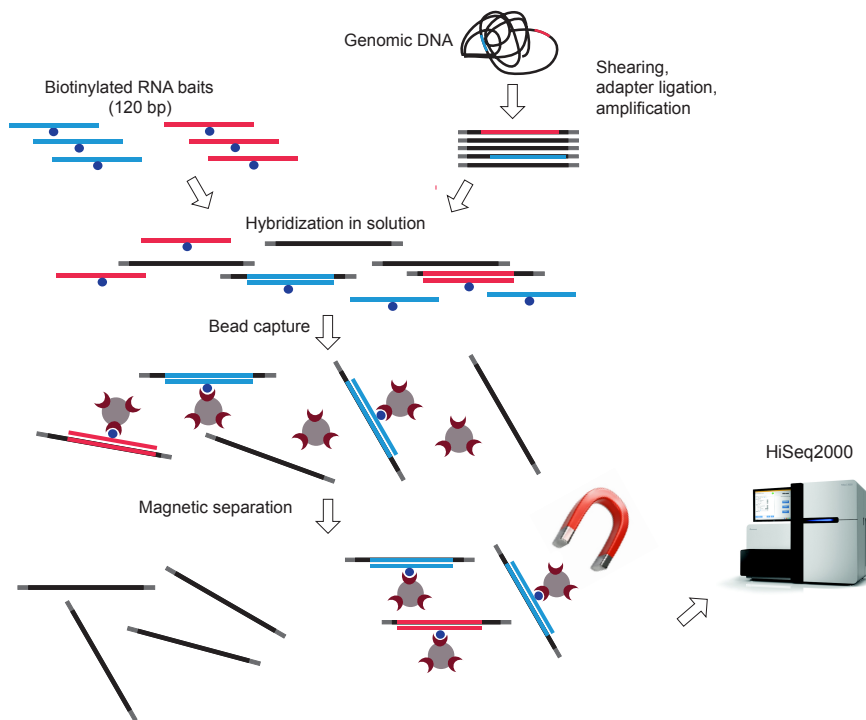


Figure 1.2 The principle of sequence capture (modified from Gnirke *et al.*, 2009). Fragmented and adapter ligated genomic DNA is hybridized in solution with RNA baits that are complementary to genomic regions of interest (blue and red). Two sequencing targets and their respective baits are shown. DNA-RNA bait hybrids are separated from the unbound fraction using streptavidin coated beads magnetic beads. The enriched DNA fractions can then be sequenced on an Illumina machine.

Sequence capture is applicable to a broad taxonomic scale and able to retrieve long informative loci. It can be applied to large genomes and even to non-model species, since the capture probes are able to hybridize also in the presence of ~25% sequence

substitutions compared to the reference sequences used for bait design (A. Lemmon, personal communication, Dresden, 2014).

Therefore, a hybridization-based enrichment approach is better suited for understanding phylogenetic relationships within Triticeae than methods that employ the digestion of DNA with restriction enzymes for genomic partitioning, e.g. genotyping by sequencing (GBS; Elshire *et al.*, 2011) or restriction site associated DNA sequencing (RAD-seq; Miller *et al.*, 2007; Baird *et al.*, 2008). These methods can only be applied to analyse shallow evolutionary relationship (i.e. within a species) due to the relatively fast evolution of restriction sites. It is also faster than PCR-based approaches, e.g. parallel-tagged amplicon sequencing that requires a laborious primer design and testing of PCR conditions (Bybee *et al.*, 2011; Brassac & Blattner, 2015).

Illumina sequencing is one of the so-called second-generation sequencing technologies that employs clonally amplified copies of the template DNA molecules of interest (Mardis, 2008; Shendure & Ji, 2008; Metzker, 2009). Other second-generation techniques are e.g. the 454 (Roche) and Solid (Life Technologies) sequencing. Illumina is the most widely applied sequencing technology at the moment (e.g. Mayer *et al.*, 2012, 2014) due to the combination of large sequencing throughput of 50-1000 Gb per run (<http://www.illumina.com>; accessed in October 2015), low sequencing cost per base, and a low error rate (Glenn, 2011). It can produce paired-end reads (i.e. bases are determined from both ends of a single template molecule) with a length of currently 100-250 bp each. The general sequencing principle for double-stranded (ds) DNA is shown in **Figure 1.3**.

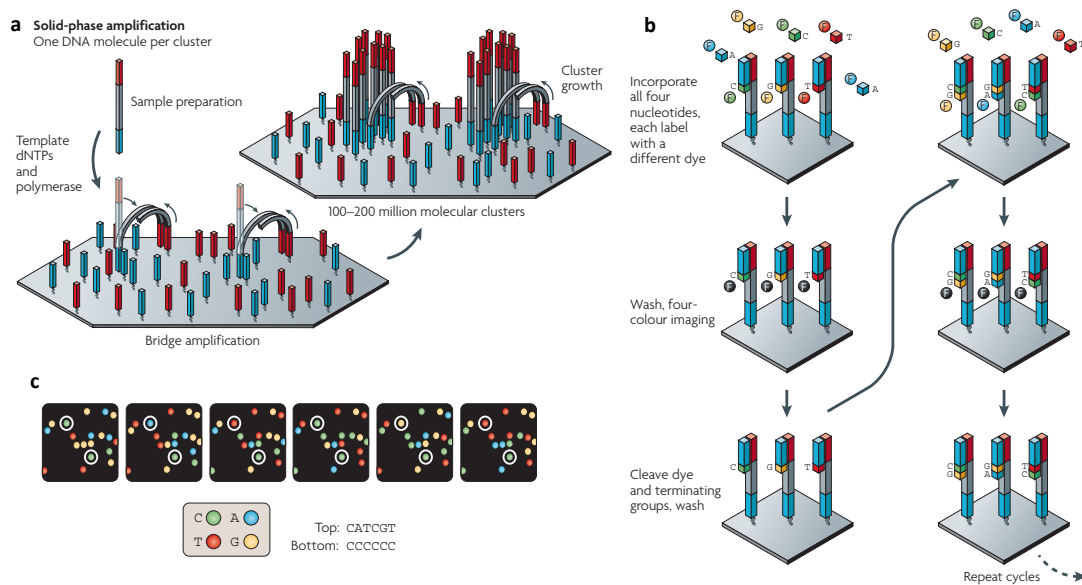


Figure 1.3 Overview of the Illumina sequencing principle (from Metzker, 2009). (a) Adapter ligated DNA molecules are immobilized on the flow cell of an Illumina sequencing platform and amplified via bridge PCR with adjacent adapters (primers). (b) Clusters of clonally amplified template molecules are sequenced by repeating cycles of incorporation of the four nucleotides each labelled with different fluorescent dyes and a terminating group, washing, imaging and cleavage of terminating groups and dyes. (c) The four-colour imaging is highlighted for two different clusters and six cycles of nucleotide incorporation and imaging.

Adapters are ligated to both ends of dsDNA fragments. These adapters are complementary to adapters immobilised on a flow cell (i.e. a glass slide with different lanes). The template DNA is denatured and the single-stranded (ss) DNA is randomly attached to the adapters on the flow cell surface. The ssDNA templates are amplified via a solid-phase bridge PCR (i.e. PCR that occurs between the immobilized adapters (primers) on the flow cell surface). This results in randomly distributed clusters of clonally amplified dsDNA templates. These molecules are denatured and an enzyme selectively removes one strand. The remaining ssDNA fragments (forward strand) in each cluster are primed (sequencing primer 1) and sequenced by synthesis: The four different nucleotides, each labelled with different fluorescent dye and with a reversible terminating group, are added. The complementary nucleotide is incorporated while not integrated nucleotides are washed away. The incorporated nucleotides are recorded for each cluster by laser excitation of the fluorescent dye. Subsequently, dye and terminating groups are cleaved off and the cycle is repeated. The sequencing template that was used to generate the forward read (R1) is then used to regenerate the complementary strand, the original template is removed, and the new strand is used to obtain the reverse read (R2) using sequencing primer 2. Two Illumina sequencing systems are available: the HiSeq and the MiSeq. Both follow the same sequencing principle. However, the MiSeq has a smaller flow cell that offers greater flexibility in instrument running.

Third generation sequencing technologies that sequence single molecules like the single-molecule real time (SMRT) sequencing technology (Pacific Biosciences) still have a lower sequencing throughput compared to Illumina, but especially SMRT is getting more attractive for researchers, because it does not introduce an amplification bias via PCR steps and constantly increases its sequencing output and read length. It is already able to retrieve reads with lengths of up to 40 kilobases (kb), which enables the recovery of haplotype sequences without phasing (Roberts *et al.*, 2013, www.pacific-biosciences.com; accessed in October 2015).

2 MATERIALS AND METHODS

2.1 Selection of taxa and accessions

In total 127 accessions spanning 15 genera and about 35 Triticeae species as well as two outgroup taxa were selected for the study. The accessions covered 24 genomic groups and were acquired from the International Center for Agricultural Research in the Dry Areas (ICARDA), the genebank of the Leibniz Institute of Plant Genetics and Crop Research (IPK), the National Small Grain Collection of the US Department of Agriculture (USDA), and the Czech Crop Research Institute. Additional seed material was collected during field trips. Multiple accessions per species and intra-specific entities were selected aiming at a good coverage of the distribution areas of these species, but also to be able to detect indications for monophyly of species, genetic variability, and the extent of incomplete lineage sorting. Only few accessions of the genus *Hordeum* were selected, since the relationships within this genus have been the focus of intense research and are well understood (e.g. Blattner, 2009; Brassac & Blattner, 2015). The included *Hordeum* accessions cover the four basic genomes described of this genus. An overview of all taxa incorporated in this work is presented in **Table 2.1**.

Table 2.1 Triticeae and outgroup species included in this study. For all species the genome (G), the number of included accessions (N), and the main native distribution according to Kilian *et al.* (2011) for *Aegilops* and eMonocot.org for other taxa is given.

Species	G	N	Distribution area
<i>Aegilops bicornis</i> (Forssk.) Jaub. & Spach	S	4	SE Mediterranean
<i>Aegilops comosa</i> Sibth. & Sm.	M	4	Balkans
<i>Aegilops longissima</i> Schweinf. & Muschl.	S	5	E Mediterranean
<i>Aegilops markgrafii</i> (Greuter) K. Hammer	C	5	NE Mediterranean
<i>Aegilops searsii</i> Feldman & Kislev ex K. Hammer	S	5	E Mediterranean
<i>Aegilops sharonensis</i> Schweinf. & Muschl.	S	1	Israel, Lebanon
<i>Aegilops speltoides</i> Tausch	B	7	E Mediterranean
<i>Aegilops tauschii</i> Coss.	D	4	SW–C Asia
<i>Aegilops umbellulata</i> Zhuk.	U	3	SE Europe, SW Asia
<i>Aegilops uniaristata</i> Vis.	N	3	SE Europe
<i>Agropyron cristatum</i> (L.) Gaertn.	P	2	S Europe, NECW Asia
<i>Amblyopyrum muticum</i> (Boiss.) Eig	T	6	Turkey
<i>Australopyrum retrofractum</i> (Vickery) A. Löve	W	4	SE Australia
<i>Dasypyrum villosum</i> (L.) P. Candargy	V	5	SW–SE Europe, Caucasus
<i>Eremopyrum distans</i> (K. Koch) Nevski	Ft	1	SE–E Europe, WC Asia
<i>Eremopyrum triticeum</i> (Gaertn.) Nevski	Ft	3	SE–E Europe, WC Asia
<i>Henrardia persica</i> (Boiss.) C.E. Hubb.	O	4	SE Europe, SW Asia
<i>Heterantherium piliferum</i> (Banks & Sol.) Hochst.	Q	4	SE Europe, SW Asia
<i>Hordeum marinum</i> Huds.	Xa	1	Mediterranean
<i>Hordeum murinum</i> L.	Xu	1	Mediterranean to C Asia
<i>Hordeum pubiflorum</i> Hook. f.	I	1	S Argentina
<i>Hordeum vulgare</i> L.	H	2	SW Asia
<i>Psathyrostachys juncea</i> (Fisch.) Nevski	Ns	6	E Europe, NC Asia
<i>Pseudoroegneria stipifolia</i> (Czern. ex Nevski) A. Löve	St	3	E Europe, N Caucasus
<i>Pseudoroegneria strigosa</i> (M. Bieb.) A. Löve	St	4	Balkans, Crimea
<i>Pseudoroegneria tauri</i> (Boiss. & Balansa) A. Löve	St	5	E Mediterranean, S Caucasus
<i>Secale cereale</i> L.	R	4	Turkey
<i>Secale strictum</i> (C. Presl) C. Presl	R	4	S Europe, SW Asia, N Africa
<i>Taeniatherum caput-medusae</i> (L.) Nevski	Ta	6	S Europe, SW Asia, N Africa
<i>Thinopyrum bessarabicum</i> (Savul. & Rayss) A. Löve	E ^b	1	SE Europe, N Caucasus
<i>Thinopyrum elongatum</i> (Host) D.R. Dewey	E ^e	2	S Europe, SW Asia, N Africa
<i>Triticum monococcum</i> L.	A	1	Turkey
<i>Triticum urartu</i> Tumanian ex Gandilyan	A	5	E Mediterranean, Caucasus
<i>Brachypodium distachyon</i> (L.) P. Beauv.		1	S Europe, SW Asia, N Africa
<i>Bromus tectorum</i> L.		1	Europe, SW Asia, N Africa

Note: Different genebanks adopt different taxonomic treatments that may vary in the number of sub(species) recognized. More comprehensive information about the used accessions, including the name in the donor genebank and the country of origin is provided in **Table S.1**.

The plant material was grown for seed propagation and leaf harvests for DNA extraction and flow-cytometric measurements. The material was morphologically determined and herbarium vouchers were deposited in the Gatersleben Herbarium (GAT). During flowering, inflorescences were covered with plastic bags (Crispac, Baumann Saatzuchtbedarf) having holes of 0.5 mm to prevent wind-pollination (**Figure 2.1**). For species found to be obligate outcrossers more than one plant was grown from the same accession and they were planted next to each other in the field. The inflorescences of such individuals were packed under the same bag.



Figure 2.1 Growing of plant material. Seeds of the Triticeae collection under study were sown in the greenhouse and grown in the field for propagation purposes and leaf harvests at IPK in 2012 and 2013. Inflorescences were covered with perforated plastic bags to prevent from unwanted cross-pollination.

2.2 Flow-cytometric estimation of the genome size

Flow cytometric measurements were conducted for all selected accessions to determine the genome size, analyse the ploidy level and thereby verify species affiliations. All analyses followed the protocol of Doležel *et al.* (2007) for the estimation of nuclear DNA content in absolute units on a CyFlow Space flow cytometer (Partec). Fresh material of young leaves from sample and reference standard were chopped together using a sharp razor blade in Galbraith's buffer containing 50 µg/ml RNAase to release the nuclei from the cell and to degrade RNA. The use of young leaves ensures that most nuclei are in growth phase 1 (G1) of the cell cycle. The buffer contained propidium iodide (PI) as DNA-selective fluorochrome (excitation at 538 nm and emission at 630 nm) that intercalates into double-stranded DNA without a base dependent bias. A reference standard was found empirically, by testing from a set of available standards with known genome size (**Table 2.2**).

Table 2.2 Genome size reference standards used in this study. Accession numbers in the IPK Genebank and their 2C genome size in picogram is given.

Species used as internal reference standard	Accession	Genome size (pg)
<i>Glycine max</i> (L.) Merr. convar. <i>max</i> var. <i>max</i>	SOJA 392	2.5
<i>Zea mays</i> L. subsp. <i>indurata</i> (Sturtev.) Zhuk. var. <i>vulgata</i> Körn.	ZEA 3443	5.43
<i>Pisum sativum</i> L. subsp. <i>sativum</i> convar. <i>sativum</i> var. <i>ponderosum</i> Alef.	PIS 630	9.09
<i>Hordeum vulgare</i> L. subsp. <i>vulgare</i> var. <i>hybernum</i> Viborg 'Hohenfinower'	HOR 82	10.36
<i>Secale cereale</i> L. subsp. <i>cereale</i>	R 737	16.19
<i>Vicia faba</i> L. subsp. <i>minor</i> (Peterm. em. Harz) Rothm. var. <i>minor</i> Peterm. subvar. <i>minor</i>	FAB 602	26.9

A standard was considered appropriate if it had a minimum size difference of 15–20% and a maximum two-fold size difference to the genome size of the sample (**Figure 2.2**). First, the reference standard was processed alone and the standard peak was positioned on e.g. channel 100 (i.e. a quantity class for fluorescence intensity) by changing the gain values for the photomultiplier tubes. The instrument settings were saved and used for all measurements using this standard on that day. For all genome size estimations at least 7500 nuclei were counted. Only measurements with a coefficient of variation (CV) for sample and standard peak lower or equal to 4% were accepted. Samples that recurrently produced CV values >4% were repeated in Galbraith's buffer containing 1% Polyvinylpyrrolidon (vol/vol) and 0.1% Triton X-100 (vol/vol).

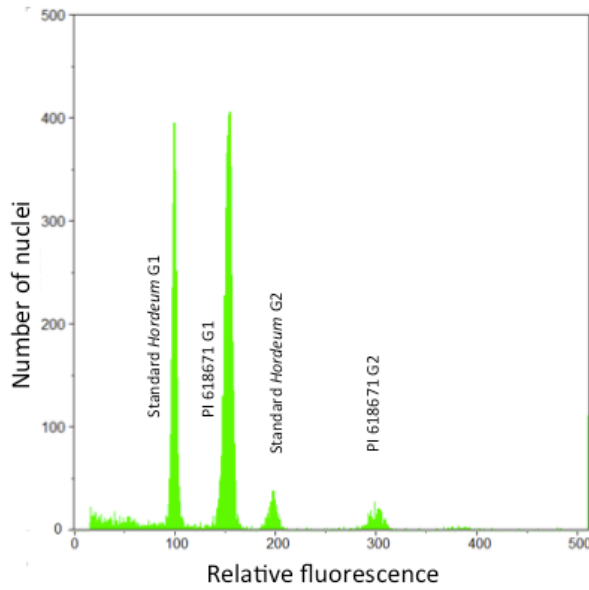


Figure 2.2 Exemplary histogram of fluorescence intensities from DNA content estimations. All measurements were performed according to Dolézel *et al.* (2007) on a Partec CyFlow Space. Appropriate reference standards for internal standardization were determined empirically. The reference standard was first run alone and the G1 peak was set to the channel 100, i.e. the fluorescence intensity class. At least 7500 nuclei were counted per measurement.

Measurements were done for all selected accessions. At least three measurements per species were carried out. Accessions of the same species were processed on at least two different days to account for instrument drifts. The genome size of individual samples was calculated as:

$$\text{Sample } 2C \text{ (pg)} = \frac{\text{Standard } 2C \text{ (pg)} \times \text{Sample mean peak position}}{\text{Reference mean peak position}}$$

The mean and the standard deviation were calculated for every ploidy level per species.

2.3 Sequence capture

2.3.1 Designing the library of sequence capture probes

The aim of this project was to develop a hybrid enrichment protocol that can be coupled with a NGS technology to simultaneously retrieve phylogenetic information from approximately 450 genes from diploid Triticeae taxa that cover all main genomic groups of the tribe. The selected genes should be equally distributed over all chromosomes of Triticeae and show orthology to more distantly related, already sequenced, grass genomes. The design of capture probes was chosen to be restricted to exons only, which show lower substitution rates than introns. This was considered to make the library of capture probes applicable to at least all taxa within Triticeae. A target enrichment protocol that uses custom 120 bp baits (i.e. SureSelectXT Target Enrichment, Agilent Technologies) was selected, since it was assumed that these baits tolerate more mismatches in respect to the target DNA than shorter baits provided by other manufacturers and, thus, are expected to work better on a broad taxonomic sampling.

For the development of a bait library, first 10,105 publicly available barley full-length complementary DNAs (fl-cDNAs) from the cultivar 'Haruna Nijo' (Matsumoto *et al.*, 2011) were retrieved from the Triticeae full-length CDS database (Mochida *et al.*, 2009). These fl-cDNAs were assembled in a putative linear gene model employing a series of bioinformatically constructed genome zippers, that compared the fully sequenced grass genomes of *Brachypodium distachyon*, rice and sorghum and used the extensive conservation of synteny between them (Mayer *et al.*, 2011). ORTHOMCL (Chen *et al.*, 2006) was used to remove loci for which orthology could not be verified between these taxa. Then one locus was selected every 0.5 cM resulting in 2,129 fl-cDNAs (approximately 300 per chromosome) that were used as a query for BLAST sequence comparison (Altschul *et al.*, 1990) against data of *Brachypodium*, rice and sorghum, barley and wheat. If a gene was matched by the BLAST search, the genomic and fl-cDNA sequences of the corresponding gene (first best hit) were included in a multiple sequence alignment (MSA) using the MUSCLE alignment algorithm (Edgar, 2004). Exon/intron boundaries were identified by the genomic DNA sequences of *Hordeum vulgare* cv. Morex and *Brachypodium distachyon* in the alignments. The loci were selected manually for bait design when the alignment met criteria like (1) a conserved exon-intron structure for most of the considered taxa in the alignment, (2) a total length of exonic region to be enriched per locus larger than 1000 bp (3) with a minimum size of single exons being 120 bp, and (4) introns separating adjacent short exons being smaller than 400 bp. Using these criteria should enable to recover a high extent of genetic diversity by not only retrieving sequence information from exons but also from introns or parts of introns next to them. Due to higher substitution rates in introns, their sequence information would provide additional phylogenetic information to the dataset and would be of high value for understanding relationships between closely related taxa. Based on these criteria and the information on chromosomal locations, alignments of 451 loci were selected for bait design (**Figure 2.3**).

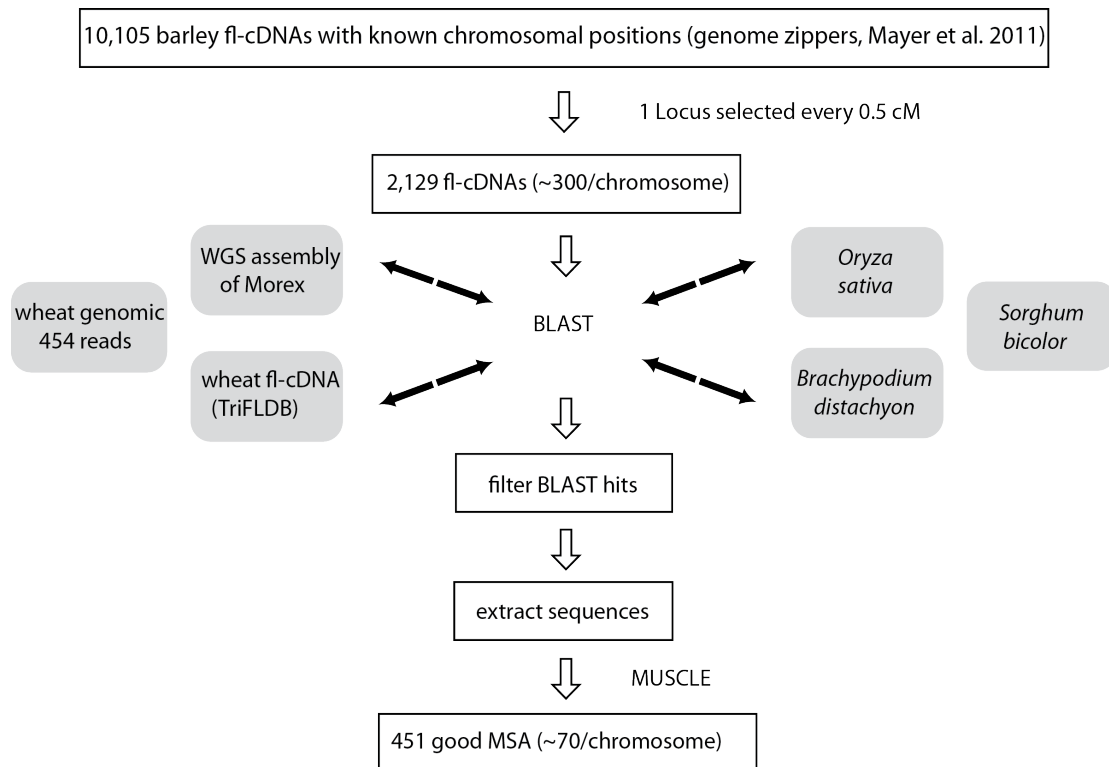


Figure 2.3 Schematic representation of the selection procedure for nuclear target loci. About 2000 barley fl-cDNAs with known chromosomal positions as established by the genome zipper were selected and used in BLAST searches against available sequence data from *Brachypodium distachyon*, rice, sorghum, wheat and the barley Morex assembly. Multiple sequence alignments (MSA) were calculated with MUSCLE and 451 good MSA were obtained.

Although the MSAs comprised also sequences from sorghum and rice, the design of capture probes was finally based only on fl-cDNAs from *Hordeum vulgare* and *Triticum aestivum*, two distantly related Triticeae taxa, and *Brachypodium distachyon*, which was used to further consider outgroup information. Capture probes for each of the 451 loci were designed on exon sequences of all three species. Also one plastid locus (i.e. *ndhF*) was included. Baits were designed to cover each exon at least three times (**Figure 2.4**). The total exonic sequence information considered in bait design amounts to 690 kb. Bait design was performed with custom PERL scripts and submitted to the web-based application eARRAY (Agilent Technologies).

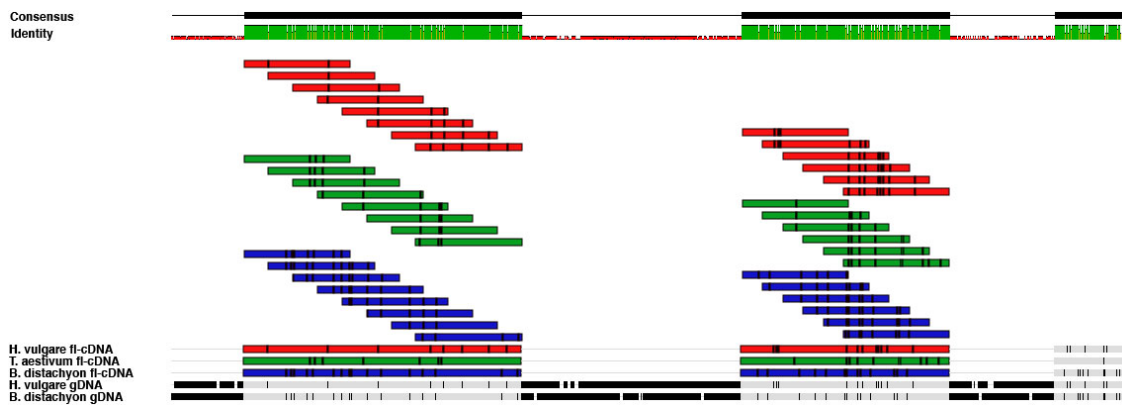


Figure 2.4 Design of sequence capture probes. The bait library was designed based on locus-wise multiple sequence alignments (MSAs) of fl-cDNA from *Hordeum vulgare*, *Triticum aestivum* and *Brachypodium distachyon*. Genomic DNA of *Hordeum* and *Brachypodium* were included in the MSA to obtain exon-intron borders. Three different sets of baits were designed based on each fl-cDNA type from the three species. Single baits are 120 bp long.

Additionally, the barley fl-cDNAs were used to retrieve functional annotation information via a local BLASTN search against the non-redundant (nr) sequence database of the National Center for Biotechnology Information (NCBI; accessed in October 2014).

2.3.2 Accomplishment of the sequence capture

The sequence capture was performed using the SureSelectXT Target Enrichment System for Illumina Paired-End Sequencing Libraries for 3 µg of genomic DNA (version 1.6, October 2013; Agilent Technologies). The instructions of the manufacturer were generally followed; adjustments to the protocol are described in the following.

2.3.2.1 Optimizing the DNA fragment length

Initially, the capture efficiency was compared when shearing the sample DNA into different average fragment length (recommended 'short fragments' of 150 bp vs. 'longer fragments' of 400 bp). By testing the performance of DNA fragments longer than recommended by the manufacturer, an enhanced capture of intronic sequences was attempted. The capture probe design and the different fragment sizes were tested on the same set of samples, covering species considered and species not considered in bait design (**Table 2.3**). The samples were sequenced on a Illumina HiSeq aiming for a sequence coverage of 100X.

Table 2.3 Species considered in tests of the bait library and different DNA fragment sizes. The species considered differ from each other in genome size (1C), basic genome (G) and ploidy level. Genome sizes were taken from the Kew Angiosperm DNA C-values database and Eilam *et al.* (2010). The species used for bait design (**bold**) were used as well as additional taxa. For each sample two different average fragment sizes were tested (150 bp vs. 400 bp).

Species	1C in pg	G	Ploidy
<i>Hordeum vulgare</i> subsp. <i>vulgare</i> cv. Morex	5.55	H	2x
<i>Brachypodium distachyon</i>	0.36		4x
<i>Aegilops speltoides</i>	5.81	S	2x
<i>Aegilops tauschii</i>	5.17	D	2x
<i>Hordeum pubiflorum</i>	4.32	I	2x
<i>Hordeum vulgare</i> subsp. <i>spontaneum</i>	5.50	H	2x
<i>Triticum urartu</i>	4.93	A	2x

Sequence reads were mapped against genomic sequences of the barley cultivar Morex as a reference. The resulting assemblies were compared and samples having longer DNA fragments were found to return more intron information than samples with shorter DNA fragments. Also a *de novo* assembly as implemented in the CLC ASSEMBLY CELL version 4.0 (CLC bio) was used to compare N50 values (i.e. a weighted median statistics of the contig length of an assembly) for the samples used to test the optimal fragment length of input DNA. A paired t-test showed significant difference in N50 values between different shearing procedures (p-value: 0.01; **Figure 2.5**) Thus, the modification of using longer fragments was kept for all future sample library preparations.

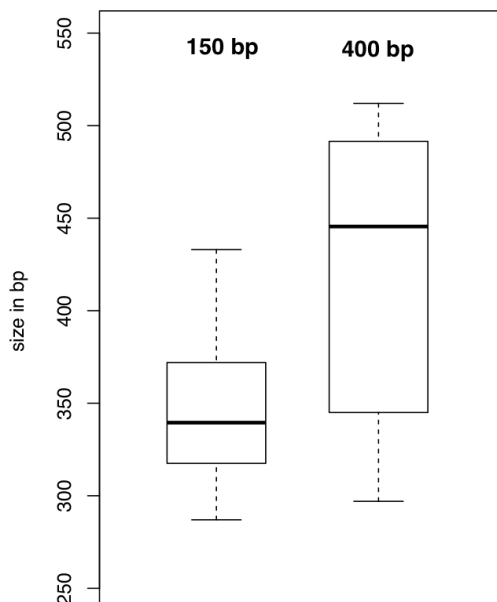


Figure 2.5 Comparison of contig N50 values for the test samples. Different shearing of the genomic DNA (average fragment length of 150 bp vs. 400 bp) resulted in different length of the sequences that could be assembled *de novo*. Larger DNA fragments resulted in significantly longer contigs.

2.3.2.2 Library preparation and Illumina sequencing

Genomic DNA was extracted either from 10 mg silica-dried leaves using the DNeasy Plant Mini Kit (Qiagen) or from 5 g of freeze-dried leaves using the Cetyltrimethylammonium bromide (CTAB) method (Doyle & Doyle, 1987). DNA quantifications were done using the Qubit dsDNA BR Assay (Life Technologies) or the Quant-iT PicoGreen dsDNA Assay Kit (Invitrogen) on a Tecan Infinite 200 microplate reader according to the manufactures instructions. The LE220 Focused-ultrasonicator (Covaris) was used to shear 3 µg genomic DNA in 130 µl TE buffer for every sample with the following settings: instantaneous ultrasonic power (PIP) 450 W, duty factor (df) 30%, cycles per burst (cpb) 200. The treatment was applied for 100 sec.

Afterwards, a sequence of enzymatic reactions was carried out, always alternating with SPRI (i.e. solid phase reversible immobilization) beads purification with SpeedBeads 3 EDAC/PA5 (Fisher Scientific). The ends of the fragmented DNA were repaired to obtain blunt 5'-phosphorylated ends. Then, dATP was attached that facilitated the ligation of adapters having a dT-overhang. Five cycles of PCR were performed to amplify only the DNA fragments carrying the adapters that also function as primer binding site. Quality assessments after fragmentation and PCR were done on a Bioanalyzer 2100 with the DNA 7500 or the High Sensitivity Kit (Agilent Technologies) for a few randomly selected samples. For the remaining samples quality control steps requiring fragment analyses were substituted by gel electrophoresis on 2% agarose gels to save expenses. PCR products were quantified and vacuum concentrated (SpeedVac, Savant) to obtain 750 ng/µl of prepped library in a final volume of 3.4 µl.

The prepped library was then incubated with sequence capture probes in solution for 24 hours. Streptavidin-coupled magnetic beads were used to select the captured fraction. Unbound DNA fragments were removed via three repetitive washing steps. The captured fragments were amplified on the magnetic beads via 12 cycles of PCR, simultaneously adding an individual-specific index to each sample. Agilent Technologies provided only 16 individual barcodes, hence at maximum 16 samples could be pooled and sequenced simultaneously on one lane of a Illumina HiSeq. However, a large set of barcodes available at IPK (following Meyer & Kircher, 2010; Himmelbach *et al.*, 2014) allowed me to circumvent this limitation and to sequence more samples concurrently. After amplification and index tagging the successful capture was assessed for a few randomly selected samples on a Bioanalyzer 2100 using a High Sensitivity Kit (Agilent Technologies). The DNA was quantified and always several samples were pooled in equimolar ratios. A final quality control on a Bioanalyzer 2100 and quantification using qPCR was done for the entire pool. The flowcell of the Illumina Hi- or MiSeq was loaded aiming for a sequencing coverage of 40X. The MiSeq platform that produced longer sequence reads was tested as another possibility to bridge larger introns. The sequencing was repeated, in case of low sequence data output. An overview of the sample preparation workflow is presented in **Figure 2.6**.

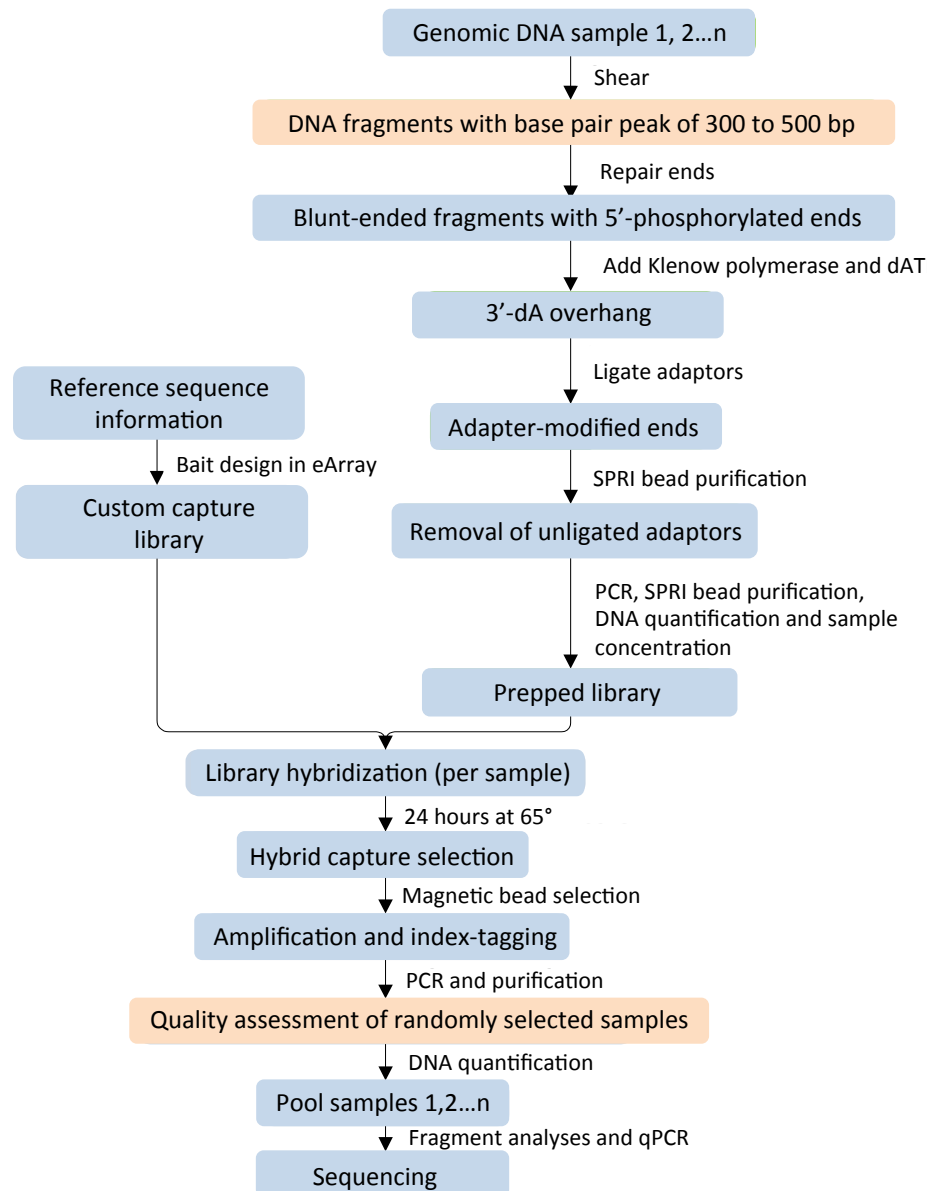


Figure 2.6 The sample preparation workflow (modified from SureSelectXT Target Enrichment Kit, Agilent Technologies). In contrast to the manufacturer instructions the genomic DNA was sheared into larger fragments with an average length of 400 bp. The sequence capture was done for each sample separately. Samples were index-tagged and pooled after the hybrid capture. Major changes compared to the manufacturer protocol are highlighted in orange.

2.4 Sequence assembly and data analyses

2.4.1 On-target assembly

The sequence assembly of the barley genome (Mayer *et al.*, 2012) was used as a reference for the primary data analysis. Since the capture probes were designed prior to its release, the exon sequences of fl-cDNAs from *Hordeum vulgare* were first aligned to the annotated barley genome assembly using BLAT (Kent, 2002) with default parameters. The physical location of an annotated exon was chosen for downstream analysis if it was the best BLAT hit and query and target sequence had an overlap of at least 60%. Exons belonging to the same gene and including introns were merged into a target locus using BEDTOOLS version 2.22.0 (Quinlan & Hall, 2010). Potentially due to incomplete annotation of the barley genome assembly, some exons of fl-cDNAs did not map to annotated exons. The best BLAT hits of these exons were also kept as target regions.

After sequence capture and Illumina sequencing the reads obtained from different runs and platforms were merged for each accession. For each sample, the sequence reads were mapped to the barley genome assembly using the Burrows-Wheeler Alignment (BWA) Tool version 0.7.8 (Li & Durbin, 2009). The parameters *k* (i.e. maximum difference in seed) and *n* (i.e. maximum edit distance) were adjusted to allow the simultaneous mapping of reads with different lengths (MiSeq and HiSeq reads). The final mismatch rate was approximately 10%. Consensus sequences were called using SAMTOOLS version 1.1. (Li *et al.*, 2009; Li, 2011) and converted into FASTA sequences using VCFUTILS and SEQTK version 1.0 (Heng Li, <https://github.com/lh3/seqtk>). Consensus sequences for each of the 451 target loci were extracted

For each accession the number of reads that mapped to the reference genome and to the on-target regions were compared. The capture performance for different species and genera was assessed using 40 “single exons” (i.e. exons that either belong to a locus, for which only a single exon was selected for bait design or exons that are separated from other exons by more than 600 bp intronic sequences). The length distribution of these purely exonic sequences was compared to the length of continuous sequence information that could be assembled for them, i.e. including adjacent intron information.

2.4.2 Off-target assembly

Although not considered in bait design, off-target regions that occur in a high copy number in the cell like the nuclear ribosomal DNA (nrDNA) tandem-repeat region and the chloroplast genome were assembled from the fraction of reads not mapping on-target.

The nrDNA region was assembled iteratively combining *de novo* assembly and read mapping. This allowed the assembly of the conserved coding regions (18S, 5.8S and 26S rRNA genes), the internal transcribed spacers (ITS) and the external transcribed spacer (ETS), which is highly variable in sequence and length among the analysed taxa. First, a *de novo* assembly of all Illumina reads was carried out for each accession using the CLC ASSEMBLY CELL version 4.3.0. saving only contigs larger than 500 bp. The

nrDNA contigs were identified by mapping to the longest Triticeae reference sequence available in NCBI (i.e. *Secale cereale* JF489233). The annotation for this sequence is spanning 6952 bp from ETS to 26S. The mapping was done in GENEIOUS version 8.0.4 (<http://www.geneious.com>; Kearse *et al.*, 2012) with medium sensitivity (i.e. a maximum number of mismatches of 30%) Next, read mappings were carried out using the BWA mem algorithm and the genus- or species-specific contigs as reference. *Hordeum vulgare* (HQ825319) and *Hordeum murinum* (KJ632437) references were downloaded from NCBI to complement the sequence information from the length-variable ETS for these taxa. The mapped reads were further used for a *de novo* assembly and consensus calling in GENEIOUS. Sequences were aligned using MAFFT version 7.017 (Kato & Standley, 2013) with default parameters. Alignment ends were trimmed according to the annotated part of the *Secale cereale* reference sequence.

The chloroplast genome was assembled using a read mapping approach only. Due to a lower read coverage compared to the nrDNA region a *de novo* strategy was not feasible. Complete chloroplast reference sequences were retrieved from NCBI for *Aegilops searsii* (KJ614415), *Aegilops sharonensis* (KJ614417, KJ614419), *Aegilops speltoides* (KJ614404), *Aegilops tauschii* (KJ614412), *Brachypodium distachyon* (EU325680), *Hordeum vulgare* (EF115541), *Secale cereale* (KC912691), *Triticum urartu* (KJ614411), *Triticum monococcum* (KC912692). An alignment of an *Aegilops sharonensis* (KJ614419) and a *Hordeum vulgare* (EF115541) sequence was used to call an artificial sequence to be used as reference for read mapping for all accessions. This sequence comprised the sequence information from all parts variable in length present in the reference sequences. Moreover, this approach allows assembling sequences that all have the same starting point of the circular plastid genome, which is the *psbA* coding DNA sequence.

The chloroplast genome assembly was entirely performed in GENEIOUS. Read pairs were set and low quality reads were trimmed. Read mapping was performed with medium sensitivity (i.e. a maximum number of mismatches per read of 30%) and two iterations of read mapping were carried out. Consensus sequences were called using the 50% majority rule for parts of the assembly that have at least 3X coverage. The average coverage of the chloroplast genome was calculated by excluding *ndhF* that was included in bait design and therefore resulted in an elevated coverage of this region. Accessions with more than 20% of missing data, which corresponds to approximately 7X coverage, were excluded. A multiple sequence alignment (MSA) was calculated using MAFFT as implemented in GENEIOUS with an elevated gap penalty of 2.3. Start- and end-regions of the chloroplast inverted repeat regions (IRs) showed an atypical substitution pattern and were removed. For phylogenetic analyses one IR was removed from the MSA, as no sequence variations were found between the inverted repeats of the same accession. A second MSA was created, by extracting 102 annotated genes (coding DNA sequences, tRNA, rRNA) of the chloroplast. The extractions were manually curated and subsequently concatenated.

2.4.3 Filtering of on-target loci and dataset partitioning

For all samples the sequences assembled for the captured loci were subsumed in locus-wise MSAs. These MSAs were visually inspected in GENEIOUS. The percentage of ambiguous sites was determined for each sequence in the MSA for each locus separately using a custom PERL script. Allelic diversity is assumed to be much lower than 1% for single- and low-copy number loci. Thus, a high percentage of ambiguous positions for sequences of the same species is assumed to reflect the presence of paralogous gene copies (for a comparison see e.g. Jakob *et al.*, 2014). The average percentages of ambiguous positions were compared for every genus. Loci showing an average value of ambiguous sites >1% in more than five diploid Triticeae genera or most accessions of *Aegilops* and *Triticum* were considered as mainly multi-copy. All remaining loci were defined as mainly low-copy number loci and used for further quality assessment while all multi-copy loci were excluded.

Ambiguous positions in MSAs of the retained low-copy number loci were coded “N” to prevent the analysis of non-homologous sequence signals. The number of parsimony-informative positions for each locus were counted in PAUP*4.0b10 (Swofford, 2002). Low-copy number loci were selected for phylogenetic inference if the locus had a total length of at least 1000 bp, contained less than 25% of missing data and comprised at least 150 parsimony-informative positions.

The access to recent genetic maps of *Hordeum vulgare* (Mascher *et al.*, 2013), *Secale cereale* (T. Schmutzer, personal communication, Gatersleben, 2015) and *Triticum aestivum* (Mayer *et al.*, 2014; Chapman *et al.*, 2015) was used to retrieve positional information of the captured loci in different Triticeae genomes. Therefore, barley fl-cDNAs used for bait design were aligned to the different genome assemblies. An overlap between query and genome assembly was defined by an alignment of more than 50% of their length to genomic contigs. Low-copy number loci fulfilling the quality criteria (dataset 1) were further divided into loci on the same chromosome in barley, wheat and rye (dataset 2), loci located on the same chromosome in barley and wheat and with known chromosomal position in barley (dataset 3), were further split into data partitions of loci in centromeric (dataset 3a) and telomeric (dataset 3b) regions. The known recombination gradient along the chromosomes of barley (Mayer *et al.*, 2012) was used to define the centromeric regions. Therefore, the recombination frequencies obtained for *Hordeum vulgare* (Mascher *et al.*, 2013) were plotted for each chromosome separately (**Figure S.2, Table E.4**). Since the changes in recombination frequencies can be described using a positive exponential function from centromeres to telomeres (Escobar *et al.*, 2011; Mayer *et al.*, 2012), centromeric regions were defined for loci in linear parts of the plot, e.g. loci having similar recombination frequencies. Telomeric regions were defined for regions with rapid changes in recombination frequencies. Additionally, exact centromer positions were obtained from M. Mascher (personal communication, Gatersleben, 2015).

2.4.4 Inference of phylogenetic trees and topological comparisons

For all low-copy number loci fulfilling the quality criteria (dataset 1) and for the nrDNA region, Bayesian gene trees were inferred separately. All Bayesian phylogenetic trees were estimated with MRBAYES version 3.2.5 (Ronquist *et al.*, 2012) applying the best DNA substitution models as suggested by PARTITIONFINDER version 1.1.1 (Lanfear *et al.*, 2012). MRBAYES was run by conducting two independent Metropolis coupled Monte Carlo Markov chain analyses each with four sequentially heated chains (temperature set to 0.05) until the standard deviation of split frequencies reached 0.009 or for a maximum of 20 million generations. Trees were sampled every 500 generations. Convergence of the runs was assessed by checking the continuous parameter values sampled from the chains for mixing in TRACER version 1.6 (Drummond & Rambaut, 2007). For a random choice of analyses convergence of the topologies was additionally checked using the compare function of the online application tool AWTY (Nylander *et al.*, 2007). A consensus tree was computed after removal (burn-in) of the first 25% of trees or more, if suggested by TRACER.

Additionally, Maximum Likelihood (ML) trees were inferred for all low-copy number genes separately (dataset 1), a partitioned datasets of concatenated loci located on the same chromosome (i.e. chromosomes 1 to 3) in barley, wheat, and rye, (dataset 2) and for the assembled chloroplast genome. ML phylogenetic trees were inferred using RAxML version 8.1 (Stamatakis, 2014) under the GTRCAT model and with 100 bootstrap replicates. All phylogenetic inferences were run on the high-performance computing cluster of the Integrative Biodiversity Research (iDiv) centre (Leipzig, Germany).

Bayesian consensus trees of individual loci were compared by pairwise calculation of the Robinson-Foulds (RF) metric (Robinson & Foulds, 1981). The RF metric is calculated by counting the number of branch subsets that occur in one tree but not the other. For each non-matched subset "1" is scored. Since both trees under comparison are scored the metric is called a symmetrical difference metric. The RF metric was shown to be a good measure to compare tree topologies of highly dissimilar trees (Kuhner & Yamato, 2015). The RF calculations were performed in R version 3.0.2 using a custom script. This script first randomly resolves polytomies using the multi2d function as implemented in the R package ape (Paradis *et al.*, 2004). Subsequently, the RF distance was calculated for each pair of trees using the RF.dist function in the phangorn package (Schliep, 2011). The distributions of RF distances were compared between centromeric and telomeric loci for each chromosome separately and between centromeric and telomeric loci from all chromosomes combined. For each data partition a test of normality was carried out using the Shapiro-Wilk normality test. The Welch Two Sample t-test was used for normally distributed datasets and the Wilcoxon rank sum test for non-normally distributed datasets to test the hypothesis if the two populations have the same means.

2.4.5 Estimation of reticulations

Rooted phylogenetic networks were constructed from individual Bayesian gene trees to detect taxa that evolved in a rather reticulate than in a bifurcating manner. These networks represent a set of several gene trees simultaneously. First, the single Bayesian gene trees were rooted in PHYUTILTY version 2.2 (Smith & Dunn, 2008) with *Brachypodium distachyon* as outgroup. Then, the source tree correction pre-process of PHYSIC_IST (Scornavacca *et al.*, 2008) was used with a correction threshold of 0.9 as suggested by Escobar *et al.* (2011) to keep only strongly supported topological conflicts. Non-frequent topological groupings were dropped. A rooted phylogenetic network was constructed that represents all clusters of taxa present in the modified gene trees using the cluster network algorithm in DENDROSCOPE3 (Huson & Rupp, 2008; Huson & Scornavacca, 2012). Networks were calculated for all quality-filtered low-copy number genes (dataset 1), for all centromeric (dataset 3a) and for all telomeric loci (dataset 3b).

2.4.6 Coalescent-based species tree estimation

The effect of gene tree conflicts due to incomplete lineage sorting was addressed using two kinds of coalescent-based methods: A short-cut coalescence method that employs individual gene trees estimated beforehand, and a Bayesian coalescence method that co-estimates gene and species trees.

ASTRAL-II (Mirarab & Warnow, 2015) is able to estimate the true species tree with high probability given a large enough number of correct gene trees under the multispecies coalescent model. This program can deal with large datasets comprising hundreds of taxa and loci. ASTRAL-II version 4.7.8 was run for three datasets of pre-estimated ML gene trees as input: For all quality-filtered loci combined (dataset 1), for all centromeric (dataset 3a) and for all telomeric loci (dataset 3b) separately. ASTRAL-II was run with multilocus bootstrapping.

A Bayesian coalescence analysis was performed in *BEAST (Heled & Drummond, 2010), a program known to provide accurate species trees and species divergence times (e.g. Mirarab *et al.*, 2014b; Zimmermann *et al.*, 2014). However, due to large computational requirements its application is limited to relatively small datasets. Thus, the analysis was performed on a reduced dataset to provide a species tree estimation for the *Aegilops-Triticum-Amblyopyrum* complex only. Therefore, MSAs comprising only sequences of *Aegilops*, *Triticum*, *Amblyopyrum muticum* and one *Hordeum vulgare* accession as outgroup were used. Based on results of earlier phylogenetic analyses of the present work that revealed no genetic distinctions between the accessions of *Triticum monococcum* and *Triticum boeoticum* both taxa were subsumed under the species name *Triticum monococcum*. The analysis was run on 28 “good quality” telomeric loci combined (four per chromosome according to the barley genetic map). Telomeric loci were chosen for the analysis since they are considered to provide phylogenetic relevant information from independently inherited genes, while centromeric loci are potentially more affected by linkage disequilibrium and selection (Petit & Excoffier, 2009; Nater *et al.*, 2015). First, the best partitioning schemes and DNA substitutions models were inferred with PARTITIONFINDER (Lanfear *et al.*, 2012) using the “greedy” algorithm. The multispecies coalescent analysis was carried out with two secondary calibration points in

million years ago (Ma) as normally distributed priors for the root of Triticeae (mean 15.32 Ma \pm 0.34) and for the *Triticum-Aegilops* clade (mean 6.55 Ma \pm 0.22), using the divergence times inferred by Marcussen *et al.* (2014). The analysis was run with the substitution models linked in BEAUTI version 1.8.2 (Drummond *et al.*, 2012), the Yule species tree prior, as well as the piecewise linear and constant root population model. Since the rate constancy was systematically rejected for all loci by the likelihood-ratio test (Huelsenbeck & Rannala, 1997), an uncorrelated lognormal clock model (Drummond *et al.* 2006; uniform ucl.d.mean: min 0, max 0.01) was used. Trees were sampled every 5000 generations. The analysis was run with three chains for 500 million generation each with *BEAST as part of the BEAST package version 1.8.2 (Drummond *et al.*, 2006). *BEAST was run using the BEAGLE library (Ayres *et al.*, 2012) on the CIPRES (Cyberinfrastructure for Phylogenetic Research) Science Gateway version 3.3 (Miller *et al.*, 2010). Effective sample size (ESS) and convergence of the analyses were assessed using TRACER version 1.6 (Rambaut *et al.*, 2014). An appropriate burn-in was estimated from each trace file, and all analyses were combined with LOGCOMBINER (Drummond *et al.*, 2012). A maximum clade credibility (MCC) tree was summarised with TREEANNOTATOR (Drummond *et al.*, 2012), and visualized with FIGTREE version 1.4.0 (<http://tree.bio.ed.ac.uk/software/figtree>).

Because the ESS values for the combined runs indicated low mixing, the analysis was repeated for the 28 telomeric loci using a divide-and-conquer approach, similar to Mirarab *et al.* (2014a) and Zimmermann *et al.* (2014). First, the loci were binned four by four according to their best DNA substitution model (**Table 2.4**) and two to four independent analyses were computed for 150 million generations each using *BEAST. A combined visualization of the species trees sets sampled from all binned analyses was done in DENSITREE version 2.0 (Bouckaert, 2010). For each bin a MCC tree was summarised with TREEANNOTATOR (Drummond *et al.*, 2012). Moreover, all species trees sets were summarised with ASTRAL-II version 4.7.8 (Mirarab & Warnow, 2015).

Table 2.4 Partitioning scheme and DNA substitution models for 28 telomeric loci. Multiple sequence alignments comprising sequences of the diploid taxa *Aegilops*, *Amblyopyrum* and *Triticum* and one *Hordeum vulgare* accession were used to infer the best partitioning schemes and DNA substitutions models. Accordingly, the loci were divided into seven different bins for the multispecies coalescence analysis. The different bins are indicated by the superscript.

Partition	DNA substitution model	Telomeric loci
1	GTR+I+G	AK250130.1 ¹ , AK249495.1 ¹ , AK250796.1 ¹ , AK248476.1 ¹ , NIASHv1006M08 ² , NIASHv1028O24 ² , NIASHv2014N04 ²
2	HKY+I+G	NIASHv2020C20 ³ , NIASHv2013C21 ³ , NIASHv2040G12 ³
3	GTR+I+G	NIASHv2105L06 ⁴ , NIASHv1026E03 ⁴ , NIASHv2040E18 ⁴ , NIASHv2032E04 ⁴
4	SYM+I+G	NIASHv2023F05 ²
5	TrN+I+G	NIASHv2112K23 ⁵
6	HKY+I+G	NIASHv2020D03 ⁶ , NIASHv2120H086 ⁶
7	GTR+I+G	NIASHv2028E10 ⁷ , NIASHv2014H03 ⁷ , NIASHv2028H24 ⁷ , AK252062.1 ⁷
8	HKY+I+G	NIASHv2082K16 ³
9	K80+I+G	NIASHv2112C18 ⁵ , NIASHv2112L06 ⁵ , NIASHv3021D10 ⁵
10	TrN+I+G	AK248704.1 ⁶ , NIASHv1117B24 ⁶

3 RESULTS

3.1 Genome sizes

Flow cytometric measurements were performed for all selected accessions to determine the genome size, the ploidy level and, thereby, to verify species affiliations. In a few cases, accessions of the same species showed the existence of di- and tetraploids, which was indicated by a two-fold variation in genome size. This was expected e.g. *Agropyron cristatum* (Asay *et al.*, 1992; Jauhar, 1992), and for *Pseudoroegneria strigosa* (Yu *et al.*, 2008). No references mentioning the existence of tetraploids in *Pseudoroegneria stipifolia* were found. For every ploidy level per species the average genome size was calculated (**Table 3.1**). The genome sizes between diploid Triticeae species showed up to two-fold variation. The smallest 2C genome size measured was 7.5 pg for *Pseudoroegneria stipifolia* while the largest was 16.3 pg for *Secale cereale*. No genome size variations within the diploid accessions of a species were detected **Figure S.1**. The genome size of diploid species of the same genus is often similar (e.g. *Triticum*, *Pseudoroegneria*, *Secale*). However, there is considerable variation in the genome sizes of different *Aegilops* species ranging from 9 pg to 14.65 pg. The existence of small non-significant variations in genome sizes of the same species but significant differences between species is in agreement with other studies (for a review see Eilam *et al.*, 2010). In the vast majority, the determined genome sizes were comparable to the data in the Kew Angiosperm DNA C-values database (<http://data.kew.org/cvalues>). However, the only accession of the diploid species *Eremopyrum distans* (Frederiksen, 1991) was found to be tetraploid.

Genome sizes

Table 3.1 Results of flow cytometric measurements. For each taxon the genomic symbol, the determined genome size and the standard deviation (SD) is shown. Also the number of measured accessions (#Nacc), and the number of individual measurements (#Nms) is depicted. Asterisks refer to measurements conducted by Jakob *et al.* (2004).

Species	Genome	Species mean	#Nacc	#Nms
<i>Aegilops bicornis</i>	S	13.37 ± 0.08	4	6
<i>Aegilops comosa</i>	M	10.54 ± 0.37	6	7
<i>Aegilops longissima</i>	S	14.65 ± 0.06	5	5
<i>Aegilops markgrafii</i>	C	9.09 ± 0.25	11	11
<i>Aegilops searsii</i>	S	12.99 ± 0.05	6	6
<i>Aegilops sharonensis</i>	S	14.56 ± 0.03	2	4
<i>Aegilops speltoides</i>	B	11.14 ± 0.17	12	12
<i>Aegilops tauschii</i>	D	9.68 ± 0.05	8	9
<i>Aegilops umbellulata</i>	U	11.84 ± 0.1	6	7
<i>Aegilops uniaristata</i>	N	10.85 ± 0.18	8	9
<i>Agropyron cristatum</i>	P	12.73 ± 0.23	2	3
<i>Agropyron cristatum</i>	PP	26.52 ± 0.36	2	3
<i>Amblyopyrum muticum</i>	T	11.24 ± 0.14	8	8
<i>Australopyrum retrofractum</i>	W	8.38 ± 0.12	4	11
<i>Dasypyrum villosum</i>	V	10.28 ± 0.25	12	13
<i>Eremopyrum distans</i>	Fd	18.88 ± 0.42	1	4
<i>Eremopyrum triticeum</i>	Ft	9.43 ± 0.06	3	4
<i>Henrardia persica</i>	O	15.78 ± 0.26	4	5
<i>Heterantherium piliferum</i>	Q	8.11 ± 0.14	4	4
<i>Hordeum marinum</i>	Xa	9.1 ± 0.5*	10	19
<i>Hordeum murinum</i>	Xu	9.2 ± 0.1	2	4
<i>Hordeum pubiflorum</i>	I	8.63 ± 0.05*	1	3
<i>Hordeum vulgare</i>	H	10.23 ± 0.06	2	3
<i>Psathyrostachys juncea</i>	Ns	14.98 ± 0.15	10	14
<i>Pseudoroegneria stipifolia</i>	St	7.3 ± 0.13	1	3
<i>Pseudoroegneria stipifolia</i>	StX	15.03 ± 0.23	2	3
<i>Pseudoroegneria strigosa</i>	St	8 ± 0.34	2	3
<i>Pseudoroegneria strigosa</i>	StX	22.6 ± 0.12	2	3
<i>Pseudoroegneria tauri</i>	St	7.5 ± 0.07	5	10
<i>Secale cereale</i>	R	16.36 ± 0.3	6	9
<i>Secale strictum</i>	R	15.78 ± 0.5	3	5
<i>Secale vavilovii</i>	R	16.15 ± 0.32	2	4
<i>Taeniatherum caput-medusae</i>	Ta	8.55 ± 0.05	8	8
<i>Thinopyrum bessarabicum</i>	E ^b	45.16 ± 0.23	1	3
<i>Thinopyrum elongatum</i>	E ^e	45.96 ± 0.56	2	3
<i>Thinopyrum elongatum</i>	E ^e	36.33 ± 1.32	1	3
<i>Triticum monococcum</i>	A	12.19 ± 0.15	21	31
<i>Triticum urartu</i>	A	11.61 ± 0.01	5	14
<i>Brachypodium distachyon</i>		1.22 ± 0.05	1	3
<i>Bromus tectorum</i>		9.72 ± 0.06	1	3

In some cases accessions revealed a genome size in conflict to other accessions of the same species. These violations in genome size could be confirmed with atypical herbarium vouchers (e.g. for accession AE 1070 *Aegilops umbellulata*). These and tetraploid accessions of *Pseudoroegneria* were excluded from further analysis. Two diploid *Thinopyrum* species, *Thinopyrum bessarabicum* and *Thinopyrum elongatum* (Jauhar, 1990), were selected for this study. The measured genome sizes of the genebank accessions and their comparison to the Kew Angiosperm DNA C-values database revealed that they are actually polyploid. A genome size variation of 20% was detected for different *Thinopyrum elongatum* accessions. The *Thinopyrum* accessions were kept in the analysis, since the genus is autopolyploid and it is the only taxon that contains the basic **E** genome.

3.2 Sequencing output and sequence assembly

3.2.1 On-target

3.2.1.1 Read statistics and capture efficiency

For 121 Triticeae accessions, covering approximately 35 Triticeae species and 24 genomic groups, and two outgroup taxa a custom sequence capture of 451 putative single-copy loci and Illumina sequencing was performed. The reads were mapped to the barley genome assembly as a reference (Mayer *et al.*, 2012) and consensus sequences of the target loci (i.e. the exons considered in bait design that belong to the same gene plus adjacent intron sequences) were extracted.

The number of sequence reads that mapped to all target loci in barley (i.e. 940 kb of exons plus adjacent introns) ranged from 67,980 to 2,191,884, with a median of 26X for the actual sequencing coverage (**Table E.1**). Of the 451 loci, 24 (5%) were not sufficiently captured (i.e. not captured in most taxa) and were excluded from further analyses. The capture performance of all accessions was assessed using 40 “single exons” (i.e. exons separated from other exons by more than 600 bp intronic sequence). Comparing the length of these purely exonic sequences with the length of sequences that could be assembled including adjacent intron information (**Figure 3.1**) showed that the capture reliably worked for all taxa. No obvious difference in capture performance between genera was found. However, the capture success showed variation between samples of the same species. Accessions sequenced with the aim of 100X showed the highest number of reads mapping to the target region, but resulted in only slightly longer assembled sequences compared to accessions of the same taxon (**Figure 3.1**). The capture efficiency was usually taxon independent, indicating no influence of probe design on capture efficiency. Up to 400 bp of flanking sequence information could be retrieved (**Table E.2**). Hence, the complete sequence of small introns could be assembled while larger introns could only be obtained partially.

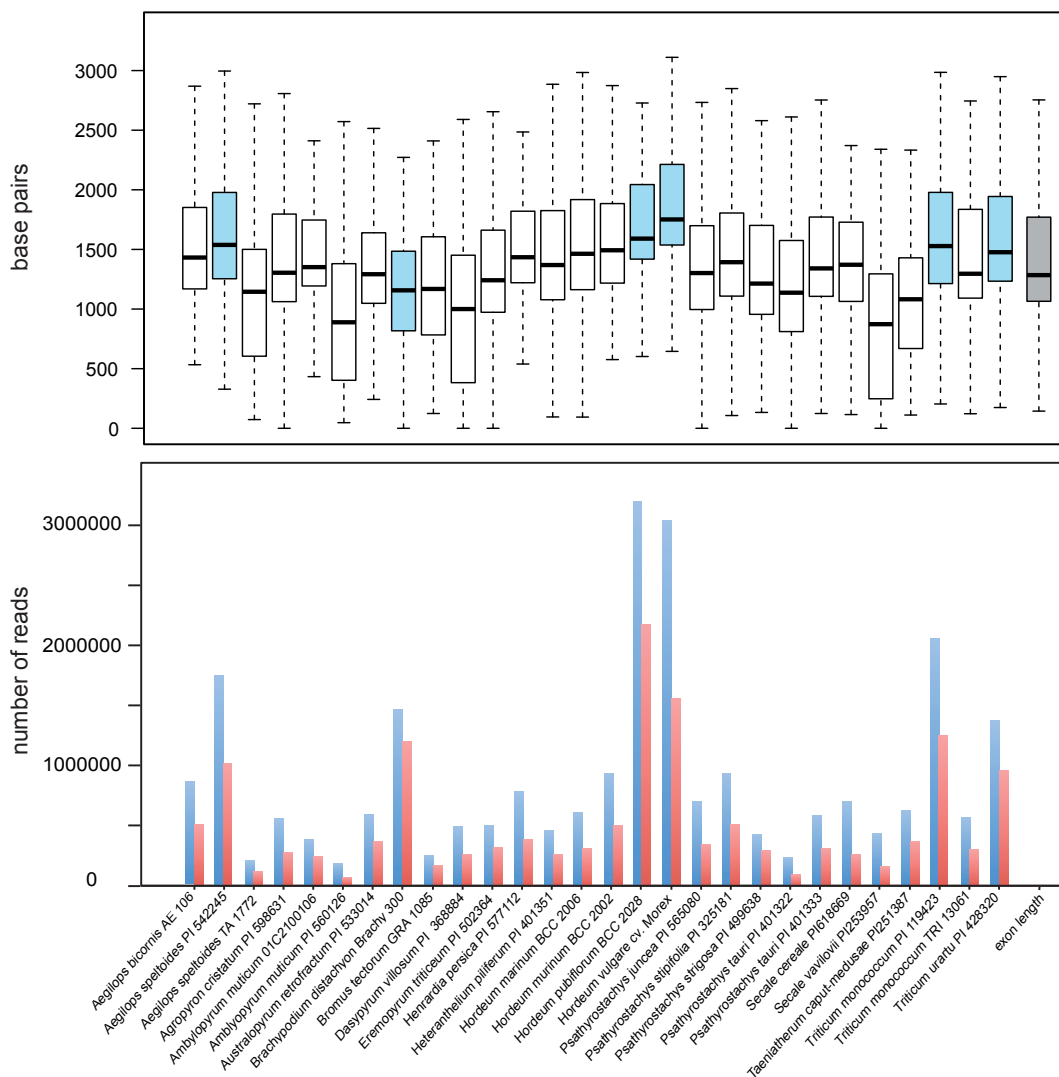


Figure 3.1 Comparison of sequencing output and capture success. Read numbers (lower part) and capture efficiency (upper part) for the same selection of accessions and covering all Triticeae genera. The number of reads that map to the barley genome assembly as reference (blue) and to the target loci (red) are shown. The capture performance for different species and genera was assessed using 40 “single exons” (i.e. exons that are separated from other exons by more than 600 bp intronic sequences). The length distribution of these purely exonic sequences (grey boxplot) was compared to the length of continuous sequences that could be assembled from individual samples. Boxplots from samples sequenced with 100X are coloured in blue. All other accessions were sequenced with 40X. Boxplots indicate that some exons were not captured, while others could be assembled including adjacent intron information.

3.2.1.2 Low-copy number loci and dataset partitioning

The sequences retrieved for the 427 well captured nuclear loci were combined into multiple sequence alignments. Visual inspection of these alignments often showed genus- or species-specific patterns of ambiguous positions. Allelic diversity is assumed to be much lower than 1%. Hence, high proportions of ambiguous positions in sequences of the same species are expected to reflect the existence of paralogous gene copies for a locus, either functional or as pseudogenes. The proportion of ambiguous positions per accession and locus was estimated (**Table E.3a**). An average

of more than 1% of ambiguous sites per genus in more than five diploid Triticeae genera and/or in many accessions of *Aegilops* and *Triticum* was detected for 85 (~20%) of the captured loci (**Figure 3.2, Table E.3b**). Therefore, these loci were considered as mainly multi-copy and excluded from further analyses. On the other hand, 341 loci (~80%) showed an average number of less than 1% of polymorphic positions in most diploid genera and/or accessions. They were considered as mainly low-copy number loci and kept in the analyses. A summary of the decisions made can be found in **Table E.3c**.

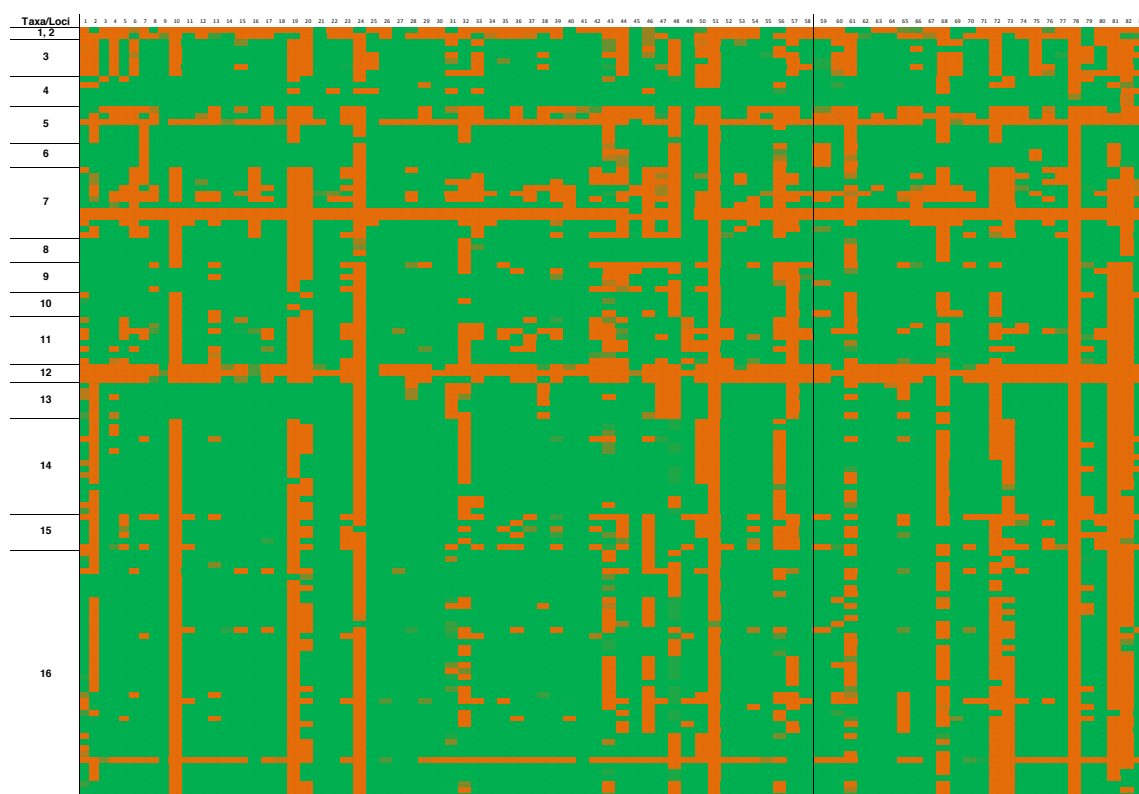


Figure 3.2 Comparison of proportions of ambiguous positions per locus. Each sequenced accessions is represented by one row. Accessions are sorted in putative phylogenetic order by genus and species. Numbers indicate the different genera: 1 *Brachypodium*, 2 *Bromus*, 3 *Psathyrostachys*, 4 *Hordeum*, 5 *Agropyron* + *Eremopyrum*, 6 *Australopyrum*, 7 *Pseudoroegneria*, 8 *Heterantherium*, 9 *Dasypyrum*, 10 *Henrardia*, 11 *Secale*, 12 *Thinopyrum*, 13 *Taeniatherum*, 14 *Triticum*, 15 *Amblyopyrum*, 16 *Aegilops*. Loci are arranged horizontally and loci with $\geq 1\%$ ambiguous positions are coloured in bright orange. Comparisons are shown for all loci of chromosome 1 of barley and a few loci of chromosome 2, separated by a thin black line. The comparison for all loci can be found in **Table E.3a**.

A comparison of the chromosomal locations of the enriched loci with the genetic maps of barley, wheat and rye showed that in these species only 134 loci are located on the same chromosome, while 369 loci are located on the same chromosome when comparing only barley and wheat. This is in agreement with Martis *et al.* (2013), where many chromosomal rearrangements have been proposed for *Secale cereale* compared to a putative common Triticeae ancestor. In contrast, only a few rearrangements have been suggested for *Hordeum vulgare* and *Triticum aestivum*. The comparison of recombination frequencies of captured loci retrieved from the barley genetic map

(**Figure S.2**) was used to detect which loci are located in centromeric and telomeric regions of the chromosomes.

Low-copy number loci were kept for phylogenetic inference if they had a total length of ≥ 1000 bp, contained less than 25% of missing data and comprised at least 150 parsimony-informative positions. Finally, the nuclear datasets for phylogenetic analyses consisted of 245 low-copy number loci fulfilling these filter criteria (dataset 1). These loci were further partitioned into loci that are located on the same chromosomes in barley, wheat and rye. In total 51 of them occur on the same chromosomes 1 to 3 in these three taxa (dataset 2). These chromosomes were reported to have undergone no or only small chromosomal rearrangements in rye (Martis *et al.*, 2013). There are 179 low-copy number loci with known chromosomal location in barley, 83 are located in centromeric (dataset 3a) and 96 in telomeric regions (dataset 3b). Chromosomal positions according to the genetic maps of barley, wheat and rye, information about alignment length, missing data and informativeness are summarised in **Table E.4** and **Figure S.3**.

3.2.2 Off-target

Reads that were not mapping on-target could be used to assemble the nrDNA tandem-repeat region and the whole chloroplast genome that occur in high-copy number within the cell.

3.2.2.1 The nrDNA tandem-repeat region

The nrDNA unit was assembled for 120 accessions by mapping the reads to a genus- or species-specific reference sequence obtained from a *de novo* assembly. The number of reads mapping to such regions varied greatly and was dependent on the sequencing coverage. Four accessions were excluded because of an insufficient amount of reads mapping. For the remaining samples the number of reads ranged from 602 to 56,968 (**Table E.1**). The coverage was ranging from 8X to 621X with a median of 38.4X. The *Brachypodium distachyon* accession was excluded, as it did not show sufficient sequence overlap in the spacer regions with the other taxa.

The final alignment consisted of 121 sequences, including the NCBI GenBank sequence of *Secale cereale*, and had a total length of 7527 bp. The ribosomal DNA was highly conserved while most variation is contained in the spacers, e.g. 80% of the parsimony-informative characters are located in the ETS (**Table 3.2**). The ETS assembled sequences of *Psathyrostachys juncea*, *Bromus tectorum* and *Hordeum marinum* were the shortest and this region was most variable for all *Hordeum* species. It showed further species-specific sequence length variations (indels i.e. insertions and/or deletions). Compared to the majority of taxa, deletions were found in e.g. *Triticum*, *Heterantherium*, *Eremopyrum* and ranged from 9 to ~200 bp. The sequences of *Aegilops markgrafii*, *Ae. umbellulata*, *Ae. speltoides*, *Agropyron cristatum*, *Australopyrum retrofractum*, and *Hordeum vulgare* revealed short (30 bp) or longer (up to 310 bp) insertions. The longer insertions contain repeat motives consisting of 27 to 32 nucleotides. Length variations found in ITS1 and ITS2 were not longer than 4 bp. In total, 6.9% of the data matrix was constituted by gaps because of sequence length variations.

Table 3.2 Alignment statistics for the nrDNA tandem-repeat region. The multiple sequence alignment consisted of 121 sequences. The alignment length, the number of variable (but parsimony-uninformative) and the number of parsimony-informative positions are shown for each partition.

Partition	Length (bp)	Non-parsimony-informative	Parsimony-informative
ETS	1696	134	788
18S rRNA	1811	12	13
ITS1	282	24	63
5.8S rRNA	110	2	2
ITS2	218	21	70
26S rRNA	3410	65	62
Total	7527	258	998

3.2.2.2 The whole chloroplast genome

Due to a lower read coverage, the chloroplast genome sequences could be assembled for 103 accessions. They were assembled via read mapping to a reference sequence that was artificially created by combining whole chloroplast genome sequences of *Hordeum vulgare* and *Aegilops sharonensis* that could be retrieved from GenBank. The new reference sequence comprised all length variation that occurred in the original sequences and had a total length of 137.7 kb. Between 81 to 97% of the reads that mapped to the chloroplast, mapped to *ndhF*, which was included in the bait design. The number of reads mapping to the chloroplast after the exclusion of reads mapping to *ndhF* ranged from 2906 to 77,400. The median coverage of the chloroplast genome was 13X with the coverage ranging from 2.8X to 61.4X and with moderate variations within different parts of the assemblies (**Table E.1**).

The final multiple sequence alignment consisted of 113 sequences, including ten GenBank reference sequences. No sequence differences were found between the inverted repeats (IR1 and IR2) of the same accession. Thus, the alignment used for phylogenetic analyses was reduced by IR2. The length of this alignment was 123,456 bp and started with the coding DNA sequence of *psbA* in the large single-copy region and ended with *ndhH* in the small single-copy region. The pairwise sequence identity was 92.2%, and 11,777 (9.6%) of the alignment positions were parsimony-informative. Due to the low sequencing coverage randomly distributed stretches of missing data are visible in the sequences. Thus, the data matrix contained 9.7% of undefined positions. Odd SNP combinations of less than 100 bp have been found in some accessions of a species, indicating misplacement of some reads in palindromic sites. Some taxa share long indels in intergenic regions, e.g. the same 900 bp deletion was found in *Pseudoroegneria*, *Thinopyrum* and *Dasypyrum*. Further, deletions ranging from 15 to 200 bp were found to be specific for *Hordeum vulgare*. A BLAST search of a 900 bp insertion unique to *Triticum monococcum* KC912692 returned mitochondrial DNA as best hit. The true occurrence of this fragment in the chloroplast genome of accessions included in this study could not be confirmed. Many short indels (3–40 bp) were found in introns of coding genes (e.g. *ysf3*). The extraction and alignment of 102 annotated

coding regions had a length of 69 kb and did not comprise the intergenic regions that contain most of the length and sequence variation.

3.3 Phylogenetic analyses

To unravel the phylogenetic relationships within Triticeae, phylogenetic analyses were performed for different types of molecular markers. The nrDNA tandem-repeat region, the whole chloroplast genome, and different combinations of low-copy number loci (e.g. centromeric vs. telomeric loci) were analysed. No particular reason for gene tree conflict was assumed for the inference of phylogenies using chromosome based concatenations of gene alignments, or the estimation of individual gene trees and the summary of the resulting gene tree topologies using network approaches. Additionally, ILS was assumed as the only source of gene tree conflict for species tree estimations using short-cut coalescence methods or a Bayesian coalescence analysis. A comparison of the results from different methods and the main topological features can be found in **Table E.6**.

3.3.1 Low-copy number nuclear gene phylogenies

The quality-filtered multiple sequence alignments of 245 low-copy number genes were used to infer individual gene trees by Bayesian phylogenetic inference under the best fitting substitution models GTR+G+I or GTR+G. The obtained consensus trees mainly indicate monophyly for the different genera or species. *Secale* appears monophyletic with *Secale strictum* diverging first, *Secale cereale* and *Secale vavilovii* fall into the same clade. *Aegilops* and *Triticum* appear as younger taxa in the tree topologies. The positions of other monophyletic groups are constantly changing when different loci are compared. Accessions of the same taxon may be widely scattered in the phylogenetic trees of certain loci (e.g. *Pseudoroegneria strigosa* in AK250796, or the grouping of *Hordeum murinum* with *Eremopyrum triticeum*, apart from all other *Hordeum* accessions in NIASHv1008C12). The gene trees often show low support or even polytomies for deeper nodes (e.g. AK252992, NIASHv116D04, NIASHv2008E12). However, the occurrence of “odd relationships involving different taxa” as well as the fact that “support values ... of deeper nodes are weaker than those of more recent nodes” was also reported for gene trees in Escobar *et al.* (2011). All individual gene trees can be found in the electronic supplement.

The Robinson-Foulds (RF) metric was used to systematically assess the degree of topological conflict between gene tree topologies. Therefore, the gene trees of 179 loci with known chromosomal location in the barley genetic map were compared. The RF metric revealed that all topologies are in conflict (**Figure 3.3, Table E.5**). In a combined analysis the difference in RF distances was significant between all centromeric and telomeric loci. A chromosome based comparison of RF distances for centromeric and telomeric loci also revealed significant differences except for chromosome 6 (**Table S.2**). The picture is most pronounced for chromosome 2, where loci on the long chromosome arm show a cluster of gene trees with larger RF distances than gene trees of loci in the

centromere. For chromosome 3 only the tips of the telomeres show an increase in RF distances. However, the centromere is often not entirely free from strongly conflicting topologies. Centromeric loci of chromosome 1 and chromosome 6 show similar RF metric distributions to telomeric loci of chromosome 2, 3, 5 and 7 (**Figure S.4**).

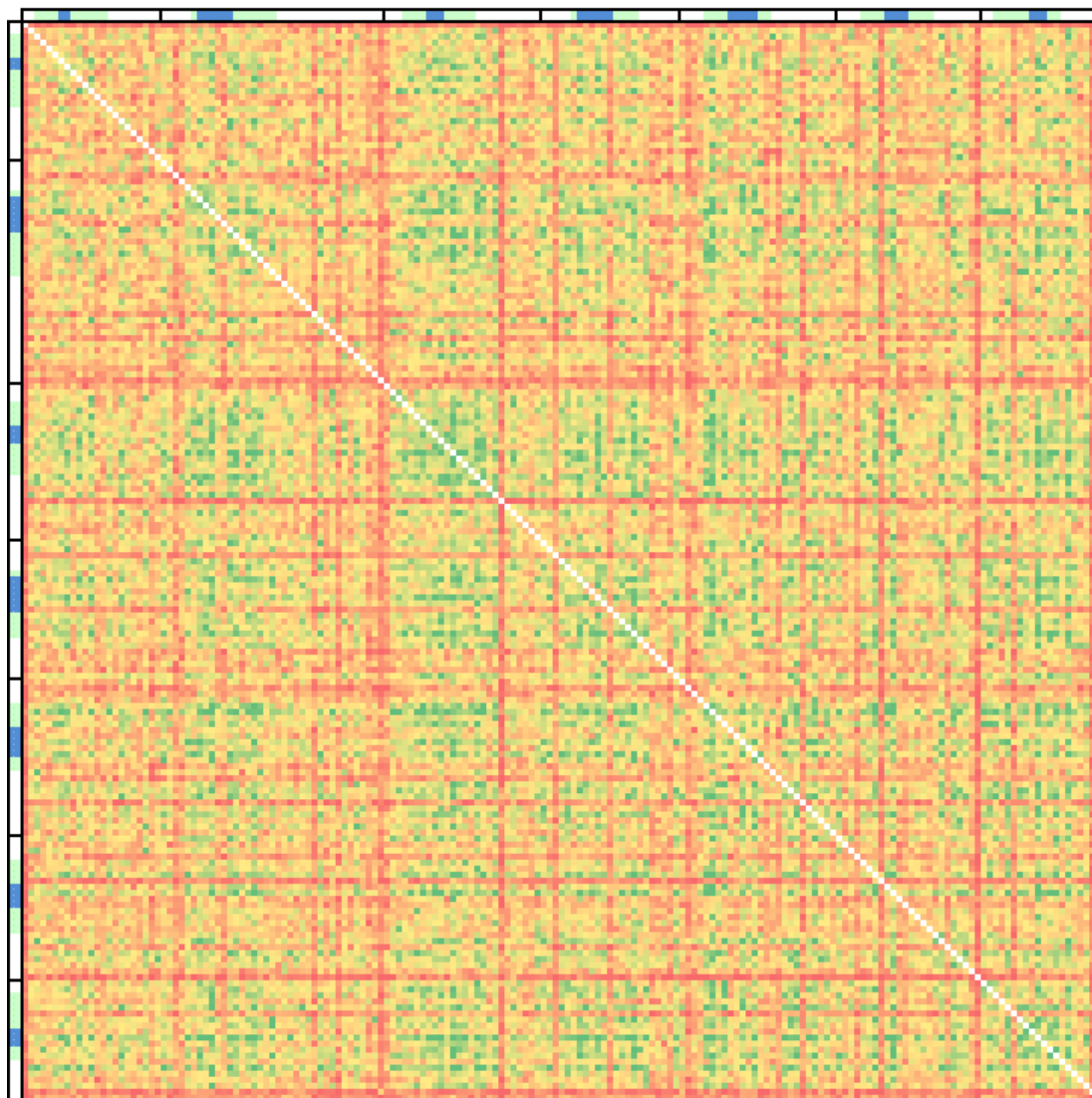


Figure 3.3 Comparison of the Robinson-Foulds (RF) metric for 179 Bayesian gene trees. Loci are ordered according to their position in the barley genetic map (Mascher *et al.*, 2013), starting with the short arm of chromosome 1. Different chromosomes are indicated by the framed blocks on the top and the left side of the plot. Centromeric regions (green) were defined comparing recombination frequencies for each chromosome (**Figure S.2**). Exact centromer positions as obtained by M. Mascher (personal communication), are highlighted in blue. Each data point refers to one pairwise tree comparison. Topological differences as assessed by the RF metric are represented by changes in colour from white (no difference), green (low tree difference), yellow (medium), and red (strong tree difference). The complete data matrix can be found in **Table E.5**.

A supermatrix approach was performed by concatenating loci located on the same chromosome in barley, wheat, and rye (dataset 2) and analysed by ML phylogenetic inference. This approach was chosen to see if loci originating from the same chromosome of barley, wheat and rye might be interpreted as linkage groups that

overall result in the same phylogeny and, hence, can be used to approximate a species tree. The supermatrix for chromosome 1 resulted from the concatenation of 14 loci and consisted of 32.8 kb, while for chromosome 2 and 3 19 loci and 18 loci were combined into supermatrices of 42.3 kb and 32.3 kb, respectively.

The three obtained tree topologies showed well-supported agreements such as the monophyly of species or genera, except for *Aegilops*. *Psathyrostachys* and *Hordeum* are positioned at the deepest splits of the tribe. Moreover, *Agropyron* and *Eremopyrum* are grouped as sister taxa with high bootstrap support. The genus *Aegilops* diverged latest, other sister species are, for example, *Ae. uniaristata* and *Ae. comosa*. Species sharing the **S** genome (**Table 2.1**) always fall into the same clade. However, there are well-supported clades in these phylogenies, making the chromosome-based topologies incongruent: *Amblyopyrum muticum* is sister species to *Ae. tauschii* on chromosome 1, while *Amblyopyrum muticum* is sister to *Ae. speltoides* on chromosome 2. The phylogeny obtained for chromosome 3 shows further well-supported conflicting resolutions, e.g. *Ae. tauschii* is sister to *Ae. uniaristata* and *Ae. comosa*. There are groupings with low support, especially at the backbone of the topology of chromosome 1 and 3. The ML tree topologies obtained for chromosome 1 and 2 are compared in **Figure S.5**. The topology obtained for chromosome 3 can be found in **Figure S.6**. Since all supermatrices returned different topologies, the usage of chromosome-based concatenations does not result in reliable estimates of a species tree in Triticeae.

3.3.2 Rooted phylogenetic networks

Rooted phylogenetic networks were constructed to identify the taxa causing the strongest phylogenetic conflicts between individual gene tree inferences. The networks were drawn for three different partitions of Bayesian consensus trees (i.e. all quality-filtered loci, all centromeric and all telomeric loci). First, the source trees were modified to keep only well supported incongruences. The cleaned source trees were used to summarise all clusters of taxa present in these trees.

The network retrieved from 245 low-copy number genes (**Figure 3.4**) showed much less reticulations than the phylogenetic networks for the centromeric and telomeric datasets (**Figure S.7** and **Figure S.8**). In this network deeper nodes are mainly unresolved. The *Aegilops-Triticum-Amblyopyrum* complex is connected by a large polytomy. Reticulations between species are only present within *Aegilops* and suggest that the MRCAs of *Ae. umbellulata*/*Ae. markgrafii* and *Ae. uniaristata*/*Ae. comosa* gave rise to *Ae. tauschii*.

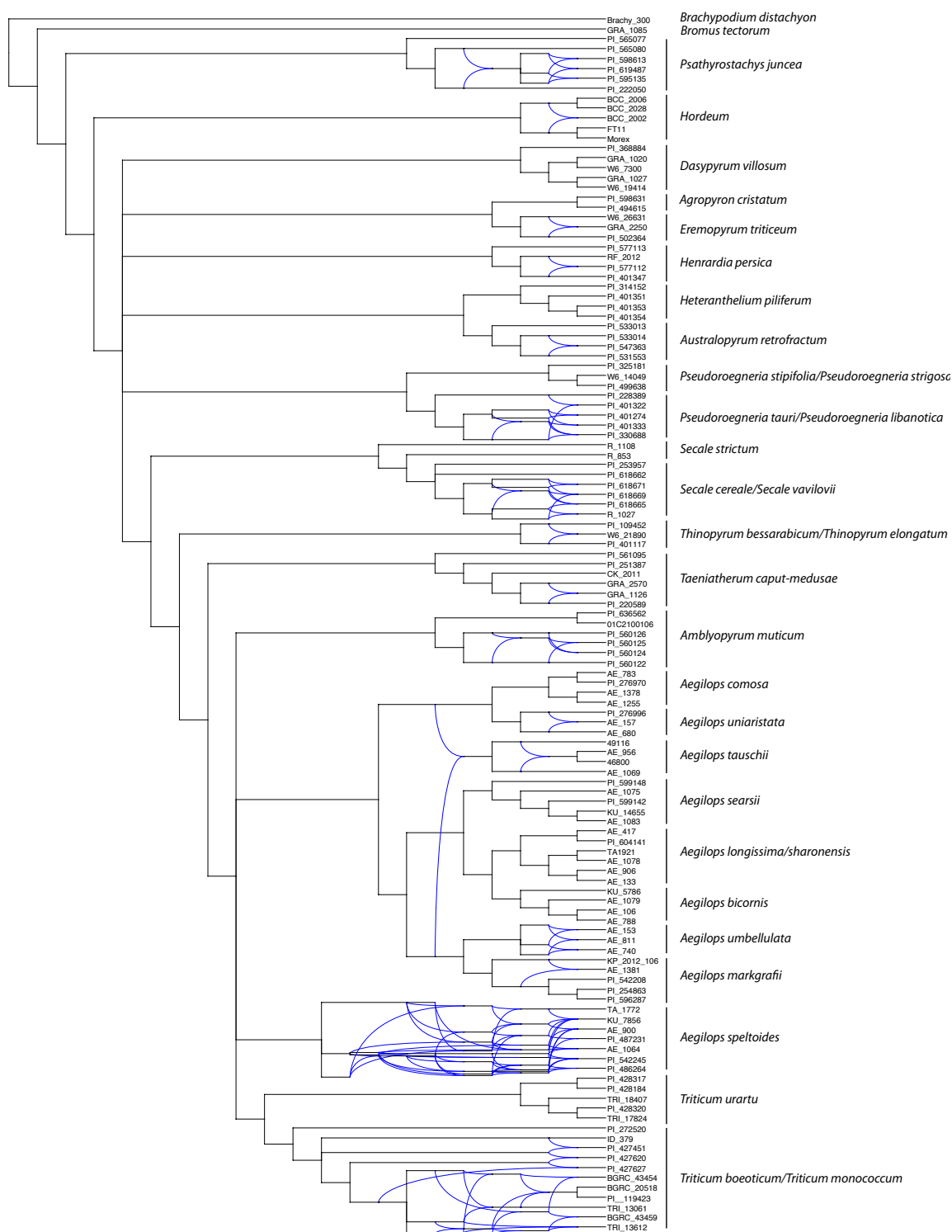


Figure 3.4 Rooted phylogenetic network that summarises 245 quality-filtered single Bayesian consensus trees. The individual Bayesian gene trees were rooted with *Brachypodium distachyon* as the outgroup. The network was constructed after the source tree correction to keep only strongly supported conflicts. Reticulations are depicted in blue.

The phylogenetic networks for the centromeric and telomeric datasets (**Figure S.7** and **Figure S.8**) show higher numbers of reticulations. A net-like formation of branches is often visible within accessions of the same species. On the intergeneric level *Psathyrostachys* and *Hordeum* show a strictly bifurcating evolution. Other genera

grouping at deeper nodes are often placed on a large polytomy and/or are involved in reticulations. In the centromeric dataset a sub-network was necessary to depict the relationships between *Australopyrum*, *Heterantherium* and *Dasypyrum*. Further reticulations in the centre of the network involve *Secale* and *Thinopyrum*, *Triticum* and *Aegilops speltoides*. In contrast, *Dasypyrum* is sister to *Pseudoroegneria* and not involved in reticulations in the telomeric dataset. *Eremopyrum*, *Australopyrum*, *Heterantherium*, *Henrardia* and *Secale* are connected net-like. The *Aegilops-Triticum-Amblyopyrum* complex is built by a large polytomy. In both datasets many reticulations were necessary to reflect their various relationships suggested by the gene trees. Reticulations involve all species of *Aegilops* or the most recent common ancestor (MRCA) as for the sister species of *Ae. comosa* + *Ae. uniaristata* and the **S**-genome group. There are topological conflicts between all networks (**Table E.6**).

3.3.3 Coalescent-based species trees

Species trees based on multilocus data were estimated using two approaches that account for incomplete lineage sorting as the only reason for gene tree conflict: a short-cut coalescence analysis was conducted, that was shown to be statistically consistent under the multispecies coalescent model even for large datasets. Additionally, a Bayesian coalescence analysis was performed that co-estimates gene and species trees, but which is limited to smaller datasets.

The summary method implemented in ASTRAL-II was used to estimate species trees based on 245 quality-filtered loci (dataset 1), 83 centromeric (dataset 3a) and 96 telomeric (dataset 3b) ML gene trees with multilocus bootstrapping. The species trees obtained from centromeric and telomeric datasets (**Figure S.9** and **Figure S.10**) show some highly supported incongruences. The well-supported placement of the sister taxa *Agropyron* and *Eremopyrum* in the centromeric dataset swaps its location with *Pseudoroegneria* in the telomeric dataset. Both species trees show a very low support for the taxa grouped in the centre of the phylogenetic tree. *Secale*, *Thinopyrum* and *Taeniatherum* appear to have originated in a mainly bifurcating manner. In the species tree based on centromeric loci the sister relationship of *Aegilops speltoides* and *Amblyopyrum muticum* is highly supported. The split of *Triticum* from all remaining *Aegilops* species has moderate support. Within *Aegilops* only a few nodes are resolved. In contrast, in the telomeric species tree *Amblyopyrum* is clearly separated from the clade comprising *Triticum* and *Aegilops*. The node separating *Ae. speltoides* and all remaining *Aegilops* species has low support. *Ae. tauschii* is sister to *Ae. umbellulata* and *Ae. markgrafii* with moderate support. The other groupings within *Aegilops* are generally better resolved. In the overall species tree (**Figure 3.5**) *Eremopyrum*, *Agropyron* and *Pseudoroegneria* are placed together with other taxa in the centre of the phylogeny with low support. *Aegilops speltoides* and *Amblyopyrum muticum* have a weakly supported sister relationship. The node separating *Triticum* and all remaining *Aegilops* taxa is also only poorly supported. There are few well-resolved groupings within the *Aegilops-Triticum-Amblyopyrum* complex like the monophyly of the **S**-genome group and the sister relationship of *Ae. markgrafii* and *Ae. umbellulata*.

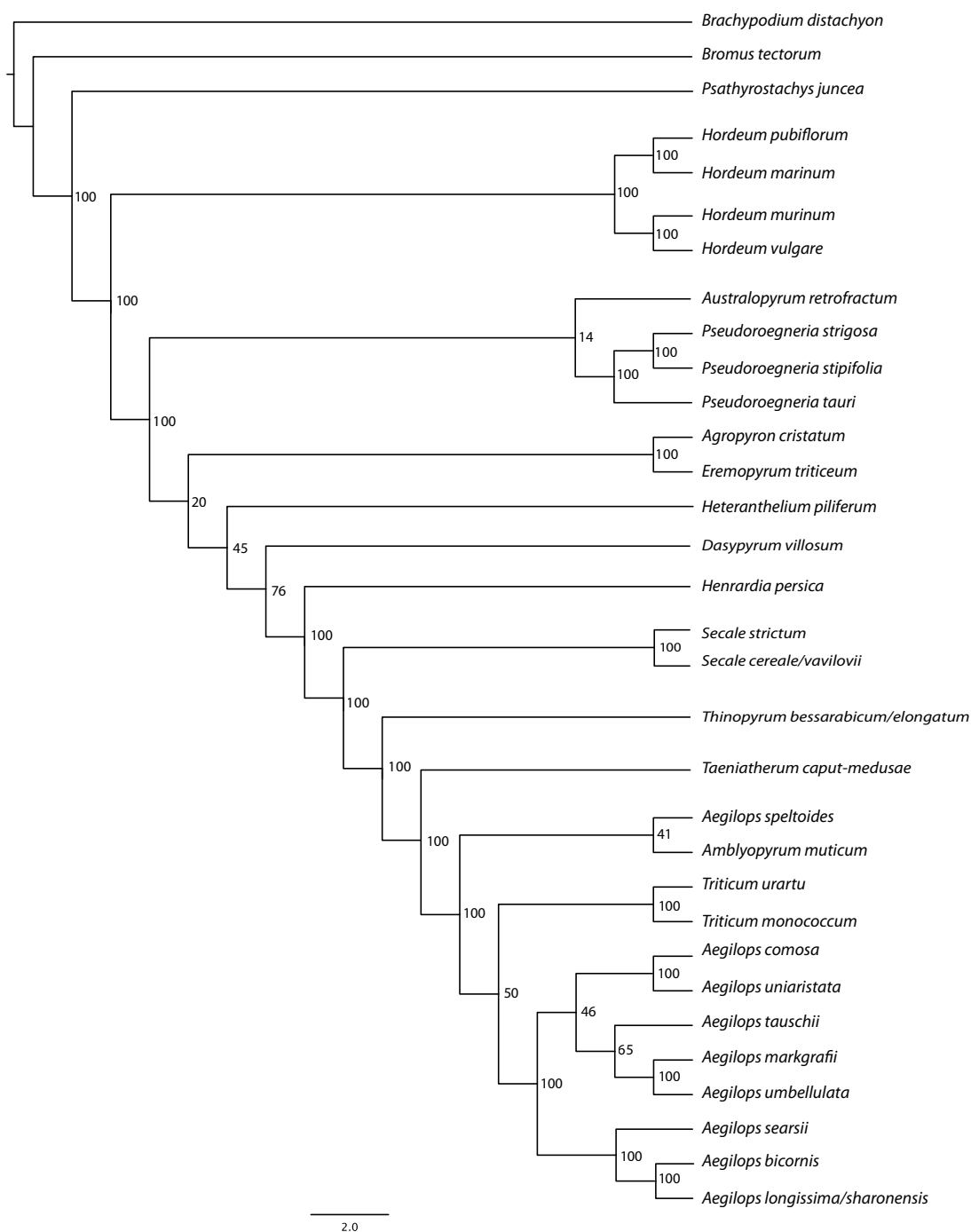


Figure 3.5 Summarised coalescent-based species tree topology estimated from 245 ML gene trees with multilocus bootstrapping. Bootstrap support values are depicted next to all nodes. Monophyletic clades were collapsed. A “/” between species names indicates that two species fell into the same clade.

A species tree and species divergence times were estimated on a reduced dataset for the *Aegilops-Triticum-Amblyopyrum* complex. The Bayesian coalescence analysis was performed in *BEAST for 28 telomeric loci combined and divided into bins according to the best partition schemes and DNA substitution models. The partitioned analysis was performed for seven bins, each comprising four loci. All species trees sets were then summarised with ASTRAL-II. Although the combined analyses showed poor mixing after

500 million generations as indicated by the ESS values, the species tree topology was concordant with the one obtained from the partitioned analysis. In this species tree topology (**Figure 3.6**) *Triticum* groups inside *Aegilops*, while *Amblyopyrum muticum* appears as sister to this clade. In contrast to all other phylogenetic analyses conducted, the *Aegilops* section *Sitopsis* appears monophyletic. Based on morphological and genomic data this section was defined for *Ae. speltoides* and the **S**-genome species *Ae. bicornis*, *Ae. searsii*, *Ae. sharonensis*, and *Ae. longissima* (Kilian *et al.*, 2011). The section is separated from the clade of all other *Aegilops* and *Triticum* species with low support. The early divergence of *Ae. tauschii* from the other *Aegilops* species in this clade is poorly supported, while the sister relationships between *Ae. comosa* and *Ae. uniaristata* and between *Ae. markgrafii* and *Ae. umbellulata* shows high support. Divergence time estimations using an uncorrelated lognormal clock and secondary calibration points on the root of all Triticeae and the *Aegilops*-*Triticum* clade resulted in two classes of species divergence times at approximately 6-5 million years ago (Ma) and 2.5 Ma.

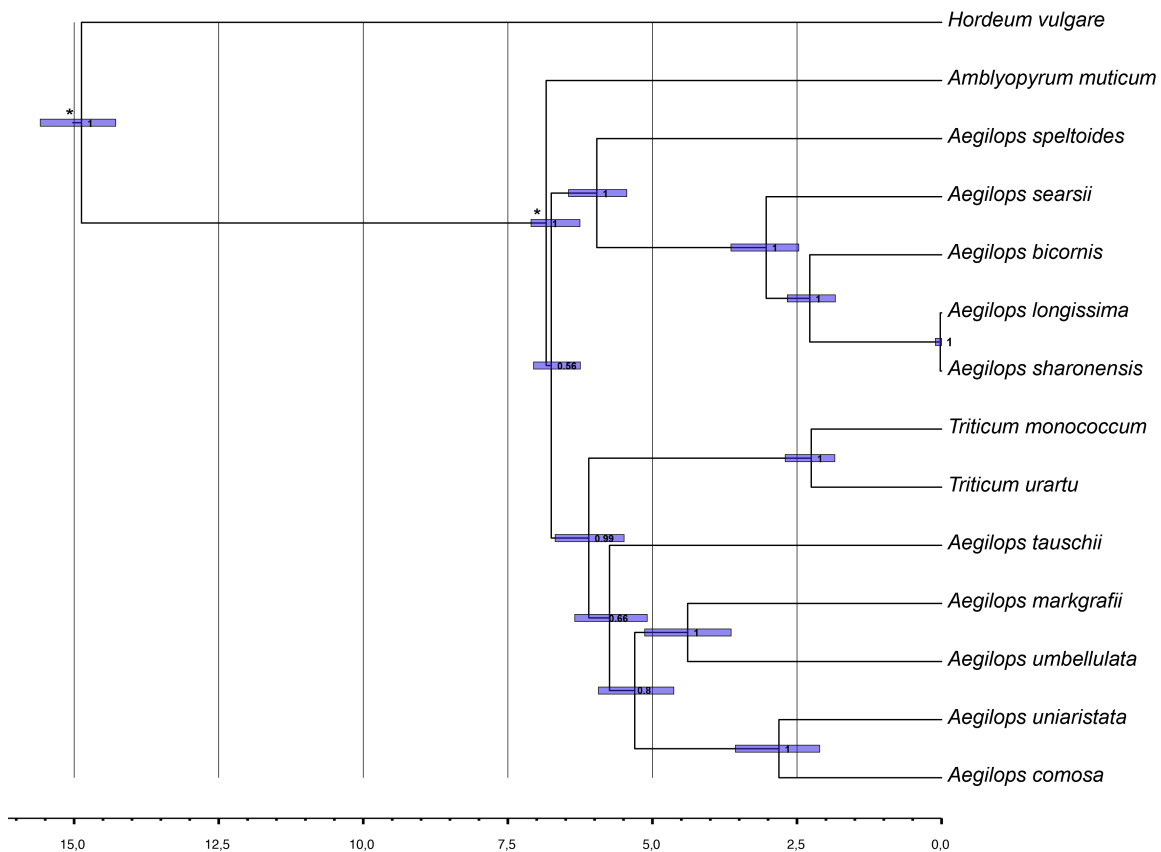


Figure 3.6 Calibrated species tree obtained from a Bayesian multispecies coalescence analysis. The analysis was run for 28 telomeric loci to investigate the diploid *Aegilops*, *Amblyopyrum muticum* and *Triticum* taxa. One *Hordeum vulgare* accession was included as outgroup. Posterior probabilities are given at the nodes. Divergence time estimates were inferred using secondary calibration (*) points for the root of the Triticeae (15.32 million years ago, Ma) and for the split between *Aegilops* and *Triticum* (6.55 Ma) taken from Marcussen *et al.* (2014). Node bars indicate the age range with 95% interval of the highest probability density.

The superimposed representation of species tree sets **Figure 3.7** summarises 389,326 species trees. The plot revealed a mixed signal especially at the backbone of the whole *Aegilops-Triticum-Amblyopyrum* clade and shows that there is no prominent species tree topology. Although with varying intensities, there is a reticulate signal for most species.

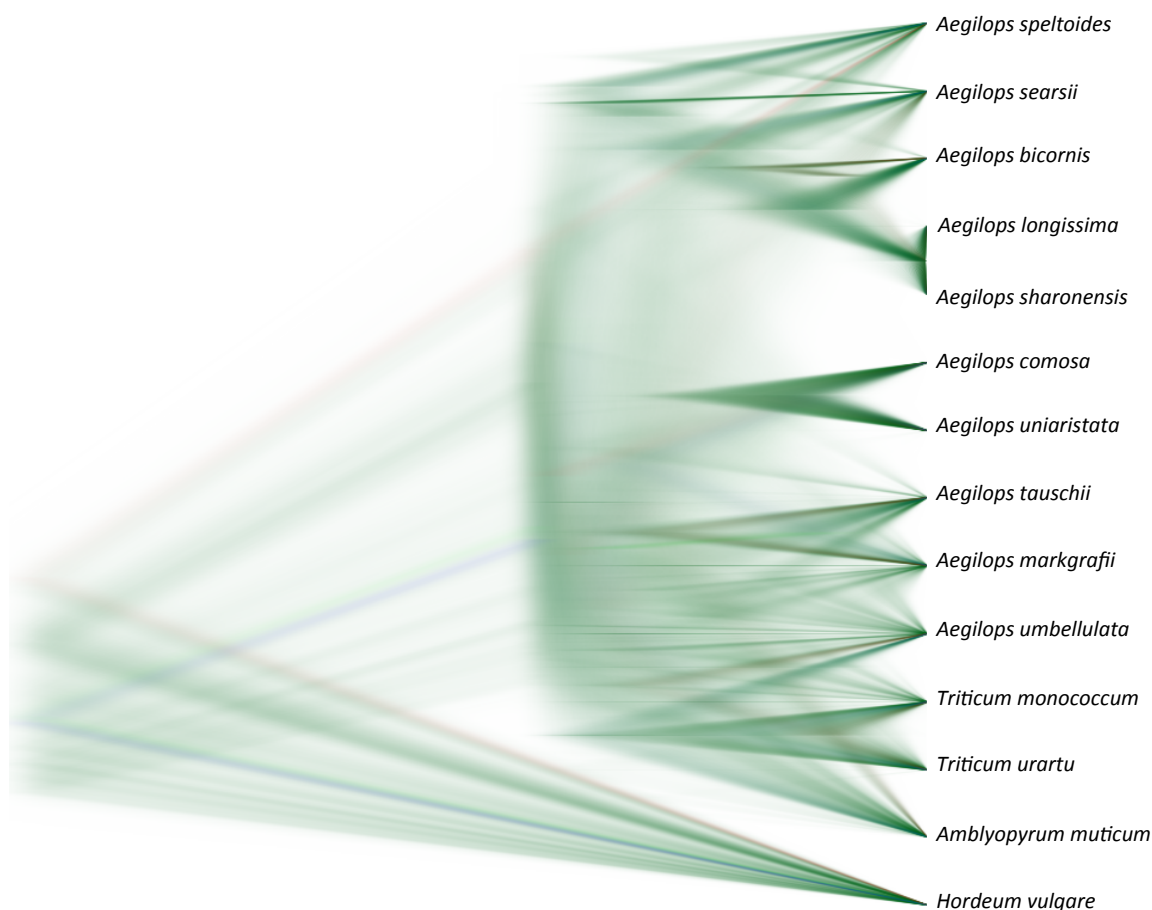


Figure 3.7 Superimposed DENSITREE representation of species tree sets obtained from the binned Bayesian coalescence analysis. In total 28 telomeric loci were used to analyse the diploid *Aegilops*, *Amblyopyrum muticum* and *Triticum* taxa. One *Hordeum vulgare* accession was included as outgroup. Colours correspond to the frequency of the topologies: from blue – most frequent, red – second most frequent, and green – least frequent.

3.3.4 The nrDNA tandem-repeat and the chloroplast phylogeny

The multiple sequence alignments of the nrDNA tandem-repeat region and the chloroplast genomes were used to reconstruct phylogenetic trees from markers known to evolve under different evolutionary constraints. The multiple sequence alignments are provided in the electronic supplement.

For the nrDNA unit three different substitution models were suggested for the six data partitions: SYM+G for the spacer regions, and K80+I and GTR+I+G for the ribosomal DNA. The topology obtained after Bayesian phylogenetic inference (**Figure 3.8**) revealed *Psathyrostachys* and *Hordeum* placed on a basal polytomy. Long branches

separate the different *Hordeum* species. *Heteranthelium* and *Dasypyrum* fall into the same clade, but together with *Australopyrum* on another polytomy. *Pseudoroegneria* is polyphyletic with *Pseudoroegneria tauri* diverging first from the sister species *Pseudoroegneria strigosa* and *Pseudoroegneria stipifolia*. *Thinopyrum bessarabicum* and *Thinopyrum elongatum* are monophyletic with high support. *Henrardia* groups as sister taxon to the clade of *Secale* and *Triticum*. *Taeniatherum* is sister species to *Amblyopyrum* and all *Aegilops* species. *Ae. speltoides*, followed by *Ae. tauschii* were the first species to diverge within *Aegilops*. *Ae. comosa* and *Ae. uniarisitata* group as sister to *Ae. umbellulata* and *Ae. markgrafii*. The clade comprising these four species is sister to the clade of the **S**-genome species.

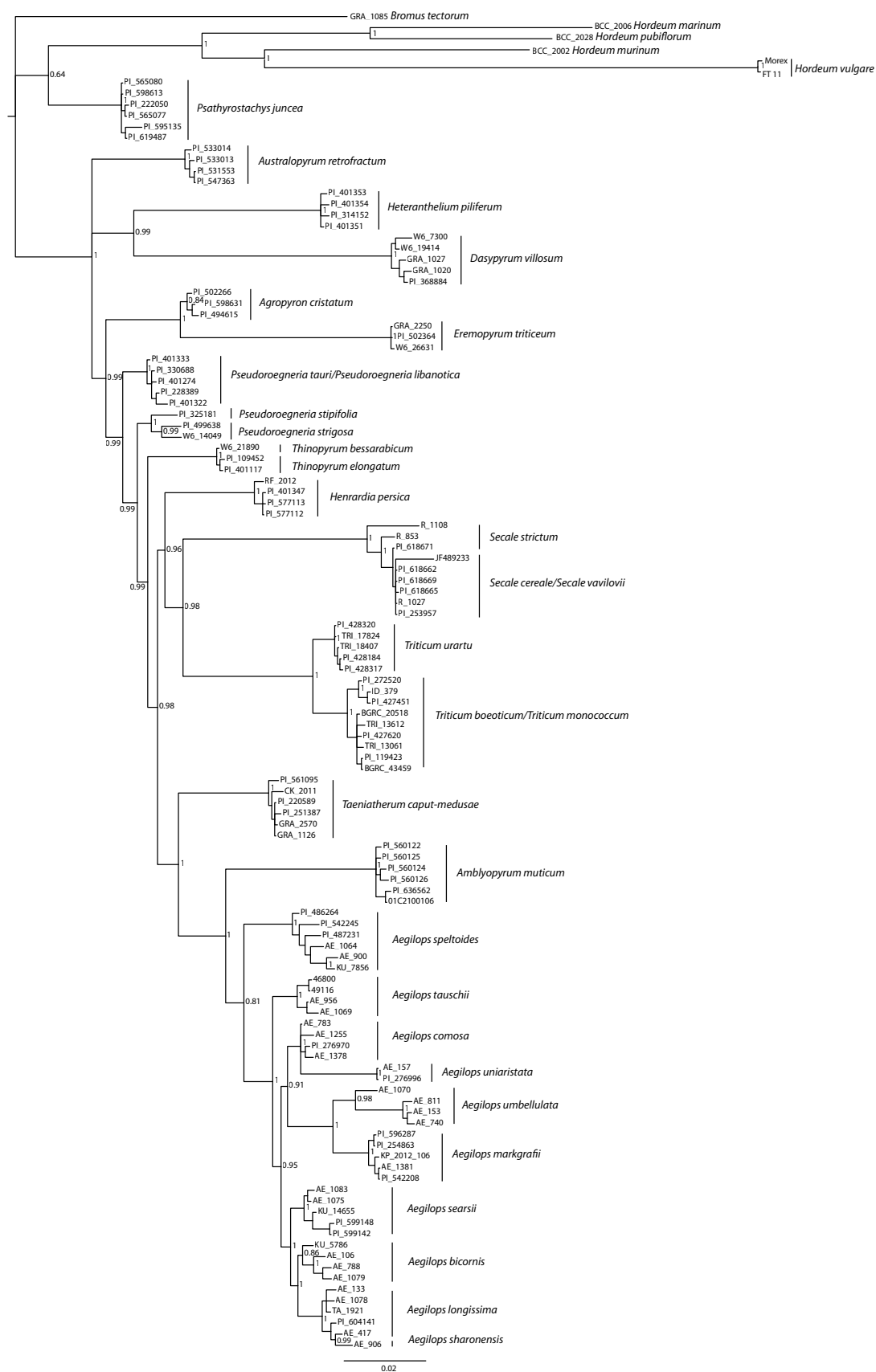


Figure 3.8 Phylogenetic tree derived from 7527 bp of the nrDNA tandem-repeat region by Bayesian phylogenetic inference. The multiple sequence alignment consisted of 120 sequenced accessions and one GenBank accession for *Secale cereale*. *Bromus tectorum* was included as an outgroup. Posterior probability values for the main clades are depicted next to the nodes.

The ML tree derived from the whole chloroplast genome alignment (**Figure 3.9**) is well resolved for deeper nodes, but due to only 9.6% of parsimony-informative characters less resolved for younger clades. *Psathyrostachys* and *Hordeum* are the most basal taxa. In contrast to phylogenetic results obtained from other methods and datasets *Thinopyrum* groups within *Pseudoroegneria* and *Aegilops speltoides* groups as sister to *Taeniatherum* (bootstrap support 85). Both appear as sister to all species in the *Aegilops-Triticum-Amblyopyrum* complex. *Amblyopyrum muticum* (T genome) falls inside *Aegilops* (without *Ae. speltoides*) and groups close to *Ae. comosa* (M), *Ae. markgrafii* (C), *Ae. umbellulata* (U), and *Ae. uniaristata* (N). There are some long branches for accessions having a high proportion of missing data. The ML tree estimated from the concatenation of annotated regions confirmed the phylogeny derived from the entire chloroplast genome, although *Taeniatherum* appeared as sister to the *Aegilops-Triticum-Amblyopyrum* complex with low support (bootstrap support 69; data not shown). With respect to the *Aegilops-Triticum-Amblyopyrum* complex the chloroplast phylogeny is in general agreement with other studies, although these mainly focus on domesticated wheat and its close relatives (Middleton *et al.*, 2014; Gornicki *et al.*, 2014; Li *et al.*, 2015a).

Figure 3.9 Phylogenetic tree derived from the whole chloroplast sequence by Maximum-Likelihood. The alignment consisted of 103 sequenced accessions and 10 GenBank sequences. One inverted repeat was removed for phylogenetic analysis. The multiple sequence alignment used for phylogenetic analysis had a length of 123 kb. *Brachypodium distachyon* was included as an outgroup. Bootstrap support values >75 are depicted next to nodes. Accession names follow the taxonomic treatment as used in the donor genebanks of the utilised seed material.



4 DISCUSSION

At this time the evolutionary history of the tribe Triticeae has not been resolved satisfactorily. Earlier molecular phylogenetic studies have been focused on a single and/or a small subset of related genera, with the main attention on economically important species and their close relatives. Moreover these studies were based on a few molecular markers providing only a partial insight into the evolution of the tribe. To overcome the limitations of previous studies, a hybridization-based enrichment approach coupled with next-generation sequencing (NGS) technology was chosen to sequence parts of 451 putative single-copy loci. Accessions covering the basic Triticeae genomes and several accessions per species were selected. The present work, for the first time, provides a phylogenetic hypothesis that is based on a comprehensive sampling of taxa and phylogenetic markers.

4.1 Seed material

The accessions included in the analyses were mainly acquired from several genebanks (i.e. ICARDA, IPK, USDA, the Czech Crop Research Institute) but additional material was collected during field trips. Multiple accessions per species and intra-specific entities were selected to achieve a good coverage of the distribution areas of these species, and to be able to detect intraspecific genetic variability.

Concerns about the condition of genebank accessions have been raised in other studies and are related to the fact that seed material is often maintained in genebanks under conditions that permit open pollination over several decades (Frederiksen & Petersen,

1998). The differential genetic behaviour of genebank material from *Hordeum vulgare* subsp. *spontaneum* in comparison to recently collected wild material led Jakob *et al.* (2014) to state that “hybridization has most probably taken place during propagation and maintenance in *ex situ* seed repositories”. Also in the scope of this study, a few selected accessions needed to be excluded due to deviations in genome size or morphological characters (e.g. in *Aegilops*, *Taeniatherum*). However, the vast majority of the material did not reveal any peculiarities and samples that were retrieved from collection trips in the course of this project always grouped with other samples of the same species. The estimation of genome sizes for the selected accessions proved to be a good strategy to detect problematic material, especially in the case of perennial Triticeae where inflorescences for morphological species determination can not always be obtained within the timeframe of a research project. Further, genome size estimations allowed the distinction between di- and polyploid accessions of the same species.

4.2 Sequence capture performance and data assembly

A set of loci was initially selected for enrichment aiming at an even distribution of loci on the chromosomes of *Hordeum vulgare*. This species was used as a proxy for the location of the loci in other Triticeae genomes due to the highly conserved synteny observed among grass genomes (Mayer *et al.*, 2011). Moreover, loci were only considered for bait design if they showed one orthologous gene and a conserved exon-intron structure in comparison to more distantly related grasses. The sequence capture probes were designed to cover 690 kb of exonic regions of 451 locus-wise MSAs comprising fl-cDNA from *Hordeum vulgare*, *Triticum aestivum* and *Brachypodium distachyon*. The average sequence identity between exons of the fl-cDNA types amounted to 84%. One set of baits was designed for each fl-cDNA type in the MSA. This intrinsic diversity of the bait library and the ability of the 120 bp long capture probes to hybridize to the target DNA in case of sequence differences (Lemmon & Lemmon, 2013) allowed its application to a broad taxonomic range.

After the sequence capture of 123 accessions, the Illumina sequence reads were mapped with an average mismatch rate of 10% to the target loci (i.e. exons and associated introns) of the reference barley genome assembly. The library of capture probes successfully retrieved sequence information for all main genomic groups of Triticeae and the two outgroup taxa *Bromus* and *Brachypodium* for 95% of the selected loci. This indicates that the bait library designed here can also work within higher taxonomic ranks. Although with some fluctuations, the sequence capture worked for all accessions. Differences in capture performance among samples of the same species indicate variations in library preparations and can result from sub-optimal performance in several steps of the protocol, such as adapter ligation, PCR amplification bias, variation in hybridization and/or DNA quantifications. Further, it was shown that an increase in sequencing coverage could accommodate for lower capture performance, an action that is favoured due to the on-going reduction in sequencing costs (Glenn, 2011), instead of repeating the time and cost-intensive library preparations.

Approximately 20% of all Illumina sequence reads mapped to the target loci. This is an on-target rate comparable to other studies that employ custom bait libraries (Kenny *et al.*, 2010), although larger on-target rates of 40-50% have been reported as well (Lord *et al.*, 2012). Additionally, a small on-target to off-target ratio may lead to a drop in the number of reads mapping on-target. In this work a bait library was designed to cover 690 kb of exonic sequences. With genome sizes ranging from approximately 4–8 Gb (1C), which corresponds to an on-target size of approximately 0.01 to 0.02% of the genome. Thus, the regions of interest were on average enriched by a factor of 1000. Hence, the relatively low rate of reads mapping on-target may be partially explained by the large genome size of the Triticeae species. The inclusion of repeat regions in bait design was further reported to lower the on-target output dramatically (Kenny *et al.*, 2010, Lord *et al.*, 2012). In this study on average 25% of all generated reads mapped to the chloroplast marker *ndhF*, which was considered in bait design. Capture probes complementary to *ndhF* find their target more frequently, since it exists in higher copy number in the cell. The following PCR steps of the enriched fraction then amplify this bias. However, in hybrid enrichment studies, the off-target fraction can provide a valuable source of other phylogenetic informative markers, e.g. transposable elements. In Triticeae the contribution of different transposable element families, so far, has only been analysed in a few studies (Middleton *et al.*, 2013; Markova & Mason-Gamer, 2015). In this work, the off-target fraction of reads was used to assemble the nrDNA tandem-repeat region and the whole chloroplast genome.

The ability of the capture probe library to tolerate mismatches and the current assembly procedure for the nuclear loci returned multiple sequence variants (i.e. homeologues and/or paralogues and pseudogenes), as identified by an increased number of polymorphic sequence positions. Because the assembly pipeline does not yet allow for disentangling of paralogous gene copies, ambiguous positions had to be masked which resulted in an overall loss of phylogenetic information. Many software tools were published that are able to phase the sequence data of heterozygous or polyploid samples (e.g. Bansal & Bafna, 2008; O'Neil & Emrich, 2012; Krasileva *et al.*, 2013; Berger *et al.*, 2014). However, they have been successfully applied only on heterozygous or tetraploid samples. Since the identified multi-copy genes may represent gene families potentially combining more than two gene copies, none of these programs fulfils the needs of the data at hand. Assuming a sequencing coverage that is high enough and sufficient sequence variation between copies, a combination of read mapping and *de novo* assembly, similar to Brassac & Blattner (2015), seems to be the best way to phase paralogues. This would also account for sequence length differences between taxa, a feature not supported by the current assembly pipeline, and possibly increase the phylogenetic resolution. However, since the bait design was based on a conserved approach, i.e. considering sequence information from more distantly related grasses and the choice of loci with conserved exon-intron boundaries, the amount of insertions and deletions might be rather low, at least in exons of the chosen loci. A phasing approach would also allow the use of species tree methods that make use of gene family data (Boussau *et al.*, 2013; de Oliveira Martins *et al.*, 2014). This approach, which was acknowledged for integrating more data, may be well suited to unravel the poorly supported relationships in the central part of the tribe's phylogeny, especially because it does not require the identification of orthologues.

4.3 Genome plasticity

4.3.1 Origin and identification of paralogues

All grasses are known to share two ancient whole-genome duplication (WGD) events (Vogel *et al.*, 2010; de Smet *et al.*, 2013) that occurred approximately 100 and 65 million years ago (Ma). In addition, large- and small-scale genome duplications (SSD) shape genomes as the result of e.g. unequal crossing over during homologous recombination or non-homologous recombination resulting from the repair of DNA double-strand breaks (Zhang, 2003; Hastings *et al.*, 2009; Murat *et al.*, 2014). Furthermore, individual genomes are shaped considerably by differential elimination or retention of duplicated genes and/or genomes. The latter can result in the birth of a gene family that consists of several paralogues.

Approximately 80% of the loci selected for sequence capture appeared as low-copy number loci, while 20% showed indications for the existence of multiple closely related sequence variants in most diploid genera. Sequence information from homeologues (i.e. in the case of *Thinopyrum*) and/or paralogues and pseudogenes could be identified by a number of polymorphic sites >1%. An allelic diversity clearly lower than 1% was found in the analysis of six single-copy loci of large populations of *Hordeum vulgare* subsp. *spontaneum* (Jakob *et al.*, 2014). Thus, single-copy loci of heterozygous individuals can be expected to show noticeably less than 1% of ambiguous positions in assembled sequences. Since sequenced accessions within a species mainly share the same combinations of polymorphic positions, this points to the existence of paralogous gene copies rather than to heterozygous loci. The sequences assembled for *Hordeum vulgare* never showed an elevated number of ambiguous positions. This shows that low-copy number loci were initially correctly inferred and that the retrieved pattern of low- and multi-copy loci indicates structural distinctions in the genomes that are likely the result of gene and/or genome duplications.

4.3.2 Chromosomal rearrangements

Whole genome sequence data that can be used to detect chromosomal rearrangement in Triticeae is limited to the economically important members wheat, barley and rye (e.g. Devos *et al.*, 1993; Qi *et al.*, 2004; Mayer *et al.*, 2011, 2012, 2014; Chapman *et al.*, 2015). Comparative genomic approaches revealed that barley and wheat chromosomes are highly syntenic. Only chromosomes 4A and 5A of bread wheat show signals of interchromosomal translocations when compared to barley, while many chromosomal rearrangements have been postulated for rye (Devos *et al.*, 1993; Moore *et al.*, 1995; Mayer *et al.*, 2011; Martis *et al.*, 2013): Large parts of chromosome 4R and 7R are structurally altered. Chromosome 1R is the only one without rearrangements compared to a hypothesized MRCA of Triticeae, wheat, and/or barley. Telomeric regions appear generally more affected by these chromosomal rearrangements than centromeric regions (Martis *et al.*, 2013).

In this study individual gene trees of low-copy number loci that could be assigned to centromeric and telomeric chromosomal locations, were subjected to topological comparisons via the Robinson-Foulds metric. Most centromeric loci showed less

conflicting topologies to each other than telomeric loci. This is concordant to findings made for loci located on chromosome 3 according to the genetic map of wheat (Escobar *et al.*, 2011) and may indicate that for most diploid Triticeae centromeric regions are less affected by recombination. Hence, they would be structurally more conserved than telomeric regions. However, loci in the centromeric regions of chromosome 1 and 6 showed strong topological conflicts throughout the chromosome. This may be an indicator that these chromosomes were affected by rearrangements and gene flow in Triticeae taxa for which no sequenced genomes yet exist.

4.3.3 Gene and/or genome duplications and functional adaptation

Duplicated genes and genomes are assumed to return to single-copy status by diploidization through time, i.e. gene duplicates can be eliminated randomly or because their expression has negative effects (Murat *et al.*, 2014). For example, the expression of all gene duplicates might imbalance the stoichiometric ratio needed to correctly form protein complexes (i.e. dosage balance hypothesis). This accounts for SSD, but may be true for WGD if the proteins interact with organelle-encoded proteins (de Smet *et al.*, 2013). Furthermore, a duplicated gene that encodes for a subunit of a protein complex might acquire mutations resulting in an inactive protein unit that competes with the gene product of the intact copy. Because active and inactive subunits are both involved in the formation of the protein complex this lowers the actual amount of active protein complexes (i.e. dominant negative effect hypothesis; de Smet *et al.*, 2013). Additionally, the acquisition of mutations in one copy might result in a functionless or unexpressed gene duplicate (i.e. pseudogene). In Triticeae, it was suggested that pseudogenes occur at a low frequency of 0.7-1%, as they are quickly excluded from the genome (Mayer *et al.*, 2014). In contrast, duplicated genes can be maintained if they adopt novel functions (neofunctionalization) or if the ancestral gene function is divided between the different copies (subfunctionalization; e.g. Moore & Purugganan, 2003; Murat *et al.*, 2014). Functional diploidization is assumed to occur within 50 million years after WGD (Pont *et al.*, 2011) and can be considered complete in diploid Triticeae, since grasses encountered the last WGD approximately 65 Ma. The existence of multi-copy loci in most taxa under study can pinpoint to old gene duplications due to WGD or SSD followed by neo- or subfunctionalization before diversification of Triticeae. It is assumed that SSD constantly occur in a genome, but most duplicates get rapidly removed, so that at any time there are many recent SSD and a few old ones (Vanneste *et al.*, 2013). This can explain why in this study ~75% of the captured loci show a paralogous signal in at least one diploid Triticeae genus. SSD are assumed to result in 300-500 duplicated genes per 10 million years per species (de Smet *et al.*, 2013). However, it is possible that this number is even higher in taxa with large genomes and a high amount of repetitive elements, which could favour gene duplications due to recombination. Between 20-30% of genes were found to have paralogues on every chromosome arm in *Triticum aestivum* (Mayer *et al.*, 2014).

Gene or genome duplications and neofunctionalization have been repeatedly suggested to play an important role in the development of evolutionary key innovations for adaptation, coevolution, and origins of biodiversity (e.g. de Smet *et al.*, 2013; Edger *et*

al., 2015). Neofunctionalization is intensively studied in the domestication related genes of crops (Purugganan & Fuller, 2009; Wang *et al.*, 2012; Renny-Byfield & Wendel, 2014). Several studies focused on the role of certain genes and their origin particularly in Triticeae (e.g. Simons *et al.*, 2006; Sakuma *et al.*, 2009, 2011; Madsen *et al.*, 2013; Pourkheirandish *et al.*, 2015). Barley, for instance, is morphologically characterized by inflorescences having three spikelets at each rachis node. Wild barley (*Hordeum vulgare* subsp. *spontaneum*) is two-rowed meaning, the central spikelet is fertile while the two lateral ones are sterile. In cultivated barley (*Hordeum vulgare* subsp. *vulgare*) the *Vrs1* gene that evolved via gene duplication from its ancestral gene *HvHox2* encodes a homeodomain-leucine zipper transcription factor and its expression results in a six-rowed spike, which produces three-times more seeds than wild barley and hence was domesticated by earlier farmers (Sakuma *et al.*, 2009, 2011). Also the development of a non-brittle rachis is the result of neofunctionalization after duplication of the two genes *Btr1* and *Btr2*. Two independent deletions have been identified to be responsible for cell-wall thickening at rachis nodes, which prevent the spike from disarticulating at maturity. Non-disarticulating spikes allow for an efficient harvesting. Therefore, early farmers selected for seeds carrying this trait (Pourkheirandish *et al.*, 2015).

Among others, these two cases of genetic modifications were established in a short time frame of approximately 12,000 years since the beginning of barley domestication. This suggests that genetic variants may be generated at a high frequency and can be rapidly fixed under certain conditions.

4.4 Phylogenetic relationships among diploid Triticeae

Phylogenetic analyses were conducted for nuclear low-copy number loci that were quality-filtered according to alignment length, proportions of missing data and phylogenetic informativeness. Selected loci were further divided into different datasets according to their chromosomal locations in genetic maps of barley, wheat and rye. The nrDNA region and the whole chloroplast genome were additionally used to obtain independent phylogenetic hypotheses from molecular markers having a different mode of evolution. There are several evolutionary reasons why gene trees can differ from the species tree (gene flow, ILS, differential gene duplication/loss and/or selection pressures). Additionally, a multitude of phylogenetic inference methods with different benefits and shortcomings exist. Therefore, several complementing phylogenetic approaches were used. Methods were employed that can make use of multiple genes and thereby do not consider any particular reasons for gene tree conflict (supermatrix and phylogenetic networks) as well as methods that explicitly consider ILS as the only reason for gene tree conflicts (short-cut coalescence methods and a Bayesian coalescence analysis). The comparison of phylogenetic results from this study to earlier ones is severely hampered, because of differences in study design and taxon sampling. Thus, in the following the discussion and comparisons to other works will be focused on selected phylogenetic groupings.

4.4.1 Main topological groupings

The results from all phylogenetic analyses of this study revealed strong incongruences for the individual loci as well as for the different multilocus datasets. Most species (depending on the taxonomic treatment) and/or all genera generally appear monophyletic. However, the relative relationships among these taxa considerably change between the analysed loci and analysis methods. The results of this study show an overall agreement that *Psathyrostachys* and *Hordeum* represent the earliest splits within the tribe. This is in agreement with many earlier studies of nuclear and plastid makers (e.g. Petersen & Seberg, 1997; Mason-Gamer *et al.*, 2002; Mason-Gamer, 2013; Bieniek *et al.*, 2014) and for nrDNA (Hsiao *et al.*, 1995). However, it is in conflict to other works (e.g. Mason-Gamer, 2005), although most single-markers analyses lack support on the backbone of the phylogeny (Petersen & Seberg, 2002; Petersen *et al.*, 2006). Escobar *et al.* (2011) published the most comprehensive molecular dataset to date, which also revealed the early divergence of *Psathyrostachys* and *Hordeum*. For the other taxa Escobar *et al.* (2011) divided the tribe into clades of taxa evolving either in a bifurcated or in a reticulated manner. My study returned net-like relationships, as indicated by the high number of considerably different topologies and reticulations in phylogenetic networks together with often poorly supported nodes, for all taxa but *Psathyrostachys* and *Hordeum*. The genera *Eremopyrum* and *Agropyron*, *Australopyrum*, *Dasyphyrum*, *Heteranthelium*, *Henrardia*, *Pseudoroegneria*, *Secale* and *Thinopyrum* occur at constantly changing positions in the central part of the phylogenies. However, there were indications that *Secale* and *Thinopyrum* separated later from this group of taxa. In agreement to Escobar *et al.* (2011) *Taeniatherum* is undoubtedly closely related to the *Aegilops-Triticum-Amblyopyrum* complex that was the latest to diverge. While dating for some nodes does exist, they are in strong conflict between published studies: Middleton *et al.* (2014) suggested the split between rye and wheat to have occurred *circa* 3-4 Ma, while Marcussen *et al.* (2014) estimated an age of *circa* 6.55 Ma for the *Aegilops-Triticum-Amblyopyrum* complex.

4.4.2 The evolution of *Australopyrum* and its implications

The **W**-genome species *Australopyrum* and several allopolyploid taxa (*Stenostachys* - **HW**, *Anthosachne* - **StYW**, *Connorochloa* - **StYHW**) are endemic to Australasia (Barkworth & Jacobs, 2011). This indicates speciation in allopatry after long-distance dispersal of an *Australopyrum* progenitor and a likely recurrent formation of allopolyploid taxa involving numerous other Triticeae species in Australasia. The formation of allopolyploid **W**-genome species might have happened either after long-distance dispersal of diploid taxa (i.e. taxa having the **H** genome from *Hordeum*, the **St** genome from *Pseudoroegneria* and the **Y** genome, which is of unknown origin) and/or of allopolyploid taxa (i.e. *Elymus* taxa with **StH** and/or **StYH** genomes) to Australasia. The chloroplast phylogeny indicates a common maternal ancestor for *Australopyrum*, *Eremopyrum*, *Agropyron* and *Henrardia*. In the tribe-wide phylogeny *Australopyrum* shows a reticulate origin with these and other taxa grouping in the central part of the topology (i.e. also with *Heteranthelium* and *Dasyphyrum*). Although these taxa have overlapping distribution areas in southern Europe and western Asia, due to the great

geographical distances, on-going gene flow can be excluded as a reason for reticulate phylogenetic signals. This may indicate ILS and/or hybridization events, which generally date back to the origin of these species, rather than to contemporary gene flow.

4.4.3 *Eremopyrum* and *Agropyron*

The sister species relationship between *Agropyron cristatum* and *Eremopyrum triticeum* was revealed from all phylogenetic analyses of this study. There were no indications of reticulations between either taxa. Morphologically they are very similar (Frederiksen, 1991) but can be distinguished, among others, by the veins of the lemma being confluent towards the apex or not (Löve, 1984). Nevertheless, both taxa differ in their life cycle and mode of pollination. *Agropyron cristatum* is outcrossing and perennial, while *Eremopyrum triticeum* is selfing and annual (Löve, 1984; Escobar *et al.*, 2010). This may efficiently prevent gene flow between them despite an overlapping distribution area in Central Asia. A sister relationship between species of *Agropyron* and *Eremopyrum* has also been proposed by other studies; although, when *Eremopyrum bonaepartis* was included, *Eremopyrum* became polyphyletic (Mason-Gamer & Kellogg, 2000; Mason-Gamer, 2005; Escobar *et al.*, 2011). *Eremopyrum bonaepartis*, a taxon not included in the present work, is known to occur at the di- and tetraploid level and different cytotypes were suggested to have different genomes (Sakamoto, 1974; Frederiksen, 1991). Thus, the clarification of relationships in *Eremopyrum* requires a more comprehensive sampling at the infrageneric level and the inclusion of polyploid accessions.

4.4.4 *Pseudoroegneria*

In the scope of this study the **St**-genome *Pseudoroegneria* appeared monophyletic, except for ribosomal data. The monophyly at the diploid level was also revealed in earlier studies (Yu *et al.*, 2008; Escobar *et al.*, 2011). Hsiao *et al.* (1995) retrieved monophyly based on ITS sequence data of two *Pseudoroegneria* species. However, the infrageneric taxon sampling of Hsiao *et al.* (1995) and the present work are only overlapping in respect to *Pseudoroegneria tauri*. Thus, both studies are not in conflict on this point. In the present work *Pseudoroegneria* is involved in the only strongly supported incongruence between the centromeric and telomeric datasets in coalescent-based analyses. The telomeric datasets, which is potentially more affected by gene flow, returns a grouping of *Pseudoroegneria*, which is closer to *Hordeum*. It was independently suggested that species of *Pseudoroegneria* were possibly shaped by introgressive events involving **H**-genome species (Mason-Gamer & Kellogg, 2000; Escobar *et al.*, 2011). Polyploids have been reported to act as bridges for gene flow between diploids in *Aegilops* (e.g. Kimber & Feldman, 1987; Kellogg *et al.*, 1996). Therefore, it has been hypothesized that the *Elymus* taxa act as passages for genes between diploid **St**- and **H**-genome species (Mason-Gamer & Kellogg, 2000). The hypothesis is reinforced by the fact that species of *Pseudoroegneria* together with species of *Hordeum* form allopolyploid species of the genus *Elymus*. Genome size measurements revealed that di- and tetraploid *Pseudoroegneria* accessions were initially selected for my study, but only diploids were finally included in phylogenetic

analyses. In contrast, other studies that reported *Pseudoroegneria* to be polyphyletic (Mason-Gamer & Kellogg, 2000) did not account for different ploidy levels within species. Especially tetraploid *Pseudoroegneria* taxa, although monogenomic, may be (partially) introgressed and therefore led *Pseudoroegneria* to appear polyphyletic in studies combining di- and tetraploids. A comprehensive sampling including di- and polyploids taxa is required to systematically test for reticulate relationships among such taxa.

4.4.5 *Secale*

The genus *Secale* harbours only diploid taxa. Several considerably different taxonomic treatments exist that vary in the number of species and subspecific entities recognized. The most recent taxonomic treatment (Frederiksen & Petersen, 1998) described three species: *S. sylvestre*, *S. strictum* and *S. cereale*. A conspecific treatment of *S. cereale* and *S. vavilovii* was based on an extensive survey of herbarium material. Also in the present work both taxa could not be distinguished genetically. Monophyly of the genus was reported repeatedly (e.g. Hsiao *et al.*, 1995; Mason-Gamer *et al.*, 2002; Petersen *et al.*, 2004) and is in agreement with findings of this study. In respect to the placement of the genus in the tribe-wide phylogeny “virtually all genera of the Triticeae have been suggested – either alone or in combination with other genera – as the sister group to *Secale*” (Petersen *et al.*, 2004). *Secale* seems only little involved in reticulations. Observed network-like structures point to the MRCA of the genus, which may have acquired strong chromosomal rearrangements compared to other Triticeae genomes. Such rearrangements have been found in *S. cereale* (Martis *et al.*, 2013) and may hamper the pairing of homoeologous chromosomes during meiosis in intergeneric hybrids and, hence, represent a barrier against gene flow. The phylogenetic relationships on the infrageneric level are still poorly understood. The results of this study show a tendency that *S. strictum* is somewhat different from *S. cereale*. Also Petersen *et al.* (2004) reported “an increased amount of evidence that *S. cereale* and *S. strictum* are not exclusive lineages”. This points to a rather recent age for these species supported by the fact that the same chloroplast sequence type is shared by all species of *Secale* included in this study. For a conclusive infrageneric taxonomic treatment *S. sylvestre* needs to be included in future investigations. *Secale sylvestre* was suggested to have diverged earliest from other *Secale* species (de Bustos & Jouve, 2002). However, its position was uncertain in Petersen *et al.* (2004).

4.4.6 *Thinopyrum*

The genus *Thinopyrum* circumscribes 12-15 perennial taxa with varying ploidy levels and genome combinations (<http://herbarium.usu.edu/triticeae/thinopyrum.htm>). Two species described as diploid, *Thinopyrum bessarabicum* and *Thinopyrum elongatum* (Jauhar, 1990), were selected for this study. The genome size of the genebank accessions revealed that they are actually polyploid. However, since *Thinopyrum* is the only taxon that carries the basic **E** genome the accessions were kept for phylogenetic inferences. The chloroplast phylogeny suggests *Pseudoroegneria* to be its maternal

parent, a result congruent with previous studies (Mahelka *et al.*, 2011; Petersen *et al.*, 2011; Mason-Gamer, 2013). Chloroplast capture was also reported in other plant groups (e.g. Bänfer *et al.*, 2006; Stegemann *et al.*, 2012). *Pseudoroegneria* and *Thinopyrum* have currently overlapping distribution areas in the Caucasian region. However, all other analyses revealed both taxa to be distinct. *Thinopyrum* often groups between *Secale* and *Taeniatherum* and the *Aegilops-Triticum-Amblyopyrum* complex. A close relationship to the *Aegilops-Triticum-Amblyopyrum* group has already been reported (Hsiao *et al.*, 1995; Petersen & Seberg, 2002; Mason-Gamer, 2005; Petersen *et al.*, 2011).

4.4.7 The *Aegilops-Triticum-Amblyopyrum* complex

It is well known that the species of *Triticum*, *Aegilops* and *Amblyopyrum muticum* are closely related and of rather recent origin (e.g. Petersen & Seberg, 1997; Petersen *et al.*, 2006; Escobar *et al.*, 2011; Marcussen *et al.*, 2014). The species divergence time of this species complex dates back to approximately 6.55 Ma (Marcussen *et al.*, 2014). To date, there is no general agreement how taxa within this species complex are related to each other, even at the diploid level. There is an on-going dispute if *Aegilops* and *Triticum* should be merged into one genus, and if *Amblyopyrum muticum* should be included into *Aegilops* (Kilian *et al.*, 2011; Li *et al.*, 2015a,b; Sandve *et al.*, 2015). Additionally to the analyses performed on a tribe-wide species set, a reduced dataset was created to analyse the *Aegilops-Triticum-Amblyopyrum* complex in particular and to obtain a calibrated species tree by a Bayesian coalescence analysis. Due to large computational requirements “only” 28 telomeric loci, four from each chromosome, were selected and analysed together. The obtained species tree is fundamentally different from the one in Marcussen *et al.* (2014) that is based on six genes for the same set of taxa as in this study. However, in the present work the obtained Bayesian coalescence tree is supported by all other phylogenetic analyses, as it shows the same well-supported nodes. Poorly supported nodes match uncertainties or reticulate signals of other analyses and are also visible in the superimposed representations of the species trees sets obtained from the multispecies coalescence analyses. The result of this analysis depicts a high extent of ambiguous signal especially at the backbone of the phylogeny. Selected taxa and relationships will be discussed in detail in below.

4.4.7.1 *Amblyopyrum*, *Aegilops speltoides* and the section *Sitopsis*

Based on nuclear data *Amblyopyrum muticum* appears to be the most distinct taxon from the *Aegilops* and *Triticum* species. In agreement with Bordbar *et al.* (2011), the chloroplast phylogeny revealed that *Amblyopyrum muticum* possesses a chloroplast genome similar to *Ae. markgrafii* (C genome), *Ae. comosa* (M), *Ae. uniaristata* (N), and *Ae. umbellulata* (U). Additionally, *Amblyopyrum muticum* has an overlapping distribution area with these species in central Turkey and Armenia. This might be explained by the existence of a common ancestor and therefore a shared chloroplast genome before divergence. Alternatively, because *Amblyopyrum muticum* is outcrossing, while the other species are selfing, it may indicate that it captured the chloroplast from one of these species or their MRCA.

Based on nuclear and chloroplast data and supported by the findings of, among others, Petersen *et al.* (2006) and Li *et al.* (2015), *Ae. speltoides* appears to be the species that diverged earliest from all other *Aegilops* species approximately 6 Ma. The Bayesian coalescence analysis was the only method that returned the *Aegilops* section *Sitopsis* to be monophyletic. However, the chloroplast data indicated that the section was polyphyletic. In contrast, the other species of *Sitopsis* (i.e. *Ae. searsii*, *Ae. bicornis*, *Ae. longissima*, *Ae. sharonensis*) always appeared monophyletic.

The superimposed set of species trees indicates some contradicting signal in the nuclear data for *Amblyopyrum muticum*, but strong conflicting signal for *Ae. speltoides* that can be an indicator of ILS and/or hybridization. Hybrid signals from early diverged outcrossers including *Amblyopyrum muticum* or *Ae. speltoides* may indicate a higher capability of these species to introgress. Moreover, it was suggested that frequent occurrence of intraspecific gene flow, which may be stronger for outcrossers, might prevent the permanent incorporation of interspecific introgressions into the genome (Petit & Excoffier, 2009). This could have led to a faster differentiation and reproductive isolation of these species compared to others.

4.4.7.2 *Triticum* and its relationships to *Aegilops*

In this work, the position of the genus *Triticum* s.str. inside the *Aegilops-Triticum-Amblyopyrum* complex is uncertain. Yet all analyses concur in that the diploid *Triticum* species are monophyletic. *T. boeoticum* and *T. monococcum*, two taxa given species rank by Dorofeev *et al.* (1979) could not be distinguished genetically, which supports the subsumed treatment by van Slageren (1994) as *T. monococcum*. Both taxa together appear in a sister relationships with *T. urartu*. Species divergence time estimates suggest that the MRCA of *Triticum* occurred approximately 6 Ma, while *T. monococcum/boeoticum* and *T. urartu* diverged about 2.5 Ma. In contrast, the ages proposed for species divergence by Middleton *et al.* (2014) differ by approximately 2 Ma (i.e. the estimates of divergence are *T. boeoticum/T. urartu*: 0.57 Ma; *T. boeoticum/T. monococcum*: 0.29 Ma). Middleton *et al.* (2014) performed the dating on chloroplast data under the assumption that chloroplast divergence may predate the species divergence. Based on the low mutation rates of chloroplast genomes in plants (e.g. Smith, 2015) and the chloroplast phylogeny obtained in this study, I consider the opposite more likely, i.e. the divergence of a chloroplast lineage after species separation. Finally, the genus *Triticum* does not appear to be genetically more distinct from *Aegilops*, than, for example, *Ae. speltoides* is different from all other *Aegilops* species. This supports taxonomic treatments that favour the unification of *Aegilops* and *Triticum* within the same genus.

4.4.7.3 *Aegilops tauschii* and species involved in its formation

Aegilops tauschii carries a **D** genome and is the species that shows the strongest hybrid signal in the genomic data. A homoploid hybrid origin of the **D**-genome lineage was suggested earlier and is the subject of a recent dispute (Marcussen *et al.*, 2014; Li *et al.*, 2015a,b; Sandve *et al.*, 2015). Although recent publications agree that the recognition of hybridization events highly depends on the taxon sampling, so far all postulated hypotheses are based on a limited choice of taxa. For example, Marcussen *et al.* (2014) suggested that a hybridization event approximately 5.5 Ma between **A**- and **B**-genome lineages gave rise to the **D**-genome lineage, in a study that strongly focused on the wild wheat progenitors *Triticum urartu* (**A**) and *Ae. speltoides* (**B**). The fact that the **D**-genome chloroplast is more closely related to all other *Aegilops* than to **A**- and **B**-genome lineages violates this hypothesis (Li *et al.*, 2015a). In the present study *Ae. tauschii* also appears to be of hybrid origin at *circa* 5.5 Ma, though the MRCA of *Ae. uniaristata*/*Ae. comosa*, *Ae. markgrafii* and *Ae. umbellulata* were involved in its formation. The phylogenetic networks based on different datasets result in a varying amount of reticulations involving also other *Aegilops* species (i.e. the MRCA of the section *Sitopsis* without *Ae. speltoides*) that may point to ILS rather than to a hybrid signal. *Aegilops tauschii* has a current distribution distinct from other diploid *Aegilops* with its centre along the southern coastline of the Caspian Sea and Azerbaijan (Kilian *et al.*, 2011). Hence, only limited, if any, on-going gene flow is to be expected.

The descendants of species likely involved in the hybrid origin of *Ae. tauschii*, formed well-supported sister species relationships and diverged more recently (approximately 2.5-4.5 Ma). The low amounts of ambiguous signal argues for speciations with strongly limited gene flow, possibly starting from a small isolated and genetically differentiated founding population resulting in low amounts of ILS. The sister species relationship of *Ae. comosa* and *Ae. uniaristata* confirms their traditional unification in the section *Comopyrum* (Kilian *et al.*, 2011). The sister grouping of *Ae. markgrafii* and *Ae. umbellulata* was (partially) also retrieved in other studies (Dvořák & Zhang, 1992; Petersen *et al.*, 2006). Based on morphological and genomic data these two species were placed in different sections (*Aegilops* and *Cylindropyrum*; Kilian *et al.*, 2011).

5 CONCLUSIONS

The aim of this project was to obtain a deeper understanding of evolutionary relationships among diploid members of the grass tribe Triticeae. A hybridization-based enrichment approach coupled with next-generation sequencing was developed to retrieve phylogenetic information from several hundred low-copy number loci from a comprehensive set of Triticeae taxa. Different partitions of loci and analysis procedures were used to assess if more molecular phylogenetic information can contribute to a clarified picture of phylogenetic relationships between Triticeae. This knowledge could then be used to make future classificatory decisions that in turn reduce recent taxonomic confusion within the tribe, e.g. if the genera *Aegilops* and *Triticum*, or *Amblyopyrum* and *Aegilops*, respectively, should be treated separately or unified under the same taxon. The present work provides the most comprehensive molecular dataset of the tribe available to date and provides new insights in the taxonomically and evolutionary complex Triticeae.

5.1 Hybridization-based enrichment approach for Triticeae

The design of sequence capture probes established in the scope of this project was based on exonic sequences of fl-cDNA from two relatively distantly related Triticeae species (i.e. *Hordeum vulgare* and *Triticum aestivum*) and *Brachypodium distachyon* as outgroup taxon. The probe design successfully retrieved sequence information from the target loci for all monogenomic Triticeae and outgroups included in the study. A shearing of genomic DNA into longer fragments than recommended by the manufacturer resulted

in more phylogenetically informative sequences, as in addition to the exons considered in bait design adjacent intron information could be assembled as well. Despite some fluctuations in the capture performance and a relatively low rate of reads mapping on-target, 95% of the initially selected loci could be assembled. An increase in sequencing coverage could accommodate for less successful sequence capture library preparations. Moreover, the access to a large set of barcodes allowed an efficient sequencing of several hundred samples simultaneously on the same Illumina flow cell. Although this approach is able to retrieve sequence information from several different taxa and loci with the same set of baits, their design and the assembly of the large amount of sequence data requires advanced bioinformatic knowledge that constitute a challenge to the final implementation of this method. The current assembly pipeline represents a compromise: It was used to assemble several hundred phylogenetic informative loci automatically, but was not, for example, able to disentangle paralogous gene copies.

Although the costs for high-throughput sequencing techniques are constantly dropping while the read length increases, due to the large genome sizes and the high repeat content that amounts to approximately 80% in Triticeae (e.g. Mayer *et al.*, 2012, 2014; Middleton *et al.*, 2013), sequencing the whole genome of many Triticeae species and several accessions per species will persist to be an obstacle in the near future. Single molecule sequencing technologies that are able to generate long sequence reads still have a lower sequencing throughput and a higher error rate (e.g. SMRT from Pacific Biosciences, MinION from Oxford Nanopore Technologies) compared to technologies of the second-generation (e.g. Illumina). Therefore, a high coverage is needed to level out sequencing errors, which in turn results in higher costs to sequence several large-genome Triticeae. To date, (draft) genome sequences have been published for the economically important representatives barley, wheat and rye and a few closely related species. The generation of the genomic sequences were based on flow sorting of chromosomes and/or whole genome shotgun sequencing (Mayer *et al.*, 2012, 2014; Jia *et al.*, 2013; Ling *et al.*, 2013), or involved the development of mapping populations (Martis *et al.*, 2013; Mascher *et al.*, 2013; Chapman *et al.*, 2015). In any case, large conglomerates of scientists were needed to establish the genome assemblies. Moreover, robust phylogenetic inferences rely on sequence information from several accessions per species. Due to the challenges related to Triticeae genome sequencing, a hybridization-based enrichment approach will remain the best strategy to obtain phylogenetically relevant sequence information of large genomic fractions from numerous Triticeae taxa and several accessions per species in the near future.

5.2 Markers and methods for phylogenetic inferences

Phylogenetic analyses were conducted for nuclear low-copy number loci aiming at an even distribution over the seven chromosomes of the Triticeae genomes. The loci were analysed individually and divided into different datasets according to their chromosomal locations in the genetic maps of barley, wheat and rye. Furthermore, the nrDNA tandem-repeat region and the whole chloroplast genome were assembled to obtain independent phylogenetic hypotheses. Several phylogenetic inference methods were applied to account for biological or analytical causes for conflicting tree topologies.

However, none of the marker(s) and approaches returned a clearly resolved phylogeny for Triticeae. Not even two individual gene tree topologies were congruent with each other. Additionally, the methods that integrated information from multiple loci, as well as the nrDNA region and the whole chloroplast genome analysis retrieved unique topologies. The nrDNA region did not provide more information than a single nuclear low-copy number locus. Although bi-parentally inherited, one of the parental copies will be randomly homogenized through time (Álvarez & Wendel, 2003). In contrast, the whole chloroplast genome data provides additional evidence for the interpretation of phylogenies, since it points to the maternal lineage of a species (Sang, 2002). In the present work it provided indications of shared ancestry (i.e. *Australopyrum*, *Eremopyrum*, *Henrardia*, etc.), ancient hybridization events (i.e. *Amblyopyrum*) or the misled hypotheses about hybridizations (of e.g. *Aegilops tauschii*; Li *et al.*, 2015a). Single markers can have different evolutionary histories and provide only little insight into species relationships. Thus, there is consensus that the use of multiple nuclear coding single- or low-copy number genes is a good strategy for species tree reconstructions (Maddison, 1997; Sang, 2002; Degnan & Rosenberg, 2009). However, the best choice and number of loci required to arrive at a robust phylogeny is still under debate. Some authors recommend choosing loci by means of phylogenetic informativeness (e.g. Gatesy & Springer, 2013, 2014; Salichos & Rokas, 2013), while others advocate the selection of loci in respect to clock-likeness and/or inference-based measures of model violation to return more robust phylogenetic results (Doyle *et al.*, 2015). Additionally, it was argued that the inclusion of more loci improves the accuracy of certain phylogenetic methods. For example, short-cut coalescence methods have been found to be more robust to gene tree estimation error or recombination if more loci are included (Xi *et al.*, 2015; Mirarab & Warnow, 2015). However, by adding more loci the stochastic error can be reduced but in turn the systematic error might be increased. Therefore, the consideration of more data might not be sufficient to solve difficult phylogenetic questions (Philippe *et al.*, 2011; Doyle *et al.*, 2015).

Here I considered only loci that passed a certain threshold of minimal phylogenetic informativeness and made use of their putative chromosomal locations. Significantly lower tree conflict was observed in centromeric compared to telomeric regions. I assume that this is best explained by linkage disequilibrium for centromeric loci and the reduced neutral variability at these linked sites (see also Charlesworth *et al.*, 1993; Nater *et al.*, 2015). Although telomeric loci are potentially more affected by recombination, they more likely provide several autonomous hypotheses for species tree estimations. Additionally, it was suggested that a high rate of intra-specific recombination prevents the permanent fixation of interspecific introgressions (Petit & Excoffier, 2009) and, hence, is superior for species tree inferences. Nevertheless, the comparison of centromeric and telomeric datasets resulted in only one supported topological conflict in multilocus analyses for the Triticeae taxa under study (i.e. the placement of the genera *Agropyron* and *Pseudoroegneria* swapped in coalescent-based analyses). This shows that centromeric loci can also be used as a proxy for species tree relationships. However, multispecies coalescence methods assume free recombination between loci (Heled & Drummond, 2010; Liu *et al.*, 2015). Thus, the linked nature of centromeric loci may mislead attempts of species tree inference and divergence time estimations based on these loci.

To analyse the relationships of the often-debated *Aegilops-Triticum-Amblyopyrum* complex, a Bayesian multispecies coalescence analysis was performed on 28 telomeric loci for these taxa. In the present work, the results are in agreement among all analyses integrating different combination of low-copy number loci. The same taxa are subject to topological changes and/or have poorly supported nodes. In comparison to a recently published Bayesian coalescence species tree based on the same set of taxa and six genes (Marcussen *et al.*, 2014), the species tree obtained in this work resulted in a largely different phylogeny but with generally higher support values. The large congruence among all performed phylogenetic analyses of this work, the agreement with groupings from earlier studies and the current distribution areas of the taxa (Kilian *et al.* 2011) indicates that the use of the 28 telomeric loci returned a reliable species tree hypothesis for the *Aegilops-Triticum-Amblyopyrum* complex. Moreover, the Bayesian coalescence analysis was especially suitable to illustrate the origins of conflicting signal and, additionally, provided age estimates for the species divergences. Thus, a similar coalescence analysis for the other, earlier diverged, Triticeae taxa can be useful to gain deeper understanding of the speciation events that shaped the tribe. Yet, the minimum and/or maximum number of telomeric loci necessary to arrive at a robust phylogeny still needs to be explored.

Independent of the method used, the frequently found incongruences between tree topologies suggest a species radiation accompanied with ILS and/or introgressive events. However, it is not possible to assess the degree of both biological processes and to distinguish between them. There are analysis tools that claim to be able to disentangle both mechanisms. They are based on the assumption that the split of alleles involved in ILS always predates the speciation event while hybridization may occur before and/or after speciation. Hence, the minimum genetic distances of genes should be smaller for some hybridization events than for ILS. However, this requires making strong assumptions of population sizes and divergences times (Joly, 2012), data that is not available for Triticeae. Another reasons for gene tree conflict is the sampling of paralogues. The selection of only low-copy number loci does not eliminate the chance of orthologue misidentification. Different copies may have been restored to a single-copy status after duplication in different taxa as the result of drift or selection. Yet, the establishment of a phasing strategy for multi-copy loci would allow the application of tools that can infer species trees from the data of whole gene families for which orthologues do not need to be identified. Also, since paralogues can be included, such tools make use of more data and may result in better-resolved phylogenies.

5.3 Phylogenetic relationships among diploid Triticeae

5.3.1 The main clades and their estimated ages

The MRCA of the tribe probably occurred approximately 15 Ma (Marcussen *et al.*, 2014). In agreement with earlier findings (e.g. Hsiao *et al.*, 1995; Escobar *et al.*, 2011), also in my analyses the genera *Psathyrostachys* and *Hordeum* appear well differentiated and diverged earliest from other taxa of the tribe. In this study, all other taxa show indications of reticulations. There are two agglomerates of poorly supported nodes and/or net-like

structures in the tribe-wide phylogeny. These phylogenetic uncertainties can be indicators of two independent rapid species radiation events that were accompanied by strong incomplete lineage sorting and/or homoploid hybrid speciation. The older one involved all species but *Psathyrostachys* and *Hordeum* and probably took place between 10-7 Ma, since the MRCA of *Hordeum* occurred approximately 9.2 Ma (Brassac & Blattner, 2015). The second radiation event encompasses the more recently diverged *Aegilops-Triticum-Amblyopyrum* complex. It can be assumed to have taken place approximately 6.55 Ma (Marcussen *et al.*, 2014).

The two consolidations of uncertain nodes can be assumed to depict historic events as species and/or genera are genetically well differentiated from other taxa, which is indicated by the formation of monophyletic groups. Thus, recent gene flow could be identified by the formation of polyphyletic clades. Additionally, the species showed species-specific genome sizes and nrDNA sequence types. Two cases of chloroplast capture (i.e. for *Thinopyrum* and *Amblyopyrum*) were reported that indicate either common ancestry or hybridization events. Species that diverged after the first radiation event have their own chloroplast type, while the chloroplast genomes of the *Aegilops-Triticum-Amblyopyrum* complex are less well differentiated, which is due to a shorter time for diversification since species separation. The *Aegilops-Triticum-Amblyopyrum* complex appears monophyletic for all multilocus analyses. Sister species relationships of more recently diverged lineages are less affected by reticulate signal. This holds for *Agropyron cristatum* and *Eremopyrum triticeum*, but also for several relationships within the *Aegilops-Triticum-Amblyopyrum* complex: *Ae. markgrafii* and *Ae. umbellulata* (MRCA occurred approximately 4.5 Ma), *Ae. uniaristata* and *Ae. comosa*, *Ae. bicornis* and *Ae. longissima/sharonensis*, and *Triticum urartu* and *T. monococcum* (nearly simultaneous speciations *circa* 2.5 Ma).

The strongest signal of reticulate evolution was detected for *Aegilops tauschii*. A hybrid origin of this taxon was already inferred (Marcussen *et al.*, 2014; Li *et al.*, 2015a; Sandve *et al.*, 2015). Due to the comprehensive taxon sampling that covers all diploid *Aegilops* taxa, for the first time, the MRCA of *Ae. comosa* and *Ae. uniaristata* and the MRCA of *Ae. markgrafii* and *Ae. umbellulata* could be identified as putative taxa that gave rise to *Ae. tauschii* by homoploid hybrid speciation.

5.3.2 Possible scenarios of speciation in Triticeae

The evolution of the tribe Triticeae has been largely affected by ILS and/or hybridization events. It is currently not possible to distinguish between these processes or to assess the degree of their influence on the retrieved phylogenetic picture. However, species radiation started with an ancestral population in Eurasia, as this is the cradle of Triticeae (Hsiao *et al.*, 1999). Also the beginning of species diversification of the old genus *Hordeum* was proposed to have taken place in southwest Asia (Blattner, 2006). Despite possible range shifts in the past, this is also supported by the current centre of distribution of the early-diverged genus *Psathyrostachys* in south and southwest Asia (eMonocot.org).

This ancestral pre-Triticeae population acquired a high allelic diversity over time, also as the result of a reduced intraspecific gene exchange with an increase in geographical

distance between members of the populations due to range expansions (isolation by distance; Wright, 1943). From this point, different scenarios can be imagined to have triggered species radiations of Triticeae, none of which are mutually exclusive. Long-distance dispersal of lineages that exposes them to new habitats and climates has been repeatedly shown to be the cause for species radiation (Juan *et al.*, 2000; Winkworth *et al.*, 2005; Blattner, 2006; Baldwin & Wagner, 2010; Linder *et al.*, 2014). This best explains the origin of **W**-genome species, such as *Australopyrum*, that are endemic to Australasia. But long-distance dispersal likely also applies to other speciation events in Triticeae. Moreover, the ancestral Triticeae population likely also split into sub-populations that experienced reduced gene flow, for example, because of allopatry and parapatry (i.e. complete and partial geographic isolation), two mechanisms that are believed to play a key role in most speciation events (Coyne & Orr, 2004). Climatic oscillations, for example the increasing fluctuations in the global temperature that have occurred since the end of the Pliocene and Pleistocene (Lisiecki & Raymo, 2007), have led to geographical isolations of populations. This has repeatedly resulted in species diversification and the reinforcement of reproductive isolation between 4.5 and 2.5 Ma. Additionally, founding populations may have undergone genetic bottlenecks, which then resulted in low effective population sizes. This explains the strongly supported sister species relationships of the more recently diverged taxa, e.g. the ones in the *Aegilops-Triticum-Amblyopyrum* complex that are less affected by reticulate signal. Moreover, climatic changes not only altered ecological niches, but also species extinctions rates (Crisp & Cook, 2009; Linder *et al.*, 2014), that probably selected against intermediate hybrids with lower fitness. Also the intrusion of new genetic variability into an area that is already populated was suggested to enhance species diversifications (Wagner *et al.*, 2012; Linder *et al.*, 2014). For example two populations that diverged in allopatry can hybridize when coming back into contact, potentially creating new species. Alternatively, secondary contact of the populations might result in changing selection pressures and enhance the adaptation to different ecological niches (i.e. disruptive selection; Smith, 1962).

As indicated by the diverse pattern of duplicated genes (i.e. gene families), Triticeae genomes must be highly dynamic. This offers a great potential for lineages to quickly adapt to changing environmental conditions. The intense research of neo- and subfunctionalization of duplicated genes that play a role in domestication can be used to gain a deeper understanding for the evolution of wild Triticeae. Only few genes are supposed to play a role in plant domestication (e.g. Purugganan & Fuller, 2009). Among others, it was shown by Pourkheirandish *et al.* (2015), that small genetic changes that have been acquired independently in less than 12,000 years resulted in pronounced morphological changes. Additionally, domestication of crops was frequently found to be associated with the development of reproductive barriers between crop and progenitor species (Dempewolf *et al.*, 2012). Thus, reproductive barriers and morphological changes in Triticeae probably have been acquired rapidly by neo- and/or subfunctionalization of a few duplicated genes. This can explain the strong morphological differentiation between the species, despite a lack of pronounced interspecific genetic distinctions in DNA sequences of most low-copy number nuclear genes, which in turn results in uncertainties in phylogenetic inferences.

The results retrieved in the scope of this project provide the most comprehensive picture of phylogenetic relationships of Triticeae available at the moment. However, some taxa (e.g. taxa of the small monogenomic lineages with the basic genomes **K** and **G**) could not be accessed. Future phylogenetic studies can aim at the inclusion of these species for a more complete picture. Additionally, the establishment of divergence time estimates for more Triticeae taxa can result in a better understanding of the sequence of speciation events. At best, this can be done for subsets of my dataset comprising complete infrageneric taxon sets. Furthermore, it has been suggested that tetraploid taxa may act as a bridge for gene flow between diploid species (e.g. Kellogg *et al.*, 1996). Only a combined analysis of di- and polyploid Triticeae taxa can assess the frequency of these incidents.

5.4 Implications for taxonomic treatments

The taxonomic treatment of the grass tribe Triticeae is under long-standing debate. The reasons are multifaceted and include the complex mode of evolution of genera and species, due to recurrent hybridization among species resulting in many allopolyploids, and the taxonomic representation of such relationships. The high number of existing species and genera, their worldwide distribution in temperate regions, and their economic importance made them of interest to many taxonomists around the globe. Conceptual and methodological achievements in taxonomy as well as different opinions of taxonomists resulted in the existence of various different treatments and several correct scientific names for many taxa of Triticeae (e.g. Barkworth, 2000; Barkworth & Bothmer, 2009).

The new insights into the tribe's evolutionary history presented here, show that based on several independent nuclear molecular markers monogenomic taxa form monophyletic clades. This supports frequently used generic taxonomic treatments. However, taxonomic revisions often differ in the number of described genera and (sub)species. Treatments that are based on morphological distinctions and/or the basic genomes may tend to recognize more taxa at species rank. For example, Löve (1984) recognized 37 genera, 13 of which are treated as *Aegilops* by most taxonomists today. Dorofeev *et al.* (1979) recognized 27 *Triticum* species, while van Slageren (1994) accepted six. The large molecular phylogenetic dataset at hand supports several infrageneric taxonomic treatments that describe lower number of taxa at species rank: *Pseudoroegneria tauri* and *Pseudoroegneria libanotica*, *Secale cereale* and *Secale vavilovii*, *Taeniatherum caput-medusae* and *Taeniatherum crinitum* could not be genetically differentiated from each other in my analyses. There are already taxonomic treatments that unify these taxa under the same species name and acknowledge morphological dissimilarities under lower taxonomic ranks (for more information see [ww.ipni.org](http://www.ipni.org)). For more infrageneric recommendations the taxon sampling needs to be extended, e.g. a proper understanding of the genus *Secale* requires the inclusion of *S. sylvestre*. Moreover, the taxonomic decision-making will probably be more difficult when more taxa are included. In previous studies *Eremopyrum* turned out polyphyletic if *Eremopyrum bonaepartis*, a taxon containing both di- and tetraploid cytotypes, was incorporated (Mason-Gamer, 2005; Escobar *et al.*, 2011). Furthermore, the inclusion of monogenomic but tetraploid

Conclusions

accessions may return paraphyletic clades, as noticed for *Pseudoroegneria* (Mason-Gamer & Kellogg, 2000; Escobar *et al.*, 2011). Yet, there are taxonomists that suggest the general acceptance of paraphyletic taxa (e.g. Brummitt, 2006), as this reflects the course of evolutionary history.

Another source of conflict occurs when authors disagree if a certain taxon should be included into another. The *Aegilops-Triticum-Amblyopyrum* complex harbours several levels of this conflict. (1) It is a matter of on-going dispute if *Amblyopyrum muticum* should be included into *Aegilops* as *Aegilops mutica* (van Slageren, 1994; Kilian *et al.*, 2011). In the present work it appeared most distinct from all *Aegilops* and *Triticum* species, which would allow to place it in its own genus. However, the occurrence of an *Aegilops* chloroplast type contradicts a completely separate treatment. (2) A similar discussion was dealing with the inclusion of *Aegilops speltoides* into *Aegilops*, since it was independently shown to be most distinct from all other *Aegilops* and resulted in polyphyletic clades with respect to *Aegilops* (e.g. Yamane & Kawahara, 2005; Petersen *et al.*, 2006). The exclusion of *Aegilops speltoides* from the genus was considered, since this would make *Aegilops* monophyletic (Kilian *et al.*, 2011). In the scope of this study, the traditional section *Sitopsis* could be restored, which supports the placement of *Ae. speltoides* in *Aegilops*. (3) With respect to the genus *Triticum*, a consensus on its interpretation (i.e. keeping *Aegilops* and *Triticum* separate vs. their unification in one genus) is desirable. In sum, the findings of this study suggest that *Triticum* evolved from the same MRCA as all other species of *Aegilops*. This provides an argument for the congeneric treatment of both taxa, which would result in renaming of all *Aegilops* species into *Triticum*, as the latter was described first. Although an agreement on the congeneric status of *Aegilops* and *Triticum* would solve this nomenclatural problem, the separate generic status of *Aegilops* and *Triticum* s.str. can be favoured because of clear morphological distinctions and the long tradition in keeping the taxa separate (Barkworth & Bothmer, 2009). (4) The situation within *Triticum* s.str. is more complex, since two different taxonomic treatments are adopted in different parts of the world. The taxonomic system proposed by Dorofeev *et al.* (1979) is mainly used in Eastern countries, whereas Mac Key's (1977, 1989) or the revision by van Slageren (1994) are used in Western countries. A classificatory system in the tradition of van Slageren and Mac Key that reflects the progenitors of a taxon already in its name is both self-informative and easy to learn. In this study *Triticum boeoticum* and *Triticum monococcum*, two taxa given species rank by Dorofeev *et al.* (1979) as a result of a meticulous investigation of morphological features, could not be distinguished genetically, which supports the taxonomic treatment by van Slageren (1994). To avoid loss of information related to biodiversity and genetic resources, morphological distinctions can be made under lower taxonomic ranks, e.g. subspecies or varieties in case of wild taxa.

The classificatory systems that were proposed for *Triticum* exhibit a striking example for how different opinions of taxonomist can influence the naming of plants. Deciding on a taxonomic treatment is difficult; there are usually several reasons for one or another. When working with Triticeae, the main confusion stems from the large number of taxonomic names under use for the same taxon. Although long lists of synonymous names are provided on different websites (e.g. the National Plant Germplasm System of the US Department of Agriculture and eMonocot.org), the multitude of websites that favour different treatments adds to the confusion. However, a future classificatory

system for Triticeae can only decrease current confusion in the taxonomy, if it experiences general attention and acceptance by scientists working with these taxa. Therefore, one central database could provide an easily accessible repository for valid names. The establishment of such a database is not feasible for a single or few collaborating taxonomists. The literature that needs to be considered is at least partially difficult to access and written in different languages, such as Chinese, English, German, and Russian. Taxonomists working on Triticeae would be asked to share their knowledge by completing a database like the International Plant Name Index database (www.ipni.org). This would greatly facilitate the understanding of taxonomic changes made in the past and provide access to all available information regarding a given taxon.

ABSTRACT

The grass tribe Triticeae consists of about 360 species and several subspecies in approximately 20-30 genera. The tribe harbours the important cereals, bread wheat (*Triticum aestivum*), barley (*Hordeum vulgare*), rye (*Secale cereale*) and their wild relatives. The taxonomic treatment of the tribe is under long-standing debate. The reasons therefore are multifaceted and include the complex mode of evolution of genera and species, due to recurrent hybridization among species resulting in many allopolyploids, and the taxonomic representation of such relationships. The high number of existing genera and species, their worldwide distribution in temperate regions, and their economic importance made them of interest to taxonomists around the globe, many of them arriving at different opinions regarding nomenclature. Finally, conceptual and methodological achievements in taxonomy in combination with different opinions of taxonomists resulted in the existence of various different treatments and several correct scientific names for many taxa of Triticeae. For example, although a conclusive taxonomic treatment of the taxa *Aegilops*, *Amblyopyrum* and *Triticum* is of high interest, there is no satisfactory understanding of the evolutionary relationships among these taxa available yet. Thus, generic and infrageneric treatments, e.g. to include *Aegilops* into *Triticum* are often differently interpreted. An improved picture of the course of evolutionary history can represent the starting point for a stable taxonomic treatment of the tribe's members. In my dissertation I provide new insights into the evolutionary history of the diploid members of the tribe Triticeae, as these are the tribes basic units. In addition to investigations performed on a tribe-wide taxon set, I analyse phylogenetic relationships within the *Aegilops-Triticum-Amblyopyrum* complex in more detail.

A hybridization-based enrichment approach coupled with Illumina sequencing was developed that aimed at retrieving phylogenetic information from initially 451 single-copy loci with an even distribution over the Triticeae genomes. In total, the sequence capture was performed for 123 accessions. Several accessions of 35 Triticeae species, spanning 15 genera and two outgroup taxa were included in the study. For the vast majority of the selected loci sequence information could be retrieved. However, approximately 20% of the sequenced loci showed the existence of paralogues in most taxa and indicated structural distinctions between Triticeae genomes. Although not considered in the sequence capture design, the nuclear ribosomal DNA units and whole chloroplast genomes could also be recovered and were used to obtain independent phylogenetic hypotheses. Finally, 245 nuclear low-copy number loci were used for phylogenetic inferences. The loci were analysed individually and in multilocus datasets that encompassed loci according to their chromosomal locations. Traditional model-based, phylogenetic network, and coalescent-based methods were applied to account for biological and/or analytical causes of incongruences between gene trees.

The phylogenetic results showed that species and/or genera are generally monophyletic. In accord with earlier studies, the genera *Psathyrostachys* and *Hordeum* appear well differentiated and diverged earliest from other taxa of the tribe. The relative relationships among all remaining monophyletic groups considerably changed between analyses. These uncertain phylogenetic groupings depict rather historic events of incomplete lineage sorting and/or hybridization than recent gene flow and may be

explained by the highly dynamic nature of Triticeae genomes. As a result of gene and/or genome duplications Triticeae genomes hold a great potential for lineages to quickly develop reproductive barriers and/or morphological changes by neo- and/or subfunctionalization of a few duplicated genes.

On a tribe-wide basis, the phylogenetic results support those infrageneric taxonomic treatments that describe a lower number of taxa at species rank. Other main findings show that (1) *Amblyopyrum* is most distinct from all *Aegilops* and *Triticum* species. But, due to its possession of an *Aegilops* chloroplast type it cannot be treated completely separate. (2) The traditional *Aegilops* section *Sitopsis* could be restored, which supports the placement of *Aegilops speltoides* in *Aegilops*. (3) The congeneric treatment of *Aegilops* and *Triticum* is supported, since *Triticum* evolved from within the *Aegilops* clade. (4) The recently hypothesized hybrid origin of *Aegilops tauschii* could be confirmed. For the first time, the most recent common ancestor of *Aegilops comosa* and *Aegilops uniaristata* and of *Aegilops markgrafii* and *Aegilops umbellulata* could be identified as putative progenitors that gave rise to the *Aegilops tauschii* lineage approximately 5.5 million years ago (Ma). (5) Additionally, several speciation events occurred simultaneously between 4.5 and 2.5 Ma within *Aegilops-Triticum-Amblyopyrum* complex.

ZUSAMMENFASSUNG

Die Tribus Triticeae besteht aus etwa 360 Arten mit vielen Unterarten in ungefähr 20-30 Gattungen und umfasst die Getreidearten, Brotweizen (*Triticum aestivum*), Gerste (*Hordeum vulgare*) und Roggen (*Secale cereale*), sowie ihre wilden Verwandten. Die taxonomische Einteilung der Tribus unterliegt einer andauernden Debatte. Die Gründe dafür sind vielfältig und umfassen die komplexe Evolution der Gattungen und Arten. Dazu gehören zum Beispiel wiederholte Hybridisierungen zwischen Arten welche zur Entstehung vieler allopolyploider Taxa führten und die taxonomische Darstellung solcher Beziehungen. Die hohe Zahl der Gattungen und Arten, ihre weltweite Verbreitung in gemäßigten Regionen und ihrer wirtschaftlichen Bedeutung, machte sie interessant für Taxonomen auf der ganzen Welt, die unterschiedliche nomenklatorische Konzepte verwendeten. Schließlich führten sowohl konzeptionelle und methodische Errungenschaften in der Taxonomie, als auch unterschiedliche Meinungen von Taxonomen zum gleichzeitigen Bestehen von verschiedenen taxonomischen Einteilungen und mehreren richtigen wissenschaftlichen Namen für viele Taxa der Triticeae. Obwohl, beispielsweise, eine schlüssige taxonomische Einteilung der Taxa *Aegilops*, *Amblyopyrum* und *Triticum* von großem Interesse ist, gibt es bisher kein zufriedenstellendes Verständnis über die verwandtschaftlichen Beziehungen zwischen diesen. Daher sind generische und infragenerische Einteilungen, z.B. ob *Aegilops* und *Triticum* zu einer Gattung zusammengefasst werden sollten, oft verschieden. Ein verbessertes Verständnis über den Verlauf der Evolutionsgeschichte kann den Ausgangspunkt für eine solide taxonomische Behandlung von Angehörigen der Tribus darstellen. In meiner Dissertation liefere ich neue Einblicke in die Entwicklungsgeschichte der diploiden Mitglieder der Triticeae, welche die Grundeinheiten der Tribus darstellen. Zusätzlich zu Untersuchungen der Tribus als Ganzes, untersuche ich auch die phylogenetischen Beziehungen innerhalb des *Aegilops-Triticum-Amblyopyrum* Artkomplexes im Detail.

Es wurde ein Anreicherungs-Ansatz auf dem Prinzip der Hybridisierung und verbunden mit Illumina Sequenzierung entwickelt, um phylogenetische Informationen von zunächst 451 *single-copy* Loci, die gleichmäßig über die Triticeae Genome verteilt sind, zu erhalten. Insgesamt wurde die gezielte Anreicherung von DNA für 123 Akzessionen durchgeführt. Jeweils mehrere Akzessionen von 35 Triticeae Arten, die 15 Gattungen umfassen, und zwei Außengruppen wurden in der Studie berücksichtigt. Die Anreicherung war für die überwiegende Mehrheit der gewählten Loci erfolgreich. Etwa 20% der sequenzierten Loci zeigten das Vorliegen von Paralogen in den meisten Taxa was auf strukturelle Unterschiede zwischen den Triticeae Genomen hindeutet. Obwohl nicht im Design des Anreicherungsansatzes berücksichtigt konnten auch die ribosomale DNA Einheit des Zellkerns und gesamte Chloroplastengenome gewonnen und analysiert werden. Schließlich wurden Teile von 245 Genen des Zellkerns, die in niedriger Kopienanzahl im Genom vorkommen für phylogenetische Analysen verwendet.

Die Loci wurden sowohl einzeln als auch entsprechend ihrer chromosomalen Position zu verschiedenen Datensätzen kombiniert und analysiert. Traditionell modell-basierte Methoden, phylogenetische Netzwerke und koaleszenz-basierende Verfahren wurden angewendet, um biologische und/oder analytische Ursachen für Unterschiede zwischen

Genstammbäumen zu berücksichtigen. Die phylogenetischen Ergebnisse zeigten, dass Gattungen und/oder Arten im Allgemeinen monophyletisch sind. Die Gattungen *Hordeum* and *Psathyrostachys* haben sich früh von anderen Taxa der Tribus abgespalten und erscheinen stark differenziert. Dies ist auch in Übereinstimmung mit früheren Arbeiten. Die relativen Positionen der übrigen monophyletischen Gruppen variiert beträchtlich zwischen den Analysen. Schwach unterstützte phylogenetischen Gruppierungen stellen eher historische Ereignisse unvollständiger Trennung von Abstammungslinien und/oder Hybridisierung zum Zeitpunkt der Artbildung als rezenten Genfluss dar. Diese Gruppierungen können durch die hochdynamischen Triticeae Genome erklärt werden, welche als Ergebnis von Gen- und/oder Genomduplikationen ein großes Potenzial für die schnelle Entwicklung von reproduktiven Barrieren und/oder morphologische Veränderungen durch Neo- und/oder Subfunktionalisierung von einigen wenigen duplizierten Genen innehaben.

Die Ergebnisse der phylogenetischen Analysen, welche auf die Tribus als ganzes abzielten, unterstützen die Ergebnisse solcher infragenerischer taxonomischer Einteilungen, die einer geringeren Anzahl von Taxa Artstatus zuschreiben. Andere wichtigsten Ergebnisse zeigen, dass (1) *Amblyopyrum* am deutlichsten von allen *Aegilops* und *Triticum* Arten verschieden ist. Die Art ist im Besitz eines *Aegilops* Chloroplastengenoms und kann daher von *Aegilops* nicht völlig getrennt behandelt werden. (2) Die traditionelle *Aegilops* Sektion *Sitopsis* konnte wiederhergestellt werden. Dieses Ergebnis stützt die Zugehörigkeit von *Aegilops speltoides* zu *Aegilops*. (3) Die gleichrangige Behandlung von *Aegilops* und *Triticum* wird dadurch befürwortet, dass *Triticum* innerhalb der *Aegilops*-Gruppe entstanden ist. (4) Die kürzlich aufgestellt Hypothese das *Aegilops tauschii* durch Hybridisierung entstanden ist, konnte bestätigt werden. Zum ersten Mal wurden die letzten gemeinsamen Vorfahren von *Aegilops comosa* und *Aegilops uniaristata* sowie *Aegilops markgrafii* und *Aegilops umbellulata* als mögliche Vorfahren identifiziert welche vor circa 5,5 Millionen Jahren den Vorfahren heutiger *Aegilops tauschii* bildeten. (5) Zusätzlich konnten innerhalb des *Aegilops-Triticum-Amblyopyrum* Artkomplexes mehre gleichzeitige abgelaufene Artbildungsereignisse aufgezeigt werden, die ungefähr zwischen 4,5 und 2,5 Millionen Jahren stattfanden.

REFERENCES

- Akaike H. 1974.** A new look at the statistical model identification. *IEEE Transactions on Automatic Control* **19**: 716–723.
- Altschul SF, Gish W, Miller W, Myers EW, Lipman DJ. 1990.** Basic local alignment search tool. *Journal of Molecular Biology* **215**: 403–410.
- Álvarez I, Wendel JF. 2003.** Ribosomal ITS sequences and plant phylogenetic inference. *Molecular Phylogenetics and Evolution* **29**: 417–434.
- Ané C, Larget B, Baum DA, Smith SD, Rokas A. 2007.** Bayesian estimation of concordance among gene trees. *Molecular Biology and Evolution* **24**: 412–426.
- Asay KH, Jensen KB, Hsiao C, Dewey DR. 1992.** Probable origin of standard crested wheatgrass, *Agropyron desertorum* Fisch. ex Link, Schultes. *Canadian Journal of Plant Science* **72**: 763–772.
- Ayres DL, Darling A, Zwickl DJ, Beerli P, Holder MT, Lewis PO, Huelsenbeck JP, Ronquist F, Swofford DL, Cummings MP, et al. 2012.** BEAGLE: An application programming interface and high-performance computing library for statistical phylogenetics. *Systematic Biology* **61**: 170–173.
- Baird NA, Etter PD, Atwood TS, Currey MC, Shiver AL, Lewis ZA, Selker EU, Cresko WA, Johnson EA. 2008.** Rapid SNP discovery and genetic mapping using sequenced RAD markers. *PLoS ONE* **3**: e3376.
- Baldwin BG, Sanderson MJ, Porter JM, Wojciechowski MF, Campbell CS, Donoghue MJ. 1995.** The ITS region of nuclear ribosomal DNA: A valuable source of evidence on angiosperm phylogeny. *Annals of the Missouri Botanical Garden* **82**: 247–277.
- Baldwin BG, Wagner WL. 2010.** Hawaiian angiosperm radiations of North American origin. *Annals of Botany*: **105**: 849–879.
- Bänfer G, Moog U, Fiala B, Mohamed M, Weising K, Blattner FR. 2006.** A chloroplast genealogy of myrmecophytic *Macaranga* species (Euphorbiaceae) in Southeast Asia reveals hybridization, vicariance and long-distance dispersals. *Molecular Ecology* **15**: 4409–4424.
- Bansal V, Bafna V. 2008.** HapCUT: An efficient and accurate algorithm for the haplotype assembly problem. *Bioinformatics* **24**: i153–i159.
- Barkworth ME. 2000.** Changing perceptions of the Triticeae. In: Jacobs S, Everett J, eds. *Grasses: Systematics and Evolution*. Collingwood, Victoria, Australia: CSIRO Publishing, 110–120.
- Barkworth ME, Bothmer R von. 2005.** Twenty-one years later: The impact of Löve and Dewey's genomic classification proposal. *Czech Journal of Genetics and Plant Breeding* **41**: 3–9.
- Barkworth ME, Bothmer R von. 2009.** Scientific names in the Triticeae. In: Muehlbauer GJ, Feuillet C, eds. *Plant Genetics and Genomics: Crops and Models. Genetics and Genomics of the Triticeae*. Springer US, 3–30.
- Barkworth ME, Jacobs SW. 2011.** The Triticeae (Gramineae) in Australasia. *Telopea* **13**: 37–56.
- Baum BR, Estes JR, Gupta PK. 1987.** Assessment of the genomic system of classification in the Triticeae. *American Journal of Botany* **74**: 1388–1395.

References

- Bayes T. 1763.** An essay towards solving a problem in the doctrine of chances. *Philosophical Transactions of the Royal Society of London* **53**: 370–418.
- Bayzid MS, Hunt T, Warnow T. 2014.** Disk covering methods improve phylogenomic analyses. *BMC Genomics* **15**: S7.
- Bayzid MS, Warnow T. 2013.** Naive binning improves phylogenomic analyses. *Bioinformatics* **29**: 2277–2284.
- Bennett MD, Leitch IJ. 2011.** Nuclear DNA amounts in angiosperms: Targets, trends and tomorrow. *Annals of Botany* **107**: 467–590.
- Bentham G. 1882.** Notes on Gramineae. *Journal of the Linnean Society of London, Botany* **19**: 14–134.
- Berger E, Yorukoglu D, Peng J, Berger B. 2014.** HapTree: A novel Bayesian framework for single individual polyplototyping using NGS data. *PLoS Computational Biology* **10**: e1003502.
- Bieniek W, Mizianty M, Szklarczyk M. 2014.** Sequence variation at the three chloroplast loci (*matK*, *rbcL*, *trnH-psbA*) in the Triticeae tribe (Poaceae): Comments on the relationships and utility in DNA barcoding of selected species. *Plant Systematics and Evolution* **301**: 1275–1286.
- Bininda-Emonds ORP. 2004.** The evolution of supertrees. *Trends in Ecology and Evolution* **19**: 315–322.
- Blattner FR. 2004.** Phylogenetic analysis of *Hordeum* (Poaceae) as inferred by nuclear rDNA ITS sequences. *Molecular Phylogenetics and Evolution* **33**: 289–299.
- Blattner FR. 2006.** Multiple intercontinental dispersals shaped the distribution area of *Hordeum* (Poaceae). *New Phytologist* **169**: 603–614.
- Blattner FR. 2009.** Progress in phylogenetic analysis and a new infrageneric classification of the barley genus *Hordeum* (Poaceae: Triticeae). *Breeding Science* **59**: 471–480.
- Bordbar F, Rahiminejad MR, Saeidi H, Blattner FR. 2011.** Phylogeny and genetic diversity of D-genome species of *Aegilops* and *Triticum* (Triticeae, Poaceae) from Iran based on microsatellites, ITS, and *trnL-F*. *Plant Systematics and Evolution* **291**: 117–131.
- Bothmer R von, Jacobsen N. 1985.** Origin, taxonomy and related species. In: Rasmusson DC, ed. *Barley. Agronomy Monograph* **26**: 19–56.
- Bothmer R von, Jacobsen N, Baden C, Jørgensen RB, Linde-Laursen I. 1995.** An ecogeographical study of the genus *Hordeum*. *2nd edn. IPGRI, Rome*: 129.
- Bouckaert RR. 2010.** DensiTree: Making sense of sets of phylogenetic trees. *Bioinformatics* **26**: 1372–1373.
- Boussau B, Szöllösi GJ, Duret L, Gouy M, Tannier E, Daubin V. 2013.** Genome-scale coestimation of species and gene trees. *Genome Research* **23**: 323–330.
- Bowden WM. 1959.** The taxonomy and nomenclature of the wheats, barleys, and ryes and their wild relatives. *Canadian Journal of Botany* **37**: 657–684.
- Brassac J, Blattner FR. 2015.** Species-level phylogeny and polyploid relationships in *Hordeum* (Poaceae) inferred by next-generation sequencing and *in silico* cloning of multiple nuclear loci. *Systematic Biology* **64**: 792–808.
- Brassac J, Jakob SS, Blattner FR. 2012.** Progenitor-derivative relationships of *Hordeum* polyploids (Poaceae, Triticeae) inferred from sequences of *TOPO6*, a nuclear low-copy gene region. *PLoS ONE* **7**: e33808.

- Brummitt RK. 2006.** Am I a bony fish? *Taxon* **55**: 268–269.
- Burbano HA, Hodges E, Green RE, Briggs AW, Krause J, Meyer M, Good JM, Maricic T, Johnson PLF, Xuan Z, et al. 2010.** Targeted investigation of the Neandertal genome by array-based sequence capture. *Science* **328**: 723–725.
- de Bustos A, Jouve N. 2002.** Phylogenetic relationships of the genus *Secale* based on the characterisation of rDNA ITS sequences. *Plant Systematics and Evolution* **235**: 147–154.
- Bybee SM, Bracken-Grissom H, Haynes BD, Hermansen RA, Byers RL, Clement MJ, Udall JA, Wilcox ER, Crandall KA. 2011.** Targeted amplicon sequencing (TAS): A scalable next-gen approach to multilocus, multitaxa phylogenetics. *Genome Biology and Evolution* **3**: 1312–1323.
- Chapman JA, Mascher M, Buluç A, Barry K, Georganas E, Session A, Strnadova V, Jenkins J, Sehgal S, Olikar L, et al. 2015.** A whole-genome shotgun approach for assembling and anchoring the hexaploid bread wheat genome. *Genome Biology* **16**: 26.
- Charlesworth B. 2012.** The effects of deleterious mutations on evolution at linked sites. *Genetics* **190**: 5–22.
- Charlesworth B, Morgan MT, Charlesworth D. 1993.** The effect of deleterious mutations on neutral molecular variation. *Genetics* **134**: 1289–1303.
- Chen K, Durand D, Farach-Colton M. 2000.** NOTUNG: A program for dating gene duplications and optimizing gene family trees. *Journal of Computational Biology* **7**: 429–447.
- Chen F, Mackey AJ, Stoeckert CJ, Roos DS. 2006.** OrthoMCL-DB: Querying a comprehensive multi-species collection of ortholog groups. *Nucleic Acids Research* **34**: D363–D368.
- Chor B, Hendy MD, Holland BR, Penny D. 2000.** Multiple maxima of likelihood in phylogenetic trees: An analytic approach. *Molecular Biology and Evolution* **17**: 1529–1541.
- Covas G. 1949.** Taxonomic observations on the North American species of *Hordeum*. *Madrono* **10**: 1–21.
- Coyne JA, Orr HA. 2004.** *Speciation*. Sinauer Associates Sunderland, Massachusetts.
- Cracraft J. 1983.** Species concepts and speciation analysis. In: Johnston RF, ed. *Current Ornithology*. Plenum Press, 159–187.
- Crisp MD, Cook LG. 2009.** Explosive radiation or cryptic mass extinction? Interpreting signatures in molecular phylogenies. *Evolution* **63**: 2257–2265.
- Cronn R, Knaus BJ, Liston A, Maughan PJ, Parks M, Syring JV, Udall J. 2012.** Targeted enrichment strategies for next-generation plant biology. *American Journal of Botany* **99**: 291–311.
- Cruickshank TE, Hahn MW. 2014.** Reanalysis suggests that genomic islands of speciation are due to reduced diversity, not reduced gene flow. *Molecular Ecology* **23**: 3133–3157.
- Cummings N, King R, Rickers A, Kaspi A, Lunke S, Haviv I, Jowett J. 2010.** Combining target enrichment with barcode multiplexing for high throughput SNP discovery. *BMC Genomics* **11**: 641.
- Degnan JH, Rosenberg NA. 2009.** Gene tree discordance, phylogenetic inference and the multispecies coalescent. *Trends in Ecology and Evolution* **24**: 332–340.
- Dempewolf H, Hodgins KA, Rummell SE, Ellstrand NC, Rieseberg LH. 2012.** Reproductive isolation during domestication. *The Plant Cell* **24**: 2710–2717.

References

- Devos KM, Atkinson MD, Chinoy CN, Francis HA, Harcourt RL, Koebner RMD, Liu CJ, Masojć P, Xie DX, Gale MD. 1993.** Chromosomal rearrangements in the rye genome relative to that of wheat. *Theoretical and Applied Genetics* **85**: 673–680.
- Dewey DR. 1984.** The genomic system of classification as a guide to intergeneric hybridization with the perennial Triticeae. In: Gustafson JP, ed. *Gene Manipulation in Plant Improvement*. Stadler Genetics Symposia Series, Springer US, 209–279.
- Doležel J. 2005.** Plant DNA flow cytometry and estimation of nuclear genome size. *Annals of Botany* **95**: 99–110.
- Doležel J, Greilhuber J, Suda J. 2007.** Estimation of nuclear DNA content in plants using flow cytometry. *Nature Protocols* **2**: 2233–2244.
- Dorofeev VF, Filatenko AA, Migushova EF, Udaczin RA, Jakubziner MM. 1979.** Wheat. In: Dorofeev VF, Korovina ON, eds. *Flora of Cultivated Plants* **1**: 346.
- Doyle JJ, Doyle JL. 1987.** Genomic plant DNA preparation from fresh tissue-CTAB method. *Phytochemical Bulletin* **19**: 11–15.
- Doyle JJ, Doyle JL. 1999.** Nuclear protein-coding genes in phylogeny reconstruction and homology assessment: Some examples from Leguminosae. *Molecular Systematics and Plant Evolution. Systematics Association Special Volume* **57**: 229–254.
- Doyle VP, Young RE, Naylor GJP, Brown JM. 2015.** Can we identify genes with increased phylogenetic reliability? *Systematic Biology* **64**: 824–837.
- Drummond AJ, Ho SY, Phillips MJ, Rambaut A. 2006.** Relaxed phylogenetics and dating with confidence. *PLoS Biology* **4**: 699.
- Drummond AJ, Rambaut A. 2007.** BEAST: Bayesian evolutionary analysis by sampling trees. *BMC Evolutionary Biology* **7**: 214.
- Drummond AJ, Suchard MA, Xie D, Rambaut A. 2012.** Bayesian phylogenetics with BEAUti and the BEAST 1.7. *Molecular Biology and Evolution* **29**: 1969–1973.
- Dubcovsky J, Dvořák J. 1995.** Ribosomal RNA multigene loci: Nomads of the Triticeae genomes. *Genetics* **140**: 1367–1377.
- Dvořák J, Zhang H-B. 1992.** Reconstruction of the phylogeny of the genus *Triticum* from variation in repeated nucleotide sequences. *Theoretical and Applied Genetics* **84**: 419–429.
- Eddy SR. 2012.** The C-value paradox, junk DNA and ENCODE. *Current Biology* **22**: R898–R899.
- Edgar RC. 2004.** MUSCLE: Multiple sequence alignment with high accuracy and high throughput. *Nucleic Acids Research* **32**: 1792–1797.
- Edger PP, Heidel-Fischer HM, Bekaert M, Rota J, Glöckner G, Platts AE, Heckel DG, Der JP, Wafula EK, Tang M, et al. 2015.** The butterfly plant arms-race escalated by gene and genome duplications. *Proceedings of the National Academy of Sciences USA* **112**: 8362–8366.
- Eilam T, Anikster Y, Millet E, Manisterski J, Feldman M. 2010.** Genome size in diploids, allopolyploids, and autopolyploids of Mediterranean Triticeae. *Journal of Botany* **2010**: 1–12.
- Elshire RJ, Glaubitz JC, Sun Q, Poland JA, Kawamoto K, Buckler ES, Mitchell SE. 2011.** A robust, simple genotyping-by-sequencing (GBS) approach for high diversity species. *PLoS ONE* **6**: e19379.

- Escobar JS, Cenci A, Bolognini J, Haudry A, Laurent S, David J, Glémin S. 2010.** An integrative test of the dead-end hypothesis of selfing evolution in Triticeae (Poaceae): Selfing evolution in grasses. *Evolution* **64**: 2855–2872.
- Escobar JS, Scornavacca C, Cenci A, Guilhaumon C, Santoni S, Douzery EJ, Ranwez V, Glémin S, David J. 2011.** Multigenic phylogeny and analysis of tree incongruences in Triticeae (Poaceae). *BMC Evolutionary Biology* **11**: 181.
- Faircloth BC, Branstetter MG, White ND, Brady SG. 2015.** Target enrichment of ultraconserved elements from arthropods provides a genomic perspective on relationships among Hymenoptera. *Molecular Ecology Resources* **15**: 489–501.
- Fan X, Liu J, Sha L-N, Sun G-L, Hu Z-Q, Zeng J, Kang H-Y, Zhang H-Q, Wang Y, Wang X-L, et al. 2014.** Evolutionary pattern of rDNA following polyploidy in *Leymus* (Triticeae: Poaceae). *Molecular Phylogenetics and Evolution* **77**: 296–306.
- Farooq S, Iqbal N, Shah TM. 1990.** Promotion of homoeologous chromosome pairing in hybrids of *Triticum aestivum* × *Aegilops variabilis*. *Genome* **33**: 825–828.
- Feldman M, Levy AA. 2012.** Genome evolution due to allopolyploidization in wheat. *Genetics* **192**: 763–774.
- Felsenstein J. 1981.** Evolutionary trees from DNA sequences: A maximum likelihood approach. *Journal of Molecular Evolution* **17**: 368–376.
- Flaksberger KA. 1935.** Wheat. In: Wulff EV, ed. *Flora of Cultivated Plants*. Moscow and St Petersburg, Russia: State Agricultural Publishing Co., 19–434.
- Francis AR, Steel M. 2015.** Tree-like reticulation networks: When do tree-like distances also support reticulate evolution? *Mathematical Biosciences* **259**: 12–19.
- Frederiksen S. 1991.** Taxonomic studies in *Eremopyrum* (Poaceae). *Nordic Journal of Botany* **11**: 271–285.
- Frederiksen S, Petersen G. 1998.** A taxonomic revision of *Secale* (Triticeae, Poaceae). *Nordic Journal of Botany* **18**: 399–420.
- Friesen N, Herden T, Schoenfelder P. 2015.** *Allium canariense* (Amaryllidaceae), a species endemic to the Canary Islands. *Phytotaxa* **221**: 1–20.
- Fu Y, Springer NM, Gerhardt DJ, Ying K, Yeh C-T, Wu W, Swanson-Wagner R, D'Ascenzo M, Millard T, Freeberg L, et al. 2010.** Repeat subtraction-mediated sequence capture from a complex genome: Sequence capture in maize. *The Plant Journal* **62**: 898–909.
- Gatesy J, Springer MS. 2013.** Concatenation versus coalescence versus 'concatalescence'. *Proceedings of the National Academy of Sciences USA* **110**: E1179.
- Gatesy J, Springer MS. 2014.** Phylogenetic analysis at deep timescales: Unreliable gene trees, bypassed hidden support, and the coalescence/concatalescence conundrum. *Molecular Phylogenetics and Evolution* **80**: 231–266.
- Glenn TC. 2011.** Field guide to next-generation DNA sequencers. *Molecular Ecology Resources* **11**: 759–769.
- Gnrke A, Melnikov A, Maguire J, Rogov P, LeProust EM, Brockman W, Fennell T, Giannoukos G, Fisher S, Russ C, et al. 2009.** Solution hybrid selection with ultra-long oligonucleotides for massively parallel targeted sequencing. *Nature Biotechnology* **27**: 182–189.
- Golovnina KA, Glushkov SA, Blinov AG, Mayorov VI, Adkison LR, Goncharov NP. 2007.** Molecular phylogeny of the genus *Triticum* L. *Plant Systematics and Evolution* **264**: 195–216.

References

- Goncharov NP. 2002.** *Comparative genetics of wheats and their related species*. Novosibirsk, Russia: Siberian University Press.
- Goncharov NP. 2011.** Genus *Triticum* L. taxonomy: The present and the future. *Plant Systematics and Evolution* **295**: 1–11.
- Gornicki P, Zhu H, Wang J, Challa GS, Zhang Z, Gill BS, Li W. 2014.** The chloroplast view of the evolution of polyploid wheat. *New Phytologist* **204**: 704–714.
- Gottschalk W. 1973.** The genetic control of meiosis. *Genetics* **74**: 99.
- Grover CE, Salmon A, Wendel JF. 2012.** Targeted sequence capture as a powerful tool for evolutionary analysis. *American Journal of Botany* **99**: 312–319.
- Guindon S, Gascuel O. 2003.** A simple, fast, and accurate algorithm to estimate large phylogenies by Maximum Likelihood. *Systematic Biology* **52**: 696–704.
- Hackel E. 1887.** Gramineae. In: Engler A, Prantl KAE, eds. *Die natürlichen Pflanzenfamilien*. Leipzig, Germany: Wilhelm Engelmann, 1–97.
- Haeseler A von. 2012.** Do we still need supertrees? *BMC Biology* **10**: 13.
- Hammer K, Filatenko AA, Pistrick K. 2011.** Taxonomic remarks on *Triticum* L. and *×Triticosecale* Wittm. *Genetic Resources and Crop Evolution* **58**: 3–10.
- Hasegawa M, Kishino H, Yano T. 1985.** Dating of the human-ape splitting by a molecular clock of mitochondrial DNA. *Journal of Molecular Evolution* **22**: 160–174.
- Hastings PJ, Lupski JR, Rosenberg SM, Ira G. 2009.** Mechanisms of change in gene copy number. *Nature Reviews Genetics* **10**: 551–564.
- Heled J, Drummond AJ. 2010.** Bayesian inference of species trees from multilocus data. *Molecular Biology and Evolution* **27**: 570–580.
- Himmelbach A, Knauff M, Stein N. 2014.** Plant sequence capture optimised for Illumina sequencing. *Bio-protocol* **4**: e1166.
- Hitchcock AS. 1935.** *Manual of the grasses of the United States*. Washington, D.C., USA: U.S. Government Printing Office.
- Hitchcock AS. 1951.** *Manual of the grasses of the United States. Edition 2*. Revised by Chase A. Washington, D.C., USA: U.S. Government Printing Office.
- Holder M, Lewis PO. 2003.** Phylogeny estimation: Traditional and Bayesian approaches. *Nature Reviews Genetics* **4**: 275–284.
- Hsiao C, Chatterton NJ, Asay KH, Jensen KB. 1995.** Phylogenetic relationships of the monogenomic species of the wheat tribe, Triticeae (Poaceae), inferred from nuclear rDNA (internal transcribed spacer) sequences. *Genome* **38**: 211–223.
- Hsiao C, Jacobs SWL, Chatterton NJ, Asay KH. 1999.** A molecular phylogeny of the grass family (Poaceae) based on the sequences of nuclear ribosomal DNA (ITS). *Australian Systematic Botany* **11**: 667–688.
- Hudson RR. 1990.** Gene genealogies and the coalescent process. *Oxford Surveys in Evolutionary Biology* **7**: 44.
- Huelsenbeck JP, Rannala B. 1997.** Phylogenetic methods come of age: Testing hypotheses in an evolutionary context. *Science* **276**: 227–232.

- Huson DH. 1998.** SplitsTree: Analyzing and visualizing evolutionary data. *Bioinformatics* **14**: 68–73.
- Huson DH, Bryant D. 2006.** Application of phylogenetic networks in evolutionary studies. *Molecular Biology and Evolution* **23**: 254–267.
- Huson DH, Rupp R. 2008.** Summarizing multiple gene trees using cluster networks. *Algorithms in Bioinformatics*. Springer, 296–305.
- Huson DH, Scornavacca C. 2011.** A survey of combinatorial methods for phylogenetic networks. *Genome Biology and Evolution* **3**: 23–35.
- Huson DH, Scornavacca C. 2012.** Dendroscope 3: An interactive tool for rooted phylogenetic trees and networks. *Systematic Biology* **61**: 1061–1067.
- Jakob SS, Blattner FR. 2010.** Two extinct diploid progenitors were involved in allopolyploid formation in the *Hordeum murinum* (Poaceae: Triticeae) taxon complex. *Molecular Phylogenetics and Evolution* **55**: 650–659.
- Jakob SS, Meister A, Blattner FR. 2004.** The considerable genome size variation of *Hordeum* species (Poaceae) is linked to phylogeny, life form, ecology, and speciation rates. *Molecular Biology and Evolution* **21**: 860–869.
- Jakob SS, Rödder D, Engler JO, Shaaf S, Özkan H, Blattner FR, Kilian B. 2014.** Evolutionary history of wild barley (*Hordeum vulgare* subsp. *spontaneum*) analyzed using multilocus sequence data and paleodistribution modeling. *Genome Biology and Evolution* **6**: 685–702.
- Jarvie JK, Barkworth ME. 1990.** Isozyme similarity in *Thinopyrum* and its relatives (Triticeae: Gramineae). *Genome* **33**: 885–891.
- Jauhar PP. 1990.** Multidisciplinary approach to genome analysis in the diploid species, *Thinopyrum bessarabicum* and *Th. elongatum* (*Lophopyrum elongatum*), of the Triticeae. *Theoretical and Applied Genetics* **80**: 523–536.
- Jauhar PP. 1992.** Chromosome pairing in hybrids between hexaploid bread wheat and tetraploid crested wheatgrass (*Agropyron cristatum*). *Hereditas* **116**: 107–109.
- Jia J, Zhao S, Kong X, Li Y, Zhao G, He W, Appels R, Pfeifer M, Tao Y, Zhang X, et al. 2013.** *Aegilops tauschii* draft genome sequence reveals a gene repertoire for wheat adaptation. *Nature* **496**: 91–95.
- Joly S. 2012.** JML: Testing hybridization from species trees. *Molecular Ecology Resources* **12**: 179–184.
- Juan C, Emerson BC, Oromí P, Hewitt GM. 2000.** Colonization and diversification: Towards a phylogeographic synthesis for the Canary Islands. *Trends in Ecology and Evolution* **15**: 104–109.
- Kaplan NL, Hudson RR, Langley CH. 1989.** The ‘hitchhiking effect’ revisited. *Genetics* **123**: 887–899.
- Katoh K, Standley DM. 2013.** MAFFT multiple sequence alignment software version 7: Improvements in performance and usability. *Molecular Biology and Evolution* **30**: 772–780.
- Kearse M, Moir R, Wilson A, Stones-Havas S, Cheung M, Sturrock S, Buxton S, Cooper A, Markowitz S, Duran C, et al. 2012.** Geneious Basic: An integrated and extendable desktop software platform for the organization and analysis of sequence data. *Bioinformatics* **28**: 1647–1649.
- Kellogg EA. 1989.** Comments on genomic genera in the Triticeae (Poaceae). *American Journal of Botany* **76**: 796–805.

References

- Kellogg EA. 1992.** Tools for studying the chloroplast genome in the Triticeae (Gramineae): An *EcoRI* map, a diagnostic deletion, and support for *Bromus* as an outgroup. *American Journal of Botany* **79**: 186–197.
- Kellogg EA, Appels R, Mason-Gamer RJ. 1996.** When genes tell different stories: The diploid genera of Triticeae (Gramineae). *Systematic Botany* **21**: 321–347.
- Kenny EM, Cormican P, Gilks WP, Gates AS, O'Dushlaine CT, Pinto C, Corvin AP, Gill M, Morris DW. 2010.** Multiplex target enrichment using DNA indexing for ultra-high throughput SNP detection. *DNA Research* **18**: 31–38.
- Kent WJ. 2002.** BLAT-The BLAST-like alignment tool. *Genome Research* **12**: 656–664.
- Kihara H. 1930.** Genomanalyse bei *Triticum* und *Aegilops*. *Cytologia* **1**: 263–284.
- Kilian B, Mammen K, Millet E, Sharma R, Graner A, Salamini F, Hammer K, Özkan H. 2011.** *Aegilops*. In: Kole C, ed. *Wild Crop Relatives: Genomic and Breeding Resources*. Springer Berlin Heidelberg, 1–76.
- Kilian B, Martin W, Salamini F. 2010.** Genetic diversity, evolution and domestication of wheat and barley in the Fertile Crescent. In: Glaubrecht M, ed. *Evolution in Action*. Springer Berlin Heidelberg, 137–166.
- Kimber G, Feldman M. 1987.** Wild wheat. An introduction. *Special Report, College of Agriculture, University of Missouri-Columbia*.
- Kingman JFC. 1982.** The coalescent. *Stochastic Processes and their Applications* **13**: 235–248.
- Knowles LL, Kubatko LS. 2011.** Estimating species trees: An introduction to concepts and models. In: Knowles LL and Kubatko LS, eds. *Estimating Species Trees: Practical and Theoretical Aspects*. Hoboken, NJ, USA: John Wiley & Sons, 1–14.
- Krasileva KV, Buffalo V, Bailey P, Pearce S, Ayling S, Tabbita F, Soria M, Wang S, Akhunov E, Uauy C, et al. 2013.** Separating homeologs by phasing in the tetraploid wheat transcriptome. *Genome Biology* **14**: R66.
- Kubatko LS. 2009.** Identifying hybridization events in the presence of coalescence via model selection. *Systematic Biology* **58**: 478–488.
- Kubatko LS, Carstens BC, Knowles LL. 2009.** STEM: Species tree estimation using Maximum Likelihood for gene trees under coalescence. *Bioinformatics* **25**: 971–973.
- Kubatko LS, Degnan JH. 2007.** Inconsistency of phylogenetic estimates from concatenated data under coalescence. *Systematic Biology* **56**: 17–24.
- Kuhner MK, Yamato J. 2015.** Practical performance of tree comparison metrics. *Systematic Biology* **64**: 205–214.
- Kupczok A, Schmidt HA, Haeseler A von. 2010.** Accuracy of phylogeny reconstruction methods combining overlapping gene data sets. *Algorithms for Molecular Biology* **5**: 37.
- Lanfear R, Calcott B, Ho SYW, Guindon S. 2012.** PartitionFinder: Combined selection of partitioning schemes and substitution models for phylogenetic analyses. *Molecular Biology and Evolution* **29**: 1695–1701.
- Larget BR, Kotha SK, Dewey CN, Ané C. 2010.** BUCKy: Gene tree/species tree reconciliation with Bayesian concordance analysis. *Bioinformatics* **26**: 2910–2911.
- Lemmon EM, Lemmon AR. 2013.** High-throughput genomic data in systematics and phylogenetics. *Annual Review of Ecology, Evolution, and Systematics* **44**: 99–121.

- Li S. 1996.** Phylogenetic tree construction using Markov chain Monte carlo. *PhD Dissertation, Ohio State University, Columbus.*
- Li H. 2011.** A statistical framework for SNP calling, mutation discovery, association mapping and population genetical parameter estimation from sequencing data. *Bioinformatics* **27**: 2987–2993.
- Li H, Durbin R. 2009.** Fast and accurate short read alignment with Burrows–Wheeler transform. *Bioinformatics* **25**: 1754–1760.
- Li H, Handsaker B, Wysoker A, Fennell T, Ruan J, Homer N, Marth G, Abecasis G, Durbin R, 1000 Genome Project Data Processing Subgroup. 2009.** The Sequence Alignment/Map format and SAMtools. *Bioinformatics* **25**: 2078–2079.
- Li L-F, Liu B, Olsen KM, Wendel JF. 2015a.** A re-evaluation of the homoploid hybrid origin of *Aegilops tauschii*, the donor of the wheat D-subgenome. *New Phytologist* **208**: 4–8.
- Li L-F, Liu B, Olsen KM, Wendel JF. 2015b.** Multiple rounds of ancient and recent hybridizations have occurred within the *Aegilops–Triticum* complex. *New Phytologist*: **208**: 11–12.
- Linder HP, Rabosky DL, Antonelli A, Wüest RO, Ohlemüller R. 2014.** Disentangling the influence of climatic and geological changes on species radiations. *Journal of Biogeography* **41**: 1313–1325.
- Ling H-Q, Zhao S, Liu D, Wang J, Sun H, Zhang C, Fan H, Li D, Dong L, Tao Y, et al. 2013.** Draft genome of the wheat A-genome progenitor *Triticum urartu*. *Nature* **496**: 87–90.
- Linnaeus C von. 1753.** *Species Plantarum*. Laurentii Salvi Stockholm.
- Liò P, Goldman N. 1998.** Models of molecular evolution and phylogeny. *Genome Research* **8**: 1233–1244.
- Lisiecki LE, Raymo ME. 2007.** Plio–Pleistocene climate evolution: Trends and transitions in glacial cycle dynamics. *Quaternary Science Reviews* **26**: 56–69.
- Liu L. 2008.** BEST: Bayesian estimation of species trees under the coalescent model. *Bioinformatics* **24**: 2542–2543.
- Liu L, Xi Z, Wu S, Davis CC, Edwards SV. 2015.** Estimating phylogenetic trees from genome-scale data. *Annals of the New York Academy of Sciences*: 10.1111/nyas.12747.
- Liu L, Yu L, Edwards SV. 2010.** A maximum pseudo-likelihood approach for estimating species trees under the coalescent model. *BMC Evolutionary Biology* **10**: 302.
- Lord J, Turton J, Medway C, Shi H, Brown K, Lowe J, Mann D, Pickering-Brown S, Kalsheker N, Passmore P, et al. 2012.** Next generation sequencing of CLU, PICALM and CR1: Pitfalls and potential solutions. *International Journal of Molecular Epidemiology and Genetics* **3**: 262–275.
- Löve A. 1982.** Generic evolution of the wheatgrasses. *Biologisches Zentralblatt* **101**: 199–212.
- Löve A. 1984.** Conspectus of the Triticeae. *Feddes Repertorium* **95**: 425–521.
- Mac Key J. 1966.** Species relationship in *Triticum*. *Hereditas* **2**: 237–276.
- Mac Key J. 1977.** Sec. *Dicoccoides* Flaksb. of wheat, its phylogeny, diversification and subdivision. *Proceedings of the Symposium on Extended Availability of Wheat Genetics Resources*. Bari, 5–46.
- Mac Key J. 1989.** Genus *Triticum* and its systematics. In: Shumny VK, ed. *Vavilov's legacy in Modern Biology*. Moscow, SSSR: Nauka, 170–185.

References

- Mac Key J. 2005.** Wheat: Its concept, evolution and taxonomy. In: Royo C, Nachit M, Di Fonzo N, Pfeiffer W, Araus J, Slafer G, eds. *Durum Wheat Breeding. Current Approaches and Future Strategies*. Binghamton, NY, USA: Food Products Press, 3–61.
- Maddison WP. 1997.** Gene trees in species trees. *Systematic Biology* **46**: 523–536.
- Madsen CK, Dionisio G, Holme IB, Holm PB, Brinch-Pedersen H. 2013.** High mature grain phytase activity in the Triticeae has evolved by duplication followed by neofunctionalization of the purple acid phosphatase phytase (*PAPhy*) gene. *Journal of Experimental Botany* **64**: 3111–3123.
- Mahelka V, Kopecký D, Palvstová L. 2011.** On the genome constitution and evolution of intermediate wheatgrass (*Thinopyrum intermedium*: Poaceae, Triticeae). *BMC Evolutionary Biology* **11**: 127.
- Mallet J. 2007.** Hybrid speciation. *Nature* **446**: 279–283.
- Mamanova L, Coffey AJ, Scott CE, Kozarewa I, Turner EH, Kumar A, Howard E, Shendure J, Turner DJ. 2010.** Target-enrichment strategies for next-generation sequencing. *Nature Methods* **7**: 111–118.
- Marcussen T, Sandve SR, Heier L, Spannagl M, Pfeifer M, Jakobsen KS, Wulff BBH, Steuernagel B, Mayer KFX, Olsen O-A, et al. 2014.** Ancient hybridizations among the ancestral genomes of bread wheat. *Science* **345**: 1250092.
- Mardis ER. 2008.** Next-generation DNA sequencing methods. *Annual Review of Genomics and Human Genetics* **9**: 387–402.
- Markova DN, Mason-Gamer RJ. 2015.** The role of vertical and horizontal transfer in the evolutionary dynamics of *Pf1*-like transposable elements in Triticeae. *PLoS ONE* **10**: e0137648.
- Martis MM, Klemme S, Banaei-Moghaddam AM, Blattner FR, Macas J, Schmutzer T, Scholz U, Gundlach H, Wicker T, Šimková H, et al. 2012.** Selfish supernumerary chromosome reveals its origin as a mosaic of host genome and organellar sequences. *Proceedings of the National Academy of Sciences USA* **109**: 13343–13346.
- Martis MM, Zhou R, Haseneyer G, Schmutzer T, Vrána J, Kubaláková M, König S, Kugler KG, Scholz U, Hackauf B, et al. 2013.** Reticulate evolution of the rye genome. *The Plant Cell* **25**: 3685–3698.
- Mascher M, Muehlbauer GJ, Rokhsar DS, Chapman J, Schmutz J, Barry K, Muñoz-Amatriaín M, Close TJ, Wise RP, Schulman AH, et al. 2013.** Anchoring and ordering NGS contig assemblies by population sequencing (POPSEQ). *The Plant Journal* **76**: 718–727.
- Mason-Gamer RJ. 2004.** Reticulate evolution, introgression, and intertribal gene capture in an allohexaploid grass. *Systematic Biology* **53**: 25–37.
- Mason-Gamer RJ. 2005.** The β -amylase genes of grasses and a phylogenetic analysis of the Triticeae (Poaceae). *American Journal of Botany* **92**: 1045–1058.
- Mason-Gamer RJ. 2008.** Allohexaploidy, introgression, and the complex phylogenetic history of *Elymus repens* (Poaceae). *Molecular Phylogenetics and Evolution* **47**: 598–611.
- Mason-Gamer RJ. 2013.** Phylogeny of a genomically diverse group of *Elymus* (Poaceae) allopolyploids reveals multiple levels of reticulation. *PLoS ONE* **8**: e78449.
- Mason-Gamer RJ, Kellogg EA. 1996.** Testing for phylogenetic conflict among molecular data sets in the tribe Triticeae (Gramineae). *Systematic Biology* **45**: 524–545.

- Mason-Gamer RJ, Kellogg EA. 2000.** Phylogenetic analysis of the Triticeae using the starch synthase gene, and a preliminary analysis of some North American *Elymus* species. In: Jacobs S, Everett J, eds. *Grasses. Systematics and Evolution*. Collingwood, Victoria, Australia: CSIRO Publishing, 102–109.
- Mason-Gamer RJ, Orme NL, Anderson CM. 2002.** Phylogenetic analysis of North American *Elymus* and the monogenomic Triticeae (Poaceae) using three chloroplast DNA data sets. *Genome* **45**: 991–1002.
- Matsumoto T, Tanaka T, Sakai H, Amano N, Kanamori H, Kurita K, Kikuta A, Kamiya K, Yamamoto M, Ikawa H, et al. 2011.** Comprehensive sequence analysis of 24,783 barley full-length cDNAs derived from 12 clone libraries. *Plant Physiology* **156**: 20–28.
- Matsuoka Y. 2011.** Evolution of polyploid *Triticum* wheats under cultivation: The role of domestication, natural hybridization and allopolyploid speciation in their diversification. *Plant and Cell Physiology* **52**: 750–764.
- Mayer KFX, Martis M, Hedley PE, Šimková H, Liu H, Morris JA, Steuernagel B, Taudien S, Roessner S, Gundlach H, et al. 2011.** Unlocking the barley genome by chromosomal and comparative genomics. *The Plant Cell* **23**: 1249–1263.
- Mayer KFX, Rogers J, Dole el J, Pozniak C, Eversole K, Feuillet C, Gill B, Friebe B, Lukaszewski AJ, Sourdille P, et al. 2014.** A chromosome-based draft sequence of the hexaploid bread wheat (*Triticum aestivum*) genome. *Science* **345**: 1251788.
- Mayer KFX, Waugh R, Brown JW, Schulman A, Langridge P, Platzer M, Fincher GB, Muehlbauer GJ, Sato K, Close TJ. 2012.** A physical, genetic and functional sequence assembly of the barley genome. *Nature* **491**: 711–716.
- Mayr E. 1942.** *Systematics and the Origin of Species, from the Viewpoint of a Zoologist*. Harvard University Press.
- McCormack JE, Hird SM, Zellmer AJ, Carstens BC, Brumfield RT. 2013.** Applications of next-generation sequencing to phylogeography and phylogenetics. *Molecular Phylogenetics and Evolution* **66**: 526–538.
- McIntyre CL. 1988.** Variation at isozyme loci in Triticeae. *Plant Systematics and Evolution* **160**: 123–142.
- McNeill J, Barrie FR, Buck WR, Demoulin V, Greuter W, Hawksworth DL, Herendeen PS, Knapp S, Marhold K, Prado J, et al. 2012.** *International Code of Nomenclature for Algae, Fungi, and Plants (Melbourne Code)*. A.R.G. Gantner Verlag KG, Ruggell, Liechtenstein.
- Metropolis N, Rosenbluth AW, Rosenbluth MN, Teller AH, Teller E. 1953.** Equation of state calculations by fast computing machines. *The Journal of Chemical Physics* **21**: 1087–1092.
- Metzker ML. 2009.** Sequencing technologies — the next generation. *Nature Reviews Genetics* **11**: 31–46.
- Meyer M, Kircher M. 2010.** Illumina sequencing library preparation for highly multiplexed target capture and sequencing. *Cold Spring Harbor Protocols* **2010**: t5448.
- Middleton CP, Senerchia N, Stein N, Akhunov ED, Keller B, Wicker T, Kilian B. 2014.** Sequencing of chloroplast genomes from wheat, barley, rye and their relatives provides a detailed insight into the evolution of the Triticeae tribe. *PLoS ONE* **9**: e85761.
- Middleton CP, Stein N, Keller B, Kilian B, Wicker T. 2013.** Comparative analysis of genome composition in Triticeae reveals strong variation in transposable element dynamics and nucleotide diversity. *The Plant Journal* **73**: 347–356.

References

- Miller MR, Atwood TS, Eames BF, Eberhart JK, Yan Y-L, Postlethwait JH, Johnson EA. 2007.** RAD marker microarrays enable rapid mapping of zebrafish mutations. *Genome Biology* **8**: R105.
- Miller MA, Pfeiffer W, Schwartz T. 2010.** Creating the CIPRES Science Gateway for inference of large phylogenetic trees. Gateway Computing Environments Workshop (GCE), 2010.1–8.
- Mirarab S, Bayzid MS, Boussau B, Warnow T. 2014a.** Statistical binning enables an accurate coalescent-based estimation of the avian tree. *Science* **346**: 1250463.
- Mirarab S, Bayzid MS, Warnow T. 2014b.** Evaluating summary methods for multilocus species tree estimation in the presence of incomplete lineage sorting. *Systematic Biology* doi: 10.1093/sysbio/syu063.
- Mirarab S, Reaz R, Bayzid MS, Zimmermann T, Swenson MS, Warnow T. 2014c.** ASTRAL: Genome-scale coalescent-based species tree estimation. *Bioinformatics* **30**: i541–i548.
- Mirarab S, Warnow T. 2015.** ASTRAL-II: Coalescent-based species tree estimation with many hundreds of taxa and thousands of genes. *Bioinformatics* **31**: i44–i52.
- Mochida K, Shinozaki K. 2013.** Unlocking Triticeae genomics to sustainably feed the future. *Plant and Cell Physiology* **54**: 1931–1950.
- Mochida K, Yoshida T, Sakurai T, Ogihara Y, Shinozaki K. 2009.** TriFLDB: A database of clustered full-length coding sequences from Triticeae with applications to comparative grass genomics. *Plant Physiology* **150**: 1135–1146.
- Monte JV, McIntyre CL, Gustafson JP. 1993.** Analysis of phylogenetic relationships in the Triticeae tribe using RFLPs. *Theoretical and Applied Genetics* **86**: 649–655.
- Moore G. 2009.** Early stages of meiosis in wheat and the role of *Ph1*. In: Muehlbauer GJ, Feuillet C, eds. *Genetics and Genomics of the Triticeae*. Springer, 237–252.
- Moore G, Devos KM, Wang Z, Gale MD. 1995.** Cereal genome evolution: Grasses, line up and form a circle. *Current Biology* **5**: 737–739.
- Moore RC, Purugganan MD. 2003.** The early stages of duplicate gene evolution. *Proceedings of the National Academy of Sciences USA* **100**: 15682–15687.
- Murat F, Zhang R, Guizard S, Flores R, Armero A, Pont C, Steinbach D, Quesneville H, Cooke R, Salse J. 2014.** Shared subgenome dominance following polyploidization explains grass genome evolutionary plasticity from a seven protochromosome ancestor with 16K protogenes. *Genome Biology and Evolution* **6**: 12–33.
- Nguyen N, Mirarab S, Warnow T. 2012.** MRL and SuperFine+MRL: New supertree methods. *Algorithms for Molecular Biology* **7**: 1–13.
- Nater A, Burri R, Kawakami T, Smeds L, Ellegren H. 2015.** Resolving evolutionary relationships in closely related species with whole-genome sequencing data. *Systematic Biology*: syv045.
- Nevski SA. 1934.** Agrostological studies IV. The systematics of the tribe Hordeae. *Flora / Sistematika Vysshikh Rasteniin 1. Trudy Botanicheskogo Instituta Adakademii Nauk SSSR* **1**: 9–32.
- Nevski SA. 1941.** Beiträge zur Kenntnis der wildwachsenden Gersten im Zusammenhang mit der Frage über den Ursprung von *Hordeum vulgare* L. und *Hordeum distichon* L. (Versuch einer Monographie der Gattung *Hordeum*). *Trudy Botanicheskogo Instituta Akademii Nauk SSSR* **5**: 65–255.

- Nosil P, Funk DJ, Ortiz-Barrientos D. 2009.** Divergent selection and heterogeneous genomic divergence. *Molecular Ecology* **18**: 375–402.
- Nylander JAA, Wilgenbusch JC, Warren DL, Swofford DL. 2007.** AWTY (Are we there yet?): A system for graphical exploration of MCMC convergence in Bayesian phylogenetics. *Bioinformatics* **24**: 581–583.
- Ogihara Y, Tsunewaki K. 1988.** Diversity and evolution of chloroplast DNA in *Triticum* and *Aegilops* as revealed by restriction fragment analysis. *Theoretical and Applied Genetics* **76**: 321–332.
- de Oliveira Martins L, Mallo D, Posada D. 2014.** A Bayesian supertree model for genome-wide species tree reconstruction. *Systematic Biology*: doi: 10.1093/sysbio/syu082.
- O’Neil T, Emrich SJ. 2012.** Haplotype and minimum-chimerism consensus determination using short sequence data. *BMC Genomics* **13**: S4.
- Padial JM, Miralles A, De la Riva I, Vences M. 2010.** The integrative future of taxonomy. *Frontiers in Zoology* **7**: 1–14.
- Paradis E, Claude J, Strimmer K. 2004.** APE: Analyses of phylogenetics and evolution in R language. *Bioinformatics* **20**: 289–290.
- Petersen G, Seberg O. 1997.** Phylogenetic analysis of the Triticeae (Poaceae) based on *rpoA* sequence data. *Molecular Phylogenetics and Evolution* **7**: 217–230.
- Petersen G, Seberg O. 2000.** Phylogenetic evidence for excision of *Stowaway* Miniature Inverted-repeat Transposable Elements in Triticeae (Poaceae). *Molecular Biology and Evolution* **17**: 1589–1596.
- Petersen G, Seberg O. 2002.** Molecular evolution and phylogenetic application of *DMC1*. *Molecular Phylogenetics and Evolution* **22**: 43–50.
- Petersen G, Seberg O. 2009.** *Stowaway* MITEs in *Hordeum* (Poaceae): Evolutionary history, ancestral elements and classification. *Cladistics* **25**: 198–208.
- Petersen G, Seberg O, Aagesen L, Frederiksen S. 2004.** An empirical test of the treatment of indels during optimization alignment based on the phylogeny of the genus *Secale* (Poaceae). *Molecular Phylogenetics and Evolution* **30**: 733–742.
- Petersen G, Seberg O, Salomon B. 2011.** The origin of the H, St, W, and Y genomes in allotetraploid species of *Elymus* L. and *Stenostachys* Turcz. (Poaceae: Triticeae). *Plant Systematics and Evolution* **291**: 197–210.
- Petersen G, Seberg O, Yde M, Berthelsen K. 2006.** Phylogenetic relationships of *Triticum* and *Aegilops* and evidence for the origin of the A, B, and D genomes of common wheat (*Triticum aestivum*). *Molecular Phylogenetics and Evolution* **39**: 70–82.
- Petit RJ, Excoffier L. 2009.** Gene flow and species delimitation. *Trends in Ecology and Evolution* **24**: 386–393.
- Philippe H, Brinkmann H, Lavrov DV, Littlewood DTJ, Manuel M, Wörheide G, Baurain D. 2011.** Resolving difficult phylogenetic questions: Why more sequences are not enough. *PLoS Biology* **9**: e1000602.
- Pont C, Murat F, Confolent C, Balzergue S, Salse J. 2011.** RNA-seq in grain unveils fate of neo- and paleopolyploidization events in bread wheat (*Triticum aestivum* L.). *Genome Biology* **12**: 1–19.

References

- Posada D. 2008.** jModelTest: Phylogenetic model averaging. *Molecular Biology and Evolution* **25**: 1253–1256.
- Posada D. 2009.** Selection of models of DNA evolution with jModelTest. *Bioinformatics for DNA Sequence Analysis*. Springer, 93–112.
- Posada D, Crandall KA. 2001.** Selecting the best-fit model of nucleotide substitution. *Systematic Biology* **50**: 580–601.
- Pourkheirandish M, Hensel G, Kilian B, Senthil N, Chen G, Sameri M, Azhaguvel P, Sakuma S, Dhanagond S, Sharma R, et al. 2015.** Evolution of the grain dispersal system in barley. *Cell* **162**: 527–539.
- Purugganan MD, Fuller DQ. 2009.** The nature of selection during plant domestication. *Nature* **457**: 843–848.
- Qi LL, Echalié B, Chao S, Lazo GR, Butler GE, Anderson OD, Akhunov ED, Dvořák J, Linkiewicz AM, Ratnasiri A. 2004.** A chromosome bin map of 16,000 expressed sequence tag loci and distribution of genes among the three genomes of polyploid wheat. *Genetics* **168**: 701–712.
- de Queiroz K. 2007.** Species concepts and species delimitation. *Systematic Biology* **56**: 879–886.
- Quinlan AR, Hall IM. 2010.** BEDTools: A flexible suite of utilities for comparing genomic features. *Bioinformatics* **26**: 841–842.
- Rambaut A, Suchard M, Xie W, Drummond A. 2014.** *Tracer v. 1.6*. Institute of Evolutionary Biology, University of Edinburgh, UK: available from <http://beast.bio.ed.ac.uk/Tracer>
- Rannala B, Yang Z. 1996.** Probability distribution of molecular evolutionary trees: A new method of phylogenetic inference. *Journal of Molecular Evolution* **43**: 304–311.
- Renny-Byfield S, Wendel JF. 2014.** Doubling down on genomes: Polyploidy and crop plants. *American Journal of Botany* **101**: 1711–1725.
- Reveal JL. 2004.** Latest news on vascular plant family nomenclature: Earlier validation of certain tribal names in Poaceae, version 27 Nov 2004. <http://www.plantsystematics.org/reveal/pbio/fam/NEWS.html> (accessed March 12th, 2015).
- Reveal JL. 2011.** *Indices Nominum Supragenericorum Plantarum Vascularium*, version 17 Feb. 2011. <http://www.plantsystematics.org/reveal/pbio/fam/famPO-PZ.html> (accessed March 12th, 2015).
- Rieseberg LH. 1997.** Hybrid origins of plant species. *Annual Review of Ecology and Systematics* **28**: 359–389.
- Rieseberg LH, Wendel JF. 1993.** Introgression and its consequences in plants. In: Harrison RG, ed. *Hybrid zones and the evolutionary process*. Oxford University Press, 70–109.
- Roberts RJ, Carneiro MO, Schatz MC. 2013.** The advantages of SMRT sequencing. *Genome Biology* **14**: 405.
- Robinson D, Foulds LR. 1981.** Comparison of phylogenetic trees. *Mathematical Biosciences* **53**: 131–147.
- Robinson JP, Grégori G. 2007.** Principles of flow cytometry. In: Doležel J, Greilhuber J, Suda J, eds. *Flow Cytometry with Plant Cells: Analysis of Genes, Chromosomes and Genomes*. John Wiley & Sons, 19–40.

- Roch S, Steel M. 2014.** Likelihood-based tree reconstruction on a concatenation of alignments can be positively misleading. *arXiv:1409.2051*.
- Roch S, Warnow T. 2015.** On the robustness to gene tree estimation error (or lack thereof) of coalescent-based species tree methods. *Systematic Biology* **64**: 663–676.
- Ronquist F, Huelsenbeck JP. 2003.** MrBayes 3: Bayesian phylogenetic inference under mixed models. *Bioinformatics* **19**: 1572–1574.
- Ronquist F, van der Mark P, Huelsenbeck JP, Salemi M, Vandamme A-M. 2009.** Bayesian phylogenetic analysis using MrBayes. In: Lemey P, Salemi M, Vandamme A-M, eds. *The Phylogenetic Handbook: A Practical Approach to Phylogenetic Analysis and Hypothesis Testing*. Cambridge University Press, 210–266.
- Ronquist F, Teslenko M, van der Mark P, Ayres DL, Darling A, Höhna S, Larget B, Liu L, Suchard MA, Huelsenbeck JP. 2012.** MrBayes 3.2: Efficient Bayesian phylogenetic inference and model choice across a large model space. *Systematic Biology* **61**: 539–542.
- Rosen DE. 1979.** Fishes from the uplands and intermontane basins of Guatemala: Revisionary studies and comparative geography. *Bulletin of the American Museum of Natural History* **162**: 5.
- Saitou N, Nei M. 1987.** The neighbor-joining method: A new method for reconstructing phylogenetic trees. *Molecular Biology and Evolution* **4**: 406–425.
- Sakamoto S. 1974.** Intergeneric hybridization among three species of *Heterantherium*, *Eremopyrum* and *Hordeum*, and its significance for the genetic relationships within the tribe Triticeae. *New Phytologist* **73**: 341–350.
- Sakuma S, Pourkheirandish M, Matsumoto T, Koba T, Komatsuda T. 2009.** Duplication of a well-conserved homeodomain-leucine zipper transcription factor gene in barley generates a copy with more specific functions. *Functional & Integrative Genomics* **10**: 123–133.
- Sakuma S, Salomon B, Komatsuda T. 2011.** The domestication syndrome genes responsible for the major changes in plant form in the Triticeae crops. *Plant and Cell Physiology* **52**: 738–749.
- Salichos L, Rokas A. 2013.** Inferring ancient divergences requires genes with strong phylogenetic signals. *Nature* **497**: 327–331.
- Salmon A, Udall JA, Jeddelloh JA, Wendel J. 2012.** Targeted capture of homoeologous coding and noncoding sequence in polyploid cotton. *G3: Genes|Genomes|Genetics* **2**: 921–930.
- Sandve SR, Marcussen T, Mayer K, Jakobsen KS, Heier L, Steuernagel B, Wulff BBH, Olsen OA. 2015.** Chloroplast phylogeny of *Triticum/Aegilops* species is not incongruent with an ancient homoploid hybrid origin of the ancestor of the bread wheat D-genome. *New Phytologist* **208**: 9–10.
- Sang T. 2002.** Utility of low-copy nuclear gene sequences in plant phylogenetics. *Critical Reviews in Biochemistry and Molecular Biology* **37**: 121–147.
- Schliep KP. 2011.** phangorn: Phylogenetic analysis in R. *Bioinformatics* **27**: 592–593.
- Schneider J, Döring E, Hilu KW, Röser M. 2009.** Phylogenetic structure of the grass subfamily Pooideae based on comparison of plastid *matK* gene-3' *trnK* exon and nuclear ITS sequences. *Taxon* **58**: 405–424.
- Schulte LJ, Clark JL, Novak SJ, Jeffries SK, Smith JF. 2015.** Speciation within *Columnnea* section *Angustiflora* (Gesneriaceae): Islands, pollinators and climate. *Molecular Phylogenetics and Evolution* **84**: 125–144.
- Schwarz G. 1978.** Estimating the dimension of a model. *The Annals of Statistics* **6**: 461–464.

References

- Scornavacca C, Berry V, Lefort V, Douzery EJ, Ranwez V. 2008.** PhySIC_IST: Cleaning source trees to infer more informative supertrees. *BMC Bioinformatics* **9**: 413.
- Seberg O, Frederiksen S. 2001.** A phylogenetic analysis of the monogenomic Triticeae (Poaceae) based on morphology. *Botanical Journal of the Linnean Society* **136**: 75–97.
- Seberg O, Petersen G. 1998.** A critical review of concepts and methods used in classical genome analysis. *The Botanical Review* **64**: 372–417.
- Shendure J, Ji H. 2008.** Next-generation DNA sequencing. *Nature Biotechnology* **26**: 1135–1145.
- Simons KJ, Fellers JP, Trick HN, Zhang Z, Tai Y-S, Gill BS, Faris JD. 2006.** Molecular Characterization of the Major Wheat Domestication Gene Q. *Genetics* **172**: 547–555.
- van Slageren MW. 1994.** *Wild wheats: A monograph of Aegilops L. and Amblyopyrum (Jaub. & Spach) Eig (Poaceae)*. Wageningen Agricultural University Papers.
- de Smet R, Adams KL, Vandepoele K, van Montagu MCE, Maere S, van der Peer Y. 2013.** Convergent gene loss following gene and genome duplications creates single-copy families in flowering plants. *Proceedings of the National Academy of Sciences USA* **110**: 2898–2903.
- Smith JM. 1962.** Disruptive selection, polymorphism and sympatric speciation. *Nature* **195**: 60–62.
- Smith DR. 2015.** Mutation rates in plastid genomes: They are lower than you might think. *Genome Biology and Evolution* **7**: 1227–1234.
- Smith SA, Dunn CW. 2008.** Phyutility: A phyloinformatics tool for trees, alignments and molecular data. *Bioinformatics* **24**: 715–716.
- Soltis DE, Soltis PS. 1999.** Polyploidy: Recurrent formation and genome evolution. *Trends in Ecology and Evolution* **14**: 348–352.
- Soreng RJ, Davis JI, Doyle JJ. 1990.** A phylogenetic analysis of chloroplast DNA restriction site variation in Poaceae subfamily Pooideae. *Plant Systematics and Evolution* **172**: 83–97.
- Stamatakis A. 2014.** RAxML version 8: A tool for phylogenetic analysis and post-analysis of large phylogenies. *Bioinformatics* **30**: 1312–1313.
- Stebbins GL. 1956.** Taxonomy and the evolution of genera, with special reference to the family Gramineae. *Evolution*: 235–245.
- Steffen S, Ball P, Mucina L, Kadereit G. 2015.** Phylogeny, biogeography and ecological diversification of *Sarcocornia* (Salicornioideae, Amaranthaceae). *Annals of Botany* **115**: 353–368.
- Stegemann S, Keuthe M, Greiner S, Bock R. 2012.** Horizontal transfer of chloroplast genomes between plant species. *Proceedings of the National Academy of Sciences USA* **109**: 2434–2438.
- Stephens JD, Rogers WL, Heyduk K, Cruse-Sanders JM, Determann RO, Glenn TC, Malmberg RL. 2015a.** Resolving phylogenetic relationships of the recently radiated carnivorous plant genus *Sarracenia* using target enrichment. *Molecular Phylogenetics and Evolution* **85**: 76–87.
- Stephens JD, Rogers WL, Mason CM, Donovan LA, Malmberg RL. 2015b.** Species tree estimation of diploid *Helianthus* (Asteraceae) using target enrichment. *American Journal of Botany* **102**: 910–920.
- Stewart C-B. 1993.** The powers and pitfalls of parsimony. *Nature* **361**: 603–607.

- Stoof-Leichsenring KR, Bernhardt N, Pestryakova LA, Epp LS, Herzsuh U, Tiedemann R. 2014.** A combined paleolimnological/genetic analysis of diatoms reveals divergent evolutionary lineages of *Staurosira* and *Staurosirella* (Bacillariophyta) in Siberian lake sediments along a latitudinal transect. *Journal of Paleolimnology* **52**: 77–93.
- Strimmer K, Haeseler A von, Salemi M, Vandamme A-M. 2009.** Genetic distances and nucleotide substitution models. In: Lemey P, Salemi M, Vandamme A-M, eds. *The Phylogenetic Handbook: A Practical Approach to Phylogenetic Analysis and Hypothesis Testing*. Cambridge University Press, 111–141.
- Swenson MS, Suri R, Linder CR, Warnow T. 2012.** SuperFine: Fast and accurate supertree estimation. *Systematic Biology* **61**: 214–227.
- Swofford DL. 2002.** PAUP*. Phylogenetic analysis using parsimony (* and other methods). Version 4.b10. *Sinauer Associates, Sunderland Massachusetts*.
- Tavaré S. 1986.** Some probabilistic and statistical problems in the analysis of DNA sequences. *Lectures on Mathematics in the Life Sciences* **17**: 57–86.
- Than C, Ruths D, Nakhleh L. 2008.** PhyloNet: A software package for analyzing and reconstructing reticulate evolutionary relationships. *BMC Bioinformatics* **9**: 322.
- Thomas CA. 1971.** The genetic organization of chromosomes. *Annual Review of Genetics* **5**: 237–256.
- Tzvelev NN. 1976.** *Zlaki SSSR (Grasses of the Soviet Union)*. Leningrad, SSSR: Nauka.
- Vanneste K, van de Peer Y de, Maere S. 2013.** Inference of genome duplications from age distributions revisited. *Molecular Biology and Evolution* **30**: 177–190.
- Via S, West J. 2008.** The genetic mosaic suggests a new role for hitchhiking in ecological speciation. *Molecular Ecology* **17**: 4334–4345.
- Vogel JP, Garvin DF, Mockler TC, Schmutz J, Rokhsar D, Bevan MW, Barry K, Lucas S, Harmon-Smith M, Lail K, et al. 2010.** Genome sequencing and analysis of the model grass *Brachypodium distachyon*. *Nature* **463**: 763–768.
- Wagner CE, Harmon LJ, Seehausen O. 2012.** Ecological opportunity and sexual selection together predict adaptive radiation. *Nature* **487**: 366–369.
- Wang RRC, Bothmer R von, Dvorak J, Fedak G, Linde-Laursen I, Muramatsu M. 1994.** Genome symbols in the Triticeae (Poaceae). *Proceedings of the 2nd International Triticeae Symposium*, Logan, Utah, USA: 20–24.
- Wang Y, Wang X, Paterson AH. 2012.** Genome and gene duplications and gene expression divergence: A view from plants. *Annals of the New York Academy of Sciences* **1256**: 1–14.
- Watson L, Clifford HT, Dallwitz MJ. 1985.** The classification of Poaceae: Subfamilies and supertribes. *Australian Journal of Botany* **33**: 433–484.
- Welker CAD, Kellogg EA, Prado J. 2014.** Andropogoneae versus Sacchareae (Poaceae: Panicoideae): The end of a great controversy. *Taxon* **63**: 643–646.
- Wendel JF, Schnabel A, Seelanan T. 1995.** Bidirectional interlocus concerted evolution following allopolyploid speciation in cotton (*Gossypium*). *Proceedings of the National Academy of Sciences USA* **92**: 280–284.
- Whelan S, Liò P, Goldman N. 2001.** Molecular phylogenetics: State-of-the-art methods for looking into the past. *Trends in Genetics* **17**: 262–272.

References

- Wiley EO, Lieberman BS. 2011.** *Phylogenetics: Theory and Practice of Phylogenetic Systematics*. Hoboken, NJ, USA: John Wiley & Sons.
- Winkworth RC, Wagstaff SJ, Glenny D, Lockhart PJ. 2005.** Evolution of the New Zealand mountain flora: Origins, diversification and dispersal. *Organisms Diversity & Evolution* **5**: 237–247.
- Wright S. 1943.** Isolation by distance. *Genetics* **28**: 114.
- Xi Z, Liu L, Davis CC. 2015.** Genes with minimal phylogenetic information are problematic for coalescent analyses when gene tree estimation is biased. *Molecular Phylogenetics and Evolution* **92**: 63–71.
- Yamane K, Kawahara T. 2005.** Intra- and interspecific phylogenetic relationships among diploid *Triticum-Aegilops* species (Poaceae) based on base-pair substitutions, indels, and microsatellites in chloroplast noncoding sequences. *American Journal of Botany* **92**: 1887–1898.
- Yan C, Sun G. 2012.** Multiple origins of allopolyploid wheatgrass *Elymus caninus* revealed by *RPB2*, *PepC* and *TrnD/T* genes. *Molecular Phylogenetics and Evolution* **64**: 441–451.
- Yen C, Yang JL. 2009.** Historical review and prospect of taxonomy of tribe Triticeae Dumortier (Poaceae). *Breeding Science* **59**: 513–518.
- Yen C, Yang J-L, Yen Y. 2005.** Hitoshi Kihara, Áskell Löve and the modern genetic concept of the genera in the tribe Triticeae (Poaceae). *Acta Phytotaxonomica Sinica* **43**: 82–93.
- Yu H, Fan X, Zhang C, Ding C, Wang X, Zhou Y. 2008.** Phylogenetic relationships of species in *Pseudoroegneria* (Poaceae: Triticeae) and related genera inferred from nuclear rDNA ITS (internal transcribed spacer) sequences. *Biologia* **63**: 498–505.
- Zhang J. 2003.** Evolution by gene duplication: An update. *Trends in Ecology and Evolution* **18**: 292–298.
- Zimmermann T, Mirarab S, Warnow T. 2014.** BBCA: Improving the scalability of *BEAST using random binning. *BMC Genomics* **15**: S11.
- Zohary D, Hopf M, Weiss E. 2012.** *Domestication of Plants in the Old World: The Origin and Spread of Domesticated Plants in Southwest Asia, Europe, and the Mediterranean Basin*. Oxford University Press.

ACKNOWLEDGEMENTS

At this point I would like to express my sincere thanks to my supervisor Dr. Frank Blattner for his encouragements, patience, and all advises given during the entire project period and, therefore, that his office door is always open for us.

I am very thankful to Prof. Dr. Dirk Albach at the Carl von Ossietzky Universität Oldenburg for agreeing to supervise my Ph.D. thesis and for his help related to all bureaucratic matters.

I would like to thank Dr. Benjamin Kilian who provided the seed material. I am also grateful for all the advice and support he provided through my time as Ph.D. student.

I am deeply indebted to Brunhilde Wedemeier and Christina Koch for their great help with the greenhouse and fieldwork, and for the excellent technical assistance with the flow cytometric measurements. I am also grateful for invaluable practical advices from Jörg Fuchs and Petra Sarhanova when setting up the flow cytometer. I thank Dr. Klaus Pistrick and the entire herbarium staff at IPK i.e. Carola Kahlau, Ute Riedel, Birgit Schaefer, Martina Fischer for mounting the large number herbarium vouchers. Furthermore, I thank Dr. Klaus Pistrick for valuable discussions on nomenclatural issues.

I thank Ina Faustman, Manuela Knauff, Ute Krajewski, Katrin Trnka, Petra Oswald, Birgit Kränzlin, Brunhilde Wedemeier and Kerstin Wolf for the excellent technical assistance in the lab. I want to thank Dr. Lothar Altschmied and Dr. Axel Himmelbach who helped establishing the sequence capture protocol at IPK and Dr. Ronny Brandt for his reliability and ambitiousness when setting up the Illumina runs.

I thank Dr. Matthias Pfeifer, Dr. Klaus Mayer, Dr. Eva-Maria Willing, Dr. Korbinian Schneeberger for their assistance and helpful discussion in the initial decision-making which loci to enrich and I especially thank Eva-Maria Willing who performed the final bait design. I am grateful Dr. Eva-Maria Willing, Dr. Korbinian Schneeberger and, especially, Dr. Xue Dong for their essential contributions in setting up the pipeline for the on-target assembly. I thank Dr. Martin Mascher, Sebastian Beier and Thomas Schmutzer and Dr. Eva Bauer for kindly providing the genomic locations of the selected loci in the genetic maps of barley, wheat and rye.

I am deeply grateful to Dr. Hart Poskar for long afternoons and evenings he spent with me PERL scripting to automatize the initial steps of data handling. Thanks to him I learned how to solve following challenges on my own. I also thank him for valuable suggestions on the manuscript that helped to improve this thesis. I am also indebted to Dr. Hart Poskar and Christian Krause who taught me how to efficiently run jobs on the computer cluster of iDiv.

I would like to thank Dr. Jonathan Brassac for his invaluable contribution in setting up the coalescent-based analyses. I want to thank him for all lively discussions, his inexhaustible patience and providing constructive criticism that greatly improved this thesis. I also want to thank all members of the ETX working group for the warm working atmosphere.

Financial support from the DFG and the IPK Gatersleben is acknowledged.

I am grateful to all member of the Ph.D. Student Board of IPK. Next to jointly organizing events for the Ph.D. students at IPK, I made friends and had encouraging discussions that helped to get through difficult project phases. Particularly, I want to thank Jonathan Brassac, Arvid Diehn, Diana Gierth, Katja Herrmann, Markus Meier and Nicole Schmid.

I want to thank those who made the IPK Club a place to recover and to learn so much about different cultures and cuisines. I am grateful to Jonathan Brassac, Arvid Diehn, Takayoshii Ishii, Tiina Liiving, Hart Poskar, Martin Mau, André Marques, Celia Maria Municio, Quddoos ul Haq Muqaddasi, Marco Pellino, Mian Abdur Rehman Arif, Petra Sarhanova, Nicole Schmid and many others.

Finally, I am grateful to my parents, my sister, Sandra, Nancy and Annett for their permanent support and encouragements during all my studies.

ABBREVIATIONS

2C	DNA content of a diploid cell before DNA replication
AIC	Akaike information criterion
BCA	Bayesian concordance analysis
BI	Bayesian phylogenetic inference
BIC	Bayesian information criterion
BLAST	basic local alignment search tool
BLAT	Blast like alignment tool
bp	base pair
BWA	Burrows-Wheeler Alignment Tool
CV	coefficient of variation
DNA	deoxyribonucleic acid
ds	double-stranded
e.g.	<i>exempli gratia</i> , for example
ESS	effective sample size
ETS	external transcribed spacer
FCM	Flow cytometry
fl-cDNAs	full-length complementary DNAs
FSC	forward side scatter
Gb	giga base pairs
GTEE	gene tree estimation error
GTR	general time reversible model
HKY	Hasegawa, Kishino and Yano
i.e.	<i>id est</i> , that is
ICARDA	International Center for Agricultural Research in the Dry Areas
ICN	International Code of Nomenclature for algae, fungi and plants
ILS	incomplete lineage sorting
IPK	Leibniz Institute of Plant Genetics and Crop Research
IPNI	The International Plant Name Index
IR	inverted repeat
ITS	internal transcribed spacer
K80	Kimura 2-parameter
kb	kilo base pairs
Ma	million years ago

Mb	mega base pairs
MCC	maximum clade credibility
MCMC	Markov chain Monte Carlo
ML	Maximum-Likelihood
MRP	matrix representation with parsimony
MSA	multiple sequence alignment
NSGC	National Small Grain Collection of the US Department of Agriculture
NCBI	National Center for Biotechnology Information
NGS	next-generation sequencing
nrDNA	nuclear ribosomal DNA
PCR	polymerase chain reaction
PI	propidium iodide
PMT	photomultiplier tubes
qPCR	quantitative real-time PCR
RF	Robinson-Foulds
RNA	ribonucleic acid
SD	standard deviation
s.l.	<i>sensu lato</i> , in the broad sense
s.str.	<i>sensu stricto</i> , in the narrow sense
SMRT	single-molecule real time sequencing technology
SPRI	solid phase reversible immobilization
ss	single-stranded
SSC	side scatter
SSD	small-scale genome duplications
SYM	symmetrical model
USDA	US Department of Agriculture
USSR	Union of Soviet Socialist Republics
vs.	<i>versus</i> , against
WGD	whole genome duplication

FIGURES

Figure 1.1	Schematic overview of the cuvette in a flow cytometer	25
Figure 1.2	The principle of sequence capture	26
Figure 1.3	Overview of the Illumina sequencing principle	27
Figure 2.1	Growing of plant material.....	31
Figure 2.2	Exemplary histogram of fluorescence intensities from DNA content estimations	33
Figure 2.3	Schematic representation of the selection procedure for nuclear target loci	35
Figure 2.4	Design of sequence capture probes.....	36
Figure 2.5	Comparison of contig N50 values for the test samples.....	37
Figure 2.6	The sample preparation workflow.....	39
Figure 3.1	Comparison of sequencing output and capture success.....	50
Figure 3.2	Comparison of proportions of ambiguous positions per locus.....	51
Figure 3.3	Comparison of the Robinson-Foulds (RF) metric for 179 Bayesian gene trees.	55
Figure 3.4	Rooted phylogenetic network that summarises 245 quality-filtered single Bayesian consensus trees	57
Figure 3.5	Summarised coalescent-based species tree topology estimated from 245 ML gene trees	59
Figure 3.6	Calibrated species tree obtained from a multispecies coalescence analysis	60
Figure 3.7	Superimposed DENSITREE representation of species tree sets obtained from the binned Bayesian coalescence analysis.....	61
Figure 3.8	Phylogenetic tree derived from the nrDNA tandem-repeat region by Bayesian phylogenetic inference.....	63
Figure 3.9	Phylogenetic tree derived from the whole chloroplast sequence by Maximum-Likelihood	64
Figure S.1	Genome sizes of diploid Triticeae species determined by flow cytometry	129
Figure S.2	Recombination frequency per chromosome and locus according to the barley genetic map	130
Figure S.3	Characteristics of quality-filtered loci.....	131
Figure S.4	The distributions of Robinson-Foulds (RF) distances obtained from pairwise comparisons of individual Bayesian consensus trees	132
Figure S.5	Comparison of ML trees derived from concatenations of 14 and 19 low-copy number loci located on chromosome 1 and chromosome 2 in <i>Hordeum vulgare</i> , <i>Secale cereale</i> , and <i>Triticum aestivum</i>	133

Figure S.6 ML tree derived from concatenations of 18 low-copy number loci located on chromosome 3 in *Hordeum vulgare*, *Secale cereale*, and *Triticum aestivum* 134

Figure S.7 Rooted phylogenetic network constructed from 83 centromeric loci..... 135

Figure S.8 Rooted phylogenetic network constructed from 96 telomeric loci 136

Figure S.9 Summarised coalescent-based species tree estimated with Astral-II from 83 centromeric ML gene trees..... 137

Figure S.10 Summarised coalescent-based species tree estimated with Astral-II from 96 telomeric ML gene trees..... 138

TABLES

Table 1.1	List of genera and genomes in Triticeae.....	7
Table 2.1	Triticeae and outgroup species included in this study.....	30
Table 2.2	Genome size reference standards used in this study	32
Table 2.3	Species considered in tests of the bait library and different DNA fragment sizes.....	37
Table 2.4	Partitioning scheme and DNA substitution models for 28 telomeric loci..	46
Table 3.1	Results of flow cytometric measurements.....	48
Table 3.2	Alignment statistics for the nrDNA tandem-repeat region.....	53
Table S.2	Detailed information about selected accessions.....	119
Table S.2	Summary of statistical comparisons of Robinson-Foulds (RF) distances... ..	131

Tables in the electronic supplement:

Table E.1	Read statistics for 123 sequenced accessions
Table E.2	Capture efficiency for 40 single-exons
Table E.3	Identification of low-copy number loci
Table E.4	Summary statistics of all loci considered in bait design
Table E.5	Robinson-Foulds metric for 179 genes with known chromosomal location
Table E.6	Comparison of phylogenetic results

SUPPLEMENTARY INFORMATION

Table S.1 Detailed information of all selected accessions. Basic genomes (G), origin of accessions, and type of data generated during this project (GZ - genome size, SC - sequence capture, V - herbarium voucher) are given.

Species	Subspecies/variety/cultivar	Synonym	Accession	G	Material source	Country of origin	Data
<i>Aegilops bicornis</i> (Forssk.) Jaub. & Spach			AE 788	S	Genebank IPK Gatersleben	Libya	GZ/SC/V
			KU 5786		KOMUGI, Japan	Egypt	GZ/SC/V
	var. <i>bicornis</i>		AE 106		Genebank IPK Gatersleben	Russian Federation	GZ/SC/V
	var. <i>mutica</i> (Asch.) Eig		AE 1079		Genebank IPK Gatersleben	Jordan	GZ/SC/V
	subsp. <i>comosa</i> (Boiss.) Eig		AE 1255	M	Genebank IPK Gatersleben	Greece	GZ/SC/V
<i>Aegilops comosa</i> Sibth. & Sm.	subsp. <i>comosa</i> var. <i>comosa</i>		AE 1378		Genebank IPK Gatersleben	Greece	GZ/SC/V
	subsp. <i>heldreichii</i> (Boiss.) Eig		AE 783		Genebank IPK Gatersleben	Greece	GZ/SC/V
	var. <i>comosa</i>		PI 276970		USDA NSGC, Aberdeen, USA	Greece	GZ/SC/V
	var. <i>subventricosa</i>		PI 551042		USDA NSGC, Aberdeen, USA	Greece	GZ/V
	var. <i>subventricosa</i>		PI 551075		USDA NSGC, Aberdeen, USA	Greece	GZ/V
<i>Aegilops longissima</i> Schweinf. & Muschl.			AE 417	S	Genebank IPK Gatersleben	Israel	GZ/SC/V
			PI 604141		USDA NSGC, Aberdeen, USA	Israel	GZ/SC/V
			TA 1921		WGRC, Kansas, USA	Jordan	GZ/SC/V
	subsp. <i>longissima</i> (Eig) K. Hammer		AE 1078		Genebank IPK Gatersleben	Jordan	GZ/SC/V
	subsp. <i>sharonensis</i> var. <i>major</i> (Eig) K. Hammer		AE 133		Genebank IPK Gatersleben	NA	GZ/SC/V
<i>Aegilops markgrafii</i> (Greuter) K. Hammer			AE 1082	C	Genebank IPK Gatersleben	Syrian Arab Republic	GZ/V
			AE 1094		Genebank IPK Gatersleben	Turkey	GZ/V
			AE 1381		Genebank IPK Gatersleben	Greece	GZ/SC/V
			PI 254863		USDA NSGC, Aberdeen, USA	Iraq	GZ/SC/V
		PI 542208		USDA NSGC, Aberdeen, USA	Turkey	GZ/SC/V	

Table S.1 (continued).

Species	Subspecies/variety/cultivar	Synonym	Accession	G	Material source	Country of origin	Data
<i>Aegilops searsii</i> Feldman & Kislev ex K. Hammer			PI 551132		USDA NSGC, Aberdeen, USA	Greece	GZ/V
			PI 551136		USDA NSGC, Aberdeen, USA	Greece	GZ/V
			PI 596287		USDA NSGC, Aberdeen, USA	Turkey	GZ/SC/V
	var. <i>markgrafii</i> (Boiss.) K. Hammer		AE 744		Genebank IPK Gatersleben	Turkey	GZ/V
	var. <i>markgrafii</i> (Boiss.) K. Hammer		KP 2012106		Klaus Pistrick	Greece	GZ/SC/V
	var. <i>polypathera</i> (Boiss.) K. Hammer		AE 819		Genebank IPK Gatersleben	Turkey	GZ/V
			AE 1072	S	Genebank IPK Gatersleben	Jordan	GZ/V
			AE 1075		Genebank IPK Gatersleben	Jordan	GZ/SC/V
			AE 1083		Genebank IPK Gatersleben	Syrian Arab Republic	GZ/SC/V
			KU 14655		KOMUGI, Japan	Israel	GZ/SC/V
<i>Aegilops sharonensis</i> Schweinf. & Muschl.			PI 599142		USDA NSGC, Aberdeen, USA	Jordan	GZ/SC/V
			PI 599148		USDA NSGC, Aberdeen, USA	Syrian Arab Republic	GZ/SC/V
			AE 906	S	Genebank IPK Gatersleben	Israel	GZ/SC/V
			AE 319		Genebank IPK Gatersleben	Israel	GZ/V
<i>Aegilops speltoides</i> Tausch			AE 1085	B	Genebank IPK Gatersleben	Syrian Arab Republic	GZ/V
			AE 747		Genebank IPK Gatersleben	Turkey	GZ/V
			KU 7856		KOMUGI, Japan	Iraq	GZ/SC/V
			TA 1772		WGRC	Turkey	GZ/SC/V
	var. <i>speltoides</i>		PI 542245		USDA NSGC, Aberdeen, USA	Turkey	GZ/SC/V
	subsp. <i>ligustica</i> (Savign.) Zhuk.		AE 921		Genebank IPK Gatersleben	Iraq	GZ/V
	subsp. <i>ligustica</i> (Savign.) Zhuk.		PI 487231		USDA NSGC, Aberdeen, USA	Syrian Arab Republic	GZ/SC/V

Table S.1 (continued).

Species	Subspecies/variety/cultivar	Synonym	Accession	G	Material source	Country of origin	Data
<i>Aegilops tauschii</i> Coss.	subsp. <i>ligustica</i> var. <i>ligustica</i> (Savign.) Bormm.		AE 918		Genebank IPK Gatersleben	Turkey	GZV
	subsp. <i>ligustica</i> var. <i>ligustica</i> (Savign.) Bormm.		PI 486264		USDA NSGC, Aberdeen, USA	Turkey	GZ/ISCV
	subsp. <i>speltoides</i> (Savign.) Bormm.		AE 1064		Genebank IPK Gatersleben	Syrian Arab Republic	GZ/ISCV
	subsp. <i>speltoides</i> (Savign.) Bormm.		AE 900		Genebank IPK Gatersleben	Iraq	GZ/ISCV
	subsp. <i>speltoides</i> (Savign.) Bormm.		NGB 9854		Nordic Genetic Resource Center	NA	GZV
			46800	D	ICARDA	Turkey	GZ/ISC
<i>Aegilops tauschii</i> var. <i>meyeri</i> (Griseb.) Tzvelev			48508		ICARDA	Turkmenistan	GZV
			49116		ICARDA	Iran	GZ/ISCV
			AE 1039		Genebank IPK Gatersleben	Tajikistan	GZV
			AE 1090		Genebank IPK Gatersleben	Kazakhstan	GZV
			AE 956		Genebank IPK Gatersleben	Tajikistan	GZ/ISCV
			AE 1038		Genebank IPK Gatersleben	Tajikistan	GZV
			AE 1069		Genebank IPK Gatersleben	Syrian Arab Republic	GZ/ISCV
			AE 153	U	Genebank IPK Gatersleben	Iran	GZ/ISCV
			AE 740		Genebank IPK Gatersleben	Turkey	GZ/ISCV
			AE 811		Genebank IPK Gatersleben	Azerbaijan	GZ/ISCV
<i>Aegilops umbellulata</i> Zhuk.			PI 560774		USDA NSGC, Aberdeen, USA	Turkey	GZV
			PI 573516		USDA NSGC, Aberdeen, USA	Turkey	GZV
			PI560774		USDA NSGC, Aberdeen, USA	Turkey	GZV

Table S.1 (continued).

Species	Subspecies/variety/cultivar	Synonym	Accession	G	Material source	Country of origin	Data	
<i>Aegilops uniaristata</i> Vis.			AE 157	N	Genebank IPK Gatersleben	Former Soviet Union	GZ/SCV	
			AE 680		Genebank IPK Gatersleben	Italy	GZ/SCV	
			AE 156		Genebank IPK Gatersleben	Former Soviet Union	GZV	
			PI 276996		USDA NSGC, Aberdeen, USA	Turkey	GZ/SCV	
			PI 374326		USDA NSGC, Aberdeen, USA	Turkey	GZV	
			PI 554418		USDA NSGC, Aberdeen, USA	NA	GZV	
			PI 554419		USDA NSGC, Aberdeen, USA	Turkey	GZV	
			PI 554421		USDA NSGC, Aberdeen, USA	Turkey	GZV	
<i>Agropyron cristatum</i> (L.) Gaertn.			NB 2012012A	PP	Nadine Bernhardt	Russian Federation	GZV	
			PI 494615	P	USDA NSGC, Aberdeen, USA	Romania	GZ/SC	
			PI 598631	P	USDA NSGC, Aberdeen, USA	Kazakhstan	GZ/SC	
		subsp. <i>tarbagataicum</i> (N. Plotn.) Tzvelev		W6 25117	PP	USDA NSGC, Aberdeen, USA	Kazakhstan	GZV
<i>Amblyopyrum muticum</i> (Boiss.) Eig.			PI 560122	T	USDA NSGC, Aberdeen, USA	Turkey	GZ/SCV	
			PI 560124		USDA NSGC, Aberdeen, USA	Turkey	GZ/SCV	
			PI 560125		USDA NSGC, Aberdeen, USA	Turkey	GZ/SCV	
			PI 560126		USDA NSGC, Aberdeen, USA	Turkey	GZ/SCV	
			PI 636562		USDA NSGC, Aberdeen, USA	Turkey	GZ/SCV	
			PI 560121		USDA NSGC, Aberdeen, USA	Turkey	GZV	
			PI 598388		USDA NSGC, Aberdeen, USA	Turkey	GZV	
		var. <i>lofiacea</i> (Jaub. et Sp.) Eig		01C2100106		EVIGEZ, Czech Republic	Turkey	GZ/SCV

Table S.1 (continued).

Species	Subspecies/Variety/cultivar	Synonym	Accession	G	Material source	Country of origin	Data
<i>Australopyrum retrofractum</i> (Vickery) A. Löve			PI 531553	W	USDA NSGC, Aberdeen, USA	Australia	GZ/SCN
			PI 533013		USDA NSGC, Aberdeen, USA	Australia	GZ/SCN
			PI 533014		USDA NSGC, Aberdeen, USA	Australia	GZ/SCN
			PI 547363		USDA NSGC, Aberdeen, USA	Australia	GZ/SCN
<i>Brachypodium distachyon</i> (L.) P. Beauv.			Brachy 300		Andreas Houben, IPK Gatersleben	NA	GZ/SCN
			GRA 1085		Genebank IPK Gatersleben	Libya	GZ/SCN
<i>Dasyphyrum vilosum</i> (L.) P. Candargy			GRA 1020	V	Genebank IPK Gatersleben	Italy	GZ/SCN
			GRA 1027		Genebank IPK Gatersleben	Bulgaria	GZ/SCN
			GRA 2262		Genebank IPK Gatersleben	Turkey	GZV
			GRA 2707		Genebank IPK Gatersleben	Italy	GZV
			GRA 2991		Genebank IPK Gatersleben	Greece	GZV
			PI 368884		USDA NSGC, Aberdeen, USA	Turkey	GZ/SCN
			PI 470279		USDA NSGC, Aberdeen, USA	Turkey	GZV
			W6 19414		USDA NSGC, Aberdeen, USA	Bulgaria	GZ/SCN
			W6 21717		USDA NSGC, Aberdeen, USA	Ukraine	GZV
			W6 7267		USDA NSGC, Aberdeen, USA	Greece	GZV
		W6 7284		USDA NSGC, Aberdeen, USA	Greece	GZV	
		W6 7300		USDA NSGC, Aberdeen, USA	Greece	GZ/SCN	

Table S.1 (continued).

Species	Subspecies/variety/cultivar	Synonym	Accession	G	Material source	Country of origin	Data
<i>Erenopyrum distans</i> (K. Koch) Nevski			PI 193264	FdX	USDA NSGC, Aberdeen, USA	Afghanistan	GZISC/V
<i>Erenopyrum triticeum</i> (Gaertn.) Nevski			GRA 2250 PI 502364 W6 26631	Ft	Genebank IPK Gatersleben USDA NSGC, Aberdeen, USA USDA NSGC, Aberdeen, USA	Kazakhstan Russian Federation Kazakhstan	GZISC/V GZISC/V GZISC/V
<i>Henrardia persica</i> (Boiss.) C.E. Hubb.			PI 401347 PI 577112 PI 577113 RF 2012 1	O	USDA NSGC, Aberdeen, USA USDA NSGC, Aberdeen, USA USDA NSGC, Aberdeen, USA Reinhard Fritzsich	Iran Turkey Turkey Iran	GZISC/V GZISC/V GZISC/V GZISC/V
<i>Heteranthellium piliferum</i> (Banks & Sol.) Hochst.		<i>Heteranthellium</i> spp.	PI 314152 PI 401351 PI 401353 PI 401354	Q	USDA NSGC, Aberdeen, USA USDA NSGC, Aberdeen, USA USDA NSGC, Aberdeen, USA USDA NSGC, Aberdeen, USA	Uzbekistan Iran Iran Iran	GZISC/V GZISC/V GZISC/V GZISC/V
<i>Hordeum marinum</i> Huds. <i>Hordeum murinum</i> L. <i>Hordeum pubiflorum</i> Hook. f. <i>Hordeum vulgare</i> L.	subsp. <i>marinum</i> subsp. <i>glaucum</i> (Steud.) Tzvelev subsp. <i>pubiflorum</i> subsp. <i>spontaneum</i> (C. Koch) Theill cv. Morex		BCC 2006 BCC 2002 BCC 2028 FT11 Morex	Xa Xu I H H	International Barley Core Collection International Barley Core Collection International Barley Core Collection Benjamin Kilian, IPK Gatersleben Benjamin Kilian, IPK Gatersleben	Spain Tunisia Argentina NA NA	GZISC/V GZISC/V GZISC/V GZISC/V GZISC/V
<i>Psathyrostachys juncea</i> (Fisch.) Nevski			PI 222050 PI 476299 PI 565055	Ns	USDA NSGC, Aberdeen, USA USDA NSGC, Aberdeen, USA USDA NSGC, Aberdeen, USA	Afghanistan NA Russian Federation	GZISC/V GZV GZV

Table S.1 (continued).

Species	Subspecies/variety/cultivar	Synonym	Accession	G	Material source	Country of origin	Data
<i>Pseudoroegneria stipifolia</i> (Czern. ex Nevski) A. Löve			PI 565077		USDA NSGC, Aberdeen, USA	China	GZSCV
		<i>Psathyrostachys</i> spp.	PI 565080		USDA NSGC, Aberdeen, USA	Russian Federation	GZSCV
			PI 595135		USDA NSGC, Aberdeen, USA	China	GZSCV
			PI 598613		USDA NSGC, Aberdeen, USA	Kazakhstan	GZSCV
			PI 598615		USDA NSGC, Aberdeen, USA	Kazakhstan	GZV
			PI 619487		USDA NSGC, Aberdeen, USA	Mongolia	GZSC
			W6 19786		USDA NSGC, Aberdeen, USA	Mongolia	GZV
<i>Pseudoroegneria strigosa</i> (M. Bieb.) A. Löve			PI 325181	St	USDA NSGC, Aberdeen, USA	Russian Federation	GZSCV
			PI 440095	StX	USDA NSGC, Aberdeen, USA	Russian Federation	GZSCV
			PI 531751	StX	USDA NSGC, Aberdeen, USA	Ukraine	GZSCV
<i>Pseudoroegneria strigosa</i> (M. Bieb.) A. Löve			PI 499638		USDA NSGC, Aberdeen, USA	China	GZSCV
		subsp. <i>aegilopsides</i> (Drobow) A. Löve	W6 14049	St	USDA NSGC, Aberdeen, USA	Russian Federation	GZSCV
		subsp. <i>aegilopsides</i> (Drobow) A. Löve	PI 639805	StX	USDA NSGC, Aberdeen, USA	Mongolia	GZSCV
<i>Pseudoroegneria tauri</i> (Boiss. & Balansa) A. Löve			PI 595172	StX	USDA NSGC, Aberdeen, USA	China	GZSCV
			PI 401322	St	USDA NSGC, Aberdeen, USA	Iran	GZSC
			PI 401333		USDA NSGC, Aberdeen, USA	Iran	GZSCV
			PI 228389		USDA NSGC, Aberdeen, USA	Iran	GZSCV
		<i>Pseudoroegneria libanotica</i> (Hack.) D.R.Dewey			USDA NSGC, Aberdeen, USA	Iran	GZSCV
		subsp. <i>libanotica</i> (Hack.) A. Löve			USDA NSGC, Aberdeen, USA	Iran	GZSCV
		subsp. <i>libanotica</i> (Hack.) A. Löve	PI 330688		USDA NSGC, Aberdeen, USA	Iran	GZSCV

Table S.1 (continued).

Species	Subspecies/variety/cultivar	Synonym	Accession	G	Material source	Country of origin	Data
<i>Secale cereale</i> L.	subsp. <i>ilbanotica</i> (Hack.) A. Löve	<i>Pseudoroegneria ilbanotica</i> (Hack.) D.R.Dewey	PI 401274		USDA NSGC, Aberdeen, USA	Iran	GZISC/V
	subsp. <i>afghanicum</i> (Vavilov) K. Hammer		PI 618662	R	USDA NSGC, Aberdeen, USA	Armenia	GZISC/V
	subsp. <i>ancestrale</i> Zhuk.		PI 618664		USDA NSGC, Aberdeen, USA	Sweden	GZ/V
	subsp. <i>ancestrale</i> Zhuk.		PI 618665		USDA NSGC, Aberdeen, USA	NA	GZISC/V
	subsp. <i>ancestrale</i> Zhuk.		PI 618666		USDA NSGC, Aberdeen, USA	Turkey	GZ/V
	subsp. <i>rigidum</i> Vavilov & Antropov		PI 618669		USDA NSGC, Aberdeen, USA	Turkey	GZISC/V
<i>Secale strictum</i> (C. Presl) C. Presl	subsp. <i>segetale</i> Zhuk.		PI 618671		USDA NSGC, Aberdeen, USA	Turkey	GZISC/V
			R 1174	R	Genebank IPK Gatersleben	Bulgaria	GZ/V
	subsp. <i>kuprijanovii</i> (Grossh.) K. Hammer		R 1108		Genebank IPK Gatersleben	Kazakhstan	GZISC/V
<i>Secale vavilovii</i> Grossh.	subsp. <i>strictum</i> (Grossh.) K. Hammer		R 853		Genebank IPK Gatersleben	Italy	GZISC/V
			PI 253957	R	USDA NSGC, Aberdeen, USA	Afghanistan	GZISC/V
			R 1027		Genebank IPK Gatersleben	Italy	GZISC/V
<i>Taeniatherum caput-medusae</i> (L.) Nevski			CK 2011	Ta	Christina Koch	Greece	GZISC/V
			GRA 1126		Genebank IPK Gatersleben	Tajikistan	GZISC/V
			PI 577709		USDA NSGC, Aberdeen, USA	Turkey	GZ/V
			PI 577710		USDA NSGC, Aberdeen, USA	Turkey	GZ/V
	subsp. <i>crinitum</i> (Schreb.) Meldertis	<i>Taeniatherum crinitum</i> (Schreb.) Nevski	GRA 2570		Genebank IPK Gatersleben	Kazakhstan	GZISC/V

Table S.1 (continued).

Species	Subspecies/variety/cultivar	Synonym	Accession	G	Material source	Country of origin	Data
	<i>subsp. crinitum</i> (Schreb.) Meldertis		PI 567095		USDA NSGC, Aberdeen, USA	Turkey	GZ/SC/V
<i>Triticopyrum bessarabicum</i> (Savul. & Rayss) A. Löve			W6 10232	E ^b	USDA NSGC, Aberdeen, USA	Russian Federation	GZ/V
			W6 21890		USDA NSGC, Aberdeen, USA	Ukraine	GZ/SC
<i>Triticopyrum elongatum</i> (Host) D.R. Dewey			PI 109452	E ^o	USDA NSGC, Aberdeen, USA	Turkey	GZ/SC
			PI 401117		USDA NSGC, Aberdeen, USA	Iran	GZ/SC
			PI 535580		USDA NSGC, Aberdeen, USA	Tunisia	GZ/V
			PI 595139		USDA NSGC, Aberdeen, USA	China	GZ
<i>Triticum monococcum</i> L.			BGRC 43454	A	Genebank IPK Gatersleben	Germany	GZ/SC/V
			BGRC 43459		Genebank IPK Gatersleben	Switzerland	GZ/SC/V
<i>subsp. monococcum</i>			PI 119423		USDA NSGC, Aberdeen, USA	Turkey	GZ/SC/V
			TRI 13061		Genebank IPK Gatersleben	Italy	GZ/SC/V
			TRI 13612		Genebank IPK Gatersleben	Georgia	GZ/SC/V
			TRI 17054		Genebank IPK Gatersleben	Spain	GZ/V
<i>var. hohensteinii</i> Flaksb.			TRI 13483		Genebank IPK Gatersleben	Italy	GZ/V
<i>var. macedonicum</i> Papag.			TRI 2009		Genebank IPK Gatersleben	Turkey	GZ/V
<i>var. vulgare</i> Körn.			NGB 5164		Nordic Genetic Resource Center	NA	GZ/V
<i>var. vulgare</i> Körn.			TRI 1990		Genebank IPK Gatersleben	Albania	GZ/V
<i>var. vulgare</i> Körn.			TRI 1997		Genebank IPK Gatersleben	Bulgaria	GZ/V
<i>var. vulgare</i> Körn.			TRI 617		Genebank IPK Gatersleben	Albania	GZ/V
<i>var. vulgare</i> Körn.			TRI 645		Genebank IPK Gatersleben	Greece	GZ/V
<i>subsp. aegilopoides</i> (Link) Theil.			BGRC 20518		Genebank IPK Gatersleben	Balkans	GZ/SC/V
		<i>Triticum boeoticum</i> Boiss.*					

Table S.1 (continued).

Species	Subspecies/variety/cultivar	Synonym	Accession	G	Material source	Country of origin	Data
	subsp. <i>aegilopoides</i> (Link) Thell.	<i>Triticum boeoticum</i> Boiss.*	ID 379		WGRC, Kansas, USA	Lebanon	GZ/SCV
	subsp. <i>aegilopoides</i> (Link) Thell.	<i>Triticum boeoticum</i> Boiss.*	PI 272520		USDA NSGC, Aberdeen, USA	Hungary	GZ/SCV
	subsp. <i>aegilopoides</i> (Link) Thell.	<i>Triticum boeoticum</i> Boiss.*	PI 427451		USDA NSGC, Aberdeen, USA	Turkey	GZ/SCV
	subsp. <i>aegilopoides</i> (Link) Thell.	<i>Triticum boeoticum</i> Boiss.*	PI 427620		USDA NSGC, Aberdeen, USA	Turkey	GZ/SCV
	subsp. <i>aegilopoides</i> (Link) Thell.	<i>Triticum boeoticum</i> Boiss.*	PI 427627		USDA NSGC, Aberdeen, USA	Turkey	GZ/SCV
	subsp. <i>aegilopoides</i> (Link) Thell.		PI 427963		USDA NSGC, Aberdeen, USA	Turkey	GZV
	subsp. <i>aegilopoides</i> (Link) Thell.		PI 427986		USDA NSGC, Aberdeen, USA	Turkey	GZV
<i>Triticum urartu</i> Tumanian ex Gandilyan			PI 428184	A	USDA NSGC, Aberdeen, USA	Turkey	GZ/SCV
			PI 428317		USDA NSGC, Aberdeen, USA	Iran	GZ/SCV
			PI 428320		USDA NSGC, Aberdeen, USA	Lebanon	GZ/SCV
	var. <i>spontaneocalbum</i> Tumanian ex Dorof. & Filat.		TRI 17824		Genebank IPK Gatersleben	Lebanon	GZ/SCV
	var. <i>spontaneocalbum</i> Tumanian ex Dorof. & Filat.		TRI 18407		Genebank IPK Gatersleben	Syrian Arab Republic	GZ/SCV

Note: Species names used in phylogenetic analyses followed taxonomic treatments of the donor genebanks. Synonyms are given for accessions of taxa having different names in different genebanks. Asterisks indicate synonyms used in phylogenetic analyses based on morphological characterisation by AA Filatenko.

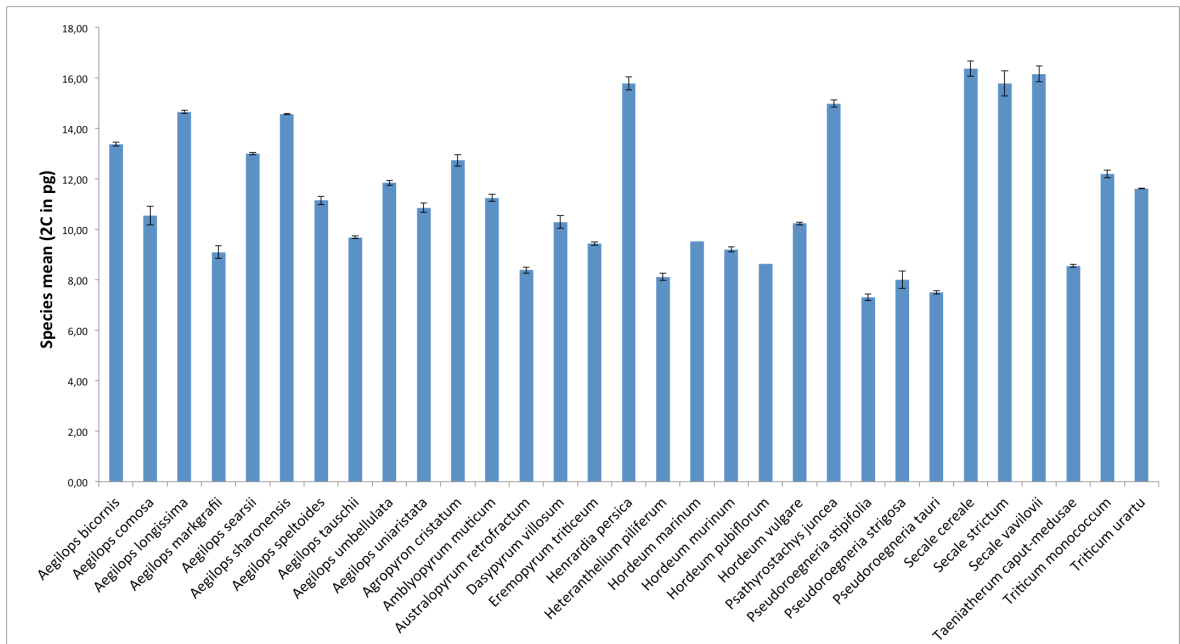


Figure S.1 Genome sizes of diploid Triticeae species determined by flow cytometry in the scope of this study. 2C species means in pg and standard deviations between measurements are shown.

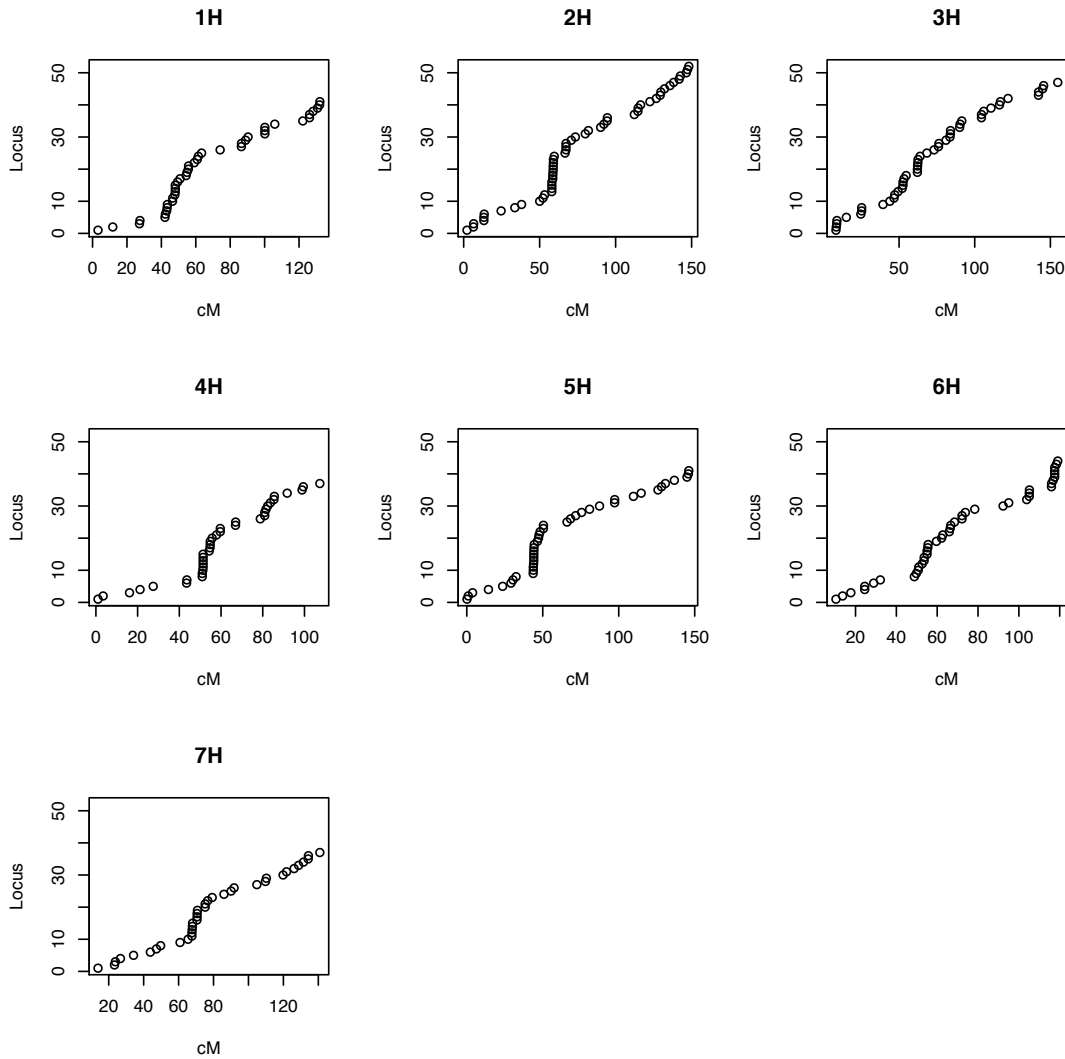


Figure S.2 The recombination frequencies in cM are plotted per chromosome for all captured loci with known position in the barley genetic map (Mascher *et al.*, 2013). Loci are ordered according to their position on the individual chromosomes, starting with short chromosome arms. The recombination gradient along the chromosomes can be described using a positive exponential function from centromer to telomer. Centromeric regions were defined for loci that have similar recombination frequencies and are surrounded by loci with a rapid drop or increase in recombination frequency. More detailed information can be found in **Table E.4**.

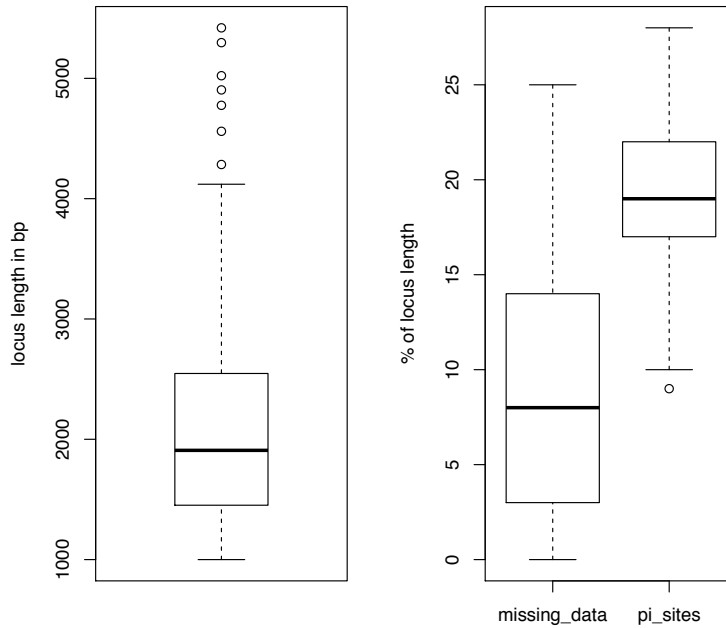


Figure S.3 Characteristics of quality-filtered loci. The length distribution in bp (left panel) and the distribution of missing data and parsimony-informative sites (pi-sites) in % (right panel) is shown for the 245 loci that were used for phylogenetic inferences, after exclusion of loci with a length <1000 bp, missing data of >25 % and less than 150 parsimony-informative positions.

Table S.2 Summary of statistical comparisons of Robinson-Foulds (RF) distances. Bayesian consensus trees were inferred from individual gene alignments. The distributions of RF distances from pairwise consensus trees comparisons were compared for chromosome-based datasets for centromeric and telomeric loci and for all loci combined. The Welch Two Sample t-test was used for normal-distributed datasets and the Wilcoxon rank sum test for non-normal distributed datasets to test the hypothesis if the RF distributions of centromeric and telomeric loci have the same means.

Test/Dataset	Chr 1	Chr 2	Chr 3	Chr 4	Chr 5	Chr 6	Chr 7	All
Shapiro-Wilk normality test	0.5673	0.0074	0.0036	0.2002	0.6981	0.6391	0.0552	0.1888
Welch Two Sample t-test	0.0003	-		1.97E-005	9.43E-06	0.9597	0.0008	2.2E-16
Wilcoxon rank sum test	-	2.2E-16	2.54E-09	-	-	-	-	-

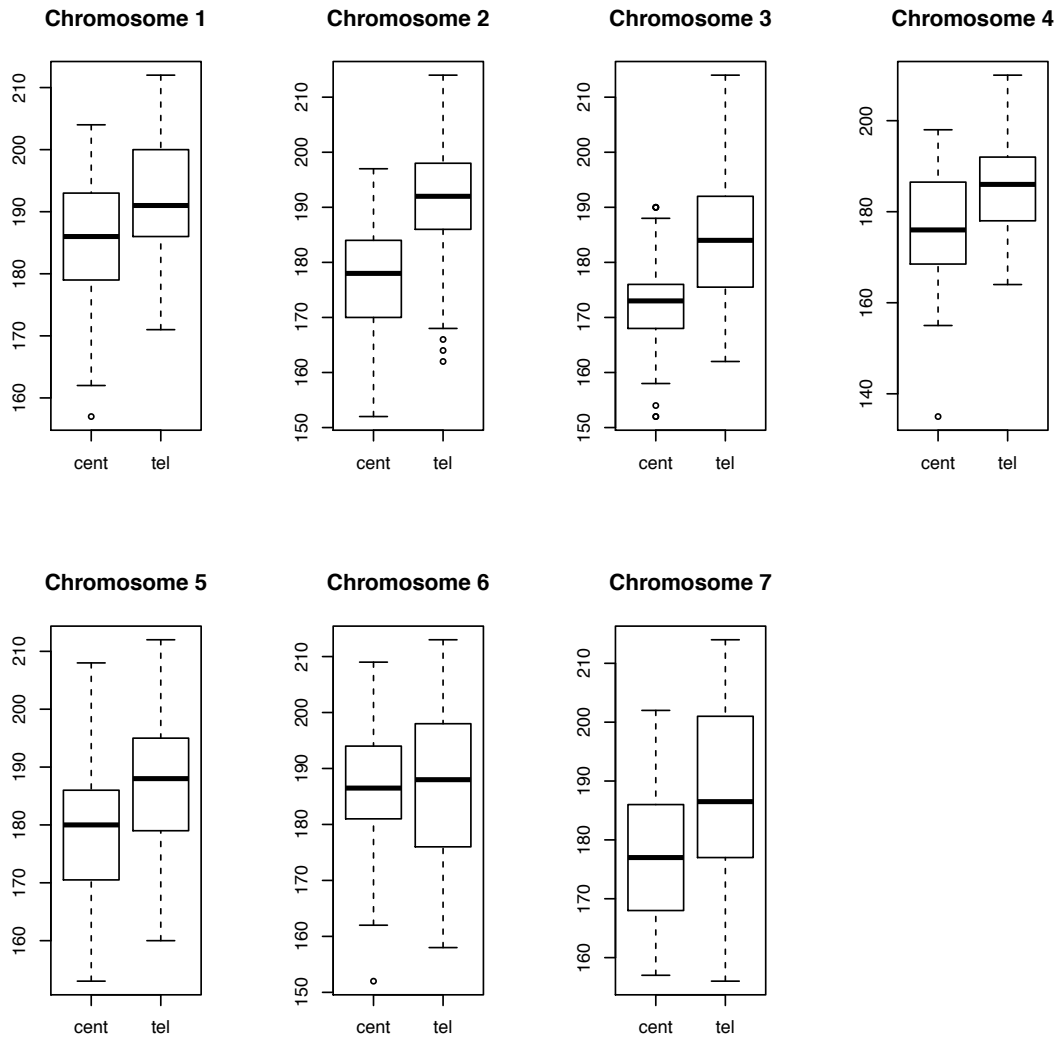


Figure S.4 The distributions of Robinson-Foulds (RF) distances obtained from pairwise comparisons of individual Bayesian consensus trees. The RF distances were plotted for centromeric compared to telomeric loci for the same chromosome.



Figure S.5 Comparison of ML trees derived from concatenations of 14 and 19 low-copy number loci that are located on chromosome 1 (left) and chromosome 2 (right) in *Hordeum vulgare*, *Secale cereale*, and *Triticum aestivum*, respectively. *Brachypodium distachyon* and *Bromus tectorum* were included as outgroups. Bootstrap support values are depicted next to the nodes if they were lower than 100. Monophyletic clades of the same species or genus were collapsed. The size of the clade is proportional to the number of included accessions. Taxa involved in topological conflicts between the two trees are connected with solid lines.



Figure S.6 ML tree derived from concatenations of 18 low-copy number loci that are located on chromosome 3 in *Hordeum vulgare*, *Secale cereale*, and *Triticum aestivum*, respectively. *Brachypodium distachyon* and *Bromus tectorum* were included as outgroups. Bootstrap support values are depicted for all nodes. Accession names follow the taxonomic treatment used in the donor genebanks of the utilised seed material.



Figure S.7 Rooted phylogenetic network constructed from 83 centromeric loci. The network was built using a cluster network algorithm that summarises single Bayesian gene trees with *Brachypodium distachyon* as outgroup after application of a source tree correction to keep only strongly supported conflicts. Accession names follow the taxonomic treatment used in the donor genebanks of the utilised seed material.

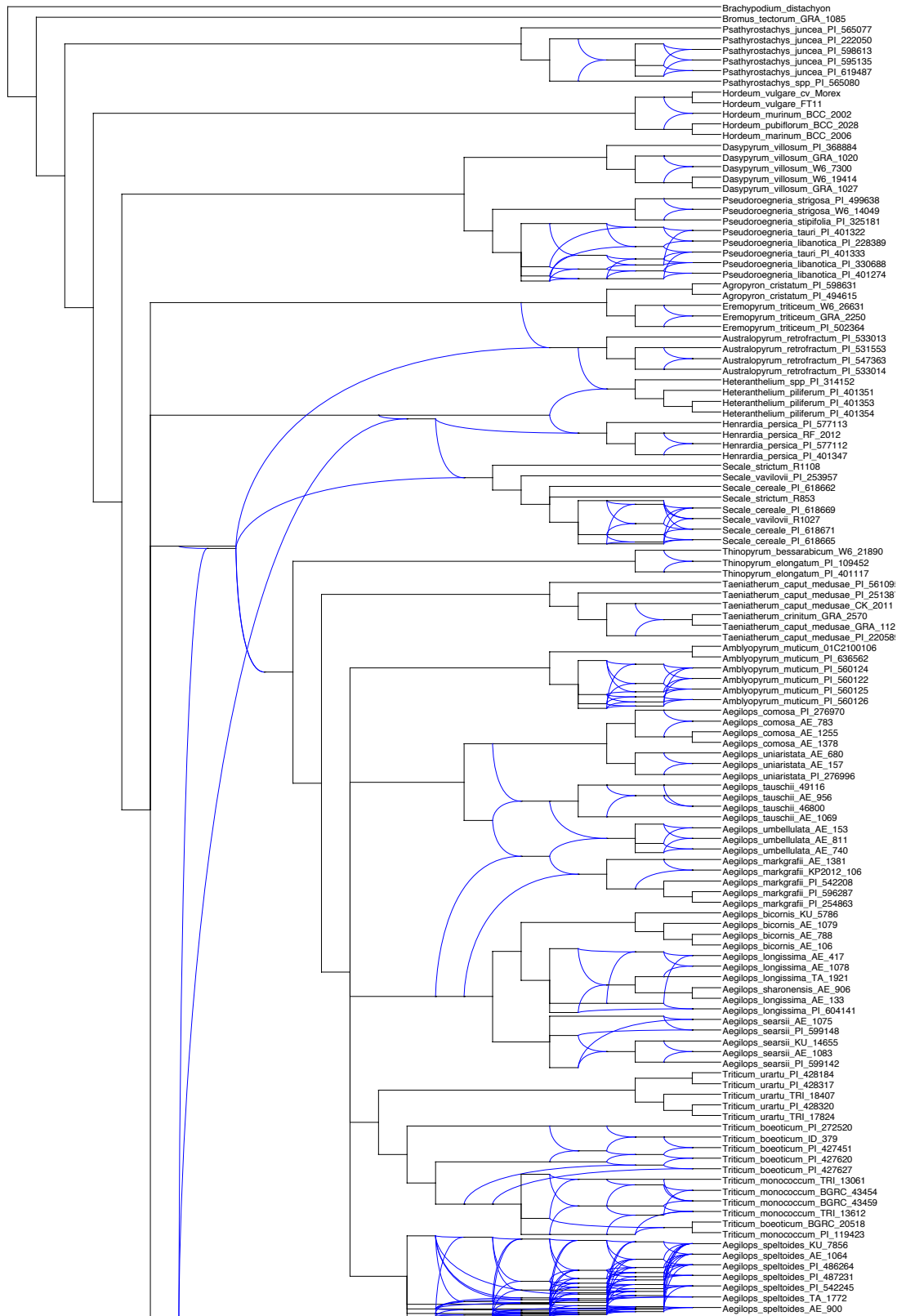


Figure S.8 Rooted phylogenetic network constructed from 96 telomeric loci. The network was built using a cluster network algorithm that summarises single Bayesian gene trees with *Brachypodium distachyon* as outgroup after application of a source tree correction to keep only strongly supported conflicts. Accession names follow the taxonomic treatment used in the donor genebanks of the utilised seed material.

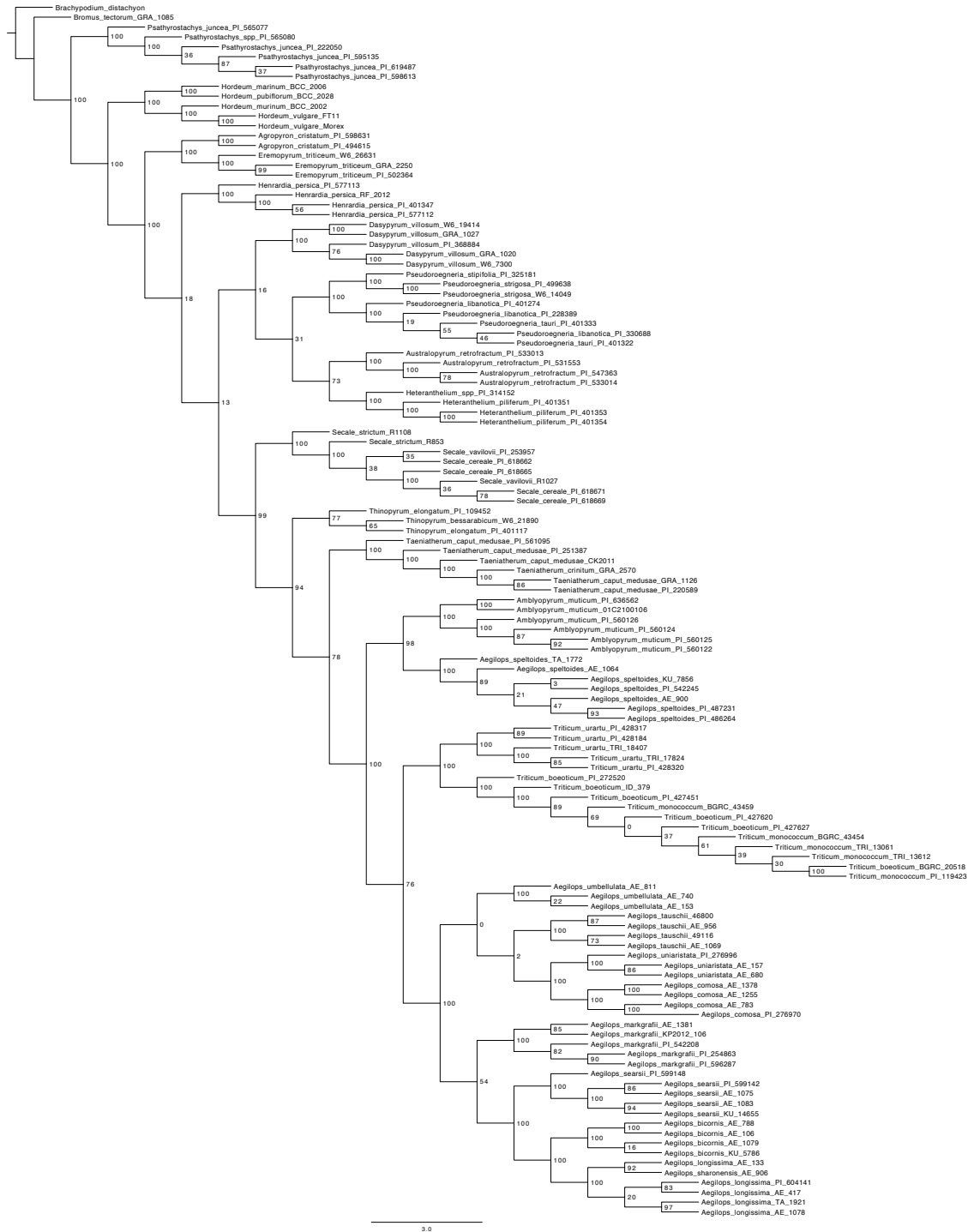


Figure S.9 Summarised coalescent-based species tree estimated with Astral-II from 83 centromeric ML gene trees with multilocus bootstrapping. Bootstrap support values are depicted for each node. Accession names follow the taxonomic treatment under use in the donor genebanks of the used seed material.

Supplementary information

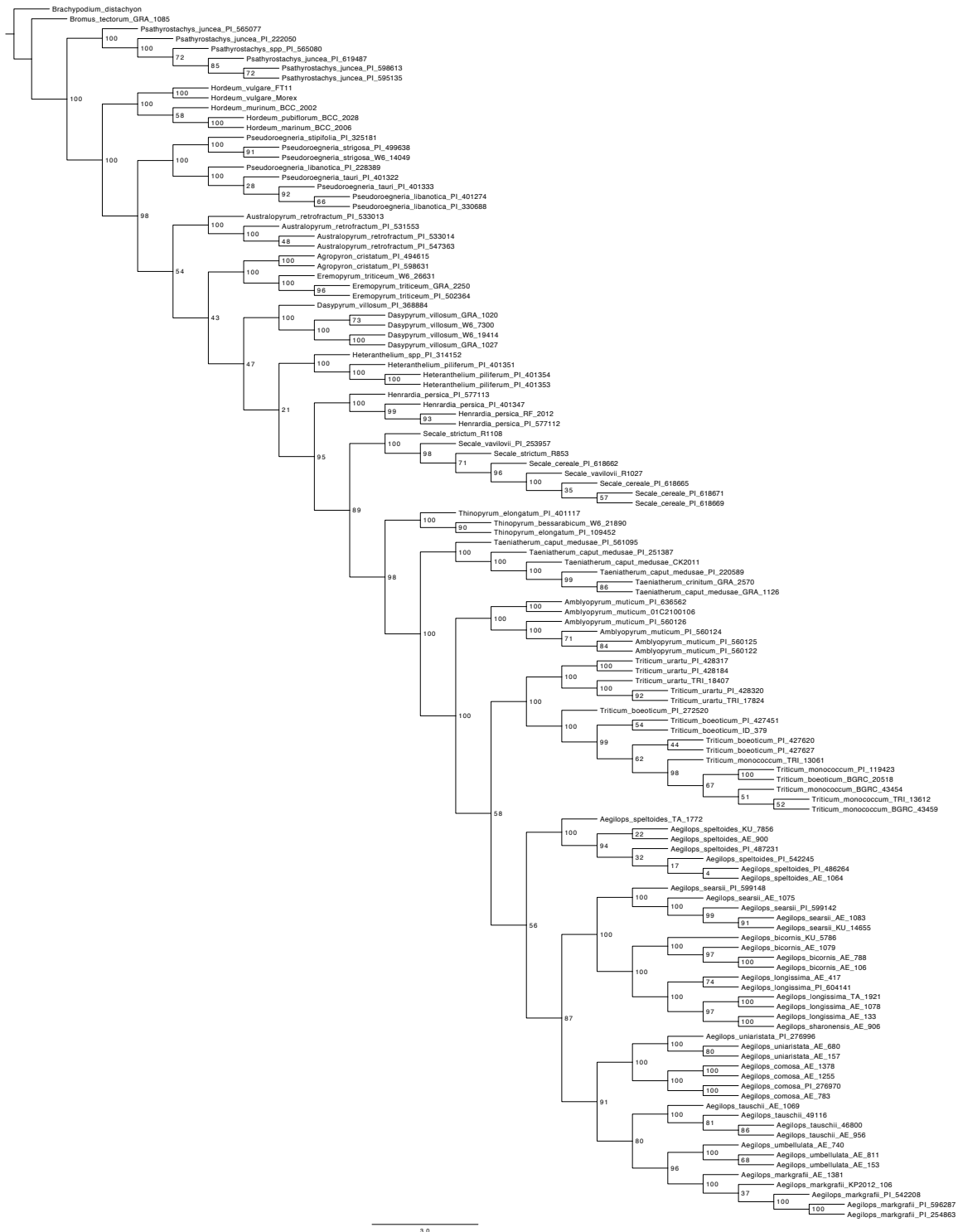


Figure S.10 Summarised coalescent-based species tree estimated with Astral-II from 96 telomeric ML gene trees with multilocus bootstrapping. Bootstrap support values are depicted for each node nodes. Accession names follow the taxonomic treatment used in the donor genebanks of the utilised seed material.

CURRICULUM VITAE & PUBLICATIONS

PERSONAL INFORMATION

Name Nadine Bernhardt

Date of birth 31st August 1985

Nationality German

Residency Steinholzstraße 6
D-06484 Quedlinburg
Germany

STUDY AND PROFESSIONAL EXPERIENCE

Jun 2011 – present Ph.D. Student at Leibniz Institute of Plant Genetics and Crop Research (IPK), Gatersleben

“Analysis of phylogenetic relationships among Triticeae grasses”

Apr 2010 - Feb 2011 Master thesis: “Genetic assessment of environmental freshwater samples from northern Yakutia (Arctic Russia)” in collaboration with the Alfred-Wegener Institute (AWI) Potsdam

Oct 2009 - Jan 2011 Scientific assistant in the unit of Evolutionary Biology at the University of Potsdam

Apr 2009 - Sept 2009 Scientific assistant in the unit of Evolutionary Ecology at the Leibniz Institute for Zoo- and Wildlife Research, Berlin

Nov 2008 – Feb 2011 Member of the “Evolution across Scales” core group (Master program funded by Volkswagen Foundation at the University of Potsdam)

Oct 2008 - Feb 2011 Study of Cellular and Molecular Biology at the University of Potsdam
Degree: Master of Science

Oct 2005 - Sept 2008 Study of Life Science at the University of Potsdam
Degree: Bachelor of Science

Bachelor thesis:
“Phylogeny and phylogeography of Southern Chinese cave crickets of the genus *Diestrammena*”

SOCIAL COMMITMENT AT IPK (selected contributions)

Jun 2011 – Oct 2014

Member of the Ph.D. Student Board (PSB) at IPK
Gatersleben:

Accountant for PSB budget

Plant Science Student Conference (PSSC) organisations

Invitation of international guest speakers

Public relations

PUBLICATIONS

Bernhardt N. 2015. Taxonomic treatments of Triticeae and the wheat genus *Triticum* In: Molnar M, Ceoloni C, Doležel J, eds. *Alien Introgression in Wheat: Cytogenetics, Molecular Biology, and Genomics*. Switzerland: Springer International Publishing: in press.

Diehn TA, Pommerrenig B, Bernhardt N, Hartmann A, Bienert GP. 2015. Genome-wide identification of aquaporin (AQP) encoding genes in cabbage (*Brassica oleracea*) sheds light on AQP evolution in *Brassica* crops and Arabidopsis. *Frontiers in Plant Science* **6**:166.

Stoof-Leichsenring KR, Bernhardt N, Pestryakova LA, Epp LS, Herzschuh U, Tiedemann R. 2014. A combined paleolimnological/genetic analysis of diatoms reveals divergent evolutionary lineages of *Staurosira* and *Staurosirella* (Bacillariophyta) in Siberian lake sediments along a latitudinal transect. *Journal of Paleolimnology* **52**: 77–93.

Ketmaier V, Di Russo C, Rampini M, Bernhardt N, Tiedemann R, Cobolli C. 2013. Molecular divergence and evolutionary relationships among Aemodogryllinae from Southern China, Laos and Thailand (Orthoptera, Rhaphidophoridae). *Subterranean Biology* **10**: 25–35.

Eigenständigkeitserklärung

Ich versichere hiermit, dass ich die vorliegende Arbeit selbständig verfasst und nur die angegebenen Quellen und Hilfsmittel benutzt habe. Stellen, die anderen Werken wörtlich oder inhaltlich entsprechen wurden als solche kenntlich gemacht.

Nadine Bernhardt

Gatersleben, den 30. Oktober 2015

Table E.1. The number of all Illumina reads and the number of reads mapping to the barley genome assembly as reference, the nrDNA unit and the chloroplast genome are given for each accession. Also the maximum read length and the coverage are shown.

Genus	Species	Accessions	#All reads		#Reads mapped to barley genome	#Reads mapped on target loci	Coverage of target loci	#Reads mapping to ETS	Coverage ETS	#Nucleotides mapping to chloroplast*	#Approximate number of reads	
			with length	Maximum read length							mapping to chloroplast*	Coverage chloroplast*
Aegilops	bicornis	AE106	2342636	101	854558	505773	49	2519	35	1554051	155411	
Aegilops	bicornis	AE1079	980490	251	240225	118928	18	2023	50	2392624	239397	
Aegilops	bicornis	AE1078	1382684	251	413177	233628	23	3708	50	1234083	123419	
Aegilops	bicornis	KU5786	1052112	251	258471	152564	23	1894	45	1634602	163482	
Aegilops	comosa	AE1255	1662111	101	6030390	3235384	35	2686	36	1723613	1723613	
Aegilops	comosa	AE1378	1040022	251	309851	162602	18	892	12	2105078	210515	
Aegilops	comosa	AE783	1370520	101	509226	236718	23	2056	28	1803319	1803319	
Aegilops	comosa	PI276970	1535036	101	528101	383207	38	2905	39	1904319	1904319	
Aegilops	longissima	AE1078	1531104	101	538684	241400	24	1700	23	2068545	206855	
Aegilops	longissima	AE1533	1509868	101	545028	318715	19	2417	32	2293375	2293375	
Aegilops	longissima	AE147	1104536	251	251003	139024	20	1781	43	226021	226601	
Aegilops	longissima	PI604141	909718	251	220470	105610	16	2023	50	2660275	2660319	
Aegilops	longissima	TA1921	2157408	101	622930	325399	32	6515	88	1883917	1883914	
Aegilops	markgrafii	AE1381	1417326	101	489891	272380	27	5520	74	2046224	2046215	
Aegilops	markgrafii	KP2012106	148212	101	171710	286940	28	551	51	1816247	1816247	
Aegilops	markgrafii	PI254863	75344	101	255370	163241	16	1323	18	582532	582532	
Aegilops	markgrafii	PI542208	1951450	101	684006	512817	50	3061	41	1202975	1202975	
Aegilops	markgrafii	PI969287	1445684	101	459007	311235	30	4983	67	694642	69465	
Aegilops	searsii	AE1075	1279234	101	484919	225710	22	1075	14	452369	4524	
Aegilops	searsii	AE1083	2854684	101	1047749	560236	55	5457	74	3038953	3038953	
Aegilops	searsii	KU14655	2034700	101	732409	407763	40	2640	34	1851415	1851415	
Aegilops	searsii	PI991142	2056704	101	765096	345100	34	2454	33	2087533	2087515	
Aegilops	searsii	PI991148	531734	251	156184	89289	13	1164	26	1165526	1165526	
Aegilops	sharonensis	AE908	1442400	101	503504	240256	23	2884	39	1931488	1931514	
Aegilops	speltoides	PI244245	6087670	101	1740356	1012503	99	56968	622	4893515	4893536	
Aegilops	speltoides	AE1064	1453114	101	453482	216480	21	3334	34	223659	223659	
Aegilops	speltoides	AE900	1345864	101	470331	218185	21	2255	29	1434063	1434110	
Aegilops	speltoides	KU7856	1025276	251	236703	134480	20	3663	79	2053936	205395	
Aegilops	speltoides	PH48264	1282114	101	768132	350945	34	6177	76	3302967	3303024	
Aegilops	speltoides	PH487231	1045002	101	369587	269169	26	1597	20	56904	56964	
Aegilops	speltoides	TA172	1045002	101	332923	203560	17	NA	NA	620183	620183	
Aegilops	tauschii	49116	1044804	251	351121	211862	25	1442	26	998422	99847	
Aegilops	tauschii	46800	5246326	101	1589953	1207088	118	11988	166	4312866	431291	
Aegilops	tauschii	AE1069	808876	101	302543	161792	16	3937	52	156778	1567811	
Aegilops	tauschii	AE956	1609978	101	582186	331210	32	2205	29	1813419	1813419	
Aegilops	umbellulata	AE1070	1527133	101	583048	293509	28	3948	53	1811904	1811913	
Aegilops	umbellulata	AE153	1458722	101	542828	293716	29	3279	44	2107632	2107615	
Aegilops	umbellulata	AE740	887398	251	211695	134318	20	3223	76	1520525	1520611	
Aegilops	umbellulata	AE811	550552	251	148580	67980	10	2417	45	1921929	1921919	
Aegilops	uniaristata	AE157	1526276	101	515763	329243	32	5028	68	1816247	1816213	
Aegilops	uniaristata	AE930	1395556	101	463024	241502	33	3189	34	91603	91603	
Aegilops	uniaristata	PI276996	1504362	101	503372	312159	31	3783	51	1057737	1057787	
Aegilops	mutica	O1C2100106	1137568	101	386021	238650	23	1195	15	1073190	107328	
Agropyron	cristatum	NA94615	1506226	101	524258	283810	28	602	8	1913960	1913919	
Agropyron	cristatum	PI98631	1548816	101	556337	278100	27	1913	25	1350940	1350910	
Amblyopyrum	muticum	PI5680122	4271322	101	2715127	171214	14	1284	16	229710	229710	
Amblyopyrum	muticum	PI5680124	450520	101	234269	96141	14	2477	31	1250849	1250819	
Amblyopyrum	muticum	PI5680125	1006444	251	264058	158886	14	3333	67	6251214	6251245	
Amblyopyrum	muticum	PI5680126	766074	251	182628	70601	10	4530	90	4080578	4080630	
Amblyopyrum	muticum	PI636562	1471886	101	525984	195808	19	2480	31	2978353	29784	
Amblyopyrum	retrofractum	PI533013	1532024	101	316312	252062	25	2186	28	95620	95620	
Amblyopyrum	retrofractum	PI533013	985110	251	247806	176466	26	2743	62	1819135	1819112	
Amblyopyrum	retrofractum	PI533014	1558592	101	586865	369408	36	2175	28	1810995	1811013	
Amblyopyrum	retrofractum	PI547363	1471110	101	540757	347568	34	1729	22	1668686	1668712	
Brachypodium	dactylochyon	GR1020	6742070	101	1457568	1195077	115	90175*	1211*	NA	NA	
Brachypodium	dactylochyon	GRA1005	554505	101	249912	146790	14	16170	20	72659	7267	
Dasyphyllum	villosum	PI20402	1224502	101	382412	148281	15	1566	19	2998620	2998322	
Dasyphyllum	villosum	PIA1027	1268702	101	423080	207802	20	4051	49	1747466	1747513	
Dasyphyllum	villosum	PI368884	1441982	101	488427	259931	25	2322	28	1149647	114968	
Dasyphyllum	villosum	WE19414	1051818	251	268143	111864	16	2240	48	4520841	4520833	
Dasyphyllum	villosum	W67300	1522714	101	459882	243591	24	1885	23	1779382	1779382	
Dasyphyllum	villosum	PI193284	1465150	101	483007	271592	26	2143	33	1481818	1481818	
Eremopyrum	triticeum	GRA2250	1469540	101	547982	227483	22	1999	27	3268324	3268324	
Eremopyrum	triticeum	PI502364	1470992	101	501062	318177	31	2173	29	1034305	103438	
Eremopyrum	triticeum	WE26631	1898994	101	318876	87225	9	7092	95	1991411	1991411	
Henardia	persica	PH401547	1483936	101	476382	179821	18	3884	49	2621621	2621619	
Henardia	persica	PI571112	2431874	101	751810	429712	37	2338	37	2576102	2576102	
Henardia	persica	PI577113	1513262	101	367952	113365	11	4669	59	1511631	1511611	
Henardia	persica	RF2012	1601610	101	571886	322213	23	978	12	2792720	2792720	
Heteranthellium	pilliferum	PH401351	1229914	101	460850	259566	25	2675	35	2713430	2713420	
Heteranthellium	pilliferum	PH401353	2057022	101	707318	425131	42	5176	65	1734538	1734513	
Heteranthellium	pilliferum	PH401354	2677113	101	819340	453348	45	6493	83	3263653	3263653	
Heteranthellium	sp.	PI314152	1581468	101	558709	310184	30	3246	41	1327508	1327508	
Hordeum	marinum	BCC2006	1444234	101	606384	309059	30	3029	43	2366394	2366394	
Hordeum	marinum	BCC2002	2210648	101	932454	498123	49	2884	41	3805947	3805928	
Hordeum	pubiflorum	BCC2028	9023276	101	3179106	2160154	213	15429	208	7475277	7475354	
Hordeum	spodiopogon	FT11	1111	101	8136324	519019	49	43304	319	8456888	8456888	
Hordeum	vulgare	Morex	6140588	101	3023222	1546686	154	40929	447	5894289	5894843	
Psathyrostachys	juncea	PI222050	1142906	101	415345	193001	19	844	12	1105106	110518	
Psathyrostachys	juncea	PI565077	1069284	251	264735	142507	21	935	21	1743918	1743913	
Psathyrostachys	juncea	PI595135	1340214	101	455838	246050	24	1453	21	1196212	119628	
Psathyrostachys	juncea	PI598813	1270724	101	423565	223586	22	1011	11	9237398	9237398	
Psathyrostachys	juncea	PI619487	986792	101	328030	185385	18	950	13	916135	91617	
Psathyrostachys	juncea	PI565080	1851384	101	697783	345370	34	2815	40	2402855	2402917	
Pseudoroegneria	libanotica	PI228389	825106	101	302083	188898	19	967	12	963807	96387	
Pseudoroegneria	libanotica	PI230688	3483976	101	1187769	861718	84	5382	69	1036325	103638	
Pseudoroegneria	stipifolia	PH401274	803731	101	269661	151106	15	1304	20	3921816	3921816	
Pseudoroegneria	stipifolia	PI325181	2668316	101	932961	503646	49	2093	27	2362960	2363017	
Pseudoroegneria	stipifolia	PH440095	1496784	101	539406	441184	43	1410	18	600712	60074	
Pseudoroegneria	stipifolia	PI531751	1542944	101	561863	409467	40	1050	13	905166	905166	
Pseudoroegneria	stipifolia	PH499638	1183568	101	424706	289935	28	1026	13	718579	71867	
Pseudoroegneria	stipifolia	PI951172	1547156	101	515752	312357	32	943	11	1657152	1657152	
Pseudoroegneria	stipifolia	PI639805	1508014	101	602816	378524	37	761	9	1256505	1256519	
Pseudoroegneria	stipifolia	WE14049	1704892	101	599961	391032	38	1341	17	1350132	1350130	
Pseudoroegneria	tauri	PH401322	990396	101	234353	91509	9	2399	31	1068746	106878	
Pseudoroegneria	tauri	PH401333	1738204	101	584205	310916	31	2851	37	2960173	296021	
Secale	cereale	PI61862	618350	251	189223	92961	14	2479	28	1412815	1412810	
Secale	cereale	PI618665	1403368	101	370709	132819	13	3625	44	1657273	1657312	
Secale	cereale	PI618669	2144668	101	697028	352522	25	7048	84	3626396	362624	
Secale	cereale	PI618671	1128554	101	339038	162969	16	1354	16	1099046	109908	
Secale	cereale	R1108	1513528									

Table E.2 Capture performance per accession assessed using 40 "single exons" (i.e. exons that are separated from other exons by more than 600 bp intronic sequences).

Locus	Accession	Mapped exon length in barley (bp)	Assembled exon length (bp)	% of mapped exon length that could be assembled	Extended target (bp)
AK249824.1	Aegilops_bicornis_AE106	2054	2395	117%	601
AK249824.1	Aegilops_bicornis_AE1079	2054	2192	107%	601
AK249824.1	Aegilops_bicornis_AE788	2054	2345	114%	601
AK249824.1	Aegilops_bicornis_KU-5786	2054	2205	107%	601
AK249824.1	Aegilops_comosa_AE1255	2054	2409	117%	601
AK249824.1	Aegilops_comosa_AE1378	2054	2225	108%	601
AK249824.1	Aegilops_comosa_AE783	2054	2445	119%	601
AK249824.1	Aegilops_comosa_PI276970	2054	2182	106%	601
AK249824.1	Aegilops_longissima_AE1078	2054	2407	117%	601
AK249824.1	Aegilops_longissima_AE133	2054	2377	116%	601
AK249824.1	Aegilops_longissima_AE417	2054	2253	110%	601
AK249824.1	Aegilops_longissima_PI604141	2054	2166	105%	601
AK249824.1	Aegilops_longissima_TA1921	2054	2314	113%	601
AK249824.1	Aegilops_markgrafii_AE1381	2054	2394	117%	601
AK249824.1	Aegilops_markgrafii_KP-2012-106	2054	2257	110%	601
AK249824.1	Aegilops_markgrafii_PI254863	2054	2173	106%	601
AK249824.1	Aegilops_markgrafii_PI542208	2054	2410	117%	601
AK249824.1	Aegilops_markgrafii_PI596287	2054	2430	118%	601
AK249824.1	Aegilops_mutica_01C2100106	2054	2411	117%	601
AK249824.1	Aegilops_searsii_AE1075	2054	2280	111%	601
AK249824.1	Aegilops_searsii_AE1083	2054	2421	118%	601
AK249824.1	Aegilops_searsii_KU-14655	2054	2460	120%	601
AK249824.1	Aegilops_searsii_PI599142	2054	2338	114%	601
AK249824.1	Aegilops_searsii_PI599148	2054	2016	98%	601
AK249824.1	Aegilops_sharonensis_AE90691	2054	2314	113%	601
AK249824.1	Aegilops_speltooides_3776	2054	2489	121%	601
AK249824.1	Aegilops_speltooides_AE1064	2054	2339	114%	601
AK249824.1	Aegilops_speltooides_AE900	2054	2365	115%	601
AK249824.1	Aegilops_speltooides_KU-7856	2054	2232	109%	601
AK249824.1	Aegilops_speltooides_PI486264	2054	2439	119%	601
AK249824.1	Aegilops_speltooides_PI487231	2054	2334	114%	601
AK249824.1	Aegilops_speltooides_TA1772	2054	2109	103%	601
AK249824.1	Aegilops_tauschii_49116	2054	2256	110%	601
AK249824.1	Aegilops_tauschii_937	2054	2582	126%	601
AK249824.1	Aegilops_tauschii_AE1069	2054	2343	114%	601
AK249824.1	Aegilops_tauschii_AE956	2054	2422	118%	601
AK249824.1	Aegilops_umbellulata_AE1070	2054	2272	111%	601
AK249824.1	Aegilops_umbellulata_AE153	2054	2369	115%	601
AK249824.1	Aegilops_umbellulata_AE740	2054	2096	102%	601
AK249824.1	Aegilops_umbellulata_AE811	2054	1847	90%	601
AK249824.1	Aegilops_uniaristata_AE157	2054	2517	123%	601
AK249824.1	Aegilops_uniaristata_AE680	2054	2386	116%	601
AK249824.1	Aegilops_uniaristata_PI276996	2054	2100	102%	601
AK249824.1	Agropyron_cristatum_PI494615	2054	2386	116%	601
AK249824.1	Agropyron_cristatum_PI598631	2054	2319	113%	601
AK249824.1	Amblyopyrum_muticum_PI560122	2054	1973	96%	601
AK249824.1	Amblyopyrum_muticum_PI560124	2054	2113	103%	601
AK249824.1	Amblyopyrum_muticum_PI560125	2054	2073	101%	601
AK249824.1	Amblyopyrum_muticum_PI560126	2054	1912	93%	601
AK249824.1	Amblyopyrum_muticum_PI636562	2054	2285	111%	601
AK249824.1	Australopyrum_retrofractum_PI531553	2054	2291	112%	601
AK249824.1	Australopyrum_retrofractum_PI533013	2054	2145	104%	601
AK249824.1	Australopyrum_retrofractum_PI533014	2054	2290	111%	601
AK249824.1	Australopyrum_retrofractum_PI547363	2054	2406	117%	601
AK249824.1	Brachypodium_distachyon	2054	2064	100%	601
AK249824.1	Bromus_tectorum_GRA1085	2054	2095	102%	601
AK249824.1	Dasyphyrum_villosum_GRA1020	2054	2278	111%	601
AK249824.1	Dasyphyrum_villosum_GRA1027	2054	2281	111%	601
AK249824.1	Dasyphyrum_villosum_PI368884	2054	2076	101%	601
AK249824.1	Dasyphyrum_villosum_W619414	2054	2211	108%	601
AK249824.1	Dasyphyrum_villosum_W67300	2054	2377	116%	601
AK249824.1	Eremopyrum_distans_PI193264	2054	2323	113%	601
AK249824.1	Eremopyrum_triticeum_GRA2250	2054	2554	124%	601
AK249824.1	Eremopyrum_triticeum_PI502364	2054	2249	109%	601
AK249824.1	Eremopyrum_triticeum_W626631	2054	2216	108%	601
AK249824.1	Henrardia_persica_PI401347	2054	2387	116%	601
AK249824.1	Henrardia_persica_PI577112	2054	2394	117%	601
AK249824.1	Henrardia_persica_PI577113	2054	2232	109%	601
AK249824.1	Henrardia_persica_RF2012	2054	2398	117%	601
AK249824.1	Heteranthelium_piliferum_PI401351	2054	2406	117%	601
AK249824.1	Heteranthelium_piliferum_PI401353	2054	2371	115%	601
AK249824.1	Heteranthelium_piliferum_PI401354	2054	2418	118%	601
AK249824.1	Heteranthelium_sp_PI314152	2054	2226	108%	601
AK249824.1	Hordeum_marinum_BCC2006	2054	2372	115%	601
AK249824.1	Hordeum_marinum_BCC2002	2054	2476	121%	601
AK249824.1	Hordeum_pubiflorum_2028	2054	2570	125%	601
AK249824.1	Hordeum_spontaneum_FT11	2054	2606	127%	601
AK249824.1	Hordeum_vulgare_Morex	2054	2576	125%	601
AK249824.1	Psathyrostachys_juncea_PI222050	2054	2277	111%	601

Locus	Accession	Mapped exon length in barley (bp)	Assembled exon length (bp)	% of mapped exon length that could be assembled	Extended target (bp)
AK249824.1	Psathyrostachys_juncea_PI565077	2054	2104	102%	601
AK249824.1	Psathyrostachys_juncea_PI595135	2054	2236	109%	601
AK249824.1	Psathyrostachys_juncea_PI598613	2054	2294	112%	601
AK249824.1	Psathyrostachys_juncea_PI619487	2054	2395	117%	601
AK249824.1	Psathyrostachys_sp_PI565080	2054	2369	115%	601
AK249824.1	Pseudoroegneria_libanotica_PI228389	2054	2189	107%	601
AK249824.1	Pseudoroegneria_libanotica_PI330688	2054	2222	108%	601
AK249824.1	Pseudoroegneria_libanotica_PI401274	2054	2306	112%	601
AK249824.1	Pseudoroegneria_stipifolia_PI325181	2054	2403	117%	601
AK249824.1	Pseudoroegneria_stipifolia_PI440095	2054	2294	112%	601
AK249824.1	Pseudoroegneria_stipifolia_PI531751	2054	2368	115%	601
AK249824.1	Pseudoroegneria_strigosa_PI499638	2054	2261	110%	601
AK249824.1	Pseudoroegneria_strigosa_PI595172	2054	2398	117%	601
AK249824.1	Pseudoroegneria_strigosa_W614049	2054	2374	116%	601
AK249824.1	Pseudoroegneria_strigosa_PI639805	2054	2300	112%	601
AK249824.1	Pseudoroegneria_strigosa_PI639805	2054	2460	120%	601
AK249824.1	Pseudoroegneria_tauri_PI401322	2054	2247	109%	601
AK249824.1	Pseudoroegneria_tauri_PI401333	2054	2430	118%	601
AK249824.1	Secale_cereale_PI618662	2054	1995	97%	601
AK249824.1	Secale_cereale_PI618665	2054	2152	105%	601
AK249824.1	Secale_cereale_PI618669	2054	2371	115%	601
AK249824.1	Secale_cereale_PI618671	2054	2275	111%	601
AK249824.1	Secale_strictum_R1108	2054	2124	103%	601
AK249824.1	Secale_strictum_R853	2054	2325	113%	601
AK249824.1	Secale_vavilovii_PI253957	2054	1742	85%	601
AK249824.1	Secale_vavilovii_R1027	2054	2149	105%	601
AK249824.1	Taeniatherum_caput-medusae_CK2011	2054	2370	115%	601
AK249824.1	Taeniatherum_caput-medusae_GRA1126	2054	2570	125%	601
AK249824.1	Taeniatherum_caput-medusae_PI220589	2054	2340	114%	601
AK249824.1	Taeniatherum_caput-medusae_PI251387	2054	2163	105%	601
AK249824.1	Taeniatherum_caput-medusae_PI561095	2054	2158	105%	601
AK249824.1	Taeniatherum_crinatum_GRA2570	2054	2491	121%	601
AK249824.1	Thinopyrum_bessarabicum_W621890	2054	2286	111%	601
AK249824.1	Thinopyrum_elongatum_PI109452	2054	2376	116%	601
AK249824.1	Thinopyrum_elongatum_PI401117	2054	2219	108%	601
AK249824.1	Triticum_boeoticum_1613	2054	2591	126%	601
AK249824.1	Triticum_boeoticum_1688	2054	2347	114%	601
AK249824.1	Triticum_boeoticum_ID379	2054	2274	111%	601
AK249824.1	Triticum_boeoticum_PI272520	2054	2208	107%	601
AK249824.1	Triticum_boeoticum_PI427451	2054	2377	116%	601
AK249824.1	Triticum_boeoticum_PI427620	2054	2437	119%	601
AK249824.1	Triticum_monococcum_2205	2054	2386	116%	601
AK249824.1	Triticum_monococcum_2208	2054	2286	111%	601
AK249824.1	Triticum_monococcum_2271	2054	2544	124%	601
AK249824.1	Triticum_monococcum_TR113061	2054	2337	114%	601
AK249824.1	Triticum_monococcum_TR113612	2054	2407	117%	601
AK249824.1	Triticum_urartu_1307	2054	2418	118%	601
AK249824.1	Triticum_urartu_PI428184	2054	2096	102%	601
AK249824.1	Triticum_urartu_PI428317	2054	2053	100%	601
AK249824.1	Triticum_urartu_TR117824	2054	2256	110%	601
AK249824.1	Triticum_urartu_TR118407	2054	2444	119%	601
AK249999.1	Aegilops_bicornis_AE106	246	539	219%	601
AK249999.1	Aegilops_bicornis_AE1079	246	300	122%	601
AK249999.1	Aegilops_bicornis_AE788	246	516	210%	601
AK249999.1	Aegilops_bicornis_KU-5786	246	217	88%	601
AK249999.1	Aegilops_comosa_AE1255	246	645	262%	601
AK249999.1	Aegilops_comosa_AE1378	246	455	185%	601
AK249999.1	Aegilops_comosa_AE783	246	567	230%	601
AK249999.1	Aegilops_comosa_PI276970	246	327	133%	601
AK249999.1	Aegilops_longissima_AE1078	246	433	176%	601
AK249999.1	Aegilops_longissima_AE133	246	405	165%	601
AK249999.1	Aegilops_longissima_AE417	246	396	161%	601
AK249999.1	Aegilops_longissima_PI604141	246	244	99%	601
AK249999.1	Aegilops_longissima_TA1921	246	359	146%	601
AK249999.1	Aegilops_markgrafii_AE1381	246	424	172%	601
AK249999.1	Aegilops_markgrafii_KP-2012-106	246	355	144%	601
AK249999.1	Aegilops_markgrafii_PI254863	246	336	137%	601
AK249999.1	Aegilops_markgrafii_PI542208	246	455	185%	601
AK249999.1	Aegilops_markgrafii_PI596287	246	442	180%	601
AK249999.1	Aegilops_mutica_01C2100106	246	433	176%	601
AK249999.1	Aegilops_searsii_AE1075	246	398	162%	601
AK249999.1	Aegilops_searsii_AE1083	246	525	213%	601
AK249999.1	Aegilops_searsii_KU-14655	246	527	214%	601
AK249999.1	Aegilops_searsii_PI599142	246	419	170%	601
AK249999.1	Aegilops_searsii_PI599148	246	299	122%	601
AK249999.1	Aegilops_sharonensis_AE90691	246	525	213%	601
AK249999.1	Aegilops_speltoides_3776	246	603	245%	601
AK249999.1	Aegilops_speltoides_AE1064	246	368	150%	601
AK249999.1	Aegilops_speltoides_AE900	246	424	172%	601
AK249999.1	Aegilops_speltoides_KU-7856	246	372	151%	601
AK249999.1	Aegilops_speltoides_PI486264	246	492	200%	601
AK249999.1	Aegilops_speltoides_PI487231	246	332	135%	601
AK249999.1	Aegilops_speltoides_TA1772	246	262	107%	601
AK249999.1	Aegilops_tauschii_49116	246	386	157%	601
AK249999.1	Aegilops_tauschii_937	246	646	263%	601
AK249999.1	Aegilops_tauschii_AE1069	246	385	157%	601

Locus	Accession	Mapped exon length in barley (bp)	Assembled exon length (bp)	% of mapped exon length that could be assembled	Extended target (bp)
AK249999.1	Aegilops_tauschii_AE956	246	525	213%	601
AK249999.1	Aegilops_umbellulata_AE1070	246	544	221%	601
AK249999.1	Aegilops_umbellulata_AE153	246	537	218%	601
AK249999.1	Aegilops_umbellulata_AE740	246	258	105%	601
AK249999.1	Aegilops_umbellulata_AE811	246	205	83%	601
AK249999.1	Aegilops_uniaristata_AE157	246	422	172%	601
AK249999.1	Aegilops_uniaristata_AE680	246	607	247%	601
AK249999.1	Aegilops_uniaristata_PI276996	246	328	133%	601
AK249999.1	Agropyron_cristatum_PI494615	246	448	182%	601
AK249999.1	Agropyron_cristatum_PI598631	246	493	200%	601
AK249999.1	Amblyopyrum_muticum_PI560122	246	190	77%	601
AK249999.1	Amblyopyrum_muticum_PI560124	246	195	79%	601
AK249999.1	Amblyopyrum_muticum_PI560125	246	157	64%	601
AK249999.1	Amblyopyrum_muticum_PI560126	246	184	75%	601
AK249999.1	Amblyopyrum_muticum_PI636562	246	407	165%	601
AK249999.1	Australopyrum_retrofractum_PI531553	246	326	133%	601
AK249999.1	Australopyrum_retrofractum_PI533013	246	311	126%	601
AK249999.1	Australopyrum_retrofractum_PI533014	246	496	202%	601
AK249999.1	Australopyrum_retrofractum_PI547363	246	586	238%	601
AK249999.1	Brachypodium_distachyon	246	257	104%	601
AK249999.1	Bromus_tectorum_GRA1085	246	374	152%	601
AK249999.1	Dasyphyrum_villosum_GRA1020	246	348	141%	601
AK249999.1	Dasyphyrum_villosum_GRA1027	246	407	165%	601
AK249999.1	Dasyphyrum_villosum_PI368884	246	259	105%	601
AK249999.1	Dasyphyrum_villosum_W619414	246	302	123%	601
AK249999.1	Dasyphyrum_villosum_W67300	246	464	189%	601
AK249999.1	Eremopyrum_distans_PI193264	246	556	226%	601
AK249999.1	Eremopyrum_triticeum_GRA2250	246	476	193%	601
AK249999.1	Eremopyrum_triticeum_PI502364	246	471	191%	601
AK249999.1	Eremopyrum_triticeum_W626631	246	356	145%	601
AK249999.1	Henrardia_persica_PI401347	246	425	173%	601
AK249999.1	Henrardia_persica_PI577112	246	543	221%	601
AK249999.1	Henrardia_persica_PI577113	246	390	159%	601
AK249999.1	Henrardia_persica_RF2012	246	424	172%	601
AK249999.1	Heterantherium_piliferum_PI401351	246	507	206%	601
AK249999.1	Heterantherium_piliferum_PI401353	246	609	248%	601
AK249999.1	Heterantherium_piliferum_PI401354	246	663	270%	601
AK249999.1	Heterantherium_sp._PI314152	246	357	145%	601
AK249999.1	Hordeum_marinum_BCC2006	246	500	203%	601
AK249999.1	Hordeum_murinum_BCC2002	246	646	263%	601
AK249999.1	Hordeum_pubiflorum_2028	246	641	261%	601
AK249999.1	Hordeum_spontaneum_FT11	246	813	330%	601
AK249999.1	Hordeum_vulgare_Morex	246	782	318%	601
AK249999.1	Psathyrostachys_junceae_PI222050	246	400	163%	601
AK249999.1	Psathyrostachys_junceae_PI565077	246	381	155%	601
AK249999.1	Psathyrostachys_junceae_PI595135	246	512	208%	601
AK249999.1	Psathyrostachys_junceae_PI598613	246	444	180%	601
AK249999.1	Psathyrostachys_junceae_PI619487	246	560	228%	601
AK249999.1	Psathyrostachys_sp._PI565080	246	360	146%	601
AK249999.1	Pseudoroegneria_libanotica_PI228389	246	231	94%	601
AK249999.1	Pseudoroegneria_libanotica_PI330688	246	421	171%	601
AK249999.1	Pseudoroegneria_libanotica_PI401274	246	494	201%	601
AK249999.1	Pseudoroegneria_stipifolia_PI325181	246	617	251%	601
AK249999.1	Pseudoroegneria_stipifolia_PI440095	246	505	205%	601
AK249999.1	Pseudoroegneria_stipifolia_PI531751	246	432	176%	601
AK249999.1	Pseudoroegneria_strigosa_PI499638	246	363	148%	601
AK249999.1	Pseudoroegneria_strigosa_PI595172	246	599	243%	601
AK249999.1	Pseudoroegneria_strigosa_W614049	246	552	224%	601
AK249999.1	Pseudoroegneria_strigosa_PI639805	246	382	155%	601
AK249999.1	Pseudoroegneria_strigosa_PI639805	246	577	235%	601
AK249999.1	Pseudoroegneria_tauri_PI401322	246	325	132%	601
AK249999.1	Pseudoroegneria_tauri_PI401333	246	523	213%	601
AK249999.1	Secale_cereale_PI618662	246	145	59%	601
AK249999.1	Secale_cereale_PI618665	246	277	113%	601
AK249999.1	Secale_cereale_PI618669	246	580	236%	601
AK249999.1	Secale_cereale_PI618671	246	389	158%	601
AK249999.1	Secale_strictum_R1108	246	185	75%	601
AK249999.1	Secale_strictum_R853	246	353	143%	601
AK249999.1	Secale_vavilovii_PI253957	246	206	84%	601
AK249999.1	Secale_vavilovii_R1027	246	188	76%	601
AK249999.1	Taeniatherum_caput-medusae_CK2011	246	556	226%	601
AK249999.1	Taeniatherum_caput-medusae_GRA1126	246	604	246%	601
AK249999.1	Taeniatherum_caput-medusae_PI220589	246	433	176%	601
AK249999.1	Taeniatherum_caput-medusae_PI251387	246	362	147%	601
AK249999.1	Taeniatherum_caput-medusae_PI561095	246	257	104%	601
AK249999.1	Taeniatherum_crinatum_GRA2570	246	470	191%	601
AK249999.1	Thinopyrum_bessarabicum_W621890	246	361	147%	601
AK249999.1	Thinopyrum_elongatum_PI109452	246	600	244%	601
AK249999.1	Thinopyrum_elongatum_PI401117	246	294	120%	601
AK249999.1	Triticum_boeoticum_1613	246	800	325%	601
AK249999.1	Triticum_boeoticum_1688	246	564	229%	601
AK249999.1	Triticum_boeoticum_ID379	246	304	124%	601
AK249999.1	Triticum_boeoticum_PI272520	246	384	156%	601
AK249999.1	Triticum_boeoticum_PI427451	246	525	213%	601
AK249999.1	Triticum_boeoticum_PI427620	246	545	222%	601
AK249999.1	Triticum_monococcum_2205	246	558	227%	601

Locus	Accession	Mapped exon length in barley (bp)	Assembled exon length (bp)	% of mapped exon length that could be assembled	Extended target (bp)
AK249999.1	Triticum_monococcum_2208	246	499	203%	601
AK249999.1	Triticum_monococcum_2271	246	730	297%	601
AK249999.1	Triticum_monococcum_TRI13061	246	455	185%	601
AK249999.1	Triticum_monococcum_TRI13612	246	473	192%	601
AK249999.1	Triticum_urartu_1307	246	749	304%	601
AK249999.1	Triticum_urartu_PI428184	246	312	127%	601
AK249999.1	Triticum_urartu_PI428317	246	97	39%	601
AK249999.1	Triticum_urartu_TRI17824	246	494	201%	601
AK249999.1	Triticum_urartu_TRI18407	246	509	207%	601
AK250429.1	Aegilops_bicornis_AE106	273	673	247%	601
AK250429.1	Aegilops_bicornis_AE1079	273	362	133%	601
AK250429.1	Aegilops_bicornis_AE788	273	603	221%	601
AK250429.1	Aegilops_bicornis_KU-5786	273	472	173%	601
AK250429.1	Aegilops_comosa_AE1255	273	589	216%	601
AK250429.1	Aegilops_comosa_AE1378	273	470	172%	601
AK250429.1	Aegilops_comosa_AE783	273	565	207%	601
AK250429.1	Aegilops_comosa_PI276970	273	371	136%	601
AK250429.1	Aegilops_longissima_AE1078	273	484	177%	601
AK250429.1	Aegilops_longissima_AE133	273	503	184%	601
AK250429.1	Aegilops_longissima_AE417	273	455	167%	601
AK250429.1	Aegilops_longissima_PI604141	273	357	131%	601
AK250429.1	Aegilops_longissima_TA1921	273	541	198%	601
AK250429.1	Aegilops_markgrafii_AE1381	273	615	225%	601
AK250429.1	Aegilops_markgrafii_KP-2012-106	273	624	229%	601
AK250429.1	Aegilops_markgrafii_PI254863	273	355	130%	601
AK250429.1	Aegilops_markgrafii_PI542208	273	539	197%	601
AK250429.1	Aegilops_markgrafii_PI596287	273	505	185%	601
AK250429.1	Aegilops_mutica_01C2100106	273	486	178%	601
AK250429.1	Aegilops_searsii_AE1075	273	429	157%	601
AK250429.1	Aegilops_searsii_AE1083	273	625	229%	601
AK250429.1	Aegilops_searsii_KU-14655	273	623	228%	601
AK250429.1	Aegilops_searsii_PI599142	273	359	132%	601
AK250429.1	Aegilops_searsii_PI599148	273	374	137%	601
AK250429.1	Aegilops_sharonensis_AE90691	273	624	229%	601
AK250429.1	Aegilops_speltoides_3776	273	589	216%	601
AK250429.1	Aegilops_speltoides_AE1064	273	515	189%	601
AK250429.1	Aegilops_speltoides_AE900	273	358	131%	601
AK250429.1	Aegilops_speltoides_KU-7856	273	300	110%	601
AK250429.1	Aegilops_speltoides_PI486264	273	464	170%	601
AK250429.1	Aegilops_speltoides_PI487231	273	419	153%	601
AK250429.1	Aegilops_speltoides_TA1772	273	364	133%	601
AK250429.1	Aegilops_tauschii_49116	273	442	162%	601
AK250429.1	Aegilops_tauschii_937	273	719	263%	601
AK250429.1	Aegilops_tauschii_AE1069	273	505	185%	601
AK250429.1	Aegilops_tauschii_AE956	273	522	191%	601
AK250429.1	Aegilops_umbellulata_AE1070	273	528	193%	601
AK250429.1	Aegilops_umbellulata_AE153	273	610	223%	601
AK250429.1	Aegilops_umbellulata_AE740	273	359	132%	601
AK250429.1	Aegilops_umbellulata_AE811	273	262	96%	601
AK250429.1	Aegilops_uniaristata_AE157	273	617	226%	601
AK250429.1	Aegilops_uniaristata_AE680	273	607	222%	601
AK250429.1	Aegilops_uniaristata_PI276996	273	384	141%	601
AK250429.1	Agropyron_cristatum_PI494615	273	657	241%	601
AK250429.1	Agropyron_cristatum_PI598631	273	530	194%	601
AK250429.1	Amblyopyrum_muticum_PI560122	273	187	68%	601
AK250429.1	Amblyopyrum_muticum_PI560124	273	217	79%	601
AK250429.1	Amblyopyrum_muticum_PI560125	273	301	110%	601
AK250429.1	Amblyopyrum_muticum_PI560126	273	320	117%	601
AK250429.1	Amblyopyrum_muticum_PI636562	273	553	203%	601
AK250429.1	Australopyrum_retrofractum_PI531553	273	441	162%	601
AK250429.1	Australopyrum_retrofractum_PI533013	273	525	192%	601
AK250429.1	Australopyrum_retrofractum_PI533014	273	574	210%	601
AK250429.1	Australopyrum_retrofractum_PI547363	273	701	257%	601
AK250429.1	Brachypodium_distachyon	273	553	203%	601
AK250429.1	Bromus_tectorum_GRA1085	273	524	192%	601
AK250429.1	Dasyphyrum_villosum_GRA1020	273	356	130%	601
AK250429.1	Dasyphyrum_villosum_GRA1027	273	468	171%	601
AK250429.1	Dasyphyrum_villosum_PI368884	273	366	134%	601
AK250429.1	Dasyphyrum_villosum_W619414	273	290	106%	601
AK250429.1	Dasyphyrum_villosum_W67300	273	596	218%	601
AK250429.1	Eremopyrum_distans_PI193264	273	558	204%	601
AK250429.1	Eremopyrum_triticeum_GRA2250	273	573	210%	601
AK250429.1	Eremopyrum_triticeum_PI502364	273	415	152%	601
AK250429.1	Eremopyrum_triticeum_W626631	273	354	130%	601
AK250429.1	Henrardia_persica_PI401347	273	520	190%	601
AK250429.1	Henrardia_persica_PI577112	273	563	206%	601
AK250429.1	Henrardia_persica_PI577113	273	460	168%	601
AK250429.1	Henrardia_persica_RF2012	273	574	210%	601
AK250429.1	Heterantherium_piliferum_PI401351	273	627	230%	601
AK250429.1	Heterantherium_piliferum_PI401353	273	743	272%	601
AK250429.1	Heterantherium_piliferum_PI401354	273	751	275%	601
AK250429.1	Heterantherium_sp._PI314152	273	573	210%	601
AK250429.1	Hordeum_marinum_BCC2006	273	481	176%	601
AK250429.1	Hordeum_murinum_BCC2002	273	688	252%	601
AK250429.1	Hordeum_pubiflorum_2028	273	602	221%	601
AK250429.1	Hordeum_spontaneum_FT11	273	648	237%	601

Locus	Accession	Mapped exon length in barley (bp)	Assembled exon length (bp)	% of mapped exon length that could be assembled	Extended target (bp)
AK250429.1	Hordeum_vulgare_Morex	273	842	308%	601
AK250429.1	Psathyrostachys_junceae_PI222050	273	544	199%	601
AK250429.1	Psathyrostachys_junceae_PI565077	273	352	129%	601
AK250429.1	Psathyrostachys_junceae_PI595135	273	537	197%	601
AK250429.1	Psathyrostachys_junceae_PI598613	273	614	225%	601
AK250429.1	Psathyrostachys_junceae_PI619487	273	603	221%	601
AK250429.1	Psathyrostachys_sp_PI565080	273	431	158%	601
AK250429.1	Pseudoroegneria_libanotica_PI228389	273	358	131%	601
AK250429.1	Pseudoroegneria_libanotica_PI330688	273	429	157%	601
AK250429.1	Pseudoroegneria_libanotica_PI401274	273	512	188%	601
AK250429.1	Pseudoroegneria_stipifolia_PI325181	273	595	218%	601
AK250429.1	Pseudoroegneria_stipifolia_PI440095	273	582	213%	601
AK250429.1	Pseudoroegneria_stipifolia_PI531751	273	417	153%	601
AK250429.1	Pseudoroegneria_strigosa_PI499638	273	420	154%	601
AK250429.1	Pseudoroegneria_strigosa_PI595172	273	483	177%	601
AK250429.1	Pseudoroegneria_strigosa_W614049	273	546	200%	601
AK250429.1	Pseudoroegneria_strigosa_PI639805	273	414	152%	601
AK250429.1	Pseudoroegneria_strigosa_PI639805	273	568	208%	601
AK250429.1	Pseudoroegneria_tauri_PI401322	273	416	152%	601
AK250429.1	Pseudoroegneria_tauri_PI401333	273	406	149%	601
AK250429.1	Secale_cereale_PI618662	273	278	102%	601
AK250429.1	Secale_cereale_PI618665	273	589	216%	601
AK250429.1	Secale_cereale_PI618669	273	586	215%	601
AK250429.1	Secale_cereale_PI618671	273	561	205%	601
AK250429.1	Secale_strictum_R1108	273	297	109%	601
AK250429.1	Secale_strictum_R853	273	563	206%	601
AK250429.1	Secale_vavilovii_PI253957	273	224	82%	601
AK250429.1	Secale_vavilovii_R1027	273	325	119%	601
AK250429.1	Taeniatherum_caput-medusae_CK2011	273	527	193%	601
AK250429.1	Taeniatherum_caput-medusae_GRA1126	273	577	211%	601
AK250429.1	Taeniatherum_caput-medusae_PI220589	273	544	199%	601
AK250429.1	Taeniatherum_caput-medusae_PI251387	273	332	122%	601
AK250429.1	Taeniatherum_caput-medusae_PI561095	273	204	75%	601
AK250429.1	Taeniatherum_crinatum_GRA2570	273	615	225%	601
AK250429.1	Thinopyrum_bessarabicum_W621890	273	518	190%	601
AK250429.1	Thinopyrum_elongatum_PI109452	273	556	204%	601
AK250429.1	Thinopyrum_elongatum_PI401117	273	365	134%	601
AK250429.1	Triticum_boeoticum_1613	273	696	255%	601
AK250429.1	Triticum_boeoticum_1688	273	633	232%	601
AK250429.1	Triticum_boeoticum_ID379	273	424	155%	601
AK250429.1	Triticum_boeoticum_PI272520	273	357	131%	601
AK250429.1	Triticum_boeoticum_PI427451	273	619	227%	601
AK250429.1	Triticum_boeoticum_PI427620	273	641	235%	601
AK250429.1	Triticum_monococcum_2205	273	592	217%	601
AK250429.1	Triticum_monococcum_2208	273	593	217%	601
AK250429.1	Triticum_monococcum_2271	273	740	271%	601
AK250429.1	Triticum_monococcum_TRI13061	273	614	225%	601
AK250429.1	Triticum_monococcum_TRI13612	273	587	215%	601
AK250429.1	Triticum_urartu_1307	273	684	251%	601
AK250429.1	Triticum_urartu_PI428184	273	386	141%	601
AK250429.1	Triticum_urartu_PI428317	273	362	133%	601
AK250429.1	Triticum_urartu_TRI17824	273	610	223%	601
AK250429.1	Triticum_urartu_TRI18407	273	615	225%	601
AK250497.1	Aegilops_bicornis_AE106	184	100	54%	601
AK250497.1	Aegilops_bicornis_AE1079	184	0	0%	601
AK250497.1	Aegilops_bicornis_AE788	184	50	27%	601
AK250497.1	Aegilops_bicornis_KU-5786	184	0	0%	601
AK250497.1	Aegilops_comosa_AE1255	184	143	78%	601
AK250497.1	Aegilops_comosa_AE1378	184	121	66%	601
AK250497.1	Aegilops_comosa_AE783	184	192	104%	601
AK250497.1	Aegilops_longissima_AE1078	184	0	0%	601
AK250497.1	Aegilops_longissima_AE133	184	72	39%	601
AK250497.1	Aegilops_longissima_AE417	184	0	0%	601
AK250497.1	Aegilops_longissima_PI604141	184	31	17%	601
AK250497.1	Aegilops_longissima_TA1921	184	0	0%	601
AK250497.1	Aegilops_markgrafii_AE1381	184	165	90%	601
AK250497.1	Aegilops_markgrafii_KP-2012-106	184	125	68%	601
AK250497.1	Aegilops_markgrafii_PI254863	184	0	0%	601
AK250497.1	Aegilops_markgrafii_PI542208	184	89	48%	601
AK250497.1	Aegilops_markgrafii_PI596287	184	101	55%	601
AK250497.1	Aegilops_mutica_01C2100106	184	0	0%	601
AK250497.1	Aegilops_searsii_AE1075	184	125	68%	601
AK250497.1	Aegilops_searsii_AE1083	184	162	88%	601
AK250497.1	Aegilops_searsii_KU-14655	184	85	46%	601
AK250497.1	Aegilops_searsii_PI599142	184	0	0%	601
AK250497.1	Aegilops_sharonensis_AE90691	184	101	55%	601
AK250497.1	Aegilops_speltioides_3776	184	328	178%	601
AK250497.1	Aegilops_speltioides_AE1064	184	101	55%	601
AK250497.1	Aegilops_speltioides_AE900	184	173	94%	601
AK250497.1	Aegilops_speltioides_KU-7856	184	0	0%	601
AK250497.1	Aegilops_speltioides_PI486264	184	146	79%	601
AK250497.1	Aegilops_speltioides_PI487231	184	168	91%	601
AK250497.1	Aegilops_tauschii_49116	184	0	0%	601
AK250497.1	Aegilops_tauschii_937	184	281	153%	601
AK250497.1	Aegilops_tauschii_AE1069	184	156	85%	601
AK250497.1	Aegilops_tauschii_AE956	184	186	101%	601

Locus	Accession	Mapped exon length in barley (bp)	Assembled exon length (bp)	% of mapped exon length that could be assembled	Extended target (bp)
AK250497.1	Aegilops_umbellulata_AE1070	184	101	55%	601
AK250497.1	Aegilops_umbellulata_AE153	184	50	27%	601
AK250497.1	Aegilops_umbellulata_AE740	184	0	0%	601
AK250497.1	Aegilops_uniaristata_AE157	184	0	0%	601
AK250497.1	Aegilops_uniaristata_AE680	184	132	72%	601
AK250497.1	Aegilops_uniaristata_PI276996	184	0	0%	601
AK250497.1	Agropyron_cristatum_PI494615	184	149	81%	601
AK250497.1	Agropyron_cristatum_PI598631	184	0	0%	601
AK250497.1	Amblyopyrum_muticum_PI560122	184	0	0%	601
AK250497.1	Amblyopyrum_muticum_PI560124	184	0	0%	601
AK250497.1	Amblyopyrum_muticum_PI636562	184	62	34%	601
AK250497.1	Australopyrum_retrofractum_PI533013	184	0	0%	601
AK250497.1	Australopyrum_retrofractum_PI533014	184	0	0%	601
AK250497.1	Australopyrum_retrofractum_PI547363	184	0	0%	601
AK250497.1	Brachypodium_distachyon	184	165	90%	601
AK250497.1	Bromus_tectorum_GRA1085	184	124	67%	601
AK250497.1	Dasypyrum_villosum_GRA1020	184	0	0%	601
AK250497.1	Dasypyrum_villosum_GRA1027	184	0	0%	601
AK250497.1	Dasypyrum_villosum_PI368884	184	0	0%	601
AK250497.1	Dasypyrum_villosum_W619414	184	0	0%	601
AK250497.1	Dasypyrum_villosum_W67300	184	73	40%	601
AK250497.1	Eremopyrum_distans_PI193264	184	97	53%	601
AK250497.1	Eremopyrum_triticeum_GRA2250	184	0	0%	601
AK250497.1	Eremopyrum_triticeum_PI502364	184	135	73%	601
AK250497.1	Eremopyrum_triticeum_W626631	184	0	0%	601
AK250497.1	Henrardia_persica_PI401347	184	0	0%	601
AK250497.1	Henrardia_persica_PI577112	184	111	60%	601
AK250497.1	Henrardia_persica_PI577113	184	0	0%	601
AK250497.1	Henrardia_persica_RF2012	184	126	68%	601
AK250497.1	Heterantherium_piliferum_PI401351	184	95	52%	601
AK250497.1	Heterantherium_piliferum_PI401353	184	162	88%	601
AK250497.1	Heterantherium_piliferum_PI401354	184	119	65%	601
AK250497.1	Heterantherium_sp_PI314152	184	97	53%	601
AK250497.1	Hordeum_marinum_BCC2006	184	94	51%	601
AK250497.1	Hordeum_marinum_BCC2002	184	36	20%	601
AK250497.1	Hordeum_pubiflorum_2028	184	356	193%	601
AK250497.1	Hordeum_spontaneum_FT11	184	653	355%	601
AK250497.1	Hordeum_vulgare_Morex	184	645	351%	601
AK250497.1	Psathyrostachys_junceae_PI222050	184	0	0%	601
AK250497.1	Psathyrostachys_junceae_PI565077	184	0	0%	601
AK250497.1	Psathyrostachys_junceae_PI595135	184	0	0%	601
AK250497.1	Psathyrostachys_junceae_PI598613	184	149	81%	601
AK250497.1	Psathyrostachys_junceae_PI619487	184	51	28%	601
AK250497.1	Psathyrostachys_sp_PI565080	184	0	0%	601
AK250497.1	Pseudoroegneria_libanotica_PI330688	184	101	55%	601
AK250497.1	Pseudoroegneria_libanotica_PI401274	184	0	0%	601
AK250497.1	Pseudoroegneria_stipifolia_PI325181	184	107	58%	601
AK250497.1	Pseudoroegneria_stipifolia_PI440095	184	88	48%	601
AK250497.1	Pseudoroegneria_stipifolia_PI531751	184	0	0%	601
AK250497.1	Pseudoroegneria_strigosa_PI499638	184	133	72%	601
AK250497.1	Pseudoroegneria_strigosa_PI595172	184	16	9%	601
AK250497.1	Pseudoroegneria_strigosa_W614049	184	178	97%	601
AK250497.1	Pseudoroegneria_strigosa_PI639805	184	0	0%	601
AK250497.1	Pseudoroegneria_strigosa_PI639805	184	73	40%	601
AK250497.1	Pseudoroegneria_tauri_PI401322	184	0	0%	601
AK250497.1	Pseudoroegneria_tauri_PI401333	184	124	67%	601
AK250497.1	Secale_cereale_PI618665	184	158	86%	601
AK250497.1	Secale_cereale_PI618669	184	115	63%	601
AK250497.1	Secale_cereale_PI618671	184	0	0%	601
AK250497.1	Secale_strictum_R853	184	0	0%	601
AK250497.1	Secale_vavilovii_R1027	184	0	0%	601
AK250497.1	Taeniatherum_caput-medusae_CK2011	184	188	102%	601
AK250497.1	Taeniatherum_caput-medusae_GRA1126	184	101	55%	601
AK250497.1	Taeniatherum_caput-medusae_PI220589	184	135	73%	601
AK250497.1	Taeniatherum_crinatum_GRA2570	184	153	83%	601
AK250497.1	Thinopyrum_bessarabicum_W621890	184	51	28%	601
AK250497.1	Thinopyrum_elongatum_PI109452	184	53	29%	601
AK250497.1	Thinopyrum_elongatum_PI401117	184	96	52%	601
AK250497.1	Triticum_boeoticum_1613	184	204	111%	601
AK250497.1	Triticum_boeoticum_1688	184	139	76%	601
AK250497.1	Triticum_boeoticum_ID379	184	101	55%	601
AK250497.1	Triticum_boeoticum_PI272520	184	0	0%	601
AK250497.1	Triticum_boeoticum_PI427451	184	118	64%	601
AK250497.1	Triticum_boeoticum_PI427620	184	174	95%	601
AK250497.1	Triticum_monococcum_2205	184	126	68%	601
AK250497.1	Triticum_monococcum_2208	184	117	64%	601
AK250497.1	Triticum_monococcum_2271	184	204	111%	601
AK250497.1	Triticum_monococcum_TRI13061	184	122	66%	601
AK250497.1	Triticum_monococcum_TRI13612	184	175	95%	601
AK250497.1	Triticum_urartu_1307	184	174	95%	601
AK250497.1	Triticum_urartu_PI428184	184	0	0%	601
AK250497.1	Triticum_urartu_TRI17824	184	146	79%	601
AK250497.1	Triticum_urartu_TRI18407	184	69	38%	601
AK251050.1	Aegilops_bicornis_AE106	1464	1810	124%	601
AK251050.1	Aegilops_bicornis_AE1079	1464	1573	107%	601
AK251050.1	Aegilops_bicornis_AE788	1464	1686	115%	601

Locus	Accession	Mapped exon length in barley (bp)	Assembled exon length (bp)	% of mapped exon length that could be assembled	Extended target (bp)
AK251050.1	Aegilops_bicornis_KU-5786	1464	1555	106%	601
AK251050.1	Aegilops_comosa_AE1255	1464	1886	129%	601
AK251050.1	Aegilops_comosa_AE1378	1464	1655	113%	601
AK251050.1	Aegilops_comosa_AE783	1464	1615	110%	601
AK251050.1	Aegilops_comosa_PI276970	1464	1516	104%	601
AK251050.1	Aegilops_longissima_AE1078	1464	1636	112%	601
AK251050.1	Aegilops_longissima_AE133	1464	1727	118%	601
AK251050.1	Aegilops_longissima_AE417	1464	1446	99%	601
AK251050.1	Aegilops_longissima_PI604141	1464	1504	103%	601
AK251050.1	Aegilops_longissima_TA1921	1464	1689	115%	601
AK251050.1	Aegilops_markgrafii_AE1381	1464	1771	121%	601
AK251050.1	Aegilops_markgrafii_KP-2012-106	1464	1670	114%	601
AK251050.1	Aegilops_markgrafii_PI254863	1464	1578	108%	601
AK251050.1	Aegilops_markgrafii_PI542208	1464	1761	120%	601
AK251050.1	Aegilops_markgrafii_PI596287	1464	1664	114%	601
AK251050.1	Aegilops_mutica_01C2100106	1464	1761	120%	601
AK251050.1	Aegilops_searsii_AE1075	1464	1720	117%	601
AK251050.1	Aegilops_searsii_AE1083	1464	1865	127%	601
AK251050.1	Aegilops_searsii_KU-14655	1464	1827	125%	601
AK251050.1	Aegilops_searsii_PI599142	1464	1684	115%	601
AK251050.1	Aegilops_searsii_PI599148	1464	1487	102%	601
AK251050.1	Aegilops_sharonensis_AE90691	1464	1776	121%	601
AK251050.1	Aegilops_speltoides_3776	1464	1994	136%	601
AK251050.1	Aegilops_speltoides_AE1064	1464	1796	123%	601
AK251050.1	Aegilops_speltoides_AE900	1464	1681	115%	601
AK251050.1	Aegilops_speltoides_KU-7856	1464	1554	106%	601
AK251050.1	Aegilops_speltoides_PI486264	1464	1920	131%	601
AK251050.1	Aegilops_speltoides_PI487231	1464	1707	117%	601
AK251050.1	Aegilops_speltoides_TA1772	1464	1582	108%	601
AK251050.1	Aegilops_tauschii_49116	1464	1718	117%	601
AK251050.1	Aegilops_tauschii_937	1464	1992	136%	601
AK251050.1	Aegilops_tauschii_AE1069	1464	1662	114%	601
AK251050.1	Aegilops_tauschii_AE956	1464	1764	120%	601
AK251050.1	Aegilops_umbellulata_AE1070	1464	1633	112%	601
AK251050.1	Aegilops_umbellulata_AE153	1464	1789	122%	601
AK251050.1	Aegilops_umbellulata_AE740	1464	1460	100%	601
AK251050.1	Aegilops_umbellulata_AE811	1464	1396	95%	601
AK251050.1	Aegilops_uniaristata_AE157	1464	1883	129%	601
AK251050.1	Aegilops_uniaristata_AE680	1464	1764	120%	601
AK251050.1	Aegilops_uniaristata_PI276996	1464	1568	107%	601
AK251050.1	Agropyron_cristatum_PI494615	1464	1772	121%	601
AK251050.1	Agropyron_cristatum_PI598631	1464	1783	122%	601
AK251050.1	Amblyopyrum_muticum_PI560122	1464	1453	99%	601
AK251050.1	Amblyopyrum_muticum_PI560124	1464	1529	104%	601
AK251050.1	Amblyopyrum_muticum_PI560125	1464	1448	99%	601
AK251050.1	Amblyopyrum_muticum_PI560126	1464	1383	94%	601
AK251050.1	Amblyopyrum_muticum_PI636562	1464	1770	121%	601
AK251050.1	Australopyrum_retrofractum_PI531553	1464	1593	109%	601
AK251050.1	Australopyrum_retrofractum_PI533013	1464	1656	113%	601
AK251050.1	Australopyrum_retrofractum_PI533014	1464	1573	107%	601
AK251050.1	Australopyrum_retrofractum_PI547363	1464	1813	124%	601
AK251050.1	Brachypodium_distachyon	1464	1625	111%	601
AK251050.1	Bromus_tectorum_GRA1085	1464	1595	109%	601
AK251050.1	Dasyphyrum_villosum_GRA1020	1464	1707	117%	601
AK251050.1	Dasyphyrum_villosum_GRA1027	1464	1698	116%	601
AK251050.1	Dasyphyrum_villosum_PI368884	1464	1532	105%	601
AK251050.1	Dasyphyrum_villosum_W619414	1464	1501	103%	601
AK251050.1	Dasyphyrum_villosum_W67300	1464	1691	116%	601
AK251050.1	Eremopyrum_distans_PI193264	1464	1668	114%	601
AK251050.1	Eremopyrum_triticeum_GRA2250	1464	1760	120%	601
AK251050.1	Eremopyrum_triticeum_PI502364	1464	1622	111%	601
AK251050.1	Eremopyrum_triticeum_W626631	1464	1561	107%	601
AK251050.1	Henrardia_persica_PI401347	1464	1738	119%	601
AK251050.1	Henrardia_persica_PI577112	1464	1735	119%	601
AK251050.1	Henrardia_persica_PI577113	1464	1668	114%	601
AK251050.1	Henrardia_persica_RF2012	1464	1667	114%	601
AK251050.1	Heterantherium_piliferum_PI401351	1464	1719	117%	601
AK251050.1	Heterantherium_piliferum_PI401353	1464	1811	124%	601
AK251050.1	Heterantherium_piliferum_PI401354	1464	1868	128%	601
AK251050.1	Heterantherium_sp_PI314152	1464	1670	114%	601
AK251050.1	Hordeum_marinum_BCC2006	1464	1811	124%	601
AK251050.1	Hordeum_murinum_BCC2002	1464	1793	122%	601
AK251050.1	Hordeum_pubiflorum_2028	1464	2017	138%	601
AK251050.1	Hordeum_spontanum_FT11	1464	2051	140%	601
AK251050.1	Hordeum_vulgare_Morex	1464	2065	141%	601
AK251050.1	Psathyrostachys_junceae_PI222050	1464	1588	108%	601
AK251050.1	Psathyrostachys_junceae_PI565077	1464	1541	105%	601
AK251050.1	Psathyrostachys_junceae_PI595135	1464	1791	122%	601
AK251050.1	Psathyrostachys_junceae_PI598613	1464	1634	112%	601
AK251050.1	Psathyrostachys_junceae_PI619487	1464	1725	118%	601
AK251050.1	Psathyrostachys_sp_PI565080	1464	1712	117%	601
AK251050.1	Pseudoroegneria_libanotica_PI228389	1464	1353	92%	601
AK251050.1	Pseudoroegneria_libanotica_PI330688	1464	1528	104%	601
AK251050.1	Pseudoroegneria_libanotica_PI401274	1464	1714	117%	601
AK251050.1	Pseudoroegneria_stipifolia_PI325181	1464	1781	122%	601
AK251050.1	Pseudoroegneria_stipifolia_PI440095	1464	1711	117%	601

Locus	Accession	Mapped exon length in barley (bp)	Assembled exon length (bp)	% of mapped exon length that could be assembled	Extended target (bp)
AK251050.1	Pseudoroegneria_stipifolia_PI531751	1464	1737	119%	601
AK251050.1	Pseudoroegneria_strigosa_PI499638	1464	1627	111%	601
AK251050.1	Pseudoroegneria_strigosa_PI595172	1464	1678	115%	601
AK251050.1	Pseudoroegneria_strigosa_W614049	1464	1712	117%	601
AK251050.1	Pseudoroegneria_strigosa_PI639805	1464	1603	109%	601
AK251050.1	Pseudoroegneria_strigosa_PI639805	1464	1811	124%	601
AK251050.1	Pseudoroegneria_tauri_PI401322	1464	1614	110%	601
AK251050.1	Pseudoroegneria_tauri_PI401333	1464	1712	117%	601
AK251050.1	Secale_cereale_PI618662	1464	1444	99%	601
AK251050.1	Secale_cereale_PI618665	1464	1536	105%	601
AK251050.1	Secale_cereale_PI618669	1464	1717	117%	601
AK251050.1	Secale_cereale_PI618671	1464	1810	124%	601
AK251050.1	Secale_strictum_R1108	1464	1500	102%	601
AK251050.1	Secale_strictum_R853	1464	1684	115%	601
AK251050.1	Secale_vavilovii_PI253957	1464	1257	86%	601
AK251050.1	Secale_vavilovii_R1027	1464	1538	105%	601
AK251050.1	Taeniatherum_caput-medusae_CK2011	1464	1772	121%	601
AK251050.1	Taeniatherum_caput-medusae_GRA1126	1464	1820	124%	601
AK251050.1	Taeniatherum_caput-medusae_PI220589	1464	1709	117%	601
AK251050.1	Taeniatherum_caput-medusae_PI251387	1464	1452	99%	601
AK251050.1	Taeniatherum_caput-medusae_PI561095	1464	1425	97%	601
AK251050.1	Taeniatherum_crinatum_GRA2570	1464	1745	119%	601
AK251050.1	Thinopyrum_bessarabicum_W621890	1464	1626	111%	601
AK251050.1	Thinopyrum_elongatum_PI109452	1464	1811	124%	601
AK251050.1	Thinopyrum_elongatum_PI401117	1464	1556	106%	601
AK251050.1	Triticum_boeoticum_1613	1464	1996	136%	601
AK251050.1	Triticum_boeoticum_1688	1464	1843	126%	601
AK251050.1	Triticum_boeoticum_ID379	1464	1561	107%	601
AK251050.1	Triticum_boeoticum_PI272520	1464	1609	110%	601
AK251050.1	Triticum_boeoticum_PI427451	1464	1727	118%	601
AK251050.1	Triticum_boeoticum_PI427620	1464	1738	119%	601
AK251050.1	Triticum_monococcum_2205	1464	1722	118%	601
AK251050.1	Triticum_monococcum_2208	1464	1759	120%	601
AK251050.1	Triticum_monococcum_2271	1464	1967	134%	601
AK251050.1	Triticum_monococcum_TR113061	1464	1860	127%	601
AK251050.1	Triticum_monococcum_TR113612	1464	1814	124%	601
AK251050.1	Triticum_urartu_1307	1464	1958	134%	601
AK251050.1	Triticum_urartu_PI428184	1464	1592	109%	601
AK251050.1	Triticum_urartu_PI428317	1464	1562	107%	601
AK251050.1	Triticum_urartu_TR117824	1464	1789	122%	601
AK251050.1	Triticum_urartu_TR118407	1464	1825	125%	601
AK251526.1	Aegilops_bicornis_AE106	1921	2138	111%	601
AK251526.1	Aegilops_bicornis_AE1079	1921	1941	101%	601
AK251526.1	Aegilops_bicornis_AE788	1921	2176	113%	601
AK251526.1	Aegilops_bicornis_KU-5786	1921	1926	100%	601
AK251526.1	Aegilops_comosa_AE1255	1921	2176	113%	601
AK251526.1	Aegilops_comosa_AE1378	1921	2112	110%	601
AK251526.1	Aegilops_comosa_AE783	1921	2063	107%	601
AK251526.1	Aegilops_comosa_PI276970	1921	1866	97%	601
AK251526.1	Aegilops_longissima_AE1078	1921	2096	109%	601
AK251526.1	Aegilops_longissima_AE133	1921	2184	114%	601
AK251526.1	Aegilops_longissima_AE417	1921	2047	107%	601
AK251526.1	Aegilops_longissima_PI604141	1921	1873	98%	601
AK251526.1	Aegilops_longissima_TA1921	1921	2119	110%	601
AK251526.1	Aegilops_markgrafii_AE1381	1921	2081	108%	601
AK251526.1	Aegilops_markgrafii_KP-2012-106	1921	2088	109%	601
AK251526.1	Aegilops_markgrafii_PI254863	1921	2049	107%	601
AK251526.1	Aegilops_markgrafii_PI542208	1921	2232	116%	601
AK251526.1	Aegilops_markgrafii_PI596287	1921	2309	120%	601
AK251526.1	Aegilops_mutica_01C2100106	1921	2177	113%	601
AK251526.1	Aegilops_searsii_AE1075	1921	2072	108%	601
AK251526.1	Aegilops_searsii_AE1083	1921	2258	118%	601
AK251526.1	Aegilops_searsii_KU-14655	1921	2188	114%	601
AK251526.1	Aegilops_searsii_PI599142	1921	2112	110%	601
AK251526.1	Aegilops_searsii_PI599148	1921	1930	100%	601
AK251526.1	Aegilops_sharonensis_AE90691	1921	2198	114%	601
AK251526.1	Aegilops_speltoides_3776	1921	2258	118%	601
AK251526.1	Aegilops_speltoides_AE1064	1921	2148	112%	601
AK251526.1	Aegilops_speltoides_AE900	1921	2116	110%	601
AK251526.1	Aegilops_speltoides_KU-7856	1921	1863	97%	601
AK251526.1	Aegilops_speltoides_PI486264	1921	2191	114%	601
AK251526.1	Aegilops_speltoides_PI487231	1921	2168	113%	601
AK251526.1	Aegilops_speltoides_TA1772	1921	1984	103%	601
AK251526.1	Aegilops_tauschii_49116	1921	2134	111%	601
AK251526.1	Aegilops_tauschii_937	1921	2253	117%	601
AK251526.1	Aegilops_tauschii_AE1069	1921	2027	106%	601
AK251526.1	Aegilops_tauschii_AE956	1921	2131	111%	601
AK251526.1	Aegilops_umbellulata_AE1070	1921	2151	112%	601
AK251526.1	Aegilops_umbellulata_AE153	1921	2184	114%	601
AK251526.1	Aegilops_umbellulata_AE740	1921	1942	101%	601
AK251526.1	Aegilops_umbellulata_AE811	1921	1720	90%	601
AK251526.1	Aegilops_uniaristata_AE157	1921	2172	113%	601
AK251526.1	Aegilops_uniaristata_AE680	1921	2108	110%	601
AK251526.1	Aegilops_uniaristata_PI276996	1921	1953	102%	601
AK251526.1	Agropyron_cristatum_PI494615	1921	2137	111%	601
AK251526.1	Agropyron_cristatum_PI598631	1921	2029	106%	601

Locus	Accession	Mapped exon length in barley (bp)	Assembled exon length (bp)	% of mapped exon length that could be assembled	Extended target (bp)
AK251526.1	Amblyopyrum_muticum_PI560122	1921	1967	102%	601
AK251526.1	Amblyopyrum_muticum_PI560124	1921	1717	89%	601
AK251526.1	Amblyopyrum_muticum_PI560125	1921	1898	99%	601
AK251526.1	Amblyopyrum_muticum_PI560126	1921	1923	100%	601
AK251526.1	Amblyopyrum_muticum_PI636562	1921	2062	107%	601
AK251526.1	Australopyrum_retrofractum_PI531553	1921	2023	105%	601
AK251526.1	Australopyrum_retrofractum_PI533013	1921	2023	105%	601
AK251526.1	Australopyrum_retrofractum_PI533014	1921	2088	109%	601
AK251526.1	Australopyrum_retrofractum_PI547363	1921	2204	115%	601
AK251526.1	Brachypodium_distachyon	1921	1949	101%	601
AK251526.1	Bromus_tectorum_GRA1085	1921	1935	101%	601
AK251526.1	Dasypyrum_villosum_GRA1020	1921	2126	111%	601
AK251526.1	Dasypyrum_villosum_GRA1027	1921	2225	116%	601
AK251526.1	Dasypyrum_villosum_PI368884	1921	1951	102%	601
AK251526.1	Dasypyrum_villosum_W619414	1921	2106	110%	601
AK251526.1	Dasypyrum_villosum_W67300	1921	2102	109%	601
AK251526.1	Eremopyrum_distans_PI193264	1921	1992	104%	601
AK251526.1	Eremopyrum_triticeum_GRA2250	1921	2047	107%	601
AK251526.1	Eremopyrum_triticeum_PI502364	1921	2064	107%	601
AK251526.1	Eremopyrum_triticeum_W626631	1921	1986	103%	601
AK251526.1	Henrardia_persica_PI401347	1921	2055	107%	601
AK251526.1	Henrardia_persica_PI577112	1921	2104	110%	601
AK251526.1	Henrardia_persica_PI577113	1921	2129	111%	601
AK251526.1	Henrardia_persica_RF2012	1921	2132	111%	601
AK251526.1	Heteranthelium_piliferum_PI401351	1921	2054	107%	601
AK251526.1	Heteranthelium_piliferum_PI401353	1921	2178	113%	601
AK251526.1	Heteranthelium_piliferum_PI401354	1921	2233	116%	601
AK251526.1	Heteranthelium_sp._PI314152	1921	1965	102%	601
AK251526.1	Hordeum_marinum_BCC2006	1921	2229	116%	601
AK251526.1	Hordeum_murinum_BCC2002	1921	2290	119%	601
AK251526.1	Hordeum_pubiflorum_2028	1921	2257	117%	601
AK251526.1	Hordeum_spontanum_FT11	1921	2505	130%	601
AK251526.1	Hordeum_vulgare_Morex	1921	2480	129%	601
AK251526.1	Psathyrostachys_junceae_PI222050	1921	2133	111%	601
AK251526.1	Psathyrostachys_junceae_PI565077	1921	1905	99%	601
AK251526.1	Psathyrostachys_junceae_PI595135	1921	2048	107%	601
AK251526.1	Psathyrostachys_junceae_PI598613	1921	2066	108%	601
AK251526.1	Psathyrostachys_junceae_PI619487	1921	2143	112%	601
AK251526.1	Psathyrostachys_sp._PI565080	1921	2116	110%	601
AK251526.1	Pseudoroegneria_libanotica_PI228389	1921	2037	106%	601
AK251526.1	Pseudoroegneria_libanotica_PI330688	1921	2089	109%	601
AK251526.1	Pseudoroegneria_libanotica_PI401274	1921	2147	112%	601
AK251526.1	Pseudoroegneria_stipifolia_PI325181	1921	2244	117%	601
AK251526.1	Pseudoroegneria_stipifolia_PI440095	1921	2161	112%	601
AK251526.1	Pseudoroegneria_stipifolia_PI531751	1921	2252	117%	601
AK251526.1	Pseudoroegneria_strigosa_PI499638	1921	2136	111%	601
AK251526.1	Pseudoroegneria_strigosa_PI595172	1921	1978	103%	601
AK251526.1	Pseudoroegneria_strigosa_W614049	1921	2194	114%	601
AK251526.1	Pseudoroegneria_strigosa_PI639805	1921	1939	101%	601
AK251526.1	Pseudoroegneria_strigosa_PI639805	1921	2024	105%	601
AK251526.1	Pseudoroegneria_tauri_PI401322	1921	1973	103%	601
AK251526.1	Pseudoroegneria_tauri_PI401333	1921	2097	109%	601
AK251526.1	Secale_cereale_PI618662	1921	1855	97%	601
AK251526.1	Secale_cereale_PI618665	1921	1989	104%	601
AK251526.1	Secale_cereale_PI618669	1921	2112	110%	601
AK251526.1	Secale_cereale_PI618671	1921	2044	106%	601
AK251526.1	Secale_strictum_R1108	1921	1845	96%	601
AK251526.1	Secale_strictum_R853	1921	2053	107%	601
AK251526.1	Secale_vavilovii_PI253957	1921	1732	90%	601
AK251526.1	Secale_vavilovii_R1027	1921	1893	99%	601
AK251526.1	Taeniatherum_caput-medusae_CK2011	1921	2148	112%	601
AK251526.1	Taeniatherum_caput-medusae_GRA1126	1921	2188	114%	601
AK251526.1	Taeniatherum_caput-medusae_PI220589	1921	2151	112%	601
AK251526.1	Taeniatherum_caput-medusae_PI251387	1921	1968	102%	601
AK251526.1	Taeniatherum_caput-medusae_PI561095	1921	1782	93%	601
AK251526.1	Taeniatherum_crininum_GRA2570	1921	2068	108%	601
AK251526.1	Thinopyrum_bessarabicum_W621890	1921	2007	104%	601
AK251526.1	Thinopyrum_elongatum_PI109452	1921	2051	107%	601
AK251526.1	Thinopyrum_elongatum_PI401117	1921	1874	98%	601
AK251526.1	Triticum_boeoticum_1613	1921	2252	117%	601
AK251526.1	Triticum_boeoticum_1688	1921	2247	117%	601
AK251526.1	Triticum_boeoticum_ID379	1921	2017	105%	601
AK251526.1	Triticum_boeoticum_PI272520	1921	2023	105%	601
AK251526.1	Triticum_boeoticum_PI427451	1921	2166	113%	601
AK251526.1	Triticum_boeoticum_PI427620	1921	2118	110%	601
AK251526.1	Triticum_monococcum_2205	1921	2124	111%	601
AK251526.1	Triticum_monococcum_2208	1921	2093	109%	601
AK251526.1	Triticum_monococcum_2271	1921	2241	117%	601
AK251526.1	Triticum_monococcum_TR113061	1921	2140	111%	601
AK251526.1	Triticum_monococcum_TR113612	1921	2175	113%	601
AK251526.1	Triticum_urartu_1307	1921	2253	117%	601
AK251526.1	Triticum_urartu_PI428184	1921	2110	110%	601
AK251526.1	Triticum_urartu_PI428317	1921	2078	108%	601
AK251526.1	Triticum_urartu_TR117824	1921	2152	112%	601
AK251526.1	Triticum_urartu_TR118407	1921	2141	111%	601
AK251704.1	Aegilops_bicornis_AE106	1639	2153	131%	601

Locus	Accession	Mapped exon length in barley (bp)	Assembled exon length (bp)	% of mapped exon length that could be assembled	Extended target (bp)
AK251704.1	Aegilops_bicornis_AE1079	1639	1735	106%	601
AK251704.1	Aegilops_bicornis_AE788	1639	2085	127%	601
AK251704.1	Aegilops_bicornis_KU-5786	1639	1835	112%	601
AK251704.1	Aegilops_comosa_AE1255	1639	2006	122%	601
AK251704.1	Aegilops_comosa_AE1378	1639	1818	111%	601
AK251704.1	Aegilops_comosa_AE783	1639	1954	119%	601
AK251704.1	Aegilops_comosa_PI276970	1639	1691	103%	601
AK251704.1	Aegilops_longissima_AE1078	1639	1999	122%	601
AK251704.1	Aegilops_longissima_AE133	1639	1980	121%	601
AK251704.1	Aegilops_longissima_AE417	1639	1933	118%	601
AK251704.1	Aegilops_longissima_PI604141	1639	1713	105%	601
AK251704.1	Aegilops_longissima_TA1921	1639	1951	119%	601
AK251704.1	Aegilops_markgrafii_AE1381	1639	2166	132%	601
AK251704.1	Aegilops_markgrafii_KP-2012-106	1639	2064	126%	601
AK251704.1	Aegilops_markgrafii_PI254863	1639	1976	121%	601
AK251704.1	Aegilops_markgrafii_PI542208	1639	2066	126%	601
AK251704.1	Aegilops_markgrafii_PI596287	1639	1964	120%	601
AK251704.1	Aegilops_mutica_01C2100106	1639	2029	124%	601
AK251704.1	Aegilops_searsii_AE1075	1639	1785	109%	601
AK251704.1	Aegilops_searsii_AE1083	1639	1986	121%	601
AK251704.1	Aegilops_searsii_KU-14655	1639	2085	127%	601
AK251704.1	Aegilops_searsii_PI599142	1639	2011	123%	601
AK251704.1	Aegilops_searsii_PI599148	1639	1520	93%	601
AK251704.1	Aegilops_sharonensis_AE90691	1639	2095	128%	601
AK251704.1	Aegilops_speltoides_3776	1639	1962	120%	601
AK251704.1	Aegilops_speltoides_AE1064	1639	1956	119%	601
AK251704.1	Aegilops_speltoides_AE900	1639	1935	118%	601
AK251704.1	Aegilops_speltoides_KU-7856	1639	1765	108%	601
AK251704.1	Aegilops_speltoides_PI486264	1639	2042	125%	601
AK251704.1	Aegilops_speltoides_PI487231	1639	1933	118%	601
AK251704.1	Aegilops_speltoides_TA1772	1639	1656	101%	601
AK251704.1	Aegilops_tauschii_49116	1639	1966	120%	601
AK251704.1	Aegilops_tauschii_937	1639	2106	128%	601
AK251704.1	Aegilops_tauschii_AE1069	1639	1969	120%	601
AK251704.1	Aegilops_tauschii_AE956	1639	1960	120%	601
AK251704.1	Aegilops_umbellulata_AE1070	1639	2058	126%	601
AK251704.1	Aegilops_umbellulata_AE153	1639	2067	126%	601
AK251704.1	Aegilops_umbellulata_AE740	1639	1794	109%	601
AK251704.1	Aegilops_umbellulata_AE811	1639	1832	112%	601
AK251704.1	Aegilops_uniaristata_AE157	1639	2013	123%	601
AK251704.1	Aegilops_uniaristata_AE680	1639	2005	122%	601
AK251704.1	Aegilops_uniaristata_PI276996	1639	1834	112%	601
AK251704.1	Agropyron_cristatum_PI494615	1639	1924	117%	601
AK251704.1	Agropyron_cristatum_PI598631	1639	1966	120%	601
AK251704.1	Amblyopyrum_muticum_PI560122	1639	1652	101%	601
AK251704.1	Amblyopyrum_muticum_PI560124	1639	1662	101%	601
AK251704.1	Amblyopyrum_muticum_PI560125	1639	1728	105%	601
AK251704.1	Amblyopyrum_muticum_PI560126	1639	1582	97%	601
AK251704.1	Amblyopyrum_muticum_PI636562	1639	1940	118%	601
AK251704.1	Australopyrum_retrofractum_PI531553	1639	1897	116%	601
AK251704.1	Australopyrum_retrofractum_PI533013	1639	1860	113%	601
AK251704.1	Australopyrum_retrofractum_PI533014	1639	1967	120%	601
AK251704.1	Australopyrum_retrofractum_PI547363	1639	2042	125%	601
AK251704.1	Brachypodium_distachyon	1639	0	0%	601
AK251704.1	Bromus_tectorum_GRA1085	1639	1842	112%	601
AK251704.1	Dasyphyrum_villosum_GRA1020	1639	1818	111%	601
AK251704.1	Dasyphyrum_villosum_GRA1027	1639	1983	121%	601
AK251704.1	Dasyphyrum_villosum_PI368884	1639	1647	100%	601
AK251704.1	Dasyphyrum_villosum_W619414	1639	1801	110%	601
AK251704.1	Dasyphyrum_villosum_W67300	1639	2001	122%	601
AK251704.1	Eremopyrum_distans_PI193264	1639	1863	114%	601
AK251704.1	Eremopyrum_triticeum_GRA2250	1639	2080	127%	601
AK251704.1	Eremopyrum_triticeum_PI502364	1639	1899	116%	601
AK251704.1	Eremopyrum_triticeum_W626631	1639	1801	110%	601
AK251704.1	Henrardia_persica_PI401347	1639	1875	114%	601
AK251704.1	Henrardia_persica_PI577112	1639	1977	121%	601
AK251704.1	Henrardia_persica_PI577113	1639	1935	118%	601
AK251704.1	Henrardia_persica_RF2012	1639	1916	117%	601
AK251704.1	Heteranthelium_piliferum_PI401351	1639	1967	120%	601
AK251704.1	Heteranthelium_piliferum_PI401353	1639	2080	127%	601
AK251704.1	Heteranthelium_piliferum_PI401354	1639	2107	129%	601
AK251704.1	Heteranthelium_sp_PI314152	1639	1880	115%	601
AK251704.1	Hordeum_marinum_BCC2006	1639	2050	125%	601
AK251704.1	Hordeum_marinum_BCC2002	1639	2030	124%	601
AK251704.1	Hordeum_pubiflorum_2028	1639	2133	130%	601
AK251704.1	Hordeum_spontaneum_FT11	1639	2219	135%	601
AK251704.1	Hordeum_vulgare_Morex	1639	2227	136%	601
AK251704.1	Psathyrostachys_juncea_PI222050	1639	1973	120%	601
AK251704.1	Psathyrostachys_juncea_PI565077	1639	1872	114%	601
AK251704.1	Psathyrostachys_juncea_PI595135	1639	1932	118%	601
AK251704.1	Psathyrostachys_juncea_PI598613	1639	1992	122%	601
AK251704.1	Psathyrostachys_juncea_PI619487	1639	1970	120%	601
AK251704.1	Psathyrostachys_sp_PI565080	1639	1856	113%	601
AK251704.1	Pseudoroegneria_libanotica_PI228389	1639	1819	111%	601
AK251704.1	Pseudoroegneria_libanotica_PI330688	1639	1921	117%	601
AK251704.1	Pseudoroegneria_libanotica_PI401274	1639	1957	119%	601

Locus	Accession	Mapped exon length in barley (bp)	Assembled exon length (bp)	% of mapped exon length that could be assembled	Extended target (bp)
AK251704.1	Pseudoroegneria_stipifolia_PI325181	1639	2113	129%	601
AK251704.1	Pseudoroegneria_stipifolia_PI440095	1639	2008	123%	601
AK251704.1	Pseudoroegneria_stipifolia_PI531751	1639	1883	115%	601
AK251704.1	Pseudoroegneria_strigosa_PI499638	1639	1941	118%	601
AK251704.1	Pseudoroegneria_strigosa_PI595172	1639	1854	113%	601
AK251704.1	Pseudoroegneria_strigosa_W614049	1639	2003	122%	601
AK251704.1	Pseudoroegneria_strigosa_PI639805	1639	1937	118%	601
AK251704.1	Pseudoroegneria_strigosa_PI639805	1639	1927	118%	601
AK251704.1	Pseudoroegneria_tauri_PI401322	1639	1802	110%	601
AK251704.1	Pseudoroegneria_tauri_PI401333	1639	1936	118%	601
AK251704.1	Secale_cereale_PI618662	1639	1733	106%	601
AK251704.1	Secale_cereale_PI618665	1639	1834	112%	601
AK251704.1	Secale_cereale_PI618669	1639	2023	123%	601
AK251704.1	Secale_cereale_PI618671	1639	1954	119%	601
AK251704.1	Secale_strictum_R1108	1639	1888	115%	601
AK251704.1	Secale_strictum_R853	1639	1990	121%	601
AK251704.1	Secale_vavilovii_PI253957	1639	1511	92%	601
AK251704.1	Secale_vavilovii_R1027	1639	1814	111%	601
AK251704.1	Taeniatherum_caput-medusae_CK2011	1639	2050	125%	601
AK251704.1	Taeniatherum_caput-medusae_GRA1126	1639	2121	129%	601
AK251704.1	Taeniatherum_caput-medusae_PI220589	1639	1998	122%	601
AK251704.1	Taeniatherum_caput-medusae_PI251387	1639	1868	114%	601
AK251704.1	Taeniatherum_caput-medusae_PI561095	1639	1785	109%	601
AK251704.1	Taeniatherum_crinatum_GRA2570	1639	2007	122%	601
AK251704.1	Thinopyrum_bessarabicum_W621890	1639	1788	109%	601
AK251704.1	Thinopyrum_elongatum_PI109452	1639	1992	122%	601
AK251704.1	Thinopyrum_elongatum_PI401117	1639	1688	103%	601
AK251704.1	Triticum_boeoticum_1613	1639	2207	135%	601
AK251704.1	Triticum_boeoticum_1688	1639	2054	125%	601
AK251704.1	Triticum_boeoticum_ID379	1639	1839	112%	601
AK251704.1	Triticum_boeoticum_PI272520	1639	1825	111%	601
AK251704.1	Triticum_boeoticum_PI427451	1639	2074	127%	601
AK251704.1	Triticum_boeoticum_PI427620	1639	1995	122%	601
AK251704.1	Triticum_monococcum_2205	1639	2135	130%	601
AK251704.1	Triticum_monococcum_2208	1639	2082	127%	601
AK251704.1	Triticum_monococcum_2271	1639	2213	135%	601
AK251704.1	Triticum_monococcum_TRI13061	1639	2077	127%	601
AK251704.1	Triticum_monococcum_TRI13612	1639	2080	127%	601
AK251704.1	Triticum_urartu_1307	1639	2046	125%	601
AK251704.1	Triticum_urartu_PI428184	1639	1806	110%	601
AK251704.1	Triticum_urartu_PI428317	1639	1820	111%	601
AK251704.1	Triticum_urartu_TRI17824	1639	2021	123%	601
AK251704.1	Triticum_urartu_TRI18407	1639	2025	124%	601
AK252992.1	Aegilops_bicornis_AE106	1197	1438	120%	601
AK252992.1	Aegilops_bicornis_AE1079	1197	902	75%	601
AK252992.1	Aegilops_bicornis_AE788	1197	1265	106%	601
AK252992.1	Aegilops_bicornis_KU-5786	1197	1082	90%	601
AK252992.1	Aegilops_comosa_AE1255	1197	1325	111%	601
AK252992.1	Aegilops_comosa_AE1378	1197	1304	109%	601
AK252992.1	Aegilops_comosa_AE783	1197	1249	104%	601
AK252992.1	Aegilops_comosa_PI276970	1197	1064	89%	601
AK252992.1	Aegilops_longissima_AE1078	1197	1247	104%	601
AK252992.1	Aegilops_longissima_AE133	1197	1340	112%	601
AK252992.1	Aegilops_longissima_AE417	1197	1118	93%	601
AK252992.1	Aegilops_longissima_PI604141	1197	1029	86%	601
AK252992.1	Aegilops_longissima_TA1921	1197	1292	108%	601
AK252992.1	Aegilops_markgrafii_AE1381	1197	1394	116%	601
AK252992.1	Aegilops_markgrafii_KP-2012-106	1197	1412	118%	601
AK252992.1	Aegilops_markgrafii_PI254863	1197	1266	106%	601
AK252992.1	Aegilops_markgrafii_PI542208	1197	1365	114%	601
AK252992.1	Aegilops_markgrafii_PI596287	1197	1335	112%	601
AK252992.1	Aegilops_mutica_01C2100106	1197	1340	112%	601
AK252992.1	Aegilops_searsii_AE1075	1197	1196	100%	601
AK252992.1	Aegilops_searsii_AE1083	1197	1410	118%	601
AK252992.1	Aegilops_searsii_KU-14655	1197	1341	112%	601
AK252992.1	Aegilops_searsii_PI599142	1197	1322	110%	601
AK252992.1	Aegilops_searsii_PI599148	1197	986	82%	601
AK252992.1	Aegilops_sharonensis_AE90691	1197	1288	108%	601
AK252992.1	Aegilops_speltoides_3776	1197	1445	121%	601
AK252992.1	Aegilops_speltoides_AE1064	1197	1298	108%	601
AK252992.1	Aegilops_speltoides_AE900	1197	1267	106%	601
AK252992.1	Aegilops_speltoides_KU-7856	1197	1116	93%	601
AK252992.1	Aegilops_speltoides_PI486264	1197	1356	113%	601
AK252992.1	Aegilops_speltoides_PI487231	1197	1309	109%	601
AK252992.1	Aegilops_speltoides_TA1772	1197	1023	85%	601
AK252992.1	Aegilops_tauschii_49116	1197	1176	98%	601
AK252992.1	Aegilops_tauschii_937	1197	1529	128%	601
AK252992.1	Aegilops_tauschii_AE1069	1197	1283	107%	601
AK252992.1	Aegilops_tauschii_AE956	1197	1400	117%	601
AK252992.1	Aegilops_umbellulata_AE1070	1197	1332	111%	601
AK252992.1	Aegilops_umbellulata_AE153	1197	1442	120%	601
AK252992.1	Aegilops_umbellulata_AE740	1197	1239	104%	601
AK252992.1	Aegilops_umbellulata_AE811	1197	936	78%	601
AK252992.1	Aegilops_uniaristata_AE157	1197	1388	116%	601
AK252992.1	Aegilops_uniaristata_AE680	1197	1374	115%	601
AK252992.1	Aegilops_uniaristata_PI276996	1197	1091	91%	601

Locus	Accession	Mapped exon length in barley (bp)	Assembled exon length (bp)	% of mapped exon length that could be assembled	Extended target (bp)
AK252992.1	Agropyron_cristatum_PI494615	1197	1415	118%	601
AK252992.1	Agropyron_cristatum_PI598631	1197	1259	105%	601
AK252992.1	Amblyopyrum_muticum_PI560122	1197	953	80%	601
AK252992.1	Amblyopyrum_muticum_PI560124	1197	1041	87%	601
AK252992.1	Amblyopyrum_muticum_PI560125	1197	876	73%	601
AK252992.1	Amblyopyrum_muticum_PI560126	1197	885	74%	601
AK252992.1	Amblyopyrum_muticum_PI636562	1197	1232	103%	601
AK252992.1	Australopyrum_retrofractum_PI531553	1197	1257	105%	601
AK252992.1	Australopyrum_retrofractum_PI533013	1197	1134	95%	601
AK252992.1	Australopyrum_retrofractum_PI533014	1197	1408	118%	601
AK252992.1	Australopyrum_retrofractum_PI547363	1197	1367	114%	601
AK252992.1	Brachypodium_distachyon	1197	1174	98%	601
AK252992.1	Bromus_tectorum_GRA1085	1197	1244	104%	601
AK252992.1	Dasyphyrum_villosum_GRA1020	1197	1248	104%	601
AK252992.1	Dasyphyrum_villosum_GRA1027	1197	1292	108%	601
AK252992.1	Dasyphyrum_villosum_PI368884	1197	1037	87%	601
AK252992.1	Dasyphyrum_villosum_W619414	1197	1133	95%	601
AK252992.1	Dasyphyrum_villosum_W67300	1197	1286	107%	601
AK252992.1	Eremopyrum_distans_PI193264	1197	1234	103%	601
AK252992.1	Eremopyrum_triticeum_GRA2250	1197	1332	111%	601
AK252992.1	Eremopyrum_triticeum_PI502364	1197	1258	105%	601
AK252992.1	Eremopyrum_triticeum_W626631	1197	1185	99%	601
AK252992.1	Henrardia_persica_PI401347	1197	1327	111%	601
AK252992.1	Henrardia_persica_PI577112	1197	1422	119%	601
AK252992.1	Henrardia_persica_PI577113	1197	1252	105%	601
AK252992.1	Henrardia_persica_RF2012	1197	1390	116%	601
AK252992.1	Heteranthelium_piliferum_PI401351	1197	1312	110%	601
AK252992.1	Heteranthelium_piliferum_PI401353	1197	1321	110%	601
AK252992.1	Heteranthelium_piliferum_PI401354	1197	1458	122%	601
AK252992.1	Heteranthelium_sp_PI314152	1197	1197	100%	601
AK252992.1	Hordeum_marinum_BCC2006	1197	1469	123%	601
AK252992.1	Hordeum_murinum_BCC2002	1197	1536	128%	601
AK252992.1	Hordeum_pubiflorum_2028	1197	1459	122%	601
AK252992.1	Hordeum_spontaneum_FT11	1197	1624	136%	601
AK252992.1	Hordeum_vulgare_Morex	1197	1692	141%	601
AK252992.1	Psathyrostachys_junceae_PI222050	1197	1232	103%	601
AK252992.1	Psathyrostachys_junceae_PI565077	1197	1114	93%	601
AK252992.1	Psathyrostachys_junceae_PI595135	1197	1300	109%	601
AK252992.1	Psathyrostachys_junceae_PI598613	1197	1312	110%	601
AK252992.1	Psathyrostachys_junceae_PI619487	1197	1317	110%	601
AK252992.1	Psathyrostachys_sp_PI565080	1197	1230	103%	601
AK252992.1	Pseudoroegneria_libanotica_PI228389	1197	1142	95%	601
AK252992.1	Pseudoroegneria_libanotica_PI330688	1197	1278	107%	601
AK252992.1	Pseudoroegneria_libanotica_PI401274	1197	1286	107%	601
AK252992.1	Pseudoroegneria_stipifolia_PI325181	1197	1376	115%	601
AK252992.1	Pseudoroegneria_stipifolia_PI440095	1197	1435	120%	601
AK252992.1	Pseudoroegneria_stipifolia_PI531751	1197	1331	111%	601
AK252992.1	Pseudoroegneria_strigosa_PI499638	1197	1161	97%	601
AK252992.1	Pseudoroegneria_strigosa_PI595172	1197	1344	112%	601
AK252992.1	Pseudoroegneria_strigosa_W614049	1197	1305	109%	601
AK252992.1	Pseudoroegneria_strigosa_PI639805	1197	1240	104%	601
AK252992.1	Pseudoroegneria_strigosa_PI639805	1197	1331	111%	601
AK252992.1	Pseudoroegneria_tauri_PI401322	1197	1146	96%	601
AK252992.1	Pseudoroegneria_tauri_PI401333	1197	1414	118%	601
AK252992.1	Secale_cereale_PI618662	1197	789	66%	601
AK252992.1	Secale_cereale_PI618665	1197	1285	107%	601
AK252992.1	Secale_cereale_PI618669	1197	1361	114%	601
AK252992.1	Secale_cereale_PI618671	1197	1361	114%	601
AK252992.1	Secale_strictum_R1108	1197	1103	92%	601
AK252992.1	Secale_strictum_R853	1197	1315	110%	601
AK252992.1	Secale_vavilovii_PI253957	1197	873	73%	601
AK252992.1	Secale_vavilovii_R1027	1197	1115	93%	601
AK252992.1	Taeniatherum_caput-medusae_CK2011	1197	1284	107%	601
AK252992.1	Taeniatherum_caput-medusae_GRA1126	1197	1581	132%	601
AK252992.1	Taeniatherum_caput-medusae_PI220589	1197	1341	112%	601
AK252992.1	Taeniatherum_caput-medusae_PI251387	1197	882	74%	601
AK252992.1	Taeniatherum_caput-medusae_PI561095	1197	769	64%	601
AK252992.1	Taeniatherum_crinium_GRA2570	1197	1314	110%	601
AK252992.1	Thinopyrum_bessarabicum_W621890	1197	1247	104%	601
AK252992.1	Thinopyrum_elongatum_PI109452	1197	1330	111%	601
AK252992.1	Thinopyrum_elongatum_PI401117	1197	1041	87%	601
AK252992.1	Triticum_boeoticum_1613	1197	1477	123%	601
AK252992.1	Triticum_boeoticum_1688	1197	1416	118%	601
AK252992.1	Triticum_boeoticum_ID379	1197	1140	95%	601
AK252992.1	Triticum_boeoticum_PI272520	1197	1165	97%	601
AK252992.1	Triticum_boeoticum_PI427451	1197	1399	117%	601
AK252992.1	Triticum_boeoticum_PI427620	1197	1242	104%	601
AK252992.1	Triticum_monococcum_2205	1197	1323	111%	601
AK252992.1	Triticum_monococcum_2208	1197	1414	118%	601
AK252992.1	Triticum_monococcum_2271	1197	1530	128%	601
AK252992.1	Triticum_monococcum_TRI13061	1197	1241	104%	601
AK252992.1	Triticum_monococcum_TRI13612	1197	1362	114%	601
AK252992.1	Triticum_urartu_1307	1197	1503	126%	601
AK252992.1	Triticum_urartu_PI428184	1197	1148	96%	601
AK252992.1	Triticum_urartu_PI428317	1197	1159	97%	601
AK252992.1	Triticum_urartu_TRI17824	1197	1408	118%	601

Locus	Accession	Mapped exon length in barley (bp)	Assembled exon length (bp)	% of mapped exon length that could be assembled	Extended target (bp)	
AK252992.1	Triticum_urartu_TRI18407		1197	1441	120%	601
NIASHv1003D08	Aegilops_bicornis_AE106		1000	1394	139%	601
NIASHv1003D08	Aegilops_bicornis_AE1079		1000	1070	107%	601
NIASHv1003D08	Aegilops_bicornis_AE788		1000	1335	134%	601
NIASHv1003D08	Aegilops_bicornis_KU-5786		1000	1207	121%	601
NIASHv1003D08	Aegilops_comosa_AE1255		1000	1354	135%	601
NIASHv1003D08	Aegilops_comosa_AE1378		1000	1195	120%	601
NIASHv1003D08	Aegilops_comosa_AE783		1000	1226	123%	601
NIASHv1003D08	Aegilops_comosa_PI276970		1000	1041	104%	601
NIASHv1003D08	Aegilops_longissima_AE1078		1000	1270	127%	601
NIASHv1003D08	Aegilops_longissima_AE133		1000	1298	130%	601
NIASHv1003D08	Aegilops_longissima_AE417		1000	1042	104%	601
NIASHv1003D08	Aegilops_longissima_PI604141		1000	1146	115%	601
NIASHv1003D08	Aegilops_longissima_TA1921		1000	1291	129%	601
NIASHv1003D08	Aegilops_markgrafii_AE1381		1000	1406	141%	601
NIASHv1003D08	Aegilops_markgrafii_KP-2012-106		1000	1441	144%	601
NIASHv1003D08	Aegilops_markgrafii_PI254863		1000	1166	117%	601
NIASHv1003D08	Aegilops_markgrafii_PI542208		1000	1436	144%	601
NIASHv1003D08	Aegilops_markgrafii_PI596287		1000	1392	139%	601
NIASHv1003D08	Aegilops_mutica_01C2100106		1000	1340	134%	601
NIASHv1003D08	Aegilops_searsii_AE1075		1000	1183	118%	601
NIASHv1003D08	Aegilops_searsii_AE1083		1000	1458	146%	601
NIASHv1003D08	Aegilops_searsii_KU-14655		1000	1381	138%	601
NIASHv1003D08	Aegilops_searsii_PI599142		1000	1362	136%	601
NIASHv1003D08	Aegilops_searsii_PI599148		1000	916	92%	601
NIASHv1003D08	Aegilops_sharonensis_AE90691		1000	1343	134%	601
NIASHv1003D08	Aegilops_speltooides_3776		1000	1496	150%	601
NIASHv1003D08	Aegilops_speltooides_AE1064		1000	1216	122%	601
NIASHv1003D08	Aegilops_speltooides_AE900		1000	1325	133%	601
NIASHv1003D08	Aegilops_speltooides_KU-7856		1000	1025	103%	601
NIASHv1003D08	Aegilops_speltooides_PI486264		1000	1324	132%	601
NIASHv1003D08	Aegilops_speltooides_PI487231		1000	1348	135%	601
NIASHv1003D08	Aegilops_speltooides_TA1772		1000	1155	116%	601
NIASHv1003D08	Aegilops_tauschii_49116		1000	1270	127%	601
NIASHv1003D08	Aegilops_tauschii_937		1000	1577	158%	601
NIASHv1003D08	Aegilops_tauschii_AE1069		1000	1249	125%	601
NIASHv1003D08	Aegilops_tauschii_AE956		1000	1336	134%	601
NIASHv1003D08	Aegilops_umbellulata_AE1070		1000	1387	139%	601
NIASHv1003D08	Aegilops_umbellulata_AE153		1000	1369	137%	601
NIASHv1003D08	Aegilops_umbellulata_AE740		1000	1134	113%	601
NIASHv1003D08	Aegilops_umbellulata_AE811		1000	824	82%	601
NIASHv1003D08	Aegilops_uniaristata_AE157		1000	1325	133%	601
NIASHv1003D08	Aegilops_uniaristata_AE680		1000	1415	142%	601
NIASHv1003D08	Aegilops_uniaristata_PI276996		1000	1235	124%	601
NIASHv1003D08	Agropyron_cristatum_PI494615		1000	1272	127%	601
NIASHv1003D08	Agropyron_cristatum_PI598631		1000	1260	126%	601
NIASHv1003D08	Amblyopyrum_muticum_PI560122		1000	1038	104%	601
NIASHv1003D08	Amblyopyrum_muticum_PI560124		1000	1042	104%	601
NIASHv1003D08	Amblyopyrum_muticum_PI560125		1000	914	91%	601
NIASHv1003D08	Amblyopyrum_muticum_PI560126		1000	724	72%	601
NIASHv1003D08	Amblyopyrum_muticum_PI636562		1000	1327	133%	601
NIASHv1003D08	Australopyrum_retrofractum_PI531553		1000	1240	124%	601
NIASHv1003D08	Australopyrum_retrofractum_PI533013		1000	1027	103%	601
NIASHv1003D08	Australopyrum_retrofractum_PI533014		1000	1249	125%	601
NIASHv1003D08	Australopyrum_retrofractum_PI547363		1000	1247	125%	601
NIASHv1003D08	Brachypodium_distachyon		1000	730	73%	601
NIASHv1003D08	Bromus_tectorum_GRA1085		1000	1226	123%	601
NIASHv1003D08	Dasyphyrum_villosum_GRA1020		1000	1248	125%	601
NIASHv1003D08	Dasyphyrum_villosum_GRA1027		1000	1335	134%	601
NIASHv1003D08	Dasyphyrum_villosum_PI368884		1000	963	96%	601
NIASHv1003D08	Dasyphyrum_villosum_W619414		1000	1084	108%	601
NIASHv1003D08	Dasyphyrum_villosum_W67300		1000	1380	138%	601
NIASHv1003D08	Eremopyrum_distans_PI193264		1000	1280	128%	601
NIASHv1003D08	Eremopyrum_triticeum_GRA2250		1000	1379	138%	601
NIASHv1003D08	Eremopyrum_triticeum_PI502364		1000	1220	122%	601
NIASHv1003D08	Eremopyrum_triticeum_W626631		1000	1321	132%	601
NIASHv1003D08	Henrardia_persica_PI401347		1000	1243	124%	601
NIASHv1003D08	Henrardia_persica_PI577112		1000	1399	140%	601
NIASHv1003D08	Henrardia_persica_PI577113		1000	1236	124%	601
NIASHv1003D08	Henrardia_persica_RF2012		1000	1301	130%	601
NIASHv1003D08	Heteranthelium_piliferum_PI401351		1000	1370	137%	601
NIASHv1003D08	Heteranthelium_piliferum_PI401353		1000	1366	137%	601
NIASHv1003D08	Heteranthelium_piliferum_PI401354		1000	1447	145%	601
NIASHv1003D08	Heteranthelium_sp_PI314152		1000	1236	124%	601
NIASHv1003D08	Hordeum_marinum_BCC2006		1000	1553	155%	601
NIASHv1003D08	Hordeum_marinum_BCC2002		1000	1337	134%	601
NIASHv1003D08	Hordeum_pubiflorum_2028		1000	1600	160%	601
NIASHv1003D08	Hordeum_spontanum_FT11		1000	1523	152%	601
NIASHv1003D08	Hordeum_vulgare_Morex		1000	1601	160%	601
NIASHv1003D08	Psathyrostachys_junceae_PI222050		1000	1159	116%	601
NIASHv1003D08	Psathyrostachys_junceae_PI565077		1000	1161	116%	601
NIASHv1003D08	Psathyrostachys_junceae_PI595135		1000	1308	131%	601
NIASHv1003D08	Psathyrostachys_junceae_PI598613		1000	1403	140%	601
NIASHv1003D08	Psathyrostachys_junceae_PI619487		1000	1401	140%	601
NIASHv1003D08	Psathyrostachys_sp_PI565080		1000	1296	130%	601
NIASHv1003D08	Pseudoroegneria_libanotica_PI228389		1000	1125	113%	601

Locus	Accession	Mapped exon length in barley (bp)	Assembled exon length (bp)	% of mapped exon length that could be assembled	Extended target (bp)
NIASHv1003D08	Pseudoroegneria_libanotica_PI330688	1000	1131	113%	601
NIASHv1003D08	Pseudoroegneria_libanotica_PI401274	1000	1239	124%	601
NIASHv1003D08	Pseudoroegneria_stipifolia_PI325181	1000	1291	129%	601
NIASHv1003D08	Pseudoroegneria_stipifolia_PI440095	1000	1341	134%	601
NIASHv1003D08	Pseudoroegneria_stipifolia_PI531751	1000	1225	123%	601
NIASHv1003D08	Pseudoroegneria_strigosa_PI499638	1000	1272	127%	601
NIASHv1003D08	Pseudoroegneria_strigosa_PI595172	1000	1272	127%	601
NIASHv1003D08	Pseudoroegneria_strigosa_W614049	1000	1302	130%	601
NIASHv1003D08	Pseudoroegneria_strigosa_PI639805	1000	1288	129%	601
NIASHv1003D08	Pseudoroegneria_strigosa_PI639805	1000	1315	132%	601
NIASHv1003D08	Pseudoroegneria_tauri_PI401322	1000	1094	109%	601
NIASHv1003D08	Pseudoroegneria_tauri_PI401333	1000	1279	128%	601
NIASHv1003D08	Secale_cereale_PI618662	1000	837	84%	601
NIASHv1003D08	Secale_cereale_PI618665	1000	1308	131%	601
NIASHv1003D08	Secale_cereale_PI618669	1000	1472	147%	601
NIASHv1003D08	Secale_cereale_PI618671	1000	1191	119%	601
NIASHv1003D08	Secale_strictum_R1108	1000	1052	105%	601
NIASHv1003D08	Secale_strictum_R853	1000	1346	135%	601
NIASHv1003D08	Secale_vavilovii_PI253957	1000	694	69%	601
NIASHv1003D08	Secale_vavilovii_R1027	1000	1098	110%	601
NIASHv1003D08	Taeniatherum_caput-medusae_CK2011	1000	1404	140%	601
NIASHv1003D08	Taeniatherum_caput-medusae_GRA1126	1000	1398	140%	601
NIASHv1003D08	Taeniatherum_caput-medusae_PI220589	1000	1254	125%	601
NIASHv1003D08	Taeniatherum_caput-medusae_PI251387	1000	1043	104%	601
NIASHv1003D08	Taeniatherum_caput-medusae_PI561095	1000	1055	106%	601
NIASHv1003D08	Taeniatherum_crinutum_GRA2570	1000	1355	136%	601
NIASHv1003D08	Thinopyrum_bessarabicum_W621890	1000	1302	130%	601
NIASHv1003D08	Thinopyrum_elongatum_PI109452	1000	1250	125%	601
NIASHv1003D08	Thinopyrum_elongatum_PI401117	1000	999	100%	601
NIASHv1003D08	Triticum_boeoticum_1613	1000	1449	145%	601
NIASHv1003D08	Triticum_boeoticum_1688	1000	1386	139%	601
NIASHv1003D08	Triticum_boeoticum_ID379	1000	1152	115%	601
NIASHv1003D08	Triticum_boeoticum_PI272520	1000	1077	108%	601
NIASHv1003D08	Triticum_boeoticum_PI427451	1000	1450	145%	601
NIASHv1003D08	Triticum_boeoticum_PI427620	1000	1292	129%	601
NIASHv1003D08	Triticum_monococcum_2205	1000	1375	138%	601
NIASHv1003D08	Triticum_monococcum_2208	1000	1394	139%	601
NIASHv1003D08	Triticum_monococcum_2271	1000	1526	153%	601
NIASHv1003D08	Triticum_monococcum_TR113061	1000	1297	130%	601
NIASHv1003D08	Triticum_monococcum_TR113612	1000	1360	136%	601
NIASHv1003D08	Triticum_urartu_1307	1000	1482	148%	601
NIASHv1003D08	Triticum_urartu_PI428184	1000	1048	105%	601
NIASHv1003D08	Triticum_urartu_PI428317	1000	1092	109%	601
NIASHv1003D08	Triticum_urartu_TR117824	1000	1342	134%	601
NIASHv1003D08	Triticum_urartu_TR118407	1000	1419	142%	601
NIASHv1004I13	Aegilops_bicornis_AE106	922	1022	111%	601
NIASHv1004I13	Aegilops_bicornis_AE1079	922	779	84%	601
NIASHv1004I13	Aegilops_bicornis_AE788	922	946	103%	601
NIASHv1004I13	Aegilops_bicornis_KU-5786	922	533	58%	601
NIASHv1004I13	Aegilops_comosa_AE1255	922	996	108%	601
NIASHv1004I13	Aegilops_comosa_AE1378	922	682	74%	601
NIASHv1004I13	Aegilops_comosa_AE783	922	991	107%	601
NIASHv1004I13	Aegilops_comosa_PI276970	922	695	75%	601
NIASHv1004I13	Aegilops_longissima_AE1078	922	689	75%	601
NIASHv1004I13	Aegilops_longissima_AE133	922	948	103%	601
NIASHv1004I13	Aegilops_longissima_AE417	922	425	46%	601
NIASHv1004I13	Aegilops_longissima_PI604141	922	604	66%	601
NIASHv1004I13	Aegilops_longissima_TA1921	922	932	101%	601
NIASHv1004I13	Aegilops_markgrafii_AE1381	922	1039	113%	601
NIASHv1004I13	Aegilops_markgrafii_KP-2012-106	922	952	103%	601
NIASHv1004I13	Aegilops_markgrafii_PI254863	922	513	56%	601
NIASHv1004I13	Aegilops_markgrafii_PI542208	922	979	106%	601
NIASHv1004I13	Aegilops_markgrafii_PI596287	922	1008	109%	601
NIASHv1004I13	Aegilops_mutica_01C2100106	922	1019	111%	601
NIASHv1004I13	Aegilops_searsii_AE1075	922	844	92%	601
NIASHv1004I13	Aegilops_searsii_AE1083	922	1024	111%	601
NIASHv1004I13	Aegilops_searsii_KU-14655	922	985	107%	601
NIASHv1004I13	Aegilops_searsii_PI599142	922	797	86%	601
NIASHv1004I13	Aegilops_searsii_PI599148	922	359	39%	601
NIASHv1004I13	Aegilops_sharonensis_AE90691	922	937	102%	601
NIASHv1004I13	Aegilops_speltoides_3776	922	1100	119%	601
NIASHv1004I13	Aegilops_speltoides_AE1064	922	961	104%	601
NIASHv1004I13	Aegilops_speltoides_AE900	922	997	108%	601
NIASHv1004I13	Aegilops_speltoides_KU-7856	922	639	69%	601
NIASHv1004I13	Aegilops_speltoides_PI486264	922	992	108%	601
NIASHv1004I13	Aegilops_speltoides_PI487231	922	1040	113%	601
NIASHv1004I13	Aegilops_speltoides_TA1772	922	565	61%	601
NIASHv1004I13	Aegilops_tauschii_49116	922	806	87%	601
NIASHv1004I13	Aegilops_tauschii_937	922	1073	116%	601
NIASHv1004I13	Aegilops_tauschii_AE1069	922	761	83%	601
NIASHv1004I13	Aegilops_tauschii_AE956	922	986	107%	601
NIASHv1004I13	Aegilops_umbellulata_AE1070	922	1004	109%	601
NIASHv1004I13	Aegilops_umbellulata_AE153	922	1051	114%	601
NIASHv1004I13	Aegilops_umbellulata_AE740	922	638	69%	601
NIASHv1004I13	Aegilops_umbellulata_AE811	922	364	39%	601
NIASHv1004I13	Aegilops_uniaristata_AE157	922	1012	110%	601

Locus	Accession	Mapped exon length in barley (bp)	Assembled exon length (bp)	% of mapped exon length that could be assembled	Extended target (bp)
NIASHv1004i13	Aegilops_uniaristata_AE680	922	1011	110%	601
NIASHv1004i13	Aegilops_uniaristata_PI276996	922	672	73%	601
NIASHv1004i13	Agropyron_cristatum_PI494615	922	997	108%	601
NIASHv1004i13	Agropyron_cristatum_PI598631	922	1000	108%	601
NIASHv1004i13	Amblyopyrum_muticum_PI560122	922	324	35%	601
NIASHv1004i13	Amblyopyrum_muticum_PI560124	922	382	41%	601
NIASHv1004i13	Amblyopyrum_muticum_PI560125	922	39	4%	601
NIASHv1004i13	Amblyopyrum_muticum_PI560126	922	349	38%	601
NIASHv1004i13	Amblyopyrum_muticum_PI636562	922	911	99%	601
NIASHv1004i13	Australopyrum_retrofractum_PI531553	922	1026	111%	601
NIASHv1004i13	Australopyrum_retrofractum_PI533013	922	828	90%	601
NIASHv1004i13	Australopyrum_retrofractum_PI533014	922	1030	112%	601
NIASHv1004i13	Australopyrum_retrofractum_PI547363	922	1107	120%	601
NIASHv1004i13	Brachypodium_distachyon	922	920	100%	601
NIASHv1004i13	Bromus_tectorum_GRA1085	922	984	107%	601
NIASHv1004i13	Dasypyrum_villosum_GRA1020	922	952	103%	601
NIASHv1004i13	Dasypyrum_villosum_GRA1027	922	921	100%	601
NIASHv1004i13	Dasypyrum_villosum_PI368884	922	600	65%	601
NIASHv1004i13	Dasypyrum_villosum_W619414	922	649	70%	601
NIASHv1004i13	Dasypyrum_villosum_W67300	922	1012	110%	601
NIASHv1004i13	Eremopyrum_distans_PI193264	922	857	93%	601
NIASHv1004i13	Eremopyrum_triticeum_GRA2250	922	1117	121%	601
NIASHv1004i13	Eremopyrum_triticeum_PI502364	922	1040	113%	601
NIASHv1004i13	Eremopyrum_triticeum_W626631	922	663	72%	601
NIASHv1004i13	Henrardia_persica_PI401347	922	975	106%	601
NIASHv1004i13	Henrardia_persica_PI577112	922	1163	126%	601
NIASHv1004i13	Henrardia_persica_PI577113	922	962	104%	601
NIASHv1004i13	Henrardia_persica_RF2012	922	1078	117%	601
NIASHv1004i13	Heteranthelium_piliferum_PI401351	922	1037	112%	601
NIASHv1004i13	Heteranthelium_piliferum_PI401353	922	1110	120%	601
NIASHv1004i13	Heteranthelium_piliferum_PI401354	922	1157	125%	601
NIASHv1004i13	Heteranthelium_sp._PI314152	922	933	101%	601
NIASHv1004i13	Hordeum_marinum_BCC2006	922	1022	111%	601
NIASHv1004i13	Hordeum_marinum_BCC2002	922	1018	110%	601
NIASHv1004i13	Hordeum_pubiflorum_2028	922	1170	127%	601
NIASHv1004i13	Hordeum_spontanum_FT11	922	1249	135%	601
NIASHv1004i13	Hordeum_vulgare_Morex	922	1255	136%	601
NIASHv1004i13	Psathyrostachys_junceae_PI222050	922	936	102%	601
NIASHv1004i13	Psathyrostachys_junceae_PI565077	922	649	70%	601
NIASHv1004i13	Psathyrostachys_junceae_PI595135	922	1004	109%	601
NIASHv1004i13	Psathyrostachys_junceae_PI598613	922	998	108%	601
NIASHv1004i13	Psathyrostachys_junceae_PI619487	922	972	105%	601
NIASHv1004i13	Psathyrostachys_sp._PI565080	922	980	106%	601
NIASHv1004i13	Pseudoroegneria_libanotica_PI228389	922	550	60%	601
NIASHv1004i13	Pseudoroegneria_libanotica_PI330688	922	884	96%	601
NIASHv1004i13	Pseudoroegneria_libanotica_PI401274	922	990	107%	601
NIASHv1004i13	Pseudoroegneria_stipifolia_PI325181	922	1002	109%	601
NIASHv1004i13	Pseudoroegneria_stipifolia_PI440095	922	1000	108%	601
NIASHv1004i13	Pseudoroegneria_stipifolia_PI531751	922	990	107%	601
NIASHv1004i13	Pseudoroegneria_strigosa_PI499638	922	945	102%	601
NIASHv1004i13	Pseudoroegneria_strigosa_PI595172	922	1038	113%	601
NIASHv1004i13	Pseudoroegneria_strigosa_W614049	922	1001	109%	601
NIASHv1004i13	Pseudoroegneria_strigosa_PI639805	922	905	98%	601
NIASHv1004i13	Pseudoroegneria_strigosa_PI639805	922	992	108%	601
NIASHv1004i13	Pseudoroegneria_tauri_PI401322	922	840	91%	601
NIASHv1004i13	Pseudoroegneria_tauri_PI401333	922	1026	111%	601
NIASHv1004i13	Secale_cereale_PI618662	922	375	41%	601
NIASHv1004i13	Secale_cereale_PI618665	922	805	87%	601
NIASHv1004i13	Secale_cereale_PI618669	922	1045	113%	601
NIASHv1004i13	Secale_cereale_PI618671	922	979	106%	601
NIASHv1004i13	Secale_strictum_R1108	922	842	91%	601
NIASHv1004i13	Secale_strictum_R853	922	934	101%	601
NIASHv1004i13	Secale_vavilovii_PI253957	922	363	39%	601
NIASHv1004i13	Secale_vavilovii_R1027	922	885	96%	601
NIASHv1004i13	Taeniatherum_caput-medusae_CK2011	922	915	99%	601
NIASHv1004i13	Taeniatherum_caput-medusae_GRA1126	922	1009	109%	601
NIASHv1004i13	Taeniatherum_caput-medusae_PI220589	922	1013	110%	601
NIASHv1004i13	Taeniatherum_caput-medusae_PI251387	922	713	77%	601
NIASHv1004i13	Taeniatherum_caput-medusae_PI561095	922	420	46%	601
NIASHv1004i13	Taeniatherum_crinatum_GRA2570	922	971	105%	601
NIASHv1004i13	Thinopyrum_bessarabicum_W621890	922	886	96%	601
NIASHv1004i13	Thinopyrum_elongatum_PI109452	922	977	106%	601
NIASHv1004i13	Thinopyrum_elongatum_PI401117	922	514	56%	601
NIASHv1004i13	Triticum_boeoticum_1613	922	1138	123%	601
NIASHv1004i13	Triticum_boeoticum_1688	922	1061	115%	601
NIASHv1004i13	Triticum_boeoticum_ID379	922	748	81%	601
NIASHv1004i13	Triticum_boeoticum_PI272520	922	865	94%	601
NIASHv1004i13	Triticum_boeoticum_PI427451	922	1039	113%	601
NIASHv1004i13	Triticum_boeoticum_PI427620	922	1032	112%	601
NIASHv1004i13	Triticum_monococcum_2205	922	1004	109%	601
NIASHv1004i13	Triticum_monococcum_2208	922	1029	112%	601
NIASHv1004i13	Triticum_monococcum_2271	922	1107	120%	601
NIASHv1004i13	Triticum_monococcum_TR113061	922	985	107%	601
NIASHv1004i13	Triticum_monococcum_TR113612	922	1081	117%	601
NIASHv1004i13	Triticum_urartu_1307	922	1055	114%	601
NIASHv1004i13	Triticum_urartu_PI428184	922	575	62%	601

Locus	Accession	Mapped exon length in barley (bp)	Assembled exon length (bp)	% of mapped exon length that could be assembled	Extended target (bp)
NIASHv1004113	Triticum_urartu_P1428317	922	383	42%	601
NIASHv1004113	Triticum_urartu_TRI17824	922	1089	118%	601
NIASHv1004113	Triticum_urartu_TRI18407	922	1008	109%	601
NIASHv1005K14	Aegilops_bicornis_AE106	1054	1158	110%	601
NIASHv1005K14	Aegilops_bicornis_AE1079	1054	910	86%	601
NIASHv1005K14	Aegilops_bicornis_AE788	1054	975	93%	601
NIASHv1005K14	Aegilops_bicornis_KU-5786	1054	694	66%	601
NIASHv1005K14	Aegilops_comosa_AE1255	1054	1078	102%	601
NIASHv1005K14	Aegilops_comosa_AE1378	1054	978	93%	601
NIASHv1005K14	Aegilops_comosa_AE783	1054	953	90%	601
NIASHv1005K14	Aegilops_comosa_PI276970	1054	621	59%	601
NIASHv1005K14	Aegilops_longissima_AE1078	1054	888	84%	601
NIASHv1005K14	Aegilops_longissima_AE133	1054	1091	104%	601
NIASHv1005K14	Aegilops_longissima_AE417	1054	851	81%	601
NIASHv1005K14	Aegilops_longissima_PI604141	1054	843	80%	601
NIASHv1005K14	Aegilops_longissima_TA1921	1054	969	92%	601
NIASHv1005K14	Aegilops_markgrafii_AE1381	1054	1142	108%	601
NIASHv1005K14	Aegilops_markgrafii_KP-2012-106	1054	1066	101%	601
NIASHv1005K14	Aegilops_markgrafii_PI254863	1054	837	79%	601
NIASHv1005K14	Aegilops_markgrafii_PI542208	1054	1073	102%	601
NIASHv1005K14	Aegilops_markgrafii_PI596287	1054	1089	103%	601
NIASHv1005K14	Aegilops_mutica_01C2100106	1054	1095	104%	601
NIASHv1005K14	Aegilops_searsii_AE1075	1054	840	80%	601
NIASHv1005K14	Aegilops_searsii_AE1083	1054	1050	100%	601
NIASHv1005K14	Aegilops_searsii_KU-14655	1054	1084	103%	601
NIASHv1005K14	Aegilops_searsii_PI599142	1054	946	90%	601
NIASHv1005K14	Aegilops_searsii_PI599148	1054	595	56%	601
NIASHv1005K14	Aegilops_sharonensis_AE90691	1054	1052	100%	601
NIASHv1005K14	Aegilops_speltoides_3776	1054	1196	113%	601
NIASHv1005K14	Aegilops_speltoides_AE1064	1054	1034	98%	601
NIASHv1005K14	Aegilops_speltoides_AE900	1054	1025	97%	601
NIASHv1005K14	Aegilops_speltoides_KU-7856	1054	812	77%	601
NIASHv1005K14	Aegilops_speltoides_PI486264	1054	1149	109%	601
NIASHv1005K14	Aegilops_speltoides_PI487231	1054	1056	100%	601
NIASHv1005K14	Aegilops_speltoides_TA1772	1054	624	59%	601
NIASHv1005K14	Aegilops_tauschii_49116	1054	892	85%	601
NIASHv1005K14	Aegilops_tauschii_937	1054	1220	116%	601
NIASHv1005K14	Aegilops_tauschii_AE1069	1054	975	93%	601
NIASHv1005K14	Aegilops_tauschii_AE956	1054	1040	99%	601
NIASHv1005K14	Aegilops_umbellulata_AE1070	1054	1044	99%	601
NIASHv1005K14	Aegilops_umbellulata_AE153	1054	1067	101%	601
NIASHv1005K14	Aegilops_umbellulata_AE740	1054	690	65%	601
NIASHv1005K14	Aegilops_umbellulata_AE811	1054	268	25%	601
NIASHv1005K14	Aegilops_uniaristata_AE157	1054	1029	98%	601
NIASHv1005K14	Aegilops_uniaristata_AE680	1054	1140	108%	601
NIASHv1005K14	Aegilops_uniaristata_PI276996	1054	642	61%	601
NIASHv1005K14	Agropyron_cristatum_PI494615	1054	1073	102%	601
NIASHv1005K14	Agropyron_cristatum_PI598631	1054	1087	103%	601
NIASHv1005K14	Amblyopyrum_muticum_PI560122	1054	607	58%	601
NIASHv1005K14	Amblyopyrum_muticum_PI560124	1054	524	50%	601
NIASHv1005K14	Amblyopyrum_muticum_PI560125	1054	349	33%	601
NIASHv1005K14	Amblyopyrum_muticum_PI560126	1054	648	61%	601
NIASHv1005K14	Amblyopyrum_muticum_PI636562	1054	990	94%	601
NIASHv1005K14	Australopyrum_retrofractum_PI531553	1054	981	93%	601
NIASHv1005K14	Australopyrum_retrofractum_PI533013	1054	809	77%	601
NIASHv1005K14	Australopyrum_retrofractum_PI533014	1054	1033	98%	601
NIASHv1005K14	Australopyrum_retrofractum_PI547363	1054	1008	96%	601
NIASHv1005K14	Brachypodium_distachyon	1054	1015	96%	601
NIASHv1005K14	Bromus_tectorum_GRA1085	1054	739	70%	601
NIASHv1005K14	Dasyphyrum_villosum_GRA1020	1054	969	92%	601
NIASHv1005K14	Dasyphyrum_villosum_GRA1027	1054	994	94%	601
NIASHv1005K14	Dasyphyrum_villosum_PI368884	1054	370	35%	601
NIASHv1005K14	Dasyphyrum_villosum_W619414	1054	561	53%	601
NIASHv1005K14	Dasyphyrum_villosum_W67300	1054	1077	102%	601
NIASHv1005K14	Eremopyrum_distans_PI193264	1054	964	91%	601
NIASHv1005K14	Eremopyrum_triticeum_GRA2250	1054	1015	96%	601
NIASHv1005K14	Eremopyrum_triticeum_PI502364	1054	1010	96%	601
NIASHv1005K14	Eremopyrum_triticeum_W626631	1054	820	78%	601
NIASHv1005K14	Henrardia_persica_PI401347	1054	968	92%	601
NIASHv1005K14	Henrardia_persica_PI577112	1054	1145	109%	601
NIASHv1005K14	Henrardia_persica_PI577113	1054	909	86%	601
NIASHv1005K14	Henrardia_persica_RF2012	1054	1005	95%	601
NIASHv1005K14	Heterantherium_piliferum_PI401351	1054	1059	100%	601
NIASHv1005K14	Heterantherium_piliferum_PI401353	1054	1067	101%	601
NIASHv1005K14	Heterantherium_piliferum_PI401354	1054	1152	109%	601
NIASHv1005K14	Heterantherium_sp_PI314152	1054	977	93%	601
NIASHv1005K14	Hordeum_marinum_BCC2006	1054	1167	111%	601
NIASHv1005K14	Hordeum_marinum_BCC2002	1054	1132	107%	601
NIASHv1005K14	Hordeum_pubiflorum_2028	1054	1378	131%	601
NIASHv1005K14	Hordeum_spontaneum_FT11	1054	1579	150%	601
NIASHv1005K14	Hordeum_vulgare_Morex	1054	1579	150%	601
NIASHv1005K14	Psathyrostachys_juncea_PI222050	1054	1093	104%	601
NIASHv1005K14	Psathyrostachys_juncea_PI565077	1054	686	65%	601
NIASHv1005K14	Psathyrostachys_juncea_PI595135	1054	1041	99%	601
NIASHv1005K14	Psathyrostachys_juncea_PI598613	1054	1018	97%	601
NIASHv1005K14	Psathyrostachys_juncea_PI619487	1054	1070	102%	601

Locus	Accession	Mapped exon length in barley (bp)	Assembled exon length (bp)	% of mapped exon length that could be assembled	Extended target (bp)
NIASHv1005K14	Psathyrostachys_sp_PI565080	1054	964	91%	601
NIASHv1005K14	Pseudoroegneria_libanotica_PI228389	1054	681	65%	601
NIASHv1005K14	Pseudoroegneria_libanotica_PI330688	1054	988	94%	601
NIASHv1005K14	Pseudoroegneria_libanotica_PI401274	1054	965	92%	601
NIASHv1005K14	Pseudoroegneria_stipifolia_PI325181	1054	1075	102%	601
NIASHv1005K14	Pseudoroegneria_stipifolia_PI440095	1054	1048	99%	601
NIASHv1005K14	Pseudoroegneria_stipifolia_PI531751	1054	1008	96%	601
NIASHv1005K14	Pseudoroegneria_strigosa_PI499638	1054	966	92%	601
NIASHv1005K14	Pseudoroegneria_strigosa_PI595172	1054	1089	103%	601
NIASHv1005K14	Pseudoroegneria_strigosa_W614049	1054	1098	104%	601
NIASHv1005K14	Pseudoroegneria_strigosa_PI639805	1054	1004	95%	601
NIASHv1005K14	Pseudoroegneria_strigosa_PI639805	1054	936	89%	601
NIASHv1005K14	Pseudoroegneria_tauri_PI401322	1054	729	69%	601
NIASHv1005K14	Pseudoroegneria_tauri_PI401333	1054	1108	105%	601
NIASHv1005K14	Secale_cereale_PI618662	1054	434	41%	601
NIASHv1005K14	Secale_cereale_PI618665	1054	933	89%	601
NIASHv1005K14	Secale_cereale_PI618669	1054	1083	103%	601
NIASHv1005K14	Secale_cereale_PI618671	1054	786	75%	601
NIASHv1005K14	Secale_strictum_R1108	1054	789	75%	601
NIASHv1005K14	Secale_strictum_R853	1054	881	84%	601
NIASHv1005K14	Secale_vavilovii_PI253957	1054	154	15%	601
NIASHv1005K14	Secale_vavilovii_R1027	1054	898	85%	601
NIASHv1005K14	Taeniatherum_caput-medusae_CK2011	1054	1071	102%	601
NIASHv1005K14	Taeniatherum_caput-medusae_GRA1126	1054	1213	115%	601
NIASHv1005K14	Taeniatherum_caput-medusae_PI220589	1054	1104	105%	601
NIASHv1005K14	Taeniatherum_caput-medusae_PI251387	1054	625	59%	601
NIASHv1005K14	Taeniatherum_caput-medusae_PI561095	1054	483	46%	601
NIASHv1005K14	Taeniatherum_crinatum_GRA2570	1054	1055	100%	601
NIASHv1005K14	Thinopyrum_bessarabicum_W621890	1054	955	91%	601
NIASHv1005K14	Thinopyrum_elongatum_PI109452	1054	1016	96%	601
NIASHv1005K14	Thinopyrum_elongatum_PI401117	1054	875	83%	601
NIASHv1005K14	Triticum_boeoticum_1613	1054	1219	116%	601
NIASHv1005K14	Triticum_boeoticum_1688	1054	997	95%	601
NIASHv1005K14	Triticum_boeoticum_ID379	1054	869	82%	601
NIASHv1005K14	Triticum_boeoticum_PI272520	1054	783	74%	601
NIASHv1005K14	Triticum_boeoticum_PI427451	1054	1116	106%	601
NIASHv1005K14	Triticum_boeoticum_PI427620	1054	1110	105%	601
NIASHv1005K14	Triticum_monococcum_2205	1054	1134	108%	601
NIASHv1005K14	Triticum_monococcum_2208	1054	1055	100%	601
NIASHv1005K14	Triticum_monococcum_2271	1054	1215	115%	601
NIASHv1005K14	Triticum_monococcum_TR113061	1054	1074	102%	601
NIASHv1005K14	Triticum_monococcum_TR113612	1054	1140	108%	601
NIASHv1005K14	Triticum_urartu_1307	1054	1242	118%	601
NIASHv1005K14	Triticum_urartu_PI428184	1054	834	79%	601
NIASHv1005K14	Triticum_urartu_PI428317	1054	722	69%	601
NIASHv1005K14	Triticum_urartu_TR117824	1054	1112	106%	601
NIASHv1005K14	Triticum_urartu_TR118407	1054	1084	103%	601
NIASHv1006N15	Aegilops_bicornis_AE106	1811	2251	124%	601
NIASHv1006N15	Aegilops_bicornis_AE1079	1811	1950	108%	601
NIASHv1006N15	Aegilops_bicornis_AE788	1811	2031	112%	601
NIASHv1006N15	Aegilops_bicornis_KU-5786	1811	2068	114%	601
NIASHv1006N15	Aegilops_comosa_AE1255	1811	2130	118%	601
NIASHv1006N15	Aegilops_comosa_AE1378	1811	2083	115%	601
NIASHv1006N15	Aegilops_comosa_AE783	1811	2077	115%	601
NIASHv1006N15	Aegilops_comosa_PI276970	1811	2018	111%	601
NIASHv1006N15	Aegilops_longissima_AE1078	1811	1979	109%	601
NIASHv1006N15	Aegilops_longissima_AE133	1811	2133	118%	601
NIASHv1006N15	Aegilops_longissima_AE417	1811	1920	106%	601
NIASHv1006N15	Aegilops_longissima_PI604141	1811	1922	106%	601
NIASHv1006N15	Aegilops_longissima_TA1921	1811	2032	112%	601
NIASHv1006N15	Aegilops_markgrafii_AE1381	1811	2176	120%	601
NIASHv1006N15	Aegilops_markgrafii_KP-2012-106	1811	2211	122%	601
NIASHv1006N15	Aegilops_markgrafii_PI254863	1811	2006	111%	601
NIASHv1006N15	Aegilops_markgrafii_PI542208	1811	2218	122%	601
NIASHv1006N15	Aegilops_markgrafii_PI596287	1811	2189	121%	601
NIASHv1006N15	Aegilops_mutica_01C2100106	1811	2121	117%	601
NIASHv1006N15	Aegilops_searsii_AE1075	1811	2087	115%	601
NIASHv1006N15	Aegilops_searsii_AE1083	1811	2203	122%	601
NIASHv1006N15	Aegilops_searsii_KU-14655	1811	2152	119%	601
NIASHv1006N15	Aegilops_searsii_PI599142	1811	2131	118%	601
NIASHv1006N15	Aegilops_searsii_PI599148	1811	1816	100%	601
NIASHv1006N15	Aegilops_sharonensis_AE90691	1811	2148	119%	601
NIASHv1006N15	Aegilops_speltoides_3776	1811	2177	120%	601
NIASHv1006N15	Aegilops_speltoides_AE1064	1811	2045	113%	601
NIASHv1006N15	Aegilops_speltoides_AE900	1811	2064	114%	601
NIASHv1006N15	Aegilops_speltoides_KU-7856	1811	1890	104%	601
NIASHv1006N15	Aegilops_speltoides_PI486264	1811	2139	118%	601
NIASHv1006N15	Aegilops_speltoides_PI487231	1811	2119	117%	601
NIASHv1006N15	Aegilops_speltoides_TA1772	1811	1855	102%	601
NIASHv1006N15	Aegilops_tauschii_49116	1811	2084	115%	601
NIASHv1006N15	Aegilops_tauschii_937	1811	2160	119%	601
NIASHv1006N15	Aegilops_tauschii_AE1069	1811	2018	111%	601
NIASHv1006N15	Aegilops_tauschii_AE956	1811	2080	115%	601
NIASHv1006N15	Aegilops_umbellulata_AE1070	1811	2079	115%	601
NIASHv1006N15	Aegilops_umbellulata_AE153	1811	2061	114%	601
NIASHv1006N15	Aegilops_umbellulata_AE740	1811	1899	105%	601

Locus	Accession	Mapped exon length in barley (bp)	Assembled exon length (bp)	% of mapped exon length that could be assembled	Extended target (bp)
NIASHv1006N15	Aegilops_umbellulata_AE811	1811	1883	104%	601
NIASHv1006N15	Aegilops_uniaristata_AE157	1811	2176	120%	601
NIASHv1006N15	Aegilops_uniaristata_AE680	1811	2079	115%	601
NIASHv1006N15	Aegilops_uniaristata_PI276996	1811	1874	103%	601
NIASHv1006N15	Agropyron_cristatum_PI494615	1811	2242	124%	601
NIASHv1006N15	Agropyron_cristatum_PI598631	1811	2041	113%	601
NIASHv1006N15	Amblyopyrum_muticum_PI560122	1811	1799	99%	601
NIASHv1006N15	Amblyopyrum_muticum_PI560124	1811	1786	99%	601
NIASHv1006N15	Amblyopyrum_muticum_PI560125	1811	1819	100%	601
NIASHv1006N15	Amblyopyrum_muticum_PI560126	1811	1671	92%	601
NIASHv1006N15	Amblyopyrum_muticum_PI636562	1811	2162	119%	601
NIASHv1006N15	Australopyrum_retrofractum_PI531553	1811	2091	115%	601
NIASHv1006N15	Australopyrum_retrofractum_PI533013	1811	1987	110%	601
NIASHv1006N15	Australopyrum_retrofractum_PI533014	1811	2159	119%	601
NIASHv1006N15	Australopyrum_retrofractum_PI547363	1811	2172	120%	601
NIASHv1006N15	Brachypodium_distachyon	1811	21	1%	601
NIASHv1006N15	Bromus_tectorum_GRA1085	1811	1875	104%	601
NIASHv1006N15	Dasypyrum_villosum_GRA1020	1811	2095	116%	601
NIASHv1006N15	Dasypyrum_villosum_GRA1027	1811	2130	118%	601
NIASHv1006N15	Dasypyrum_villosum_PI368884	1811	1914	106%	601
NIASHv1006N15	Dasypyrum_villosum_W619414	1811	1913	106%	601
NIASHv1006N15	Dasypyrum_villosum_W67300	1811	2161	119%	601
NIASHv1006N15	Eremopyrum_distans_PI193264	1811	2047	113%	601
NIASHv1006N15	Eremopyrum_triticeum_GRA2250	1811	2133	118%	601
NIASHv1006N15	Eremopyrum_triticeum_PI502364	1811	2053	113%	601
NIASHv1006N15	Eremopyrum_triticeum_W626631	1811	1990	110%	601
NIASHv1006N15	Henrardia_persica_PI401347	1811	2037	112%	601
NIASHv1006N15	Henrardia_persica_PI577112	1811	2140	118%	601
NIASHv1006N15	Henrardia_persica_PI577113	1811	2004	111%	601
NIASHv1006N15	Henrardia_persica_RF2012	1811	2003	111%	601
NIASHv1006N15	Heterantherium_piliferum_PI401351	1811	2165	120%	601
NIASHv1006N15	Heterantherium_piliferum_PI401353	1811	2172	120%	601
NIASHv1006N15	Heterantherium_piliferum_PI401354	1811	2188	121%	601
NIASHv1006N15	Heterantherium_sp._PI314152	1811	2173	120%	601
NIASHv1006N15	Hordeum_marinum_BCC2006	1811	2182	120%	601
NIASHv1006N15	Hordeum_murinum_BCC2002	1811	2266	125%	601
NIASHv1006N15	Hordeum_pubiflorum_2028	1811	2291	127%	601
NIASHv1006N15	Hordeum_spontanum_FT11	1811	2398	132%	601
NIASHv1006N15	Hordeum_vulgare_Morex	1811	2317	128%	601
NIASHv1006N15	Psathyrostachys_junceae_PI222050	1811	2133	118%	601
NIASHv1006N15	Psathyrostachys_junceae_PI565077	1811	1835	101%	601
NIASHv1006N15	Psathyrostachys_junceae_PI595135	1811	2096	116%	601
NIASHv1006N15	Psathyrostachys_junceae_PI598613	1811	2142	118%	601
NIASHv1006N15	Psathyrostachys_junceae_PI619487	1811	2050	113%	601
NIASHv1006N15	Psathyrostachys_sp._PI565080	1811	1999	110%	601
NIASHv1006N15	Pseudoroegneria_libanotica_PI228389	1811	1884	104%	601
NIASHv1006N15	Pseudoroegneria_libanotica_PI330688	1811	2104	116%	601
NIASHv1006N15	Pseudoroegneria_libanotica_PI401274	1811	2145	118%	601
NIASHv1006N15	Pseudoroegneria_stipifolia_PI325181	1811	2179	120%	601
NIASHv1006N15	Pseudoroegneria_stipifolia_PI440095	1811	2182	120%	601
NIASHv1006N15	Pseudoroegneria_stipifolia_PI531751	1811	2111	117%	601
NIASHv1006N15	Pseudoroegneria_strigosa_PI499638	1811	2025	112%	601
NIASHv1006N15	Pseudoroegneria_strigosa_PI595172	1811	2054	113%	601
NIASHv1006N15	Pseudoroegneria_strigosa_W614049	1811	2163	119%	601
NIASHv1006N15	Pseudoroegneria_strigosa_PI639805	1811	2092	116%	601
NIASHv1006N15	Pseudoroegneria_strigosa_PI639805	1811	2037	112%	601
NIASHv1006N15	Pseudoroegneria_tauri_PI401322	1811	1993	110%	601
NIASHv1006N15	Pseudoroegneria_tauri_PI401333	1811	2056	114%	601
NIASHv1006N15	Secale_cereale_PI618662	1811	1858	103%	601
NIASHv1006N15	Secale_cereale_PI618665	1811	2053	113%	601
NIASHv1006N15	Secale_cereale_PI618669	1811	2106	116%	601
NIASHv1006N15	Secale_cereale_PI618671	1811	2116	117%	601
NIASHv1006N15	Secale_strictum_R1108	1811	1956	108%	601
NIASHv1006N15	Secale_strictum_R853	1811	2142	118%	601
NIASHv1006N15	Secale_vavilovii_PI253957	1811	1606	89%	601
NIASHv1006N15	Secale_vavilovii_R1027	1811	1878	104%	601
NIASHv1006N15	Taeniatherum_caput-medusae_CK2011	1811	2069	114%	601
NIASHv1006N15	Taeniatherum_caput-medusae_GRA1126	1811	2202	122%	601
NIASHv1006N15	Taeniatherum_caput-medusae_PI220589	1811	2081	115%	601
NIASHv1006N15	Taeniatherum_caput-medusae_PI251387	1811	1908	105%	601
NIASHv1006N15	Taeniatherum_caput-medusae_PI561095	1811	1810	100%	601
NIASHv1006N15	Taeniatherum_crininum_GRA2570	1811	2080	115%	601
NIASHv1006N15	Thinopyrum_bessarabicum_W621890	1811	2050	113%	601
NIASHv1006N15	Thinopyrum_elongatum_PI109452	1811	2135	118%	601
NIASHv1006N15	Thinopyrum_elongatum_PI401117	1811	1951	108%	601
NIASHv1006N15	Triticum_boeoticum_1613	1811	2305	127%	601
NIASHv1006N15	Triticum_boeoticum_1688	1811	2163	119%	601
NIASHv1006N15	Triticum_boeoticum_ID379	1811	1932	107%	601
NIASHv1006N15	Triticum_boeoticum_PI272520	1811	1919	106%	601
NIASHv1006N15	Triticum_boeoticum_PI427451	1811	2148	119%	601
NIASHv1006N15	Triticum_boeoticum_PI427620	1811	2125	117%	601
NIASHv1006N15	Triticum_monococcum_2205	1811	2106	116%	601
NIASHv1006N15	Triticum_monococcum_2208	1811	2108	116%	601
NIASHv1006N15	Triticum_monococcum_2271	1811	2270	125%	601
NIASHv1006N15	Triticum_monococcum_TRI13061	1811	2130	118%	601
NIASHv1006N15	Triticum_monococcum_TRI13612	1811	2147	119%	601

Locus	Accession	Mapped exon length in barley (bp)	Assembled exon length (bp)	% of mapped exon length that could be assembled	Extended target (bp)
NIASHv1006N15	Triticum_urartu_1307	1811	2186	121%	601
NIASHv1006N15	Triticum_urartu_PI428184	1811	1969	109%	601
NIASHv1006N15	Triticum_urartu_PI428317	1811	1986	110%	601
NIASHv1006N15	Triticum_urartu_TRI17824	1811	2144	118%	601
NIASHv1006N15	Triticum_urartu_TRI18407	1811	2207	122%	601
NIASHv1007B04	Aegilops_bicornis_AE106	1408	1577	112%	601
NIASHv1007B04	Aegilops_bicornis_AE1079	1408	1423	101%	601
NIASHv1007B04	Aegilops_bicornis_AE788	1408	1519	108%	601
NIASHv1007B04	Aegilops_bicornis_KU-5786	1408	1441	102%	601
NIASHv1007B04	Aegilops_comosa_AE1255	1408	1583	112%	601
NIASHv1007B04	Aegilops_comosa_AE1378	1408	1462	104%	601
NIASHv1007B04	Aegilops_comosa_AE783	1408	1562	111%	601
NIASHv1007B04	Aegilops_comosa_PI276970	1408	1405	100%	601
NIASHv1007B04	Aegilops_longissima_AE1078	1408	1461	104%	601
NIASHv1007B04	Aegilops_longissima_AE133	1408	1474	105%	601
NIASHv1007B04	Aegilops_longissima_AE417	1408	1473	105%	601
NIASHv1007B04	Aegilops_longissima_PI604141	1408	1365	97%	601
NIASHv1007B04	Aegilops_longissima_TA1921	1408	1545	110%	601
NIASHv1007B04	Aegilops_markgrafii_AE1381	1408	1641	117%	601
NIASHv1007B04	Aegilops_markgrafii_KP-2012-106	1408	1560	111%	601
NIASHv1007B04	Aegilops_markgrafii_PI254863	1408	1441	102%	601
NIASHv1007B04	Aegilops_markgrafii_PI542208	1408	1669	119%	601
NIASHv1007B04	Aegilops_markgrafii_PI596287	1408	1460	104%	601
NIASHv1007B04	Aegilops_mutica_01C2100106	1408	1684	120%	601
NIASHv1007B04	Aegilops_searsii_AE1075	1408	1422	101%	601
NIASHv1007B04	Aegilops_searsii_AE1083	1408	1659	118%	601
NIASHv1007B04	Aegilops_searsii_KU-14655	1408	1587	113%	601
NIASHv1007B04	Aegilops_searsii_PI599142	1408	1458	104%	601
NIASHv1007B04	Aegilops_searsii_PI599148	1408	1377	98%	601
NIASHv1007B04	Aegilops_sharonensis_AE90691	1408	1481	105%	601
NIASHv1007B04	Aegilops_speltoides_3776	1408	1745	124%	601
NIASHv1007B04	Aegilops_speltoides_AE1064	1408	1620	115%	601
NIASHv1007B04	Aegilops_speltoides_AE900	1408	1549	110%	601
NIASHv1007B04	Aegilops_speltoides_KU-7856	1408	1472	105%	601
NIASHv1007B04	Aegilops_speltoides_PI486264	1408	1583	112%	601
NIASHv1007B04	Aegilops_speltoides_PI487231	1408	1549	110%	601
NIASHv1007B04	Aegilops_speltoides_TA1772	1408	1437	102%	601
NIASHv1007B04	Aegilops_tauschii_49116	1408	1451	103%	601
NIASHv1007B04	Aegilops_tauschii_937	1408	1691	120%	601
NIASHv1007B04	Aegilops_tauschii_AE1069	1408	1450	103%	601
NIASHv1007B04	Aegilops_tauschii_AE956	1408	1538	109%	601
NIASHv1007B04	Aegilops_umbellulata_AE1070	1408	1547	110%	601
NIASHv1007B04	Aegilops_umbellulata_AE153	1408	1537	109%	601
NIASHv1007B04	Aegilops_umbellulata_AE740	1408	1449	103%	601
NIASHv1007B04	Aegilops_umbellulata_AE811	1408	1283	91%	601
NIASHv1007B04	Aegilops_uniaristata_AE157	1408	1642	117%	601
NIASHv1007B04	Aegilops_uniaristata_AE680	1408	1537	109%	601
NIASHv1007B04	Aegilops_uniaristata_PI276996	1408	1425	101%	601
NIASHv1007B04	Agropyron_cristatum_PI494615	1408	1626	115%	601
NIASHv1007B04	Agropyron_cristatum_PI598631	1408	1601	114%	601
NIASHv1007B04	Amblyopyrum_muticum_PI560122	1408	1415	100%	601
NIASHv1007B04	Amblyopyrum_muticum_PI560124	1408	1427	101%	601
NIASHv1007B04	Amblyopyrum_muticum_PI560125	1408	1411	100%	601
NIASHv1007B04	Amblyopyrum_muticum_PI560126	1408	1429	101%	601
NIASHv1007B04	Amblyopyrum_muticum_PI636562	1408	1581	112%	601
NIASHv1007B04	Australopyrum_retrofractum_PI531553	1408	1471	104%	601
NIASHv1007B04	Australopyrum_retrofractum_PI533013	1408	1481	105%	601
NIASHv1007B04	Australopyrum_retrofractum_PI533014	1408	1523	108%	601
NIASHv1007B04	Australopyrum_retrofractum_PI547363	1408	1573	112%	601
NIASHv1007B04	Brachypodium_distachyon	1408	1408	100%	601
NIASHv1007B04	Bromus_tectorum_GRA1085	1408	1436	102%	601
NIASHv1007B04	Dasyphyrum_villosum_GRA1020	1408	1517	108%	601
NIASHv1007B04	Dasyphyrum_villosum_GRA1027	1408	1652	117%	601
NIASHv1007B04	Dasyphyrum_villosum_PI368884	1408	1371	97%	601
NIASHv1007B04	Dasyphyrum_villosum_W619414	1408	1472	105%	601
NIASHv1007B04	Dasyphyrum_villosum_W67300	1408	1558	111%	601
NIASHv1007B04	Eremopyrum_distans_PI193264	1408	1548	110%	601
NIASHv1007B04	Eremopyrum_triticeum_GRA2250	1408	1550	110%	601
NIASHv1007B04	Eremopyrum_triticeum_PI502364	1408	1470	104%	601
NIASHv1007B04	Eremopyrum_triticeum_W626631	1408	1471	104%	601
NIASHv1007B04	Henrardia_persica_PI401347	1408	1574	112%	601
NIASHv1007B04	Henrardia_persica_PI577112	1408	1541	109%	601
NIASHv1007B04	Henrardia_persica_PI577113	1408	1480	105%	601
NIASHv1007B04	Henrardia_persica_RF2012	1408	1512	107%	601
NIASHv1007B04	Heteranthelium_piliferum_PI401351	1408	1488	106%	601
NIASHv1007B04	Heteranthelium_piliferum_PI401353	1408	1558	111%	601
NIASHv1007B04	Heteranthelium_piliferum_PI401354	1408	1521	108%	601
NIASHv1007B04	Heteranthelium_sp_PI314152	1408	1465	104%	601
NIASHv1007B04	Hordeum_marinum_BCC2006	1408	1504	107%	601
NIASHv1007B04	Hordeum_murinum_BCC2002	1408	1891	134%	601
NIASHv1007B04	Hordeum_pubiflorum_2028	1408	1487	106%	601
NIASHv1007B04	Hordeum_spontaneum_FT11	1408	1949	138%	601
NIASHv1007B04	Hordeum_vulgare_Morex	1408	1954	139%	601
NIASHv1007B04	Psathyrostachys_junceae_PI222050	1408	1516	108%	601
NIASHv1007B04	Psathyrostachys_junceae_PI565077	1408	1373	98%	601
NIASHv1007B04	Psathyrostachys_junceae_PI595135	1408	1538	109%	601

Locus	Accession	Mapped exon length in barley (bp)	Assembled exon length (bp)	% of mapped exon length that could be assembled	Extended target (bp)
NIASHv1007B04	Psathyrostachys_junca_P1619487	1408	1234	88%	601
NIASHv1007B04	Psathyrostachys_sp_P1565080	1408	1477	105%	601
NIASHv1007B04	Pseudoroegneria_libanotica_P1228389	1408	1550	110%	601
NIASHv1007B04	Pseudoroegneria_libanotica_P1330688	1408	1539	109%	601
NIASHv1007B04	Pseudoroegneria_libanotica_P1401274	1408	1523	108%	601
NIASHv1007B04	Pseudoroegneria_stipifolia_P1325181	1408	1633	116%	601
NIASHv1007B04	Pseudoroegneria_stipifolia_P1440095	1408	1507	107%	601
NIASHv1007B04	Pseudoroegneria_stipifolia_P1531751	1408	1512	107%	601
NIASHv1007B04	Pseudoroegneria_strigosa_P1499638	1408	1487	106%	601
NIASHv1007B04	Pseudoroegneria_strigosa_P1595172	1408	1452	103%	601
NIASHv1007B04	Pseudoroegneria_strigosa_W614049	1408	1693	120%	601
NIASHv1007B04	Pseudoroegneria_strigosa_P1639805	1408	1431	102%	601
NIASHv1007B04	Pseudoroegneria_strigosa_P1639805	1408	1462	104%	601
NIASHv1007B04	Pseudoroegneria_tauri_P1401322	1408	1534	109%	601
NIASHv1007B04	Pseudoroegneria_tauri_P1401333	1408	1588	113%	601
NIASHv1007B04	Secale_cereale_P1618662	1408	1373	98%	601
NIASHv1007B04	Secale_cereale_P1618665	1408	1487	106%	601
NIASHv1007B04	Secale_cereale_P1618669	1408	1552	110%	601
NIASHv1007B04	Secale_cereale_P1618671	1408	1684	120%	601
NIASHv1007B04	Secale_strictum_R1108	1408	1425	101%	601
NIASHv1007B04	Secale_strictum_R853	1408	1523	108%	601
NIASHv1007B04	Secale_vavilovii_P1253957	1408	1333	95%	601
NIASHv1007B04	Secale_vavilovii_R1027	1408	1426	101%	601
NIASHv1007B04	Taeniatherum_caput-medusae_CK2011	1408	1569	111%	601
NIASHv1007B04	Taeniatherum_caput-medusae_GRA1126	1408	1569	111%	601
NIASHv1007B04	Taeniatherum_caput-medusae_P1220589	1408	1530	109%	601
NIASHv1007B04	Taeniatherum_caput-medusae_P1251387	1408	1390	99%	601
NIASHv1007B04	Taeniatherum_caput-medusae_P1561095	1408	1432	102%	601
NIASHv1007B04	Taeniatherum_crinatum_GRA2570	1408	1555	110%	601
NIASHv1007B04	Thinopyrum_bessarabicum_W621890	1408	1461	104%	601
NIASHv1007B04	Thinopyrum_elongatum_P1109452	1408	1575	112%	601
NIASHv1007B04	Thinopyrum_elongatum_P1401117	1408	1416	101%	601
NIASHv1007B04	Triticum_boeoticum_1613	1408	1718	122%	601
NIASHv1007B04	Triticum_boeoticum_1688	1408	1530	109%	601
NIASHv1007B04	Triticum_boeoticum_ID379	1408	1482	105%	601
NIASHv1007B04	Triticum_boeoticum_P1272520	1408	1417	101%	601
NIASHv1007B04	Triticum_boeoticum_P1427451	1408	1602	114%	601
NIASHv1007B04	Triticum_boeoticum_P1427620	1408	1519	108%	601
NIASHv1007B04	Triticum_monococcum_2205	1408	1483	105%	601
NIASHv1007B04	Triticum_monococcum_2208	1408	1491	106%	601
NIASHv1007B04	Triticum_monococcum_2271	1408	1670	119%	601
NIASHv1007B04	Triticum_monococcum_TRI13061	1408	1510	107%	601
NIASHv1007B04	Triticum_monococcum_TRI13612	1408	1552	110%	601
NIASHv1007B04	Triticum_urartu_1307	1408	1613	115%	601
NIASHv1007B04	Triticum_urartu_P1428184	1408	1473	105%	601
NIASHv1007B04	Triticum_urartu_P1428317	1408	1480	105%	601
NIASHv1007B04	Triticum_urartu_TRI17824	1408	1489	106%	601
NIASHv1007B04	Triticum_urartu_TRI18407	1408	1585	113%	601
NIASHv1012O21	Aegilops_bicornis_AE106	1593	1722	108%	601
NIASHv1012O21	Aegilops_bicornis_AE1079	1593	1611	101%	601
NIASHv1012O21	Aegilops_bicornis_AE788	1593	1742	109%	601
NIASHv1012O21	Aegilops_bicornis_KU-5786	1593	1687	106%	601
NIASHv1012O21	Aegilops_comosa_AE1255	1593	1714	108%	601
NIASHv1012O21	Aegilops_comosa_AE1378	1593	1613	101%	601
NIASHv1012O21	Aegilops_comosa_AE783	1593	1722	108%	601
NIASHv1012O21	Aegilops_comosa_P1276970	1593	1628	102%	601
NIASHv1012O21	Aegilops_longissima_AE1078	1593	1733	109%	601
NIASHv1012O21	Aegilops_longissima_AE133	1593	1720	108%	601
NIASHv1012O21	Aegilops_longissima_AE417	1593	1530	96%	601
NIASHv1012O21	Aegilops_longissima_P1604141	1593	1598	100%	601
NIASHv1012O21	Aegilops_longissima_TA1921	1593	1704	107%	601
NIASHv1012O21	Aegilops_markgrafii_AE1381	1593	1752	110%	601
NIASHv1012O21	Aegilops_markgrafii_KP-2012-106	1593	1758	110%	601
NIASHv1012O21	Aegilops_markgrafii_P1542208	1593	1627	102%	601
NIASHv1012O21	Aegilops_markgrafii_P1542208	1593	1785	112%	601
NIASHv1012O21	Aegilops_markgrafii_P1596287	1593	1780	112%	601
NIASHv1012O21	Aegilops_mutica_01C2100106	1593	1660	104%	601
NIASHv1012O21	Aegilops_searsii_AE1075	1593	1630	102%	601
NIASHv1012O21	Aegilops_searsii_AE1083	1593	1775	111%	601
NIASHv1012O21	Aegilops_searsii_KU-14655	1593	1792	112%	601
NIASHv1012O21	Aegilops_searsii_P1599142	1593	1701	107%	601
NIASHv1012O21	Aegilops_searsii_P1599148	1593	1482	93%	601
NIASHv1012O21	Aegilops_sharonensis_AE90691	1593	1754	110%	601
NIASHv1012O21	Aegilops_speltoides_3776	1593	1769	111%	601
NIASHv1012O21	Aegilops_speltoides_AE1064	1593	1717	108%	601
NIASHv1012O21	Aegilops_speltoides_AE900	1593	1663	104%	601
NIASHv1012O21	Aegilops_speltoides_KU-7856	1593	1472	92%	601
NIASHv1012O21	Aegilops_speltoides_P1486264	1593	1724	108%	601
NIASHv1012O21	Aegilops_speltoides_P1487231	1593	1712	107%	601
NIASHv1012O21	Aegilops_speltoides_TA1772	1593	1563	98%	601
NIASHv1012O21	Aegilops_tauschii_49116	1593	1737	109%	601
NIASHv1012O21	Aegilops_tauschii_937	1593	1852	116%	601
NIASHv1012O21	Aegilops_tauschii_AE1069	1593	1732	109%	601
NIASHv1012O21	Aegilops_tauschii_AE956	1593	1694	106%	601
NIASHv1012O21	Aegilops_umbellulata_AE1070	1593	1739	109%	601
NIASHv1012O21	Aegilops_umbellulata_AE153	1593	1756	110%	601

Locus	Accession	Mapped exon length in barley (bp)	Assembled exon length (bp)	% of mapped exon length that could be assembled	Extended target (bp)
NIASHv1012021	Aegilops_umbellulata_AE740	1593	1576	99%	601
NIASHv1012021	Aegilops_umbellulata_AE811	1593	1344	84%	601
NIASHv1012021	Aegilops_uniaristata_AE157	1593	1774	111%	601
NIASHv1012021	Aegilops_uniaristata_AE680	1593	1729	109%	601
NIASHv1012021	Aegilops_uniaristata_PI276996	1593	1577	99%	601
NIASHv1012021	Agropyron_cristatum_PI494615	1593	1630	102%	601
NIASHv1012021	Agropyron_cristatum_PI598631	1593	1645	103%	601
NIASHv1012021	Amblyopyrum_muticum_PI560122	1593	1493	94%	601
NIASHv1012021	Amblyopyrum_muticum_PI560124	1593	1404	88%	601
NIASHv1012021	Amblyopyrum_muticum_PI560125	1593	1391	87%	601
NIASHv1012021	Amblyopyrum_muticum_PI560126	1593	1038	65%	601
NIASHv1012021	Amblyopyrum_muticum_PI636562	1593	1631	102%	601
NIASHv1012021	Australopyrum_retrofractum_PI531553	1593	1685	106%	601
NIASHv1012021	Australopyrum_retrofractum_PI533013	1593	1551	97%	601
NIASHv1012021	Australopyrum_retrofractum_PI533014	1593	1673	105%	601
NIASHv1012021	Australopyrum_retrofractum_PI547363	1593	1716	108%	601
NIASHv1012021	Brachypodium_distachyon	1593	1333	84%	601
NIASHv1012021	Bromus_tectorum_GRA1085	1593	1604	101%	601
NIASHv1012021	Dasypyrum_villosum_GRA1020	1593	1683	106%	601
NIASHv1012021	Dasypyrum_villosum_GRA1027	1593	1634	103%	601
NIASHv1012021	Dasypyrum_villosum_PI368884	1593	1592	100%	601
NIASHv1012021	Dasypyrum_villosum_W619414	1593	1405	88%	601
NIASHv1012021	Dasypyrum_villosum_W67300	1593	1744	109%	601
NIASHv1012021	Eremopyrum_distans_PI193264	1593	1614	101%	601
NIASHv1012021	Eremopyrum_triticeum_GRA2250	1593	1692	106%	601
NIASHv1012021	Eremopyrum_triticeum_PI502364	1593	1618	102%	601
NIASHv1012021	Eremopyrum_triticeum_W626631	1593	1529	96%	601
NIASHv1012021	Henrardia_persica_PI401347	1593	1592	100%	601
NIASHv1012021	Henrardia_persica_PI577112	1593	1678	105%	601
NIASHv1012021	Henrardia_persica_PI577113	1593	1697	107%	601
NIASHv1012021	Henrardia_persica_RF2012	1593	1627	102%	601
NIASHv1012021	Heteranthelium_piliferum_PI401351	1593	1725	108%	601
NIASHv1012021	Heteranthelium_piliferum_PI401353	1593	1768	111%	601
NIASHv1012021	Heteranthelium_piliferum_PI401354	1593	1832	115%	601
NIASHv1012021	Heteranthelium_sp._PI314152	1593	1715	108%	601
NIASHv1012021	Hordeum_marinum_BCC2006	1593	1969	124%	601
NIASHv1012021	Hordeum_murinum_BCC2002	1593	1777	112%	601
NIASHv1012021	Hordeum_pubiflorum_2028	1593	1925	121%	601
NIASHv1012021	Hordeum_spontaneum_FT11	1593	2153	135%	601
NIASHv1012021	Hordeum_vulgare_Morex	1593	2157	135%	601
NIASHv1012021	Psathyrostachys_junceae_PI222050	1593	1802	113%	601
NIASHv1012021	Psathyrostachys_junceae_PI565077	1593	1559	98%	601
NIASHv1012021	Psathyrostachys_junceae_PI595135	1593	1731	109%	601
NIASHv1012021	Psathyrostachys_junceae_PI598613	1593	1791	112%	601
NIASHv1012021	Psathyrostachys_junceae_PI619487	1593	1777	112%	601
NIASHv1012021	Psathyrostachys_sp._PI565080	1593	1680	105%	601
NIASHv1012021	Pseudoroegneria_libanotica_PI228389	1593	1630	102%	601
NIASHv1012021	Pseudoroegneria_libanotica_PI330688	1593	1786	112%	601
NIASHv1012021	Pseudoroegneria_libanotica_PI401274	1593	1813	114%	601
NIASHv1012021	Pseudoroegneria_stipifolia_PI325181	1593	1694	106%	601
NIASHv1012021	Pseudoroegneria_stipifolia_PI440095	1593	1747	110%	601
NIASHv1012021	Pseudoroegneria_stipifolia_PI531751	1593	1709	107%	601
NIASHv1012021	Pseudoroegneria_strigosa_PI499638	1593	1703	107%	601
NIASHv1012021	Pseudoroegneria_strigosa_PI595172	1593	1696	106%	601
NIASHv1012021	Pseudoroegneria_strigosa_W614049	1593	1887	118%	601
NIASHv1012021	Pseudoroegneria_strigosa_PI639805	1593	1631	102%	601
NIASHv1012021	Pseudoroegneria_strigosa_PI639805	1593	1628	102%	601
NIASHv1012021	Pseudoroegneria_tauri_PI401322	1593	1700	107%	601
NIASHv1012021	Pseudoroegneria_tauri_PI401333	1593	1762	111%	601
NIASHv1012021	Secale_cereale_PI618662	1593	1363	86%	601
NIASHv1012021	Secale_cereale_PI618665	1593	1650	104%	601
NIASHv1012021	Secale_cereale_PI618669	1593	1663	104%	601
NIASHv1012021	Secale_cereale_PI618671	1593	1683	106%	601
NIASHv1012021	Secale_strictum_R1108	1593	1498	94%	601
NIASHv1012021	Secale_strictum_R853	1593	1680	105%	601
NIASHv1012021	Secale_vavilovii_PI253957	1593	1367	86%	601
NIASHv1012021	Secale_vavilovii_R1027	1593	1529	96%	601
NIASHv1012021	Taeniatherum_caput-medusae_CK2011	1593	1723	108%	601
NIASHv1012021	Taeniatherum_caput-medusae_GRA1126	1593	1795	113%	601
NIASHv1012021	Taeniatherum_caput-medusae_PI220589	1593	1725	108%	601
NIASHv1012021	Taeniatherum_caput-medusae_PI251387	1593	1487	93%	601
NIASHv1012021	Taeniatherum_caput-medusae_PI561095	1593	1405	88%	601
NIASHv1012021	Taeniatherum_crinatum_GRA2570	1593	1794	113%	601
NIASHv1012021	Thinopyrum_bessarabicum_W621890	1593	1642	103%	601
NIASHv1012021	Thinopyrum_elongatum_PI109452	1593	1695	106%	601
NIASHv1012021	Thinopyrum_elongatum_PI401117	1593	1446	91%	601
NIASHv1012021	Triticum_boeoticum_1613	1593	1861	117%	601
NIASHv1012021	Triticum_boeoticum_1688	1593	1774	111%	601
NIASHv1012021	Triticum_boeoticum_ID379	1593	1671	105%	601
NIASHv1012021	Triticum_boeoticum_PI272520	1593	1664	104%	601
NIASHv1012021	Triticum_boeoticum_PI427451	1593	1781	112%	601
NIASHv1012021	Triticum_boeoticum_PI427620	1593	1742	109%	601
NIASHv1012021	Triticum_monococcum_2205	1593	1743	109%	601
NIASHv1012021	Triticum_monococcum_2208	1593	1793	113%	601
NIASHv1012021	Triticum_monococcum_2271	1593	1902	119%	601
NIASHv1012021	Triticum_monococcum_TR113061	1593	1812	114%	601

Locus	Accession	Mapped exon length in barley (bp)	Assembled exon length (bp)	% of mapped exon length that could be assembled	Extended target (bp)
NIASHv1012021	Triticum_monococcum_TRI13612	1593	1749	110%	601
NIASHv1012021	Triticum_urartu_1307	1593	1888	119%	601
NIASHv1012021	Triticum_urartu_PI428184	1593	1506	95%	601
NIASHv1012021	Triticum_urartu_PI428317	1593	1650	104%	601
NIASHv1012021	Triticum_urartu_TRI17824	1593	1719	108%	601
NIASHv1012021	Triticum_urartu_TRI18407	1593	1779	112%	601
NIASHv1026E03	Aegilops_bicornis_AE106	1906	2023	106%	601
NIASHv1026E03	Aegilops_bicornis_AE1079	1906	1256	66%	601
NIASHv1026E03	Aegilops_bicornis_AE788	1906	2048	107%	601
NIASHv1026E03	Aegilops_bicornis_KU-5786	1906	1359	71%	601
NIASHv1026E03	Aegilops_comosa_AE1255	1906	2043	107%	601
NIASHv1026E03	Aegilops_comosa_AE1378	1906	1591	83%	601
NIASHv1026E03	Aegilops_comosa_AE783	1906	1948	102%	601
NIASHv1026E03	Aegilops_comosa_PI276970	1906	1270	67%	601
NIASHv1026E03	Aegilops_longissima_AE1078	1906	1750	92%	601
NIASHv1026E03	Aegilops_longissima_AE133	1906	1869	98%	601
NIASHv1026E03	Aegilops_longissima_AE417	1906	1422	75%	601
NIASHv1026E03	Aegilops_longissima_PI604141	1906	1306	69%	601
NIASHv1026E03	Aegilops_longissima_TA1921	1906	2052	108%	601
NIASHv1026E03	Aegilops_markgrafii_AE1381	1906	1910	100%	601
NIASHv1026E03	Aegilops_markgrafii_KP-2012-106	1906	1814	95%	601
NIASHv1026E03	Aegilops_markgrafii_PI254863	1906	1359	71%	601
NIASHv1026E03	Aegilops_markgrafii_PI542208	1906	2107	111%	601
NIASHv1026E03	Aegilops_markgrafii_PI596287	1906	2072	109%	601
NIASHv1026E03	Aegilops_mutica_01C2100106	1906	1868	98%	601
NIASHv1026E03	Aegilops_searsii_AE1075	1906	1835	96%	601
NIASHv1026E03	Aegilops_searsii_AE1083	1906	2083	109%	601
NIASHv1026E03	Aegilops_searsii_KU-14655	1906	2008	105%	601
NIASHv1026E03	Aegilops_searsii_PI599142	1906	1738	91%	601
NIASHv1026E03	Aegilops_searsii_PI599148	1906	1280	67%	601
NIASHv1026E03	Aegilops_sharonensis_AE90691	1906	1962	103%	601
NIASHv1026E03	Aegilops_speltoides_3776	1906	2172	114%	601
NIASHv1026E03	Aegilops_speltoides_AE1064	1906	1655	87%	601
NIASHv1026E03	Aegilops_speltoides_AE900	1906	1976	104%	601
NIASHv1026E03	Aegilops_speltoides_KU-7856	1906	1674	88%	601
NIASHv1026E03	Aegilops_speltoides_PI486264	1906	2011	106%	601
NIASHv1026E03	Aegilops_speltoides_PI487231	1906	1819	95%	601
NIASHv1026E03	Aegilops_speltoides_TA1772	1906	1145	60%	601
NIASHv1026E03	Aegilops_tauschii_49116	1906	1714	90%	601
NIASHv1026E03	Aegilops_tauschii_937	1906	2218	116%	601
NIASHv1026E03	Aegilops_tauschii_AE1069	1906	2018	106%	601
NIASHv1026E03	Aegilops_tauschii_AE956	1906	2055	108%	601
NIASHv1026E03	Aegilops_umbellulata_AE1070	1906	1913	100%	601
NIASHv1026E03	Aegilops_umbellulata_AE153	1906	1922	101%	601
NIASHv1026E03	Aegilops_umbellulata_AE740	1906	1405	74%	601
NIASHv1026E03	Aegilops_umbellulata_AE811	1906	1224	64%	601
NIASHv1026E03	Aegilops_uniaristata_AE157	1906	2019	106%	601
NIASHv1026E03	Aegilops_uniaristata_AE680	1906	2100	110%	601
NIASHv1026E03	Aegilops_uniaristata_PI276996	1906	1440	76%	601
NIASHv1026E03	Agropyron_cristatum_PI494615	1906	2094	110%	601
NIASHv1026E03	Agropyron_cristatum_PI598631	1906	1936	102%	601
NIASHv1026E03	Amblyopyrum_muticum_PI560122	1906	1181	62%	601
NIASHv1026E03	Amblyopyrum_muticum_PI560124	1906	1297	68%	601
NIASHv1026E03	Amblyopyrum_muticum_PI560125	1906	1243	65%	601
NIASHv1026E03	Amblyopyrum_muticum_PI560126	1906	1110	58%	601
NIASHv1026E03	Amblyopyrum_muticum_PI636562	1906	1656	87%	601
NIASHv1026E03	Australopyrum_retrofractum_PI531553	1906	1826	96%	601
NIASHv1026E03	Australopyrum_retrofractum_PI533013	1906	1593	84%	601
NIASHv1026E03	Australopyrum_retrofractum_PI533014	1906	1913	100%	601
NIASHv1026E03	Australopyrum_retrofractum_PI547363	1906	1892	99%	601
NIASHv1026E03	Brachypodium_distachyon	1906	1980	104%	601
NIASHv1026E03	Bromus_tectorum_GRA1085	1906	1834	96%	601
NIASHv1026E03	Dasyphyrum_villosum_GRA1020	1906	1687	89%	601
NIASHv1026E03	Dasyphyrum_villosum_GRA1027	1906	1563	82%	601
NIASHv1026E03	Dasyphyrum_villosum_PI368884	1906	1364	72%	601
NIASHv1026E03	Dasyphyrum_villosum_W619414	1906	1278	67%	601
NIASHv1026E03	Dasyphyrum_villosum_W67300	1906	1741	91%	601
NIASHv1026E03	Eremopyrum_distans_PI193264	1906	2052	108%	601
NIASHv1026E03	Eremopyrum_triticeum_GRA2250	1906	2011	106%	601
NIASHv1026E03	Eremopyrum_triticeum_PI502364	1906	1782	93%	601
NIASHv1026E03	Eremopyrum_triticeum_W626631	1906	1640	86%	601
NIASHv1026E03	Henrardia_persica_PI401347	1906	2019	106%	601
NIASHv1026E03	Henrardia_persica_PI577112	1906	2086	109%	601
NIASHv1026E03	Henrardia_persica_PI577113	1906	1961	103%	601
NIASHv1026E03	Henrardia_persica_RF2012	1906	2007	105%	601
NIASHv1026E03	Heteranthelium_piliferum_PI401351	1906	1892	99%	601
NIASHv1026E03	Heteranthelium_piliferum_PI401353	1906	2009	105%	601
NIASHv1026E03	Heteranthelium_piliferum_PI401354	1906	2104	110%	601
NIASHv1026E03	Heteranthelium_sp_PI314152	1906	1898	100%	601
NIASHv1026E03	Hordeum_marinum_BCC2006	1906	2176	114%	601
NIASHv1026E03	Hordeum_marinum_BCC2002	1906	2137	112%	601
NIASHv1026E03	Hordeum_pubiflorum_2028	1906	2263	119%	601
NIASHv1026E03	Hordeum_spontanum_FT11	1906	2316	122%	601
NIASHv1026E03	Hordeum_vulgare_Morex	1906	2327	122%	601
NIASHv1026E03	Psathyrostachys_juncea_PI222050	1906	1798	94%	601
NIASHv1026E03	Psathyrostachys_juncea_PI565077	1906	1411	74%	601

Locus	Accession	Mapped exon length in barley (bp)	Assembled exon length (bp)	% of mapped exon length that could be assembled	Extended target (bp)
NIASHv1026E03	Psathyrostachys_junceae_PI595135	1906	2031	107%	601
NIASHv1026E03	Psathyrostachys_junceae_PI598613	1906	1831	96%	601
NIASHv1026E03	Psathyrostachys_junceae_PI619487	1906	2115	111%	601
NIASHv1026E03	Psathyrostachys_sp_PI565080	1906	1937	102%	601
NIASHv1026E03	Pseudoroegneria_libanotica_PI228389	1906	1498	79%	601
NIASHv1026E03	Pseudoroegneria_libanotica_PI330688	1906	1705	89%	601
NIASHv1026E03	Pseudoroegneria_libanotica_PI401274	1906	1978	104%	601
NIASHv1026E03	Pseudoroegneria_stipifolia_PI325181	1906	2064	108%	601
NIASHv1026E03	Pseudoroegneria_stipifolia_PI440095	1906	2088	110%	601
NIASHv1026E03	Pseudoroegneria_stipifolia_PI531751	1906	1898	100%	601
NIASHv1026E03	Pseudoroegneria_strigosa_PI499638	1906	1866	98%	601
NIASHv1026E03	Pseudoroegneria_strigosa_PI595172	1906	1859	98%	601
NIASHv1026E03	Pseudoroegneria_strigosa_W614049	1906	2070	109%	601
NIASHv1026E03	Pseudoroegneria_strigosa_PI639805	1906	1773	93%	601
NIASHv1026E03	Pseudoroegneria_strigosa_PI639805	1906	1756	92%	601
NIASHv1026E03	Pseudoroegneria_tauri_PI401322	1906	1536	81%	601
NIASHv1026E03	Pseudoroegneria_tauri_PI401333	1906	2023	106%	601
NIASHv1026E03	Secale_cereale_PI618662	1906	1313	69%	601
NIASHv1026E03	Secale_cereale_PI618665	1906	1892	99%	601
NIASHv1026E03	Secale_cereale_PI618669	1906	1997	105%	601
NIASHv1026E03	Secale_cereale_PI618671	1906	1936	102%	601
NIASHv1026E03	Secale_strictum_R1108	1906	1663	87%	601
NIASHv1026E03	Secale_strictum_R853	1906	1774	93%	601
NIASHv1026E03	Secale_vavilovii_PI253957	1906	1229	64%	601
NIASHv1026E03	Secale_vavilovii_R1027	1906	1813	95%	601
NIASHv1026E03	Taeniatherum_caput-medusae_CK2011	1906	1981	104%	601
NIASHv1026E03	Taeniatherum_caput-medusae_GRA1126	1906	2207	116%	601
NIASHv1026E03	Taeniatherum_caput-medusae_PI220589	1906	1903	100%	601
NIASHv1026E03	Taeniatherum_caput-medusae_PI251387	1906	1370	72%	601
NIASHv1026E03	Taeniatherum_caput-medusae_PI561095	1906	1137	60%	601
NIASHv1026E03	Taeniatherum_cnitium_GRA2570	1906	2072	109%	601
NIASHv1026E03	Thinopyrum_bessarabicum_W621890	1906	1589	83%	601
NIASHv1026E03	Thinopyrum_elongatum_PI109452	1906	1809	95%	601
NIASHv1026E03	Thinopyrum_elongatum_PI401117	1906	1450	76%	601
NIASHv1026E03	Triticum_boeoticum_1613	1906	2159	113%	601
NIASHv1026E03	Triticum_boeoticum_1688	1906	2012	106%	601
NIASHv1026E03	Triticum_boeoticum_ID379	1906	1591	83%	601
NIASHv1026E03	Triticum_boeoticum_PI272520	1906	1735	91%	601
NIASHv1026E03	Triticum_boeoticum_PI427451	1906	2037	107%	601
NIASHv1026E03	Triticum_boeoticum_PI427620	1906	1995	105%	601
NIASHv1026E03	Triticum_monococcum_2205	1906	2047	107%	601
NIASHv1026E03	Triticum_monococcum_2208	1906	2048	107%	601
NIASHv1026E03	Triticum_monococcum_2271	1906	2049	108%	601
NIASHv1026E03	Triticum_monococcum_TRI13061	1906	1992	105%	601
NIASHv1026E03	Triticum_monococcum_TRI13612	1906	2028	106%	601
NIASHv1026E03	Triticum_urartu_1307	1906	2167	114%	601
NIASHv1026E03	Triticum_urartu_PI428184	1906	1428	75%	601
NIASHv1026E03	Triticum_urartu_PI428317	1906	1629	85%	601
NIASHv1026E03	Triticum_urartu_TRI17824	1906	2103	110%	601
NIASHv1026E03	Triticum_urartu_TRI18407	1906	1941	102%	601
NIASHv1027H02	Aegilops_bicornis_AE106	1328	1180	89%	601
NIASHv1027H02	Aegilops_bicornis_AE1079	1328	715	54%	601
NIASHv1027H02	Aegilops_bicornis_AE788	1328	1113	84%	601
NIASHv1027H02	Aegilops_bicornis_KU-5786	1328	347	26%	601
NIASHv1027H02	Aegilops_comosa_AE1255	1328	1272	96%	601
NIASHv1027H02	Aegilops_comosa_AE1378	1328	862	65%	601
NIASHv1027H02	Aegilops_comosa_AE783	1328	1017	77%	601
NIASHv1027H02	Aegilops_comosa_PI276970	1328	539	41%	601
NIASHv1027H02	Aegilops_longissima_AE1078	1328	937	71%	601
NIASHv1027H02	Aegilops_longissima_AE133	1328	1185	89%	601
NIASHv1027H02	Aegilops_longissima_AE417	1328	503	38%	601
NIASHv1027H02	Aegilops_longissima_PI604141	1328	497	37%	601
NIASHv1027H02	Aegilops_longissima_TA1921	1328	876	66%	601
NIASHv1027H02	Aegilops_markgrafii_AE1381	1328	1162	88%	601
NIASHv1027H02	Aegilops_markgrafii_KP-2012-106	1328	979	74%	601
NIASHv1027H02	Aegilops_markgrafii_PI254863	1328	877	66%	601
NIASHv1027H02	Aegilops_markgrafii_PI542208	1328	1146	86%	601
NIASHv1027H02	Aegilops_markgrafii_PI596287	1328	1219	92%	601
NIASHv1027H02	Aegilops_mutica_01C2100106	1328	1262	95%	601
NIASHv1027H02	Aegilops_searsii_AE1075	1328	729	55%	601
NIASHv1027H02	Aegilops_searsii_AE1083	1328	1363	103%	601
NIASHv1027H02	Aegilops_searsii_KU-14655	1328	1083	82%	601
NIASHv1027H02	Aegilops_searsii_PI599142	1328	859	65%	601
NIASHv1027H02	Aegilops_searsii_PI599148	1328	462	35%	601
NIASHv1027H02	Aegilops_sharonensis_AE90691	1328	1092	82%	601
NIASHv1027H02	Aegilops_speltoides_3776	1328	1308	98%	601
NIASHv1027H02	Aegilops_speltoides_AE1064	1328	1088	82%	601
NIASHv1027H02	Aegilops_speltoides_AE900	1328	1068	80%	601
NIASHv1027H02	Aegilops_speltoides_KU-7856	1328	824	62%	601
NIASHv1027H02	Aegilops_speltoides_PI486264	1328	1012	76%	601
NIASHv1027H02	Aegilops_speltoides_PI487231	1328	1030	78%	601
NIASHv1027H02	Aegilops_speltoides_TA1772	1328	598	45%	601
NIASHv1027H02	Aegilops_tauschii_49116	1328	909	68%	601
NIASHv1027H02	Aegilops_tauschii_937	1328	1413	106%	601
NIASHv1027H02	Aegilops_tauschii_AE1069	1328	1042	78%	601
NIASHv1027H02	Aegilops_tauschii_AE956	1328	1277	96%	601

Locus	Accession	Mapped exon length in barley (bp)	Assembled exon length (bp)	% of mapped exon length that could be assembled	Extended target (bp)
NIASHv1027H02	Aegilops_umbellulata_AE1070	1328	1183	89%	601
NIASHv1027H02	Aegilops_umbellulata_AE153	1328	1197	90%	601
NIASHv1027H02	Aegilops_umbellulata_AE740	1328	882	66%	601
NIASHv1027H02	Aegilops_umbellulata_AE811	1328	536	40%	601
NIASHv1027H02	Aegilops_uniaristata_AE157	1328	1267	95%	601
NIASHv1027H02	Aegilops_uniaristata_AE680	1328	1293	97%	601
NIASHv1027H02	Aegilops_uniaristata_PI276996	1328	833	63%	601
NIASHv1027H02	Agropyron_cristatum_PI494615	1328	1335	101%	601
NIASHv1027H02	Agropyron_cristatum_PI598631	1328	1131	85%	601
NIASHv1027H02	Amblyopyrum_muticum_PI560122	1328	502	38%	601
NIASHv1027H02	Amblyopyrum_muticum_PI560124	1328	652	49%	601
NIASHv1027H02	Amblyopyrum_muticum_PI560125	1328	145	11%	601
NIASHv1027H02	Amblyopyrum_muticum_PI560126	1328	209	16%	601
NIASHv1027H02	Amblyopyrum_muticum_PI636562	1328	1028	77%	601
NIASHv1027H02	Australopyrum_retrofractum_PI531553	1328	1070	81%	601
NIASHv1027H02	Australopyrum_retrofractum_PI533013	1328	826	62%	601
NIASHv1027H02	Australopyrum_retrofractum_PI533014	1328	1281	96%	601
NIASHv1027H02	Australopyrum_retrofractum_PI547363	1328	1021	77%	601
NIASHv1027H02	Brachypodium_distachyon	1328	1176	89%	601
NIASHv1027H02	Bromus_tectorum_GRA1085	1328	885	67%	601
NIASHv1027H02	Dasyphyrum_villosum_GRA1020	1328	856	64%	601
NIASHv1027H02	Dasyphyrum_villosum_GRA1027	1328	1020	77%	601
NIASHv1027H02	Dasyphyrum_villosum_PI368884	1328	395	30%	601
NIASHv1027H02	Dasyphyrum_villosum_W619414	1328	709	53%	601
NIASHv1027H02	Dasyphyrum_villosum_W67300	1328	1160	87%	601
NIASHv1027H02	Eremopyrum_distans_PI193264	1328	1032	78%	601
NIASHv1027H02	Eremopyrum_triticum_GRA2250	1328	997	75%	601
NIASHv1027H02	Eremopyrum_triticum_PI502364	1328	1069	80%	601
NIASHv1027H02	Eremopyrum_triticum_W626631	1328	964	73%	601
NIASHv1027H02	Henrardia_persica_PI401347	1328	1012	76%	601
NIASHv1027H02	Henrardia_persica_PI577112	1328	1313	99%	601
NIASHv1027H02	Henrardia_persica_PI577113	1328	1048	79%	601
NIASHv1027H02	Henrardia_persica_RF2012	1328	1182	89%	601
NIASHv1027H02	Heterantherium_piliferum_PI401351	1328	1368	103%	601
NIASHv1027H02	Heterantherium_piliferum_PI401353	1328	1234	93%	601
NIASHv1027H02	Heterantherium_piliferum_PI401354	1328	1430	108%	601
NIASHv1027H02	Heterantherium_sp_PI314152	1328	970	73%	601
NIASHv1027H02	Hordeum_marinum_BCC2006	1328	1272	96%	601
NIASHv1027H02	Hordeum_murinum_BCC2002	1328	1450	109%	601
NIASHv1027H02	Hordeum_pubiflorum_2028	1328	1536	116%	601
NIASHv1027H02	Hordeum_spontanum_FT11	1328	1684	127%	601
NIASHv1027H02	Hordeum_vulgare_Morex	1328	1672	126%	601
NIASHv1027H02	Psathyrostachys_juncea_PI222050	1328	950	72%	601
NIASHv1027H02	Psathyrostachys_juncea_PI565077	1328	392	30%	601
NIASHv1027H02	Psathyrostachys_juncea_PI595135	1328	1183	89%	601
NIASHv1027H02	Psathyrostachys_juncea_PI598613	1328	1139	86%	601
NIASHv1027H02	Psathyrostachys_juncea_PI619487	1328	1091	82%	601
NIASHv1027H02	Psathyrostachys_sp_PI565080	1328	1049	79%	601
NIASHv1027H02	Pseudoroegneria_libanotica_PI228389	1328	680	51%	601
NIASHv1027H02	Pseudoroegneria_libanotica_PI330688	1328	1024	77%	601
NIASHv1027H02	Pseudoroegneria_libanotica_PI401274	1328	1075	81%	601
NIASHv1027H02	Pseudoroegneria_stipifolia_PI325181	1328	1188	89%	601
NIASHv1027H02	Pseudoroegneria_stipifolia_PI440095	1328	1321	99%	601
NIASHv1027H02	Pseudoroegneria_stipifolia_PI531751	1328	1039	78%	601
NIASHv1027H02	Pseudoroegneria_strigosa_PI499638	1328	1004	76%	601
NIASHv1027H02	Pseudoroegneria_strigosa_PI595172	1328	1048	79%	601
NIASHv1027H02	Pseudoroegneria_strigosa_W614049	1328	1171	88%	601
NIASHv1027H02	Pseudoroegneria_strigosa_PI639805	1328	1171	88%	601
NIASHv1027H02	Pseudoroegneria_strigosa_PI639805	1328	1181	89%	601
NIASHv1027H02	Pseudoroegneria_tauri_PI401322	1328	991	75%	601
NIASHv1027H02	Pseudoroegneria_tauri_PI401333	1328	1105	83%	601
NIASHv1027H02	Secale_cereale_PI618662	1328	447	34%	601
NIASHv1027H02	Secale_cereale_PI618665	1328	1178	89%	601
NIASHv1027H02	Secale_cereale_PI618669	1328	1126	85%	601
NIASHv1027H02	Secale_cereale_PI618671	1328	1095	82%	601
NIASHv1027H02	Secale_strictum_R1108	1328	663	50%	601
NIASHv1027H02	Secale_strictum_R853	1328	894	67%	601
NIASHv1027H02	Secale_vavilovii_PI253957	1328	271	20%	601
NIASHv1027H02	Secale_vavilovii_R1027	1328	818	62%	601
NIASHv1027H02	Taeniatherum_caput-medusae_CK2011	1328	1153	87%	601
NIASHv1027H02	Taeniatherum_caput-medusae_GRA1126	1328	1200	90%	601
NIASHv1027H02	Taeniatherum_caput-medusae_PI220589	1328	1065	80%	601
NIASHv1027H02	Taeniatherum_caput-medusae_PI251387	1328	915	69%	601
NIASHv1027H02	Taeniatherum_caput-medusae_PI561095	1328	323	24%	601
NIASHv1027H02	Taeniatherum_crinatum_GRA2570	1328	1117	84%	601
NIASHv1027H02	Thinopyrum_bessarabicum_W621890	1328	845	64%	601
NIASHv1027H02	Thinopyrum_elongatum_PI109452	1328	1069	80%	601
NIASHv1027H02	Thinopyrum_elongatum_PI401117	1328	791	60%	601
NIASHv1027H02	Triticum_boeoticum_1613	1328	1238	93%	601
NIASHv1027H02	Triticum_boeoticum_1688	1328	1220	92%	601
NIASHv1027H02	Triticum_boeoticum_ID379	1328	658	50%	601
NIASHv1027H02	Triticum_boeoticum_PI272520	1328	735	55%	601
NIASHv1027H02	Triticum_boeoticum_PI427451	1328	1040	78%	601
NIASHv1027H02	Triticum_boeoticum_PI427620	1328	1246	94%	601
NIASHv1027H02	Triticum_monococcum_2205	1328	1207	91%	601
NIASHv1027H02	Triticum_monococcum_2208	1328	1227	92%	601

Locus	Accession	Mapped exon length in barley (bp)	Assembled exon length (bp)	% of mapped exon length that could be assembled	Extended target (bp)
NIASHv1027H02	Triticum_monococcum_2271	1328	1339	101%	601
NIASHv1027H02	Triticum_monococcum_TRI13061	1328	1109	84%	601
NIASHv1027H02	Triticum_monococcum_TRI13612	1328	1230	93%	601
NIASHv1027H02	Triticum_urartu_1307	1328	1336	101%	601
NIASHv1027H02	Triticum_urartu_PI428184	1328	668	50%	601
NIASHv1027H02	Triticum_urartu_PI428317	1328	570	43%	601
NIASHv1027H02	Triticum_urartu_TRI17824	1328	1113	84%	601
NIASHv1027H02	Triticum_urartu_TRI18407	1328	1201	90%	601
NIASHv1042L097	Aegilops_bicornis_AE106	154	533	346%	601
NIASHv1042L097	Aegilops_bicornis_AE1079	154	245	159%	601
NIASHv1042L097	Aegilops_bicornis_AE788	154	435	282%	601
NIASHv1042L097	Aegilops_bicornis_KU-5786	154	276	179%	601
NIASHv1042L097	Aegilops_comosa_AE1255	154	495	321%	601
NIASHv1042L097	Aegilops_comosa_AE1378	154	383	249%	601
NIASHv1042L097	Aegilops_comosa_AE783	154	485	315%	601
NIASHv1042L097	Aegilops_comosa_PI276970	154	414	269%	601
NIASHv1042L097	Aegilops_longissima_AE1078	154	473	307%	601
NIASHv1042L097	Aegilops_longissima_AE133	154	417	271%	601
NIASHv1042L097	Aegilops_longissima_AE417	154	238	155%	601
NIASHv1042L097	Aegilops_longissima_PI604141	154	384	249%	601
NIASHv1042L097	Aegilops_longissima_TA1921	154	428	278%	601
NIASHv1042L097	Aegilops_markgrafii_AE1381	154	466	303%	601
NIASHv1042L097	Aegilops_markgrafii_KP-2012-106	154	507	329%	601
NIASHv1042L097	Aegilops_markgrafii_PI254863	154	229	149%	601
NIASHv1042L097	Aegilops_markgrafii_PI542208	154	580	377%	601
NIASHv1042L097	Aegilops_markgrafii_PI596287	154	491	319%	601
NIASHv1042L097	Aegilops_mutica_01C2100106	154	594	386%	601
NIASHv1042L097	Aegilops_searsii_AE1075	154	210	136%	601
NIASHv1042L097	Aegilops_searsii_AE1083	154	607	394%	601
NIASHv1042L097	Aegilops_searsii_KU-14655	154	486	316%	601
NIASHv1042L097	Aegilops_searsii_PI599142	154	347	225%	601
NIASHv1042L097	Aegilops_searsii_PI599148	154	228	148%	601
NIASHv1042L097	Aegilops_sharonensis_AE90691	154	449	292%	601
NIASHv1042L097	Aegilops_speltoides_3776	154	678	440%	601
NIASHv1042L097	Aegilops_speltoides_AE1064	154	480	312%	601
NIASHv1042L097	Aegilops_speltoides_AE900	154	397	258%	601
NIASHv1042L097	Aegilops_speltoides_KU-7856	154	331	215%	601
NIASHv1042L097	Aegilops_speltoides_PI486264	154	523	340%	601
NIASHv1042L097	Aegilops_speltoides_PI487231	154	452	294%	601
NIASHv1042L097	Aegilops_speltoides_TA1772	154	73	47%	601
NIASHv1042L097	Aegilops_tauschii_49116	154	520	338%	601
NIASHv1042L097	Aegilops_tauschii_937	154	663	431%	601
NIASHv1042L097	Aegilops_tauschii_AE1069	154	403	262%	601
NIASHv1042L097	Aegilops_tauschii_AE956	154	535	347%	601
NIASHv1042L097	Aegilops_umbellulata_AE1070	154	483	314%	601
NIASHv1042L097	Aegilops_umbellulata_AE153	154	461	299%	601
NIASHv1042L097	Aegilops_umbellulata_AE740	154	248	161%	601
NIASHv1042L097	Aegilops_umbellulata_AE811	154	144	94%	601
NIASHv1042L097	Aegilops_uniaristata_AE157	154	529	344%	601
NIASHv1042L097	Aegilops_uniaristata_AE680	154	555	360%	601
NIASHv1042L097	Aegilops_uniaristata_PI276996	154	171	111%	601
NIASHv1042L097	Agropyron_cristatum_PI494615	154	571	371%	601
NIASHv1042L097	Agropyron_cristatum_PI598631	154	498	323%	601
NIASHv1042L097	Amblyopyrum_muticum_PI560122	154	192	125%	601
NIASHv1042L097	Amblyopyrum_muticum_PI560124	154	122	79%	601
NIASHv1042L097	Amblyopyrum_muticum_PI560125	154	201	131%	601
NIASHv1042L097	Amblyopyrum_muticum_PI560126	154	84	55%	601
NIASHv1042L097	Amblyopyrum_muticum_PI636562	154	508	330%	601
NIASHv1042L097	Australopyrum_retrofractum_PI531553	154	423	275%	601
NIASHv1042L097	Australopyrum_retrofractum_PI533013	154	285	185%	601
NIASHv1042L097	Australopyrum_retrofractum_PI533014	154	537	349%	601
NIASHv1042L097	Australopyrum_retrofractum_PI547363	154	406	264%	601
NIASHv1042L097	Brachypodium_distachyon	154	489	318%	601
NIASHv1042L097	Bromus_tectorum_GRA1085	154	517	336%	601
NIASHv1042L097	Dasyphyrum_villosum_GRA1020	154	318	206%	601
NIASHv1042L097	Dasyphyrum_villosum_GRA1027	154	410	266%	601
NIASHv1042L097	Dasyphyrum_villosum_PI368884	154	159	103%	601
NIASHv1042L097	Dasyphyrum_villosum_W619414	154	238	155%	601
NIASHv1042L097	Dasyphyrum_villosum_W67300	154	475	308%	601
NIASHv1042L097	Eremopyrum_distans_PI193264	154	416	270%	601
NIASHv1042L097	Eremopyrum_triticeum_GRA2250	154	509	331%	601
NIASHv1042L097	Eremopyrum_triticeum_PI502364	154	474	308%	601
NIASHv1042L097	Eremopyrum_triticeum_W626631	154	262	170%	601
NIASHv1042L097	Henrardia_persica_PI401347	154	515	334%	601
NIASHv1042L097	Henrardia_persica_PI577112	154	553	359%	601
NIASHv1042L097	Henrardia_persica_PI577113	154	359	233%	601
NIASHv1042L097	Henrardia_persica_RF2012	154	517	336%	601
NIASHv1042L097	Heteranthelium_piliferum_PI401351	154	522	339%	601
NIASHv1042L097	Heteranthelium_piliferum_PI401353	154	722	469%	601
NIASHv1042L097	Heteranthelium_piliferum_PI401354	154	713	463%	601
NIASHv1042L097	Heteranthelium_sp_PI314152	154	457	297%	601
NIASHv1042L097	Hordeum_marinum_BCC2006	154	558	362%	601
NIASHv1042L097	Hordeum_murinum_BCC2002	154	588	382%	601
NIASHv1042L097	Hordeum_pubiflorum_2028	154	755	490%	601
NIASHv1042L097	Hordeum_spontaneum_FT11	154	706	458%	601
NIASHv1042L097	Hordeum_vulgare_Morex	154	740	481%	601

Locus	Accession	Mapped exon length in barley (bp)	Assembled exon length (bp)	% of mapped exon length that could be assembled	Extended target (bp)
NIASHv1042L097	Psathyrostachys_junceae_PI222050	154	349	227%	601
NIASHv1042L097	Psathyrostachys_junceae_PI565077	154	374	243%	601
NIASHv1042L097	Psathyrostachys_junceae_PI595135	154	510	331%	601
NIASHv1042L097	Psathyrostachys_junceae_PI598613	154	443	288%	601
NIASHv1042L097	Psathyrostachys_junceae_PI619487	154	556	361%	601
NIASHv1042L097	Psathyrostachys_sp_PI565080	154	421	273%	601
NIASHv1042L097	Pseudoroegneria_libanotica_PI228389	154	291	189%	601
NIASHv1042L097	Pseudoroegneria_libanotica_PI330688	154	501	325%	601
NIASHv1042L097	Pseudoroegneria_libanotica_PI401274	154	425	276%	601
NIASHv1042L097	Pseudoroegneria_stipifolia_PI325181	154	598	388%	601
NIASHv1042L097	Pseudoroegneria_stipifolia_PI440095	154	491	319%	601
NIASHv1042L097	Pseudoroegneria_stipifolia_PI531751	154	381	247%	601
NIASHv1042L097	Pseudoroegneria_strigosa_PI499638	154	476	309%	601
NIASHv1042L097	Pseudoroegneria_strigosa_PI595172	154	401	260%	601
NIASHv1042L097	Pseudoroegneria_strigosa_W614049	154	433	281%	601
NIASHv1042L097	Pseudoroegneria_strigosa_PI639805	154	382	248%	601
NIASHv1042L097	Pseudoroegneria_strigosa_PI639805	154	502	326%	601
NIASHv1042L097	Pseudoroegneria_tauri_PI401322	154	339	220%	601
NIASHv1042L097	Pseudoroegneria_tauri_PI401333	154	572	371%	601
NIASHv1042L097	Secale_cereale_PI618662	154	0	0%	601
NIASHv1042L097	Secale_cereale_PI618665	154	450	292%	601
NIASHv1042L097	Secale_cereale_PI618669	154	519	337%	601
NIASHv1042L097	Secale_cereale_PI618671	154	478	310%	601
NIASHv1042L097	Secale_strictum_R1108	154	291	189%	601
NIASHv1042L097	Secale_strictum_R853	154	388	252%	601
NIASHv1042L097	Secale_vavilovii_PI253957	154	32	21%	601
NIASHv1042L097	Secale_vavilovii_R1027	154	358	232%	601
NIASHv1042L097	Taeniatherum_caput-medusae_CK2011	154	507	329%	601
NIASHv1042L097	Taeniatherum_caput-medusae_GRA1126	154	630	409%	601
NIASHv1042L097	Taeniatherum_caput-medusae_PI220589	154	512	332%	601
NIASHv1042L097	Taeniatherum_caput-medusae_PI251387	154	111	72%	601
NIASHv1042L097	Taeniatherum_caput-medusae_PI561095	154	254	165%	601
NIASHv1042L097	Taeniatherum_crinatum_GRA2570	154	480	312%	601
NIASHv1042L097	Thinopyrum_bessarabicum_W621890	154	395	256%	601
NIASHv1042L097	Thinopyrum_elongatum_PI109452	154	434	282%	601
NIASHv1042L097	Thinopyrum_elongatum_PI401117	154	47	31%	601
NIASHv1042L097	Triticum_boeoticum_1613	154	702	456%	601
NIASHv1042L097	Triticum_boeoticum_1688	154	642	417%	601
NIASHv1042L097	Triticum_boeoticum_ID379	154	292	190%	601
NIASHv1042L097	Triticum_boeoticum_PI272520	154	193	125%	601
NIASHv1042L097	Triticum_boeoticum_PI427451	154	575	373%	601
NIASHv1042L097	Triticum_boeoticum_PI427620	154	477	310%	601
NIASHv1042L097	Triticum_monococcum_2205	154	474	308%	601
NIASHv1042L097	Triticum_monococcum_2208	154	505	328%	601
NIASHv1042L097	Triticum_monococcum_2271	154	716	465%	601
NIASHv1042L097	Triticum_monococcum_TRI13061	154	430	279%	601
NIASHv1042L097	Triticum_monococcum_TRI13612	154	484	314%	601
NIASHv1042L097	Triticum_urartu_1307	154	679	441%	601
NIASHv1042L097	Triticum_urartu_PI428184	154	323	210%	601
NIASHv1042L097	Triticum_urartu_PI428317	154	166	108%	601
NIASHv1042L097	Triticum_urartu_TRI17824	154	588	382%	601
NIASHv1042L097	Triticum_urartu_TRI18407	154	611	397%	601
NIASHv1078F01	Aegilops_bicornis_AE106	991	1183	119%	601
NIASHv1078F01	Aegilops_bicornis_AE1079	991	995	100%	601
NIASHv1078F01	Aegilops_bicornis_AE788	991	1164	117%	601
NIASHv1078F01	Aegilops_bicornis_KU-5786	991	1070	108%	601
NIASHv1078F01	Aegilops_comosa_AE1255	991	1173	118%	601
NIASHv1078F01	Aegilops_comosa_AE1378	991	986	99%	601
NIASHv1078F01	Aegilops_comosa_AE783	991	1144	115%	601
NIASHv1078F01	Aegilops_comosa_PI276970	991	965	97%	601
NIASHv1078F01	Aegilops_longissima_AE1078	991	1063	107%	601
NIASHv1078F01	Aegilops_longissima_AE133	991	1117	113%	601
NIASHv1078F01	Aegilops_longissima_AE417	991	940	95%	601
NIASHv1078F01	Aegilops_longissima_PI604141	991	867	87%	601
NIASHv1078F01	Aegilops_longissima_TA1921	991	1183	119%	601
NIASHv1078F01	Aegilops_markgrafii_AE1381	991	1071	108%	601
NIASHv1078F01	Aegilops_markgrafii_KP-2012-106	991	1139	115%	601
NIASHv1078F01	Aegilops_markgrafii_PI254863	991	1084	109%	601
NIASHv1078F01	Aegilops_markgrafii_PI542208	991	1186	120%	601
NIASHv1078F01	Aegilops_markgrafii_PI596287	991	1159	117%	601
NIASHv1078F01	Aegilops_mutica_01C2100106	991	1210	122%	601
NIASHv1078F01	Aegilops_searsii_AE1075	991	1010	102%	601
NIASHv1078F01	Aegilops_searsii_AE1083	991	1164	117%	601
NIASHv1078F01	Aegilops_searsii_KU-14655	991	1112	112%	601
NIASHv1078F01	Aegilops_searsii_PI599142	991	1155	117%	601
NIASHv1078F01	Aegilops_searsii_PI599148	991	891	90%	601
NIASHv1078F01	Aegilops_sharonensis_AE90691	991	1123	113%	601
NIASHv1078F01	Aegilops_speltoides_3776	991	1189	120%	601
NIASHv1078F01	Aegilops_speltoides_AE1064	991	1068	108%	601
NIASHv1078F01	Aegilops_speltoides_AE900	991	1104	111%	601
NIASHv1078F01	Aegilops_speltoides_KU-7856	991	982	99%	601
NIASHv1078F01	Aegilops_speltoides_PI486264	991	1049	106%	601
NIASHv1078F01	Aegilops_speltoides_PI487231	991	1054	106%	601
NIASHv1078F01	Aegilops_speltoides_TA1772	991	1030	104%	601
NIASHv1078F01	Aegilops_tauschii_49116	991	1151	116%	601
NIASHv1078F01	Aegilops_tauschii_937	991	1291	130%	601

Locus	Accession	Mapped exon length in barley (bp)	Assembled exon length (bp)	% of mapped exon length that could be assembled	Extended target (bp)
NIASHv1078F01	Aegilops_tauschii_AE1069	991	1099	111%	601
NIASHv1078F01	Aegilops_tauschii_AE956	991	1098	111%	601
NIASHv1078F01	Aegilops_umbellulata_AE1070	991	1148	116%	601
NIASHv1078F01	Aegilops_umbellulata_AE153	991	1107	112%	601
NIASHv1078F01	Aegilops_umbellulata_AE740	991	977	99%	601
NIASHv1078F01	Aegilops_umbellulata_AE811	991	941	95%	601
NIASHv1078F01	Aegilops_uniaristata_AE157	991	1119	113%	601
NIASHv1078F01	Aegilops_uniaristata_AE680	991	1097	111%	601
NIASHv1078F01	Aegilops_uniaristata_PI276996	991	964	97%	601
NIASHv1078F01	Agropyron_cristatum_PI494615	991	1172	118%	601
NIASHv1078F01	Agropyron_cristatum_PI598631	991	1220	123%	601
NIASHv1078F01	Amblyopyrum_muticum_PI560122	991	1041	105%	601
NIASHv1078F01	Amblyopyrum_muticum_PI560124	991	971	98%	601
NIASHv1078F01	Amblyopyrum_muticum_PI560125	991	1028	104%	601
NIASHv1078F01	Amblyopyrum_muticum_PI560126	991	976	98%	601
NIASHv1078F01	Amblyopyrum_muticum_PI636562	991	1108	112%	601
NIASHv1078F01	Australopyrum_retrofractum_PI531553	991	1076	109%	601
NIASHv1078F01	Australopyrum_retrofractum_PI533013	991	1011	102%	601
NIASHv1078F01	Australopyrum_retrofractum_PI533014	991	1207	122%	601
NIASHv1078F01	Australopyrum_retrofractum_PI547363	991	1174	118%	601
NIASHv1078F01	Brachypodium_distachyon	991	938	95%	601
NIASHv1078F01	Bromus_tectorum_GRA1085	991	1145	116%	601
NIASHv1078F01	Dasypyrum_villosum_GRA1020	991	1093	110%	601
NIASHv1078F01	Dasypyrum_villosum_GRA1027	991	1134	114%	601
NIASHv1078F01	Dasypyrum_villosum_PI368884	991	963	97%	601
NIASHv1078F01	Dasypyrum_villosum_W619414	991	1077	109%	601
NIASHv1078F01	Dasypyrum_villosum_W67300	991	1176	119%	601
NIASHv1078F01	Eremopyrum_distans_PI193264	991	1165	118%	601
NIASHv1078F01	Eremopyrum_triticeum_GRA2250	991	1197	121%	601
NIASHv1078F01	Eremopyrum_triticeum_PI502364	991	1192	120%	601
NIASHv1078F01	Eremopyrum_triticeum_W626631	991	1034	104%	601
NIASHv1078F01	Henrardia_persica_PI401347	991	1250	126%	601
NIASHv1078F01	Henrardia_persica_PI577112	991	1303	131%	601
NIASHv1078F01	Henrardia_persica_PI577113	991	1217	123%	601
NIASHv1078F01	Henrardia_persica_RF2012	991	1258	127%	601
NIASHv1078F01	Heteranthelium_piliferum_PI401351	991	1238	125%	601
NIASHv1078F01	Heteranthelium_piliferum_PI401353	991	1195	121%	601
NIASHv1078F01	Heteranthelium_piliferum_PI401354	991	1163	117%	601
NIASHv1078F01	Heteranthelium_sp_PI314152	991	975	98%	601
NIASHv1078F01	Hordeum_marinum_BCC2006	991	1376	139%	601
NIASHv1078F01	Hordeum_murinum_BCC2002	991	1237	125%	601
NIASHv1078F01	Hordeum_pubiflorum_2028	991	1423	144%	601
NIASHv1078F01	Hordeum_spontanum_FT11	991	1592	161%	601
NIASHv1078F01	Hordeum_vulgare_Morex	991	1592	161%	601
NIASHv1078F01	Psathyrostachys_junceae_PI222050	991	1146	116%	601
NIASHv1078F01	Psathyrostachys_junceae_PI565077	991	1009	102%	601
NIASHv1078F01	Psathyrostachys_junceae_PI595135	991	1137	115%	601
NIASHv1078F01	Psathyrostachys_junceae_PI598613	991	1167	118%	601
NIASHv1078F01	Psathyrostachys_junceae_PI619487	991	1211	122%	601
NIASHv1078F01	Psathyrostachys_sp_PI565080	991	1267	128%	601
NIASHv1078F01	Pseudoroegneria_libanotica_PI228389	991	1007	102%	601
NIASHv1078F01	Pseudoroegneria_libanotica_PI330688	991	1134	114%	601
NIASHv1078F01	Pseudoroegneria_libanotica_PI401274	991	1134	114%	601
NIASHv1078F01	Pseudoroegneria_stipifolia_PI325181	991	1197	121%	601
NIASHv1078F01	Pseudoroegneria_stipifolia_PI440095	991	1179	119%	601
NIASHv1078F01	Pseudoroegneria_stipifolia_PI531751	991	1174	118%	601
NIASHv1078F01	Pseudoroegneria_strigosa_PI499638	991	1117	113%	601
NIASHv1078F01	Pseudoroegneria_strigosa_PI595172	991	1065	107%	601
NIASHv1078F01	Pseudoroegneria_strigosa_W614049	991	1166	118%	601
NIASHv1078F01	Pseudoroegneria_strigosa_PI639805	991	1099	111%	601
NIASHv1078F01	Pseudoroegneria_strigosa_PI639805	991	1195	121%	601
NIASHv1078F01	Pseudoroegneria_tauri_PI401322	991	1082	109%	601
NIASHv1078F01	Pseudoroegneria_tauri_PI401333	991	1135	115%	601
NIASHv1078F01	Secale_cereale_PI618662	991	961	97%	601
NIASHv1078F01	Secale_cereale_PI618665	991	1018	103%	601
NIASHv1078F01	Secale_cereale_PI618669	991	1188	120%	601
NIASHv1078F01	Secale_cereale_PI618671	991	1143	115%	601
NIASHv1078F01	Secale_strictum_R1108	991	928	94%	601
NIASHv1078F01	Secale_strictum_R853	991	1014	102%	601
NIASHv1078F01	Secale_vavilovii_PI253957	991	911	92%	601
NIASHv1078F01	Secale_vavilovii_R1027	991	903	91%	601
NIASHv1078F01	Taeniatherum_caput-medusae_CK2011	991	1231	124%	601
NIASHv1078F01	Taeniatherum_caput-medusae_GRA1126	991	1259	127%	601
NIASHv1078F01	Taeniatherum_caput-medusae_PI220589	991	1175	119%	601
NIASHv1078F01	Taeniatherum_caput-medusae_PI251387	991	1082	109%	601
NIASHv1078F01	Taeniatherum_caput-medusae_PI561095	991	1002	101%	601
NIASHv1078F01	Taeniatherum_crininum_GRA2570	991	1209	122%	601
NIASHv1078F01	Thinopyrum_bessarabicum_W621890	991	1025	103%	601
NIASHv1078F01	Thinopyrum_elongatum_PI109452	991	1270	128%	601
NIASHv1078F01	Thinopyrum_elongatum_PI401117	991	989	100%	601
NIASHv1078F01	Triticum_boeoticum_1613	991	1261	127%	601
NIASHv1078F01	Triticum_boeoticum_1688	991	1063	107%	601
NIASHv1078F01	Triticum_boeoticum_ID379	991	922	93%	601
NIASHv1078F01	Triticum_boeoticum_PI272520	991	1008	102%	601
NIASHv1078F01	Triticum_boeoticum_PI427451	991	1175	119%	601
NIASHv1078F01	Triticum_boeoticum_PI427620	991	1140	115%	601

Locus	Accession	Mapped exon length in barley (bp)	Assembled exon length (bp)	% of mapped exon length that could be assembled	Extended target (bp)
NIASHv1078F01	Triticum_monococcum_2205	991	1186	120%	601
NIASHv1078F01	Triticum_monococcum_2208	991	1060	107%	601
NIASHv1078F01	Triticum_monococcum_2271	991	1212	122%	601
NIASHv1078F01	Triticum_monococcum_TRI13061	991	1133	114%	601
NIASHv1078F01	Triticum_monococcum_TRI13612	991	1124	113%	601
NIASHv1078F01	Triticum_urartu_1307	991	1182	119%	601
NIASHv1078F01	Triticum_urartu_PI428184	991	1016	103%	601
NIASHv1078F01	Triticum_urartu_PI428317	991	895	90%	601
NIASHv1078F01	Triticum_urartu_TRI17824	991	1138	115%	601
NIASHv1078F01	Triticum_urartu_TRI18407	991	1125	114%	601
NIASHv1100G15	Aegilops_bicornis_AE106	1143	1242	109%	601
NIASHv1100G15	Aegilops_bicornis_AE1079	1143	928	81%	601
NIASHv1100G15	Aegilops_bicornis_AE788	1143	1154	101%	601
NIASHv1100G15	Aegilops_bicornis_KU-5786	1143	1017	89%	601
NIASHv1100G15	Aegilops_comosa_AE1255	1143	1215	106%	601
NIASHv1100G15	Aegilops_comosa_AE1378	1143	1151	101%	601
NIASHv1100G15	Aegilops_comosa_AE783	1143	1150	101%	601
NIASHv1100G15	Aegilops_comosa_PI276970	1143	1015	89%	601
NIASHv1100G15	Aegilops_longissima_AE1078	1143	1185	104%	601
NIASHv1100G15	Aegilops_longissima_AE133	1143	1179	103%	601
NIASHv1100G15	Aegilops_longissima_AE417	1143	1138	100%	601
NIASHv1100G15	Aegilops_longissima_PI604141	1143	960	84%	601
NIASHv1100G15	Aegilops_longissima_TA1921	1143	1154	101%	601
NIASHv1100G15	Aegilops_markgrafii_AE1381	1143	1164	102%	601
NIASHv1100G15	Aegilops_markgrafii_KP-2012-106	1143	1148	100%	601
NIASHv1100G15	Aegilops_markgrafii_PI254863	1143	979	86%	601
NIASHv1100G15	Aegilops_markgrafii_PI542208	1143	1210	106%	601
NIASHv1100G15	Aegilops_markgrafii_PI596287	1143	1211	106%	601
NIASHv1100G15	Aegilops_mutica_01C2100106	1143	1210	106%	601
NIASHv1100G15	Aegilops_searsii_AE1075	1143	1164	102%	601
NIASHv1100G15	Aegilops_searsii_AE1083	1143	1250	109%	601
NIASHv1100G15	Aegilops_searsii_KU-14655	1143	1180	103%	601
NIASHv1100G15	Aegilops_searsii_PI599142	1143	1181	103%	601
NIASHv1100G15	Aegilops_searsii_PI599148	1143	758	66%	601
NIASHv1100G15	Aegilops_sharonensis_AE90691	1143	1154	101%	601
NIASHv1100G15	Aegilops_speltoides_3776	1143	1317	115%	601
NIASHv1100G15	Aegilops_speltoides_AE1064	1143	1233	108%	601
NIASHv1100G15	Aegilops_speltoides_AE900	1143	1150	101%	601
NIASHv1100G15	Aegilops_speltoides_KU-7856	1143	892	78%	601
NIASHv1100G15	Aegilops_speltoides_PI486264	1143	1226	107%	601
NIASHv1100G15	Aegilops_speltoides_PI487231	1143	1171	102%	601
NIASHv1100G15	Aegilops_speltoides_TA1772	1143	1010	88%	601
NIASHv1100G15	Aegilops_tauschii_49116	1143	1108	97%	601
NIASHv1100G15	Aegilops_tauschii_937	1143	1275	112%	601
NIASHv1100G15	Aegilops_tauschii_AE1069	1143	1141	100%	601
NIASHv1100G15	Aegilops_tauschii_AE956	1143	1210	106%	601
NIASHv1100G15	Aegilops_umbellulata_AE1070	1143	1169	102%	601
NIASHv1100G15	Aegilops_umbellulata_AE153	1143	1179	103%	601
NIASHv1100G15	Aegilops_umbellulata_AE740	1143	787	69%	601
NIASHv1100G15	Aegilops_umbellulata_AE811	1143	676	59%	601
NIASHv1100G15	Aegilops_uniaristata_AE157	1143	1244	109%	601
NIASHv1100G15	Aegilops_uniaristata_AE680	1143	1190	104%	601
NIASHv1100G15	Aegilops_uniaristata_PI276996	1143	965	84%	601
NIASHv1100G15	Agropyron_cristatum_PI494615	1143	1236	108%	601
NIASHv1100G15	Agropyron_cristatum_PI598631	1143	1180	103%	601
NIASHv1100G15	Amblyopyrum_muticum_PI560122	1143	966	85%	601
NIASHv1100G15	Amblyopyrum_muticum_PI560124	1143	1070	94%	601
NIASHv1100G15	Amblyopyrum_muticum_PI560125	1143	849	74%	601
NIASHv1100G15	Amblyopyrum_muticum_PI560126	1143	860	75%	601
NIASHv1100G15	Amblyopyrum_muticum_PI636562	1143	1187	104%	601
NIASHv1100G15	Australopyrum_retrofractum_PI531553	1143	1120	98%	601
NIASHv1100G15	Australopyrum_retrofractum_PI533013	1143	1072	94%	601
NIASHv1100G15	Australopyrum_retrofractum_PI533014	1143	1154	101%	601
NIASHv1100G15	Australopyrum_retrofractum_PI547363	1143	1154	101%	601
NIASHv1100G15	Brachypodium_distachyon	1143	1178	103%	601
NIASHv1100G15	Bromus_tectorum_GRA1085	1143	1116	98%	601
NIASHv1100G15	Dasyphyrum_villosum_GRA1020	1143	1142	100%	601
NIASHv1100G15	Dasyphyrum_villosum_GRA1027	1143	1154	101%	601
NIASHv1100G15	Dasyphyrum_villosum_PI368884	1143	797	70%	601
NIASHv1100G15	Dasyphyrum_villosum_W619414	1143	1041	91%	601
NIASHv1100G15	Dasyphyrum_villosum_W67300	1143	1136	99%	601
NIASHv1100G15	Eremopyrum_distans_PI193264	1143	1145	100%	601
NIASHv1100G15	Eremopyrum_triticeum_GRA2250	1143	1151	101%	601
NIASHv1100G15	Eremopyrum_triticeum_PI502364	1143	1151	101%	601
NIASHv1100G15	Eremopyrum_triticeum_W626631	1143	1142	100%	601
NIASHv1100G15	Henrardia_persica_PI401347	1143	1151	101%	601
NIASHv1100G15	Henrardia_persica_PI577112	1143	1210	106%	601
NIASHv1100G15	Henrardia_persica_PI577113	1143	1210	106%	601
NIASHv1100G15	Henrardia_persica_RF2012	1143	1151	101%	601
NIASHv1100G15	Heterantherium_piliferum_PI401351	1143	1151	101%	601
NIASHv1100G15	Heterantherium_piliferum_PI401353	1143	1151	101%	601
NIASHv1100G15	Heterantherium_piliferum_PI401354	1143	1212	106%	601
NIASHv1100G15	Heterantherium_sp_PI314152	1143	1142	100%	601
NIASHv1100G15	Hordeum_marinum_BCC2006	1143	1273	111%	601
NIASHv1100G15	Hordeum_marinum_BCC2002	1143	1420	124%	601
NIASHv1100G15	Hordeum_pubiflorum_2028	1143	1419	124%	601

Locus	Accession	Mapped exon length in barley (bp)	Assembled exon length (bp)	% of mapped exon length that could be assembled	Extended target (bp)
NIASHv1100G15	Hordeum_spontaneum_FT11	1143	1682	147%	601
NIASHv1100G15	Hordeum_vulgare_Morex	1143	1683	147%	601
NIASHv1100G15	Psathyrostachys_junceae_PI222050	1143	1132	99%	601
NIASHv1100G15	Psathyrostachys_junceae_PI565077	1143	978	86%	601
NIASHv1100G15	Psathyrostachys_junceae_PI595135	1143	1206	106%	601
NIASHv1100G15	Psathyrostachys_junceae_PI598613	1143	1151	101%	601
NIASHv1100G15	Psathyrostachys_junceae_PI619487	1143	1160	101%	601
NIASHv1100G15	Psathyrostachys_sp_PI565080	1143	1132	99%	601
NIASHv1100G15	Pseudoroegneria_libanotica_PI228389	1143	1041	91%	601
NIASHv1100G15	Pseudoroegneria_libanotica_PI330688	1143	1060	93%	601
NIASHv1100G15	Pseudoroegneria_libanotica_PI401274	1143	1202	105%	601
NIASHv1100G15	Pseudoroegneria_stipifolia_PI325181	1143	1132	99%	601
NIASHv1100G15	Pseudoroegneria_stipifolia_PI440095	1143	1180	103%	601
NIASHv1100G15	Pseudoroegneria_stipifolia_PI531751	1143	1131	99%	601
NIASHv1100G15	Pseudoroegneria_strigosa_PI499638	1143	1144	100%	601
NIASHv1100G15	Pseudoroegneria_strigosa_PI595172	1143	1199	105%	601
NIASHv1100G15	Pseudoroegneria_strigosa_W614049	1143	1207	106%	601
NIASHv1100G15	Pseudoroegneria_strigosa_PI639805	1143	1145	100%	601
NIASHv1100G15	Pseudoroegneria_strigosa_PI639805	1143	1212	106%	601
NIASHv1100G15	Pseudoroegneria_tauri_PI401322	1143	1053	92%	601
NIASHv1100G15	Pseudoroegneria_tauri_PI401333	1143	1151	101%	601
NIASHv1100G15	Secale_cereale_PI618662	1143	916	80%	601
NIASHv1100G15	Secale_cereale_PI618665	1143	1145	100%	601
NIASHv1100G15	Secale_cereale_PI618669	1143	1184	104%	601
NIASHv1100G15	Secale_cereale_PI618671	1143	1140	100%	601
NIASHv1100G15	Secale_strictum_R1108	1143	1017	89%	601
NIASHv1100G15	Secale_strictum_R853	1143	1151	101%	601
NIASHv1100G15	Secale_vavilovii_PI253957	1143	488	43%	601
NIASHv1100G15	Secale_vavilovii_R1027	1143	1060	93%	601
NIASHv1100G15	Taeniatherum_caput-medusae_CK2011	1143	1192	104%	601
NIASHv1100G15	Taeniatherum_caput-medusae_GRA1126	1143	1202	105%	601
NIASHv1100G15	Taeniatherum_caput-medusae_PI220589	1143	1189	104%	601
NIASHv1100G15	Taeniatherum_caput-medusae_PI251387	1143	1036	91%	601
NIASHv1100G15	Taeniatherum_caput-medusae_PI561095	1143	775	68%	601
NIASHv1100G15	Taeniatherum_crinatum_GRA2570	1143	1191	104%	601
NIASHv1100G15	Thinopyrum_bessarabicum_W621890	1143	1134	99%	601
NIASHv1100G15	Thinopyrum_elongatum_PI109452	1143	1200	105%	601
NIASHv1100G15	Thinopyrum_elongatum_PI401117	1143	611	53%	601
NIASHv1100G15	Triticum_boeoticum_1613	1143	1207	106%	601
NIASHv1100G15	Triticum_boeoticum_1688	1143	1174	103%	601
NIASHv1100G15	Triticum_boeoticum_ID379	1143	1136	99%	601
NIASHv1100G15	Triticum_boeoticum_PI272520	1143	1138	100%	601
NIASHv1100G15	Triticum_boeoticum_PI427451	1143	1213	106%	601
NIASHv1100G15	Triticum_boeoticum_PI427620	1143	1213	106%	601
NIASHv1100G15	Triticum_monococcum_2205	1143	1148	100%	601
NIASHv1100G15	Triticum_monococcum_2208	1143	1189	104%	601
NIASHv1100G15	Triticum_monococcum_2271	1143	1207	106%	601
NIASHv1100G15	Triticum_monococcum_TR113061	1143	1218	107%	601
NIASHv1100G15	Triticum_monococcum_TR113612	1143	1207	106%	601
NIASHv1100G15	Triticum_urartu_1307	1143	1225	107%	601
NIASHv1100G15	Triticum_urartu_PI428184	1143	1048	92%	601
NIASHv1100G15	Triticum_urartu_PI428317	1143	982	86%	601
NIASHv1100G15	Triticum_urartu_TR117824	1143	1204	105%	601
NIASHv1100G15	Triticum_urartu_TR118407	1143	1230	108%	601
NIASHv1129O23	Aegilops_bicornis_AE106	144	540	375%	601
NIASHv1129O23	Aegilops_bicornis_AE1079	144	198	138%	601
NIASHv1129O23	Aegilops_bicornis_AE788	144	516	358%	601
NIASHv1129O23	Aegilops_bicornis_KU-5786	144	313	217%	601
NIASHv1129O23	Aegilops_comosa_AE1255	144	539	374%	601
NIASHv1129O23	Aegilops_comosa_AE1378	144	294	204%	601
NIASHv1129O23	Aegilops_comosa_AE783	144	393	273%	601
NIASHv1129O23	Aegilops_comosa_PI276970	144	288	200%	601
NIASHv1129O23	Aegilops_longissima_AE1078	144	330	229%	601
NIASHv1129O23	Aegilops_longissima_AE133	144	403	280%	601
NIASHv1129O23	Aegilops_longissima_AE417	144	364	253%	601
NIASHv1129O23	Aegilops_longissima_PI604141	144	242	168%	601
NIASHv1129O23	Aegilops_longissima_TA1921	144	440	306%	601
NIASHv1129O23	Aegilops_markgrafii_AE1381	144	552	383%	601
NIASHv1129O23	Aegilops_markgrafii_KP-2012-106	144	434	301%	601
NIASHv1129O23	Aegilops_markgrafii_PI254863	144	238	165%	601
NIASHv1129O23	Aegilops_markgrafii_PI542208	144	629	437%	601
NIASHv1129O23	Aegilops_markgrafii_PI596287	144	448	311%	601
NIASHv1129O23	Aegilops_mutica_01C2100106	144	628	436%	601
NIASHv1129O23	Aegilops_searsii_AE1075	144	283	197%	601
NIASHv1129O23	Aegilops_searsii_AE1083	144	624	433%	601
NIASHv1129O23	Aegilops_searsii_KU-14655	144	620	431%	601
NIASHv1129O23	Aegilops_searsii_PI599142	144	352	244%	601
NIASHv1129O23	Aegilops_searsii_PI599148	144	236	164%	601
NIASHv1129O23	Aegilops_sharonensis_AE90691	144	495	344%	601
NIASHv1129O23	Aegilops_speltoides_3776	144	601	417%	601
NIASHv1129O23	Aegilops_speltoides_AE1064	144	577	401%	601
NIASHv1129O23	Aegilops_speltoides_AE900	144	511	355%	601
NIASHv1129O23	Aegilops_speltoides_KU-7856	144	310	215%	601
NIASHv1129O23	Aegilops_speltoides_PI486264	144	556	386%	601
NIASHv1129O23	Aegilops_speltoides_PI487231	144	398	276%	601
NIASHv1129O23	Aegilops_speltoides_TA1772	144	258	179%	601

Locus	Accession	Mapped exon length in barley (bp)	Assembled exon length (bp)	% of mapped exon length that could be assembled	Extended target (bp)
NIASHv1129O23	Aegilops_tauschii_49116	144	373	259%	601
NIASHv1129O23	Aegilops_tauschii_937	144	691	480%	601
NIASHv1129O23	Aegilops_tauschii_AE1069	144	322	224%	601
NIASHv1129O23	Aegilops_tauschii_AE956	144	507	352%	601
NIASHv1129O23	Aegilops_umbellulata_AE1070	144	437	303%	601
NIASHv1129O23	Aegilops_umbellulata_AE153	144	599	416%	601
NIASHv1129O23	Aegilops_umbellulata_AE740	144	245	170%	601
NIASHv1129O23	Aegilops_umbellulata_AE811	144	226	157%	601
NIASHv1129O23	Aegilops_uniaristata_AE157	144	649	451%	601
NIASHv1129O23	Aegilops_uniaristata_AE680	144	505	351%	601
NIASHv1129O23	Aegilops_uniaristata_PI276996	144	237	165%	601
NIASHv1129O23	Agropyron_cristatum_PI494615	144	422	293%	601
NIASHv1129O23	Agropyron_cristatum_PI598631	144	498	346%	601
NIASHv1129O23	Amblyopyrum_muticum_PI560122	144	212	147%	601
NIASHv1129O23	Amblyopyrum_muticum_PI560124	144	214	149%	601
NIASHv1129O23	Amblyopyrum_muticum_PI560125	144	264	183%	601
NIASHv1129O23	Amblyopyrum_muticum_PI560126	144	199	138%	601
NIASHv1129O23	Amblyopyrum_muticum_PI636562	144	523	363%	601
NIASHv1129O23	Australopyrum_retrofractum_PI531553	144	242	168%	601
NIASHv1129O23	Australopyrum_retrofractum_PI533013	144	277	192%	601
NIASHv1129O23	Australopyrum_retrofractum_PI533014	144	475	330%	601
NIASHv1129O23	Australopyrum_retrofractum_PI547363	144	544	378%	601
NIASHv1129O23	Bromus_tectorum_GRA1085	144	232	161%	601
NIASHv1129O23	Dasyphyrum_villosum_GRA1020	144	352	244%	601
NIASHv1129O23	Dasyphyrum_villosum_GRA1027	144	414	288%	601
NIASHv1129O23	Dasyphyrum_villosum_PI368884	144	194	135%	601
NIASHv1129O23	Dasyphyrum_villosum_W619414	144	300	208%	601
NIASHv1129O23	Dasyphyrum_villosum_W67300	144	521	362%	601
NIASHv1129O23	Eremopyrum_distans_PI193264	144	448	311%	601
NIASHv1129O23	Eremopyrum_triticeum_GRA2250	144	460	319%	601
NIASHv1129O23	Eremopyrum_triticeum_PI502364	144	372	258%	601
NIASHv1129O23	Eremopyrum_triticeum_W626631	144	338	235%	601
NIASHv1129O23	Henrardia_persica_PI401347	144	328	228%	601
NIASHv1129O23	Henrardia_persica_PI577112	144	539	374%	601
NIASHv1129O23	Henrardia_persica_PI577113	144	236	164%	601
NIASHv1129O23	Henrardia_persica_RF2012	144	283	197%	601
NIASHv1129O23	Heteranthelium_piliferum_PI401351	144	463	322%	601
NIASHv1129O23	Heteranthelium_piliferum_PI401353	144	532	369%	601
NIASHv1129O23	Heteranthelium_piliferum_PI401354	144	563	391%	601
NIASHv1129O23	Heteranthelium_sp_PI314152	144	529	367%	601
NIASHv1129O23	Hordeum_marinum_BCC2006	144	621	431%	601
NIASHv1129O23	Hordeum_marinum_BCC2002	144	576	400%	601
NIASHv1129O23	Hordeum_pubiflorum_2028	144	609	423%	601
NIASHv1129O23	Hordeum_spontaneum_FT11	144	725	503%	601
NIASHv1129O23	Hordeum_vulgare_Morex	144	707	491%	601
NIASHv1129O23	Psathyrostachys_junceae_PI222050	144	488	339%	601
NIASHv1129O23	Psathyrostachys_junceae_PI565077	144	294	204%	601
NIASHv1129O23	Psathyrostachys_junceae_PI595135	144	539	374%	601
NIASHv1129O23	Psathyrostachys_junceae_PI598613	144	542	376%	601
NIASHv1129O23	Psathyrostachys_junceae_PI619487	144	613	426%	601
NIASHv1129O23	Psathyrostachys_sp_PI565080	144	333	231%	601
NIASHv1129O23	Pseudoroegneria_libanotica_PI228389	144	208	144%	601
NIASHv1129O23	Pseudoroegneria_libanotica_PI330688	144	288	200%	601
NIASHv1129O23	Pseudoroegneria_libanotica_PI401274	144	298	207%	601
NIASHv1129O23	Pseudoroegneria_stipifolia_PI325181	144	554	385%	601
NIASHv1129O23	Pseudoroegneria_stipifolia_PI440095	144	490	340%	601
NIASHv1129O23	Pseudoroegneria_stipifolia_PI531751	144	492	342%	601
NIASHv1129O23	Pseudoroegneria_strigosa_PI499638	144	392	272%	601
NIASHv1129O23	Pseudoroegneria_strigosa_PI595172	144	573	398%	601
NIASHv1129O23	Pseudoroegneria_strigosa_W614049	144	577	401%	601
NIASHv1129O23	Pseudoroegneria_strigosa_PI639805	144	429	298%	601
NIASHv1129O23	Pseudoroegneria_strigosa_PI639805	144	630	438%	601
NIASHv1129O23	Pseudoroegneria_tauri_PI401322	144	241	167%	601
NIASHv1129O23	Pseudoroegneria_tauri_PI401333	144	498	346%	601
NIASHv1129O23	Secale_cereale_PI618662	144	160	111%	601
NIASHv1129O23	Secale_cereale_PI618665	144	322	224%	601
NIASHv1129O23	Secale_cereale_PI618669	144	477	331%	601
NIASHv1129O23	Secale_cereale_PI618671	144	423	294%	601
NIASHv1129O23	Secale_strictum_R1108	144	241	167%	601
NIASHv1129O23	Secale_strictum_R853	144	238	165%	601
NIASHv1129O23	Secale_vavilovii_PI253957	144	0	0%	601
NIASHv1129O23	Secale_vavilovii_R1027	144	168	117%	601
NIASHv1129O23	Taeniatherum_caput-medusae_CK2011	144	532	369%	601
NIASHv1129O23	Taeniatherum_caput-medusae_GRA1126	144	583	405%	601
NIASHv1129O23	Taeniatherum_caput-medusae_PI220589	144	483	335%	601
NIASHv1129O23	Taeniatherum_caput-medusae_PI251387	144	197	137%	601
NIASHv1129O23	Taeniatherum_caput-medusae_PI561095	144	199	138%	601
NIASHv1129O23	Taeniatherum_crinatum_GRA2570	144	534	371%	601
NIASHv1129O23	Thinopyrum_bessarabicum_W621890	144	246	171%	601
NIASHv1129O23	Thinopyrum_elongatum_PI109452	144	501	348%	601
NIASHv1129O23	Thinopyrum_elongatum_PI401117	144	222	154%	601
NIASHv1129O23	Triticum_boeoticum_1613	144	704	489%	601
NIASHv1129O23	Triticum_boeoticum_1688	144	562	390%	601
NIASHv1129O23	Triticum_boeoticum_ID379	144	253	176%	601
NIASHv1129O23	Triticum_boeoticum_PI272520	144	337	234%	601
NIASHv1129O23	Triticum_boeoticum_PI427451	144	447	310%	601

Locus	Accession	Mapped exon length in barley (bp)	Assembled exon length (bp)	% of mapped exon length that could be assembled	Extended target (bp)
NIASHv1129O23	Triticum_boeoticum_PI427620	144	524	364%	601
NIASHv1129O23	Triticum_monococcum_2205	144	575	399%	601
NIASHv1129O23	Triticum_monococcum_2208	144	610	424%	601
NIASHv1129O23	Triticum_monococcum_2271	144	683	474%	601
NIASHv1129O23	Triticum_monococcum_TR113061	144	505	351%	601
NIASHv1129O23	Triticum_monococcum_TR113612	144	596	414%	601
NIASHv1129O23	Triticum_urartu_1307	144	573	398%	601
NIASHv1129O23	Triticum_urartu_PI428184	144	291	202%	601
NIASHv1129O23	Triticum_urartu_PI428317	144	219	152%	601
NIASHv1129O23	Triticum_urartu_TR117824	144	468	325%	601
NIASHv1129O23	Triticum_urartu_TR118407	144	428	297%	601
NIASHv2008P1	Aegilops_bicornis_AE106	1268	1426	112%	601
NIASHv2008P1	Aegilops_bicornis_AE1079	1268	373	29%	601
NIASHv2008P1	Aegilops_bicornis_AE788	1268	1261	99%	601
NIASHv2008P1	Aegilops_bicornis_KU-5786	1268	718	57%	601
NIASHv2008P1	Aegilops_comosa_AE1255	1268	1287	101%	601
NIASHv2008P1	Aegilops_comosa_AE1378	1268	1186	94%	601
NIASHv2008P1	Aegilops_comosa_AE783	1268	1161	92%	601
NIASHv2008P1	Aegilops_comosa_PI276970	1268	711	56%	601
NIASHv2008P1	Aegilops_longissima_AE1078	1268	1048	83%	601
NIASHv2008P1	Aegilops_longissima_AE133	1268	1333	105%	601
NIASHv2008P1	Aegilops_longissima_AE417	1268	505	40%	601
NIASHv2008P1	Aegilops_longissima_PI604141	1268	489	39%	601
NIASHv2008P1	Aegilops_longissima_TA1921	1268	1130	89%	601
NIASHv2008P1	Aegilops_markgrafii_AE1381	1268	1302	103%	601
NIASHv2008P1	Aegilops_markgrafii_KP-2012-106	1268	1372	108%	601
NIASHv2008P1	Aegilops_markgrafii_PI254863	1268	833	66%	601
NIASHv2008P1	Aegilops_markgrafii_PI542208	1268	1438	113%	601
NIASHv2008P1	Aegilops_markgrafii_PI596287	1268	1384	109%	601
NIASHv2008P1	Aegilops_mutica_01C2100106	1268	1279	101%	601
NIASHv2008P1	Aegilops_searsii_AE1075	1268	795	63%	601
NIASHv2008P1	Aegilops_searsii_AE1083	1268	1292	102%	601
NIASHv2008P1	Aegilops_searsii_KU-14655	1268	1280	101%	601
NIASHv2008P1	Aegilops_searsii_PI599142	1268	960	76%	601
NIASHv2008P1	Aegilops_searsii_PI599148	1268	500	39%	601
NIASHv2008P1	Aegilops_sharonensis_AE90691	1268	1288	102%	601
NIASHv2008P1	Aegilops_speltoides_3776	1268	1528	121%	601
NIASHv2008P1	Aegilops_speltoides_AE1064	1268	1339	106%	601
NIASHv2008P1	Aegilops_speltoides_AE900	1268	1270	100%	601
NIASHv2008P1	Aegilops_speltoides_KU-7856	1268	956	75%	601
NIASHv2008P1	Aegilops_speltoides_PI486264	1268	1339	106%	601
NIASHv2008P1	Aegilops_speltoides_PI487231	1268	1277	101%	601
NIASHv2008P1	Aegilops_speltoides_TA1772	1268	915	72%	601
NIASHv2008P1	Aegilops_tauschii_49116	1268	1087	86%	601
NIASHv2008P1	Aegilops_tauschii_937	1268	1517	120%	601
NIASHv2008P1	Aegilops_tauschii_AE1069	1268	1115	88%	601
NIASHv2008P1	Aegilops_tauschii_AE956	1268	1254	99%	601
NIASHv2008P1	Aegilops_umbellulata_AE1070	1268	1225	97%	601
NIASHv2008P1	Aegilops_umbellulata_AE153	1268	1338	106%	601
NIASHv2008P1	Aegilops_umbellulata_AE740	1268	738	58%	601
NIASHv2008P1	Aegilops_umbellulata_AE811	1268	389	31%	601
NIASHv2008P1	Aegilops_uniaristata_AE157	1268	1429	113%	601
NIASHv2008P1	Aegilops_uniaristata_AE680	1268	1321	104%	601
NIASHv2008P1	Aegilops_uniaristata_PI276996	1268	1014	80%	601
NIASHv2008P1	Agropyron_cristatum_PI494615	1268	1310	103%	601
NIASHv2008P1	Agropyron_cristatum_PI598631	1268	1216	96%	601
NIASHv2008P1	Amblyopyrum_muticum_PI560122	1268	557	44%	601
NIASHv2008P1	Amblyopyrum_muticum_PI560124	1268	552	44%	601
NIASHv2008P1	Amblyopyrum_muticum_PI560125	1268	385	30%	601
NIASHv2008P1	Amblyopyrum_muticum_PI560126	1268	514	41%	601
NIASHv2008P1	Amblyopyrum_muticum_PI636562	1268	1269	100%	601
NIASHv2008P1	Australopyrum_retrofractum_PI531553	1268	1195	94%	601
NIASHv2008P1	Australopyrum_retrofractum_PI533013	1268	753	59%	601
NIASHv2008P1	Australopyrum_retrofractum_PI533014	1268	1379	109%	601
NIASHv2008P1	Australopyrum_retrofractum_PI547363	1268	1362	107%	601
NIASHv2008P1	Brachypodium_distachyon	1268	1257	99%	601
NIASHv2008P1	Bromus_tectorum_GRA1085	1268	908	72%	601
NIASHv2008P1	Dasyphyrum_villosum_GRA1020	1268	1116	88%	601
NIASHv2008P1	Dasyphyrum_villosum_GRA1027	1268	1094	86%	601
NIASHv2008P1	Dasyphyrum_villosum_PI368884	1268	666	53%	601
NIASHv2008P1	Dasyphyrum_villosum_W619414	1268	690	54%	601
NIASHv2008P1	Dasyphyrum_villosum_W67300	1268	1301	103%	601
NIASHv2008P1	Eremopyrum_distans_PI193264	1268	1195	94%	601
NIASHv2008P1	Eremopyrum_triticeum_GRA2250	1268	1274	100%	601
NIASHv2008P1	Eremopyrum_triticeum_PI502364	1268	1225	97%	601
NIASHv2008P1	Eremopyrum_triticeum_W626631	1268	992	78%	601
NIASHv2008P1	Henrardia_persica_PI401347	1268	1257	99%	601
NIASHv2008P1	Henrardia_persica_PI577112	1268	1405	111%	601
NIASHv2008P1	Henrardia_persica_PI577113	1268	1052	83%	601
NIASHv2008P1	Henrardia_persica_RF2012	1268	1373	108%	601
NIASHv2008P1	Heterantherium_piliferum_PI401351	1268	1247	98%	601
NIASHv2008P1	Heterantherium_piliferum_PI401353	1268	1397	110%	601
NIASHv2008P1	Heterantherium_piliferum_PI401354	1268	1409	111%	601
NIASHv2008P1	Heterantherium_sp_PI314152	1268	1138	90%	601
NIASHv2008P1	Hordeum_marinum_BCC2006	1268	1523	120%	601
NIASHv2008P1	Hordeum_marinum_BCC2002	1268	1378	109%	601

Locus	Accession	Mapped exon length in barley (bp)	Assembled exon length (bp)	% of mapped exon length that could be assembled	Extended target (bp)
NIASHv2008P1	Hordeum_pubiflorum_2028	1268	1552	122%	601
NIASHv2008P1	Hordeum_spontaneum_FT11	1268	1688	133%	601
NIASHv2008P1	Hordeum_vulgare_Morex	1268	1678	132%	601
NIASHv2008P1	Psathyrostachys_junceae_PI222050	1268	1277	101%	601
NIASHv2008P1	Psathyrostachys_junceae_PI565077	1268	888	70%	601
NIASHv2008P1	Psathyrostachys_junceae_PI595135	1268	1239	98%	601
NIASHv2008P1	Psathyrostachys_junceae_PI598613	1268	1437	113%	601
NIASHv2008P1	Psathyrostachys_junceae_PI619487	1268	1247	98%	601
NIASHv2008P1	Psathyrostachys_sp_PI565080	1268	1369	108%	601
NIASHv2008P1	Pseudoroegneria_libanotica_PI228389	1268	1148	91%	601
NIASHv2008P1	Pseudoroegneria_libanotica_PI330688	1268	1332	105%	601
NIASHv2008P1	Pseudoroegneria_libanotica_PI401274	1268	1301	103%	601
NIASHv2008P1	Pseudoroegneria_stipifolia_PI325181	1268	1457	115%	601
NIASHv2008P1	Pseudoroegneria_stipifolia_PI440095	1268	1338	106%	601
NIASHv2008P1	Pseudoroegneria_stipifolia_PI531751	1268	1308	103%	601
NIASHv2008P1	Pseudoroegneria_strigosa_PI499638	1268	1175	93%	601
NIASHv2008P1	Pseudoroegneria_strigosa_PI595172	1268	1344	106%	601
NIASHv2008P1	Pseudoroegneria_strigosa_W614049	1268	1341	106%	601
NIASHv2008P1	Pseudoroegneria_strigosa_PI639805	1268	1315	104%	601
NIASHv2008P1	Pseudoroegneria_strigosa_PI639805	1268	1360	107%	601
NIASHv2008P1	Pseudoroegneria_tauri_PI401322	1268	1128	89%	601
NIASHv2008P1	Pseudoroegneria_tauri_PI401333	1268	1451	114%	601
NIASHv2008P1	Secale_cereale_PI618662	1268	190	15%	601
NIASHv2008P1	Secale_cereale_PI618665	1268	1175	93%	601
NIASHv2008P1	Secale_cereale_PI618669	1268	1304	103%	601
NIASHv2008P1	Secale_cereale_PI618671	1268	1224	97%	601
NIASHv2008P1	Secale_strictum_R1108	1268	796	63%	601
NIASHv2008P1	Secale_strictum_R853	1268	910	72%	601
NIASHv2008P1	Secale_vavilovii_PI253957	1268	0	0%	601
NIASHv2008P1	Secale_vavilovii_R1027	1268	964	76%	601
NIASHv2008P1	Taeniatherum_caput-medusae_CK2011	1268	1252	99%	601
NIASHv2008P1	Taeniatherum_caput-medusae_GRA1126	1268	1396	110%	601
NIASHv2008P1	Taeniatherum_caput-medusae_PI220589	1268	1208	95%	601
NIASHv2008P1	Taeniatherum_caput-medusae_PI251387	1268	767	60%	601
NIASHv2008P1	Taeniatherum_caput-medusae_PI561095	1268	390	31%	601
NIASHv2008P1	Taeniatherum_crinatum_GRA2570	1268	1424	112%	601
NIASHv2008P1	Thinopyrum_bessarabicum_W621890	1268	1180	93%	601
NIASHv2008P1	Thinopyrum_elongatum_PI109452	1268	1388	109%	601
NIASHv2008P1	Thinopyrum_elongatum_PI401117	1268	914	72%	601
NIASHv2008P1	Triticum_boeoticum_1613	1268	1494	118%	601
NIASHv2008P1	Triticum_boeoticum_1688	1268	1334	105%	601
NIASHv2008P1	Triticum_boeoticum_ID379	1268	789	62%	601
NIASHv2008P1	Triticum_boeoticum_PI272520	1268	1086	86%	601
NIASHv2008P1	Triticum_boeoticum_PI427451	1268	1340	106%	601
NIASHv2008P1	Triticum_boeoticum_PI427620	1268	1271	100%	601
NIASHv2008P1	Triticum_monococcum_2205	1268	1393	110%	601
NIASHv2008P1	Triticum_monococcum_2208	1268	1282	101%	601
NIASHv2008P1	Triticum_monococcum_2271	1268	1436	113%	601
NIASHv2008P1	Triticum_monococcum_TRI13061	1268	1175	93%	601
NIASHv2008P1	Triticum_monococcum_TRI13612	1268	1428	113%	601
NIASHv2008P1	Triticum_urartu_1307	1268	1446	114%	601
NIASHv2008P1	Triticum_urartu_PI428184	1268	855	67%	601
NIASHv2008P1	Triticum_urartu_PI428317	1268	581	46%	601
NIASHv2008P1	Triticum_urartu_TRI17824	1268	1445	114%	601
NIASHv2008P1	Triticum_urartu_TRI18407	1268	1446	114%	601
NIASHv2017D1	Aegilops_bicornis_AE106	2082	1681	81%	601
NIASHv2017D1	Aegilops_bicornis_AE1079	2082	322	15%	601
NIASHv2017D1	Aegilops_bicornis_AE788	2082	1417	68%	601
NIASHv2017D1	Aegilops_bicornis_KU-5786	2082	483	23%	601
NIASHv2017D1	Aegilops_comosa_AE1255	2082	1827	88%	601
NIASHv2017D1	Aegilops_comosa_AE1378	2082	1116	54%	601
NIASHv2017D1	Aegilops_comosa_AE783	2082	1458	70%	601
NIASHv2017D1	Aegilops_comosa_PI276970	2082	644	31%	601
NIASHv2017D1	Aegilops_longissima_AE1078	2082	744	36%	601
NIASHv2017D1	Aegilops_longissima_AE133	2082	1437	69%	601
NIASHv2017D1	Aegilops_longissima_AE417	2082	432	21%	601
NIASHv2017D1	Aegilops_longissima_PI604141	2082	277	13%	601
NIASHv2017D1	Aegilops_longissima_TA1921	2082	1333	64%	601
NIASHv2017D1	Aegilops_markgrafii_AE1381	2082	1612	77%	601
NIASHv2017D1	Aegilops_markgrafii_KP-2012-106	2082	1686	81%	601
NIASHv2017D1	Aegilops_markgrafii_PI254863	2082	587	28%	601
NIASHv2017D1	Aegilops_markgrafii_PI542208	2082	1573	76%	601
NIASHv2017D1	Aegilops_markgrafii_PI596287	2082	1872	90%	601
NIASHv2017D1	Aegilops_mutica_01C2100106	2082	1700	82%	601
NIASHv2017D1	Aegilops_searsii_AE1075	2082	1209	58%	601
NIASHv2017D1	Aegilops_searsii_AE1083	2082	1754	84%	601
NIASHv2017D1	Aegilops_searsii_KU-14655	2082	1507	72%	601
NIASHv2017D1	Aegilops_searsii_PI599142	2082	962	46%	601
NIASHv2017D1	Aegilops_searsii_PI599148	2082	4	0%	601
NIASHv2017D1	Aegilops_sharonensis_AE90691	2082	1436	69%	601
NIASHv2017D1	Aegilops_speltoides_3776	2082	2070	99%	601
NIASHv2017D1	Aegilops_speltoides_AE1064	2082	1329	64%	601
NIASHv2017D1	Aegilops_speltoides_AE900	2082	1544	74%	601
NIASHv2017D1	Aegilops_speltoides_KU-7856	2082	654	31%	601
NIASHv2017D1	Aegilops_speltoides_PI486264	2082	1630	78%	601
NIASHv2017D1	Aegilops_speltoides_PI487231	2082	1553	75%	601

Locus	Accession	Mapped exon length in barley (bp)	Assembled exon length (bp)	% of mapped exon length that could be assembled	Extended target (bp)
NIASHv2017D1	Aegilops_speltoides_TA1772	2082	480	23%	601
NIASHv2017D1	Aegilops_tauschii_49116	2082	797	38%	601
NIASHv2017D1	Aegilops_tauschii_937	2082	2016	97%	601
NIASHv2017D1	Aegilops_tauschii_AE1069	2082	1479	71%	601
NIASHv2017D1	Aegilops_tauschii_AE956	2082	1632	78%	601
NIASHv2017D1	Aegilops_umbellulata_AE1070	2082	1287	62%	601
NIASHv2017D1	Aegilops_umbellulata_AE153	2082	1756	84%	601
NIASHv2017D1	Aegilops_umbellulata_AE740	2082	909	44%	601
NIASHv2017D1	Aegilops_umbellulata_AE811	2082	289	14%	601
NIASHv2017D1	Aegilops_uniaristata_AE157	2082	1728	83%	601
NIASHv2017D1	Aegilops_uniaristata_AE680	2082	1699	82%	601
NIASHv2017D1	Aegilops_uniaristata_PI276996	2082	642	31%	601
NIASHv2017D1	Agropyron_cristatum_PI494615	2082	1743	84%	601
NIASHv2017D1	Agropyron_cristatum_PI598631	2082	1710	82%	601
NIASHv2017D1	Amblyopyrum_muticum_PI560122	2082	971	47%	601
NIASHv2017D1	Amblyopyrum_muticum_PI560124	2082	652	31%	601
NIASHv2017D1	Amblyopyrum_muticum_PI560125	2082	903	43%	601
NIASHv2017D1	Amblyopyrum_muticum_PI560126	2082	736	35%	601
NIASHv2017D1	Amblyopyrum_muticum_PI636562	2082	1160	56%	601
NIASHv2017D1	Australopyrum_retrofractum_PI531553	2082	1416	68%	601
NIASHv2017D1	Australopyrum_retrofractum_PI533013	2082	578	28%	601
NIASHv2017D1	Australopyrum_retrofractum_PI533014	2082	1735	83%	601
NIASHv2017D1	Australopyrum_retrofractum_PI547363	2082	1547	74%	601
NIASHv2017D1	Brachypodium_distachyon	2082	1610	77%	601
NIASHv2017D1	Bromus_tectorum_GRA1085	2082	911	44%	601
NIASHv2017D1	Dasyphyrum_villosum_GRA1020	2082	1189	57%	601
NIASHv2017D1	Dasyphyrum_villosum_GRA1027	2082	1278	61%	601
NIASHv2017D1	Dasyphyrum_villosum_PI368884	2082	309	15%	601
NIASHv2017D1	Dasyphyrum_villosum_W619414	2082	450	22%	601
NIASHv2017D1	Dasyphyrum_villosum_W67300	2082	1307	63%	601
NIASHv2017D1	Eremopyrum_distans_PI193264	2082	1328	64%	601
NIASHv2017D1	Eremopyrum_triticeum_GRA2250	2082	1635	79%	601
NIASHv2017D1	Eremopyrum_triticeum_PI502364	2082	1182	57%	601
NIASHv2017D1	Eremopyrum_triticeum_W626631	2082	1137	55%	601
NIASHv2017D1	Henrardia_persica_PI401347	2082	1441	69%	601
NIASHv2017D1	Henrardia_persica_PI577112	2082	1808	87%	601
NIASHv2017D1	Henrardia_persica_PI577113	2082	966	46%	601
NIASHv2017D1	Henrardia_persica_RF2012	2082	1512	73%	601
NIASHv2017D1	Heteranthelium_piliferum_PI401351	2082	1542	74%	601
NIASHv2017D1	Heteranthelium_piliferum_PI401353	2082	1783	86%	601
NIASHv2017D1	Heteranthelium_piliferum_PI401354	2082	1770	85%	601
NIASHv2017D1	Heteranthelium_sp_PI314152	2082	1586	76%	601
NIASHv2017D1	Hordeum_marinum_BCC2006	2082	1867	90%	601
NIASHv2017D1	Hordeum_murinum_BCC2002	2082	1727	83%	601
NIASHv2017D1	Hordeum_pubiflorum_2028	2082	1942	93%	601
NIASHv2017D1	Hordeum_spontanum_FT11	2082	2280	110%	601
NIASHv2017D1	Hordeum_vulgare_Morex	2082	2199	106%	601
NIASHv2017D1	Psathyrostachys_junceae_PI222050	2082	1539	74%	601
NIASHv2017D1	Psathyrostachys_junceae_PI565077	2082	574	28%	601
NIASHv2017D1	Psathyrostachys_junceae_PI595135	2082	1814	87%	601
NIASHv2017D1	Psathyrostachys_junceae_PI598613	2082	1650	79%	601
NIASHv2017D1	Psathyrostachys_junceae_PI619487	2082	1674	80%	601
NIASHv2017D1	Psathyrostachys_sp_PI565080	2082	1461	70%	601
NIASHv2017D1	Pseudoroegneria_libanotica_PI228389	2082	952	46%	601
NIASHv2017D1	Pseudoroegneria_libanotica_PI330688	2082	1280	61%	601
NIASHv2017D1	Pseudoroegneria_libanotica_PI401274	2082	1809	87%	601
NIASHv2017D1	Pseudoroegneria_stipifolia_PI325181	2082	1716	82%	601
NIASHv2017D1	Pseudoroegneria_stipifolia_PI440095	2082	1693	81%	601
NIASHv2017D1	Pseudoroegneria_stipifolia_PI531751	2082	1546	74%	601
NIASHv2017D1	Pseudoroegneria_strigosa_PI499638	2082	1032	50%	601
NIASHv2017D1	Pseudoroegneria_strigosa_PI595172	2082	1602	77%	601
NIASHv2017D1	Pseudoroegneria_strigosa_W614049	2082	1751	84%	601
NIASHv2017D1	Pseudoroegneria_strigosa_PI639805	2082	1386	67%	601
NIASHv2017D1	Pseudoroegneria_strigosa_PI639805	2082	1597	77%	601
NIASHv2017D1	Pseudoroegneria_tauri_PI401322	2082	1022	49%	601
NIASHv2017D1	Pseudoroegneria_tauri_PI401333	2082	1702	82%	601
NIASHv2017D1	Secale_cereale_PI618662	2082	304	15%	601
NIASHv2017D1	Secale_cereale_PI618665	2082	1594	77%	601
NIASHv2017D1	Secale_cereale_PI618669	2082	1505	72%	601
NIASHv2017D1	Secale_cereale_PI618671	2082	1768	85%	601
NIASHv2017D1	Secale_strictum_R1108	2082	616	30%	601
NIASHv2017D1	Secale_strictum_R853	2082	953	46%	601
NIASHv2017D1	Secale_vavilovii_PI253957	2082	801	38%	601
NIASHv2017D1	Secale_vavilovii_R1027	2082	996	48%	601
NIASHv2017D1	Taeniatherum_caput-medusae_CK2011	2082	1358	65%	601
NIASHv2017D1	Taeniatherum_caput-medusae_GRA1126	2082	1765	85%	601
NIASHv2017D1	Taeniatherum_caput-medusae_PI220589	2082	1557	75%	601
NIASHv2017D1	Taeniatherum_caput-medusae_PI251387	2082	298	14%	601
NIASHv2017D1	Taeniatherum_caput-medusae_PI561095	2082	56	3%	601
NIASHv2017D1	Taeniatherum_crininum_GRA2570	2082	1674	80%	601
NIASHv2017D1	Thinopyrum_bessarabicum_W621890	2082	1609	77%	601
NIASHv2017D1	Thinopyrum_elongatum_PI109452	2082	1721	83%	601
NIASHv2017D1	Thinopyrum_elongatum_PI401117	2082	1240	60%	601
NIASHv2017D1	Triticum_boeoticum_1613	2082	2033	98%	601
NIASHv2017D1	Triticum_boeoticum_1688	2082	1361	65%	601
NIASHv2017D1	Triticum_boeoticum_ID379	2082	810	39%	601

Locus	Accession	Mapped exon length in barley (bp)	Assembled exon length (bp)	% of mapped exon length that could be assembled	Extended target (bp)
NIASHv2017D1	Triticum_boeoticum_PI272520	2082	435	21%	601
NIASHv2017D1	Triticum_boeoticum_PI427451	2082	1647	79%	601
NIASHv2017D1	Triticum_boeoticum_PI427620	2082	1450	70%	601
NIASHv2017D1	Triticum_monococcum_2205	2082	1553	75%	601
NIASHv2017D1	Triticum_monococcum_2208	2082	1503	72%	601
NIASHv2017D1	Triticum_monococcum_2271	2082	1893	91%	601
NIASHv2017D1	Triticum_monococcum_TRI13061	2082	1559	75%	601
NIASHv2017D1	Triticum_monococcum_TRI13612	2082	1473	71%	601
NIASHv2017D1	Triticum_urartu_1307	2082	1889	91%	601
NIASHv2017D1	Triticum_urartu_PI428184	2082	382	18%	601
NIASHv2017D1	Triticum_urartu_PI428317	2082	560	27%	601
NIASHv2017D1	Triticum_urartu_TRI17824	2082	1642	79%	601
NIASHv2017D1	Triticum_urartu_TRI18407	2082	1737	83%	601
NIASHv2017N01	Aegilops_bicornis_AE106	2035	2270	112%	601
NIASHv2017N01	Aegilops_bicornis_AE1079	2035	1921	94%	601
NIASHv2017N01	Aegilops_bicornis_AE788	2035	2215	109%	601
NIASHv2017N01	Aegilops_bicornis_KU-5786	2035	2088	103%	601
NIASHv2017N01	Aegilops_comosa_AE1255	2035	2394	118%	601
NIASHv2017N01	Aegilops_comosa_AE1378	2035	2242	110%	601
NIASHv2017N01	Aegilops_comosa_AE783	2035	2312	114%	601
NIASHv2017N01	Aegilops_comosa_PI276970	2035	2092	103%	601
NIASHv2017N01	Aegilops_longissima_AE1078	2035	2189	108%	601
NIASHv2017N01	Aegilops_longissima_AE133	2035	2295	113%	601
NIASHv2017N01	Aegilops_longissima_AE417	2035	2068	102%	601
NIASHv2017N01	Aegilops_longissima_PI604141	2035	2047	101%	601
NIASHv2017N01	Aegilops_longissima_TA1921	2035	2290	113%	601
NIASHv2017N01	Aegilops_markgrafii_AE1381	2035	2395	118%	601
NIASHv2017N01	Aegilops_markgrafii_KP-2012-106	2035	2214	109%	601
NIASHv2017N01	Aegilops_markgrafii_PI254863	2035	2004	98%	601
NIASHv2017N01	Aegilops_markgrafii_PI542208	2035	2262	111%	601
NIASHv2017N01	Aegilops_markgrafii_PI596287	2035	2275	112%	601
NIASHv2017N01	Aegilops_mutica_01C2100106	2035	2365	116%	601
NIASHv2017N01	Aegilops_searsii_AE1075	2035	2218	109%	601
NIASHv2017N01	Aegilops_searsii_AE1083	2035	2357	116%	601
NIASHv2017N01	Aegilops_searsii_KU-14655	2035	2377	117%	601
NIASHv2017N01	Aegilops_searsii_PI599142	2035	2265	111%	601
NIASHv2017N01	Aegilops_searsii_PI599148	2035	1970	97%	601
NIASHv2017N01	Aegilops_sharonensis_AE90691	2035	2290	113%	601
NIASHv2017N01	Aegilops_speltoides_3776	2035	2399	118%	601
NIASHv2017N01	Aegilops_speltoides_AE1064	2035	2363	116%	601
NIASHv2017N01	Aegilops_speltoides_AE900	2035	2276	112%	601
NIASHv2017N01	Aegilops_speltoides_KU-7856	2035	2167	106%	601
NIASHv2017N01	Aegilops_speltoides_PI486264	2035	2351	116%	601
NIASHv2017N01	Aegilops_speltoides_PI487231	2035	2311	114%	601
NIASHv2017N01	Aegilops_speltoides_TA1772	2035	2101	103%	601
NIASHv2017N01	Aegilops_tauschii_49116	2035	2183	107%	601
NIASHv2017N01	Aegilops_tauschii_937	2035	2448	120%	601
NIASHv2017N01	Aegilops_tauschii_AE1069	2035	2307	113%	601
NIASHv2017N01	Aegilops_tauschii_AE956	2035	2396	118%	601
NIASHv2017N01	Aegilops_umbellulata_AE1070	2035	2271	112%	601
NIASHv2017N01	Aegilops_umbellulata_AE153	2035	2323	114%	601
NIASHv2017N01	Aegilops_umbellulata_AE740	2035	2167	106%	601
NIASHv2017N01	Aegilops_umbellulata_AE811	2035	1644	81%	601
NIASHv2017N01	Aegilops_uniaristata_AE157	2035	2418	119%	601
NIASHv2017N01	Aegilops_uniaristata_AE680	2035	2284	112%	601
NIASHv2017N01	Aegilops_uniaristata_PI276996	2035	1854	91%	601
NIASHv2017N01	Agropyron_cristatum_PI494615	2035	2320	114%	601
NIASHv2017N01	Agropyron_cristatum_PI598631	2035	2230	110%	601
NIASHv2017N01	Amblyopyrum_muticum_PI560122	2035	1950	96%	601
NIASHv2017N01	Amblyopyrum_muticum_PI560124	2035	1826	90%	601
NIASHv2017N01	Amblyopyrum_muticum_PI560125	2035	1887	93%	601
NIASHv2017N01	Amblyopyrum_muticum_PI560126	2035	1894	93%	601
NIASHv2017N01	Amblyopyrum_muticum_PI636562	2035	2310	114%	601
NIASHv2017N01	Australopyrum_retrofractum_PI531553	2035	2216	109%	601
NIASHv2017N01	Australopyrum_retrofractum_PI533013	2035	2201	108%	601
NIASHv2017N01	Australopyrum_retrofractum_PI533014	2035	2243	110%	601
NIASHv2017N01	Australopyrum_retrofractum_PI547363	2035	2231	110%	601
NIASHv2017N01	Brachypodium_distachyon	2035	2091	103%	601
NIASHv2017N01	Bromus_tectorum_GRA1085	2035	2018	99%	601
NIASHv2017N01	Dasyphyrum_villosum_GRA1020	2035	2205	108%	601
NIASHv2017N01	Dasyphyrum_villosum_GRA1027	2035	2252	111%	601
NIASHv2017N01	Dasyphyrum_villosum_PI368884	2035	2007	99%	601
NIASHv2017N01	Dasyphyrum_villosum_W619414	2035	2116	104%	601
NIASHv2017N01	Dasyphyrum_villosum_W67300	2035	2293	113%	601
NIASHv2017N01	Eremopyrum_distans_PI193264	2035	2216	109%	601
NIASHv2017N01	Eremopyrum_triticeum_GRA2250	2035	2346	115%	601
NIASHv2017N01	Eremopyrum_triticeum_PI502364	2035	2203	108%	601
NIASHv2017N01	Eremopyrum_triticeum_W626631	2035	2149	106%	601
NIASHv2017N01	Henrardia_persica_PI401347	2035	2290	113%	601
NIASHv2017N01	Henrardia_persica_PI577112	2035	2385	117%	601
NIASHv2017N01	Henrardia_persica_PI577113	2035	2217	109%	601
NIASHv2017N01	Henrardia_persica_RF2012	2035	2247	110%	601
NIASHv2017N01	Heterantherium_piliferum_PI401351	2035	2269	111%	601
NIASHv2017N01	Heterantherium_piliferum_PI401353	2035	2376	117%	601
NIASHv2017N01	Heterantherium_piliferum_PI401354	2035	2454	121%	601
NIASHv2017N01	Heterantherium_sp_PI314152	2035	2230	110%	601

Locus	Accession	Mapped exon length in barley (bp)	Assembled exon length (bp)	% of mapped exon length that could be assembled	Extended target (bp)
NIASHv2017N01	Hordeum_marinum_BCC2006	2035	2395	118%	601
NIASHv2017N01	Hordeum_murinum_BCC2002	2035	2454	121%	601
NIASHv2017N01	Hordeum_pubiflorum_2028	2035	2589	127%	601
NIASHv2017N01	Hordeum_spontaneum_FT11	2035	2609	128%	601
NIASHv2017N01	Hordeum_vulgare_Morex	2035	2496	123%	601
NIASHv2017N01	Psathyrostachys_junceae_P1222050	2035	2231	110%	601
NIASHv2017N01	Psathyrostachys_junceae_P1565077	2035	2213	109%	601
NIASHv2017N01	Psathyrostachys_junceae_P1595135	2035	2340	115%	601
NIASHv2017N01	Psathyrostachys_junceae_P1598613	2035	2284	112%	601
NIASHv2017N01	Psathyrostachys_junceae_P1619487	2035	2343	115%	601
NIASHv2017N01	Psathyrostachys_sp_P1565080	2035	2231	110%	601
NIASHv2017N01	Pseudoroegneria_libanotica_P1228389	2035	2190	108%	601
NIASHv2017N01	Pseudoroegneria_libanotica_P1330688	2035	2246	110%	601
NIASHv2017N01	Pseudoroegneria_libanotica_P1401274	2035	2393	118%	601
NIASHv2017N01	Pseudoroegneria_stipifolia_P1325181	2035	2368	116%	601
NIASHv2017N01	Pseudoroegneria_stipifolia_P1440095	2035	2288	112%	601
NIASHv2017N01	Pseudoroegneria_stipifolia_P1531751	2035	2210	109%	601
NIASHv2017N01	Pseudoroegneria_strigosa_P1499638	2035	2186	107%	601
NIASHv2017N01	Pseudoroegneria_strigosa_P1595172	2035	2207	108%	601
NIASHv2017N01	Pseudoroegneria_strigosa_W614049	2035	2317	114%	601
NIASHv2017N01	Pseudoroegneria_strigosa_P1639805	2035	2162	106%	601
NIASHv2017N01	Pseudoroegneria_strigosa_P1639805	2035	2231	110%	601
NIASHv2017N01	Pseudoroegneria_tauri_P1401322	2035	2167	106%	601
NIASHv2017N01	Pseudoroegneria_tauri_P1401333	2035	2318	114%	601
NIASHv2017N01	Secale_cereale_P1618662	2035	2018	99%	601
NIASHv2017N01	Secale_cereale_P1618665	2035	2230	110%	601
NIASHv2017N01	Secale_cereale_P1618669	2035	2339	115%	601
NIASHv2017N01	Secale_cereale_P1618671	2035	2236	110%	601
NIASHv2017N01	Secale_strictum_R1108	2035	2159	106%	601
NIASHv2017N01	Secale_strictum_R853	2035	2184	107%	601
NIASHv2017N01	Secale_vavilovii_P1253957	2035	1621	80%	601
NIASHv2017N01	Secale_vavilovii_R1027	2035	2176	107%	601
NIASHv2017N01	Taeniatherum_caput-medusae_CK2011	2035	2277	112%	601
NIASHv2017N01	Taeniatherum_caput-medusae_GRA1126	2035	2373	117%	601
NIASHv2017N01	Taeniatherum_caput-medusae_P1220589	2035	2293	113%	601
NIASHv2017N01	Taeniatherum_caput-medusae_P1251387	2035	2157	106%	601
NIASHv2017N01	Taeniatherum_caput-medusae_P1561095	2035	1869	92%	601
NIASHv2017N01	Taeniatherum_crinatum_GRA2570	2035	2291	113%	601
NIASHv2017N01	Thinopyrum_besarabicum_W621890	2035	2118	104%	601
NIASHv2017N01	Thinopyrum_elongatum_P1109452	2035	2199	108%	601
NIASHv2017N01	Thinopyrum_elongatum_P1401117	2035	2108	104%	601
NIASHv2017N01	Triticum_boeoticum_1613	2035	2550	125%	601
NIASHv2017N01	Triticum_boeoticum_1688	2035	2275	112%	601
NIASHv2017N01	Triticum_boeoticum_ID379	2035	2112	104%	601
NIASHv2017N01	Triticum_boeoticum_P1272520	2035	2107	104%	601
NIASHv2017N01	Triticum_boeoticum_P1427451	2035	2347	115%	601
NIASHv2017N01	Triticum_boeoticum_P1427620	2035	2295	113%	601
NIASHv2017N01	Triticum_monococcum_2205	2035	2249	111%	601
NIASHv2017N01	Triticum_monococcum_2208	2035	2359	116%	601
NIASHv2017N01	Triticum_monococcum_2271	2035	2449	120%	601
NIASHv2017N01	Triticum_monococcum_TRI13061	2035	2318	114%	601
NIASHv2017N01	Triticum_monococcum_TRI13612	2035	2402	118%	601
NIASHv2017N01	Triticum_urartu_1307	2035	2401	118%	601
NIASHv2017N01	Triticum_urartu_P1428184	2035	2181	107%	601
NIASHv2017N01	Triticum_urartu_P1428317	2035	2130	105%	601
NIASHv2017N01	Triticum_urartu_TRI17824	2035	2409	118%	601
NIASHv2017N01	Triticum_urartu_TRI18407	2035	2347	115%	601
NIASHv2029G1	Aegilops_bicornis_AE106	1076	993	92%	601
NIASHv2029G1	Aegilops_bicornis_AE1079	1076	275	26%	601
NIASHv2029G1	Aegilops_bicornis_AE788	1076	632	59%	601
NIASHv2029G1	Aegilops_bicornis_KU-5786	1076	147	14%	601
NIASHv2029G1	Aegilops_comosa_AE1255	1076	865	80%	601
NIASHv2029G1	Aegilops_comosa_AE1378	1076	348	32%	601
NIASHv2029G1	Aegilops_comosa_AE783	1076	791	74%	601
NIASHv2029G1	Aegilops_comosa_P1276970	1076	379	35%	601
NIASHv2029G1	Aegilops_longissima_AE1078	1076	330	31%	601
NIASHv2029G1	Aegilops_longissima_AE133	1076	768	71%	601
NIASHv2029G1	Aegilops_longissima_AE417	1076	70	7%	601
NIASHv2029G1	Aegilops_longissima_P1604141	1076	189	18%	601
NIASHv2029G1	Aegilops_longissima_TA1921	1076	700	65%	601
NIASHv2029G1	Aegilops_markgrafii_AE1381	1076	559	52%	601
NIASHv2029G1	Aegilops_markgrafii_KP-2012-106	1076	563	52%	601
NIASHv2029G1	Aegilops_markgrafii_P1254863	1076	41	4%	601
NIASHv2029G1	Aegilops_markgrafii_P1542208	1076	884	82%	601
NIASHv2029G1	Aegilops_markgrafii_P1596287	1076	939	87%	601
NIASHv2029G1	Aegilops_mutica_01C2100106	1076	729	68%	601
NIASHv2029G1	Aegilops_searsii_AE1075	1076	169	16%	601
NIASHv2029G1	Aegilops_searsii_AE1083	1076	920	86%	601
NIASHv2029G1	Aegilops_searsii_KU-14655	1076	587	55%	601
NIASHv2029G1	Aegilops_searsii_P1599142	1076	545	51%	601
NIASHv2029G1	Aegilops_searsii_P1599148	1076	236	22%	601
NIASHv2029G1	Aegilops_sharonensis_AE90691	1076	587	55%	601
NIASHv2029G1	Aegilops_speltoides_3776	1076	1200	112%	601
NIASHv2029G1	Aegilops_speltoides_AE1064	1076	501	47%	601
NIASHv2029G1	Aegilops_speltoides_AE900	1076	608	57%	601
NIASHv2029G1	Aegilops_speltoides_KU-7856	1076	263	24%	601

Locus	Accession	Mapped exon length in barley (bp)	Assembled exon length (bp)	% of mapped exon length that could be assembled	Extended target (bp)
NIASHv2029G1	Aegilops_speltoides_PI486264	1076	965	90%	601
NIASHv2029G1	Aegilops_speltoides_PI487231	1076	878	82%	601
NIASHv2029G1	Aegilops_speltoides_TA1772	1076	174	16%	601
NIASHv2029G1	Aegilops_tauschii_49116	1076	505	47%	601
NIASHv2029G1	Aegilops_tauschii_937	1076	1055	98%	601
NIASHv2029G1	Aegilops_tauschii_AE1069	1076	475	44%	601
NIASHv2029G1	Aegilops_tauschii_AE956	1076	748	70%	601
NIASHv2029G1	Aegilops_umbellulata_AE1070	1076	405	38%	601
NIASHv2029G1	Aegilops_umbellulata_AE153	1076	750	70%	601
NIASHv2029G1	Aegilops_umbellulata_AE740	1076	101	9%	601
NIASHv2029G1	Aegilops_umbellulata_AE811	1076	0	0%	601
NIASHv2029G1	Aegilops_uniaristata_AE157	1076	987	92%	601
NIASHv2029G1	Aegilops_uniaristata_AE680	1076	894	83%	601
NIASHv2029G1	Aegilops_uniaristata_PI276996	1076	43	4%	601
NIASHv2029G1	Agropyron_cristatum_PI494615	1076	574	53%	601
NIASHv2029G1	Agropyron_cristatum_PI598631	1076	529	49%	601
NIASHv2029G1	Amblyopyrum_muticum_PI560122	1076	0	0%	601
NIASHv2029G1	Amblyopyrum_muticum_PI560124	1076	0	0%	601
NIASHv2029G1	Amblyopyrum_muticum_PI560125	1076	182	17%	601
NIASHv2029G1	Amblyopyrum_muticum_PI560126	1076	47	4%	601
NIASHv2029G1	Amblyopyrum_muticum_PI636562	1076	542	50%	601
NIASHv2029G1	Australopyrum_retrofractum_PI531553	1076	404	38%	601
NIASHv2029G1	Australopyrum_retrofractum_PI533013	1076	105	10%	601
NIASHv2029G1	Australopyrum_retrofractum_PI533014	1076	622	58%	601
NIASHv2029G1	Australopyrum_retrofractum_PI547363	1076	665	62%	601
NIASHv2029G1	Brachypodium_distachyon	1076	791	74%	601
NIASHv2029G1	Bromus_tectorum_GRA1085	1076	392	36%	601
NIASHv2029G1	Dasyphyrum_villosum_GRA1020	1076	390	36%	601
NIASHv2029G1	Dasyphyrum_villosum_GRA1027	1076	490	46%	601
NIASHv2029G1	Dasyphyrum_villosum_PI368884	1076	0	0%	601
NIASHv2029G1	Dasyphyrum_villosum_W619414	1076	253	24%	601
NIASHv2029G1	Dasyphyrum_villosum_W67300	1076	484	45%	601
NIASHv2029G1	Eremopyrum_distans_PI193264	1076	513	48%	601
NIASHv2029G1	Eremopyrum_triticeum_GRA2250	1076	762	71%	601
NIASHv2029G1	Eremopyrum_triticeum_PI502364	1076	582	54%	601
NIASHv2029G1	Eremopyrum_triticeum_W626631	1076	228	21%	601
NIASHv2029G1	Henrardia_persica_PI401347	1076	450	42%	601
NIASHv2029G1	Henrardia_persica_PI577112	1076	949	88%	601
NIASHv2029G1	Henrardia_persica_PI577113	1076	312	29%	601
NIASHv2029G1	Henrardia_persica_RF2012	1076	691	64%	601
NIASHv2029G1	Heteranthelium_piliferum_PI401351	1076	648	60%	601
NIASHv2029G1	Heteranthelium_piliferum_PI401353	1076	984	91%	601
NIASHv2029G1	Heteranthelium_piliferum_PI401354	1076	1019	95%	601
NIASHv2029G1	Heteranthelium_sp._PI314152	1076	308	29%	601
NIASHv2029G1	Hordeum_marinum_BCC2006	1076	799	74%	601
NIASHv2029G1	Hordeum_murinum_BCC2002	1076	949	88%	601
NIASHv2029G1	Hordeum_pubiflorum_2028	1076	1258	117%	601
NIASHv2029G1	Hordeum_spontaneum_FT11	1076	1452	135%	601
NIASHv2029G1	Hordeum_vulgare_Morex	1076	1478	137%	601
NIASHv2029G1	Psathyrostachys_junceae_PI222050	1076	495	46%	601
NIASHv2029G1	Psathyrostachys_junceae_PI565077	1076	14	1%	601
NIASHv2029G1	Psathyrostachys_junceae_PI595135	1076	772	72%	601
NIASHv2029G1	Psathyrostachys_junceae_PI598613	1076	677	63%	601
NIASHv2029G1	Psathyrostachys_junceae_PI619487	1076	543	50%	601
NIASHv2029G1	Psathyrostachys_sp._PI565080	1076	422	39%	601
NIASHv2029G1	Pseudoroegneria_libanotica_PI228389	1076	282	26%	601
NIASHv2029G1	Pseudoroegneria_libanotica_PI330688	1076	472	44%	601
NIASHv2029G1	Pseudoroegneria_libanotica_PI401274	1076	698	65%	601
NIASHv2029G1	Pseudoroegneria_stipifolia_PI325181	1076	932	87%	601
NIASHv2029G1	Pseudoroegneria_stipifolia_PI440095	1076	817	76%	601
NIASHv2029G1	Pseudoroegneria_stipifolia_PI531751	1076	634	59%	601
NIASHv2029G1	Pseudoroegneria_strigosa_PI499638	1076	526	49%	601
NIASHv2029G1	Pseudoroegneria_strigosa_PI595172	1076	696	65%	601
NIASHv2029G1	Pseudoroegneria_strigosa_W614049	1076	975	91%	601
NIASHv2029G1	Pseudoroegneria_strigosa_PI639805	1076	730	68%	601
NIASHv2029G1	Pseudoroegneria_strigosa_PI639805	1076	656	61%	601
NIASHv2029G1	Pseudoroegneria_tauri_PI401322	1076	451	42%	601
NIASHv2029G1	Pseudoroegneria_tauri_PI401333	1076	620	58%	601
NIASHv2029G1	Secale_cereale_PI618662	1076	32	3%	601
NIASHv2029G1	Secale_cereale_PI618665	1076	323	30%	601
NIASHv2029G1	Secale_cereale_PI618669	1076	675	63%	601
NIASHv2029G1	Secale_cereale_PI618671	1076	610	57%	601
NIASHv2029G1	Secale_strictum_R1108	1076	295	27%	601
NIASHv2029G1	Secale_strictum_R853	1076	310	29%	601
NIASHv2029G1	Secale_vavilovii_PI253957	1076	0	0%	601
NIASHv2029G1	Secale_vavilovii_R1027	1076	204	19%	601
NIASHv2029G1	Taeniatherum_caput-medusae_CK2011	1076	705	66%	601
NIASHv2029G1	Taeniatherum_caput-medusae_GRA1126	1076	707	66%	601
NIASHv2029G1	Taeniatherum_caput-medusae_PI220589	1076	739	69%	601
NIASHv2029G1	Taeniatherum_caput-medusae_PI251387	1076	180	17%	601
NIASHv2029G1	Taeniatherum_caput-medusae_PI561095	1076	0	0%	601
NIASHv2029G1	Taeniatherum_crinium_GRA2570	1076	875	81%	601
NIASHv2029G1	Thinopyrum_bessarabicum_W621890	1076	516	48%	601
NIASHv2029G1	Thinopyrum_elongatum_PI109452	1076	511	47%	601
NIASHv2029G1	Thinopyrum_elongatum_PI401117	1076	250	23%	601
NIASHv2029G1	Triticum_boeoticum_1613	1076	1140	106%	601

Locus	Accession	Mapped exon length in barley (bp)	Assembled exon length (bp)	% of mapped exon length that could be assembled	Extended target (bp)
NIASHv2029G1	Triticum_boeoticum_1688	1076	808	75%	601
NIASHv2029G1	Triticum_boeoticum_ID379	1076	87	8%	601
NIASHv2029G1	Triticum_boeoticum_PI272520	1076	291	27%	601
NIASHv2029G1	Triticum_boeoticum_PI427451	1076	1000	93%	601
NIASHv2029G1	Triticum_boeoticum_PI427620	1076	737	68%	601
NIASHv2029G1	Triticum_monococcum_2205	1076	987	92%	601
NIASHv2029G1	Triticum_monococcum_2208	1076	663	62%	601
NIASHv2029G1	Triticum_monococcum_2271	1076	1161	108%	601
NIASHv2029G1	Triticum_monococcum_TRI113061	1076	840	78%	601
NIASHv2029G1	Triticum_monococcum_TRI113612	1076	826	77%	601
NIASHv2029G1	Triticum_urartu_1307	1076	1173	109%	601
NIASHv2029G1	Triticum_urartu_PI428184	1076	0	0%	601
NIASHv2029G1	Triticum_urartu_PI428317	1076	120	11%	601
NIASHv2029G1	Triticum_urartu_TRI17824	1076	737	68%	601
NIASHv2029G1	Triticum_urartu_TRI18407	1076	971	90%	601
NIASHv2039I23	Aegilops_bicornis_AE106	1300	1267	97%	601
NIASHv2039I23	Aegilops_bicornis_AE1079	1300	896	69%	601
NIASHv2039I23	Aegilops_bicornis_AE788	1300	1278	98%	601
NIASHv2039I23	Aegilops_bicornis_KU-5786	1300	794	61%	601
NIASHv2039I23	Aegilops_comosa_AE1255	1300	1334	103%	601
NIASHv2039I23	Aegilops_comosa_AE1378	1300	1102	85%	601
NIASHv2039I23	Aegilops_comosa_AE783	1300	1205	93%	601
NIASHv2039I23	Aegilops_comosa_PI276970	1300	1041	80%	601
NIASHv2039I23	Aegilops_longissima_AE1078	1300	1077	83%	601
NIASHv2039I23	Aegilops_longissima_AE133	1300	1206	93%	601
NIASHv2039I23	Aegilops_longissima_AE417	1300	710	55%	601
NIASHv2039I23	Aegilops_longissima_PI604141	1300	645	50%	601
NIASHv2039I23	Aegilops_longissima_TA1921	1300	1125	87%	601
NIASHv2039I23	Aegilops_markgrafii_AE1381	1300	1264	97%	601
NIASHv2039I23	Aegilops_markgrafii_KP-2012-106	1300	1188	91%	601
NIASHv2039I23	Aegilops_markgrafii_PI254863	1300	849	65%	601
NIASHv2039I23	Aegilops_markgrafii_PI542208	1300	1209	93%	601
NIASHv2039I23	Aegilops_markgrafii_PI596287	1300	1283	99%	601
NIASHv2039I23	Aegilops_mutica_01C2100106	1300	1287	99%	601
NIASHv2039I23	Aegilops_searsii_AE1075	1300	1147	88%	601
NIASHv2039I23	Aegilops_searsii_AE1083	1300	1275	98%	601
NIASHv2039I23	Aegilops_searsii_KU-14655	1300	1335	103%	601
NIASHv2039I23	Aegilops_searsii_PI599142	1300	1155	89%	601
NIASHv2039I23	Aegilops_searsii_PI599148	1300	278	21%	601
NIASHv2039I23	Aegilops_sharonensis_AE90691	1300	1179	91%	601
NIASHv2039I23	Aegilops_speltoides_3776	1300	1361	105%	601
NIASHv2039I23	Aegilops_speltoides_AE1064	1300	1226	94%	601
NIASHv2039I23	Aegilops_speltoides_AE900	1300	1220	94%	601
NIASHv2039I23	Aegilops_speltoides_KU-7856	1300	920	71%	601
NIASHv2039I23	Aegilops_speltoides_PI486264	1300	1285	99%	601
NIASHv2039I23	Aegilops_speltoides_PI487231	1300	1154	89%	601
NIASHv2039I23	Aegilops_speltoides_TA1772	1300	827	64%	601
NIASHv2039I23	Aegilops_tauschii_49116	1300	1163	89%	601
NIASHv2039I23	Aegilops_tauschii_937	1300	1508	116%	601
NIASHv2039I23	Aegilops_tauschii_AE1069	1300	1174	90%	601
NIASHv2039I23	Aegilops_tauschii_AE956	1300	1300	100%	601
NIASHv2039I23	Aegilops_umbellulata_AE1070	1300	1270	98%	601
NIASHv2039I23	Aegilops_umbellulata_AE153	1300	1282	99%	601
NIASHv2039I23	Aegilops_umbellulata_AE740	1300	986	76%	601
NIASHv2039I23	Aegilops_umbellulata_AE811	1300	586	45%	601
NIASHv2039I23	Aegilops_uniaristata_AE157	1300	1486	114%	601
NIASHv2039I23	Aegilops_uniaristata_AE680	1300	1249	96%	601
NIASHv2039I23	Aegilops_uniaristata_PI276996	1300	767	59%	601
NIASHv2039I23	Agropyron_cristatum_PI494615	1300	1245	96%	601
NIASHv2039I23	Agropyron_cristatum_PI598631	1300	1208	93%	601
NIASHv2039I23	Amblyopyrum_muticum_PI560122	1300	730	56%	601
NIASHv2039I23	Amblyopyrum_muticum_PI560124	1300	529	41%	601
NIASHv2039I23	Amblyopyrum_muticum_PI560125	1300	640	49%	601
NIASHv2039I23	Amblyopyrum_muticum_PI560126	1300	442	34%	601
NIASHv2039I23	Amblyopyrum_muticum_PI636562	1300	1230	95%	601
NIASHv2039I23	Australopyrum_retrofractum_PI531553	1300	1084	83%	601
NIASHv2039I23	Australopyrum_retrofractum_PI533013	1300	865	67%	601
NIASHv2039I23	Australopyrum_retrofractum_PI533014	1300	1358	104%	601
NIASHv2039I23	Australopyrum_retrofractum_PI547363	1300	1259	97%	601
NIASHv2039I23	Brachypodium_distachyon	1300	1263	97%	601
NIASHv2039I23	Bromus_tectorum_GRA1085	1300	992	76%	601
NIASHv2039I23	Dasyphyrum_villosum_GRA1020	1300	1213	93%	601
NIASHv2039I23	Dasyphyrum_villosum_GRA1027	1300	1252	96%	601
NIASHv2039I23	Dasyphyrum_villosum_PI368884	1300	610	47%	601
NIASHv2039I23	Dasyphyrum_villosum_W619414	1300	660	51%	601
NIASHv2039I23	Dasyphyrum_villosum_W67300	1300	1145	88%	601
NIASHv2039I23	Eremopyrum_distans_PI193264	1300	1339	103%	601
NIASHv2039I23	Eremopyrum_triticeum_GRA2250	1300	1305	100%	601
NIASHv2039I23	Eremopyrum_triticeum_PI502364	1300	1057	81%	601
NIASHv2039I23	Eremopyrum_triticeum_W626631	1300	1038	80%	601
NIASHv2039I23	Henrardia_persica_PI401347	1300	1310	101%	601
NIASHv2039I23	Henrardia_persica_PI577112	1300	1350	104%	601
NIASHv2039I23	Henrardia_persica_PI577113	1300	1242	96%	601
NIASHv2039I23	Henrardia_persica_RF2012	1300	1311	101%	601
NIASHv2039I23	Heteranthelium_piliferum_PI401351	1300	1192	92%	601
NIASHv2039I23	Heteranthelium_piliferum_PI401353	1300	1460	112%	601

Locus	Accession	Mapped exon length in barley (bp)	Assembled exon length (bp)	% of mapped exon length that could be assembled	Extended target (bp)
NIASHv2039l23	Heteranthelium_piliferum_PI401354	1300	1346	104%	601
NIASHv2039l23	Heteranthelium_sp_PI314152	1300	1094	84%	601
NIASHv2039l23	Hordeum_marinum_BCC2006	1300	1275	98%	601
NIASHv2039l23	Hordeum_murinum_BCC2002	1300	1386	107%	601
NIASHv2039l23	Hordeum_pubiflorum_2028	1300	1581	122%	601
NIASHv2039l23	Hordeum_spontaneum_FT11	1300	1794	138%	601
NIASHv2039l23	Hordeum_vulgare_Morex	1300	1759	135%	601
NIASHv2039l23	Psathyrostachys_junceae_PI222050	1300	1245	96%	601
NIASHv2039l23	Psathyrostachys_junceae_PI565077	1300	952	73%	601
NIASHv2039l23	Psathyrostachys_junceae_PI595135	1300	1225	94%	601
NIASHv2039l23	Psathyrostachys_junceae_PI598613	1300	1267	97%	601
NIASHv2039l23	Psathyrostachys_junceae_PI619487	1300	1332	102%	601
NIASHv2039l23	Psathyrostachys_sp_PI565080	1300	1132	87%	601
NIASHv2039l23	Pseudoroegneria_libanotica_PI228389	1300	1007	77%	601
NIASHv2039l23	Pseudoroegneria_libanotica_PI330688	1300	1191	92%	601
NIASHv2039l23	Pseudoroegneria_libanotica_PI401274	1300	1253	96%	601
NIASHv2039l23	Pseudoroegneria_stipifolia_PI325181	1300	1295	100%	601
NIASHv2039l23	Pseudoroegneria_stipifolia_PI440095	1300	1416	109%	601
NIASHv2039l23	Pseudoroegneria_stipifolia_PI531751	1300	1231	95%	601
NIASHv2039l23	Pseudoroegneria_strigosa_PI499638	1300	1178	91%	601
NIASHv2039l23	Pseudoroegneria_strigosa_PI595172	1300	1329	102%	601
NIASHv2039l23	Pseudoroegneria_strigosa_W614049	1300	1278	98%	601
NIASHv2039l23	Pseudoroegneria_strigosa_PI639805	1300	1180	91%	601
NIASHv2039l23	Pseudoroegneria_strigosa_PI639805	1300	1099	85%	601
NIASHv2039l23	Pseudoroegneria_tauri_PI401322	1300	1075	83%	601
NIASHv2039l23	Pseudoroegneria_tauri_PI401333	1300	1313	101%	601
NIASHv2039l23	Secale_cereale_PI618662	1300	840	65%	601
NIASHv2039l23	Secale_cereale_PI618665	1300	1155	89%	601
NIASHv2039l23	Secale_cereale_PI618669	1300	1330	102%	601
NIASHv2039l23	Secale_cereale_PI618671	1300	1398	108%	601
NIASHv2039l23	Secale_strictum_R1108	1300	739	57%	601
NIASHv2039l23	Secale_strictum_R853	1300	1116	86%	601
NIASHv2039l23	Secale_vavilovii_PI253957	1300	547	42%	601
NIASHv2039l23	Secale_vavilovii_R1027	1300	905	70%	601
NIASHv2039l23	Taeniatherum_caput-medusae_CK2011	1300	1205	93%	601
NIASHv2039l23	Taeniatherum_caput-medusae_GRA1126	1300	1270	98%	601
NIASHv2039l23	Taeniatherum_caput-medusae_PI220589	1300	1249	96%	601
NIASHv2039l23	Taeniatherum_caput-medusae_PI251387	1300	799	61%	601
NIASHv2039l23	Taeniatherum_caput-medusae_PI561095	1300	180	14%	601
NIASHv2039l23	Taeniatherum_crinatum_GRA2570	1300	1260	97%	601
NIASHv2039l23	Thinopyrum_bessarabicum_W621890	1300	1177	91%	601
NIASHv2039l23	Thinopyrum_elongatum_PI109452	1300	1225	94%	601
NIASHv2039l23	Thinopyrum_elongatum_PI401117	1300	839	65%	601
NIASHv2039l23	Triticum_boeoticum_1613	1300	1345	103%	601
NIASHv2039l23	Triticum_boeoticum_1688	1300	1185	91%	601
NIASHv2039l23	Triticum_boeoticum_ID379	1300	847	65%	601
NIASHv2039l23	Triticum_boeoticum_PI272520	1300	881	68%	601
NIASHv2039l23	Triticum_boeoticum_PI427451	1300	1343	103%	601
NIASHv2039l23	Triticum_boeoticum_PI427620	1300	1300	100%	601
NIASHv2039l23	Triticum_monococcum_2205	1300	1312	101%	601
NIASHv2039l23	Triticum_monococcum_2208	1300	1149	88%	601
NIASHv2039l23	Triticum_monococcum_2271	1300	1394	107%	601
NIASHv2039l23	Triticum_monococcum_TRI13061	1300	1295	100%	601
NIASHv2039l23	Triticum_monococcum_TRI13612	1300	1272	98%	601
NIASHv2039l23	Triticum_urartu_1307	1300	1389	107%	601
NIASHv2039l23	Triticum_urartu_PI428184	1300	872	67%	601
NIASHv2039l23	Triticum_urartu_PI428317	1300	945	73%	601
NIASHv2039l23	Triticum_urartu_TRI17824	1300	1313	101%	601
NIASHv2039l23	Triticum_urartu_TRI18407	1300	1233	95%	601
NIASHv2041B21	Aegilops_bicornis_AE106	1185	1261	106%	601
NIASHv2041B21	Aegilops_bicornis_AE1079	1185	837	71%	601
NIASHv2041B21	Aegilops_bicornis_AE788	1185	1145	97%	601
NIASHv2041B21	Aegilops_bicornis_KU-5786	1185	794	67%	601
NIASHv2041B21	Aegilops_comosa_AE1255	1185	1291	109%	601
NIASHv2041B21	Aegilops_comosa_AE1378	1185	1053	89%	601
NIASHv2041B21	Aegilops_comosa_AE783	1185	1120	95%	601
NIASHv2041B21	Aegilops_comosa_PI276970	1185	973	82%	601
NIASHv2041B21	Aegilops_longissima_AE1078	1185	1092	92%	601
NIASHv2041B21	Aegilops_longissima_AE133	1185	1119	94%	601
NIASHv2041B21	Aegilops_longissima_AE417	1185	974	82%	601
NIASHv2041B21	Aegilops_longissima_PI604141	1185	945	80%	601
NIASHv2041B21	Aegilops_longissima_TA1921	1185	1251	106%	601
NIASHv2041B21	Aegilops_markgrafii_AE1381	1185	1267	107%	601
NIASHv2041B21	Aegilops_markgrafii_KP-2012-106	1185	1269	107%	601
NIASHv2041B21	Aegilops_markgrafii_PI254863	1185	991	84%	601
NIASHv2041B21	Aegilops_markgrafii_PI542208	1185	1389	117%	601
NIASHv2041B21	Aegilops_markgrafii_PI596287	1185	1314	111%	601
NIASHv2041B21	Aegilops_mutica_01C2100106	1185	1363	115%	601
NIASHv2041B21	Aegilops_searsii_AE1075	1185	1173	99%	601
NIASHv2041B21	Aegilops_searsii_AE1083	1185	1375	116%	601
NIASHv2041B21	Aegilops_searsii_KU-14655	1185	1278	108%	601
NIASHv2041B21	Aegilops_searsii_PI599142	1185	1310	111%	601
NIASHv2041B21	Aegilops_searsii_PI599148	1185	850	72%	601
NIASHv2041B21	Aegilops_sharonensis_AE90691	1185	1312	111%	601
NIASHv2041B21	Aegilops_speltoides_3776	1185	1548	131%	601
NIASHv2041B21	Aegilops_speltoides_AE1064	1185	1202	101%	601

Locus	Accession	Mapped exon length in barley (bp)	Assembled exon length (bp)	% of mapped exon length that could be assembled	Extended target (bp)
NIASHv2041B21	Aegilops_speltooides_AE900	1185	1265	107%	601
NIASHv2041B21	Aegilops_speltooides_KU-7856	1185	922	78%	601
NIASHv2041B21	Aegilops_speltooides_PI486264	1185	1365	115%	601
NIASHv2041B21	Aegilops_speltooides_PI487231	1185	1251	106%	601
NIASHv2041B21	Aegilops_speltooides_TA1772	1185	901	76%	601
NIASHv2041B21	Aegilops_tauschii_49116	1185	1169	99%	601
NIASHv2041B21	Aegilops_tauschii_937	1185	1482	125%	601
NIASHv2041B21	Aegilops_tauschii_AE1069	1185	1315	111%	601
NIASHv2041B21	Aegilops_tauschii_AE956	1185	1372	116%	601
NIASHv2041B21	Aegilops_umbellulata_AE1070	1185	1216	103%	601
NIASHv2041B21	Aegilops_umbellulata_AE153	1185	1270	107%	601
NIASHv2041B21	Aegilops_umbellulata_AE740	1185	936	79%	601
NIASHv2041B21	Aegilops_umbellulata_AE811	1185	857	72%	601
NIASHv2041B21	Aegilops_uniaristata_AE157	1185	1480	125%	601
NIASHv2041B21	Aegilops_uniaristata_AE680	1185	1341	113%	601
NIASHv2041B21	Aegilops_uniaristata_PI276996	1185	928	78%	601
NIASHv2041B21	Agropyron_cristatum_PI494615	1185	1261	106%	601
NIASHv2041B21	Agropyron_cristatum_PI598631	1185	1349	114%	601
NIASHv2041B21	Amblyopyrum_muticum_PI560122	1185	880	74%	601
NIASHv2041B21	Amblyopyrum_muticum_PI560124	1185	898	76%	601
NIASHv2041B21	Amblyopyrum_muticum_PI560125	1185	882	74%	601
NIASHv2041B21	Amblyopyrum_muticum_PI560126	1185	601	51%	601
NIASHv2041B21	Amblyopyrum_muticum_PI636562	1185	1257	106%	601
NIASHv2041B21	Australopyrum_retrofractum_PI531553	1185	1292	109%	601
NIASHv2041B21	Australopyrum_retrofractum_PI533013	1185	1114	94%	601
NIASHv2041B21	Australopyrum_retrofractum_PI533014	1185	1347	114%	601
NIASHv2041B21	Australopyrum_retrofractum_PI547363	1185	1246	105%	601
NIASHv2041B21	Brachypodium_distachyon	1185	1157	98%	601
NIASHv2041B21	Bromus_tectorum_GRA1085	1185	1036	87%	601
NIASHv2041B21	Dasypyrum_villosum_GRA1020	1185	1210	102%	601
NIASHv2041B21	Dasypyrum_villosum_GRA1027	1185	1277	108%	601
NIASHv2041B21	Dasypyrum_villosum_PI368884	1185	699	59%	601
NIASHv2041B21	Dasypyrum_villosum_W619414	1185	725	61%	601
NIASHv2041B21	Dasypyrum_villosum_W67300	1185	1157	98%	601
NIASHv2041B21	Eremopyrum_distans_PI193264	1185	1388	117%	601
NIASHv2041B21	Eremopyrum_triticeum_GRA2250	1185	1397	118%	601
NIASHv2041B21	Eremopyrum_triticeum_PI502364	1185	1267	107%	601
NIASHv2041B21	Eremopyrum_triticeum_W626631	1185	1206	102%	601
NIASHv2041B21	Henrardia_persica_PI401347	1185	1256	106%	601
NIASHv2041B21	Henrardia_persica_PI577112	1185	1454	123%	601
NIASHv2041B21	Henrardia_persica_PI577113	1185	1095	92%	601
NIASHv2041B21	Henrardia_persica_RF2012	1185	1299	110%	601
NIASHv2041B21	Heteranthelium_piliferum_PI401351	1185	1239	105%	601
NIASHv2041B21	Heteranthelium_piliferum_PI401353	1185	1430	121%	601
NIASHv2041B21	Heteranthelium_piliferum_PI401354	1185	1359	115%	601
NIASHv2041B21	Heteranthelium_sp_PI314152	1185	1159	98%	601
NIASHv2041B21	Hordeum_marinum_BCC2006	1185	1453	123%	601
NIASHv2041B21	Hordeum_marinum_BCC2002	1185	1363	115%	601
NIASHv2041B21	Hordeum_pubiflorum_2028	1185	1643	139%	601
NIASHv2041B21	Hordeum_spontanum_FT11	1185	1746	147%	601
NIASHv2041B21	Hordeum_vulgare_Morex	1185	1769	149%	601
NIASHv2041B21	Psathyrostachys_juncea_PI222050	1185	1266	107%	601
NIASHv2041B21	Psathyrostachys_juncea_PI565077	1185	1117	94%	601
NIASHv2041B21	Psathyrostachys_juncea_PI595135	1185	1280	108%	601
NIASHv2041B21	Psathyrostachys_juncea_PI598613	1185	1271	107%	601
NIASHv2041B21	Psathyrostachys_juncea_PI619487	1185	1376	116%	601
NIASHv2041B21	Psathyrostachys_sp_PI565080	1185	1222	103%	601
NIASHv2041B21	Pseudoroegneria_libanotica_PI228389	1185	925	78%	601
NIASHv2041B21	Pseudoroegneria_libanotica_PI330688	1185	1041	88%	601
NIASHv2041B21	Pseudoroegneria_libanotica_PI401274	1185	1421	120%	601
NIASHv2041B21	Pseudoroegneria_stipifolia_PI325181	1185	1305	110%	601
NIASHv2041B21	Pseudoroegneria_stipifolia_PI440095	1185	1322	112%	601
NIASHv2041B21	Pseudoroegneria_stipifolia_PI531751	1185	1206	102%	601
NIASHv2041B21	Pseudoroegneria_strigosa_PI499638	1185	1144	97%	601
NIASHv2041B21	Pseudoroegneria_strigosa_PI595172	1185	1289	109%	601
NIASHv2041B21	Pseudoroegneria_strigosa_W614049	1185	1347	114%	601
NIASHv2041B21	Pseudoroegneria_strigosa_PI639805	1185	1251	106%	601
NIASHv2041B21	Pseudoroegneria_strigosa_PI639805	1185	1389	117%	601
NIASHv2041B21	Pseudoroegneria_tauri_PI401322	1185	962	81%	601
NIASHv2041B21	Pseudoroegneria_tauri_PI401333	1185	1199	101%	601
NIASHv2041B21	Secale_cereale_PI618662	1185	810	68%	601
NIASHv2041B21	Secale_cereale_PI618665	1185	1196	101%	601
NIASHv2041B21	Secale_cereale_PI618669	1185	1302	110%	601
NIASHv2041B21	Secale_cereale_PI618671	1185	1285	108%	601
NIASHv2041B21	Secale_strictum_R1108	1185	1030	87%	601
NIASHv2041B21	Secale_strictum_R853	1185	1159	98%	601
NIASHv2041B21	Secale_vavilovii_PI253957	1185	501	42%	601
NIASHv2041B21	Secale_vavilovii_R1027	1185	1020	86%	601
NIASHv2041B21	Taeniatherum_caput-medusae_CK2011	1185	1305	110%	601
NIASHv2041B21	Taeniatherum_caput-medusae_GRA1126	1185	1451	122%	601
NIASHv2041B21	Taeniatherum_caput-medusae_PI220589	1185	1317	111%	601
NIASHv2041B21	Taeniatherum_caput-medusae_PI251387	1185	789	67%	601
NIASHv2041B21	Taeniatherum_caput-medusae_PI561095	1185	708	60%	601
NIASHv2041B21	Taeniatherum_crinatum_GRA2570	1185	1270	107%	601
NIASHv2041B21	Thinopyrum_bessarabicum_W621890	1185	985	83%	601
NIASHv2041B21	Thinopyrum_elongatum_PI109452	1185	1264	107%	601

Locus	Accession	Mapped exon length in barley (bp)	Assembled exon length (bp)	% of mapped exon length that could be assembled	Extended target (bp)
NIASHv2041B21	Thinopyrum_elongatum_PI401117	1185	898	76%	601
NIASHv2041B21	Triticum_boeoticum_1613	1185	1555	131%	601
NIASHv2041B21	Triticum_boeoticum_1688	1185	1334	113%	601
NIASHv2041B21	Triticum_boeoticum_ID379	1185	1005	85%	601
NIASHv2041B21	Triticum_boeoticum_PI272520	1185	795	67%	601
NIASHv2041B21	Triticum_boeoticum_PI427451	1185	1346	114%	601
NIASHv2041B21	Triticum_boeoticum_PI427620	1185	1308	110%	601
NIASHv2041B21	Triticum_monococcum_2205	1185	1336	113%	601
NIASHv2041B21	Triticum_monococcum_2208	1185	1410	119%	601
NIASHv2041B21	Triticum_monococcum_2271	1185	1481	125%	601
NIASHv2041B21	Triticum_monococcum_TRI13061	1185	1208	102%	601
NIASHv2041B21	Triticum_monococcum_TRI13612	1185	1261	106%	601
NIASHv2041B21	Triticum_urartu_1307	1185	1471	124%	601
NIASHv2041B21	Triticum_urartu_PI428184	1185	919	78%	601
NIASHv2041B21	Triticum_urartu_PI428317	1185	942	79%	601
NIASHv2041B21	Triticum_urartu_TRI17824	1185	1345	114%	601
NIASHv2041B21	Triticum_urartu_TRI18407	1185	1273	107%	601
NIASHv2044I15	Aegilops_bicornis_AE106	1143	1467	128%	601
NIASHv2044I15	Aegilops_bicornis_AE1079	1143	1213	106%	601
NIASHv2044I15	Aegilops_bicornis_AE788	1143	1469	129%	601
NIASHv2044I15	Aegilops_bicornis_KU-5786	1143	1275	112%	601
NIASHv2044I15	Aegilops_comosa_AE1255	1143	1470	129%	601
NIASHv2044I15	Aegilops_comosa_AE1378	1143	1428	125%	601
NIASHv2044I15	Aegilops_comosa_AE783	1143	1558	136%	601
NIASHv2044I15	Aegilops_comosa_PI276970	1143	1099	96%	601
NIASHv2044I15	Aegilops_longissima_AE1078	1143	1383	121%	601
NIASHv2044I15	Aegilops_longissima_AE133	1143	1367	120%	601
NIASHv2044I15	Aegilops_longissima_AE417	1143	1273	111%	601
NIASHv2044I15	Aegilops_longissima_PI604141	1143	1146	100%	601
NIASHv2044I15	Aegilops_longissima_TA1921	1143	1356	119%	601
NIASHv2044I15	Aegilops_markgrafii_AE1381	1143	1527	134%	601
NIASHv2044I15	Aegilops_markgrafii_KP-2012-106	1143	1525	133%	601
NIASHv2044I15	Aegilops_markgrafii_PI254863	1143	1261	110%	601
NIASHv2044I15	Aegilops_markgrafii_PI542208	1143	1528	134%	601
NIASHv2044I15	Aegilops_markgrafii_PI596287	1143	1505	132%	601
NIASHv2044I15	Aegilops_mutica_01C2100106	1143	1485	130%	601
NIASHv2044I15	Aegilops_searsii_AE1075	1143	1290	113%	601
NIASHv2044I15	Aegilops_searsii_AE1083	1143	1598	140%	601
NIASHv2044I15	Aegilops_searsii_KU-14655	1143	1548	135%	601
NIASHv2044I15	Aegilops_searsii_PI599142	1143	1400	122%	601
NIASHv2044I15	Aegilops_searsii_PI599148	1143	1210	106%	601
NIASHv2044I15	Aegilops_sharonensis_AE90691	1143	1429	125%	601
NIASHv2044I15	Aegilops_speltoides_3776	1143	1648	144%	601
NIASHv2044I15	Aegilops_speltoides_AE1064	1143	1448	127%	601
NIASHv2044I15	Aegilops_speltoides_AE900	1143	1375	120%	601
NIASHv2044I15	Aegilops_speltoides_KU-7856	1143	1362	119%	601
NIASHv2044I15	Aegilops_speltoides_PI486264	1143	1358	119%	601
NIASHv2044I15	Aegilops_speltoides_PI487231	1143	1441	126%	601
NIASHv2044I15	Aegilops_speltoides_TA1772	1143	1227	107%	601
NIASHv2044I15	Aegilops_tauschii_49116	1143	1417	124%	601
NIASHv2044I15	Aegilops_tauschii_937	1143	1680	147%	601
NIASHv2044I15	Aegilops_tauschii_AE1069	1143	1450	127%	601
NIASHv2044I15	Aegilops_tauschii_AE956	1143	1380	121%	601
NIASHv2044I15	Aegilops_umbellulata_AE1070	1143	1441	126%	601
NIASHv2044I15	Aegilops_umbellulata_AE153	1143	1459	128%	601
NIASHv2044I15	Aegilops_umbellulata_AE740	1143	1276	112%	601
NIASHv2044I15	Aegilops_umbellulata_AE811	1143	1216	106%	601
NIASHv2044I15	Aegilops_uniaristata_AE157	1143	1514	132%	601
NIASHv2044I15	Aegilops_uniaristata_AE680	1143	1452	127%	601
NIASHv2044I15	Aegilops_uniaristata_PI276996	1143	1201	105%	601
NIASHv2044I15	Agropyron_cristatum_PI494615	1143	1567	137%	601
NIASHv2044I15	Agropyron_cristatum_PI598631	1143	1361	119%	601
NIASHv2044I15	Amblyopyrum_muticum_PI560122	1143	1171	102%	601
NIASHv2044I15	Amblyopyrum_muticum_PI560124	1143	1172	103%	601
NIASHv2044I15	Amblyopyrum_muticum_PI560125	1143	1159	101%	601
NIASHv2044I15	Amblyopyrum_muticum_PI560126	1143	1186	104%	601
NIASHv2044I15	Amblyopyrum_muticum_PI636562	1143	1386	121%	601
NIASHv2044I15	Australopyrum_retrofractum_PI531553	1143	1445	126%	601
NIASHv2044I15	Australopyrum_retrofractum_PI533013	1143	1405	123%	601
NIASHv2044I15	Australopyrum_retrofractum_PI533014	1143	1534	134%	601
NIASHv2044I15	Australopyrum_retrofractum_PI547363	1143	1559	136%	601
NIASHv2044I15	Brachypodium_distachyon	1143	1103	97%	601
NIASHv2044I15	Bromus_tectorum_GRA1085	1143	1352	118%	601
NIASHv2044I15	Dasyphyrum_villosum_GRA1020	1143	1322	116%	601
NIASHv2044I15	Dasyphyrum_villosum_GRA1027	1143	1316	115%	601
NIASHv2044I15	Dasyphyrum_villosum_PI368884	1143	1135	99%	601
NIASHv2044I15	Dasyphyrum_villosum_W619414	1143	1214	106%	601
NIASHv2044I15	Dasyphyrum_villosum_W67300	1143	1357	119%	601
NIASHv2044I15	Eremopyrum_distans_PI193264	1143	1471	129%	601
NIASHv2044I15	Eremopyrum_triticeum_GRA2250	1143	1434	125%	601
NIASHv2044I15	Eremopyrum_triticeum_PI502364	1143	1322	116%	601
NIASHv2044I15	Eremopyrum_triticeum_W626631	1143	1346	118%	601
NIASHv2044I15	Henrardia_persica_PI401347	1143	1502	131%	601
NIASHv2044I15	Henrardia_persica_PI577112	1143	1447	127%	601
NIASHv2044I15	Henrardia_persica_PI577113	1143	1260	110%	601
NIASHv2044I15	Henrardia_persica_RF2012	1143	1545	135%	601

Locus	Accession	Mapped exon length in barley (bp)	Assembled exon length (bp)	% of mapped exon length that could be assembled	Extended target (bp)
NIASHv2044i15	Heteranthelium_piliferum_PI401351	1143	1378	121%	601
NIASHv2044i15	Heteranthelium_piliferum_PI401353	1143	1537	134%	601
NIASHv2044i15	Heteranthelium_piliferum_PI401354	1143	1528	134%	601
NIASHv2044i15	Heteranthelium_sp._PI314152	1143	1352	118%	601
NIASHv2044i15	Hordeum_marinum_BCC2006	1143	1537	134%	601
NIASHv2044i15	Hordeum_murinum_BCC2002	1143	1626	142%	601
NIASHv2044i15	Hordeum_pubiflorum_2028	1143	1702	149%	601
NIASHv2044i15	Hordeum_spontaneum_FT11	1143	1744	153%	601
NIASHv2044i15	Hordeum_vulgare_Morex	1143	1744	153%	601
NIASHv2044i15	Psathyrostachys_juncea_PI222050	1143	1378	121%	601
NIASHv2044i15	Psathyrostachys_juncea_PI565077	1143	1433	125%	601
NIASHv2044i15	Psathyrostachys_juncea_PI595135	1143	1572	138%	601
NIASHv2044i15	Psathyrostachys_juncea_PI598613	1143	1503	131%	601
NIASHv2044i15	Psathyrostachys_juncea_PI619487	1143	1535	134%	601
NIASHv2044i15	Psathyrostachys_sp._PI565080	1143	1420	124%	601
NIASHv2044i15	Pseudoroegneria_libanotica_PI228389	1143	1244	109%	601
NIASHv2044i15	Pseudoroegneria_libanotica_PI330688	1143	1396	122%	601
NIASHv2044i15	Pseudoroegneria_libanotica_PI401274	1143	1468	128%	601
NIASHv2044i15	Pseudoroegneria_stipifolia_PI325181	1143	1410	123%	601
NIASHv2044i15	Pseudoroegneria_stipifolia_PI440095	1143	1359	119%	601
NIASHv2044i15	Pseudoroegneria_stipifolia_PI531751	1143	1399	122%	601
NIASHv2044i15	Pseudoroegneria_strigosa_PI499638	1143	1276	112%	601
NIASHv2044i15	Pseudoroegneria_strigosa_PI595172	1143	1395	122%	601
NIASHv2044i15	Pseudoroegneria_strigosa_W614049	1143	1505	132%	601
NIASHv2044i15	Pseudoroegneria_strigosa_PI639805	1143	1354	118%	601
NIASHv2044i15	Pseudoroegneria_strigosa_PI639805	1143	1525	133%	601
NIASHv2044i15	Pseudoroegneria_tauri_PI401322	1143	1268	111%	601
NIASHv2044i15	Pseudoroegneria_tauri_PI401333	1143	1369	120%	601
NIASHv2044i15	Secale_cereale_PI618662	1143	1125	98%	601
NIASHv2044i15	Secale_cereale_PI618665	1143	1352	118%	601
NIASHv2044i15	Secale_cereale_PI618669	1143	1382	121%	601
NIASHv2044i15	Secale_cereale_PI618671	1143	1323	116%	601
NIASHv2044i15	Secale_strictum_R1108	1143	1203	105%	601
NIASHv2044i15	Secale_strictum_R853	1143	1222	107%	601
NIASHv2044i15	Secale_vavilovii_PI253957	1143	1035	91%	601
NIASHv2044i15	Secale_vavilovii_R1027	1143	1138	100%	601
NIASHv2044i15	Taeniatherum_caput-medusae_CK2011	1143	1486	130%	601
NIASHv2044i15	Taeniatherum_caput-medusae_GRA1126	1143	1572	138%	601
NIASHv2044i15	Taeniatherum_caput-medusae_PI220589	1143	1551	136%	601
NIASHv2044i15	Taeniatherum_caput-medusae_PI251387	1143	1403	123%	601
NIASHv2044i15	Taeniatherum_caput-medusae_PI561095	1143	1259	110%	601
NIASHv2044i15	Taeniatherum_crinittum_GRA2570	1143	1478	129%	601
NIASHv2044i15	Thinopyrum_bessarabicum_W621890	1143	1284	112%	601
NIASHv2044i15	Thinopyrum_elongatum_PI109452	1143	1480	129%	601
NIASHv2044i15	Thinopyrum_elongatum_PI401117	1143	1214	106%	601
NIASHv2044i15	Triticum_boeoticum_1613	1143	1664	146%	601
NIASHv2044i15	Triticum_boeoticum_1688	1143	1534	134%	601
NIASHv2044i15	Triticum_boeoticum_ID379	1143	1298	114%	601
NIASHv2044i15	Triticum_boeoticum_PI272520	1143	1309	115%	601
NIASHv2044i15	Triticum_boeoticum_PI427451	1143	1474	129%	601
NIASHv2044i15	Triticum_boeoticum_PI427620	1143	1457	127%	601
NIASHv2044i15	Triticum_monococcum_2205	1143	1553	136%	601
NIASHv2044i15	Triticum_monococcum_2208	1143	1547	135%	601
NIASHv2044i15	Triticum_monococcum_2271	1143	1672	146%	601
NIASHv2044i15	Triticum_monococcum_TRI13061	1143	1479	129%	601
NIASHv2044i15	Triticum_monococcum_TRI13612	1143	1562	137%	601
NIASHv2044i15	Triticum_urartu_1307	1143	1468	128%	601
NIASHv2044i15	Triticum_urartu_PI428184	1143	1289	113%	601
NIASHv2044i15	Triticum_urartu_PI428317	1143	1275	112%	601
NIASHv2044i15	Triticum_urartu_TRI17824	1143	1393	122%	601
NIASHv2044i15	Triticum_urartu_TRI18407	1143	1474	129%	601
NIASHv2058P13	Aegilops_bicornis_AE106	1116	930	83%	601
NIASHv2058P13	Aegilops_bicornis_AE1079	1116	394	35%	601
NIASHv2058P13	Aegilops_bicornis_AE788	1116	871	78%	601
NIASHv2058P13	Aegilops_bicornis_KU-5786	1116	294	26%	601
NIASHv2058P13	Aegilops_comosa_AE1255	1116	1013	91%	601
NIASHv2058P13	Aegilops_comosa_AE1378	1116	790	71%	601
NIASHv2058P13	Aegilops_comosa_AE783	1116	923	83%	601
NIASHv2058P13	Aegilops_comosa_PI276970	1116	662	59%	601
NIASHv2058P13	Aegilops_longissima_AE1078	1116	616	55%	601
NIASHv2058P13	Aegilops_longissima_AE133	1116	918	82%	601
NIASHv2058P13	Aegilops_longissima_AE417	1116	532	48%	601
NIASHv2058P13	Aegilops_longissima_PI604141	1116	254	23%	601
NIASHv2058P13	Aegilops_longissima_TA1921	1116	774	69%	601
NIASHv2058P13	Aegilops_markgrafii_AE1381	1116	1009	90%	601
NIASHv2058P13	Aegilops_markgrafii_KP-2012-106	1116	708	63%	601
NIASHv2058P13	Aegilops_markgrafii_PI254863	1116	242	22%	601
NIASHv2058P13	Aegilops_markgrafii_PI542208	1116	970	87%	601
NIASHv2058P13	Aegilops_markgrafii_PI596287	1116	922	83%	601
NIASHv2058P13	Aegilops_mutica_01C2100106	1116	1006	90%	601
NIASHv2058P13	Aegilops_searsii_AE1075	1116	843	76%	601
NIASHv2058P13	Aegilops_searsii_AE1083	1116	1018	91%	601
NIASHv2058P13	Aegilops_searsii_KU-14655	1116	978	88%	601
NIASHv2058P13	Aegilops_searsii_PI599142	1116	793	71%	601
NIASHv2058P13	Aegilops_searsii_PI599148	1116	431	39%	601
NIASHv2058P13	Aegilops_sharonensis_AE90691	1116	924	83%	601

Locus	Accession	Mapped exon length in barley (bp)	Assembled exon length (bp)	% of mapped exon length that could be assembled	Extended target (bp)
NIASHv2058P13	Aegilops_speltooides_3776	1116	1145	103%	601
NIASHv2058P13	Aegilops_speltooides_AE1064	1116	844	76%	601
NIASHv2058P13	Aegilops_speltooides_AE900	1116	892	80%	601
NIASHv2058P13	Aegilops_speltooides_KU-7856	1116	392	35%	601
NIASHv2058P13	Aegilops_speltooides_PI486264	1116	876	78%	601
NIASHv2058P13	Aegilops_speltooides_PI487231	1116	949	85%	601
NIASHv2058P13	Aegilops_speltooides_TA1772	1116	387	35%	601
NIASHv2058P13	Aegilops_tauschii_49116	1116	602	54%	601
NIASHv2058P13	Aegilops_tauschii_937	1116	1202	108%	601
NIASHv2058P13	Aegilops_tauschii_AE1069	1116	805	72%	601
NIASHv2058P13	Aegilops_tauschii_AE956	1116	853	76%	601
NIASHv2058P13	Aegilops_umbellulata_AE1070	1116	921	83%	601
NIASHv2058P13	Aegilops_umbellulata_AE153	1116	880	79%	601
NIASHv2058P13	Aegilops_umbellulata_AE740	1116	538	48%	601
NIASHv2058P13	Aegilops_umbellulata_AE811	1116	10	1%	601
NIASHv2058P13	Aegilops_uniaristata_AE157	1116	1001	90%	601
NIASHv2058P13	Aegilops_uniaristata_AE680	1116	948	85%	601
NIASHv2058P13	Aegilops_uniaristata_PI276996	1116	640	57%	601
NIASHv2058P13	Agropyron_cristatum_PI494615	1116	837	75%	601
NIASHv2058P13	Agropyron_cristatum_PI598631	1116	805	72%	601
NIASHv2058P13	Amblyopyrum_muticum_PI560122	1116	490	44%	601
NIASHv2058P13	Amblyopyrum_muticum_PI560124	1116	445	40%	601
NIASHv2058P13	Amblyopyrum_muticum_PI560125	1116	312	28%	601
NIASHv2058P13	Amblyopyrum_muticum_PI560126	1116	300	27%	601
NIASHv2058P13	Amblyopyrum_muticum_PI636562	1116	869	78%	601
NIASHv2058P13	Australopyrum_retrofractum_PI531553	1116	793	71%	601
NIASHv2058P13	Australopyrum_retrofractum_PI533013	1116	606	54%	601
NIASHv2058P13	Australopyrum_retrofractum_PI533014	1116	965	86%	601
NIASHv2058P13	Australopyrum_retrofractum_PI547363	1116	901	81%	601
NIASHv2058P13	Brachypodium_distachyon	1116	839	75%	601
NIASHv2058P13	Bromus_tectorum_GRA1085	1116	777	70%	601
NIASHv2058P13	Dasypyrum_villosum_GRA1020	1116	761	68%	601
NIASHv2058P13	Dasypyrum_villosum_GRA1027	1116	833	75%	601
NIASHv2058P13	Dasypyrum_villosum_PI368884	1116	418	37%	601
NIASHv2058P13	Dasypyrum_villosum_W619414	1116	348	31%	601
NIASHv2058P13	Dasypyrum_villosum_W67300	1116	879	79%	601
NIASHv2058P13	Eremopyrum_distans_PI193264	1116	834	75%	601
NIASHv2058P13	Eremopyrum_triticeum_GRA2250	1116	802	72%	601
NIASHv2058P13	Eremopyrum_triticeum_PI502364	1116	876	78%	601
NIASHv2058P13	Eremopyrum_triticeum_W626631	1116	830	74%	601
NIASHv2058P13	Henrardia_persica_PI401347	1116	997	89%	601
NIASHv2058P13	Henrardia_persica_PI577112	1116	993	89%	601
NIASHv2058P13	Henrardia_persica_PI577113	1116	908	81%	601
NIASHv2058P13	Henrardia_persica_RF2012	1116	895	80%	601
NIASHv2058P13	Heteranthelium_piliferum_PI401351	1116	874	78%	601
NIASHv2058P13	Heteranthelium_piliferum_PI401353	1116	937	84%	601
NIASHv2058P13	Heteranthelium_piliferum_PI401354	1116	947	85%	601
NIASHv2058P13	Heteranthelium_sp_PI314152	1116	699	63%	601
NIASHv2058P13	Hordeum_marinum_BCC2006	1116	987	88%	601
NIASHv2058P13	Hordeum_murinum_BCC2002	1116	992	89%	601
NIASHv2058P13	Hordeum_pubiflorum_2028	1116	1159	104%	601
NIASHv2058P13	Hordeum_spontaneum_FT11	1116	1374	123%	601
NIASHv2058P13	Hordeum_vulgare_Morex	1116	1363	122%	601
NIASHv2058P13	Psathyrostachys_juncea_PI222050	1116	815	73%	601
NIASHv2058P13	Psathyrostachys_juncea_PI565077	1116	112	10%	601
NIASHv2058P13	Psathyrostachys_juncea_PI595135	1116	864	77%	601
NIASHv2058P13	Psathyrostachys_juncea_PI598613	1116	908	81%	601
NIASHv2058P13	Psathyrostachys_juncea_PI619487	1116	912	82%	601
NIASHv2058P13	Psathyrostachys_sp_PI565080	1116	800	72%	601
NIASHv2058P13	Pseudoroegneria_libanotica_PI228389	1116	494	44%	601
NIASHv2058P13	Pseudoroegneria_libanotica_PI330688	1116	786	70%	601
NIASHv2058P13	Pseudoroegneria_libanotica_PI401274	1116	789	71%	601
NIASHv2058P13	Pseudoroegneria_stipifolia_PI325181	1116	959	86%	601
NIASHv2058P13	Pseudoroegneria_stipifolia_PI440095	1116	962	86%	601
NIASHv2058P13	Pseudoroegneria_stipifolia_PI531751	1116	922	83%	601
NIASHv2058P13	Pseudoroegneria_strigosa_PI499638	1116	824	74%	601
NIASHv2058P13	Pseudoroegneria_strigosa_PI595172	1116	929	83%	601
NIASHv2058P13	Pseudoroegneria_strigosa_W614049	1116	880	79%	601
NIASHv2058P13	Pseudoroegneria_strigosa_PI639805	1116	840	75%	601
NIASHv2058P13	Pseudoroegneria_strigosa_PI639805	1116	934	84%	601
NIASHv2058P13	Pseudoroegneria_tauri_PI401322	1116	705	63%	601
NIASHv2058P13	Pseudoroegneria_tauri_PI401333	1116	889	80%	601
NIASHv2058P13	Secale_cereale_PI618662	1116	444	40%	601
NIASHv2058P13	Secale_cereale_PI618665	1116	782	70%	601
NIASHv2058P13	Secale_cereale_PI618669	1116	862	77%	601
NIASHv2058P13	Secale_cereale_PI618671	1116	845	76%	601
NIASHv2058P13	Secale_strictum_R1108	1116	694	62%	601
NIASHv2058P13	Secale_strictum_R853	1116	882	79%	601
NIASHv2058P13	Secale_vavilovii_PI253957	1116	49	4%	601
NIASHv2058P13	Secale_vavilovii_R1027	1116	720	65%	601
NIASHv2058P13	Taeniatherum_caput-medusae_CK2011	1116	890	80%	601
NIASHv2058P13	Taeniatherum_caput-medusae_GRA1126	1116	918	82%	601
NIASHv2058P13	Taeniatherum_caput-medusae_PI220589	1116	838	75%	601
NIASHv2058P13	Taeniatherum_caput-medusae_PI251387	1116	601	54%	601
NIASHv2058P13	Taeniatherum_caput-medusae_PI561095	1116	228	20%	601
NIASHv2058P13	Taeniatherum_crinutum_GRA2570	1116	962	86%	601

Locus	Accession	Mapped exon length in barley (bp)	Assembled exon length (bp)	% of mapped exon length that could be assembled	Extended target (bp)
NIASHv2058P13	Thinopyrum_bessarabicum_W621890	1116	785	70%	601
NIASHv2058P13	Thinopyrum_elongatum_P1109452	1116	936	84%	601
NIASHv2058P13	Thinopyrum_elongatum_P1401117	1116	419	38%	601
NIASHv2058P13	Triticum_boeoticum_1613	1116	1082	97%	601
NIASHv2058P13	Triticum_boeoticum_1688	1116	956	86%	601
NIASHv2058P13	Triticum_boeoticum_ID379	1116	608	54%	601
NIASHv2058P13	Triticum_boeoticum_PI272520	1116	736	66%	601
NIASHv2058P13	Triticum_boeoticum_PI427451	1116	937	84%	601
NIASHv2058P13	Triticum_boeoticum_PI427620	1116	822	74%	601
NIASHv2058P13	Triticum_monococcum_2205	1116	945	85%	601
NIASHv2058P13	Triticum_monococcum_2208	1116	933	84%	601
NIASHv2058P13	Triticum_monococcum_2271	1116	1042	93%	601
NIASHv2058P13	Triticum_monococcum_TR113061	1116	825	74%	601
NIASHv2058P13	Triticum_monococcum_TR113612	1116	859	77%	601
NIASHv2058P13	Triticum_urartu_1307	1116	1193	107%	601
NIASHv2058P13	Triticum_urartu_PI428184	1116	512	46%	601
NIASHv2058P13	Triticum_urartu_PI428317	1116	484	43%	601
NIASHv2058P13	Triticum_urartu_TR117824	1116	959	86%	601
NIASHv2058P13	Triticum_urartu_TR118407	1116	850	76%	601
NIASHv2082K16	Aegilops_bicornis_AE106	2754	2675	97%	601
NIASHv2082K16	Aegilops_bicornis_AE1079	2754	2162	79%	601
NIASHv2082K16	Aegilops_bicornis_AE788	2754	2537	92%	601
NIASHv2082K16	Aegilops_bicornis_KU-5786	2754	1980	72%	601
NIASHv2082K16	Aegilops_comosa_AE1255	2754	2799	102%	601
NIASHv2082K16	Aegilops_comosa_AE1378	2754	2482	90%	601
NIASHv2082K16	Aegilops_comosa_AE783	2754	2721	99%	601
NIASHv2082K16	Aegilops_comosa_PI276970	2754	2483	90%	601
NIASHv2082K16	Aegilops_longissima_AE1078	2754	2365	86%	601
NIASHv2082K16	Aegilops_longissima_AE133	2754	2424	88%	601
NIASHv2082K16	Aegilops_longissima_AE417	2754	2099	76%	601
NIASHv2082K16	Aegilops_longissima_PI604141	2754	1982	72%	601
NIASHv2082K16	Aegilops_longissima_TA1921	2754	2507	91%	601
NIASHv2082K16	Aegilops_markgrafii_AE1381	2754	2834	103%	601
NIASHv2082K16	Aegilops_markgrafii_KP-2012-106	2754	2730	99%	601
NIASHv2082K16	Aegilops_markgrafii_PI254863	2754	2603	95%	601
NIASHv2082K16	Aegilops_markgrafii_PI542208	2754	2645	96%	601
NIASHv2082K16	Aegilops_markgrafii_PI596287	2754	2792	101%	601
NIASHv2082K16	Aegilops_mutica_01C2100106	2754	2737	99%	601
NIASHv2082K16	Aegilops_searsii_AE1075	2754	2412	88%	601
NIASHv2082K16	Aegilops_searsii_AE1083	2754	2790	101%	601
NIASHv2082K16	Aegilops_searsii_KU-14655	2754	2749	100%	601
NIASHv2082K16	Aegilops_searsii_PI599142	2754	2397	87%	601
NIASHv2082K16	Aegilops_searsii_PI599148	2754	1811	66%	601
NIASHv2082K16	Aegilops_sharonensis_AE90691	2754	2600	94%	601
NIASHv2082K16	Aegilops_speltoides_3776	2754	2908	106%	601
NIASHv2082K16	Aegilops_speltoides_AE1064	2754	2683	97%	601
NIASHv2082K16	Aegilops_speltoides_AE900	2754	2464	89%	601
NIASHv2082K16	Aegilops_speltoides_KU-7856	2754	2058	75%	601
NIASHv2082K16	Aegilops_speltoides_PI486264	2754	2894	105%	601
NIASHv2082K16	Aegilops_speltoides_PI487231	2754	2722	99%	601
NIASHv2082K16	Aegilops_speltoides_TA1772	2754	2166	79%	601
NIASHv2082K16	Aegilops_tauschii_49116	2754	2426	88%	601
NIASHv2082K16	Aegilops_tauschii_937	2754	2900	105%	601
NIASHv2082K16	Aegilops_tauschii_AE1069	2754	2452	89%	601
NIASHv2082K16	Aegilops_tauschii_AE956	2754	2569	93%	601
NIASHv2082K16	Aegilops_umbellulata_AE1070	2754	2601	94%	601
NIASHv2082K16	Aegilops_umbellulata_AE153	2754	2702	98%	601
NIASHv2082K16	Aegilops_umbellulata_AE740	2754	2355	86%	601
NIASHv2082K16	Aegilops_umbellulata_AE811	2754	2131	77%	601
NIASHv2082K16	Aegilops_uniaristata_AE157	2754	2726	99%	601
NIASHv2082K16	Aegilops_uniaristata_AE680	2754	2751	100%	601
NIASHv2082K16	Aegilops_uniaristata_PI276996	2754	2489	90%	601
NIASHv2082K16	Agropyron_cristatum_PI494615	2754	2812	102%	601
NIASHv2082K16	Agropyron_cristatum_PI598631	2754	2766	100%	601
NIASHv2082K16	Amblyopyrum_muticum_PI560122	2754	2009	73%	601
NIASHv2082K16	Amblyopyrum_muticum_PI560124	2754	1911	69%	601
NIASHv2082K16	Amblyopyrum_muticum_PI560125	2754	1735	63%	601
NIASHv2082K16	Amblyopyrum_muticum_PI560126	2754	1822	66%	601
NIASHv2082K16	Amblyopyrum_muticum_PI636562	2754	2577	94%	601
NIASHv2082K16	Australopyrum_retrofractum_PI531553	2754	2515	91%	601
NIASHv2082K16	Australopyrum_retrofractum_PI533013	2754	2443	89%	601
NIASHv2082K16	Australopyrum_retrofractum_PI533014	2754	2899	105%	601
NIASHv2082K16	Australopyrum_retrofractum_PI547363	2754	2686	98%	601
NIASHv2082K16	Brachypodium_distachyon	2754	2272	82%	601
NIASHv2082K16	Bromus_tectorum_GRA1085	2754	2221	81%	601
NIASHv2082K16	Dasyphyrum_villosum_GRA1020	2754	2492	90%	601
NIASHv2082K16	Dasyphyrum_villosum_GRA1027	2754	2540	92%	601
NIASHv2082K16	Dasyphyrum_villosum_PI368884	2754	1828	66%	601
NIASHv2082K16	Dasyphyrum_villosum_W619414	2754	2416	88%	601
NIASHv2082K16	Dasyphyrum_villosum_W67300	2754	2753	100%	601
NIASHv2082K16	Eremopyrum_distans_PI193264	2754	2567	93%	601
NIASHv2082K16	Eremopyrum_triticeum_GRA2250	2754	2920	106%	601
NIASHv2082K16	Eremopyrum_triticeum_PI502364	2754	2655	96%	601
NIASHv2082K16	Eremopyrum_triticeum_W626631	2754	2736	99%	601
NIASHv2082K16	Henrardia_persica_PI401347	2754	2737	99%	601
NIASHv2082K16	Henrardia_persica_PI577112	2754	2811	102%	601

Locus	Accession	Mapped exon length in barley (bp)	Assembled exon length (bp)	% of mapped exon length that could be assembled	Extended target (bp)
NIASHv2082K16	Henrardia_persica_PI577113	2754	2443	89%	601
NIASHv2082K16	Henrardia_persica_RF2012	2754	2861	104%	601
NIASHv2082K16	Heterantherium_piliferum_PI401351	2754	2810	102%	601
NIASHv2082K16	Heterantherium_piliferum_PI401353	2754	2881	105%	601
NIASHv2082K16	Heterantherium_piliferum_PI401354	2754	2953	107%	601
NIASHv2082K16	Heterantherium_sp_PI314152	2754	2649	96%	601
NIASHv2082K16	Hordeum_marinum_BCC2006	2754	2984	108%	601
NIASHv2082K16	Hordeum_murinum_BCC2002	2754	2783	101%	601
NIASHv2082K16	Hordeum_pubiflorum_2028	2754	3121	113%	601
NIASHv2082K16	Hordeum_spontaneum_FT11	2754	3234	117%	601
NIASHv2082K16	Hordeum_vulgare_Morex	2754	3266	119%	601
NIASHv2082K16	Psathyrostachys_juncea_PI222050	2754	2819	102%	601
NIASHv2082K16	Psathyrostachys_juncea_PI565077	2754	2522	92%	601
NIASHv2082K16	Psathyrostachys_juncea_PI595135	2754	2992	109%	601
NIASHv2082K16	Psathyrostachys_juncea_PI598613	2754	2907	106%	601
NIASHv2082K16	Psathyrostachys_juncea_PI619487	2754	2866	104%	601
NIASHv2082K16	Psathyrostachys_sp_PI565080	2754	2733	99%	601
NIASHv2082K16	Pseudoroegneria_libanotica_PI228389	2754	2590	94%	601
NIASHv2082K16	Pseudoroegneria_libanotica_PI306688	2754	2686	98%	601
NIASHv2082K16	Pseudoroegneria_libanotica_PI401274	2754	2720	99%	601
NIASHv2082K16	Pseudoroegneria_stipifolia_PI325181	2754	2820	102%	601
NIASHv2082K16	Pseudoroegneria_stipifolia_PI440095	2754	2858	104%	601
NIASHv2082K16	Pseudoroegneria_stipifolia_PI531751	2754	2596	94%	601
NIASHv2082K16	Pseudoroegneria_strigosa_PI499638	2754	2580	94%	601
NIASHv2082K16	Pseudoroegneria_strigosa_PI595172	2754	2617	95%	601
NIASHv2082K16	Pseudoroegneria_strigosa_W614049	2754	2831	103%	601
NIASHv2082K16	Pseudoroegneria_strigosa_PI639805	2754	2733	99%	601
NIASHv2082K16	Pseudoroegneria_strigosa_PI639805	2754	2666	97%	601
NIASHv2082K16	Pseudoroegneria_tauri_PI401322	2754	2498	91%	601
NIASHv2082K16	Pseudoroegneria_tauri_PI401333	2754	2753	100%	601
NIASHv2082K16	Secale_cereale_PI618662	2754	2239	81%	601
NIASHv2082K16	Secale_cereale_PI618665	2754	2698	98%	601
NIASHv2082K16	Secale_cereale_PI618669	2754	2875	104%	601
NIASHv2082K16	Secale_cereale_PI618671	2754	2854	104%	601
NIASHv2082K16	Secale_strictum_R1108	2754	2412	88%	601
NIASHv2082K16	Secale_strictum_R853	2754	2770	101%	601
NIASHv2082K16	Secale_vavilovii_PI253957	2754	2105	76%	601
NIASHv2082K16	Secale_vavilovii_R1027	2754	2577	94%	601
NIASHv2082K16	Taeniatherum_caput-medusae_CK2011	2754	2754	100%	601
NIASHv2082K16	Taeniatherum_caput-medusae_GRA1126	2754	2688	98%	601
NIASHv2082K16	Taeniatherum_caput-medusae_PI220589	2754	2836	103%	601
NIASHv2082K16	Taeniatherum_caput-medusae_PI251387	2754	2333	85%	601
NIASHv2082K16	Taeniatherum_caput-medusae_PI561095	2754	1955	71%	601
NIASHv2082K16	Taeniatherum_crinatum_GRA2570	2754	2756	100%	601
NIASHv2082K16	Thinopyrum_bessarabicum_W621890	2754	2559	93%	601
NIASHv2082K16	Thinopyrum_elongatum_PI109452	2754	2797	102%	601
NIASHv2082K16	Thinopyrum_elongatum_PI401117	2754	2179	79%	601
NIASHv2082K16	Triticum_boeoticum_1613	2754	2872	104%	601
NIASHv2082K16	Triticum_boeoticum_1688	2754	2695	98%	601
NIASHv2082K16	Triticum_boeoticum_ID379	2754	2273	83%	601
NIASHv2082K16	Triticum_boeoticum_PI272520	2754	2322	84%	601
NIASHv2082K16	Triticum_boeoticum_PI427451	2754	2723	99%	601
NIASHv2082K16	Triticum_boeoticum_PI427620	2754	2809	102%	601
NIASHv2082K16	Triticum_monococcum_2205	2754	2693	98%	601
NIASHv2082K16	Triticum_monococcum_2208	2754	2702	98%	601
NIASHv2082K16	Triticum_monococcum_2271	2754	2866	104%	601
NIASHv2082K16	Triticum_monococcum_TRI13061	2754	2687	98%	601
NIASHv2082K16	Triticum_monococcum_TRI13612	2754	2777	101%	601
NIASHv2082K16	Triticum_urartu_1307	2754	2949	107%	601
NIASHv2082K16	Triticum_urartu_PI428184	2754	2194	80%	601
NIASHv2082K16	Triticum_urartu_PI428317	2754	2169	79%	601
NIASHv2082K16	Triticum_urartu_TRI17824	2754	2814	102%	601
NIASHv2082K16	Triticum_urartu_TRI18407	2754	2744	100%	601
NIASHv2082M12	Aegilops_bicornis_AE106	1730	1894	109%	601
NIASHv2082M12	Aegilops_bicornis_AE1079	1730	1327	77%	601
NIASHv2082M12	Aegilops_bicornis_AE788	1730	1798	104%	601
NIASHv2082M12	Aegilops_bicornis_KU-5786	1730	1273	74%	601
NIASHv2082M12	Aegilops_comosa_AE1255	1730	1746	101%	601
NIASHv2082M12	Aegilops_comosa_AE1378	1730	1594	92%	601
NIASHv2082M12	Aegilops_comosa_AE783	1730	1709	99%	601
NIASHv2082M12	Aegilops_comosa_PI276970	1730	1492	86%	601
NIASHv2082M12	Aegilops_longissima_AE1078	1730	1431	83%	601
NIASHv2082M12	Aegilops_longissima_AE133	1730	1761	102%	601
NIASHv2082M12	Aegilops_longissima_AE417	1730	1433	83%	601
NIASHv2082M12	Aegilops_longissima_PI604141	1730	1301	75%	601
NIASHv2082M12	Aegilops_longissima_TA1921	1730	1817	105%	601
NIASHv2082M12	Aegilops_markgrafii_AE1381	1730	1742	101%	601
NIASHv2082M12	Aegilops_markgrafii_KP-2012-106	1730	1780	103%	601
NIASHv2082M12	Aegilops_markgrafii_PI254863	1730	1406	81%	601
NIASHv2082M12	Aegilops_markgrafii_PI542208	1730	1742	101%	601
NIASHv2082M12	Aegilops_markgrafii_PI596287	1730	1870	108%	601
NIASHv2082M12	Aegilops_mutica_01C2100106	1730	1732	100%	601
NIASHv2082M12	Aegilops_searsii_AE1075	1730	1389	80%	601
NIASHv2082M12	Aegilops_searsii_AE1083	1730	1899	110%	601
NIASHv2082M12	Aegilops_searsii_KU-14655	1730	1782	103%	601
NIASHv2082M12	Aegilops_searsii_PI599142	1730	1567	91%	601

Locus	Accession	Mapped exon length in barley (bp)	Assembled exon length (bp)	% of mapped exon length that could be assembled	Extended target (bp)
NIASHv2082M12	Aegilops_searsii_P1599148	1730	1208	70%	601
NIASHv2082M12	Aegilops_sharonensis_AE90691	1730	1877	108%	601
NIASHv2082M12	Aegilops_speltoides_3776	1730	1922	111%	601
NIASHv2082M12	Aegilops_speltoides_AE1064	1730	1611	93%	601
NIASHv2082M12	Aegilops_speltoides_AE900	1730	1809	105%	601
NIASHv2082M12	Aegilops_speltoides_KU-7856	1730	1372	79%	601
NIASHv2082M12	Aegilops_speltoides_PI486264	1730	1831	106%	601
NIASHv2082M12	Aegilops_speltoides_PI487231	1730	1795	104%	601
NIASHv2082M12	Aegilops_speltoides_TA1772	1730	1438	83%	601
NIASHv2082M12	Aegilops_tauschii_49116	1730	1556	90%	601
NIASHv2082M12	Aegilops_tauschii_937	1730	1954	113%	601
NIASHv2082M12	Aegilops_tauschii_AE1069	1730	1663	96%	601
NIASHv2082M12	Aegilops_tauschii_AE956	1730	1824	105%	601
NIASHv2082M12	Aegilops_umbellulata_AE1070	1730	1566	91%	601
NIASHv2082M12	Aegilops_umbellulata_AE153	1730	1745	101%	601
NIASHv2082M12	Aegilops_umbellulata_AE740	1730	1268	73%	601
NIASHv2082M12	Aegilops_umbellulata_AE811	1730	1166	67%	601
NIASHv2082M12	Aegilops_uniaristata_AE157	1730	1858	107%	601
NIASHv2082M12	Aegilops_uniaristata_AE680	1730	1772	102%	601
NIASHv2082M12	Aegilops_uniaristata_PI276996	1730	1173	68%	601
NIASHv2082M12	Agropyron_cristatum_PI494615	1730	1833	106%	601
NIASHv2082M12	Agropyron_cristatum_PI598631	1730	1810	105%	601
NIASHv2082M12	Amblyopyrum_muticum_PI560122	1730	1156	67%	601
NIASHv2082M12	Amblyopyrum_muticum_PI560124	1730	1336	77%	601
NIASHv2082M12	Amblyopyrum_muticum_PI560125	1730	1219	70%	601
NIASHv2082M12	Amblyopyrum_muticum_PI560126	1730	1073	62%	601
NIASHv2082M12	Amblyopyrum_muticum_PI636562	1730	1685	97%	601
NIASHv2082M12	Australopyrum_retrofractum_PI531553	1730	1532	89%	601
NIASHv2082M12	Australopyrum_retrofractum_PI533013	1730	1337	77%	601
NIASHv2082M12	Australopyrum_retrofractum_PI533014	1730	1812	105%	601
NIASHv2082M12	Australopyrum_retrofractum_PI547363	1730	1834	106%	601
NIASHv2082M12	Brachypodium_distachyon	1730	1562	90%	601
NIASHv2082M12	Bromus_tectorum_GRA1085	1730	1608	93%	601
NIASHv2082M12	Dasypyrum_villosum_GRA1020	1730	1810	105%	601
NIASHv2082M12	Dasypyrum_villosum_GRA1027	1730	1821	105%	601
NIASHv2082M12	Dasypyrum_villosum_PI368884	1730	1247	72%	601
NIASHv2082M12	Dasypyrum_villosum_W619414	1730	1004	58%	601
NIASHv2082M12	Dasypyrum_villosum_W67300	1730	1605	93%	601
NIASHv2082M12	Eremopyrum_distans_PI193264	1730	1763	102%	601
NIASHv2082M12	Eremopyrum_triticeum_GRA2250	1730	1652	95%	601
NIASHv2082M12	Eremopyrum_triticeum_PI502364	1730	1576	91%	601
NIASHv2082M12	Eremopyrum_triticeum_W626631	1730	1460	84%	601
NIASHv2082M12	Henrardia_persica_PI401347	1730	1716	99%	601
NIASHv2082M12	Henrardia_persica_PI577112	1730	1833	106%	601
NIASHv2082M12	Henrardia_persica_PI577113	1730	1805	104%	601
NIASHv2082M12	Henrardia_persica_RF2012	1730	1806	104%	601
NIASHv2082M12	Heterantherium_piliferum_PI401351	1730	1847	107%	601
NIASHv2082M12	Heterantherium_piliferum_PI401353	1730	1910	110%	601
NIASHv2082M12	Heterantherium_piliferum_PI401354	1730	1846	107%	601
NIASHv2082M12	Heterantherium_sp_PI314152	1730	1824	105%	601
NIASHv2082M12	Hordeum_marinum_BCC2006	1730	1800	104%	601
NIASHv2082M12	Hordeum_murinum_BCC2002	1730	1878	109%	601
NIASHv2082M12	Hordeum_pubiflorum_2028	1730	2071	120%	601
NIASHv2082M12	Hordeum_spontaneum_FT11	1730	2250	130%	601
NIASHv2082M12	Hordeum_vulgare_Morex	1730	2185	126%	601
NIASHv2082M12	Psathyrostachys_juncea_PI222050	1730	1693	98%	601
NIASHv2082M12	Psathyrostachys_juncea_PI565077	1730	1140	66%	601
NIASHv2082M12	Psathyrostachys_juncea_PI595135	1730	1682	97%	601
NIASHv2082M12	Psathyrostachys_juncea_PI598613	1730	1777	103%	601
NIASHv2082M12	Psathyrostachys_juncea_PI619487	1730	1666	96%	601
NIASHv2082M12	Psathyrostachys_sp_PI565080	1730	1686	97%	601
NIASHv2082M12	Pseudoroegneria_libanotica_PI228389	1730	1384	80%	601
NIASHv2082M12	Pseudoroegneria_libanotica_PI330688	1730	1633	94%	601
NIASHv2082M12	Pseudoroegneria_libanotica_PI401274	1730	1833	106%	601
NIASHv2082M12	Pseudoroegneria_stipifolia_PI325181	1730	1830	106%	601
NIASHv2082M12	Pseudoroegneria_stipifolia_PI440095	1730	1788	103%	601
NIASHv2082M12	Pseudoroegneria_stipifolia_PI531751	1730	1663	96%	601
NIASHv2082M12	Pseudoroegneria_strigosa_PI499638	1730	1700	98%	601
NIASHv2082M12	Pseudoroegneria_strigosa_PI595172	1730	1647	95%	601
NIASHv2082M12	Pseudoroegneria_strigosa_W614049	1730	1768	102%	601
NIASHv2082M12	Pseudoroegneria_strigosa_PI639805	1730	1630	94%	601
NIASHv2082M12	Pseudoroegneria_strigosa_PI639805	1730	1741	101%	601
NIASHv2082M12	Pseudoroegneria_tauri_PI401322	1730	1479	85%	601
NIASHv2082M12	Pseudoroegneria_tauri_PI401333	1730	1781	103%	601
NIASHv2082M12	Secale_cereale_PI618662	1730	1189	69%	601
NIASHv2082M12	Secale_cereale_PI618665	1730	1660	96%	601
NIASHv2082M12	Secale_cereale_PI618669	1730	1740	101%	601
NIASHv2082M12	Secale_cereale_PI618671	1730	1903	110%	601
NIASHv2082M12	Secale_strictum_R1108	1730	1430	83%	601
NIASHv2082M12	Secale_strictum_R853	1730	1523	88%	601
NIASHv2082M12	Secale_vavilovii_PI253957	1730	950	55%	601
NIASHv2082M12	Secale_vavilovii_R1027	1730	1433	83%	601
NIASHv2082M12	Taeniatherum_caput-medusae_CK2011	1730	1771	102%	601
NIASHv2082M12	Taeniatherum_caput-medusae_GRA1126	1730	1803	104%	601
NIASHv2082M12	Taeniatherum_caput-medusae_PI220589	1730	1711	99%	601
NIASHv2082M12	Taeniatherum_caput-medusae_PI251387	1730	1309	76%	601

Locus	Accession	Mapped exon length in barley (bp)	Assembled exon length (bp)	% of mapped exon length that could be assembled	Extended target (bp)
NIASHv2082M12	Taeniatherum_caput-medusae_PI561095	1730	1107	64%	601
NIASHv2082M12	Taeniatherum_crinatum_GRA2570	1730	1735	100%	601
NIASHv2082M12	Thinopyrum_bessarabicum_W621890	1730	1510	87%	601
NIASHv2082M12	Thinopyrum_elongatum_P1109452	1730	1760	102%	601
NIASHv2082M12	Thinopyrum_elongatum_P1401117	1730	1379	80%	601
NIASHv2082M12	Triticum_boeoticum_1613	1730	1865	108%	601
NIASHv2082M12	Triticum_boeoticum_1688	1730	1835	106%	601
NIASHv2082M12	Triticum_boeoticum_ID379	1730	1460	84%	601
NIASHv2082M12	Triticum_boeoticum_PI272520	1730	1438	83%	601
NIASHv2082M12	Triticum_boeoticum_PI427451	1730	1770	102%	601
NIASHv2082M12	Triticum_boeoticum_PI427620	1730	1795	104%	601
NIASHv2082M12	Triticum_monococcum_2205	1730	1804	104%	601
NIASHv2082M12	Triticum_monococcum_2208	1730	1865	108%	601
NIASHv2082M12	Triticum_monococcum_2271	1730	1873	108%	601
NIASHv2082M12	Triticum_monococcum_TRI13061	1730	1769	102%	601
NIASHv2082M12	Triticum_monococcum_TRI13612	1730	1698	98%	601
NIASHv2082M12	Triticum_urartu_1307	1730	1930	112%	601
NIASHv2082M12	Triticum_urartu_PI428184	1730	1349	78%	601
NIASHv2082M12	Triticum_urartu_PI428317	1730	1432	83%	601
NIASHv2082M12	Triticum_urartu_TRI17824	1730	1922	111%	601
NIASHv2082M12	Triticum_urartu_TRI18407	1730	1893	109%	601
NIASHv2090C08	Aegilops_bicornis_AE106	2603	2869	110%	601
NIASHv2090C08	Aegilops_bicornis_AE1079	2603	2609	100%	601
NIASHv2090C08	Aegilops_bicornis_AE788	2603	2915	112%	601
NIASHv2090C08	Aegilops_bicornis_KU-5786	2603	2440	94%	601
NIASHv2090C08	Aegilops_comosa_AE1255	2603	2886	111%	601
NIASHv2090C08	Aegilops_comosa_AE1378	2603	2785	107%	601
NIASHv2090C08	Aegilops_comosa_AE783	2603	2803	108%	601
NIASHv2090C08	Aegilops_comosa_PI276970	2603	2665	102%	601
NIASHv2090C08	Aegilops_longissima_AE1078	2603	2751	106%	601
NIASHv2090C08	Aegilops_longissima_AE133	2603	2870	110%	601
NIASHv2090C08	Aegilops_longissima_AE417	2603	2591	100%	601
NIASHv2090C08	Aegilops_longissima_PI604141	2603	2481	95%	601
NIASHv2090C08	Aegilops_longissima_TA1921	2603	2787	107%	601
NIASHv2090C08	Aegilops_markgrafii_AE1381	2603	2849	109%	601
NIASHv2090C08	Aegilops_markgrafii_KP-2012-106	2603	2910	112%	601
NIASHv2090C08	Aegilops_markgrafii_PI254863	2603	2722	105%	601
NIASHv2090C08	Aegilops_markgrafii_PI542208	2603	2860	110%	601
NIASHv2090C08	Aegilops_markgrafii_PI596287	2603	2856	110%	601
NIASHv2090C08	Aegilops_mutica_01C2100106	2603	2880	111%	601
NIASHv2090C08	Aegilops_searsii_AE1075	2603	2695	104%	601
NIASHv2090C08	Aegilops_searsii_AE1083	2603	2973	114%	601
NIASHv2090C08	Aegilops_searsii_KU-14655	2603	2837	109%	601
NIASHv2090C08	Aegilops_searsii_PI599142	2603	2922	112%	601
NIASHv2090C08	Aegilops_searsii_PI599148	2603	2406	92%	601
NIASHv2090C08	Aegilops_sharonensis_AE90691	2603	2805	108%	601
NIASHv2090C08	Aegilops_speltoides_3776	2603	2996	115%	601
NIASHv2090C08	Aegilops_speltoides_AE1064	2603	2733	105%	601
NIASHv2090C08	Aegilops_speltoides_AE900	2603	2804	108%	601
NIASHv2090C08	Aegilops_speltoides_KU-7856	2603	2584	99%	601
NIASHv2090C08	Aegilops_speltoides_PI486264	2603	2816	108%	601
NIASHv2090C08	Aegilops_speltoides_PI487231	2603	2703	104%	601
NIASHv2090C08	Aegilops_speltoides_TA1772	2603	2721	105%	601
NIASHv2090C08	Aegilops_tauschii_49116	2603	2782	107%	601
NIASHv2090C08	Aegilops_tauschii_937	2603	3039	117%	601
NIASHv2090C08	Aegilops_tauschii_AE1069	2603	2822	108%	601
NIASHv2090C08	Aegilops_tauschii_AE956	2603	2845	109%	601
NIASHv2090C08	Aegilops_umbellulata_AE1070	2603	2822	108%	601
NIASHv2090C08	Aegilops_umbellulata_AE153	2603	2850	109%	601
NIASHv2090C08	Aegilops_umbellulata_AE740	2603	2592	100%	601
NIASHv2090C08	Aegilops_umbellulata_AE811	2603	2655	102%	601
NIASHv2090C08	Aegilops_uniaristata_AE157	2603	3012	116%	601
NIASHv2090C08	Aegilops_uniaristata_AE680	2603	2890	111%	601
NIASHv2090C08	Aegilops_uniaristata_PI276996	2603	2714	104%	601
NIASHv2090C08	Agropyron_cristatum_PI494615	2603	2856	110%	601
NIASHv2090C08	Agropyron_cristatum_PI598631	2603	2807	108%	601
NIASHv2090C08	Amblyopyrum_muticum_PI560122	2603	2536	97%	601
NIASHv2090C08	Amblyopyrum_muticum_PI560124	2603	2462	95%	601
NIASHv2090C08	Amblyopyrum_muticum_PI560125	2603	2550	98%	601
NIASHv2090C08	Amblyopyrum_muticum_PI560126	2603	2572	99%	601
NIASHv2090C08	Amblyopyrum_muticum_PI636562	2603	2843	109%	601
NIASHv2090C08	Australopyrum_retrofractum_PI531553	2603	2769	106%	601
NIASHv2090C08	Australopyrum_retrofractum_PI533013	2603	2734	105%	601
NIASHv2090C08	Australopyrum_retrofractum_PI533014	2603	2811	108%	601
NIASHv2090C08	Australopyrum_retrofractum_PI547363	2603	2892	111%	601
NIASHv2090C08	Brachypodium_distachyon	2603	1648	63%	601
NIASHv2090C08	Bromus_tectorum_GRA1085	2603	2410	93%	601
NIASHv2090C08	Dasyphyrum_villosum_GRA1020	2603	2790	107%	601
NIASHv2090C08	Dasyphyrum_villosum_GRA1027	2603	2792	107%	601
NIASHv2090C08	Dasyphyrum_villosum_PI368884	2603	2590	100%	601
NIASHv2090C08	Dasyphyrum_villosum_W619414	2603	2557	98%	601
NIASHv2090C08	Dasyphyrum_villosum_W67300	2603	2893	111%	601
NIASHv2090C08	Eremopyrum_distans_PI193264	2603	2853	110%	601
NIASHv2090C08	Eremopyrum_triticeum_GRA2250	2603	2919	112%	601
NIASHv2090C08	Eremopyrum_triticeum_PI502364	2603	2720	104%	601
NIASHv2090C08	Eremopyrum_triticeum_W626631	2603	2710	104%	601

Locus	Accession	Mapped exon length in barley (bp)	Assembled exon length (bp)	% of mapped exon length that could be assembled	Extended target (bp)
NIASHv2090C08	Henrardia_persica_PI401347	2603	2806	108%	601
NIASHv2090C08	Henrardia_persica_PI577112	2603	2831	109%	601
NIASHv2090C08	Henrardia_persica_PI577113	2603	2772	106%	601
NIASHv2090C08	Henrardia_persica_RF2012	2603	2747	106%	601
NIASHv2090C08	Heterantherium_piliferum_PI401351	2603	2885	111%	601
NIASHv2090C08	Heterantherium_piliferum_PI401353	2603	2899	111%	601
NIASHv2090C08	Heterantherium_piliferum_PI401354	2603	2890	111%	601
NIASHv2090C08	Heterantherium_sp_PI314152	2603	2718	104%	601
NIASHv2090C08	Hordeum_marinum_BCC2006	2603	2917	112%	601
NIASHv2090C08	Hordeum_murinum_BCC2002	2603	2874	110%	601
NIASHv2090C08	Hordeum_pubiflorum_2028	2603	3088	119%	601
NIASHv2090C08	Hordeum_spontaneum_FT11	2603	3192	123%	601
NIASHv2090C08	Hordeum_vulgare_Morex	2603	3111	120%	601
NIASHv2090C08	Psathyrostachys_junceae_PI222050	2603	2887	111%	601
NIASHv2090C08	Psathyrostachys_junceae_PI565077	2603	2609	100%	601
NIASHv2090C08	Psathyrostachys_junceae_PI595135	2603	2919	112%	601
NIASHv2090C08	Psathyrostachys_junceae_PI598613	2603	2874	110%	601
NIASHv2090C08	Psathyrostachys_junceae_PI619487	2603	2889	111%	601
NIASHv2090C08	Psathyrostachys_sp_PI565080	2603	2755	106%	601
NIASHv2090C08	Pseudoroegneria_libanotica_PI228389	2603	2647	102%	601
NIASHv2090C08	Pseudoroegneria_libanotica_PI330688	2603	2817	108%	601
NIASHv2090C08	Pseudoroegneria_libanotica_PI401274	2603	2820	108%	601
NIASHv2090C08	Pseudoroegneria_stipifolia_PI325181	2603	2849	109%	601
NIASHv2090C08	Pseudoroegneria_stipifolia_PI440095	2603	2774	107%	601
NIASHv2090C08	Pseudoroegneria_stipifolia_PI531751	2603	2790	107%	601
NIASHv2090C08	Pseudoroegneria_strigosa_PI499638	2603	2823	108%	601
NIASHv2090C08	Pseudoroegneria_strigosa_PI595172	2603	2762	106%	601
NIASHv2090C08	Pseudoroegneria_strigosa_W614049	2603	2876	110%	601
NIASHv2090C08	Pseudoroegneria_strigosa_PI639805	2603	2697	104%	601
NIASHv2090C08	Pseudoroegneria_strigosa_PI639805	2603	2778	107%	601
NIASHv2090C08	Pseudoroegneria_tauri_PI401322	2603	2611	100%	601
NIASHv2090C08	Pseudoroegneria_tauri_PI401333	2603	2812	108%	601
NIASHv2090C08	Secale_cereale_PI618662	2603	2306	89%	601
NIASHv2090C08	Secale_cereale_PI618665	2603	2796	107%	601
NIASHv2090C08	Secale_cereale_PI618669	2603	2901	111%	601
NIASHv2090C08	Secale_cereale_PI618671	2603	2771	106%	601
NIASHv2090C08	Secale_strictum_R1108	2603	2486	96%	601
NIASHv2090C08	Secale_strictum_R853	2603	2823	108%	601
NIASHv2090C08	Secale_vavilovii_PI253957	2603	2340	90%	601
NIASHv2090C08	Secale_vavilovii_R1027	2603	2708	104%	601
NIASHv2090C08	Taeniatherum_caput-medusae_CK2011	2603	2781	107%	601
NIASHv2090C08	Taeniatherum_caput-medusae_GRA1126	2603	2858	110%	601
NIASHv2090C08	Taeniatherum_caput-medusae_PI220589	2603	2801	108%	601
NIASHv2090C08	Taeniatherum_caput-medusae_PI251387	2603	2677	103%	601
NIASHv2090C08	Taeniatherum_caput-medusae_PI561095	2603	2539	98%	601
NIASHv2090C08	Taeniatherum_crinatum_GRA2570	2603	2826	109%	601
NIASHv2090C08	Thinopyrum_bessarabicum_W621890	2603	2765	106%	601
NIASHv2090C08	Thinopyrum_elongatum_PI109452	2603	2842	109%	601
NIASHv2090C08	Thinopyrum_elongatum_PI401117	2603	2620	101%	601
NIASHv2090C08	Triticum_boeoticum_1613	2603	2964	114%	601
NIASHv2090C08	Triticum_boeoticum_1688	2603	2809	108%	601
NIASHv2090C08	Triticum_boeoticum_ID379	2603	2652	102%	601
NIASHv2090C08	Triticum_boeoticum_PI272520	2603	2608	100%	601
NIASHv2090C08	Triticum_boeoticum_PI427451	2603	2893	111%	601
NIASHv2090C08	Triticum_boeoticum_PI427620	2603	2849	109%	601
NIASHv2090C08	Triticum_monococcum_2205	2603	2859	110%	601
NIASHv2090C08	Triticum_monococcum_2208	2603	2919	112%	601
NIASHv2090C08	Triticum_monococcum_2271	2603	2985	115%	601
NIASHv2090C08	Triticum_monococcum_TR113061	2603	2745	105%	601
NIASHv2090C08	Triticum_monococcum_TR113612	2603	2924	112%	601
NIASHv2090C08	Triticum_urartu_1307	2603	2926	112%	601
NIASHv2090C08	Triticum_urartu_PI428184	2603	2662	102%	601
NIASHv2090C08	Triticum_urartu_PI428317	2603	2597	100%	601
NIASHv2090C08	Triticum_urartu_TR117824	2603	2777	107%	601
NIASHv2090C08	Triticum_urartu_TR118407	2603	2976	114%	601
NIASHv2101A14	Aegilops_bicornis_AE106	1488	1018	68%	601
NIASHv2101A14	Aegilops_bicornis_AE1079	1488	167	11%	601
NIASHv2101A14	Aegilops_bicornis_AE788	1488	987	66%	601
NIASHv2101A14	Aegilops_bicornis_KU-5786	1488	348	23%	601
NIASHv2101A14	Aegilops_comosa_AE1255	1488	1331	89%	601
NIASHv2101A14	Aegilops_comosa_AE1378	1488	639	43%	601
NIASHv2101A14	Aegilops_comosa_AE783	1488	231	16%	601
NIASHv2101A14	Aegilops_comosa_PI276970	1488	219	15%	601
NIASHv2101A14	Aegilops_longissima_AE1078	1488	533	36%	601
NIASHv2101A14	Aegilops_longissima_AE133	1488	1161	78%	601
NIASHv2101A14	Aegilops_longissima_AE417	1488	86	6%	601
NIASHv2101A14	Aegilops_longissima_PI604141	1488	411	28%	601
NIASHv2101A14	Aegilops_longissima_TA1921	1488	516	35%	601
NIASHv2101A14	Aegilops_markgrafii_AE1381	1488	1075	72%	601
NIASHv2101A14	Aegilops_markgrafii_KP-2012-106	1488	1075	72%	601
NIASHv2101A14	Aegilops_markgrafii_PI254863	1488	102	7%	601
NIASHv2101A14	Aegilops_markgrafii_PI542208	1488	1057	71%	601
NIASHv2101A14	Aegilops_markgrafii_PI596287	1488	1237	83%	601
NIASHv2101A14	Aegilops_mutica_01C2100106	1488	1327	89%	601
NIASHv2101A14	Aegilops_searsii_AE1075	1488	923	62%	601
NIASHv2101A14	Aegilops_searsii_AE1083	1488	1319	89%	601

Locus	Accession	Mapped exon length in barley (bp)	Assembled exon length (bp)	% of mapped exon length that could be assembled	Extended target (bp)
NIASHv2101A14	Aegilops_searsii_KU-14655	1488	937	63%	601
NIASHv2101A14	Aegilops_searsii_PI599142	1488	542	36%	601
NIASHv2101A14	Aegilops_searsii_PI599148	1488	0	0%	601
NIASHv2101A14	Aegilops_sharonensis_AE90691	1488	1163	78%	601
NIASHv2101A14	Aegilops_speltoides_3776	1488	1429	96%	601
NIASHv2101A14	Aegilops_speltoides_AE1064	1488	1119	75%	601
NIASHv2101A14	Aegilops_speltoides_AE900	1488	1026	69%	601
NIASHv2101A14	Aegilops_speltoides_KU-7856	1488	455	31%	601
NIASHv2101A14	Aegilops_speltoides_PI486264	1488	1174	79%	601
NIASHv2101A14	Aegilops_speltoides_PI487231	1488	1035	70%	601
NIASHv2101A14	Aegilops_speltoides_TA1772	1488	178	12%	601
NIASHv2101A14	Aegilops_tauschii_49116	1488	481	32%	601
NIASHv2101A14	Aegilops_tauschii_937	1488	1470	99%	601
NIASHv2101A14	Aegilops_tauschii_AE1069	1488	808	54%	601
NIASHv2101A14	Aegilops_tauschii_AE956	1488	1212	81%	601
NIASHv2101A14	Aegilops_umbellulata_AE1070	1488	991	67%	601
NIASHv2101A14	Aegilops_umbellulata_AE153	1488	1140	77%	601
NIASHv2101A14	Aegilops_umbellulata_AE740	1488	612	41%	601
NIASHv2101A14	Aegilops_umbellulata_AE811	1488	0	0%	601
NIASHv2101A14	Aegilops_uniaristata_AE157	1488	1096	74%	601
NIASHv2101A14	Aegilops_uniaristata_AE680	1488	1217	82%	601
NIASHv2101A14	Aegilops_uniaristata_PI276996	1488	129	9%	601
NIASHv2101A14	Agropyron_cristatum_PI494615	1488	1032	69%	601
NIASHv2101A14	Agropyron_cristatum_PI598631	1488	875	59%	601
NIASHv2101A14	Amblyopyrum_muticum_PI560122	1488	119	8%	601
NIASHv2101A14	Amblyopyrum_muticum_PI560124	1488	363	24%	601
NIASHv2101A14	Amblyopyrum_muticum_PI560125	1488	79	5%	601
NIASHv2101A14	Amblyopyrum_muticum_PI560126	1488	239	16%	601
NIASHv2101A14	Amblyopyrum_muticum_PI636562	1488	728	49%	601
NIASHv2101A14	Australopyrum_retrofractum_PI531553	1488	661	44%	601
NIASHv2101A14	Australopyrum_retrofractum_PI533013	1488	128	9%	601
NIASHv2101A14	Australopyrum_retrofractum_PI533014	1488	893	60%	601
NIASHv2101A14	Australopyrum_retrofractum_PI547363	1488	813	55%	601
NIASHv2101A14	Brachypodium_distachyon	1488	267	18%	601
NIASHv2101A14	Bromus_tectorum_GRA1085	1488	306	21%	601
NIASHv2101A14	Dasypyrum_villosum_GRA1020	1488	409	27%	601
NIASHv2101A14	Dasypyrum_villosum_GRA1027	1488	877	59%	601
NIASHv2101A14	Dasypyrum_villosum_PI368884	1488	77	5%	601
NIASHv2101A14	Dasypyrum_villosum_W619414	1488	451	30%	601
NIASHv2101A14	Dasypyrum_villosum_W67300	1488	558	38%	601
NIASHv2101A14	Eremopyrum_distans_PI193264	1488	953	64%	601
NIASHv2101A14	Eremopyrum_triticeum_GRA2250	1488	833	56%	601
NIASHv2101A14	Eremopyrum_triticeum_PI502364	1488	827	56%	601
NIASHv2101A14	Eremopyrum_triticeum_W626631	1488	197	13%	601
NIASHv2101A14	Henrardia_persica_PI401347	1488	761	51%	601
NIASHv2101A14	Henrardia_persica_PI577112	1488	1263	85%	601
NIASHv2101A14	Henrardia_persica_PI577113	1488	339	23%	601
NIASHv2101A14	Henrardia_persica_RF2012	1488	672	45%	601
NIASHv2101A14	Heteranthelium_piliferum_PI401351	1488	1097	74%	601
NIASHv2101A14	Heteranthelium_piliferum_PI401353	1488	1271	85%	601
NIASHv2101A14	Heteranthelium_piliferum_PI401354	1488	1384	93%	601
NIASHv2101A14	Heteranthelium_sp_PI314152	1488	771	52%	601
NIASHv2101A14	Hordeum_marinum_BCC2006	1488	1211	81%	601
NIASHv2101A14	Hordeum_murinum_BCC2002	1488	1401	94%	601
NIASHv2101A14	Hordeum_pubiflorum_2028	1488	1543	104%	601
NIASHv2101A14	Hordeum_spontaneum_FT11	1488	1831	123%	601
NIASHv2101A14	Hordeum_vulgare_Morex	1488	1711	115%	601
NIASHv2101A14	Psathyrostachys_juncea_PI222050	1488	536	36%	601
NIASHv2101A14	Psathyrostachys_juncea_PI565077	1488	56	4%	601
NIASHv2101A14	Psathyrostachys_juncea_PI595135	1488	926	62%	601
NIASHv2101A14	Psathyrostachys_juncea_PI598613	1488	975	66%	601
NIASHv2101A14	Psathyrostachys_juncea_PI619487	1488	1044	70%	601
NIASHv2101A14	Psathyrostachys_sp_PI565080	1488	635	43%	601
NIASHv2101A14	Pseudoroegneria_libanotica_PI228389	1488	510	34%	601
NIASHv2101A14	Pseudoroegneria_libanotica_PI330688	1488	642	43%	601
NIASHv2101A14	Pseudoroegneria_libanotica_PI401274	1488	1116	75%	601
NIASHv2101A14	Pseudoroegneria_stipifolia_PI325181	1488	1295	87%	601
NIASHv2101A14	Pseudoroegneria_stipifolia_PI440095	1488	1160	78%	601
NIASHv2101A14	Pseudoroegneria_stipifolia_PI531751	1488	1080	73%	601
NIASHv2101A14	Pseudoroegneria_strigosa_PI499638	1488	659	44%	601
NIASHv2101A14	Pseudoroegneria_strigosa_PI595172	1488	1065	72%	601
NIASHv2101A14	Pseudoroegneria_strigosa_W614049	1488	1259	85%	601
NIASHv2101A14	Pseudoroegneria_strigosa_PI639805	1488	675	45%	601
NIASHv2101A14	Pseudoroegneria_strigosa_PI639805	1488	1207	81%	601
NIASHv2101A14	Pseudoroegneria_tauri_PI401322	1488	281	19%	601
NIASHv2101A14	Pseudoroegneria_tauri_PI401333	1488	712	48%	601
NIASHv2101A14	Secale_cereale_PI618662	1488	149	10%	601
NIASHv2101A14	Secale_cereale_PI618665	1488	716	48%	601
NIASHv2101A14	Secale_cereale_PI618669	1488	905	61%	601
NIASHv2101A14	Secale_cereale_PI618671	1488	850	57%	601
NIASHv2101A14	Secale_strictum_R1108	1488	340	23%	601
NIASHv2101A14	Secale_strictum_R853	1488	657	44%	601
NIASHv2101A14	Secale_vavilovii_PI253957	1488	0	0%	601
NIASHv2101A14	Secale_vavilovii_R1027	1488	297	20%	601
NIASHv2101A14	Taeniatherum_caput-medusae_CK2011	1488	1144	77%	601
NIASHv2101A14	Taeniatherum_caput-medusae_GRA1126	1488	1248	84%	601

Locus	Accession	Mapped exon length in barley (bp)	Assembled exon length (bp)	% of mapped exon length that could be assembled	Extended target (bp)
NIASHv2101A14	Taeniatherum_caput-medusae_PI220589	1488	957	64%	601
NIASHv2101A14	Taeniatherum_caput-medusae_PI251387	1488	201	14%	601
NIASHv2101A14	Taeniatherum_caput-medusae_PI561095	1488	215	14%	601
NIASHv2101A14	Taeniatherum_crinium_GRA2570	1488	1083	73%	601
NIASHv2101A14	Thinopyrum_bessarabicum_W621890	1488	482	32%	601
NIASHv2101A14	Thinopyrum_elongatum_PI109452	1488	936	63%	601
NIASHv2101A14	Thinopyrum_elongatum_PI401117	1488	175	12%	601
NIASHv2101A14	Triticum_boeoticum_1613	1488	1362	92%	601
NIASHv2101A14	Triticum_boeoticum_1688	1488	1202	81%	601
NIASHv2101A14	Triticum_boeoticum_ID379	1488	743	50%	601
NIASHv2101A14	Triticum_boeoticum_PI272520	1488	570	38%	601
NIASHv2101A14	Triticum_boeoticum_PI427451	1488	885	59%	601
NIASHv2101A14	Triticum_boeoticum_PI427620	1488	1072	72%	601
NIASHv2101A14	Triticum_monococcum_2205	1488	1221	82%	601
NIASHv2101A14	Triticum_monococcum_2208	1488	998	67%	601
NIASHv2101A14	Triticum_monococcum_2271	1488	1419	95%	601
NIASHv2101A14	Triticum_monococcum_TRI13061	1488	1234	83%	601
NIASHv2101A14	Triticum_monococcum_TRI13612	1488	1066	72%	601
NIASHv2101A14	Triticum_urartu_1307	1488	1392	94%	601
NIASHv2101A14	Triticum_urartu_PI428184	1488	406	27%	601
NIASHv2101A14	Triticum_urartu_PI428317	1488	183	12%	601
NIASHv2101A14	Triticum_urartu_TRI17824	1488	1204	81%	601
NIASHv2101A14	Triticum_urartu_TRI18407	1488	1204	81%	601
NIASHv2108K22	Aegilops_bicornis_AE106	1111	1255	113%	601
NIASHv2108K22	Aegilops_bicornis_AE1079	1111	184	17%	601
NIASHv2108K22	Aegilops_bicornis_AE788	1111	1072	96%	601
NIASHv2108K22	Aegilops_bicornis_KU-5786	1111	577	52%	601
NIASHv2108K22	Aegilops_comosa_AE1255	1111	1270	114%	601
NIASHv2108K22	Aegilops_comosa_AE1378	1111	966	87%	601
NIASHv2108K22	Aegilops_comosa_AE783	1111	986	89%	601
NIASHv2108K22	Aegilops_comosa_PI276970	1111	492	44%	601
NIASHv2108K22	Aegilops_longissima_AE1078	1111	644	58%	601
NIASHv2108K22	Aegilops_longissima_AE133	1111	1038	93%	601
NIASHv2108K22	Aegilops_longissima_AE417	1111	610	55%	601
NIASHv2108K22	Aegilops_longissima_PI604141	1111	473	43%	601
NIASHv2108K22	Aegilops_longissima_TA1921	1111	868	78%	601
NIASHv2108K22	Aegilops_markgrafii_AE1381	1111	1098	99%	601
NIASHv2108K22	Aegilops_markgrafii_KP-2012-106	1111	1132	102%	601
NIASHv2108K22	Aegilops_markgrafii_PI254863	1111	623	56%	601
NIASHv2108K22	Aegilops_markgrafii_PI542208	1111	1060	95%	601
NIASHv2108K22	Aegilops_markgrafii_PI596287	1111	1101	99%	601
NIASHv2108K22	Aegilops_mutica_01C2100106	1111	1177	106%	601
NIASHv2108K22	Aegilops_searsii_AE1075	1111	1078	97%	601
NIASHv2108K22	Aegilops_searsii_AE1083	1111	1256	113%	601
NIASHv2108K22	Aegilops_searsii_KU-14655	1111	1085	98%	601
NIASHv2108K22	Aegilops_searsii_PI599142	1111	1082	97%	601
NIASHv2108K22	Aegilops_searsii_PI599148	1111	329	30%	601
NIASHv2108K22	Aegilops_sharonensis_AE90691	1111	1000	90%	601
NIASHv2108K22	Aegilops_speltooides_3776	1111	1413	127%	601
NIASHv2108K22	Aegilops_speltooides_AE1064	1111	1084	98%	601
NIASHv2108K22	Aegilops_speltooides_AE900	1111	991	89%	601
NIASHv2108K22	Aegilops_speltooides_KU-7856	1111	566	51%	601
NIASHv2108K22	Aegilops_speltooides_PI486264	1111	1224	110%	601
NIASHv2108K22	Aegilops_speltooides_PI487231	1111	1193	107%	601
NIASHv2108K22	Aegilops_speltooides_TA1772	1111	611	55%	601
NIASHv2108K22	Aegilops_tauschii_49116	1111	634	57%	601
NIASHv2108K22	Aegilops_tauschii_937	1111	1376	124%	601
NIASHv2108K22	Aegilops_tauschii_AE1069	1111	1064	96%	601
NIASHv2108K22	Aegilops_tauschii_AE956	1111	1227	110%	601
NIASHv2108K22	Aegilops_umbellulata_AE1070	1111	1058	95%	601
NIASHv2108K22	Aegilops_umbellulata_AE153	1111	1094	98%	601
NIASHv2108K22	Aegilops_umbellulata_AE740	1111	538	48%	601
NIASHv2108K22	Aegilops_umbellulata_AE811	1111	66	6%	601
NIASHv2108K22	Aegilops_uniaristata_AE157	1111	1260	113%	601
NIASHv2108K22	Aegilops_uniaristata_AE680	1111	1130	102%	601
NIASHv2108K22	Aegilops_uniaristata_PI276996	1111	222	20%	601
NIASHv2108K22	Agropyron_cristatum_PI494615	1111	1244	112%	601
NIASHv2108K22	Agropyron_cristatum_PI598631	1111	1037	93%	601
NIASHv2108K22	Amblyopyrum_muticum_PI560122	1111	474	43%	601
NIASHv2108K22	Amblyopyrum_muticum_PI560124	1111	263	24%	601
NIASHv2108K22	Amblyopyrum_muticum_PI560125	1111	248	22%	601
NIASHv2108K22	Amblyopyrum_muticum_PI560126	1111	363	33%	601
NIASHv2108K22	Amblyopyrum_muticum_PI636562	1111	1000	90%	601
NIASHv2108K22	Australopyrum_retrofractum_PI531553	1111	785	71%	601
NIASHv2108K22	Australopyrum_retrofractum_PI533013	1111	522	47%	601
NIASHv2108K22	Australopyrum_retrofractum_PI533014	1111	808	73%	601
NIASHv2108K22	Australopyrum_retrofractum_PI547363	1111	935	84%	601
NIASHv2108K22	Brachypodium_distachyon	1111	931	84%	601
NIASHv2108K22	Bromus_tectorum_GRA1085	1111	789	71%	601
NIASHv2108K22	Dasyphyrum_villosum_GRA1020	1111	1147	103%	601
NIASHv2108K22	Dasyphyrum_villosum_GRA1027	1111	1017	92%	601
NIASHv2108K22	Dasyphyrum_villosum_PI368884	1111	220	20%	601
NIASHv2108K22	Dasyphyrum_villosum_W619414	1111	401	36%	601
NIASHv2108K22	Dasyphyrum_villosum_W67300	1111	1000	90%	601
NIASHv2108K22	Eremopyrum_distans_PI193264	1111	923	83%	601
NIASHv2108K22	Eremopyrum_triticum_GRA2250	1111	1146	103%	601

Locus	Accession	Mapped exon length in barley (bp)	Assembled exon length (bp)	% of mapped exon length that could be assembled	Extended target (bp)
NIASHv2108K22	Eremopyrum_triticeum_PI502364	1111	936	84%	601
NIASHv2108K22	Eremopyrum_triticeum_W626631	1111	671	60%	601
NIASHv2108K22	Henrardia_persica_PI401347	1111	1016	91%	601
NIASHv2108K22	Henrardia_persica_PI577112	1111	1231	111%	601
NIASHv2108K22	Henrardia_persica_PI577113	1111	783	70%	601
NIASHv2108K22	Henrardia_persica_RF2012	1111	982	88%	601
NIASHv2108K22	Heterantherium_piliferum_PI401351	1111	975	88%	601
NIASHv2108K22	Heterantherium_piliferum_PI401353	1111	1189	107%	601
NIASHv2108K22	Heterantherium_piliferum_PI401354	1111	1259	113%	601
NIASHv2108K22	Heterantherium_sp_P1314152	1111	528	48%	601
NIASHv2108K22	Hordeum_marinum_BCC2006	1111	1158	104%	601
NIASHv2108K22	Hordeum_murinum_BCC2002	1111	1198	108%	601
NIASHv2108K22	Hordeum_pubiflorum_2028	1111	1470	132%	601
NIASHv2108K22	Hordeum_spontaneum_FT11	1111	1526	137%	601
NIASHv2108K22	Hordeum_vulgare_Morex	1111	1495	135%	601
NIASHv2108K22	Psathyrostachys_junceae_PI222050	1111	954	86%	601
NIASHv2108K22	Psathyrostachys_junceae_PI565077	1111	323	29%	601
NIASHv2108K22	Psathyrostachys_junceae_PI595135	1111	1016	91%	601
NIASHv2108K22	Psathyrostachys_junceae_PI598613	1111	1033	93%	601
NIASHv2108K22	Psathyrostachys_junceae_PI619487	1111	1063	96%	601
NIASHv2108K22	Psathyrostachys_sp_PI565080	1111	1012	91%	601
NIASHv2108K22	Pseudoroegneria_libanotica_PI228389	1111	604	54%	601
NIASHv2108K22	Pseudoroegneria_libanotica_PI330688	1111	820	74%	601
NIASHv2108K22	Pseudoroegneria_libanotica_PI401274	1111	1058	95%	601
NIASHv2108K22	Pseudoroegneria_stipifolia_PI325181	1111	1085	98%	601
NIASHv2108K22	Pseudoroegneria_stipifolia_PI440095	1111	1134	102%	601
NIASHv2108K22	Pseudoroegneria_stipifolia_PI531751	1111	987	89%	601
NIASHv2108K22	Pseudoroegneria_strigosa_PI499638	1111	802	72%	601
NIASHv2108K22	Pseudoroegneria_strigosa_PI595172	1111	1114	100%	601
NIASHv2108K22	Pseudoroegneria_strigosa_W614049	1111	1274	115%	601
NIASHv2108K22	Pseudoroegneria_strigosa_PI639805	1111	948	85%	601
NIASHv2108K22	Pseudoroegneria_strigosa_PI639805	1111	967	87%	601
NIASHv2108K22	Pseudoroegneria_tauri_PI401322	1111	782	70%	601
NIASHv2108K22	Pseudoroegneria_tauri_PI401333	1111	1171	105%	601
NIASHv2108K22	Secale_cereale_PI618662	1111	116	10%	601
NIASHv2108K22	Secale_cereale_PI618665	1111	974	88%	601
NIASHv2108K22	Secale_cereale_PI618669	1111	887	80%	601
NIASHv2108K22	Secale_cereale_PI618671	1111	909	82%	601
NIASHv2108K22	Secale_strictum_R1108	1111	579	52%	601
NIASHv2108K22	Secale_strictum_R853	1111	811	73%	601
NIASHv2108K22	Secale_vavilovii_PI253957	1111	72	6%	601
NIASHv2108K22	Secale_vavilovii_R1027	1111	515	46%	601
NIASHv2108K22	Taeniatherum_caput-medusae_CK2011	1111	1229	111%	601
NIASHv2108K22	Taeniatherum_caput-medusae_GRA1126	1111	1132	102%	601
NIASHv2108K22	Taeniatherum_caput-medusae_PI220589	1111	1134	102%	601
NIASHv2108K22	Taeniatherum_caput-medusae_PI251387	1111	429	39%	601
NIASHv2108K22	Taeniatherum_caput-medusae_PI561095	1111	239	22%	601
NIASHv2108K22	Taeniatherum_crinatum_GRA2570	1111	1022	92%	601
NIASHv2108K22	Thinopyrum_bessarabicum_W621890	1111	849	76%	601
NIASHv2108K22	Thinopyrum_elongatum_PI109452	1111	1045	94%	601
NIASHv2108K22	Thinopyrum_elongatum_PI401117	1111	637	57%	601
NIASHv2108K22	Triticum_boeoticum_1613	1111	1296	117%	601
NIASHv2108K22	Triticum_boeoticum_1688	1111	1072	96%	601
NIASHv2108K22	Triticum_boeoticum_ID379	1111	558	50%	601
NIASHv2108K22	Triticum_boeoticum_PI272520	1111	387	35%	601
NIASHv2108K22	Triticum_boeoticum_PI427451	1111	1134	102%	601
NIASHv2108K22	Triticum_boeoticum_PI427620	1111	1084	98%	601
NIASHv2108K22	Triticum_monococcum_2205	1111	1168	105%	601
NIASHv2108K22	Triticum_monococcum_2208	1111	1060	95%	601
NIASHv2108K22	Triticum_monococcum_2271	1111	1296	117%	601
NIASHv2108K22	Triticum_monococcum_TRI13061	1111	1072	96%	601
NIASHv2108K22	Triticum_monococcum_TRI13612	1111	1158	104%	601
NIASHv2108K22	Triticum_urartu_1307	1111	1298	117%	601
NIASHv2108K22	Triticum_urartu_PI428184	1111	731	66%	601
NIASHv2108K22	Triticum_urartu_PI428317	1111	568	51%	601
NIASHv2108K22	Triticum_urartu_TRI17824	1111	1145	103%	601
NIASHv2108K22	Triticum_urartu_TRI18407	1111	939	85%	601
NIASHv2111B14	Aegilops_bicornis_AE106	1269	1690	133%	601
NIASHv2111B14	Aegilops_bicornis_AE1079	1269	1471	116%	601
NIASHv2111B14	Aegilops_bicornis_AE788	1269	1627	128%	601
NIASHv2111B14	Aegilops_bicornis_KU-5786	1269	1380	109%	601
NIASHv2111B14	Aegilops_comosa_AE1255	1269	1550	122%	601
NIASHv2111B14	Aegilops_comosa_AE1378	1269	1484	117%	601
NIASHv2111B14	Aegilops_comosa_AE783	1269	1610	127%	601
NIASHv2111B14	Aegilops_comosa_PI276970	1269	1453	114%	601
NIASHv2111B14	Aegilops_longissima_AE1078	1269	1573	124%	601
NIASHv2111B14	Aegilops_longissima_AE133	1269	1565	123%	601
NIASHv2111B14	Aegilops_longissima_AE417	1269	1540	121%	601
NIASHv2111B14	Aegilops_longissima_PI604141	1269	1430	113%	601
NIASHv2111B14	Aegilops_longissima_TA1921	1269	1637	129%	601
NIASHv2111B14	Aegilops_markgrafii_AE1381	1269	1661	131%	601
NIASHv2111B14	Aegilops_markgrafii_KP-2012-106	1269	1597	126%	601
NIASHv2111B14	Aegilops_markgrafii_PI254863	1269	1473	116%	601
NIASHv2111B14	Aegilops_markgrafii_PI542208	1269	1648	130%	601
NIASHv2111B14	Aegilops_markgrafii_PI596287	1269	1698	134%	601
NIASHv2111B14	Aegilops_mutica_01C2100106	1269	1590	125%	601

Locus	Accession	Mapped exon length in barley (bp)	Assembled exon length (bp)	% of mapped exon length that could be assembled	Extended target (bp)
NIASHv2111B14	Aegilops_searsii_AE1075	1269	1571	124%	601
NIASHv2111B14	Aegilops_searsii_AE1083	1269	1737	137%	601
NIASHv2111B14	Aegilops_searsii_KU-14655	1269	1692	133%	601
NIASHv2111B14	Aegilops_searsii_PI599142	1269	1591	125%	601
NIASHv2111B14	Aegilops_searsii_PI599148	1269	1353	107%	601
NIASHv2111B14	Aegilops_sharonensis_AE90691	1269	1650	130%	601
NIASHv2111B14	Aegilops_speltoides_3776	1269	1652	130%	601
NIASHv2111B14	Aegilops_speltoides_AE1064	1269	1597	126%	601
NIASHv2111B14	Aegilops_speltoides_AE900	1269	1588	125%	601
NIASHv2111B14	Aegilops_speltoides_KU-7856	1269	1434	113%	601
NIASHv2111B14	Aegilops_speltoides_PI486264	1269	1636	129%	601
NIASHv2111B14	Aegilops_speltoides_PI487231	1269	1551	122%	601
NIASHv2111B14	Aegilops_speltoides_TA1772	1269	1303	103%	601
NIASHv2111B14	Aegilops_tauschii_49116	1269	1594	126%	601
NIASHv2111B14	Aegilops_tauschii_937	1269	1731	136%	601
NIASHv2111B14	Aegilops_tauschii_AE1069	1269	1488	117%	601
NIASHv2111B14	Aegilops_tauschii_AE956	1269	1572	124%	601
NIASHv2111B14	Aegilops_umbellulata_AE1070	1269	1541	121%	601
NIASHv2111B14	Aegilops_umbellulata_AE153	1269	1566	123%	601
NIASHv2111B14	Aegilops_umbellulata_AE740	1269	1400	110%	601
NIASHv2111B14	Aegilops_umbellulata_AE811	1269	1068	84%	601
NIASHv2111B14	Aegilops_uniaristata_AE157	1269	1630	128%	601
NIASHv2111B14	Aegilops_uniaristata_AE680	1269	1546	122%	601
NIASHv2111B14	Aegilops_uniaristata_PI276996	1269	1476	116%	601
NIASHv2111B14	Agropyron_cristatum_PI494615	1269	1628	128%	601
NIASHv2111B14	Agropyron_cristatum_PI598631	1269	1520	120%	601
NIASHv2111B14	Amblyopyrum_muticum_PI560122	1269	1344	106%	601
NIASHv2111B14	Amblyopyrum_muticum_PI560124	1269	1305	103%	601
NIASHv2111B14	Amblyopyrum_muticum_PI560125	1269	1360	107%	601
NIASHv2111B14	Amblyopyrum_muticum_PI560126	1269	1378	109%	601
NIASHv2111B14	Amblyopyrum_muticum_PI636562	1269	1613	127%	601
NIASHv2111B14	Australopyrum_retrofractum_PI531553	1269	1545	122%	601
NIASHv2111B14	Australopyrum_retrofractum_PI533013	1269	1463	115%	601
NIASHv2111B14	Australopyrum_retrofractum_PI533014	1269	1608	127%	601
NIASHv2111B14	Australopyrum_retrofractum_PI547363	1269	1666	131%	601
NIASHv2111B14	Brachypodium_distachyon	1269	1391	110%	601
NIASHv2111B14	Bromus_tectorum_GRA1085	1269	139	11%	601
NIASHv2111B14	Dasypyrum_villosum_GRA1020	1269	1494	118%	601
NIASHv2111B14	Dasypyrum_villosum_GRA1027	1269	1546	122%	601
NIASHv2111B14	Dasypyrum_villosum_PI368884	1269	1348	106%	601
NIASHv2111B14	Dasypyrum_villosum_W619414	1269	1348	106%	601
NIASHv2111B14	Dasypyrum_villosum_W67300	1269	1646	130%	601
NIASHv2111B14	Eremopyrum_distans_PI193264	1269	1631	129%	601
NIASHv2111B14	Eremopyrum_triticeum_GRA2250	1269	1589	125%	601
NIASHv2111B14	Eremopyrum_triticeum_PI502364	1269	1701	134%	601
NIASHv2111B14	Eremopyrum_triticeum_W626631	1269	1536	121%	601
NIASHv2111B14	Henrardia_persica_PI401347	1269	1658	131%	601
NIASHv2111B14	Henrardia_persica_PI577112	1269	1685	133%	601
NIASHv2111B14	Henrardia_persica_PI577113	1269	1521	120%	601
NIASHv2111B14	Henrardia_persica_RF2012	1269	1632	129%	601
NIASHv2111B14	Heteranthelium_piliferum_PI401351	1269	1559	123%	601
NIASHv2111B14	Heteranthelium_piliferum_PI401353	1269	1588	125%	601
NIASHv2111B14	Heteranthelium_piliferum_PI401354	1269	1704	134%	601
NIASHv2111B14	Heteranthelium_sp_PI314152	1269	1485	117%	601
NIASHv2111B14	Hordeum_marinum_BCC2006	1269	1656	130%	601
NIASHv2111B14	Hordeum_murinum_BCC2002	1269	1618	128%	601
NIASHv2111B14	Hordeum_pubiflorum_2028	1269	1673	132%	601
NIASHv2111B14	Hordeum_spontanum_FT11	1269	1796	142%	601
NIASHv2111B14	Hordeum_vulgare_Morex	1269	1815	143%	601
NIASHv2111B14	Psathyrostachys_junceae_PI222050	1269	1624	128%	601
NIASHv2111B14	Psathyrostachys_junceae_PI565077	1269	1487	117%	601
NIASHv2111B14	Psathyrostachys_junceae_PI595135	1269	1577	124%	601
NIASHv2111B14	Psathyrostachys_junceae_PI598613	1269	1556	123%	601
NIASHv2111B14	Psathyrostachys_junceae_PI619487	1269	1708	135%	601
NIASHv2111B14	Psathyrostachys_sp_PI565080	1269	1550	122%	601
NIASHv2111B14	Pseudoroegneria_libanotica_PI228389	1269	1494	118%	601
NIASHv2111B14	Pseudoroegneria_libanotica_PI330688	1269	1456	115%	601
NIASHv2111B14	Pseudoroegneria_libanotica_PI401274	1269	1574	124%	601
NIASHv2111B14	Pseudoroegneria_stipifolia_PI325181	1269	1600	126%	601
NIASHv2111B14	Pseudoroegneria_stipifolia_PI440095	1269	1638	129%	601
NIASHv2111B14	Pseudoroegneria_stipifolia_PI531751	1269	1552	122%	601
NIASHv2111B14	Pseudoroegneria_strigosa_PI499638	1269	1612	127%	601
NIASHv2111B14	Pseudoroegneria_strigosa_PI595172	1269	1520	120%	601
NIASHv2111B14	Pseudoroegneria_strigosa_W614049	1269	1635	129%	601
NIASHv2111B14	Pseudoroegneria_strigosa_PI639805	1269	1492	118%	601
NIASHv2111B14	Pseudoroegneria_strigosa_PI639805	1269	1561	123%	601
NIASHv2111B14	Pseudoroegneria_tauri_PI401322	1269	1476	116%	601
NIASHv2111B14	Pseudoroegneria_tauri_PI401333	1269	1510	119%	601
NIASHv2111B14	Secale_cereale_PI618662	1269	1308	103%	601
NIASHv2111B14	Secale_cereale_PI618665	1269	1397	110%	601
NIASHv2111B14	Secale_cereale_PI618669	1269	1611	127%	601
NIASHv2111B14	Secale_cereale_PI618671	1269	1549	122%	601
NIASHv2111B14	Secale_strictum_R1108	1269	1438	113%	601
NIASHv2111B14	Secale_strictum_R853	1269	1461	115%	601
NIASHv2111B14	Secale_vavilovii_PI253957	1269	1060	84%	601
NIASHv2111B14	Secale_vavilovii_R1027	1269	1341	106%	601

Locus	Accession	Mapped exon length in barley (bp)	Assembled exon length (bp)	% of mapped exon length that could be assembled	Extended target (bp)
NIASHv2111B14	Taeniatherum_caput-medusae_CK2011	1269	1719	135%	601
NIASHv2111B14	Taeniatherum_caput-medusae_GRA1126	1269	1755	138%	601
NIASHv2111B14	Taeniatherum_caput-medusae_PI220589	1269	1592	125%	601
NIASHv2111B14	Taeniatherum_caput-medusae_PI251387	1269	1407	111%	601
NIASHv2111B14	Taeniatherum_caput-medusae_PI561095	1269	1398	110%	601
NIASHv2111B14	Taeniatherum_crinatum_GRA2570	1269	1640	129%	601
NIASHv2111B14	Thinopyrum_bessarabicum_W621890	1269	1607	127%	601
NIASHv2111B14	Thinopyrum_elongatum_PI1109452	1269	1544	122%	601
NIASHv2111B14	Thinopyrum_elongatum_PI401117	1269	1369	108%	601
NIASHv2111B14	Triticum_boeoticum_1613	1269	1796	142%	601
NIASHv2111B14	Triticum_boeoticum_1688	1269	1714	135%	601
NIASHv2111B14	Triticum_boeoticum_ID379	1269	1416	112%	601
NIASHv2111B14	Triticum_boeoticum_PI272520	1269	1515	119%	601
NIASHv2111B14	Triticum_boeoticum_PI427451	1269	1636	129%	601
NIASHv2111B14	Triticum_boeoticum_PI427620	1269	1642	129%	601
NIASHv2111B14	Triticum_monococcum_2205	1269	1624	128%	601
NIASHv2111B14	Triticum_monococcum_2208	1269	1667	131%	601
NIASHv2111B14	Triticum_monococcum_2271	1269	1818	143%	601
NIASHv2111B14	Triticum_monococcum_TR113061	1269	1706	134%	601
NIASHv2111B14	Triticum_monococcum_TR113612	1269	1683	133%	601
NIASHv2111B14	Triticum_urartu_1307	1269	1694	133%	601
NIASHv2111B14	Triticum_urartu_PI428184	1269	1497	118%	601
NIASHv2111B14	Triticum_urartu_PI428317	1269	1422	112%	601
NIASHv2111B14	Triticum_urartu_TR117824	1269	1620	128%	601
NIASHv2111B14	Triticum_urartu_TR118407	1269	1643	129%	601
NIASHv2112C18	Aegilops_bicornis_AE106	2323	2318	100%	601
NIASHv2112C18	Aegilops_bicornis_AE1079	2323	2208	95%	601
NIASHv2112C18	Aegilops_bicornis_AE788	2323	2333	100%	601
NIASHv2112C18	Aegilops_bicornis_KU-5786	2323	2108	91%	601
NIASHv2112C18	Aegilops_comosa_AE1255	2323	2532	109%	601
NIASHv2112C18	Aegilops_comosa_AE1378	2323	2403	103%	601
NIASHv2112C18	Aegilops_comosa_AE783	2323	2510	108%	601
NIASHv2112C18	Aegilops_comosa_PI276970	2323	2372	102%	601
NIASHv2112C18	Aegilops_longissima_AE1078	2323	2222	96%	601
NIASHv2112C18	Aegilops_longissima_AE133	2323	2266	98%	601
NIASHv2112C18	Aegilops_longissima_AE417	2323	2135	92%	601
NIASHv2112C18	Aegilops_longissima_PI604141	2323	1970	85%	601
NIASHv2112C18	Aegilops_longissima_TA1921	2323	2278	98%	601
NIASHv2112C18	Aegilops_markgrafii_AE1381	2323	2342	101%	601
NIASHv2112C18	Aegilops_markgrafii_KP-2012-106	2323	2348	101%	601
NIASHv2112C18	Aegilops_markgrafii_PI254863	2323	2268	98%	601
NIASHv2112C18	Aegilops_markgrafii_PI542208	2323	2339	101%	601
NIASHv2112C18	Aegilops_markgrafii_PI596287	2323	2345	101%	601
NIASHv2112C18	Aegilops_mutica_01C2100106	2323	2362	102%	601
NIASHv2112C18	Aegilops_searsii_AE1075	2323	2203	95%	601
NIASHv2112C18	Aegilops_searsii_AE1083	2323	2349	101%	601
NIASHv2112C18	Aegilops_searsii_KU-14655	2323	2324	100%	601
NIASHv2112C18	Aegilops_searsii_PI599142	2323	2208	95%	601
NIASHv2112C18	Aegilops_searsii_PI599148	2323	1991	86%	601
NIASHv2112C18	Aegilops_sharonensis_AE90691	2323	2302	99%	601
NIASHv2112C18	Aegilops_speltoides_3776	2323	2634	113%	601
NIASHv2112C18	Aegilops_speltoides_AE1064	2323	2337	101%	601
NIASHv2112C18	Aegilops_speltoides_AE900	2323	2342	101%	601
NIASHv2112C18	Aegilops_speltoides_KU-7856	2323	2289	99%	601
NIASHv2112C18	Aegilops_speltoides_PI486264	2323	2451	106%	601
NIASHv2112C18	Aegilops_speltoides_PI487231	2323	2365	102%	601
NIASHv2112C18	Aegilops_speltoides_TA1772	2323	2144	92%	601
NIASHv2112C18	Aegilops_tauschii_49116	2323	2433	105%	601
NIASHv2112C18	Aegilops_tauschii_937	2323	2623	113%	601
NIASHv2112C18	Aegilops_tauschii_AE1069	2323	2396	103%	601
NIASHv2112C18	Aegilops_tauschii_AE956	2323	2445	105%	601
NIASHv2112C18	Aegilops_umbellulata_AE1070	2323	2442	105%	601
NIASHv2112C18	Aegilops_umbellulata_AE153	2323	2356	101%	601
NIASHv2112C18	Aegilops_umbellulata_AE740	2323	2292	99%	601
NIASHv2112C18	Aegilops_umbellulata_AE811	2323	2085	90%	601
NIASHv2112C18	Aegilops_uniaristata_AE157	2323	2377	102%	601
NIASHv2112C18	Aegilops_uniaristata_AE680	2323	2377	102%	601
NIASHv2112C18	Aegilops_uniaristata_PI276996	2323	2334	100%	601
NIASHv2112C18	Agropyron_cristatum_PI494615	2323	2455	106%	601
NIASHv2112C18	Agropyron_cristatum_PI598631	2323	2450	105%	601
NIASHv2112C18	Amblyopyrum_muticum_PI560122	2323	2299	99%	601
NIASHv2112C18	Amblyopyrum_muticum_PI560124	2323	2111	91%	601
NIASHv2112C18	Amblyopyrum_muticum_PI560125	2323	2144	92%	601
NIASHv2112C18	Amblyopyrum_muticum_PI560126	2323	1930	83%	601
NIASHv2112C18	Amblyopyrum_muticum_PI636562	2323	2204	95%	601
NIASHv2112C18	Australopyrum_retrofractum_PI531553	2323	2393	103%	601
NIASHv2112C18	Australopyrum_retrofractum_PI533013	2323	2365	102%	601
NIASHv2112C18	Australopyrum_retrofractum_PI533014	2323	2499	108%	601
NIASHv2112C18	Australopyrum_retrofractum_PI547363	2323	2640	114%	601
NIASHv2112C18	Brachypodium_distachyon	2323	1931	83%	601
NIASHv2112C18	Bromus_tectorum_GRA1085	2323	2065	89%	601
NIASHv2112C18	Dasyphyrum_villosum_GRA1020	2323	2379	102%	601
NIASHv2112C18	Dasyphyrum_villosum_GRA1027	2323	2559	110%	601
NIASHv2112C18	Dasyphyrum_villosum_PI368884	2323	2224	96%	601
NIASHv2112C18	Dasyphyrum_villosum_W619414	2323	2245	97%	601
NIASHv2112C18	Dasyphyrum_villosum_W67300	2323	2448	105%	601

Locus	Accession	Mapped exon length in barley (bp)	Assembled exon length (bp)	% of mapped exon length that could be assembled	Extended target (bp)
NIASHv2112C18	Eremopyrum_distans_PI193264	2323	2412	104%	601
NIASHv2112C18	Eremopyrum_triticeum_GRA2250	2323	2506	108%	601
NIASHv2112C18	Eremopyrum_triticeum_PI502364	2323	2378	102%	601
NIASHv2112C18	Eremopyrum_triticeum_W626631	2323	2264	97%	601
NIASHv2112C18	Henrardia_persica_PI401347	2323	2488	107%	601
NIASHv2112C18	Henrardia_persica_PI577112	2323	2485	107%	601
NIASHv2112C18	Henrardia_persica_PI577113	2323	2381	102%	601
NIASHv2112C18	Henrardia_persica_RF2012	2323	2399	103%	601
NIASHv2112C18	Heterantherium_piliferum_PI401351	2323	2486	107%	601
NIASHv2112C18	Heterantherium_piliferum_PI401353	2323	2525	109%	601
NIASHv2112C18	Heterantherium_piliferum_PI401354	2323	2579	111%	601
NIASHv2112C18	Heterantherium_sp_P1314152	2323	2325	100%	601
NIASHv2112C18	Hordeum_marinum_BCC2006	2323	2660	115%	601
NIASHv2112C18	Hordeum_murinum_BCC2002	2323	2622	113%	601
NIASHv2112C18	Hordeum_pubiflorum_2028	2323	2728	117%	601
NIASHv2112C18	Hordeum_spontaneum_FT11	2323	2867	123%	601
NIASHv2112C18	Hordeum_vulgare_Morex	2323	2757	119%	601
NIASHv2112C18	Psathyrostachys_junceae_PI222050	2323	2495	107%	601
NIASHv2112C18	Psathyrostachys_junceae_PI565077	2323	2314	100%	601
NIASHv2112C18	Psathyrostachys_junceae_PI595135	2323	2487	107%	601
NIASHv2112C18	Psathyrostachys_junceae_PI598613	2323	2422	104%	601
NIASHv2112C18	Psathyrostachys_junceae_PI619487	2323	2556	110%	601
NIASHv2112C18	Psathyrostachys_sp_PI565080	2323	2392	103%	601
NIASHv2112C18	Pseudoroegneria_libanotica_PI228389	2323	2297	99%	601
NIASHv2112C18	Pseudoroegneria_libanotica_PI330688	2323	2429	105%	601
NIASHv2112C18	Pseudoroegneria_libanotica_PI401274	2323	2459	106%	601
NIASHv2112C18	Pseudoroegneria_stipifolia_PI325181	2323	2640	114%	601
NIASHv2112C18	Pseudoroegneria_stipifolia_PI440095	2323	2488	107%	601
NIASHv2112C18	Pseudoroegneria_stipifolia_PI531751	2323	2491	107%	601
NIASHv2112C18	Pseudoroegneria_strigosa_PI499638	2323	2485	107%	601
NIASHv2112C18	Pseudoroegneria_strigosa_PI595172	2323	2455	106%	601
NIASHv2112C18	Pseudoroegneria_strigosa_W614049	2323	2470	106%	601
NIASHv2112C18	Pseudoroegneria_strigosa_PI639805	2323	2435	105%	601
NIASHv2112C18	Pseudoroegneria_strigosa_PI639805	2323	2415	104%	601
NIASHv2112C18	Pseudoroegneria_tauri_PI401322	2323	2406	104%	601
NIASHv2112C18	Pseudoroegneria_tauri_PI401333	2323	2472	106%	601
NIASHv2112C18	Secale_cereale_PI618662	2323	2146	92%	601
NIASHv2112C18	Secale_cereale_PI618665	2323	2348	101%	601
NIASHv2112C18	Secale_cereale_PI618669	2323	2355	101%	601
NIASHv2112C18	Secale_cereale_PI618671	2323	2324	100%	601
NIASHv2112C18	Secale_strictum_R1108	2323	2196	95%	601
NIASHv2112C18	Secale_strictum_R853	2323	2297	99%	601
NIASHv2112C18	Secale_vavilovii_PI253957	2323	1872	81%	601
NIASHv2112C18	Secale_vavilovii_R1027	2323	2153	93%	601
NIASHv2112C18	Taeniatherum_caput-medusae_CK2011	2323	2273	98%	601
NIASHv2112C18	Taeniatherum_caput-medusae_GRA1126	2323	2349	101%	601
NIASHv2112C18	Taeniatherum_caput-medusae_PI220589	2323	2299	99%	601
NIASHv2112C18	Taeniatherum_caput-medusae_PI251387	2323	2210	95%	601
NIASHv2112C18	Taeniatherum_caput-medusae_PI561095	2323	2149	93%	601
NIASHv2112C18	Taeniatherum_crinatum_GRA2570	2323	2364	102%	601
NIASHv2112C18	Thinopyrum_bessarabicum_W621890	2323	2484	107%	601
NIASHv2112C18	Thinopyrum_elongatum_PI109452	2323	2414	104%	601
NIASHv2112C18	Thinopyrum_elongatum_PI401117	2323	2260	97%	601
NIASHv2112C18	Triticum_boeoticum_1613	2323	2358	102%	601
NIASHv2112C18	Triticum_boeoticum_1688	2323	2287	98%	601
NIASHv2112C18	Triticum_boeoticum_ID379	2323	2145	92%	601
NIASHv2112C18	Triticum_boeoticum_PI272520	2323	2238	96%	601
NIASHv2112C18	Triticum_boeoticum_PI427451	2323	2307	99%	601
NIASHv2112C18	Triticum_boeoticum_PI427620	2323	2362	102%	601
NIASHv2112C18	Triticum_monococcum_2205	2323	2302	99%	601
NIASHv2112C18	Triticum_monococcum_2208	2323	2281	98%	601
NIASHv2112C18	Triticum_monococcum_2271	2323	2364	102%	601
NIASHv2112C18	Triticum_monococcum_TRI13061	2323	2281	98%	601
NIASHv2112C18	Triticum_monococcum_TRI13612	2323	2285	98%	601
NIASHv2112C18	Triticum_urartu_1307	2323	2313	100%	601
NIASHv2112C18	Triticum_urartu_PI428184	2323	2293	99%	601
NIASHv2112C18	Triticum_urartu_PI428317	2323	2228	96%	601
NIASHv2112C18	Triticum_urartu_TRI17824	2323	2386	103%	601
NIASHv2112C18	Triticum_urartu_TRI18407	2323	2312	100%	601
NIASHv2140L04	Aegilops_bicornis_AE106	1053	1377	131%	601
NIASHv2140L04	Aegilops_bicornis_AE1079	1053	1010	96%	601
NIASHv2140L04	Aegilops_bicornis_AE788	1053	1315	125%	601
NIASHv2140L04	Aegilops_bicornis_KU-5786	1053	1109	105%	601
NIASHv2140L04	Aegilops_comosa_AE1255	1053	1331	126%	601
NIASHv2140L04	Aegilops_comosa_AE1378	1053	1178	112%	601
NIASHv2140L04	Aegilops_comosa_AE783	1053	1244	118%	601
NIASHv2140L04	Aegilops_comosa_PI276970	1053	1136	108%	601
NIASHv2140L04	Aegilops_longissima_AE1078	1053	1242	118%	601
NIASHv2140L04	Aegilops_longissima_AE133	1053	1312	125%	601
NIASHv2140L04	Aegilops_longissima_AE417	1053	1113	106%	601
NIASHv2140L04	Aegilops_longissima_PI604141	1053	994	94%	601
NIASHv2140L04	Aegilops_longissima_TA1921	1053	1254	119%	601
NIASHv2140L04	Aegilops_markgrafii_AE1381	1053	1316	125%	601
NIASHv2140L04	Aegilops_markgrafii_KP-2012-106	1053	1241	118%	601
NIASHv2140L04	Aegilops_markgrafii_PI254863	1053	1047	99%	601
NIASHv2140L04	Aegilops_markgrafii_PI542208	1053	1366	130%	601

Locus	Accession	Mapped exon length in barley (bp)	Assembled exon length (bp)	% of mapped exon length that could be assembled	Extended target (bp)
NIASHv2140L04	Aegilops_markgrafii_PI596287	1053	1424	135%	601
NIASHv2140L04	Aegilops_mutica_01C2100106	1053	1277	121%	601
NIASHv2140L04	Aegilops_searsii_AE1075	1053	1144	109%	601
NIASHv2140L04	Aegilops_searsii_AE1083	1053	1391	132%	601
NIASHv2140L04	Aegilops_searsii_KU-14655	1053	1344	128%	601
NIASHv2140L04	Aegilops_searsii_PI599142	1053	1242	118%	601
NIASHv2140L04	Aegilops_searsii_PI599148	1053	986	94%	601
NIASHv2140L04	Aegilops_sharonensis_AE90691	1053	1287	122%	601
NIASHv2140L04	Aegilops_speltoides_3776	1053	1383	131%	601
NIASHv2140L04	Aegilops_speltoides_AE1064	1053	1277	121%	601
NIASHv2140L04	Aegilops_speltoides_AE900	1053	1318	125%	601
NIASHv2140L04	Aegilops_speltoides_KU-7856	1053	1177	112%	601
NIASHv2140L04	Aegilops_speltoides_PI486264	1053	1332	126%	601
NIASHv2140L04	Aegilops_speltoides_PI487231	1053	1317	125%	601
NIASHv2140L04	Aegilops_speltoides_TA1772	1053	1217	116%	601
NIASHv2140L04	Aegilops_tauschii_49116	1053	1256	119%	601
NIASHv2140L04	Aegilops_tauschii_937	1053	1436	136%	601
NIASHv2140L04	Aegilops_tauschii_AE1069	1053	1338	127%	601
NIASHv2140L04	Aegilops_tauschii_AE956	1053	1335	127%	601
NIASHv2140L04	Aegilops_umbellulata_AE1070	1053	1282	122%	601
NIASHv2140L04	Aegilops_umbellulata_AE153	1053	1378	131%	601
NIASHv2140L04	Aegilops_umbellulata_AE740	1053	1113	106%	601
NIASHv2140L04	Aegilops_umbellulata_AE811	1053	989	94%	601
NIASHv2140L04	Aegilops_uniaristata_AE157	1053	1311	125%	601
NIASHv2140L04	Aegilops_uniaristata_AE680	1053	1295	123%	601
NIASHv2140L04	Aegilops_uniaristata_PI276996	1053	1086	103%	601
NIASHv2140L04	Agropyron_cristatum_PI494615	1053	1201	114%	601
NIASHv2140L04	Agropyron_cristatum_PI598631	1053	1197	114%	601
NIASHv2140L04	Amblyopyrum_muticum_PI560122	1053	1068	101%	601
NIASHv2140L04	Amblyopyrum_muticum_PI560124	1053	1086	103%	601
NIASHv2140L04	Amblyopyrum_muticum_PI560125	1053	994	94%	601
NIASHv2140L04	Amblyopyrum_muticum_PI560126	1053	889	84%	601
NIASHv2140L04	Amblyopyrum_muticum_PI636562	1053	1273	121%	601
NIASHv2140L04	Australopyrum_retrofractum_PI531553	1053	1233	117%	601
NIASHv2140L04	Australopyrum_retrofractum_PI533013	1053	1136	108%	601
NIASHv2140L04	Australopyrum_retrofractum_PI533014	1053	1327	126%	601
NIASHv2140L04	Australopyrum_retrofractum_PI547363	1053	1334	127%	601
NIASHv2140L04	Brachypodium_distachyon	1053	1079	102%	601
NIASHv2140L04	Bromus_tectorum_GRA1085	1053	1214	115%	601
NIASHv2140L04	Dasypyrum_villosum_GRA1020	1053	1326	126%	601
NIASHv2140L04	Dasypyrum_villosum_GRA1027	1053	1227	117%	601
NIASHv2140L04	Dasypyrum_villosum_PI368884	1053	1121	106%	601
NIASHv2140L04	Dasypyrum_villosum_W619414	1053	1145	109%	601
NIASHv2140L04	Dasypyrum_villosum_W67300	1053	1279	121%	601
NIASHv2140L04	Eremopyrum_distans_PI193264	1053	1225	116%	601
NIASHv2140L04	Eremopyrum_triticeum_GRA2250	1053	1235	117%	601
NIASHv2140L04	Eremopyrum_triticeum_PI502364	1053	1267	120%	601
NIASHv2140L04	Eremopyrum_triticeum_W626631	1053	1147	109%	601
NIASHv2140L04	Henrardia_persica_PI401347	1053	1269	121%	601
NIASHv2140L04	Henrardia_persica_PI577112	1053	1297	123%	601
NIASHv2140L04	Henrardia_persica_PI577113	1053	1171	111%	601
NIASHv2140L04	Henrardia_persica_RF2012	1053	1271	121%	601
NIASHv2140L04	Heteranthelium_piliferum_PI401351	1053	1270	121%	601
NIASHv2140L04	Heteranthelium_piliferum_PI401353	1053	1290	123%	601
NIASHv2140L04	Heteranthelium_piliferum_PI401354	1053	1352	128%	601
NIASHv2140L04	Heteranthelium_sp_PI314152	1053	1092	104%	601
NIASHv2140L04	Hordeum_marinum_BCC2006	1053	1458	138%	601
NIASHv2140L04	Hordeum_murinum_BCC2002	1053	1430	136%	601
NIASHv2140L04	Hordeum_pubiflorum_2028	1053	1533	146%	601
NIASHv2140L04	Hordeum_spontanum_FT11	1053	1654	157%	601
NIASHv2140L04	Hordeum_vulgare_Morex	1053	1634	155%	601
NIASHv2140L04	Psathyrostachys_juncea_PI222050	1053	1282	122%	601
NIASHv2140L04	Psathyrostachys_juncea_PI565077	1053	1131	107%	601
NIASHv2140L04	Psathyrostachys_juncea_PI595135	1053	1248	119%	601
NIASHv2140L04	Psathyrostachys_juncea_PI598613	1053	1285	122%	601
NIASHv2140L04	Psathyrostachys_juncea_PI619487	1053	1356	129%	601
NIASHv2140L04	Psathyrostachys_sp_PI565080	1053	1176	112%	601
NIASHv2140L04	Pseudoroegneria_libanotica_PI228389	1053	1085	103%	601
NIASHv2140L04	Pseudoroegneria_libanotica_PI330688	1053	1189	113%	601
NIASHv2140L04	Pseudoroegneria_libanotica_PI401274	1053	1297	123%	601
NIASHv2140L04	Pseudoroegneria_stipifolia_PI325181	1053	1335	127%	601
NIASHv2140L04	Pseudoroegneria_stipifolia_PI440095	1053	1302	124%	601
NIASHv2140L04	Pseudoroegneria_stipifolia_PI531751	1053	1195	113%	601
NIASHv2140L04	Pseudoroegneria_strigosa_PI499638	1053	1249	119%	601
NIASHv2140L04	Pseudoroegneria_strigosa_PI595172	1053	1293	123%	601
NIASHv2140L04	Pseudoroegneria_strigosa_W614049	1053	1324	126%	601
NIASHv2140L04	Pseudoroegneria_strigosa_PI639805	1053	1265	120%	601
NIASHv2140L04	Pseudoroegneria_strigosa_PI639805	1053	1251	119%	601
NIASHv2140L04	Pseudoroegneria_tauri_PI401322	1053	1175	112%	601
NIASHv2140L04	Pseudoroegneria_tauri_PI401333	1053	1243	118%	601
NIASHv2140L04	Secale_cereale_PI618662	1053	1057	100%	601
NIASHv2140L04	Secale_cereale_PI618665	1053	1185	113%	601
NIASHv2140L04	Secale_cereale_PI618669	1053	1307	124%	601
NIASHv2140L04	Secale_cereale_PI618671	1053	1329	126%	601
NIASHv2140L04	Secale_strictum_R1108	1053	1146	109%	601
NIASHv2140L04	Secale_strictum_R853	1053	1296	123%	601

Locus	Accession	Mapped exon length in barley (bp)	Assembled exon length (bp)	% of mapped exon length that could be assembled	Extended target (bp)
NIASHv2140L04	Secale_vavilovii_PI253957	1053	1140	108%	601
NIASHv2140L04	Secale_vavilovii_R1027	1053	1072	102%	601
NIASHv2140L04	Taeniatherum_caput-medusae_CK2011	1053	1305	124%	601
NIASHv2140L04	Taeniatherum_caput-medusae_GRA1126	1053	1360	129%	601
NIASHv2140L04	Taeniatherum_caput-medusae_PI220589	1053	1322	126%	601
NIASHv2140L04	Taeniatherum_caput-medusae_PI251387	1053	1134	108%	601
NIASHv2140L04	Taeniatherum_caput-medusae_PI561095	1053	1057	100%	601
NIASHv2140L04	Taeniatherum_crinium_GRA2570	1053	1374	130%	601
NIASHv2140L04	Thinopyrum_bessarabicum_W621890	1053	1213	115%	601
NIASHv2140L04	Thinopyrum_elongatum_PI109452	1053	1364	130%	601
NIASHv2140L04	Thinopyrum_elongatum_PI401117	1053	1118	106%	601
NIASHv2140L04	Triticum_boeoticum_1613	1053	1481	141%	601
NIASHv2140L04	Triticum_boeoticum_1688	1053	1313	125%	601
NIASHv2140L04	Triticum_boeoticum_ID379	1053	1149	109%	601
NIASHv2140L04	Triticum_boeoticum_PI272520	1053	1238	118%	601
NIASHv2140L04	Triticum_boeoticum_PI427451	1053	1342	127%	601
NIASHv2140L04	Triticum_boeoticum_PI427620	1053	1332	126%	601
NIASHv2140L04	Triticum_monococcum_2205	1053	1334	127%	601
NIASHv2140L04	Triticum_monococcum_2208	1053	1293	123%	601
NIASHv2140L04	Triticum_monococcum_2271	1053	1431	136%	601
NIASHv2140L04	Triticum_monococcum_TRI13061	1053	1259	120%	601
NIASHv2140L04	Triticum_monococcum_TRI13612	1053	1261	120%	601
NIASHv2140L04	Triticum_urartu_1307	1053	1460	139%	601
NIASHv2140L04	Triticum_urartu_PI428184	1053	1120	106%	601
NIASHv2140L04	Triticum_urartu_PI428317	1053	1085	103%	601
NIASHv2140L04	Triticum_urartu_TRI17824	1053	1365	130%	601
NIASHv2140L04	Triticum_urartu_TRI18407	1053	1337	127%	601
NIASHv2142K13	Aegilops_bicornis_AE106	2637	1796	68%	601
NIASHv2142K13	Aegilops_bicornis_AE1079	2637	1468	56%	601
NIASHv2142K13	Aegilops_bicornis_AE788	2637	1663	63%	601
NIASHv2142K13	Aegilops_bicornis_KU-5786	2637	1516	57%	601
NIASHv2142K13	Aegilops_comosa_AE1255	2637	1717	65%	601
NIASHv2142K13	Aegilops_comosa_AE1378	2637	1615	61%	601
NIASHv2142K13	Aegilops_comosa_AE783	2637	1738	66%	601
NIASHv2142K13	Aegilops_comosa_PI276970	2637	1534	58%	601
NIASHv2142K13	Aegilops_longissima_AE1078	2637	1606	61%	601
NIASHv2142K13	Aegilops_longissima_AE133	2637	1642	62%	601
NIASHv2142K13	Aegilops_longissima_AE417	2637	1486	56%	601
NIASHv2142K13	Aegilops_longissima_PI604141	2637	1415	54%	601
NIASHv2142K13	Aegilops_longissima_TA1921	2637	1677	64%	601
NIASHv2142K13	Aegilops_markgrafii_AE1381	2637	1757	67%	601
NIASHv2142K13	Aegilops_markgrafii_KP-2012-106	2637	1653	63%	601
NIASHv2142K13	Aegilops_markgrafii_PI254863	2637	1578	60%	601
NIASHv2142K13	Aegilops_markgrafii_PI542208	2637	1737	66%	601
NIASHv2142K13	Aegilops_markgrafii_PI596287	2637	1764	67%	601
NIASHv2142K13	Aegilops_mutica_01C2100106	2637	1704	65%	601
NIASHv2142K13	Aegilops_searsii_AE1075	2637	1621	61%	601
NIASHv2142K13	Aegilops_searsii_AE1083	2637	1775	67%	601
NIASHv2142K13	Aegilops_searsii_KU-14655	2637	1787	68%	601
NIASHv2142K13	Aegilops_searsii_PI599142	2637	1599	61%	601
NIASHv2142K13	Aegilops_searsii_PI599148	2637	1191	45%	601
NIASHv2142K13	Aegilops_sharonensis_AE90691	2637	1650	63%	601
NIASHv2142K13	Aegilops_speltoides_3776	2637	1768	67%	601
NIASHv2142K13	Aegilops_speltoides_AE1064	2637	1718	65%	601
NIASHv2142K13	Aegilops_speltoides_AE900	2637	1575	60%	601
NIASHv2142K13	Aegilops_speltoides_KU-7856	2637	1641	62%	601
NIASHv2142K13	Aegilops_speltoides_PI486264	2637	1723	65%	601
NIASHv2142K13	Aegilops_speltoides_PI487231	2637	1697	64%	601
NIASHv2142K13	Aegilops_speltoides_TA1772	2637	1409	53%	601
NIASHv2142K13	Aegilops_tauschii_49116	2637	1587	60%	601
NIASHv2142K13	Aegilops_tauschii_937	2637	1920	73%	601
NIASHv2142K13	Aegilops_tauschii_AE1069	2637	1716	65%	601
NIASHv2142K13	Aegilops_tauschii_AE956	2637	1723	65%	601
NIASHv2142K13	Aegilops_umbellulata_AE1070	2637	1642	62%	601
NIASHv2142K13	Aegilops_umbellulata_AE153	2637	925	35%	601
NIASHv2142K13	Aegilops_umbellulata_AE740	2637	1413	54%	601
NIASHv2142K13	Aegilops_umbellulata_AE811	2637	1444	55%	601
NIASHv2142K13	Aegilops_uniaristata_AE157	2637	1925	73%	601
NIASHv2142K13	Aegilops_uniaristata_AE680	2637	1763	67%	601
NIASHv2142K13	Aegilops_uniaristata_PI276996	2637	1615	61%	601
NIASHv2142K13	Agropyron_cristatum_PI494615	2637	1706	65%	601
NIASHv2142K13	Agropyron_cristatum_PI598631	2637	1702	65%	601
NIASHv2142K13	Amblyopyrum_muticum_PI560122	2637	1474	56%	601
NIASHv2142K13	Amblyopyrum_muticum_PI560124	2637	1568	59%	601
NIASHv2142K13	Amblyopyrum_muticum_PI560125	2637	1352	51%	601
NIASHv2142K13	Amblyopyrum_muticum_PI560126	2637	1348	51%	601
NIASHv2142K13	Amblyopyrum_muticum_PI636562	2637	1553	59%	601
NIASHv2142K13	Australopyrum_retrofractum_PI531553	2637	1554	59%	601
NIASHv2142K13	Australopyrum_retrofractum_PI533013	2637	1487	56%	601
NIASHv2142K13	Australopyrum_retrofractum_PI533014	2637	1663	63%	601
NIASHv2142K13	Australopyrum_retrofractum_PI547363	2637	1772	67%	601
NIASHv2142K13	Brachypodium_distachyon	2637	893	34%	601
NIASHv2142K13	Bromus_tectorum_GRA1085	2637	800	30%	601
NIASHv2142K13	Dasyphyrum_villosum_GRA1020	2637	1343	51%	601
NIASHv2142K13	Dasyphyrum_villosum_GRA1027	2637	1371	52%	601
NIASHv2142K13	Dasyphyrum_villosum_PI368884	2637	1188	45%	601

Locus	Accession	Mapped exon length in barley (bp)	Assembled exon length (bp)	% of mapped exon length that could be assembled	Extended target (bp)
NIASHv2142K13	Dasypyrum_villosum_W619414	2637	1299	49%	601
NIASHv2142K13	Dasypyrum_villosum_W67300	2637	1381	52%	601
NIASHv2142K13	Eremopyrum_distans_PI193264	2637	1498	57%	601
NIASHv2142K13	Eremopyrum_triticeum_GRA2250	2637	0	0%	601
NIASHv2142K13	Eremopyrum_triticeum_PI502364	2637	0	0%	601
NIASHv2142K13	Eremopyrum_triticeum_W626631	2637	0	0%	601
NIASHv2142K13	Henrardia_persica_PI401347	2637	1630	62%	601
NIASHv2142K13	Henrardia_persica_PI577112	2637	1708	65%	601
NIASHv2142K13	Henrardia_persica_PI577113	2637	1536	58%	601
NIASHv2142K13	Henrardia_persica_RF2012	2637	1557	59%	601
NIASHv2142K13	Heterantherium_piliferum_PI401351	2637	1804	68%	601
NIASHv2142K13	Heterantherium_piliferum_PI401353	2637	1801	68%	601
NIASHv2142K13	Heterantherium_piliferum_PI401354	2637	1796	68%	601
NIASHv2142K13	Heterantherium_sp_PI314152	2637	1656	63%	601
NIASHv2142K13	Hordeum_marinum_BCC2006	2637	1089	41%	601
NIASHv2142K13	Hordeum_murinum_BCC2002	2637	1764	67%	601
NIASHv2142K13	Hordeum_pubiflorum_2028	2637	1889	72%	601
NIASHv2142K13	Hordeum_spontaneum_FT11	2637	2406	91%	601
NIASHv2142K13	Hordeum_vulgare_Morex	2637	2415	92%	601
NIASHv2142K13	Psathyrostachys_junceae_PI222050	2637	652	25%	601
NIASHv2142K13	Psathyrostachys_junceae_PI565077	2637	778	30%	601
NIASHv2142K13	Psathyrostachys_junceae_PI595135	2637	805	31%	601
NIASHv2142K13	Psathyrostachys_junceae_PI598613	2637	786	30%	601
NIASHv2142K13	Psathyrostachys_junceae_PI619487	2637	887	34%	601
NIASHv2142K13	Psathyrostachys_sp_PI565080	2637	1308	50%	601
NIASHv2142K13	Pseudoroegneria_libanotica_PI228389	2637	1291	49%	601
NIASHv2142K13	Pseudoroegneria_libanotica_PI330688	2637	1380	52%	601
NIASHv2142K13	Pseudoroegneria_libanotica_PI401274	2637	1477	56%	601
NIASHv2142K13	Pseudoroegneria_stipifolia_PI325181	2637	1547	59%	601
NIASHv2142K13	Pseudoroegneria_stipifolia_PI440095	2637	1427	54%	601
NIASHv2142K13	Pseudoroegneria_stipifolia_PI531751	2637	1478	56%	601
NIASHv2142K13	Pseudoroegneria_strigosa_PI499638	2637	1484	56%	601
NIASHv2142K13	Pseudoroegneria_strigosa_PI595172	2637	1637	62%	601
NIASHv2142K13	Pseudoroegneria_strigosa_W614049	2637	1477	56%	601
NIASHv2142K13	Pseudoroegneria_strigosa_PI639805	2637	1385	53%	601
NIASHv2142K13	Pseudoroegneria_strigosa_PI639805	2637	1581	60%	601
NIASHv2142K13	Pseudoroegneria_tauri_PI401322	2637	1317	50%	601
NIASHv2142K13	Pseudoroegneria_tauri_PI401333	2637	1294	49%	601
NIASHv2142K13	Secale_cereale_PI618662	2637	1330	50%	601
NIASHv2142K13	Secale_cereale_PI618665	2637	1122	43%	601
NIASHv2142K13	Secale_cereale_PI618669	2637	1396	53%	601
NIASHv2142K13	Secale_cereale_PI618671	2637	1292	49%	601
NIASHv2142K13	Secale_strictum_R1108	2637	1295	49%	601
NIASHv2142K13	Secale_strictum_R853	2637	1641	62%	601
NIASHv2142K13	Secale_vavilovii_PI253957	2637	1021	39%	601
NIASHv2142K13	Secale_vavilovii_R1027	2637	1404	53%	601
NIASHv2142K13	Taeniatherum_caput-medusae_CK2011	2637	1433	54%	601
NIASHv2142K13	Taeniatherum_caput-medusae_GRA1126	2637	1411	54%	601
NIASHv2142K13	Taeniatherum_caput-medusae_PI220589	2637	1347	51%	601
NIASHv2142K13	Taeniatherum_caput-medusae_PI251387	2637	1131	43%	601
NIASHv2142K13	Taeniatherum_caput-medusae_PI561095	2637	1068	41%	601
NIASHv2142K13	Taeniatherum_crininum_GRA2570	2637	1328	50%	601
NIASHv2142K13	Thinopyrum_besarabicum_W621890	2637	1591	60%	601
NIASHv2142K13	Thinopyrum_elongatum_PI109452	2637	1574	60%	601
NIASHv2142K13	Thinopyrum_elongatum_PI401117	2637	1460	55%	601
NIASHv2142K13	Triticum_boeoticum_1613	2637	2058	78%	601
NIASHv2142K13	Triticum_boeoticum_1688	2637	1851	70%	601
NIASHv2142K13	Triticum_boeoticum_ID379	2637	1591	60%	601
NIASHv2142K13	Triticum_boeoticum_PI272520	2637	1610	61%	601
NIASHv2142K13	Triticum_boeoticum_PI427451	2637	1763	67%	601
NIASHv2142K13	Triticum_boeoticum_PI427620	2637	1703	65%	601
NIASHv2142K13	Triticum_monococcum_2205	2637	1691	64%	601
NIASHv2142K13	Triticum_monococcum_2208	2637	1726	65%	601
NIASHv2142K13	Triticum_monococcum_2271	2637	1990	75%	601
NIASHv2142K13	Triticum_monococcum_TR113061	2637	1745	66%	601
NIASHv2142K13	Triticum_monococcum_TR113612	2637	1748	66%	601
NIASHv2142K13	Triticum_urartu_1307	2637	1891	72%	601
NIASHv2142K13	Triticum_urartu_PI428184	2637	1521	58%	601
NIASHv2142K13	Triticum_urartu_PI428317	2637	1528	58%	601
NIASHv2142K13	Triticum_urartu_TR117824	2637	1690	64%	601
NIASHv2142K13	Triticum_urartu_TR118407	2637	1830	69%	601
NIASHv2146E11	Aegilops_bicornis_AE106	1329	1469	111%	601
NIASHv2146E11	Aegilops_bicornis_AE1079	1329	1212	91%	601
NIASHv2146E11	Aegilops_bicornis_AE788	1329	1391	105%	601
NIASHv2146E11	Aegilops_bicornis_KU-5786	1329	1113	84%	601
NIASHv2146E11	Aegilops_comosa_AE1255	1329	1491	112%	601
NIASHv2146E11	Aegilops_comosa_AE1378	1329	1400	105%	601
NIASHv2146E11	Aegilops_comosa_AE783	1329	1367	103%	601
NIASHv2146E11	Aegilops_comosa_PI276970	1329	1254	94%	601
NIASHv2146E11	Aegilops_longissima_AE1078	1329	1303	98%	601
NIASHv2146E11	Aegilops_longissima_AE133	1329	1504	113%	601
NIASHv2146E11	Aegilops_longissima_AE417	1329	1212	91%	601
NIASHv2146E11	Aegilops_longissima_PI604141	1329	1044	79%	601
NIASHv2146E11	Aegilops_longissima_TA1921	1329	1406	106%	601
NIASHv2146E11	Aegilops_markgrafii_AE1381	1329	1445	109%	601
NIASHv2146E11	Aegilops_markgrafii_KP-2012-106	1329	1543	116%	601

Locus	Accession	Mapped exon length in barley (bp)	Assembled exon length (bp)	% of mapped exon length that could be assembled	Extended target (bp)
NIASHv2146E11	Aegilops_markgrafii_PI254863	1329	1300	98%	601
NIASHv2146E11	Aegilops_markgrafii_PI542208	1329	1521	114%	601
NIASHv2146E11	Aegilops_markgrafii_PI596287	1329	1492	112%	601
NIASHv2146E11	Aegilops_mutica_01C2100106	1329	1448	109%	601
NIASHv2146E11	Aegilops_searsii_AE1075	1329	1339	101%	601
NIASHv2146E11	Aegilops_searsii_AE1083	1329	1578	119%	601
NIASHv2146E11	Aegilops_searsii_KU-14655	1329	1543	116%	601
NIASHv2146E11	Aegilops_searsii_PI599142	1329	1353	102%	601
NIASHv2146E11	Aegilops_searsii_PI599148	1329	1165	88%	601
NIASHv2146E11	Aegilops_sharonensis_AE90691	1329	1413	106%	601
NIASHv2146E11	Aegilops_speltoides_3776	1329	1623	122%	601
NIASHv2146E11	Aegilops_speltoides_AE1064	1329	1407	106%	601
NIASHv2146E11	Aegilops_speltoides_AE900	1329	1332	100%	601
NIASHv2146E11	Aegilops_speltoides_KU-7856	1329	1267	95%	601
NIASHv2146E11	Aegilops_speltoides_PI486264	1329	1479	111%	601
NIASHv2146E11	Aegilops_speltoides_PI487231	1329	1343	101%	601
NIASHv2146E11	Aegilops_speltoides_TA1772	1329	1310	99%	601
NIASHv2146E11	Aegilops_tauschii_49116	1329	1347	101%	601
NIASHv2146E11	Aegilops_tauschii_937	1329	1726	130%	601
NIASHv2146E11	Aegilops_tauschii_AE1069	1329	1374	103%	601
NIASHv2146E11	Aegilops_tauschii_AE956	1329	1476	111%	601
NIASHv2146E11	Aegilops_umbellulata_AE1070	1329	1475	111%	601
NIASHv2146E11	Aegilops_umbellulata_AE153	1329	1515	114%	601
NIASHv2146E11	Aegilops_umbellulata_AE740	1329	1301	98%	601
NIASHv2146E11	Aegilops_umbellulata_AE811	1329	1006	76%	601
NIASHv2146E11	Aegilops_uniaristata_AE157	1329	1538	116%	601
NIASHv2146E11	Aegilops_uniaristata_AE680	1329	1509	114%	601
NIASHv2146E11	Aegilops_uniaristata_PI276996	1329	1340	101%	601
NIASHv2146E11	Agropyron_cristatum_PI494615	1329	1538	116%	601
NIASHv2146E11	Agropyron_cristatum_PI598631	1329	1482	112%	601
NIASHv2146E11	Amblyopyrum_muticum_PI560122	1329	1070	81%	601
NIASHv2146E11	Amblyopyrum_muticum_PI560124	1329	1164	88%	601
NIASHv2146E11	Amblyopyrum_muticum_PI560125	1329	1234	93%	601
NIASHv2146E11	Amblyopyrum_muticum_PI560126	1329	1078	81%	601
NIASHv2146E11	Amblyopyrum_muticum_PI636562	1329	1421	107%	601
NIASHv2146E11	Australopyrum_retrofractum_PI531553	1329	1455	109%	601
NIASHv2146E11	Australopyrum_retrofractum_PI533013	1329	1514	114%	601
NIASHv2146E11	Australopyrum_retrofractum_PI533014	1329	1609	121%	601
NIASHv2146E11	Australopyrum_retrofractum_PI547363	1329	1636	123%	601
NIASHv2146E11	Brachypodium_distachyon	1329	796	60%	601
NIASHv2146E11	Bromus_tectorum_GRA1085	1329	1319	99%	601
NIASHv2146E11	Dasyphyrum_villosum_GRA1020	1329	1371	103%	601
NIASHv2146E11	Dasyphyrum_villosum_GRA1027	1329	1417	107%	601
NIASHv2146E11	Dasyphyrum_villosum_PI368884	1329	1282	96%	601
NIASHv2146E11	Dasyphyrum_villosum_W619414	1329	1156	87%	601
NIASHv2146E11	Dasyphyrum_villosum_W67300	1329	1435	108%	601
NIASHv2146E11	Eremopyrum_distans_PI193264	1329	1514	114%	601
NIASHv2146E11	Eremopyrum_triticeum_GRA2250	1329	1488	112%	601
NIASHv2146E11	Eremopyrum_triticeum_PI502364	1329	1490	112%	601
NIASHv2146E11	Eremopyrum_triticeum_W626631	1329	1407	106%	601
NIASHv2146E11	Henrardia_persica_PI401347	1329	1419	107%	601
NIASHv2146E11	Henrardia_persica_PI577112	1329	1550	117%	601
NIASHv2146E11	Henrardia_persica_PI577113	1329	1427	107%	601
NIASHv2146E11	Henrardia_persica_RF2012	1329	1415	106%	601
NIASHv2146E11	Heteranthelium_piliferum_PI401351	1329	1436	108%	601
NIASHv2146E11	Heteranthelium_piliferum_PI401353	1329	1477	111%	601
NIASHv2146E11	Heteranthelium_piliferum_PI401354	1329	1535	116%	601
NIASHv2146E11	Heteranthelium_sp_PI314152	1329	1442	109%	601
NIASHv2146E11	Hordeum_marinum_BCC2006	1329	1547	116%	601
NIASHv2146E11	Hordeum_murinum_BCC2002	1329	1706	128%	601
NIASHv2146E11	Hordeum_pubiflorum_2028	1329	1799	135%	601
NIASHv2146E11	Hordeum_spontaneum_FT11	1329	1915	144%	601
NIASHv2146E11	Hordeum_vulgare_Morex	1329	1907	143%	601
NIASHv2146E11	Psathyrostachys_junceae_PI222050	1329	1417	107%	601
NIASHv2146E11	Psathyrostachys_junceae_PI565077	1329	1378	104%	601
NIASHv2146E11	Psathyrostachys_junceae_PI595135	1329	1518	114%	601
NIASHv2146E11	Psathyrostachys_junceae_PI598613	1329	1521	114%	601
NIASHv2146E11	Psathyrostachys_junceae_PI619487	1329	1569	118%	601
NIASHv2146E11	Psathyrostachys_sp_PI565080	1329	1411	106%	601
NIASHv2146E11	Pseudoroegneria_libanotica_PI228389	1329	1295	97%	601
NIASHv2146E11	Pseudoroegneria_libanotica_PI330688	1329	1388	104%	601
NIASHv2146E11	Pseudoroegneria_libanotica_PI401274	1329	1441	108%	601
NIASHv2146E11	Pseudoroegneria_stipifolia_PI325181	1329	1521	114%	601
NIASHv2146E11	Pseudoroegneria_stipifolia_PI440095	1329	1502	113%	601
NIASHv2146E11	Pseudoroegneria_stipifolia_PI531751	1329	1489	112%	601
NIASHv2146E11	Pseudoroegneria_strigosa_PI499638	1329	1466	110%	601
NIASHv2146E11	Pseudoroegneria_strigosa_PI595172	1329	1380	104%	601
NIASHv2146E11	Pseudoroegneria_strigosa_W614049	1329	1527	115%	601
NIASHv2146E11	Pseudoroegneria_strigosa_PI639805	1329	1511	114%	601
NIASHv2146E11	Pseudoroegneria_strigosa_PI639805	1329	1425	107%	601
NIASHv2146E11	Pseudoroegneria_tauri_PI401322	1329	1210	91%	601
NIASHv2146E11	Pseudoroegneria_tauri_PI401333	1329	1437	108%	601
NIASHv2146E11	Secale_cereale_PI618662	1329	1114	84%	601
NIASHv2146E11	Secale_cereale_PI618665	1329	1283	97%	601
NIASHv2146E11	Secale_cereale_PI618669	1329	1537	116%	601
NIASHv2146E11	Secale_cereale_PI618671	1329	1471	111%	601

Locus	Accession	Mapped exon length in barley (bp)	Assembled exon length (bp)	% of mapped exon length that could be assembled	Extended target (bp)
NIASHv2146E11	Secale_strictum_R1108	1329	1318	99%	601
NIASHv2146E11	Secale_strictum_R853	1329	1413	106%	601
NIASHv2146E11	Secale_vavilovii_P1253957	1329	1160	87%	601
NIASHv2146E11	Secale_vavilovii_R1027	1329	1235	93%	601
NIASHv2146E11	Taeniatherum_caput-medusae_CK2011	1329	1449	109%	601
NIASHv2146E11	Taeniatherum_caput-medusae_GRA1126	1329	1553	117%	601
NIASHv2146E11	Taeniatherum_caput-medusae_PI220589	1329	1409	106%	601
NIASHv2146E11	Taeniatherum_caput-medusae_PI251387	1329	1108	83%	601
NIASHv2146E11	Taeniatherum_caput-medusae_PI561095	1329	1024	77%	601
NIASHv2146E11	Taeniatherum_crinium_GRA2570	1329	1455	109%	601
NIASHv2146E11	Thinopyrum_bessarabicum_W621890	1329	1374	103%	601
NIASHv2146E11	Thinopyrum_elongatum_PI109452	1329	1439	108%	601
NIASHv2146E11	Thinopyrum_elongatum_PI401117	1329	1282	96%	601
NIASHv2146E11	Triticum_boeoticum_1613	1329	1664	125%	601
NIASHv2146E11	Triticum_boeoticum_1688	1329	1494	112%	601
NIASHv2146E11	Triticum_boeoticum_ID379	1329	1240	93%	601
NIASHv2146E11	Triticum_boeoticum_PI272520	1329	1395	105%	601
NIASHv2146E11	Triticum_boeoticum_PI427451	1329	1490	112%	601
NIASHv2146E11	Triticum_boeoticum_PI427620	1329	1463	110%	601
NIASHv2146E11	Triticum_monococcum_2205	1329	1620	122%	601
NIASHv2146E11	Triticum_monococcum_2208	1329	1450	109%	601
NIASHv2146E11	Triticum_monococcum_2271	1329	1682	127%	601
NIASHv2146E11	Triticum_monococcum_TRI13061	1329	1529	115%	601
NIASHv2146E11	Triticum_monococcum_TRI13612	1329	1542	116%	601
NIASHv2146E11	Triticum_urartu_1307	1329	1593	120%	601
NIASHv2146E11	Triticum_urartu_PI428184	1329	1430	108%	601
NIASHv2146E11	Triticum_urartu_PI428317	1329	1032	78%	601
NIASHv2146E11	Triticum_urartu_TRI17824	1329	1537	116%	601
NIASHv2146E11	Triticum_urartu_TRI18407	1329	1530	115%	601
NIASHv3078O01	Aegilops_bicornis_AE106	1488	1513	102%	601
NIASHv3078O01	Aegilops_bicornis_AE1079	1488	1174	79%	601
NIASHv3078O01	Aegilops_bicornis_AE788	1488	1497	101%	601
NIASHv3078O01	Aegilops_bicornis_KU-5786	1488	1193	80%	601
NIASHv3078O01	Aegilops_comosa_AE1255	1488	1566	105%	601
NIASHv3078O01	Aegilops_comosa_AE1378	1488	1456	98%	601
NIASHv3078O01	Aegilops_comosa_AE783	1488	1525	102%	601
NIASHv3078O01	Aegilops_comosa_PI276970	1488	1243	84%	601
NIASHv3078O01	Aegilops_longissima_AE1078	1488	1390	93%	601
NIASHv3078O01	Aegilops_longissima_AE133	1488	1421	95%	601
NIASHv3078O01	Aegilops_longissima_AE417	1488	1087	73%	601
NIASHv3078O01	Aegilops_longissima_PI604141	1488	1128	76%	601
NIASHv3078O01	Aegilops_longissima_TA1921	1488	1410	95%	601
NIASHv3078O01	Aegilops_markgrafii_AE1381	1488	1505	101%	601
NIASHv3078O01	Aegilops_markgrafii_KP-2012-106	1488	1489	100%	601
NIASHv3078O01	Aegilops_markgrafii_PI254863	1488	1309	88%	601
NIASHv3078O01	Aegilops_markgrafii_PI542208	1488	1510	101%	601
NIASHv3078O01	Aegilops_markgrafii_PI596287	1488	1445	97%	601
NIASHv3078O01	Aegilops_mutica_01C2100106	1488	1459	98%	601
NIASHv3078O01	Aegilops_searsii_AE1075	1488	1382	93%	601
NIASHv3078O01	Aegilops_searsii_AE1083	1488	1501	101%	601
NIASHv3078O01	Aegilops_searsii_KU-14655	1488	1443	97%	601
NIASHv3078O01	Aegilops_searsii_PI599142	1488	1362	92%	601
NIASHv3078O01	Aegilops_searsii_PI599148	1488	888	60%	601
NIASHv3078O01	Aegilops_sharonensis_AE90691	1488	1445	97%	601
NIASHv3078O01	Aegilops_speltoides_3776	1488	1627	109%	601
NIASHv3078O01	Aegilops_speltoides_AE1064	1488	1462	98%	601
NIASHv3078O01	Aegilops_speltoides_AE900	1488	1399	94%	601
NIASHv3078O01	Aegilops_speltoides_KU-7856	1488	1416	95%	601
NIASHv3078O01	Aegilops_speltoides_PI486264	1488	1420	95%	601
NIASHv3078O01	Aegilops_speltoides_PI487231	1488	1396	94%	601
NIASHv3078O01	Aegilops_speltoides_TA1772	1488	1384	93%	601
NIASHv3078O01	Aegilops_tauschii_49116	1488	1311	88%	601
NIASHv3078O01	Aegilops_tauschii_937	1488	1510	101%	601
NIASHv3078O01	Aegilops_tauschii_AE1069	1488	1419	95%	601
NIASHv3078O01	Aegilops_tauschii_AE956	1488	1481	100%	601
NIASHv3078O01	Aegilops_umbellulata_AE1070	1488	1443	97%	601
NIASHv3078O01	Aegilops_umbellulata_AE153	1488	1483	100%	601
NIASHv3078O01	Aegilops_umbellulata_AE740	1488	1227	82%	601
NIASHv3078O01	Aegilops_umbellulata_AE811	1488	931	63%	601
NIASHv3078O01	Aegilops_uniaristata_AE157	1488	1535	103%	601
NIASHv3078O01	Aegilops_uniaristata_AE680	1488	1524	102%	601
NIASHv3078O01	Aegilops_uniaristata_PI276996	1488	1356	91%	601
NIASHv3078O01	Agropyron_cristatum_PI494615	1488	1429	96%	601
NIASHv3078O01	Agropyron_cristatum_PI598631	1488	1353	91%	601
NIASHv3078O01	Amblyopyrum_muticum_PI560122	1488	1129	76%	601
NIASHv3078O01	Amblyopyrum_muticum_PI560124	1488	936	63%	601
NIASHv3078O01	Amblyopyrum_muticum_PI560125	1488	1186	80%	601
NIASHv3078O01	Amblyopyrum_muticum_PI560126	1488	1014	68%	601
NIASHv3078O01	Amblyopyrum_muticum_PI636562	1488	1424	95%	601
NIASHv3078O01	Australopyrum_retrofractum_PI531553	1488	1490	107%	601
NIASHv3078O01	Australopyrum_retrofractum_PI533013	1488	1570	106%	601
NIASHv3078O01	Australopyrum_retrofractum_PI533014	1488	1511	102%	601
NIASHv3078O01	Australopyrum_retrofractum_PI547363	1488	1631	110%	601
NIASHv3078O01	Brachypodium_distachyon	1488	1048	70%	601
NIASHv3078O01	Bromus_tectorum_GRA1085	1488	1345	90%	601
NIASHv3078O01	Dasyphyrum_villosum_GRA1020	1488	1332	90%	601

Locus	Accession	Mapped exon length in barley (bp)	Assembled exon length (bp)	% of mapped exon length that could be assembled	Extended target (bp)
NIASHv3078001	Dasypyrum_villosum_GRA1027	1488	1432	96%	601
NIASHv3078001	Dasypyrum_villosum_PI368884	1488	1288	87%	601
NIASHv3078001	Dasypyrum_villosum_W619414	1488	930	63%	601
NIASHv3078001	Dasypyrum_villosum_W67300	1488	1463	98%	601
NIASHv3078001	Eremopyrum_distans_PI193264	1488	1391	93%	601
NIASHv3078001	Eremopyrum_triticeum_GRA2250	1488	1476	99%	601
NIASHv3078001	Eremopyrum_triticeum_PI502364	1488	1383	93%	601
NIASHv3078001	Eremopyrum_triticeum_W626631	1488	1252	84%	601
NIASHv3078001	Henrardia_persica_PI401347	1488	1454	98%	601
NIASHv3078001	Henrardia_persica_PI577112	1488	1521	102%	601
NIASHv3078001	Henrardia_persica_PI577113	1488	1400	94%	601
NIASHv3078001	Henrardia_persica_RF2012	1488	1524	102%	601
NIASHv3078001	Heteranthelium_piliferum_PI401351	1488	1432	96%	601
NIASHv3078001	Heteranthelium_piliferum_PI401353	1488	1456	98%	601
NIASHv3078001	Heteranthelium_piliferum_PI401354	1488	1504	101%	601
NIASHv3078001	Heteranthelium_sp_PI314152	1488	1494	100%	601
NIASHv3078001	Hordeum_marinum_BCC2006	1488	1410	95%	601
NIASHv3078001	Hordeum_murinum_BCC2002	1488	1742	117%	601
NIASHv3078001	Hordeum_pubiflorum_2028	1488	1859	125%	601
NIASHv3078001	Hordeum_spontaneum_FT11	1488	2063	139%	601
NIASHv3078001	Hordeum_vulgare_Morex	1488	1965	132%	601
NIASHv3078001	Psathyrostachys_junceae_PI222050	1488	1429	96%	601
NIASHv3078001	Psathyrostachys_junceae_PI565077	1488	1115	75%	601
NIASHv3078001	Psathyrostachys_junceae_PI595135	1488	1542	104%	601
NIASHv3078001	Psathyrostachys_junceae_PI598613	1488	1498	101%	601
NIASHv3078001	Psathyrostachys_junceae_PI619487	1488	1440	97%	601
NIASHv3078001	Psathyrostachys_sp_PI565080	1488	1543	104%	601
NIASHv3078001	Pseudoroegneria_libanotica_PI228389	1488	1347	91%	601
NIASHv3078001	Pseudoroegneria_libanotica_PI330688	1488	1499	101%	601
NIASHv3078001	Pseudoroegneria_libanotica_PI401274	1488	1498	101%	601
NIASHv3078001	Pseudoroegneria_stipifolia_PI325181	1488	1516	102%	601
NIASHv3078001	Pseudoroegneria_stipifolia_PI440095	1488	1541	104%	601
NIASHv3078001	Pseudoroegneria_stipifolia_PI531751	1488	1399	94%	601
NIASHv3078001	Pseudoroegneria_strigosa_PI499638	1488	1357	91%	601
NIASHv3078001	Pseudoroegneria_strigosa_PI595172	1488	1351	91%	601
NIASHv3078001	Pseudoroegneria_strigosa_W614049	1488	1499	101%	601
NIASHv3078001	Pseudoroegneria_strigosa_PI639805	1488	1372	92%	601
NIASHv3078001	Pseudoroegneria_strigosa_PI639805	1488	1443	97%	601
NIASHv3078001	Pseudoroegneria_tauri_PI401322	1488	1237	83%	601
NIASHv3078001	Pseudoroegneria_tauri_PI401333	1488	1512	102%	601
NIASHv3078001	Secale_cereale_PI618662	1488	885	59%	601
NIASHv3078001	Secale_cereale_PI618665	1488	1441	97%	601
NIASHv3078001	Secale_cereale_PI618669	1488	1504	101%	601
NIASHv3078001	Secale_cereale_PI618671	1488	1541	104%	601
NIASHv3078001	Secale_strictum_R1108	1488	1065	72%	601
NIASHv3078001	Secale_strictum_R853	1488	1390	93%	601
NIASHv3078001	Secale_vavilovii_PI253957	1488	870	58%	601
NIASHv3078001	Secale_vavilovii_R1027	1488	1079	73%	601
NIASHv3078001	Taeniatherum_caput-medusae_CK2011	1488	1493	100%	601
NIASHv3078001	Taeniatherum_caput-medusae_GRA1126	1488	1528	103%	601
NIASHv3078001	Taeniatherum_caput-medusae_PI220589	1488	1534	103%	601
NIASHv3078001	Taeniatherum_caput-medusae_PI251387	1488	1224	82%	601
NIASHv3078001	Taeniatherum_caput-medusae_PI561095	1488	1047	70%	601
NIASHv3078001	Taeniatherum_crinium_GRA2570	1488	1500	101%	601
NIASHv3078001	Thinopyrum_bessarabicum_W621890	1488	1280	86%	601
NIASHv3078001	Thinopyrum_elongatum_PI109452	1488	1441	97%	601
NIASHv3078001	Thinopyrum_elongatum_PI401117	1488	1365	92%	601
NIASHv3078001	Triticum_boeoticum_1613	1488	1646	111%	601
NIASHv3078001	Triticum_boeoticum_1688	1488	1498	101%	601
NIASHv3078001	Triticum_boeoticum_ID379	1488	1343	90%	601
NIASHv3078001	Triticum_boeoticum_PI272520	1488	1476	99%	601
NIASHv3078001	Triticum_boeoticum_PI427451	1488	1550	104%	601
NIASHv3078001	Triticum_boeoticum_PI427620	1488	1491	100%	601
NIASHv3078001	Triticum_monococcum_2205	1488	1480	99%	601
NIASHv3078001	Triticum_monococcum_2208	1488	1499	101%	601
NIASHv3078001	Triticum_monococcum_2271	1488	1553	104%	601
NIASHv3078001	Triticum_monococcum_TRI13061	1488	1528	103%	601
NIASHv3078001	Triticum_monococcum_TRI13612	1488	1531	103%	601
NIASHv3078001	Triticum_urartu_1307	1488	1644	110%	601
NIASHv3078001	Triticum_urartu_PI428184	1488	1313	88%	601
NIASHv3078001	Triticum_urartu_PI428317	1488	1246	84%	601
NIASHv3078001	Triticum_urartu_TRI17824	1488	1514	102%	601
NIASHv3078001	Triticum_urartu_TRI18407	1488	1534	103%	601
NIASHv3120P04	Aegilops_bicornis_AE106	1177	1344	114%	601
NIASHv3120P04	Aegilops_bicornis_AE1079	1177	825	70%	601
NIASHv3120P04	Aegilops_bicornis_AE788	1177	1363	116%	601
NIASHv3120P04	Aegilops_bicornis_KU-5786	1177	1066	91%	601
NIASHv3120P04	Aegilops_comosa_AE1255	1177	1375	117%	601
NIASHv3120P04	Aegilops_comosa_AE1378	1177	1048	89%	601
NIASHv3120P04	Aegilops_comosa_AE783	1177	1269	108%	601
NIASHv3120P04	Aegilops_comosa_PI276970	1177	923	78%	601
NIASHv3120P04	Aegilops_longissima_AE1078	1177	1035	88%	601
NIASHv3120P04	Aegilops_longissima_AE133	1177	1268	108%	601
NIASHv3120P04	Aegilops_longissima_AE417	1177	992	84%	601
NIASHv3120P04	Aegilops_longissima_PI604141	1177	923	78%	601
NIASHv3120P04	Aegilops_longissima_TA1921	1177	1185	101%	601

Locus	Accession	Mapped exon length in barley (bp)	Assembled exon length (bp)	% of mapped exon length that could be assembled	Extended target (bp)
NIASHv3120P04	Aegilops_markgrafii_AE1381	1177	1329	113%	601
NIASHv3120P04	Aegilops_markgrafii_KP-2012-106	1177	1180	100%	601
NIASHv3120P04	Aegilops_markgrafii_PI254863	1177	1057	90%	601
NIASHv3120P04	Aegilops_markgrafii_PI542208	1177	1377	117%	601
NIASHv3120P04	Aegilops_markgrafii_PI596287	1177	1345	114%	601
NIASHv3120P04	Aegilops_mutica_01C2100106	1177	1318	112%	601
NIASHv3120P04	Aegilops_searsii_AE1075	1177	1138	97%	601
NIASHv3120P04	Aegilops_searsii_AE1083	1177	1354	115%	601
NIASHv3120P04	Aegilops_searsii_KU-14655	1177	1330	113%	601
NIASHv3120P04	Aegilops_searsii_PI599142	1177	1236	105%	601
NIASHv3120P04	Aegilops_searsii_PI599148	1177	916	78%	601
NIASHv3120P04	Aegilops_sharonensis_AE90691	1177	1346	114%	601
NIASHv3120P04	Aegilops_speltoides_3776	1177	1371	116%	601
NIASHv3120P04	Aegilops_speltoides_AE1064	1177	1297	110%	601
NIASHv3120P04	Aegilops_speltoides_AE900	1177	1156	98%	601
NIASHv3120P04	Aegilops_speltoides_KU-7856	1177	1010	86%	601
NIASHv3120P04	Aegilops_speltoides_PI486264	1177	1333	113%	601
NIASHv3120P04	Aegilops_speltoides_PI487231	1177	1184	101%	601
NIASHv3120P04	Aegilops_speltoides_TA1772	1177	1118	95%	601
NIASHv3120P04	Aegilops_tauschii_49116	1177	1029	87%	601
NIASHv3120P04	Aegilops_tauschii_937	1177	1381	117%	601
NIASHv3120P04	Aegilops_tauschii_AE1069	1177	1254	107%	601
NIASHv3120P04	Aegilops_tauschii_AE956	1177	1265	107%	601
NIASHv3120P04	Aegilops_umbellulata_AE1070	1177	1249	106%	601
NIASHv3120P04	Aegilops_umbellulata_AE153	1177	1273	108%	601
NIASHv3120P04	Aegilops_umbellulata_AE740	1177	1094	93%	601
NIASHv3120P04	Aegilops_umbellulata_AE811	1177	701	60%	601
NIASHv3120P04	Aegilops_uniaristata_AE157	1177	1251	106%	601
NIASHv3120P04	Aegilops_uniaristata_AE680	1177	1249	106%	601
NIASHv3120P04	Aegilops_uniaristata_PI276996	1177	895	76%	601
NIASHv3120P04	Agropyron_cristatum_PI494615	1177	1253	106%	601
NIASHv3120P04	Agropyron_cristatum_PI598631	1177	1182	100%	601
NIASHv3120P04	Amblyopyrum_muticum_PI560122	1177	863	73%	601
NIASHv3120P04	Amblyopyrum_muticum_PI560124	1177	841	71%	601
NIASHv3120P04	Amblyopyrum_muticum_PI560125	1177	794	67%	601
NIASHv3120P04	Amblyopyrum_muticum_PI560126	1177	865	73%	601
NIASHv3120P04	Amblyopyrum_muticum_PI636562	1177	1254	107%	601
NIASHv3120P04	Australopyrum_retrofractum_PI531553	1177	1252	106%	601
NIASHv3120P04	Australopyrum_retrofractum_PI533013	1177	987	84%	601
NIASHv3120P04	Australopyrum_retrofractum_PI533014	1177	1218	103%	601
NIASHv3120P04	Australopyrum_retrofractum_PI547363	1177	1352	115%	601
NIASHv3120P04	Brachypodium_distachyon	1177	1347	114%	601
NIASHv3120P04	Bromus_tectorum_GRA1085	1177	1192	101%	601
NIASHv3120P04	Dasyphyrum_villosum_GRA1020	1177	1228	104%	601
NIASHv3120P04	Dasyphyrum_villosum_GRA1027	1177	1090	93%	601
NIASHv3120P04	Dasyphyrum_villosum_PI368884	1177	781	66%	601
NIASHv3120P04	Dasyphyrum_villosum_W619414	1177	935	79%	601
NIASHv3120P04	Dasyphyrum_villosum_W67300	1177	1188	101%	601
NIASHv3120P04	Eremopyrum_distans_PI193264	1177	1233	105%	601
NIASHv3120P04	Eremopyrum_triticeum_GRA2250	1177	1231	105%	601
NIASHv3120P04	Eremopyrum_triticeum_PI502364	1177	1154	98%	601
NIASHv3120P04	Eremopyrum_triticeum_W626631	1177	1019	87%	601
NIASHv3120P04	Henrardia_persica_PI401347	1177	1228	104%	601
NIASHv3120P04	Henrardia_persica_PI577112	1177	1254	107%	601
NIASHv3120P04	Henrardia_persica_PI577113	1177	1094	93%	601
NIASHv3120P04	Henrardia_persica_RF2012	1177	1208	103%	601
NIASHv3120P04	Heteranthelium_piliferum_PI401351	1177	1278	109%	601
NIASHv3120P04	Heteranthelium_piliferum_PI401353	1177	1384	118%	601
NIASHv3120P04	Heteranthelium_piliferum_PI401354	1177	1298	110%	601
NIASHv3120P04	Heteranthelium_sp_PI314152	1177	1239	105%	601
NIASHv3120P04	Hordeum_marinum_BCC2006	1177	1311	111%	601
NIASHv3120P04	Hordeum_marinum_BCC2002	1177	1342	114%	601
NIASHv3120P04	Hordeum_pubiflorum_2028	1177	1418	120%	601
NIASHv3120P04	Hordeum_spontanum_FT11	1177	1430	121%	601
NIASHv3120P04	Hordeum_vulgare_Morex	1177	1462	124%	601
NIASHv3120P04	Psathyrostachys_juncea_PI222050	1177	1245	106%	601
NIASHv3120P04	Psathyrostachys_juncea_PI565077	1177	999	85%	601
NIASHv3120P04	Psathyrostachys_juncea_PI595135	1177	1266	108%	601
NIASHv3120P04	Psathyrostachys_juncea_PI598613	1177	1185	101%	601
NIASHv3120P04	Psathyrostachys_juncea_PI619487	1177	1261	107%	601
NIASHv3120P04	Psathyrostachys_sp_PI565080	1177	1195	102%	601
NIASHv3120P04	Pseudoroegneria_libanotica_PI228389	1177	894	76%	601
NIASHv3120P04	Pseudoroegneria_libanotica_PI330688	1177	1081	92%	601
NIASHv3120P04	Pseudoroegneria_libanotica_PI401274	1177	1152	98%	601
NIASHv3120P04	Pseudoroegneria_stipifolia_PI325181	1177	1353	115%	601
NIASHv3120P04	Pseudoroegneria_stipifolia_PI440095	1177	1240	105%	601
NIASHv3120P04	Pseudoroegneria_stipifolia_PI531751	1177	1209	103%	601
NIASHv3120P04	Pseudoroegneria_strigosa_PI499638	1177	1161	99%	601
NIASHv3120P04	Pseudoroegneria_strigosa_PI595172	1177	1241	105%	601
NIASHv3120P04	Pseudoroegneria_strigosa_W614049	1177	1320	112%	601
NIASHv3120P04	Pseudoroegneria_strigosa_PI639805	1177	1274	108%	601
NIASHv3120P04	Pseudoroegneria_strigosa_PI639805	1177	1284	109%	601
NIASHv3120P04	Pseudoroegneria_tauri_PI401322	1177	1102	94%	601
NIASHv3120P04	Pseudoroegneria_tauri_PI401333	1177	1305	111%	601
NIASHv3120P04	Secale_cereale_PI618662	1177	815	69%	601
NIASHv3120P04	Secale_cereale_PI618665	1177	1131	96%	601

Locus	Accession	Mapped exon length in barley (bp)	Assembled exon length (bp)	% of mapped exon length that could be assembled	Extended target (bp)
NIASHv3120P04	Secale_cereale_PI618669	1177	1259	107%	601
NIASHv3120P04	Secale_cereale_PI618671	1177	1311	111%	601
NIASHv3120P04	Secale_strictum_R1108	1177	1048	89%	601
NIASHv3120P04	Secale_strictum_R853	1177	1159	98%	601
NIASHv3120P04	Secale_vavilovii_PI253957	1177	734	62%	601
NIASHv3120P04	Secale_vavilovii_R1027	1177	1193	101%	601
NIASHv3120P04	Taeniatherum_caput-medusae_CK2011	1177	1212	103%	601
NIASHv3120P04	Taeniatherum_caput-medusae_GRA1126	1177	1387	118%	601
NIASHv3120P04	Taeniatherum_caput-medusae_PI220589	1177	1355	115%	601
NIASHv3120P04	Taeniatherum_caput-medusae_PI251387	1177	1035	88%	601
NIASHv3120P04	Taeniatherum_caput-medusae_PI561095	1177	733	62%	601
NIASHv3120P04	Taeniatherum_crinitum_GRA2570	1177	1320	112%	601
NIASHv3120P04	Thinopyrum_bessarabicum_W621890	1177	972	83%	601
NIASHv3120P04	Thinopyrum_elongatum_PI109452	1177	1340	114%	601
NIASHv3120P04	Thinopyrum_elongatum_PI401117	1177	1092	93%	601
NIASHv3120P04	Triticum_boeoticum_1613	1177	1433	122%	601
NIASHv3120P04	Triticum_boeoticum_1688	1177	1338	114%	601
NIASHv3120P04	Triticum_boeoticum_ID379	1177	938	80%	601
NIASHv3120P04	Triticum_boeoticum_PI272520	1177	1019	87%	601
NIASHv3120P04	Triticum_boeoticum_PI427451	1177	1349	115%	601
NIASHv3120P04	Triticum_boeoticum_PI427620	1177	1310	111%	601
NIASHv3120P04	Triticum_monococcum_2205	1177	1339	114%	601
NIASHv3120P04	Triticum_monococcum_2208	1177	1286	109%	601
NIASHv3120P04	Triticum_monococcum_2271	1177	1403	119%	601
NIASHv3120P04	Triticum_monococcum_TRI13061	1177	1261	107%	601
NIASHv3120P04	Triticum_monococcum_TRI13612	1177	1376	117%	601
NIASHv3120P04	Triticum_urartu_1307	1177	1364	116%	601
NIASHv3120P04	Triticum_urartu_PI428184	1177	1086	92%	601
NIASHv3120P04	Triticum_urartu_PI428317	1177	927	79%	601
NIASHv3120P04	Triticum_urartu_TRI17824	1177	1352	115%	601
NIASHv3120P04	Triticum_urartu_TRI18407	1177	1396	119%	601

Table E.3c Summary of the results used to distinguish low-copy number loci from multi-copy loci.

Locus	Genera with an average of >1% ambiguities	Comment	Low-copy number locus?
AK248139.1	3		yes
AK248741.1	7		no
AK249824.1	0		yes
AK250130.1	2		yes
AK250796.1	3		yes
AK251381.1	3		yes
AK251824.1	5		yes
NIASHv1001J07	1		yes
NIASHv1005E06	0		yes
NIASHv1005J12	8		no
NIASHv1005K14	0		yes
NIASHv1006J04	0		yes
NIASHv1008C12	3		yes
NIASHv1019M02	0		yes
NIASHv1020M09	0		yes
NIASHv1027H02	1		yes
NIASHv1052M11	1		yes
NIASHv1061L09	0		yes
NIASHv1071B24	11		no
NIASHv1085J04	8		no
NIASHv1107H16	0		yes
NIASHv1111N13	0		yes
NIASHv1116D04	2		yes
NIASHv1119N16	14		no
NIASHv1122M14	0		yes
NIASHv1130O12	0		yes
NIASHv1146J02	0		yes
NIASHv2001A19	0		yes
NIASHv2008E12	1		yes
NIASHv2010L15	0		yes
NIASHv2013C21	1		yes
NIASHv2014A03	9		no
NIASHv2017D10	3		yes
NIASHv2018H13	0		yes
NIASHv2020J22	0		yes
NIASHv2032E04	1		yes
NIASHv2044I15	1		yes
NIASHv2076L24	2		yes
NIASHv2082M12	1		yes
NIASHv2091P17	1		yes
NIASHv2108E11	0		yes
NIASHv2111B14	3		yes
NIASHv2112F04	6		no
NIASHv2124L23	6		no
NIASHv2136L17	1		yes
NIASHv3001I15	5		yes
NIASHv3014F17	1		yes
NIASHv3023N20	8		no
NIASHv3057H19	1		yes
NIASHv3069O18	4		yes
NIASHv3072D13	14		no
NIASHv3074A16	0		yes
NIASHv3076L17	1		yes
NIASHv3078O01	2		yes
NIASHv3088H24	1		yes
NIASHv3101J23	7		no
NIASHv3110H12	8		no
NIASHv3145A04	0		yes
AK248567.1	2		yes
AK249570.1	2		yes
AK249620.1	9		no
AK250049.1	0		yes
AK250484.1	1		yes
AK251050.1	0		yes
AK252210.1	2		yes
AK252992.1	1		yes
AK253026.1	1		yes
NIASHv1001F12	12		no
NIASHv1002F22	2		yes
NIASHv1003G15	0		yes
NIASHv1003J03	0		yes
NIASHv1004C20	11		no
NIASHv1004J10	6		no
NIASHv1006N10	1		yes
NIASHv1019H20	1		yes
NIASHv1028G08	1		yes
NIASHv1051H15	0		yes
NIASHv1061G04	14		no
NIASHv1075J15	1		yes
NIASHv1083B11	2		yes
NIASHv1107E09	11		no
NIASHv2001C22	12		no
NIASHv2001G18	1		yes
NIASHv2001J17	2		yes
NIASHv2004I15	2		yes
NIASHv2005A17	1		yes
NIASHv2005E13	0		yes
NIASHv2014H13	4		yes

Locus	Genera with an average of >1% ambiguities	Comment	Low-copy number locus?
NIASHv2017N01	0		yes
NIASHv2017P24	0		yes
NIASHv2018P05	3		yes
NIASHv2021D08	5	number of ambiguities >1% in many Aegilops and Triticum accessions	no
NIASHv2023F05	2		yes
NIASHv2023K17	1		yes
NIASHv2029L05	1		yes
NIASHv2040G12	0		yes
NIASHv2047P10	11		no
NIASHv2052D22	6		no
NIASHv2053C08	0		yes
NIASHv2058P13	2		yes
NIASHv2059H12	0		yes
NIASHv2060P18	2		yes
NIASHv2070A04	4		yes
NIASHv2075H13	6		no
NIASHv2077K09	2		yes
NIASHv2081G06	0		yes
NIASHv2099B04	0		yes
NIASHv2112K23	3		yes
NIASHv2116I02	5		yes
NIASHv2120H08	0		yes
NIASHv2129O09	2		yes
NIASHv2139N15	0		yes
NIASHv2143E05	0		yes
NIASHv2146E12	2		yes
NIASHv2147G04	0		yes
NIASHv3015H06	2		yes
NIASHv3018N07	1		yes
NIASHv3030D11	3		yes
NIASHv3030N10	1		yes
NIASHv3043P01	0		yes
NIASHv3063K23	11		no
NIASHv3067I15	4	number of ambiguities >1% in many Aegilops and Triticum accessions	no
NIASHv3093B23	5	number of ambiguities >1% in many Aegilops and Triticum accessions	no
AK248476.1	3		yes
AK249034.1	0		yes
AK249072.1	0		yes
AK249495.1	0		yes
AK249711.1	0		yes
AK249831.1	0		yes
AK250429.1	1		yes
AK250906.1	5		yes
AK251074.1	6		no
AK251526.1	1		yes
AK252552.1	10		no
NIASHv1005I08	0		yes
NIASHv1015H21	0		yes
NIASHv1026E05	1		yes
NIASHv1036M12	0		yes
NIASHv1039I18	0		yes
NIASHv1040D23	4		yes
NIASHv1041I08	1		yes
NIASHv1047L22	0		yes
NIASHv1048I05	0		yes
NIASHv1072J22	1		yes
NIASHv1077I03	4		yes
NIASHv1078F01	14		no
NIASHv1085I06	2		yes
NIASHv1089B18	0		yes
NIASHv1116P24	1		yes
NIASHv2001G19	7		no
NIASHv2012M23	1		yes
NIASHv2019E23	0		yes
NIASHv2025P23	9		no
NIASHv2027M24	1		yes
NIASHv2028E10	5		yes
NIASHv2029G10	1		yes
NIASHv2033P01	1		yes
NIASHv2041B21	0		yes
NIASHv2043E08	0		yes
NIASHv2058L21	4		yes
NIASHv2059P15	4		yes
NIASHv2064F19	5	number of ambiguities >1% in many Aegilops and Triticum accessions	no
NIASHv2065F23	1		yes
NIASHv2066C23	0		yes
NIASHv2069D19	2		yes
NIASHv2076D08	0		yes
NIASHv2082K16	3		yes
NIASHv2084N06	0		yes
NIASHv2090C08	0		yes
NIASHv2094G16	14		no
NIASHv2114B24	1		yes
NIASHv2125M08	0		yes
NIASHv2138A02	8		no
NIASHv2142K13	13		no
NIASHv2146E09	2		yes
NIASHv2147C17	8		no
NIASHv2150G18	0		yes
NIASHv3001C05	0		yes

Locus	Genera with an average of >1% ambiguities	Comment	Low-copy number locus?
NIASHv3001L02	4		yes
NIASHv3008G09	6		no
NIASHv3031M05	7		no
NIASHv3035L02	2		yes
NIASHv3080D11	2		yes
NIASHv3095B23	3		yes
NIASHv3097A23	2		yes
NIASHv3112H19	0		yes
NIASHv3129N09	0		yes
AK249011.1	6		no
AK249571.1	0		yes
AK250844.1	0		yes
AK250867.1	3		yes
AK251061.1	0		yes
AK251704.1	1		yes
AK253053.1	0		yes
NIASHv1006N15	0		yes
NIASHv1012O21	1		yes
NIASHv1030O05	1		yes
NIASHv1046E03	0		yes
NIASHv1051M22	0		yes
NIASHv1081H14	10		no
NIASHv1100G15	1		yes
NIASHv1124F24	4		yes
NIASHv1138B11	0		yes
NIASHv2001E23	0		yes
NIASHv2004F10	1		yes
NIASHv2012M06	1		yes
NIASHv2013J06	1		yes
NIASHv2014H03	1		yes
NIASHv2015D21	5	number of ambiguities >1% in many Aegilops and Triticum accessions	no
NIASHv2023D07	0		yes
NIASHv2026H08	1		yes
NIASHv2026L21	4		yes
NIASHv2028E12	0		yes
NIASHv2028H24	1		yes
NIASHv2028O18	8		no
NIASHv2029G06	0		yes
NIASHv2030H12	1		yes
NIASHv2030L12	1		yes
NIASHv2036B23	7		no
NIASHv2039I23	0		yes
NIASHv2041H01	1		yes
NIASHv2047I02	0		yes
NIASHv2055M07	2		yes
NIASHv2075O21	1		yes
NIASHv2083N11	2		yes
NIASHv2090N15	1		yes
NIASHv2092C13	3		yes
NIASHv2098F21	7		no
NIASHv2105L06	4		yes
NIASHv2107B09	2		yes
NIASHv2108J05	0		yes
NIASHv2112C18	1		yes
NIASHv2135K21	7		no
NIASHv3063P21	2		yes
NIASHv3072B14	9		no
NIASHv3081C04	3		yes
NIASHv3090B15	1		yes
NIASHv3092A12	0		yes
NIASHv3097N06	1		yes
NIASHv3120P04	1		yes
NIASHv3126D01	0		yes
NIASHv3136D22	0		yes
NIASHv3142C22	5	number of ambiguities >1% in many Aegilops and Triticum accessions	no
NIASHv3148A06	0		yes
NIASHv3148C05	3		yes
AK248344.1	1		yes
AK248694.1	3		yes
AK248749.1	12		no
AK249063.1	5	number of ambiguities >1% in many Aegilops and Triticum accessions	no
AK250137.1	13		no
AK250803.1	5	number of ambiguities >1% in many Aegilops and Triticum accessions	no
AK251479.1	0		yes
AK251756.1	2		yes
AK251848.1	2		yes
AK251964.1	0		yes
AK252329.1	0		yes
AK252673.1	8		no
AK252793.1	4		yes
NIASHv1003D08	0		yes
NIASHv1006F09	1		yes
NIASHv1013F08	3		yes
NIASHv1013L02	10		no
NIASHv1014E15	2	number of ambiguities >1% in many Aegilops and Triticum accessions	no
NIASHv1018B08	0		yes
NIASHv1023N07	0		yes
NIASHv1026E03	3		yes
NIASHv1032N06	0		yes
NIASHv1060D16	1		yes

Locus	Genera with an average of >1% ambiguities	Comment	Low-copy number locus?
NIASHv1075J07	4		yes
NIASHv1102L13	2		yes
NIASHv1107C06	1		yes
NIASHv2005H07	3		yes
NIASHv2011K02	0		yes
NIASHv2018O04	2		yes
NIASHv2019I09	1		yes
NIASHv2019K23	5		yes
NIASHv2020D03	0		yes
NIASHv2022H18	1		yes
NIASHv2026L03	7		no
NIASHv2029C24	5	number of ambiguities >1% in many Aegilops and Triticum accessions	no
NIASHv2030A19	1		yes
NIASHv2035F19	1		yes
NIASHv2037K06	0		yes
NIASHv2040J13	0		yes
NIASHv2041B06	14		no
NIASHv2041N17	2		yes
NIASHv2057H24	2		yes
NIASHv2070G19	1		yes
NIASHv2071H16	4		yes
NIASHv2085I09	0		yes
NIASHv2090B09	1		yes
NIASHv2091G21	0		yes
NIASHv2094J13	0		yes
NIASHv2112L06	3		yes
NIASHv2118F23	3		yes
NIASHv2136O20	14		no
NIASHv2142F15	2		yes
NIASHv3021D10	2		yes
NIASHv3027P02	2		yes
NIASHv3032B09	2		yes
NIASHv3035O23	0		yes
NIASHv3046C17	11		no
NIASHv3051M12	0		yes
NIASHv3052H21	10		no
NIASHv3060N24	0		yes
NIASHv3071I18	3		yes
NIASHv3085H23	6		no
NIASHv3086G24	5	number of ambiguities >1% in many Aegilops and Triticum accessions	no
NIASHv3103E17	2		yes
NIASHv3108H21	3		yes
NIASHv3108P17	1		yes
NIASHv3114M22	3	number of ambiguities >1% in many Aegilops and Triticum accessions	no
NIASHv3137B19	1		yes
AK248195.1	5	number of ambiguities >1% in many Aegilops and Triticum accessions	no
AK248499.1	2	number of ambiguities >1% in many Aegilops and Triticum accessions	no
AK249069.1	0		yes
AK249445.1	0		yes
AK249999.1	0		yes
AK250162.1	2		yes
AK250604.1	1		yes
AK250700.1	13		no
AK251739.1	8		no
AK251798.1	3		yes
AK252587.1	0		yes
AK252796.1	1		yes
AK252870.1	0		yes
NIASHv1004I13	0		yes
NIASHv1005J14	1		yes
NIASHv1006M08	1		yes
NIASHv1010N21	11		no
NIASHv1014P15	3		yes
NIASHv1015D14	0		yes
NIASHv1028O24	1		yes
NIASHv1042L09	1		yes
NIASHv1049B23	1		yes
NIASHv1057C02	2		yes
NIASHv1059F15	1		yes
NIASHv1069I21	14		no
NIASHv1097E17	0		yes
NIASHv1120F17	1		yes
NIASHv1143K18	12		no
NIASHv2001L06	4		yes
NIASHv2005J23	1		yes
NIASHv2008P10	3		yes
NIASHv2010J23	2		yes
NIASHv2016A22	1		yes
NIASHv2016P22	0		yes
NIASHv2020C20	5		yes
NIASHv2022D03	6		no
NIASHv2023D11	13		no
NIASHv2037A03	3		yes
NIASHv2039I04	2		yes
NIASHv2040E18	2		yes
NIASHv2043F06	1		yes
NIASHv2054E12	1		yes
NIASHv2072O23	3		yes
NIASHv2073P17	5		yes
NIASHv2086D01	2		yes

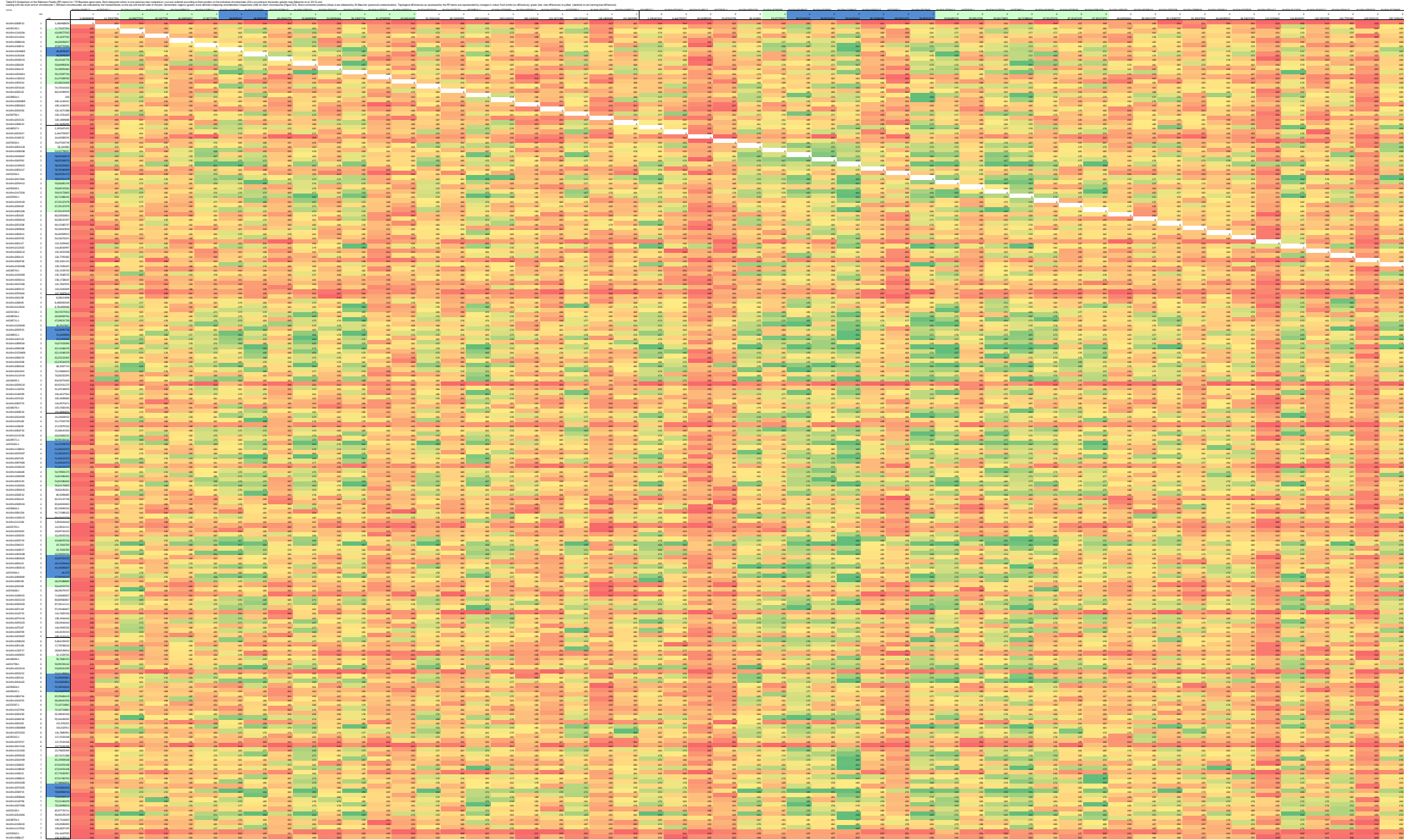
Locus	Genera with an average of >1% ambiguities	Comment	Low-copy number locus?
NIASHv2088O20	5		yes
NIASHv2101A14	0		yes
NIASHv2116K16	2		yes
NIASHv2130F02	4		yes
NIASHv2140L14	1		yes
NIASHv3003J02	4		yes
NIASHv3017A02	2		no
NIASHv3017H24	3	number of ambiguities >1% in many Aegilops and Triticum accessions	yes
NIASHv3055L19	13		no
NIASHv3081F24	0		yes
NIASHv3127P04	2		yes
AK248704.1	1		yes
AK249694.1	6		no
AK249707.1	7		no
AK250291.1	3		yes
AK252062.1	4		yes
AK252439.1	1		yes
AK252642.1	13		no
NIASHv1002C13	2		yes
NIASHv1011E07	2		yes
NIASHv1016O12	4		yes
NIASHv1033O01	0		yes
NIASHv1045G19	0		yes
NIASHv1046K18	6		no
NIASHv1071B23	3		yes
NIASHv1071N14	3		yes
NIASHv1098B12	0		yes
NIASHv1117B24	2		yes
NIASHv1119E17	1		yes
NIASHv1121G04	1		yes
NIASHv2005H17	2		yes
NIASHv2011D01	2		yes
NIASHv2013I11	7		no
NIASHv2014N04	1		yes
NIASHv2016H09	2		yes
NIASHv2027O06	0		yes
NIASHv2028J08	11		no
NIASHv2036F15	0		yes
NIASHv2040E06	7		no
NIASHv2041B24	1		yes
NIASHv2043G08	1		yes
NIASHv2058N04	2		yes
NIASHv2059N20	1		yes
NIASHv2071G08	1		yes
NIASHv2075G05	5		yes
NIASHv2076N12	13		no
NIASHv2077O03	3		yes
NIASHv2083K19	2		yes
NIASHv2088P11	0		yes
NIASHv2108I12	0		yes
NIASHv2108K22	2		yes
NIASHv2128D22	1		yes
NIASHv2128H10	0		yes
NIASHv2135D15	1		yes
NIASHv2138B20	2		yes
NIASHv2140C04	2		yes
NIASHv2140L04	6		no
NIASHv2141P06	3		yes
NIASHv2142F06	0		yes
NIASHv2146E11	2		yes
NIASHv2148A07	0		yes
NIASHv3044H03	9		no
NIASHv3051L01	2		yes
NIASHv3054B12	3		yes
NIASHv3057E16	0		yes
NIASHv3081M13	13		no
NIASHv3085K14	14		no
NIASHv3088L17	1		yes
NIASHv3100P06	3		yes

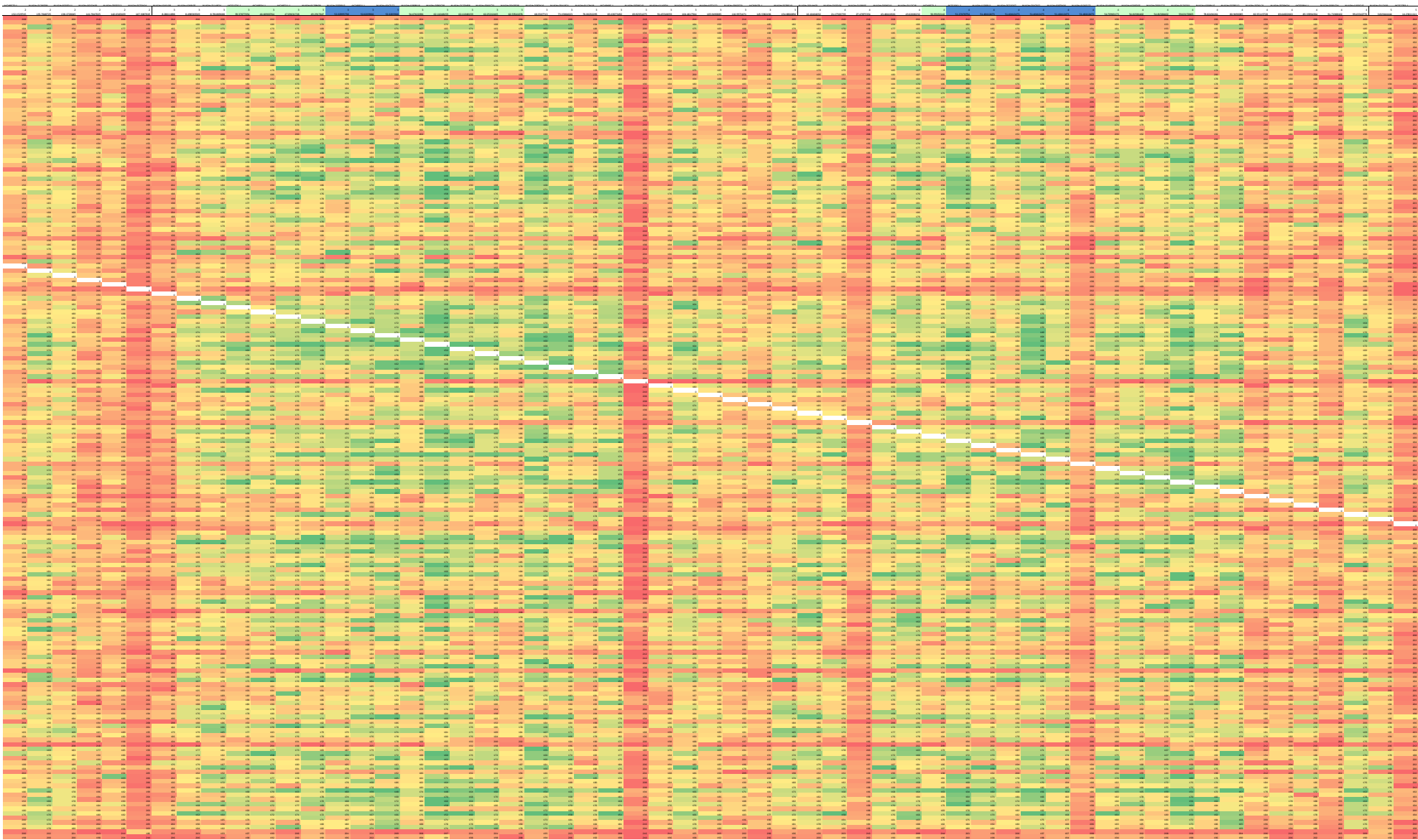
Table E.4 Overview of loci selected for the sequence capture. The barley f-cDNAs were used to retrieve functional annotation information via a local BLAST search against the non-redundant (nr) sequence database of the National Center for Biotechnology Information (NCBI); accessed in October 2014. Gene annotations presented here correspond the homologue in *Brachypodium distachyon*.

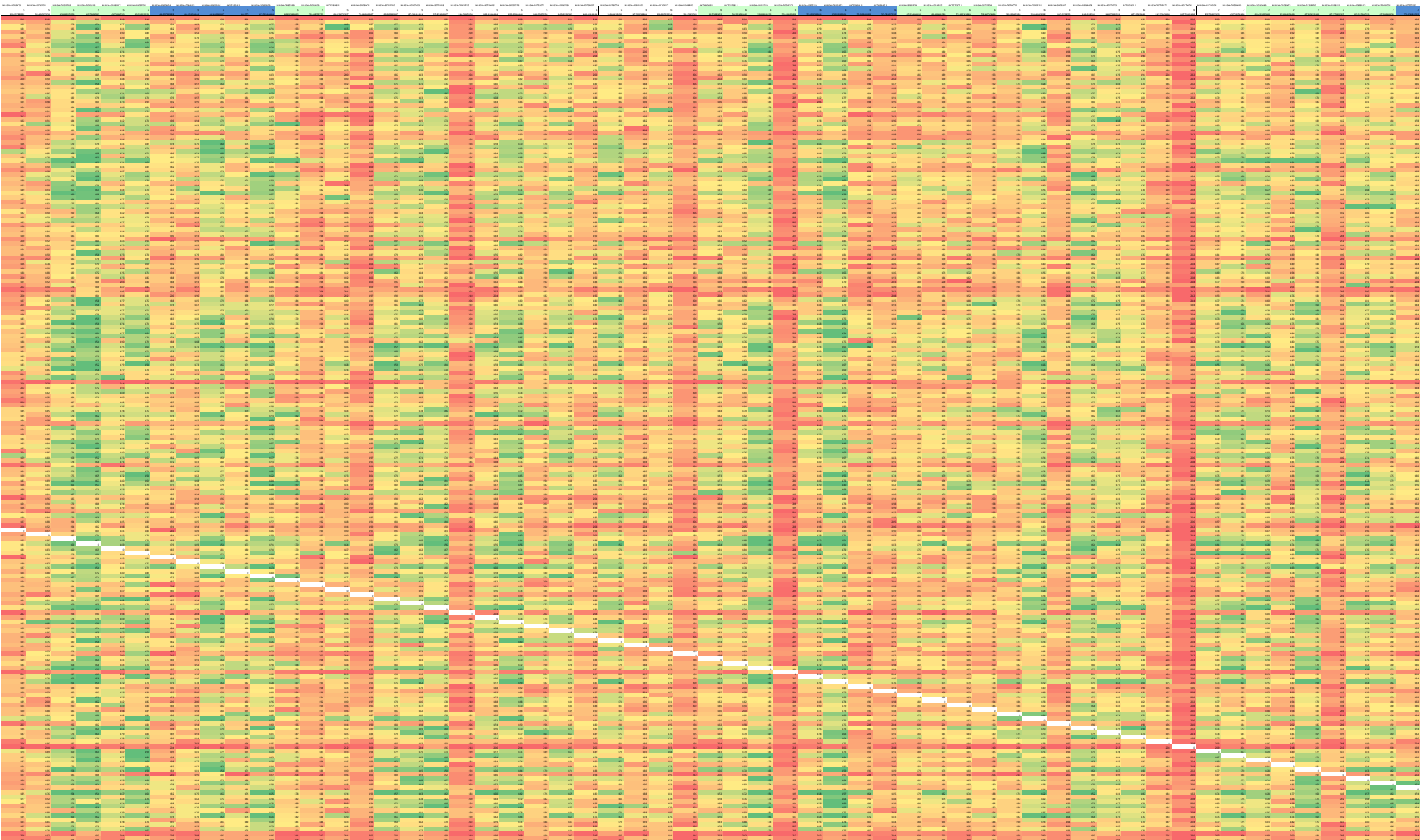
Locus	Putative function	Chromosome in barley & wheat (A/B-D)	Chromosome in barley (POPSEQ)	Chromosome in barley (POPSEQ)	Genomic location in barley (Mb)	Interfered chromosomal region in barley	Chromosome in rice	Genomic location in rice (Mb)	Alignment length (bp)	Missing data (%)	Prätranscriptomic Low-coopy sites in %	Used for phylogenetic analysis
NIASH3148205	ATPase 10, plasma membrane-type-like	4	4H	4H	85.5240793 Cent	7R	1R	1553	23.45	17.52	yes	
NIASH314840	acytoplasmic plasma membrane-associated	4	4H	4H	54.70863173 Cent	1R	1R	1033.424894	15.18	19.41	yes	
NIASH3148404	GTPase-activating protein	1	1H	1H	103.3345292	1R	1R	1400	0.48	20.81	yes	
NIASH3148424	protein transport	4	4H	4H	50.9915042							
NIASH3148422	cell division control	4	4H	4H	66.93586648 Cent	1R	1R	170.074569	3517	16.28	18.08	no
NIASH3137819	DEAD-box ATP-dependent RNA	5	5H	5H	NA	5R	5R	11.8283418	2317	45.29	13.81	yes
NIASH3138022	transcription factor POF5-like	4	4H	4H	51.40412473 Cent*			1010	13.38	22.97	yes	
NIASH3128929	probable RNA-dependent RNA	3	3H	3H	49.2917881 Cent			1549	3.78	13.44	yes	
NIASH3127704	probable RNA-dependent RNA	6	6H	6H	72.18713881 Cent	6R	6R	251.3201439	1271	9.64	23.05	yes
NIASH3126001	uncharacterized LOC100832213	4	4H	4H	59.63172862 Cent			3957	0.69	16.93	yes	
NIASH3120904	UDP-glucuronate 4-epimerase	4	4H	4H	55.73654898 Cent			1102	4.09	10.99	yes	
NIASH3114422	uncharacterized LOC10020958	5	5H	5H	NA	5R	5R	362.1431629	2469	1.20	21.79	no
NIASH3113005	ascaris protein resembling spermatin-1-like	3	3H	3H	17.847026							
NIASH3112919	L-ascorbate oxidase homologue	1	1H	1H	76.0232295 Tel	3R	3R	300.6139423	1105	0.47	13.94	yes
NIASH3110812	DNA mismatch repair protein	3	3H	3H	NA			2108	0.33	10.73	no	
NIASH3108717	uncharacterized LOC100849244	5	5H	5H	43.7604783 Cent			2028	24.81	15.97	yes	
NIASH3108421	methylase-specific RNA(cytosine-C5)-methyltransferase-like	5	5H	5H	71.6666667 Cent			1400	0.47	21.50	yes	
NIASH3103517	microtubule-associated protein	5	5H	5H	0.972222222 NA			1986	2.15	18.99	yes	
NIASH3101123	uncharacterized LOC10081690	1	1H	1H	27.26520985 Tel	1R	1R	54.77599111	1060	0.47	28.42	yes
NIASH3100906	cell division control	conflicting	7H	7H	1.628895184 NA	4R	4R	558.2496775	2763	23.56	21.39	yes
NIASH3100303	uncharacterized LOC10081690	2H	2H	2H	140.7920011							
NIASH3097908	chaperone protein ClpC2, chloroplast-like	4	4H	4H	51.40412473 Cent*			2807	11.98	21.98	yes	
NIASH3097423	uncharacterized LOC100834911	3	3H	3H	NA			1518	19.09	11.48	yes	
NIASH3095923	probable LRR receptor-like	3	3H	3H	NA			2066	7.13	21.31	yes	
NIASH3095823	transducin beta-like protein	conflicting	2H	2H	110.1863003 NA	6R	6R	5.10.4233163	4953	20.18	26.64	no
NIASH3095412	uncharacterized LOC100845761	conflicting	4H	4H	99.43342789 NA	6R	6R	99.43342789 NA	927	0.40	12.73	yes
NIASH3090915	uncharacterized LOC100845761	conflicting	4H	4H	1.02052005 Tel	4R	4R	20.28092842	741	11.11	27.13	yes
NIASH308817	26S protease regulatory subunit	7	7H	7H	134.3130031 Tel			1172	10.24	18.19	yes	
NIASH3088024	mitogen-activated protein kinase	1	1H	1H	46.00029885 Tel	1R	1R	103.7101544	2531	17.06	21.94	yes
NIASH308624	UDP-glucose 6-epimerase	5	5H	5H	126.8333333 Cent	7R	7R	231.6214778	1547	5.10	11.89	no
NIASH3085814	reticuline oxidase protein-like	7	7H	7H	70.8323222 Cent	7R	7R	1188	2.86	14.90	no	
NIASH3085812	serine/threonine-protein phosphatase	5	5H	5H	30.41666667 Tel	7R	7R	2343	5.54	19.13	yes	
NIASH3081113	probable inactive purple acid phosphatase	6	6H	6H	70.8323222 NA			1515	10.84	22.44	no	
NIASH3081104	ADP-ATP carrier, mitochondrial-like	6	6H	6H	65.92464131 Cent	6R	6R	210.3918688	1862	16.62	23.62	yes
NIASH3081004	putative transporter ans-like	4	4H	4H	91.7138012 Tel			1802	20.76	13.05	yes	
NIASH3080511	probable inactive purple acid phosphatase	3	3H	3H	NA			908	13.07	25.50	yes	
NIASH3078201	uncharacterized LOC10084174	1	1H	1H	NA	1R	1R	324.1423566	1577	7.68	27.52	yes
NIASH307617	L-ascorbate oxidase homologue	conflicting	1H	1H	NA			1438	3.90	17.73	yes	
NIASH3074116	uncharacterized LOC10020901	1H	1H	1H	74.1031816 Tel			2287	9.20	22.04	yes	
NIASH3072306	uncharacterized LOC10020901	1H	1H	1H	16.05497519							
NIASH3072023	probable glutamyl-tRNA synthetase	conflicting	1H	1H	97.5212484 NA			2060	0.52	11.80	no	
NIASH3072018	heat shock 70 kDa protein	conflicting	1H	1H	111.9602955 NA			1509	2.47	19.59	yes	
NIASH3071118	subtilisin-like protease SDD1-like	5	5H	5H	97.29166667 Tel	1R	1R	1915	2.09	19.79	yes	
NIASH3069183	uncharacterized LOC100838847	1	1H	1H	NA			2855	19.57	15.45	yes	
NIASH3067115	phosphatidylinositol 3-kinase	2	2H	2H	50.04277777 Cent	1R	1R	2171	10.27	13.54	yes	
NIASH3063921	subtilisin-like protease SDD1-like	conflicting	4H	4H	110.840451 NA	5R	5R	728.031825	2113	21.84	15.29	yes
NIASH3063923	probable LRR receptor-like	2	2H	2H	13.34447777 Tel			4015	25.42	28.84	no	
NIASH3060294	cytochrome b5-like (LOC10083454)	5	5H	5H	44.09722222 Cent*	5R	5R	134.5999866	1256	14.48	18.99	yes
NIASH3057119	glutaryl-tRNA reductase 1	1	1H	1H	NA			1640	29.53	17.07	yes	
NIASH3057116	BURP domain-containing protein	7	7H	7H	23.30028320			1455	35.71	19.93	yes	
NIASH305619	uncharacterized LOC100834473	6	6H	6H	NA			2137	0.13	15.72	yes	
NIASH3054612	patellin-4-like (LOC100834473)	7	7H	7H	110.2891218 Tel	7R	7R	359.6470132	1319	33.51	14.25	yes
NIASH3050321	ester chomolipase	conflicting	5H	5H	159.2826888 Cent	7R	7R	1617	0.77	17.92	yes	
NIASH3051112	DEAD-box ATP-dependent RNA	5	5H	5H	154.513889 NA			2296	5.40	24.09	yes	
NIASH3051101	phytylase synthase, chloroplast-like	7	7H	7H	140.8602222 Tel			1631	36.19	18.82	yes	
NIASH3050317	probable leucine carboxylase	5	5H	5H	109.65277777 Tel			1833	16.81	19.21	yes	
NIASH3044403	phosphotransaminase/psychoglucomutase-like	7	7H	7H	75.2144649 Cent	7R	7R	1280	16.28	15.48	no	
NIASH3030910	uncharacterized LOC100837141	2	2H	2H	82.08210031 Tel			1699	6.88	16.45	yes	
NIASH3030011	uncharacterized LOC100839158	2	2H	2H	138.1728045 Tel			1033	11.16	22.85	yes	
NIASH3027902	peroxisomal (S)-2-hydroxy acid	5	5H	5H	139.5922222 Tel	5R	5R	578.9076477	267	0.85	16.10	yes
NIASH3025011	uncharacterized LOC100838847	6	6H	6H	6.82789025							
NIASH3023200	probable phenylalanine-tRNA	1	1H	1H	48.0818187 Cent			242	0.72	7.44	no	
NIASH3021210	heat shock 70 kDa protein	5	5H	5H	80.80962867 Tel			1985	0.49	17.78	yes	
NIASH3020217	uncharacterized LOC100838847	5	5H	5H	46.45833333							
NIASH3018007	pentatricopeptide repeat-containing protein	2	2H	2H	58.0524074 Cent*			2694	2.27	18.15	yes	
NIASH3017004	uncharacterized LOC100838847	2	2H	2H	117.5524074 Cent*	3R	3R	485.8464828	2074	10.84	23.76	yes
NIASH3017002	probable galactaronyltransferase-like	6	6H	6H	73.79600339 Cent	6R	6R	38.2829411	887	3.92	15.32	yes
NIASH3015908	choline transporter-like protein	2	2H	2H	141.7847025 Tel			2327	6.49	23.29	yes	
NIASH3014817	uncharacterized LOC100838847	1	1H	1H	43.05948008 Cent			1867	0.84	18.47	yes	
NIASH3008909	peptide transporter PTR8-like	3	3H	3H	24.71871388 Tel			2046	15.58	20.48	yes	
NIASH3003302	uncharacterized LOC100830337	6	6H	6H	115.9170255 Tel			2378	3.68	24.43	yes	
NIASH3001301	uncharacterized LOC100839881	3	3H	3H	NA			2127	20.87	16.29	yes	
NIASH3001115	uncharacterized LOC100839881	conflicting	1H	1H	NA			856	28.85	19.98	yes	
NIASH3001008	mRNA, clone: PL018C01-A-044_G24	3	3H	3H	15.15580733	3R	3R	63.90152753	4384	77.87	5.36	yes
NIASH2150104	serine/threonine-protein kinase	6	6H	6H	54.8512749							
NIASH2150118	uncharacterized LOC100838847	3	3H	3H	53.27979037 Cent	3R	3R	209.9478988	4492	74.19	7.26	yes
NIASH2148011	peroxidase 70-kDa (LOC100838847)	7	7H	7H	24.50424958							
NIASH2148007	uncharacterized LOC100838847	7	7H	7H	NA	4R	4R	345.9008776	2513	3.54	18.92	yes
NIASH2147901	probable inactive receptor	2	2H	2H	59.63172862 Cent			1848	16.86	15.90	yes	
NIASH2147417	probable peroxidase transporter	conflicting	3H	3H	86.33144478 NA			1146	29.05	14.07	no	
NIASH2146112	26S protease regulatory subunit	2	2H	2H	24.64589235 Tel			1058	0.82	19.00	yes	
NIASH2146111	BTB/POZ domain-containing protein	2	2H	2H	13.88101889 NA			1522	3.10	23.20	yes	
NIASH2146109	U-box domain-containing protein	3	3H	3H	104.4617656 Tel	4R	4R	548.5381809	1458	0.05	14.73	yes
NIASH2143605	uncharacterized LOC100829844	2	2H	2H	NA			3236	1.57	18.80	yes	
NIASH2143603	U-box domain-containing protein	3	3H	3H	81.01903033 Cent			1043	26.00	19.43	yes	
NIASH2142715	probable cyclic nucleotide-gated ion channel	5	5H	5H	114.7685333 Tel	5R	5R	484.9329339	2286	10.31	25.49	yes
NIASH2142708	uncharacterized LOC100838847	7	7H	7H	75.21246489 Cent			2143	5.11	16.29	yes	
NIASH2141906	protein RMD5 homologue A	7	7H	7H	NA	7R	7R	197.675682	1409	1.52	16.66	yes
NIASH2140411	uncharacterized LOC100837402	6	6H	6H	117.9888888							
NIASH2140114	uncharacterized LOC100837402	6	6H	6H	52.8203988 Cent	6R	6R	123.541111	978	8.39	20.80	yes
NIASH2140104	U5 small nuclear ribonucleoprotein	7	7H	7H	126.131445 Tel	7R	7R	482.2245075	1135	0.27	16.95	no
NIASH2140004	5-3-phosphoglycerate dehydrogenase	7	7H	7H	121.8130331 Tel	2R	2R	7.84220515	2087	34.76	18.97	yes

Locus	Putative function	Chromosome in barley & wheat (AbBt)		Chromosome in barley (Genome/Type)		Chromosome in barley (Genomic location)		Chromosome in wheat (Genomic location)		Alignment length		Parasimony-informative		Low-copy		Used for phylogenetic	
		Chromosome	Region	Chromosome	Region	Chromosome	Region	Chromosome	Region	bp	bp	bp	bp	bp	bp	bp	bp
NIASH200411H1	tubulin beta-4 chain-like	conflicting	5H	134.722222 NA	5H	42.9861111	5H	591.986815	1755								
NIASH200411B	2,3-bisphosphoglycerate-independent respiratory burst	conflicting	4H	99.4332778 NA	7H	5H	42.9861111	2350				13.11				14.43	yes
NIASH200411E4	granule-bound starch synthase	conflicting	7H	73.18810198 NA	4R	5H	510.6428877	899	6.30						18.24	yes	yes
NIASH200411E1	pentatectoprotein repeat-containing	3	3H	73.18810202 NA	3H	5H	139.0972222 NA	2304	11.99						17.50	yes	yes
NIASH200411B6	pleiotropic drug resistance	conflicting	5H	43.7607478 Cent	5R	5H	185.1830879	1363	0.48						15.36	yes	yes
NIASH200411J3	alpha-alpha-trehalose-phosphatase	2	2H	122.5622687 Tel	2R	5H	517.8552581	1408	23.74						22.42	yes	yes
NIASH200411E2	putative chloride channel	2	2H	65.0249292 Tel	2R	5H	95.0429292	3344	15.05						19.97	yes	yes
NIASH20040E18	probable alpha-alpha-trehalose-phosphatase	6	6H	60.8398940 Cent	4R	7H	329.4270519	1306	8.42						15.01	no	
NIASH20040E6	T-complex protein 1 subunit	4	4H	66.9071978 Tel	4R	6H	45.7875354 Cent	1171	8.42						11.44	yes	yes
NIASH20030A1	LPT0406 protein 1, transcript	5	5H	54.8158642 Cent	4R	6H	479.1807724 no	1544	58.83						9.59	yes	yes
NIASH20030A4	26S proteasome non-ATPase	6	6H	44.2351111 Cent	6R	2H	2.119588394	3423	20.09						24.45	yes	yes
NIASH20030C9	uncharacterized LOC100838401	5	5H	NA	4R	6H	184.2148748	2532	3.83						19.30	yes	yes
NIASH20030A3	uncharacterized LOC100838820	6	6H	70.8090561 Cent	4H	7H	11.9699121	1829	8.49						20.56	no	
NIASH20030F15	uncharacterized LOC100828865	conflicting	4H	43.8805555 Cent	5H	5H	43.8805555 Cent	2862	1.29						18.37	yes	yes
NIASH20030E23	uncharacterized LOC100824880	6	6H	90.3328919 Tel	3H	3H	90.3328919 Tel	152	4.07						15.45	yes	yes
NIASH20030F19	protein VERNALIZATION INSENSITIVE	1	1H	122.1671388 Tel	1H	1H	122.1671388 Tel	1850	11.61						17.46	yes	yes
NIASH20030E4	laccase 7-like (LOC1008116)	5	5H	80.9490068 Tel	4H	4H	80.9490068 Tel	2518	39.33						12.71	yes	yes
NIASH20030L2	adenylosuccinate synthetase	4	4H	88.9846151 Tel	4H	4H	88.9846151 Tel	2375	35.83						19.88	yes	yes
NIASH20030A19	uncharacterized LOC100833308	5	5H	NA	5H	5H	NA	2728	15.95						21.04	yes	yes
NIASH20030L5	2,3-dimethylmaleate lyase-like	2	2H	2H	2H	2H	67.35127479 Cent	2149	9.42						22.29	yes	yes
NIASH20030G10	F-box protein A2G94105-like	3	3H	83.9251275 Tel	3R	3H	342.2510969	1077	19.28						19.13	yes	yes
NIASH20030C6	beta-amylase 1, chloroplastic-like	4	4H	107.365491 Tel	4H	4H	107.365491 Tel	1485	26.92						13.13	yes	yes
NIASH20030E4	chrysotholide 4-reductase-like	5	5H	NA	5H	5H	NA	1953	37.63						22.79	no	
NIASH20030I18	5-methyltetrahydrofolylglutamate-homocysteine	4	4H	3.47025498 Tel	4H	4H	3.47025498 Tel	2139	3.23						16.74	no	
NIASH20030J6	phospholipase D alpha 2-like	conflicting	7H	11.9699121 Cent	7R	2H	231.6214778	2282	25.50						18.23	no	
NIASH20030I4	tubulin-lysine isomerase-like	4	4H	83.9402266 Tel	4H	4H	83.9402266 Tel	4586	13.68						23.45	yes	yes
NIASH20030E12	uncharacterized LOC100844507	4	4H	80.9490068 Tel	4H	4H	80.9490068 Tel	1467	0.09						16.88	yes	yes
NIASH20030I10	APF-complex subunit A-like	3	3H	154.8840868 Tel	3H	3H	154.8840868 Tel	1529	12.58						20.99	yes	yes
NIASH20020C5	rRNA-dihydrouridine synthase	7	7H	79.2400954 Cent	7H	7H	79.2400954 Cent	1081	4.49						21.93	yes	yes
NIASH20020M4	probable UDP-N-acetylglucosamine-peptide	3	3H	NA	3H	3H	NA	1301	0.69						15.37	yes	yes
NIASH20020I1	uncharacterized LOC100824900	4	4H	82.3511572 NA	4H	4H	82.3511572 NA	1567	17.60						17.66	yes	yes
NIASH20020L3	cellulose synthase-like protein	conflicting	5H	79.1708522 NA	5H	5H	79.1708522 NA	2846	28.73						16.76	no	
NIASH20020H8	magnesium transporter MR5-A	4	4H	NA	4H	4H	NA	1406	0.00						13.86	yes	yes
NIASH20020F2	cytochrome P450 T1-C4-like	3	3H	25.2832861 Tel	3H	3H	25.2832861 Tel	3160	44.09						22.99	yes	yes
NIASH20020K17	4-alpha-glucanotransferase	2	2H	6.444759207 Tel	2H	2H	6.444759207 Tel	2102	1.53						22.07	yes	yes
NIASH20020F5	uncharacterized LOC100837445	2	2H	94.5461222 Tel	2H	2H	94.5461222 Tel	3539	8.24						18.24	yes	yes
NIASH20020J11	uncharacterized LOC100837445	6	6H	117.5541168 Tel	3R	4H	488.1349339	874	7.05						27.12	no	
NIASH20020D7	adenylosuccinate lyase-like	4	4H	51.40412473 Cent	4H	4H	51.40412473 Cent	2627	16.77						21.24	yes	yes
NIASH20020I16	aspartic protease-like protein	6	6H	NA	6H	6H	NA	43.073	0.00						16.69	yes	yes
NIASH20020D3	rRNA-decyl-diphosphate	6	6H	106.1869717 Tel	6R	6H	106.1869717 Tel	2345	3.22						20.09	no	
NIASH20020D8	cutin-associated NEDD8-disassociated	conflicting	2H	7.43620523 NA	7R	2H	462.6848811	3675	13.48						14.89	no	
NIASH20020E2	lysosomal beta-galactosidase-like	1H	1H	86.54295953 Cent	1R	1H	86.54295953 Cent	1000	6.07						19.45	yes	yes
NIASH20020D3	ADP-ribosylation factor GTPase-activating	5	5H	87.3811111 Tel	5H	5H	87.3811111 Tel	2292	5.84						20.99	yes	yes
NIASH20020C0	glycoproteinase-like	6	6H	92.2800328 Tel	6R	6H	92.2800328 Tel	2823	9.63						19.08	yes	yes
NIASH20019K23	K(+)-efflux antiporter 3	5	5H	29.0972222 Tel	5H	5H	29.0972222 Tel	1316	1.38						20.97	yes	yes
NIASH2001909	DUF246 domain-containing protein	5	5H	50.44225793 Cent	5H	5H	50.44225793 Cent	2033	35.1945						19.02	yes	yes
NIASH20019E1	coronatine insensitive	2	2H	90.0741443 NA	2H	2H	90.0741443 NA	1418	30.37						14.78	yes	yes
NIASH20018P5	probable protein phosphatase	2	2H	108.6188945	2H	2H	108.6188945	1493	20.96						15.94	yes	yes
NIASH20018Q4	transmembrane 8 superfamily	5	5H	NA	5H	5H	NA	1684	3.46						14.78	yes	yes
NIASH20018H3	uncharacterized LOC100827190	1H	1H	49.4342772 Cent	1H	1H	49.4342772 Cent	1253	15.31						16.60	yes	yes
NIASH20017P4	4-alpha-glucanotransferase	2	2H	NA	2H	2H	NA	1458	2.01						15.64	yes	yes
NIASH20017N1	uncharacterized LOC100849415	2	2H	58.92351205 Cent	2H	2H	58.92351205 Cent	2408	2.95						16.24	yes	yes
NIASH20017D10	ABC transporter G family member	1	1H	NA	1H	1H	NA	2598	31.94						15.59	yes	yes
NIASH20016P22	putative 1-aminopyrene-1-carboxylate	6	6H	78.39943334 Cent	6R	6H	78.39943334 Cent	529	21.88						18.90	yes	yes
NIASH20016I9	probable atanyl-ATPase	7H	7H	65.4920428 Cent	7H	7H	65.4920428 Cent	4504	10.07						15.45	yes	yes
NIASH20016A22	cytochrome 2-like (LOC100838321)	6	6H	55.0282381 Cent	6H	6H	55.0282381 Cent	2878	6.51						20.80	yes	yes
NIASH20016Q1	ubiquitin-activating enzyme	4	4H	54.30031033 Cent	4H	4H	54.30031033 Cent	5124	26.03						13.33	yes	yes
NIASH20016N21	uncharacterized LOC100829572	7H	7H	90.06529925 Tel	7R	7H	90.06529925 Tel	725	15.79						22.55	yes	yes
NIASH20016H3	endoplasmic reticulum metalloproteinase	4	4H	126.874221 NA	2R	2H	126.874221 NA	1759	0.15						16.71	yes	yes
NIASH20014H03	penicillin homology domain 32016	4	4H	16.10454032 Tel	4H	4H	16.10454032 Tel	4519	16.99						22.89	yes	yes
NIASH20014A03	glutelin type 1-like (LOC100823576)	1H	1H	131.579593 NA	1H	1H	131.579593 NA	884	5.38						20.59	no	
NIASH20013L5	LUP1022 protein A1G1640-like	4	4H	NA	4H	4H	NA	2177	4.03						17.32	yes	yes
NIASH20013I11	cockle shell protein 160	7	7H	NA	7H	7H	NA	3204	32.00						15.45	yes	yes
NIASH20013C1	probable serine/threonine-protein	1H	1H	128.186988 Tel	1R	1H	128.186988 Tel	4151	21.68						16.82	yes	yes
NIASH20012A23	uncharacterized LOC100828398	3	3H	122.0254993 Cent	3H	3H	122.0254993 Cent	2080	33.68						17.16	yes	yes
NIASH20012M06	uncharacterized LOC100828398	conflicting	4H	NA	4H	4H	NA	794.40251	1116	6.05					26.61	yes	yes
NIASH20011K02	dihydrolysozyme residue	5	5H	NA	5H	5H	NA	1888	16.54						24.53	yes	yes
NIASH20011D1	uncharacterized LOC100846183	7	7H	104.815868 Tel	7H	7H	104.815868 Tel	1453	6.91						16.99	yes	yes
NIASH20010L5	cytochrome P450 94A1-like	conflicting	1H	90.1558073 Tel	1H	3H	90.1558073 Tel	1314	24.40						13.70	yes	yes
NIASH20010J3	uncharacterized LOC100824806	6	6H	NA	6H	6H	NA	445	0.12						23.15	yes	yes
NIASH20009I0	protein-coupled amino acid	6	6H	129	6H	6H	129	4.67	1.29								

Accession	Putative function	Chromosome in barley & wheat (A/B/C)	Chromosome in barley (Genome/Type)	Chromosome in barley (POP/SC)	Genomic location in barley (Mb)	Inferred chromosomal region	Chromosome in rye	Genomic location in rye (Mb)	Alignment length (bp)	Missing data (%)	Parasimilarity sites in %	Low-copy number/focus	Used for phylogenetic analyses
NIASH1005E08	putative phosphopyruvate	1	1H	3H	48.45829231 Cent		1R	54.32769574	1568	23.71	13.78		
NIASH1004J10	UDP-glycosyltransferase 74F2-like	conflicting	2H	2H	12.39370771 NA		7R	419.4518115	1827	30.99	22.39	no	
NIASH1004I13	thioesterase reductase NTRB-like	6	6H	6H	62.14242107 Cent		6R	219.7620517	978	6.89	13.60	yes	
NIASH1004C20	probable methyltransferase	2	2H	2H	148.1586402 Tel		2R	652.1787047	1607	6.88	24.64	no	
NIASH1003J03	elongation factor G, chloroplast-like	2	2H	2H	80.02822661 Tel				2309	3.08	14.84	yes	yes
NIASH1003E15	nucleoside-triphosphatase-like	2	2H	2H	NA				1402	15.06	19.62	yes	
NIASH1003D08	uncharacterized LOC100838962	5	5H	5H	43.95833333 Cent		5R	134.3599688	1281	1.72	14.99	yes	yes
NIASH1002F22	uncharacterized LOC100838962	2	2H	2H	58.05240074 Cent				1548	35.58	15.53	yes	
NIASH1002C13	probable galactinol-1-sucrose	7	7H	7H	43.8382691 Tel				3082	28.19	18.42	yes	
NIASH1001J07	protein IQ domain 1-like (LOC100831847)	1	1H	1H	42.3512479 Cent		1R	75.76401878	2319	27.31	18.02	yes	
AK2529412	uncharacterized LOC100832399	2	2H	2H	146.597485 Tel				713	22.80	19.50	no	
AK2530531	glyceraldehyde-3-phosphate	conflicting	4H	4H	99.71671388 NA				1373	18.65	12.96	yes	yes
AK2530281	uncharacterized LOC100826062	2	2H	2H	33.67563702 Tel				1393	12.83	12.71	yes	yes
AK2529252	S-adenosylmethionine decarboxylase	2	2H	2H	66.71388102 Cent		2R	259.7920785	1731	15.32	17.97	yes	yes
AK2528701	phosphoribulokinase, chloroplast-like	6	6H	6H	NA				1163	0.20	13.84	yes	yes
AK2527961	T-complex protein 1 subunit	6	6H	6H	116.4135977 Tel				1302	28.80	19.66	yes	yes
AK2527931	uncharacterized LOC100826894	5	5H	5H	14.2381111 Tel				1179	2.70	19.25	yes	yes
AK2528731	heat shock protein 81-3-like	5	5H	5H	75.55555556 Tel				2471	17.07	8.15	no	
AK2528421	uncharacterized LOC100832399	conflicting	7H	7H	23.79603368 NA				2071	2.53	20.38	no	
AK2528711	probable beta-D-xylosidase	6	6H	6H	72.16713881 Cent		6R	246.8148195	1756	10.93	25.68	yes	yes
AK2525252	1-deoxy-D-xylulose 5-phosphate	3	3H	3H	NA				719	7.10	20.86	no	
AK2524381	mitogen-activated protein kinase 12-like	5	5H	5H	85.9773371 Tel		7R	263.03367	1680	5.00	21.85	yes	yes
AK2523291	uncharacterized LOC100833303	5	5H	5H	0.97222222 Tel				3605	36.99	14.84	yes	yes
AK2522101	probable nucleolar protein	2H	2H	2H	41.85524048 NA		2R	127.9370139	2090	7.20	24.87	yes	yes
AK2520761	mRNA, clone: PL0160C1-A-011_G07	conflicting	6H	6H	72.3796304		6R	28.2629411 no					
AK2520621	endoglycamin homology (LOC100823353)	7	7H	7H	131.4447592 Tel				3099	12.37	20.85	yes	yes
AK2519841	uncharacterized LOC100829478	5	5H	5H	44.3375 Cent		5R	150.1777208	1794	3.44	19.45	yes	yes
AK2518481	aminotransferase YxhL-like	5	5H	5H	68.29679337 Tel		5R	288.0011831	1302	4.47	18.59	yes	yes
AK2518241	uncharacterized LOC100826232	1	1H	1H	NA				692	0.96	19.94	yes	yes
AK2517881	uncharacterized LOC100836034	6	6H	6H	50.99150164 Cent		7R	11.11	1988	7.11	23.44	yes	yes
AK2517581	RNA polymerase sigma factor	conflicting	5H	5H	168.88888888 NA		7R	31.45800128	1904	11.60	25.95	yes	yes
AK2517301	AP-2 complex subunit mu-like	6	6H	6H	62.74767535 Cent				400	0.14	7.61	no	
AK2517041	uncharacterized LOC100826111	4	4H	4H	NA				1766	0.76	15.97	yes	yes
AK2515261	uncharacterized LOC100826111	3	3H	3H	39.37677008 Cent		3R	141.8428262	2340	13.91	20.38	yes	yes
AK2514781	probable leucine repeat	5	5H	5H	47.22222222 Cent				315	0.20	19.38	yes	yes
AK2513811	mRNA, clone: PL0160C1-A-059_E13	1R	1H	1H	132.062153 Tel		1R	540.6252581	314	0.54	15.29	yes	yes
AK2513221	37 kDa inner envelope membrane	4	4H	4H	1.02520005				no				
AK2510741	2,3-bisphosphoglycerate-independent	3	3H	3H	76.34509697 Tel				2996	14.33	23.70	no	
AK2510611	KH domain-containing protein	4	4H	4H	51.27478784 Cent*				2105	8.50	18.06	yes	yes
AK2510501	NADH dehydrogenase [ubiquinone]	2	2H	2H	58.92351275 Cent*				1765	5.38	15.06	yes	yes
AK2509061	conflicting	3	3H	3H	8.923512748 Tel				650	20.28	26.00	yes	yes
AK2508771	cytochrome P450 88B1-like	conflicting	4H	4H	103.753541 NA				2304	26.16	15.06	yes	yes
AK2508441	3-ketoadyl CoA synthase 10-like	4	4H	4H	85.33984354 Tel				2051	18.48	9.22	yes	yes
AK2508031	eukaryotic translation initiation	1	1H	1H	139.2311111 NA				2379	3.98	17.95	no	
AK2507861	uncharacterized LOC100830416	1	1H	1H	126.1331836 Tel				3414	8.38	23.24	yes	yes
AK2507001	peroxidase 70-like (LOC100843065)	6	6H	6H	24.50434663 Tel				1274	15.55	20.57	no	
AK2506041	elongation factor Tu, chloroplast-like	6	6H	6H	55.38243628 Cent*				1825	15.54	9.97	yes	yes
AK2504711	peroxidase 16-like (LOC100834987)	7H	7H	7H	NA		7R	294.5132883 no					
AK2504841	protein argonaute 1b-like	conflicting	2H	2H	6.758354379 NA		2R	2446	2446	3.54	19.83	yes	yes
AK2504291	selenium binding protein 1-like	3	3H	3H	116.3597374 Tel		3R	401.3088199	273	0.01	20.15	yes	yes
AK2502011	cytochrome P450 70A1-like	7	7H	7H	13.80119163 Tel		4R	512.8317938	3358	33.86	19.84	yes	yes
AK2501621	metalloid up-regulated gene	6	6H	6H	117.5541168 Tel		6R	341.6857271	1978	2.23	26.54	yes	yes
AK2501481	heat shock cognate 70 kDa	6	6H	6H	88.89101883				287	9246626 no			
AK2501371	elongation factor 2-like (LOC100836272)	conflicting	5H	5H	155.55555556 NA				2874	11.10	8.91	no	
AK2501301	transmembrane protein 638-like	1	1H	1H	11.75667394 Tel		1R	34.55379117	2894	17.10	17.66	yes	yes
AK2500491	uncharacterized LOC100846028	2	2H	2H	59.05515581 Cent		2R	231.1203861	3736	20.26	19.35	yes	yes
AK2499991	mRNA, clone: PL0160C1-A-021_L21	6	6H	6H	66.35977371 Cent		6R	222.7313322	244	0.79	15.57	yes	yes
AK2488311	uncharacterized LOC100835013	3	3H	3H	52.620396 Cent*				3114	10.59	22.00	yes	yes
AK2486241	histone lysine N-methyltransferase	1	1H	1H	100.1418431 Tel				2076	0.96	11.75	yes	yes
AK2477111	phospholipase D alpha 1-like	3	3H	3H	47.09631724 Cent		3R	163.790705	3030	6.09	18.51	yes	yes
AK2476711	putative ornithine decarboxylase	7	7H	7H	76.69971671 Cent		6R	330.6501074	1369	8.79	21.40	no	
AK2466411	cysteine synthase, chloroplast/chloroplast-like	7	7H	7H	26.71253937 Tel		4R	454.5070688	951	6.81	18.09	no	
AK2466201	uncharacterized LOC100825996	2	2H	2H	NA		2R	359.9980153	1901	4.08	16.68	no	
AK2465711	uncharacterized LOC100830952	4	4H	4H	50.99150164 Cent				1625	5.85	19.94	yes	yes
AK2465701	beta-D-xylosidase 4-like (LOC100820868)	2	2H	2H	132.1529745 Tel				2014	22.59	18.37	yes	yes
AK2464851	probable serine/threonine-protein	3	3H	3H	83.63073402 Tel				3145	14.00	21.05	yes	yes
AK2464451	protein disulfide isomerase-like	6	6H	6H	55.50470292 Cent*		6R	122.5431111	1386	6.59	21.00	yes	yes
AK2460631	actin-3-like (LOC10084890)	5	5H	5H	158.88888888 NA				1108	0.64	13.74	no	
AK2460341	dot-P-Man 6-phospho-N-acetyl-PP-Dot	3	3H	3H	46.66920784 Cent				1978	15.65	16.08	yes	yes
AK2460111	quinone oxidoreductase-like	conflicting	4H	4H	110.69405 NA		5R	752.688444	2122	27.61	20.41	no	
AK2447491	carotenoid 9, 10', 10'' cleavage	5	5H	5H	0.1388888888 Tel				800	12.33	19.50	yes	yes
AK2447411	DEAD-box ATP-dependent RNA	1	1H	1H	NA				951	9.52	11.38	no	
AK2447041	ATP-dependent zinc metalloprotease	7	7H	7H	109.7314062 Tel				1996	4.91	17.89	yes	yes
AK2486941	heat shock cognate 70 kDa	5	5H	5H	NA				2141	16.48	10.56	yes	yes
AK2486971	uncharacterized LOC100843732	2	2H	2H	2.195447426 Tel		7R	490.1205621	1452	10.95	20.45	yes	yes
AK2484991	uncharacterized LOC100835724	6	6H	6H	103.8243628 Tel		6R	322.4448005	1898	9.80	23.08	no	
AK2484761	chlorophyllide a covinase	3	3H	3H	145.5324336 Tel				1571	0.33	21.90	yes	yes
AK2483441	DEAD-box ATP-dependent RNA	5	5H	5H	NA				1956	2.06	17.48	yes	yes
AK2481951	leucine aminopeptidase 2	6	6H	6H	NA		6R	311.7988102	1194	24.24	20.02	no	
AK2481391	phosphatidate phosphatase	1	1H	1H	NA				2517	1.39	20.29	yes	yes
AK2490691	uncharacterized LOC100838403	6	6H	6H	50.7082153 Cent		6R	68.07342985	1203	0.14	16.87	yes	yes
NIASHV0035C03	probable xyloglucan glycosyltransferase	5	5H	5H	130.8944444 Tel				1842	4.55	16.23	yes	yes
NIASHV0035I02	phospholipase C-3-like (LOC100841564)	3	3H	3H	142.2093171 Tel				4809	72.58	5.16	yes	yes
NIASHV0032B09	high affinity cationic amino	5	5H	5H	23.61111111 Tel		5R	44.77698335	2515	37.43	14.99	yes	yes
NIASHV0031M05	phosphatidate cytidylyltransferase-like	conflicting	3H	3H	64.30594901 NA		3R	250.0167744	1321	12.27	15.29	no	
AK2490721	type I in												







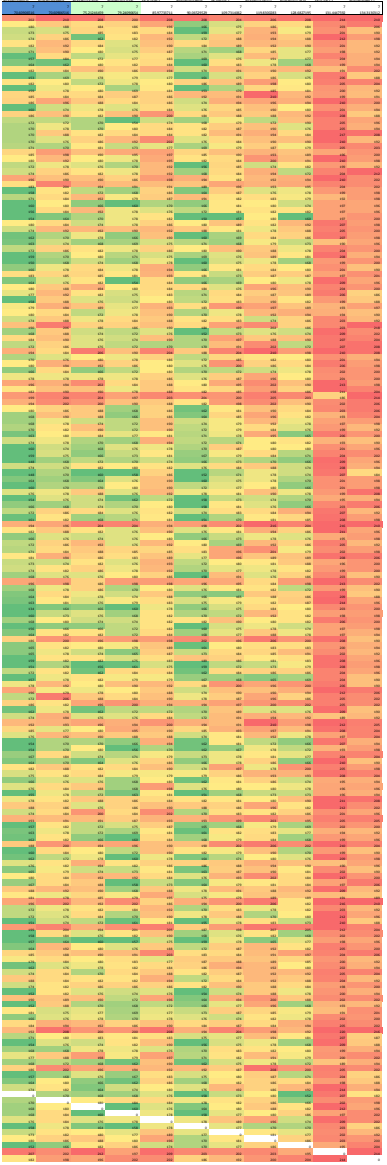


Table E.6 Comparison of topological results from different datasets and different phylogenetic methods. Loci located on the same chromosome 1,2 and 3 (Chr1-Chr3) in barley, wheat and rye were considered in chromosome-based concatenations and ML phylogenetic inference.

Method Program Dataset	Concatination & ML RAxML			Multi-genic network PhySIC_IST + Dendroscope			Coalescent-based species trees			*BEAST telomeric	BI MrBayes nrDNA unit	ML RAxML Chloroplast	
	Chr1	Chr2	Chr3	centromeric	telomeric	all	centromeric	ASTRAL-II telomeric	all				
Number of loci/partitions	14	19	18	83	96	245	83	96	245	28	6	1	
All genera monophyletic except <i>Aegilops</i>	yes	yes	yes	yes	yes	yes	yes	yes	yes	yes	–	yes	NA
<i>Psathyrostachys</i> + <i>Hordeum</i> basal	yes	yes	yes	yes	yes	yes	yes	yes	yes	yes	–	yes	yes
<i>Eremopyrum</i> + <i>Agropyron</i> sisters	yes	yes	yes	yes	yes	yes	yes	yes	yes	yes	–	yes	yes
<i>Australopyrum</i> (Au) <i>Eremopyrum</i> + <i>Agropyron</i> (Eagr) <i>Dasyphyum</i> (D) <i>Henardia</i> (Hper) <i>Heterantherium</i> (Hpil) <i>Taeniatherum</i> (Taen) <i>Thinopyrum</i> (Thin) <i>Pseudoroegneria</i> (Ps) <i>Secale</i> (S)	(Au+Hpil)	(Au,Eagr)	(D+Ps)	large polytomy; reticulation involving: Au, Hpil, D	(Ps+D)	large polytomies	Eagr basal	Ps basal			–	(Hpil+D); Ps parapythletic;	(Au, ((Eagr)+Hper), (D+Ps), Hpil S, ...)
		(S+Hper)		complex reticulations: S, Thi, Tae, <i>Aegilops</i> - <i>Amblyopyrum</i> - <i>Triticum</i>	complex reticulations: Eagr,Hper, Hpil, S, Au	(S, Thi, Taen,...)	(S, Thi, Taen,...)	(Hper, S, Thi, Taen,...)	(Hper, S, Thi, Taen,...)		–	(Thi, Hper,(S+Triticum))	Thi within Ps*
<i>Aegilops</i> monophyletic	with <i>Amblyopyrum</i>	no	with <i>Amblyopyrum</i>	no	no	no	no	yes*	no	no	yes	no	
<i>Aegilops</i> speltoides sister to <i>Amblyopyrum</i>	no	yes	yes	yes	no	no	yes	no	yes*	no	no	no	
<i>Sitopsis</i> ² monophyletic	no	no	no	no	no	no	no	no	no	yes	no	no	
<i>Sitopsis</i> monophyletic without <i>Ae. speltoides</i>	yes	yes	yes	yes	yes	yes	yes	yes	yes	yes	yes	yes	
<i>Ae. uniaristata</i> sister to <i>Ae. comosa</i>	yes	yes	yes	yes	yes	yes	yes	yes	yes	yes	yes	yes	
<i>Ae. umbellulata</i> sister to <i>Ae. markgrafii</i>	no	no	yes	complex reticulation	complex reticulation	yes	no	yes	yes	yes	yes	no	
<i>Aegilops</i> - <i>Amblyopyrum</i> - <i>Triticum</i>	(<i>Triticum</i> , <i>Taen</i> , <i>Ae. speltoides</i> , <i>Aegilops</i>)	((<i>Amblyopyrum</i> + <i>Ae. speltoides</i>), <i>Triticum</i> , <i>Aegilops</i>)	(<i>Triticum</i> ,(<i>Ae. speltoides</i> + <i>Amblyopyrum</i>), <i>Aegilops</i>)	complex reticulation	large polytomy	large polytomy	(<i>Amblyopyrum</i> + <i>Ae. speltoides</i>), (<i>Triticum</i> + <i>Aegilops</i>)	(<i>Amblyopyrum</i> ,(<i>Triticum</i> + <i>Ae. speltoides</i> *, <i>Aegilops</i>))	(<i>Amblyopyrum</i> + <i>Ae. speltoides</i> , (<i>Triticum</i> + <i>Aegilops</i>)*	(<i>Amblyopyrum</i> (<i>Aegilops</i> + <i>Triticum</i>))	(<i>Amblyopyrum</i> , <i>Aegilops</i>)	((<i>Ae. speltoides</i> + <i>Taen</i> *, <i>Triticum</i> , <i>Aegilops</i> incl. <i>Amblyopyrum</i>)	
<i>Ae. tauschii</i> sister to	<i>A. muticum</i>	<i>Ae. markgrafii</i>	<i>Ae. uniaristata</i> + <i>Ae. comosa</i>	complex reticulation within <i>Aegilops</i>	complex reticulation within <i>Aegilops</i>	complex reticulation within <i>Aegilops</i>	<i>Ae. uniaristata</i> + <i>Ae. comosa</i>	<i>Ae. markgrafii</i> + <i>Ae. umbellulata</i>	<i>Ae. markgrafii</i> + <i>Ae. umbellulata</i>	all <i>Aegilops</i> but <i>Sitopsis</i> *	all <i>Aegilops</i> but <i>Ae. speltoides</i>	all <i>Aegilops</i> but <i>Ae. speltoides</i>	

ML - Maximum Likelihood, BI - Bayesian phylogenetic inference, asterisks indicate clades with low support values.

²*Sitopsis* is a section traditionally defined for the species *Ae. bicornis*, *Ae. speltoides*, *Ae. searsii*, *Ae. sharonensis*, *Ae. longissima* based on morphological and genomic data (Kilian et al. 2011).